Development of a Protocol to Study Novel Radiotherapy-Immunotherapy Combinations in Pre-Clinical Models of Locally Advanced Rectal Cancer

Michael A. Gillespie, MBChB

Supervisors: Prof Owen Sansom and Prof Campbell Roxburgh

Thesis Submitted to the University of Glasgow
for the Degree of Doctor of Philosophy (PhD)

College of Medical, Veterinary and Life Sciences

September, 2023

University of Glasgow

CANCER RESEARCH UK | BEATSON INSTITUTE

CRUK Beatson Institute
Garscube Estate
Switchback Road
Glasgow
G61 1BD
United Kingdom

Abstract

Heterogeneous responses to neo-adjuvant chemoradiotherapy are observed in Locally Advanced Rectal Cancer (LARC). Understanding the molecular and immunological factors underpinning response to radiotherapy-based treatment strategies may promote the development of novel treatment strategies to overcome resistance mechanisms and improve response rates. Murine models of LARC and experimental platforms to deliver precise radiotherapy to small animals, will enable the pre-clinical testing and development of radiotherapy and immunotherapy combinations to guide future clinical trials.

Despite numerous technological advances in pre-clinical modelling of CRC, models which recapitulate the anatomy and mutational composition of LARC have been lacking. In Chapter 3, I describe the development of a novel orthotopic organoid transplant model which recapitulates histological features of aggressive disease, expresses common driver mutations, and maintains immunocompetence. Furthermore, the described model demonstrates reproducibility, high engraftment and is amenable to high experimental throughput.

In Chapter 4, I then utilise the developed orthotopic model of LARC to demonstrate that precise delivery of clinically relevant fractionated radiotherapy is possible in the pre-clinical setting. I then performed irradiation studies to characterise the effects of single fraction and fractionated radiotherapy to the model developed in thesis. In Chapter 4, I characterise the radio-resistance of the orthotopic model of LARC which has been developed, and identify numerous potential resistance mechanisms.

In Chapter 5, I then show the feasibility of administering fractionated radiotherapy and immunotherapy agents to an orthotopic model of LARC. Improved survival was demonstrated following treatment with fractionated radiotherapy and PD-1 inhibition. Overall, this thesis describes significant advances in the pre-clinical modelling of LARC and experimental capabilities for developing novel radiotherapy and immunotherapy combinations, which hold potential to inform the treatment scheduling of fractionated radiotherapy and PD-1 inhibition.

Contents

List of Tables

List of Figures

Acknowledgements

I wish to thank my supervisors Professor Owen Sansom and Professor Campbell Roxburgh for the opportunity to work on this exciting project, and to undertake training in scientific research. I am grateful for their generous support and guidance throughout my PhD, and for having the chance to work within the CRUK Beatson Institute. I have been very fortunate to have had extensive access to the world-leading facilities, resources and expertise available within the Institute. I have thoroughly enjoyed my time developing pre-clinical models of locally advanced rectal cancer, and developing irradiation and experimental protocols.

I would also like to thank all members of the Sansom lab for their help with all aspects of this work, particularly during such challenging times as the Covid-19 pandemic. I am extremely grateful to Tamsin Lannagan for providing invaluable advice and assistance with experiments, and for her patience and generosity in guiding me through all aspects of training in laboratory techniques and animal work. I must also thank Colin Steele for his support, expertise, experimental guidance, endless enthusiasm, and invaluable help and time in reading drafts.

This work would never have been possible without the support of the Beatson support staff and core facilities. I wish to extend my thanks to the core histology team led by Colin Nixon, Billy Clark for his assistance with RNA sequencing, and Kathryn Gilroy and Lily Hillson for their bioinformatic support and help with RNA sequencing data analysis. I am immensely thankful to Katrina Stevenson (SARRP technician) for her endless hours of support conducting irradiation experiments. I am very thankful to Dr Noori Maka (Consultant Pathologist) for kindly giving her time to help me interpret histology. I must also thank Xabier Cortes-Lavaud for performing flow cytometry, Emer Curley for performing dosimetry experiments, and Eoghan Mulholland for performing multiplex IHC.

I must thank my family for their support and patience during my PhD journey and while writing my thesis. I am grateful to my mother and father for their love and support which they have strived to provide throughout my life and career. My beautiful partner Eve has given me strength and encouragement throughout, and I am grateful for her endless patience and understanding as I dragged out the writing of this thesis. Finally, I am thankful to my two wonderful sons Benjamin and Nicholas for blessing me with happiness and motivation every day.

Author's Declaration

I confirm that all work presented in this thesis is my own, unless stated otherwise. This work has not been submitted for consideration of any other degree, either at the University of Glasgow or any other institution.

Abbreviations

4-OHT – 4-hydroxytamoxifen

5-FU – 5-Fluorouracil

AB/PAS – Alcian Blue/Periodic Acid Schiff

Alt-EJ – Alternative End-Joining

ALK – Activin Like Kinase

AOM - Azoxymethane

APC – Adenomatous Polyposis Coli

APC – Antigen Presenting Cells

ASO – Anti-sense Oligonucleotide

ATM – Ataxia Telangiectasia Mutated

ATP - Adenosine-5'-triphosphate

BrdU - 5'-bromo-2'doxyuridine

BMP – Bone Morphogenetic Proteins

BRAF – B-Rapidly Accelerated Fibrosarcoma

cCR – Clinical Complete Response

CpG – 5'-C-phosphate-G-3'

CAC – Carbonic anhydrase 1 promoter and cre recombinase

CAF – Cancer Associated Fibroblast

CALD1 – Caldesmon 1

CBCT – Cone beam Computed Tomography

CCL – Chemokine Ligand

CCR – Chemokine Receptor

CD – Cluster of Differentiation

CHK – Checkpoint Kinase

CIMP – CpG Island Methylator Phenotype

CIN – Chromosomal Instability

CK1-α – Casein Kinase 1-α

CMS – Consensus Molecular Subtype

COX - Cycloxygenase

CRC – Colorectal Cancer

CRISPR - Clustered Regularly Interspaced Short Palindromic Repeat

CRM – Circumferential Resection Margin

CRT - Chemoradiotherapy

CSC – Cancer Stem Cell

CSF – Colony Stimulating Factor

CT – Computed Tomography

CT-DNA – Circulating Tumour DNA

CTL – Cytotoxic T-Lymphocyte

CTLA-4 – Cytotoxic T-Lymphocyte Associated Protein 4

CXCR – CXC Chemokine Receptor

DAMP – Damage Associated Molecular Patterns

DC – Dendritic Cell

DCC – Deleted in Colorectal Cancer

DDR – DNA Damage Response

DMSO - Dimethyl Sulfoxide

DNA – Deoxyribonucleic Acid

DSB – Double Strand Break

DSS – Dextran Sodium Sulfate

EGFR – Epidermal Growth Factor Receptor

ELISpot – Enzyme Linked Immunosorbent Spot

EMT – Epithelial Mesenchymal Transition

ENU – N-ethyl-nitrosurea

FAP – Familial Adenomatous Polyposis

FAP – Fibroblast Activation Protein

Foxn1nu – Forkhead Box N1

FSE – Fast Spin Echo

GDF – Growth and Differentiation Factor

GEMM – Genetically Modified Mouse Model

GSK-3β – Glycogen synthase kinase - 3β

Gzm - Granzyme

HMGB – High Motility Group Box

HNPCC – Hereditary Non-Polyposis Colorectal Cancer

HP – Hyperplastic Polyp

HPMC - hydroxypropyl methycellulose

HR – Homologous Recombination

HSP – Heat Shock Protein

ICB – Immune Checkpoint Blockade

IFN – Interferon

IGFBP – Insulin-Like Growth Factor Binding Protein

IL – Interleukin

JAK – Janus Kinase

IP – intra-peritoneal

KRAS - Kirsten Rat Sarcoma Viral Oncogene Homolog

LARC – Locally Advanced Rectal Cancer

LEF1 – Lymph enhancer factor 1

LET – Linear Energy Transfer

LGR5 - Leucine-rich repeat-containing G-protein coupled receptor 5

LRP5/6 – Low density lipoprotein receptor related protein 5/6

LSL – Lox-Stop-Lox

MAP – MutY Homolog-Associated Polyposis

MAPK – Mitogen Activated Protein Kinase

MCP – Microenvironment Cell Population

MDSC – Myeloid Derived Suppressor Cells

MEK -Mitogen Activated Protein Kinase

MH – Mad Homology

MHC – Major Histocompatibility Complex

MIN – Multiple Intestinal Neoplasia

MLH – MutL Homolog

MMR – Mismatch Repair

MRI – Magnetic Resonance Imaging

MSI – Microsatellite Instability

MSS – Microsatellite Stable

Myc – Myelocytomatosis

NAR – Neoadjuvant Rectal

NCCN – National Comprehensive Cancer Network

NHEJ – Non-Homologous End-Joining

NK – Natural Killer

NOD – Non-Obese Diabetic

NSCLC – Non Small Cell Lung Cancer

NSG – NOD Scid Gamma

pCR – Pathological Complete Response

PD1 – Programmed Death 1

PDL1 – Programmed Death Ligand 1

PDO – Patient Derived Organoid

PTEN - Phosphatase and Tensin Homologue

PTSG - Prostaglandin-Endoperoxide Synthase

RAF – Rapidly Accelerated Fibrosarcoma

RAS – Rat Sarcoma Virus

RC – Rectal Cancer

RCT – Randomised Controlled Trial

RNA – Ribonucleic Acid

RNF – Ring Finger Protein

ROS – Reactive Oxygen Species

RT - Radiotherapy

SBRT – Stereotactic Body Radiation Therapy

SCID – Severe Combined Immunodeficiency

SCNA – Somatic Copy Number Alteration

SCPRT – Short-Course Pre-operative Radiotherapy

SMAD – Small Mothers Against Decapentaplegic

SSA – Sessile Serrated Adenoma

SSA – Single Strand Annealing

SSB – Single Strand Break

SSP – Sessile Serrated Polyp

STAT3 - Signal Transducer and Activator of Transcription 3 Signalling

STING – Stimulator of Interferon Genes

TAM – Tumour Associated Macrophages

TCD – Tumour Cell Density

TCF – T cell factor

TCGA – The Cancer Genome Atlas

TCR – T-Cell Receptor

TGF-β – Transforming Growth Factor beta

TGFBR – Transforming Growth Factor beta receptor

Th1 – T Helper 1

TIL – Tumour Infiltrating Lymphocyte

TLR – Toll Like Receptor

TMB – Tumour Mutational Burden

TME – Tumour Microenvironment

TNF – Tumour Necrosis Factor

TNT – Total Neoadjuvant Therapy

TP53 – Tumour Protein 53

TRG – Tumour Regression Grading

TSA – Traditional Serrated Adenoma

Wnt - Wingless-related integration site

XRCC - X-Ray Cross-Complementing

Chapter 1 – Introduction

1.1 Overview of Locally Advanced Rectal Cancer

1.1.1 Epidemiology of Colorectal Cancer

Colorectal Cancer (CRC) accounts for approximately 10% of cancer incidence and cancer-related mortality worldwide, with almost 900,000 deaths annually (Bray et al, 2018). In the UK, CRC is the fourth commonest cancer and the second commonest cause of cancer related mortality, with an incidence of approximately 42,000 cases (Cancer Research UK). Rectal Cancer (RC) represents a distinct sub-group of CRC, with differences in anatomy, clinical presentation, molecular characteristics and management strategies. RC accounts for a significant proportion of CRCs, representing 32% and 23% of male and female incidence respectively (Cancer Research UK).

Rates of CRC vary geographically, with higher incidence seen in developed countries (Dekker et al, 2019). CRC disease burden is predicted to increase globally, largely owing to rising cases in low- and middle-income countries, such that a worldwide incidence of 2.2 million cases is projected by 2030 (Arnold et al, 2017). On a global scale, recent trends in CRC incidence and mortality likely reflect increased adoption of westernised lifestyles, highlighting that disease burden is likely to increase over time. Worryingly, a rising proportion of CRCs are being found in younger individuals (<50 years), with this trend rising most rapidly in rectal cancer; 49.8% of colorectal tumours in <50s are reported to arise in the rectum (Kasi et al, 2019).

CRC survival has more than doubled in the UK over the past 40 years, with overall 5-year survival rates of 58% now observed (Cancer Research UK). Earlier stage at diagnosis leads to significantly improved outcomes, and patients with stage I and II disease have 92% and 84% 5-year survival rates respectively. Early diagnosis, with subsequent surgical resection, represents the best chance of achieving cure and disease remission for patients.

1.1.2 Research Priorities in Colorectal Cancer

Many of the current research priorities in CRC are based around improving population based screening methods, including the identification of population

subgroups at higher risk, and categorising which colorectal adenomas confer highest risk of malignant progression (Tiernan et al, 2014).

Patient outcomes worsen with increasing disease stage, with 5-year overall survival rates of 65% and 10% observed for stage III and IV disease respectively (Cancer Research UK). Current research must address the need to improve outcomes for patients with stage III and IV disease, through development of targeted therapeutic approaches and biomarkers to predict treatment response (Moorcraft et al, 2013). There is significant heterogeneity in the molecular profile of CRC, which can affect prognosis and responses to treatment, and standard of care regimens often do not result in therapeutic benefit across all patient subgroups.

Personalised medicine is focused on tailoring treatment according to an individual patient's clinical and molecular features, and CRC is currently seeing a paradigm shift towards precision medicine-based approaches, with the aim of improving response rates and survival, while minimising toxicity (Diamandis et al, 2010). Most notably, the monoclonal antibodies cetuximab and panitumumab which target epidermal growth factor receptor (EGFR), have been shown to have survival benefit in patients with refractory metastatic CRC (Cunningham et al, 2004; Saltz, 2004). However, many patients fail to respond to anti-EGFR therapies, and it has been established that KRAS (Kirsten Rat Sarcoma Viral Oncogene Homolog) mutations are associated with resistance to this treatment (Amado et al, 2008; Karapetis et al, 2008). KRAS testing is now routinely used in clinical practice, and demonstrates the implementation of personalised medicine in CRC, with anti-EGFR therapy reserved for those patients with wild-type KRAS status.

This thesis will focus on Locally Advanced Rectal Cancer (LARC), a subset of patients typically treated with neo-adjuvant radiotherapy or chemoradiotherapy (CRT), to facilitate curative margin-free surgical resection and reduce local recurrence rates (NICE, 2020). Recent years have seen a paradigm shift in the management of LARC, owing to the observation of complete tumour response to CRT in a proportion of patients (Habr-Gama et al, 2004). Recent research in LARC has focused on improving surgical cure rates, reducing distant and local recurrence, and improving the proportion of patients suitable for organ preservation strategies. In turn, it is hoped that more personalised treatment

strategies can be achieved in LARC, with management being based on biomarkers as well as clinical staging criteria.

It is evident that the mechanisms underpinning the heterogeneity of responses to CRT are incompletely understood, and that improved knowledge of the response of the tumour microenvironment to radiotherapy-based treatment strategies may aid the development of improved neo-adjuvant treatment regimens. Suitable pre-clinical models which recapitulate the molecular composition of LARC are lacking, and represent a potential tool to study the biological mechanisms of response to radiotherapy, and to test oncological therapies.

1.1.3 Aetiology of Colorectal Cancer

Hereditary, demographic, co-morbid, lifestyle and environmental factors are all known to have a role in the development of CRC. Increasing age and male sex have been shown to have a strong association with disease incidence (Dekker et al, 2019). Several modifiable environmental risk factors are associated with CRC, with cigarette smoking being associated with increased CRC incidence and mortality, with stronger associations found for rectal cancer than for colonic cancer (Botteri et al, 2008). High intake of red and processed meat is associated with significantly increased risk of CRC, with similar associations seen between colonic and rectal cancers (Chan et al, 2011). Meta-analysis data provides evidence for an association between moderate and heavy alcohol drinking and CRC, with a stronger association noted at the distal colon when compared with the proximal colon (Fedirko et al, 2011; Cai et al, 2014). Furthermore, an association between increased body mass index (BMI) and both colonic and rectal cancer has been observed in the literature, with stronger evidence existing in males (Kyrgiou et al, 2017). With an increasing global trend in the adoption of 'Westernised' lifestyles, it is likely that worldwide disease burden from both colonic and rectal cancer will increase in the coming decades.

Positive family history contributes to 10-20% of CRC cases, with increased risk known to correlate with the number and degree of relatives affected (Henrikson et al, 2015). A small subgroup of CRC patients (~5-7%) have a well-defined hereditary CRC syndrome (Syngal et al, 2015). The commonest hereditary CRC predisposing condition is Lynch syndrome, previously known as hereditary non-

polyposis colorectal cancer (HNPCC). Lynch syndrome is an autosomal dominant condition caused by mutation in one of the DNA mismatch repair (MMR) genes (MLH1, MSH2, MSH6 or PMS2) (Peltomäki and Vasen, 2004). An MMR gene defect leads to loss of DNA mismatch repair function, leading to micro-satellite instability (MSI), with the resulting accumulation in mutations predisposing to tumour formation. The presence of an MMR gene defect confers a 50-70% lifetime risk of developing CRC, with Lynch syndrome accounting for ~3% of CRC cases (Stoffel et al, 2009; Vasen et al, 2013).

Several hereditary polyposis syndromes exist which predispose to CRC, with Familial Adenomatous Polyposis (FAP) being the most common; however, this condition only occurs in 1 in 8000-10000 of the population (Plawski et al, 2013). FAP is an autosomal dominant condition caused by a heterozygous germline mutation in the adenomatous polyposis coli (APC) gene, located on chromosome 5q21, and is characterised by the development of hundreds of small colonic adenomatous polyps (Kinzler et al, 1991). Loss of heterozygosity or truncation of the second copy of the APC gene contribute to malignant transformation and a near 100% CRC risk by age 35-40 years (Lamlum et al, 1999; Galiatsatos et al, 2006). FAP patients typically undergo annual colonoscopy surveillance, with prophylactic colectomy considered in early adulthood. Other rarer polyposis syndromes exist which predispose to CRC, including MutY homolog-associated polyposis (MAP) and Peutz-Jehgers syndrome (Byrne et al, 2018). Patients with inherited polyposis syndromes require lifelong management on an individualised basis guided by a Rare Disease Collaborative Centre with expertise in such conditions; management is focused on appropriately timed colorectal surgery, intestinal and extra-intestinal surveillance, and genetic testing of family members (Clark et al, 2023).

Despite recent improvements in our understanding of the hereditary basis of CRC development, and improved screening and early detection for these patients, such cases represent the minority. In at least two thirds of patients, CRC occurs sporadically as the result of somatic mutations under the influence of both the local colonic environment and the background genetic makeup of an individual (Carethers et al, 2016). Population based screening is employed in order to detect cases of sporadic CRC at an early stage, whereby curative intervention can be offered to patients. In Scotland, the Scottish Bowel Screening Programme

invites men and women aged 50-74 to participate in 2-yearly screening through a faecal immunochemical test (FIT) (Public Health Scotland, 2017). However, despite a proportion of early CRC cases being detected through Bowel Screening Programmes, a significant proportion are diagnosed at later disease stages, with 48% of CRC patients in Scotland being diagnosed with stage III or IV disease in 2019-20 (Public Health Scotland, 2021). Colonoscopy is offered to patients with a qFIT ≥80μgHb/g rather than at positivity cut-off (≥10μgHb/g), and potentially explains the lack of substantial improvements in early detection in recent years. It remains crucial therefore, that current research focuses on developing neo-adjuvant treatment strategies in LARC based on individual and tumour characteristics, with the aim of improving clinical outcomes (Smith and Garcia-Aguilar, 2015).

1.1.4 Pathogenesis of Colorectal Cancer

Two distinct CRC development pathways exist: the 'conventional' pathway involving the 'adenoma-carcinoma sequence' (70-90%), and the serrated neoplasia pathway (10-30%). The 'adenoma-carcinoma sequence' was first proposed by Fearon and Vogelstein in 1990, and describes a stepwise accumulation of histological changes with each stage of progression being associated with key genetic alterations (Fearon and Vogelstein, 1990). The process involves four stages over an estimated period of 10-15 years, whereby normal intestinal epithelium transforms into an adenoma, then advanced adenoma with high-grade dysplasia, before eventually forming an invasive adenocarcinoma with the potential to metastasise (Figure 1.1). It is widely accepted that CRC arises from cancer stem cells (CSC) located in the base of colonic crypts, with CSCs being crucial for the initiation and maintenance of tumours; CSCs arise through accumulation of genetic alterations which result in the activation of oncogenes and inactivation of tumour-suppressor genes (Nassar et al, 2016).

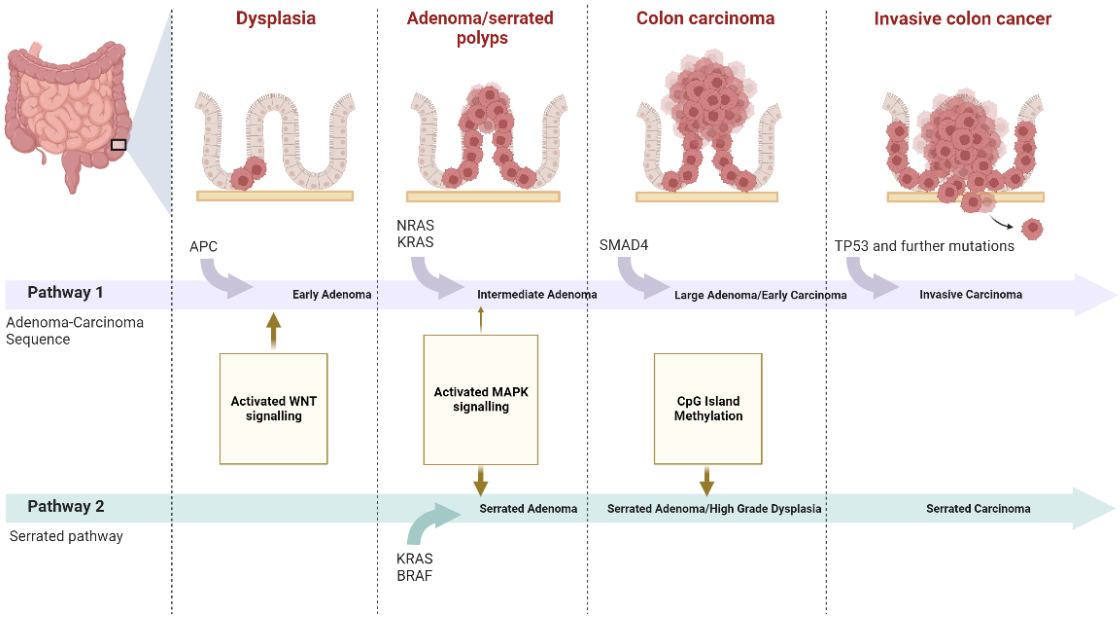

Figure 1.1: Molecular Features Associated with CRC Progression

Simplified schematic demonstrating the accumulation of mutations associated with CRC progression in both the classical 'adenoma-carcinoma' sequence and 'serrated' pathway. Figure is adapted from Fearon and Vogelstein (1990).

Fearon and Vogelstein describe the loss of the FAP locus on chromosome 5q21 in the majority of CRCs, with this mutation being the first to occur and being responsible for the formation of early adenomas. Subsequently, the FAP locus was identified as being the location of the APC (Adenomatous Polyposis Coli) tumour suppressor gene, confirming that APC loss is a key oncogenic driver in CRC progression (Groden et al, 1991; Kinzler et al 1991). Somatic APC mutations are found in ~80% of patients with sporadic CRC (Fearnhead et al, 2001).

APC has integral roles in the Wnt (Wingless related integration site) signalling pathway, which is essential for cell proliferation, tissue homeostasis and in the determination of cell fate (Logan and Nusse, 2004). The canonical Wnt signalling pathway regulates levels of β-catenin, which acts a transcriptional co-activator upon translocation to the nucleus. In the absence of Wnt signalling, a cytoplasmic β-catenin destruction complex composed of APC, Axin, CK1-α (Casein kinase 1) and GSK-3β (Glycogen synthase kinase) results in low levels of β-catenin (Figure 1.2). When the Wnt ligand binds to a core receptor complex (LRP5/6 and Frizzled) to activate Wnt signalling, Frizzled interacts with cytoplasmic Disheveled protein upstream of GSK-3β to prevent formation of the

ß-catenin degradation complex. Inhibition of ß-catenin degradation results in its stabilisation and accumulation in the cytoplasm. ß-catenin subsequently translocates to the nucleus where it combines with transcription factor T cell factor/lymph enhancer factor 1 (TCF/LEF1) to enable expression of Wnt target genes which are involved with cell proliferation, survival, differentiation and migration processes (Sansom et al, 2004; Nusse and Clevers, 2017). In the absence of functional APC, Wnt signalling is constitutively activated resulting in cytoplasmic accumulation and subsequent nuclear translocation of ß-catenin (Markowitz et al, 2009). Increased nuclear ß-catenin results in upregulation of Wnt target genes including cyclin D1 and cMYC, which influence the G1 and S phase of the cell division cycle respectively, promoting the survival and differentiation of malignant cells (He et al, 1998; Shtutman et al, 1999).

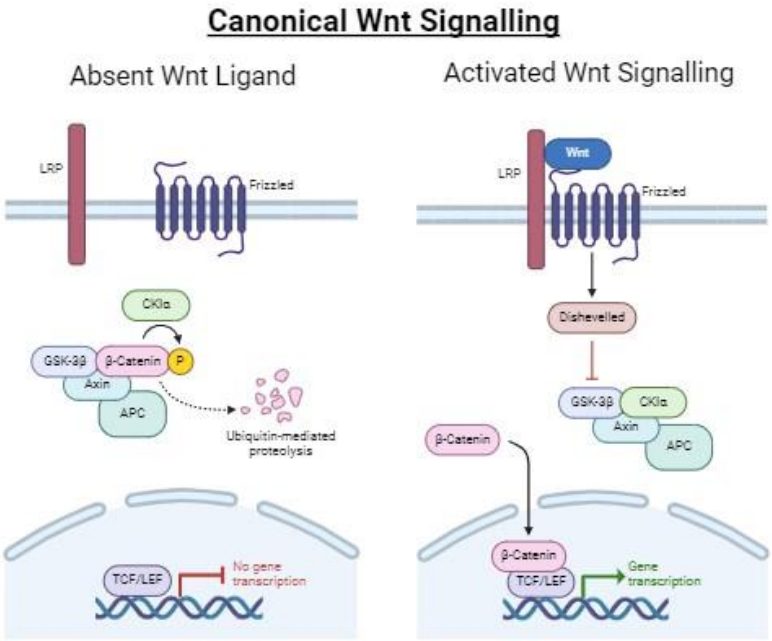

Figure 1.2: Canonical Wnt Signalling Pathway

Diagrammatic representation of the canonical Wnt signalling pathway. In the absence of Wnt ligand the ß-catenin destruction complex is constitutively active (left diagram). In the presence of Wnt (right diagram) the receptor complex recruits dishevelled and sequesters and inactivates the destruction complex which enables ß-catenin accumulation, translocation to the nucleus and subsequent regulation of its target genes. Created in Biorender. Adapted from Clevers 2006.

However, APC inactivation is not sufficient to drive progression to CRC, and resulting adenomas must accumulate additional mutations (Scott and Quirke, 1993). Fearon and Vogelstein observed that Ras (rat sarcoma virus) gene mutations were found in 50% of both intermediate adenomas and carcinomas,

but in as few as 10% of early adenomas, suggesting that Ras mutations are responsible for progression beyond the early adenomatous stage. The most frequently observed are activating mutations in the K-ras oncogene, with mutant genes at codon 12 initially being discovered in 40% of CRCs (Forrester et al, 1987). Development towards advanced adenomas have been commonly attributed to allelic deletions in chromosome 18q, found to exist in ~70% of CRCs, and containing portions of the DCC (Deleted in Colorectal Cancer), SMAD2 (Small Mothers Against Decapentaplegic) and SMAD4 genes (Fearon et al, 1990; Mehlen and Fearon, 2004). Allelic deletions in chromosome 17p, subsequently mapped to regions containing the TP53 (Tumour Protein 53) tumour suppressor gene, have been identified in as much as 75% of CRCs and are associated with late progression of advanced adenomas to adenocarcinoma (Baker et al, 1989).

In contrast to the conventional adenoma-carcinoma pathway, the alternative 'serrated' pathway is thought to account for 10-30% of CRCs, and is characterised by serrated adenomas as the initiating precursor lesion (Torlakovic and Snover, 1996; Jass, 2007). Such lesions display a 'serrated' or 'saw-toothed' appearance of the epithelial glandular crypts, and are initiated through formation of sessile serrated adenomas or polyps (SSA/SSPs), traditional serrated adenomas (TSAs) or hyperplastic polyps (HPs), which all have the potential to undergo malignant transformation (Rex et al, 2012). Activating mutations in the BRAF proto-oncogene, a member of the RAF (Rapidly Accelerated Fibrosarcoma) family of serine/threonine kinases, have been identified as a key genetic alteration in the serrated pathway, resulting in activation of the MAPK (Mitogen-Activated Protein Kinase) signalling cascade (Rajagopalan et al, 2002; Davies et al, 2002). BRAF mutation is strongly associated with both SSAs and MSI-H (Microsatellite Instability-High) CRCs, suggesting that this is a key initiating event in the 'serrated' pathway (Kambara et al, 2004). CRCs arising through the 'serrated' pathway have been shown to be associated with MSI (Hawkins and Ward, 2001). MSI occurs in a subgroup of CRC patients and is characterised by widespread mutations in microsatellite sequences, resulting from the inactivation of mismatch repair (MMR) genes which are responsible for repair of base-to-base mismatches in DNA (MLH1, MSH2, MSH6, and PMS2). Such inactivating mutations can be inherited as in Lynch syndrome (Bronner et al, 1994). Somatic inactivation of MMR genes occurs in ~15% of sporadic CRC cases,

with biallelic silencing of the MLH1 (MutL homolog) gene through hypermethylation (Herman et al, 1998).

Another common event in the 'serrated' pathway is hypermethylation of CpG islands located on the promotor regions of tumour suppressor genes, giving rise to the CpG Island Methylator Phenotype (CIMP). CpG islands are dense regions of cytosine-guanosine dinucleotides, where cytosine residues are susceptible to methylation in the promotor regions of tumour suppressor genes, with resulting epigenetic silencing and loss of gene function leading to the development of neoplastic features (Toyota et al, 1999). Toyota et al first discovered the presence of the CIMP phenotype, which is characteristic of ~15% of CRC cases, and occurs in the majority of sporadic CRCs with MSI.

Aside from the differentiation into the 'conventional' and 'serrated' pathways, CRC can be classified in terms of three major molecular pathways (Schmitt and Greten, 2021). Chromosomal instability (CIN) occurs in 80-85% of CRC cases and is characterised by aneuploidy, multiple changes in chromosome structure and copy number causing loss of heterozygosity at multiple tumour suppressor gene loci such as APC, P53 and SMAD4, with an accumulation of mutations as occurs in the classical 'adenoma-carcinoma' sequence (Markowitz and Bertagnolli, 2009).

Tumours can also be classified in terms of microsatellite stability or MMR status, with MSI/dMMR (Mismatch Repair deficient) occurring in ~15% of CRC and characterised by dysfunction of DNA MMR genes resulting in genetic hypermutability, and a predisposition to right sided CRC (Jass, 2007). Lastly, CRC can be classified according to the presence of CIMP, with CIMP tumours divided into two types: CIMP high tumours are associated with BRAF mutation and MLH1 methylation, and CIMP low tumours are associated with KRAS mutation (Shen et al, 2007).

The three major molecular pathways described are not mutually exclusive, and tumours can display features of multiple pathways. Some differences in molecular features exist between colonic and rectal cancer, with prevalence of dMMR/MSI being less frequent in rectal cancer at ~10% and CIN being a characteristic of >80% of rectal tumours (Kapiteijn et al, 2001; Fernebro et al, 2002; Cercek et al, 2020). Some evidence exists that dMMR rectal tumours are less sensitive to neoadjuvant chemotherapy when compared with pMMR tumours

(MMR proficient), while response to neoadjuvant chemoradiation is comparable (Cercek et al, 2020). Although an improved understanding of the genetic composition of CRC has been established, it has not been possible to reliably predict patient survival based on the described mutational and molecular characteristics.

1.1.5 Histopathological and Molecular Stratification of Rectal Cancer

One classification system for CRC is the TNM staging system, developed by the American Joint Committee on Cancer (AJCC) and the Union for International Cancer Control (UICC), with the 8th Edition most recently published in 2018 (Amin MB et al, 2018). This system classifies patients based on the extent of tumour infiltration into the colonic wall (T), the degree of lymph node involvement (N), and whether distant metastasis has occurred (M). Tumours can then be assigned a stage (I-IV) based on these tumour characteristics (Table 1.1).

AJCC Stage	TNM Stage	Features
0	Tis N0 M0	Tumour confined to mucosa
I	T1 N0 M0	Tumour invades submucosa
I	T2 N0 M0	Tumour invades muscularis propria
IIA	T3 N0 M0	Tumour invades subserosa; no other organs involved
IIB	T4 N0 M0	Tumour invades adjacent organs or perforates visceral peritoneum
IIIA	T1-2 N1 M0	T1-2 tumour plus metastasis to 1-3 regional lymph nodes
IIIB	T3-4 N1 M0	T3-4 tumour plus metastasis to 1-3 regional lymph nodes
IIIC	Any T stage N2 M0	Any tumour stage plus metastasis to 4 or more lymph nodes
IV	Any T stage, any N stage, M1	Any tumour and lymph node stage plus metastasis to distant organs

Table 1.1: CRC Staging and Features of AJCC and TNM Classifications

Table showing features of TNM staging systems with corresponding AJCC Stage (I-IV). T = tumour, N = lymph node, M = distant metastasis. Tis = carcinoma in-situ. Table adapted from Jass (2007).

Management decisions for patients with LARC are still largely dependent upon the TNM staging system, with consideration given to additional MRI detected features which confer higher risk: extra-mural vascular involvement (EMVI), tumour deposits and involvement of the circumferential resection margin (CRM) (Taylor et al, 2011). However, attempts have been made in recent years to move beyond TNM staging alone for patient stratification, and to account for the considerable molecular heterogeneity that exists within CRC. It is thought that the three main molecular phenotypes responsible for progression from adenoma to carcinoma are MSI, CIMP and CIN, due to genetic instability facilitating multiple tumour associated mutations (Tejpar and Van Cutsem, 2002).

Subsequently, several gene expression-based classification systems were developed to identify distinct subgroups with significant prognostic value to better stratify patients and inform individualised treatment strategies. Following this, an international consortium and large-scale data sharing of 18 CRC data-sets, combined six independent classification systems into a unifying Consensus Molecular Subtype (CMS) system (Guinney et al, 2015).

The CMS classification system allows most CRCs to be categorised into one of four subtypes (Table 1.2): CMS1 (MSI Immune), CMS2 (Canonical), CMS3 (Metabolic), and CMS4 (Mesenchymal). CMS1 tumours are characterised by genes associated with a diffuse immune infiltrate, including increased cytotoxic T-cell and Th1 (T-helper) cells. BRAF mutations frequently occur in CMS1, in keeping with its known association with MSI, CIMP high, hypermutated tumours. CMS2 tumours display epithelial differentiation and strong up-regulation of WNT and Myc (Myelocytomatosis) target genes which are classically implicated in CRC carcinogenesis. CMS3 tumours are enriched for multiple metabolic signatures in association with an increased prevalence of KRAS activating mutations, in keeping with other solid tumours (Son et al, 2013). CMS4 tumours display upregulation of genes implicated in epithelial mesenchymal transition (EMT), as well as gene signatures associated with activation of transforming growth factor β (TGF-β) signalling, angiogenesis, matrix remodelling and stromal infiltration. Guinney et al describe that prognosis is affected by CMS, with five-year survival for CRC of all stages being the highest in CMS2 at 77%, compared with 73% for CMS1, 75% for CMS3, and with CMS4 having the worst 5-year survival at 62%. Furthermore, a proportion of tumours (13%) fail to classify potentially owing to a transitional phenotype or to variation within tumours.

CMS classification is dependent upon an adequate volume of quality tissue being sampled to obtain accurate gene expression data; since the adoption of the CMS classification system, limitations have been highlighted with intra-tumoral heterogeneity and stromal sampling posing challenges in reliably stratifying tumours (Dunne et al, 2016). Application of the CMS classification system to rectal cancer also has limitations, as contributing datasets to the CMS classification described by Guinney et al contain a relatively low numbers of rectal tumours when compared with colonic tumour sites. Furthermore, it has been demonstrated that primary tumours exhibit transcriptomic differences to

their corresponding distant metastasis, highlighting that disease heterogeneity is not fully appreciated through CMS classification (Kamal et al, 2019).

	CMS 1 *MSI Immune*	**CMS 2** *Canonical*	**CMS 3** *Metabolic*	**CMS 4** *Mesenchymal*
Prevalence	14%	37%	13%	23%
Molecular Features	MSI CIMP high Hypermutation	SCNA high	Mixed MSI status SCNA low CIMP low	SCNA high
Associated mutations	BRAF		KRAS	
Characteristics	Immune infiltration and activation	WNT and Myc activation	Metabolic deregulation	Stromal infiltration TGF-ß activation Angiogenesis
Prognosis	Worse survival after relapse			Worse relapse free and overall survival

Table 1.2: Consensus Molecular Subtypes of CRC

Table showing key features and characteristics of CMS classification system of CRC. Somatic Copy Number Alteration (SCNA). Table adapted from Guinney et al (2015).

Mutational prevalence and distribution of CMS differs according to anatomical location in CRC. Rates of TP53 mutation increase with more distal tumour locations, whereas PIK3CA, BRAF and SMAD4 mutations decrease (Loree et al, 2018). Furthermore, while distribution of CMS3 and CMS4 remain relatively consistent throughout the colon and rectum, Loree et al found that a relatively higher proportion of CMS2 cases occur in the left colon and rectum, while a high distribution of CMS1 tumours is observed in the right colon when compared with the left colon and rectum.

The CMS classification system has allowed categorisation of most CRCs based on their genomic signature, with application to both basic and translational research in the hope that better understanding of each subtype will enable clinicians to devise individualised treatment strategies and improve outcomes

(Sawayama et al, 2020). Some clinical trial data has demonstrated a role for CMS classification in treatment stratification; retrospective analysis of CALBG/SWOG80405, a phase III trial investigating the addition of bevacizumab or cetuximab to standard of care chemotherapy in metastatic CRC, found that CMS1 patients treated with bevacizumab had favourable prognosis compared with cetuximab, while CMS2 patients had favourable prognosis when treated with additional cetuximab (Lenz et al, 2019). In contrast, the FIRE-3 trial demonstrated a significantly higher objective response rate in CMS2 patients for additional cetuximab plus standard of care chemotherapy in metastatic CRC, however this did not translate into a difference in PFS or OS compared with additional bevacizumab (Stintzing et al, 2019). Although the CMS classification system has aided our understanding of the molecular features, mechanisms of progression and heterogeneity of CRC, further research is necessary to analyse treatment responses in CRC in accordance with CMS classification if this system is to be used to assist with treatment stratification.

1.1.6 Surgical Management of Rectal Cancer

The current mainstay of rectal cancer treatment is surgical excision, with neoadjuvant and adjuvant therapy used in selected cases. The objectives of rectal cancer surgery are to achieve curative resection, prevent local and distant recurrence, while preserving intestinal continuity, bladder and sexual function where possible. Major resectional surgery is technically demanding due to the narrow confines of the pelvis, with difficulty in restoring intestinal continuity posing a risk of anastomotic leakage. Historically, local recurrence was a formidable problem following rectal cancer surgery, with previous surgical techniques involving blunt rectal dissection being associated with local recurrence rates in excess of 20% (Nymann et al, 1995).

Total meso-rectal excision, first described in the 1980s, is considered the gold standard surgical treatment for low and mid-rectal cancer, owing to significantly improved local recurrence and overall survival rates (Heald and Ryall, 1986). Total meso-rectal excision involves sharp dissection to achieve precise anatomical excision of the rectum within its encasing mesorectum, ensuring complete excision of draining loco-regional lymph nodes. The first series

described by Heald and Ryall, reported a local recurrence rate of 3.7% (n=115) at an average follow-up period of 4.2 years. Subsequently, larger series have demonstrated significantly improved local recurrence and overall survival rates following total meso-rectal excision when compared with earlier 'conventional' techniques (Kapiteijn et al, 2002; Martling et al, 2000). Partial mesorectal excision, with mesorectal clearance 4-5cm distal to the lower tumour border, has been shown to result in adequate oncological clearance in tumours of the upper rectum (Law et al, 2004; Lopez-Kostner et al, 1998).

Traditionally, CRC surgery has been performed through an open approach, however, over the last 20 years laparoscopic surgery for colonic cancer has offered significant benefits to patients in terms of short-term outcomes, including less blood loss, shorter hospital stays, quicker return of normal bowel function and less analgesic requirements (Veldkamp et al, 2005). Numerous studies went on to demonstrate that oncological outcomes following laparoscopic surgery were comparable with open (Jayne et al, 2007; Fleshman et al, 2007; Bagshaw et al, 2012). It is widely recognised that laparoscopic surgery for rectal cancer is more technically challenging than for colonic cancer, largely owing to the narrow confines of the pelvis and the requirement to preserve the hypogastric nerve plexus. In LARC, the COREAN Trial showed that laparoscopic surgery offered short-term benefits over open surgery for patients with cT3 mid or low rectal tumours receiving neoadjuvant CRT (Kang et al, 2010); functional outcomes such as return of normal bowel function were significantly better following laparoscopic surgery, with resection quality uncompromised. Comparable oncological outcomes were later published, with similar rates of 3-year disease-free survival (72.5% for open surgery versus 79.2% for laparoscopic surgery) and improved 3-year local recurrence (4.9% for open surgery versus 2.6% for laparoscopic surgery) (Jeong et al, 2014). Larger numbers (n=1103) were studied in the COLOR II trial, randomising patients with rectal tumours of all locations to laparoscopic or open resection, and comparable rates of local recurrence, disease-free and overall survival were seen with both approaches (Bonjer et al, 2015).

Quality of oncological resection has been a concern regarding the widespread adoption of laparoscopic surgery in rectal cancer owing to anatomical constraints. The ALaCaRT (Australasian Laparoscopic Cancer of the Rectum) trial

compared the quality of resection specimens through a composite of whether complete total meso-rectal resection, a clear circumferential margin (≥1mm), and a clear distal resection margin (≥1mm) were achieved upon pathological assessment (Stevenson et al, 2015). However, non-inferiority of laparoscopic surgery was not established in this study despite the demonstration of similar short-term and long-term outcomes in other studies. Similarly, the ACOSOG Z6051 trial failed to demonstrate non-inferiority for quality of oncological resection in stage II/III rectal cancer with the use of a laparoscopic approach (Fleshman et al, 2015).

Recently robotic assisted surgery has been used increasingly in rectal cancer surgery, with technological advantages offered through enabling precise dissection within the narrow confines of the pelvis. Initial randomised trial data demonstrated lower conversion to open rates with robotic surgery when compared with the laparoscopic approach, but with longer operating times reported (Prete et al, 2018). The ROLARR trial reported a non-significant decrease in conversion to open laparotomy rate with robotic assisted surgery (8.1% versus 12.2%), with no significant differences between robotic assisted and laparoscopic approaches being reported for other outcome measures such as circumferential resection margin (CRM) involvement, complication rates, 30-day mortality, bladder and sexual dysfunction (Jayne et al, 2017).

Despite advances in surgical technique and the benefits of laparoscopic surgery, rectal cancer surgery still poses considerable risk of morbidity to patients. Perioperative complications pose a significant risk with anastomotic leak rates for rectal surgery ranging from 5-19% (McDermott et al, 2015). Furthermore, long term functional outcomes are often compromised following rectal surgery with patients often suffering with urinary, sexual and defecatory dysfunction, and a proportion of patients requiring long term stoma formation (Giglia and Stein, 2019; Downing et al 2019). Therefore, less invasive management options with reduced morbidity, represent an attractive treatment paradigm for patient.

1.1.7 The Role of Neoadjuvant Radiotherapy in Rectal Cancer

Current UK clinical guidelines recommend that pre-operative radiotherapy or chemoradiotherapy (CRT) is offered to patients with stage II (cT3/T4) and stage

III (any cT, cN1/2) rectal cancer (NICE guideline [CG151], 2020). Preoperative RT is not recommended for patients with early rectal cancer (cT1-T2, cN0, M0), unless part of a clinical trial. These recommendations are based upon evidence from several randomised controlled trials (RCTs) showing that patients with LARC have decreased rates of local recurrence following treatment with preoperative radiotherapy or CRT. Current evidence does not show clear differences in benefit between different neo-adjuvant treatment regimens, and so recommendation is not made concerning the type or duration of radiotherapy or CRT. Two neoadjuvant strategies are commonly used in the UK – SCPRT (short-course preoperative radiotherapy) (25Gy at 5Gy/fraction over 5 consecutive days, followed by immediate surgery) and CRT (45 - 50.4Gy at 1.8Gy/fraction with concomitant 5-FU based chemotherapy over 5-6 weeks, followed by delayed surgery). However, in the UK it has been demonstrated that wide variation in practice exists, both in terms of regimen used and the time interval to surgical resection (Morris et al, 2016).

Variation in clinical practice is seen in the USA, with chemotherapy typically being administered more widely and SCPRT regimens not advocated. National Comprehensive Cancer Network (NCCN) guidelines recommend multi-modality therapy for most patients with LARC (stage II or III), consisting of surgery, preoperative CRT, and adjuvant chemotherapy (Benson et al, 2018).

Many countries, particularly within Europe, adopt a more selective approach to neoadjuvant treatment for LARC than that employed in the USA, as well as a more judicious use of adjuvant chemotherapy. Standard of care for preoperative treatment according to the European Society of Medical Oncology (ESMO) recommendations are that radiotherapy or CRT should be considered in mid and low stage II/III rectal cancers, to reduce the rate of local recurrence; furthermore, CRT is recommended where the circumferential resection margin and/or R0 resection status are predicted to be at risk (Glynne-Jones et al, 2017).

Studies were conducted as early as the 1980s to determine whether radiotherapy resulted in oncological benefit when used in addition to surgical treatment, with pre-operative radiotherapy being shown to significantly lower 5-year local recurrence rates (13% versus 22%; p=0.02) when compared with post-operative radiotherapy (Frykholm et al, 1993). Later, the Swedish Rectal Cancer Trial randomised 1168 patients to pre-operative RT (25Gy in 5 days) or surgery alone,

showing an improved local recurrence rate in the patients receiving pre-operative radiotherapy (9% versus 26%; $p<0.001$) at a median follow up of 13 years (Folkesson et al, 2005). Meta-analysis of RCTs studying pre-operative radiotherapy prior to 2000 (n=14) further demonstrated that improvement in local recurrence rates is seen with the addition of radiotherapy prior to surgery (Cammà et al, 2000). However, these early studies precede the widespread adoption of TME surgery, and so evidence to support the use of neo-adjuvant radiotherapy must account for the optimisation of surgical approach.

Following the standardisation of total meso-rectal excision surgery, further RCTs continued to demonstrate clear benefits following pre-operative radiotherapy or CRT. Numerous landmark studies following the adoption of TME surgery (summarised in Table 1.3) have demonstrated improvements in local recurrence rates when neo-adjuvant radiotherapy or CRT is administered.

The Dutch Colorectal Cancer Group showed improved 2-year local recurrence rates in rectal tumours of any T-stage following SCPRT plus surgery versus surgery alone (2.4% versus 8.2%), with no improvement in overall survival or distant metastasis rates observed (Kapiteijn et al, 2001). The MRC CR07 and NCIC-CTG C016 multi-centre RCT later addressed the question of timing of radiotherapy administration in relation to surgery, with SCPRT prior to surgery demonstrating improved 3-year local recurrence rates (4.4% versus 10.6%) when compared with surgery and post-operative CRT (Sebag-Montefiore et al, 2009). It must be noted that post-operative CRT was offered to a higher risk patient cohort with involved circumferential margin in this study, which potentially explains the poorer outcomes observed.

Following the clear improvements in local recurrence rates seen when radiotherapy is administered prior to surgery for LARC, further benefits have been achieved with the addition of radio-sensitising chemotherapy. Fluoropyrimidines, including 5-FU and capecitabine, act through inhibition of the nucleotide synthetic enzyme thymidylate synthase, and through incorporation of 5-FU metabolites into DNA and RNA, resulting in the inhibition of DNA synthesis and RNA transcription (Longley et al, 2003). It is thought that fluoropyrimidines might enhance radiosensitivity through the killing of S-phase cells, which are relatively radioresistant (Ojima et al, 2006).

Trial	Intervention	No	Inclusion	Study Endpoint	Local Recurrence	Distant - Recurrence	Overall Survival
Dutch Colorectal Cancer Group. (Kapiteijn et al, 2001)	Pre-op Short course (5x5Gy) + surgery vs surgery	1805	Operative rectal adeno-carcinoma	2 years	2.4% vs 8.2% (p<0.001)	14.8% vs 16.8% (p=0.87)	82% vs 81.8% (p=0.84)
MRC CR07/NCIC-CTG C016 (Sebag-Montefiore et al, 2007)	Pre-op Short course (5x5Gy) vs post-op CRT (45Gy + 5-FU)	1350	Operative rectal adeno-carcinoma	3 years	4.4% vs 10.6% (p<0.001)	19% vs 21%	80.3% vs 78.6% (p=0.40)
FFCD 9203 (Gerard et al, 2006)	Pre-op RT (25x1.8G) vs pre-op CRT (25x1.8Gy + 5-FU, leucovorin)	733	T3-T4, Nx, M0 rectal adeno-carcinoma	5 years	16.5% vs 8.1% (p<0.004)	-	67.9% vs 67.4% (p=0.684)
EORTC 22921 (Bosset et al, 2014)	Pre-op RT vs pre-op CRT (25x1.8Gy +/- 5-FU + folinic acid)	1011	T3-T4 resectable rectal adeno-carcinoma	10 years	22.4% vs 11.8% (p=0.0017)	39.6% vs 33.4% (p=0.52)	49.4% vs 50.7% (p=0.91)
German Rectal Cancer Study Group (Sauer et al, 2004)	Pre-op vs post-op CRT (28x1.8Gy + 5-FU)	823	T3-T4 rectal adeno-carcinoma or node +ve disease	5 years	6% vs 13% (p=0.006)	36% vs 38% (p=0.84)	76 vs 74% (p=0.80)
Polish Colorectal Study Group (Bujko et al, 2006)	Pre-op RT (5x5Gy) vs pre-op CRT (28x1.8Gy + 5-FU + leucovorin)	312	T3-T4 rectal adeno-carcinoma	4 years	9.0% vs 14.2% (p=0.170)	31.4% vs 34.6%	67.2% vs 66.2% (p=0.960)
Trans-Tasman Radiation Oncology Group trial 01.04 (Ngan et al, 2012)	Pre-op RT (5x5Gy) + adjuvant chemo vs pre-op CRT (28x1.8Gy + 5-FU) + adjuvant chemo	326	T3, N0-2, M0 rectal adeno-carcinoma	3 years	7.5% vs 4.4% (p=0.24)	27% vs 30% at 5 years (p=0.92)	74% vs 70% at 5 years (p=0.62)

Table 1.3: Key Clinical Trials in Neo-Adjuvant Radiotherapy/CRT

Table showing key features and findings of landmark clinical trials which demonstrate the benefits for neo-adjuvant radiotherapy or CRT regimens in Locally Advanced Rectal Cancer.

Early studies combining chemotherapy with preoperative radiotherapy included the Fédération Francophone de Cancérologie Digestive (FFCD) 9203 trial (1993-2003), which demonstrated improved 5-year local recurrence in the CRT group (8.1% versus 16.5%; p=0.004), with no difference in 5-year overall survival observed (Gerard et al, 2006). The EORTC 22921 trial further supported the use of neo-adjuvant CRT when compared with radiotherapy alone, with improved 10-year local recurrence rates seen (11.8% versus 22.4%; p=0.0017) (Bosset et al, 2014). The German Rectal Cancer Study Group trial highlighted the importance of treatment being administered pre-operatively, with neo-adjuvant CRT demonstrating an improved 5-year local recurrence rate (6% versus 13%;

p=0.006) when compared with post-operative CRT in patients with T3/T4 or node-positive disease (Sauer et al, 2004).

To further address the question of whether neo-adjuvant SCPRT or CRT provides optimal oncological benefit, the Polish Colorectal Study Group trial compared SCPRT with preoperative CRT, and failed to show significant differences in local recurrence, distant metastasis, or survival rates at 4-years (Bujko et al, 2006). More recently, the Trans-Tasman Radiation Oncology Group Trial 01.04 also compared SCPRT with long course CRT prior to surgery, demonstrating comparable 3-year local recurrence rates in both groups (Ngan et al, 2012). Evidence from studies to-date justify the selective use of either SCPRT or long-course CRT prior to surgical resection in LARC due to improved local recurrence rates; however, evidence fails to suggest significant benefits in long-term survival and distant metastasis rates. Until recently, the European model for management of rectal cancer was based upon MRI stratification with low-risk tumours ('the good') undergoing total meso-rectal excision alone, intermediate-risk tumours ('the bad') undergoing SCPRT, and high-risk tumours ('the ugly') undergoing CRT prior to TME (Blomqvist and Glimelius, 2008).

1.1.8 Adjuvant Chemotherapy in Rectal Cancer

Adjuvant chemotherapy has a clear role in the management of colonic cancer, with early clinical trials in the 1980s and 1990s showing survival benefit with the addition of 5-FU based chemotherapy after resection of stage III colon cancer (Haydon, 2003). Later, two pivotal trials showed improved oncological outcomes when oxaliplatin is added to fluoropyrimidine chemotherapy in the adjuvant setting. The MOSAIC trial demonstrated improved disease-free and overall survival in stage II and III colonic cancer patients receiving adjuvant chemotherapy with 5-FU, leucovorin and oxaliplatin when compared with 5-FU and leucovorin alone (André et al, 2009). Subsequently, the NSABP C07 study showed that the addition of oxaliplatin to 5-FU and leucovorin resulted in improved 5-year disease-free survival, with overall survival benefit only seen in the subset of patients <70 years old (Yothers et al, 2011). Current standard of care in the UK is that patients with stage III colorectal cancer (excluding rectal cancer patients treated with CRT), receive adjuvant chemotherapy with

capecitabine and oxaliplatin (CAPOX) or 5-FU/leucovorin and oxaliplatin (FOLFOX) for 3-6 months (NICE guideline [NG151], 2020).

Evidence to support a role for adjuvant chemotherapy following surgery for rectal cancer is less convincing, with NICE guidelines only recommending its use in stage III disease when the patient has not received pre-operative CRT. Despite a paucity of evidence, the National Comprehensive Cancer Network (NCCN) guidelines advocate the use of adjuvant chemotherapy in all patients with stage II or III disease, and so widespread use is commonplace in North America. The EORTC 22921 trial, which randomly assigned patients with T3 or T4 rectal cancer to pre-operative radiotherapy with or without concomitant chemotherapy followed by adjuvant chemotherapy or surveillance, failed to show improvement in disease-free or overall survival following adjuvant chemotherapy in any group (Bosset et al, 2014). Furthermore, meta-analysis data from four eligible trials, failed to demonstrate improvement in oncological outcome when adjuvant chemotherapy is given to patients who have undergone neoadjuvant CRT and surgery (Breugom et al, 2015). In the context of current standard of care, whereby LARC patients receive neoadjuvant therapy followed by total meso-rectal excision, evidence does not support the routine administration of adjuvant chemotherapy.

1.1.9 Organ Preservation Strategies

In recent years, organ preservation in LARC has emerged as a novel treatment paradigm, with the potential to avoid the morbidity and mortality risks associated with major surgical resection. Non-operative management was first described by Habr-Gama et al, where clinical complete response (cCR) was observed in 26.8% of patients (n=265) with T2-T4 distal rectal adenocarcinoma amenable to resection, at 8 weeks post CRT completion (Habr-Gama et al, 2004). Patients with a cCR to CRT underwent a non-operative surveillance strategy; at a mean follow-up of 57.3 months, two patients (2.8%) had developed endoluminal recurrence and a further three patients (4.2%) developed distant metastases. A recent systematic review, suggests that approximately 20% of patients may be suitable for non-operative management strategies, following treatment with neo-adjuvant CRT (Dattani et al, 2018).

Ongoing concerns exist over local regrowth and distant metastasis rates, with current evidence not yet supporting surveillance as a standard approach out with a specialised centre or well-designed clinical trial (Bernier et al, 2018). Recently, the OnCoRe project (Oncological Outcomes after Clinical Complete Response in Patients with Rectal Cancer) studying 129 patients undergoing a 'watch and wait' strategy following a cCR to CRT, found that 34% of patients developed local recurrence within 3-years; however, the majority (88%) successfully underwent salvage surgery (Renehan et al, 2016). Pooled patient data from the International Watch and Wait Database (IWWD) study, detailing outcomes of surveillance strategies following complete clinical response to CRT, showed 2-year local recurrence and 3-year distant recurrence rates of 25.2% and 8.1% respectively (Van der Valk et al, 2018). Retrospective analysis of 113 patients with cCR to CRT, who were treated conservatively at the Memorial Sloan Kettering Cancer Centre, showed that 19% of patients required salvage surgery with pelvic control achieved in 91% of patients with local relapse (Smith et al, 2019).

Despite the incidence of local recurrence following surveillance strategies, the majority of patients with a cCR following CRT do not develop local disease recurrence. Furthermore, pooled analysis data shows that patients with a pathological complete response (pCR) following CRT who have undergone surgery, have significantly improved long-term outcomes compared with non-pCR patients (Maas et al, 2010). The improved oncological outcomes following complete response to CRT, suggests a favourable biological tumour profile, and underlying mechanisms of response which warrant further research.

Total meso-rectal excision is associated with impaired functional outcomes, with ~60% of patients suffering with bowel dysfunction following low anterior resection (Emmertson and Laurberg, 2012; Juul et al, 2014). The combination of neo-adjuvant therapy and surgery also results in high morbidity rates, with negative impact on long-term functional outcomes including bowel function, faecal and urinary continence, and sexual function (Gavaruzzi et al, 2014).

Interestingly, the CARTS study (Trananal Endoscopic Microsurgery after Radiochemotherapy for Rectal Cancer) which explored the feasibility of local trans-anal excision following good response to neo-adjuvant CRT, found that 50% of patients still suffered with major bowel related symptoms, highlighting that

both neo-adjuvant therapy and local excision also result in significant morbidity (Stijns et al, 2019). The GRECCAR 2 trial compared local excision with TME in stage T2/3 low rectal tumours with good clinical response to CRT, however, failed to demonstrate superiority of local excision owing to a significant (35%) rate of patients requiring completion total meso-rectal excision (Rullier et al, 2017). The ACOSOG Z6041 trial studied T2N0 low rectal tumours treated with CRT and local excision, with a 3-year disease free survival of 86.9% rate suggesting that local excision should be considered in selected patients who refuse or are not fit for trans-abdominal resection (Garcia-Aguilar et al, 2015). More recently, the TREC study randomised T1-T2 rectal tumours to either local excision by trans-anal endoscopic microsurgery or to total meso-rectal excision following SCPRT, and showed high rates of organ preservation (70% in randomised patients, 92% in selected non-randomised patients), thus supporting the evaluation of local excision following neo-adjuvant therapy (Bach et al, 2021).

Meta-analysis data suggests a clinical complete response rate of 22.4% following standard CRT regimens (Dattani et al, 2018). Data from the Stockholm III trial which compared SCPRT with immediate surgery, SCPRT with delayed surgery (4-8 weeks) and long-course radiotherapy (25 x 2Gy), found pathological complete response rates of 0.3%, 10.4% and 2.2% respectively (Erlandsson et al, 2019). Data from the Stockholm III trial suggests a role for delayed surgery following neo-adjuvant therapy to optimise clinical/pathological response rates, and recent studies have attempted to modify and intensify standard of care regimens to exploit this. Non-operative management should be explored further, to determine optimal surveillance strategies, and so that organ preservation can be offered to patients likely to benefit. Furthermore, novel and intensified neo-adjuvant treatment strategies should be developed to enable a higher proportion of patients to undergo clinical complete response.

1.1.10 Total Neoadjuvant Therapy in Rectal Cancer

Despite the improvements in local recurrence rates following the developments in surgical technique and neo-adjuvant treatment regimens described, rates of distant metastatic recurrence and long-term disease-free survival have not

significantly improved. Long-term follow up from the Dutch Colorectal Cancer Group trial at 10-years, showed distant metastasis rates of 19% vs 24% and overall survival rates of 56% vs 57%, when comparing SCPRT and surgery with surgery alone (van Gijn et al, 2011). Similarly, long-term follow up of the German CAO/ARO/AIO-94 trial failed to demonstrate improvements in 10-year distant metastasis (29.8% vs 29.6%) and overall survival rates (59.6% vs 59.9%), when comparing pre-operative CRT with post-operative CRT respectively (Sauer et al, 2012).

Recent interest in 'Total Neoadjuvant Therapy' (TNT) strategies have developed, in the hope that earlier delivery of full-dose systemic therapy will eliminate micro-metastases at an earlier stage, potentially improving disease-free survival and distant metastatic recurrence rates. Additional 'induction' chemotherapy cycles can be administered prior to the standard CRT regimen, or after as 'consolidation' chemotherapy (Ludmir et al, 2017). Several studies have investigated the effects of both 'induction' and 'consolidation' TNT regimens in Locally Advanced Rectal Cancer, and are summarised in Table 1.4.

The Spanish GCR-3 trial investigated the effect of induction CAPOX chemotherapy (capecitabine and oxaliplatin), with no significant benefits in pathological complete response or 5-year overall survival rates observed (Fernandez-Martos et al, 2015). A larger retrospective study conducted at the Memorial Sloan Kettering Cancer Centre demonstrated an improved combined clinical and pathological response rate following induction chemotherapy when compared with adjuvant chemotherapy (Cercek et al, 2018). In comparison to post-operative chemotherapy, it is felt that systemic chemotherapy pre-operatively might better treat early micro-metastases thus reducing distant relapse rates, improve tolerance and compliance rates, reduce local recurrence, and allow earlier closure of de-functioning ileostomy.

Multiple trials have assessed the role of 'consolidation chemotherapy,' administered after CRT and prior to surgery. The non-randomised Timing of Rectal Cancer Response to Chemoradiation Consortium Study, found that pCR (Pathological Complete Response) rates increased as increasing cycles of mFOLFOX consolidation chemotherapy were administered, with an impressive pCR rate of 38% observed in patients receiving 6 cycles of mFOLFOX chemotherapy (Garcia-Aguilar et al, 2015). The Polish Colorectal Study Group

showed improved pCR and 3-year overall survival when SCPRT and consolidation chemotherapy were compared with CRT plus surgery (Bujko et al, 2016).

With evidence to suggest that both ‘induction’ and ‘consolidation’ chemotherapy strategies can improve rates of pathological and clinical complete responses, it remains unclear which TNT strategy results in optimal oncological benefit. The German Rectal Cancer Study Group CAO/ARO/AIO-12 randomised trial found an improved pCR rate of 25% following ‘consolidation’ chemotherapy when compared with 17% in the ‘induction’ chemotherapy group (Fokas et al, 2019). However, with long-term outcome data being limited, it remains unclear which is the optimal TNT regimen. The recent Organ Preservation in Patients with Rectal Adenocarcinoma Treated with Total Neoadjuvant Therapy Study (OPRA), compared ‘induction’ or ‘consolidation’ chemotherapy, and found 3-year total meso-rectal excision free survival rates of 41% and 53% respectively, highlighting that organ preservation is achievable in a high proportion of patients treated with TNT (Garcia-Aguilar J et al, 2022).

Study	Intervention	No	Inclusion	Study Endpoint	Response Rate	Overall Survival
Spanish GCR-3 Trial (Fernandez-Martos et al, 2015)	Induction CAPOX + CRT + surgery vs CRT + surgery + adjuvant CAPOX	108	T3-T4 and or node +ve mid or distal rectal adeno-carcinoma	5 years	pCR rate: 14.3% vs 13.5% (p=0.94)	75% vs 78% (p=0.64)
Memorial Sloan Kettering study - retrospective Cercek et al, 2018)	Induction CAPOX + CRT + surgery vs CRT + surgery + adjuvant chemo	628	T3-T4 or node +ve rectal adeno-carcinoma	pCR or sustained clinical response at 12 months	pCR or sustained cCR: 36% vs 21%	-
TIMING NCT00335816 Trial (Garcia-Aguilar et al, 2015)	CRT + surgery vs CRT + 2, 4 or 6 cycles of consolidation mFOLFOX + surgery	259	T3-T4 or node +ve rectal adeno-carcinoma	pCR at surgical resection	pCR: 18% vs 25% vs 30% vs 38% (p=0.0036)	-
Polish Colorectal Study Group NCT00833131 (Bujko et al, 2016)	SCRT + consolidation FOLFOX + surgery vs CRT + surgery	515	Primary or recurrent T3-T4 rectal adenocarcinoma	pCR and R0 resection rate (plus 3 year survival)	pCR: 16% vs 12% (p=0.17)	73% vs 65% (p=0.046)
German Rectal Cancer Study Group CAO/ARO/AIO-12 Trial (Fokas et al, 2019)	Induction FOLFOX + CRT + surgery vs CRT + consolidation FOLFOX + surgery	306	T3-T4 or node +ve mid or low rectal adenocarcinoma (excluding T3a tumours in mid rectum)	pCR in resection specimen	pCR: 17% vs 25% (p=0.071)	-
Prodige-23 Trial (Conroy et al, 2021)	CRT + surgery + adjuvant chemo vs induction mFOLFIRINOX + CRT + surgery + adjuvant chemo	461	T3-T4, Nx, M0 rectal adenocarcinoma	3 years DFS	11.7% vs 27.5% (p<0.001)	68.5% vs 75.7% Disease-Free Survival (p=0.034)
OPRA Trial NCT02008656 (Garcia-Aguilar et al, 2022)	Induction vs Consolidation FOLFOX/CAPOX + CRT + surgery or surveillance	324	T3-T4 or node +ve rectal adeno-carcinoma	3-year disease free survival (plus total meso-rectal excision free survival)	TME free survival: 41% vs 53% (p=0.01)	91% vs 93% (p=0.39)

Table 1.4: Clinical Trials in 'Total Neo-Adjuvant Therapy'

Table showing key features and findings of clinical trials which investigating both 'induction' and 'consolidation' TNT regimens in in Locally Advanced Rectal Cancer. Capecitabine and Oxaliplatin (CAPOX). Fluorouracil, oxaliplatin, folinic acid (FOLFOX). Pathological Complete Response (pCR). Microscopically margin-negative resection (R0).

Modified TNT approaches have been described very recently; the Rectal cancer and Preoperative Induction Therapy Followed by Dedicated Operation Trial (RAPIDO) compared SCPRT followed by 18 weeks of systemic chemotherapy prior to surgery, with patients undergoing standard of care CRT plus surgery and optional adjuvant chemotherapy in LARC patients with high-risk features (Bahadoer et al, 2021). Significantly improved 3-year disease related treatment failure rates were observed in the experimental group (23.7% versus 30.4%, p=0.019), with most treatment failures occurring due to distant metastasis

(20.0% versus 26.8%; p=0.0048). pCR was also significantly improved in the experimental group (28% versus 14%; p<0.0001).

Early evidence shows that additional chemotherapy in the neo-adjuvant setting can improve pathological and clinical response rates, with short term outcomes showing improved disease-free survival and distant metastasis rates in some studies. The CAO/ARO/AIO-12 Trial suggests a superiority of 'consolidation' chemotherapy when compared with 'induction' regimens to improve pathological response rates, potentially due to an increased interval between administration of radiotherapy and surgical intervention; this is also supported by the higher 3-year total meso-rectal excision free survival observed in the 'consolidation' group of the OPRA trial. Longer term follow-up data and current trials will address whether TNT regimens lead to long-term oncological improvements in distant metastasis and disease-free survival rates, and which treatment regimens offer optimum efficacy.

1.1.11 Quantification of Response to Radiotherapy in Rectal Cancer

Variable tumour responses are observed following treatment with neoadjuvant radiotherapy and CRT regimens in LARC. Tumour regression grading (TRG) following neoadjuvant treatment is based upon histological analysis of post resection tumour specimens, and numerous TRG systems have been described. These systems are based upon quantitatively determining the quantity of viable tumour remaining after treatment in relation to the quantity of fibrotic tissue within the tumour, and ranges from a complete lack of regression to complete response with no viable tumour remaining (Dworak et al, 1997). In the grading system described by Dworak, five groups of tumour regression are described: grade 0, no regression; grade 1, minor regression (fibrosis in ≤ 25% of the tumour mass); grade 2, moderate regression (fibrosis in 26-50% of the tumour mass); grade 3, good regression (fibrosis outgrowing tumour mass); grade 4, total regression (no viable tumour cells, with fibrotic mass only). Numerous similar TRG systems have been described, including the Mandard system, and scales proposed by both Memorial Sloak Kettering Cancer Centre (MSKCC) and AJCC (Mandard et al, 1994; Quah et al, 2008; Trakarnsanga et al, 2014). Patients with complete and intermediate responses, have been shown to have significantly

improved oncological outcomes in patients following neoadjuvant CRT, as assessed by 10-year distant metastasis and disease-free survival (Fokas et al, 2014).

Studies to determine improved oncological outcomes associated with favourable TRG involve long follow-up rates of up-to 10 years, which potentially hinders progress in clinical research. The neo-adjuvant rectal score (NAR score) was developed as a surrogate short-term endpoint to determine treatment efficacy in a shorter time period. The NAR score serves as a continuous variable with possible scores ranging from 0-100, where higher scores represent poorer prognosis, and is calculated using a formula including pathological node status (pN), clinical tumour stage prior to therapy (cT) and pathological tumour stage post therapy (pT). The NAR score accounts for tumour downstaging by incorporating the treatment effect on T stage, with the score being shown to better predict overall survival in rectal cancer trials than rates of ypCR (George Jr et al, 2015). Although grading systems and the NAR score can predict patients who will have a favourable long-term oncological outcome following treatment, predictive biomarkers of response prior to therapy would be beneficial to enable prediction of patients likely to respond to treatment, as well as identifying those whose tumours are unlikely to respond to current standard of care regimens.

1.2 Emerging Treatment Targets in Locally Advanced Rectal Cancer

1.2.1 Immune Checkpoint Inhibition

Improved understanding of the immune response to malignant cells has led to the development of immunotherapy agents, with the aim of exploiting components of the immune system for therapeutic benefit (Koebel et al, 2007). Immune checkpoint molecules exist within the host immune system, with Programmed Cell Death Protein 1 (PD-1) and Cytotoxic T-Lymphocyte Associated Protein 4 (CTLA-4) being the most developed treatment targets in clinical practice (Wei et al, 2018). T-cells are an important component of anti-tumour immunity, with T-cell receptors (TCRs) recognising tumour antigens and subsequently killing tumour cells. T-cell responses are regulated by immune checkpoints, which function under normal physiological conditions to prevent autoimmunity and to protect normal tissues, however, they can also restrict the

immune response to cancer (Mellman et al, 2011; Pardoll, 2012). Expression of checkpoint proteins can become dysregulated by tumours and represent an important mechanism of immune resistance and evasion. Blockade of immune checkpoints allows anti-tumour immune responses to be exploited, with recent success being seen in a variety of solid tumours (Vanneman et al, 2012).

Immune checkpoint blockade exploiting the PD-1 pathway has achieved recent clinical success. The PD-1 receptor is expressed on the surface of T-cells and regulates T-cell activation through interaction with its corresponding ligands PD-L1 and PD-L2, which are expressed on tumour cells, with a negative co-stimulatory signal occurring upon binding to attenuate T-cell activation (Figure 1.2) (Ishida et al, 1992). PD-L1 expression on tumour cells has been found to be poorly prognostic in a variety of cancer types including malignant melanoma (Hino et al, 2010). The interaction of PD-L1 expressed on tumour cells with PD-1 receptors on activated T-cells, has been shown to lead to inhibition and death of cytotoxic T-lymphocytes, representing a mechanism of tumour resistance and active immune evasion (Dong et al, 2002). PD-1 regulates effector T-cell activity in both normal tissue and tumour, and blockade of this axis can potentially enhance anti-tumour activity through increased survival of cytotoxic T-lymphocytes in the tumour microenvironment, leading to increased cytotoxic killing of tumour cells.

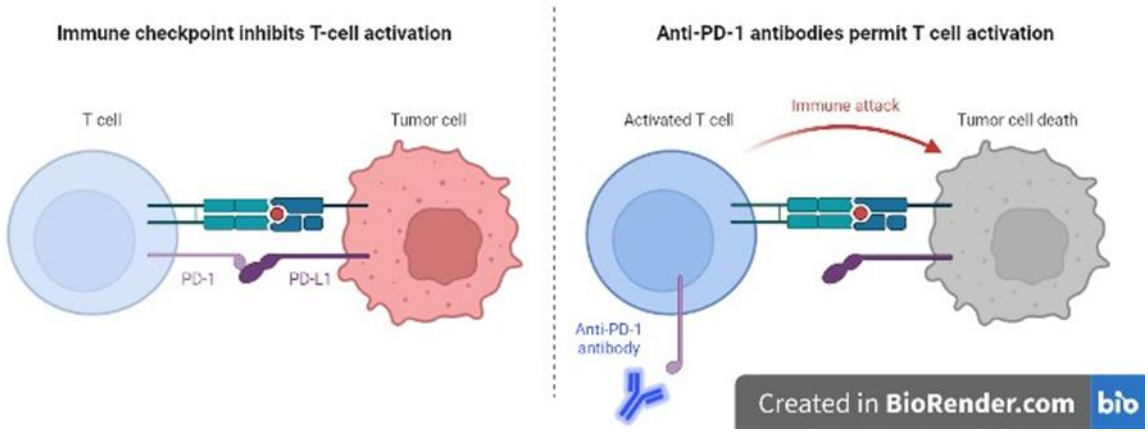

Figure 1.3: Programmed Death-1 Immune Checkpoint

Simplified schematic demonstrating the mechanism of T-cell inactivation through engagement of the T-cell PD-1 receptor with the PD-L1 ligand on tumour cells. Schematic representation of the mechanism of immune checkpoint blockade with anti-PD-1 antibodies to enable T-cell activation. Figure is adapted from Wei et al (2018).

CTLA-4 blockade has also achieved clinical efficacy in numerous solid malignancies. CTLA-4 is expressed on T-cells and dampens T-cell receptor signalling through competition with the co-stimulatory molecule CD28 for its B7 ligand binding site on antigen presenting cells (APCs), resulting in attenuation of T-cell activation (Schwartz, 1992). Furthermore, CTLA-4 has a role in the down regulation of T helper cell activity and enhancement of immunosuppressive Treg activity (Rowshanravan et al, 2018). Early pre-clinical models showed that CTLA-4 blocking antibodies caused significant anti-tumour responses in mice bearing immunogenic tumours, with mice bearing poorly immunogenic tumours failing to respond (Leach et al, 1996).

1.2.2 Immune Checkpoint Inhibition in CRC

The first significant clinical breakthrough for immune-checkpoint blockade was reported in a phase III trial in stage III/IV metastatic melanoma patients with unresectable disease refractory to standard therapies; treatment with ipilimumab, a CTLA-4 blocking human monoclonal antibody, resulted in significantly improved overall survival (Hodi et al, 2010). Ipilimumab has subsequently been shown to result in improved recurrence-free survival, overall survival and distant metastasis rates, when given as adjuvant therapy for high-risk stage III melanoma (Eggermont et al, 2016). Improved progression free survival has been reported in stage IIIb or IV non-small cell lung cancer patients, when phased ipilimumab is added to standard chemotherapy with paclitaxel and carboplatin (Lynch et al, 2012). Nivolumab has also demonstrated modest survival benefit in advanced non-small cell lung cancer (NSCLC) patients who had shown disease progression during or after first-line chemotherapy (Brahmer et al, 2015). Furthermore, pembrolizumab, another humanised monoclonal antibody against PD-1, has been shown to offer longer progression-free and overall survival than platinum-based chemotherapy, for previously untreated advanced NSCLC (Reck et al, 2016). However, toxicity is a common feature following treatment with ICB, with immune related adverse effects reported in 60-65% of patients, most commonly affecting skin, gastrointestinal tract, liver and endocrine organs (Boutros et al, 2012). By demonstrating durable responses in a subset of patients, ICB represents a significant treatment breakthrough in metastatic melanoma, a disease classically typified by dismal prognosis.

The potential for immunotherapy to induce long term durable responses in a subset of patients with solid tumours, has led to increasing interest in identifying biomarkers to distinguish which tumours will respond to this therapy. Initial responses to immune checkpoint inhibition were observed in melanoma and NSCLC, tumours which typically have high mutational burdens often owing to the effects of smoking and ultraviolet light (Alexandrov et al, 2013). It is thought that higher tumour mutation burden (TMB), reflecting the number of non-synonymous single nucleotide variants in a tumour, might result in the generation of more immunogenic tumour associated antigens thus correlating with response to immune checkpoint blockade (Havel et al, 2019). In patients with metastatic melanoma treated with immune checkpoint blockade, whole exome sequencing revealed that higher TMB was associated with improved clinical response (Snyder et al, 2014).

Initial reports of immunotherapy in the setting of CRC are confined to dMMR tumours, which typically show poor response to standard chemotherapy. dMMR tumours are considered to be MSI-H, with high tumour mutational burden, and displaying numerous tumour neoantigens which are targeted by the host immune system resulting in high levels of TILs (Fabrizio et al, 2018). dMMR in CRC tumours is associated with up-regulation of immune checkpoint markers in the tumour microenvironment, including PD-1, PD-L1, and CTLA-4, highlighting that ICB is a promising treatment strategy with potential efficacy in selective patient groups (Llosa et al, 2015). Checkmate 142, a phase 2 study using the PD-1 inhibitor nivolumab in treatment refractory dMMR/MSI-H metastatic CRC patients, showed disease control in 69% of patients for at least 12 weeks (Overman et al, 2017). This study went on to show a role for dual immunotherapy with nivolumab plus low dose ipilimumab (CTLA-4 inhibition) in treatment naïve dMMR metastatic CRC patients, with 13% achieving complete response while objective response was seen in 69% of patients at median follow up of 29 months (Lenz et al, 2022). Following these trials, the FDA granted approval in 2017 for the use of pembrolizumab and nivolumab for second line treatment in dMMR-MSI-H metastatic CRC patients (Ganesh et al, 2019). Very recently a study of single agent dostarlimab (anti-PD1 monoclonal antibody) in stage II/III rectal adenocarcinoma with dMMR status, has published exceptional results with 100% (n=12) of patients undergoing complete clinical response and

avoiding both CRT and surgical intervention (Cercek et al, 2022). These results highlight the potential benefit of administering immunotherapy early in the treatment pathway when immunocompetence is maintained, with less efficacy likely to be present against metastatic disease when immune escape mechanisms have developed.

Despite encouraging results in metastatic CRC patients with dMMR/MSI-H tumour status, only ~15% of CRCs are dMMR (Boland et al, 1998); furthermore, only 2-4% of metastatic CRC cases exhibit dMMR status (Venderbosch et al, 2014). Some efficacy has been shown recently with combined PD-1 and CTLA-4 inhibition in refractory metastatic CRC patients unselected for MMR status, with a modest survival benefit (6.6 months median versus 4.1 months) following dual immunotherapy (Chen et al, 2020). Recently, both pMMR and dMMR patients were treated at an early disease stage, with dual neo-adjuvant immunotherapy administered in early-stage colon cancer; a degree of pathological response was observed in 100% of dMMR patients, and in 27% of pMMR patients (Chalabi et al, 2020). The use of immunotherapy in CRC is an area of ongoing interest, with numerous trials ongoing to evaluate ICB in the context of both pMMR and dMMR colorectal cancer (Cohen et al, 2020).

1.2.3 Targeting the PD-1 Axis in Combination with Radiotherapy

Tissue changes induced during neoplastic transformation are sensed by the innate immune system (Dunn et al, 2004). Interferon-γ is produced by natural killer (NK) and γδ T-cells, promoting cytotoxicity of macrophages, resulting in destruction of incipient tumour cells (Street et al, 2001). The cytocidal activity of the innate immune system leads to release of tumour associated antigens for cross presentation by dendritic cells (DCs) (Schreiber et al, 2011). DCs process these antigens into peptides which are then loaded into MHC (Major Histocompatibility Complex) class I and II molecules, which are recognised by CD8+ and CD4+ T cells triggering an adaptive immune response against neoplastic cells. The concept of an ‘equilibrium’ phase can be achieved, whereby a balance between proliferation of tumour cells and killing by T-cells is reached and tumours can be maintained at a sub-clinical stage for a period of time (Koebel et al, 2007). When incomplete elimination of tumours occurs,

surviving cells can generate escape mutants, with resistance to immune rejection being critical for tumours to become clinically detectable, and 'avoiding immune destruction' is one of the key hallmarks of cancer described by Hanahan and Weinberg (Hanahan and Weinberg, 2011). Despite tumours evolving mechanisms of immune evasion, both the innate and adaptive immune system remain active and still play a role in halting tumour progression, with genomically unstable cancer cells continuing to produce neoantigens which can be recognised by T-cells (Segal et al, 2008). Both radiotherapy and immunotherapy agents can augment the anti-tumour effects of the immune system, and optimising therapeutic strategies and combinations is currently a subject of evolving interest in LARC.

Recently, interest has evolved in combining immunotherapy agents with radiotherapy, to exploit the immune priming effects of irradiation (Formenti and Demaria, 2013). It is known that radiotherapy induces tumour cell death, resulting in the priming of tumour antigens by DCs with subsequent presentation by MHC molecules, followed by expansion and activation of cytotoxic T-cells. Early pre-clinical studies suggested that T-cells played an important role in the tumour response to ionising radiation, when reduced therapeutic efficacy was seen in irradiated mice lacking in T-cells (Slone et al, 1979). It was later discovered that neoantigen associated peptides released from apoptotic cells are 'cross-primed' by DCs resulting in CD8+ cytotoxic T-Lymphocyte (CTL) stimulation (Albert et al, 1998). With both radiotherapy and immunotherapy agents having the potential to augment the anti-tumour effects of the immune system, understanding the immunological effects of these treatments is an area of evolving interest in LARC, so that therapeutic strategies and combinations can be optimised to improve neo-adjuvant treatment options for patients.

Rare clinical reports of 'abscopal' effects (at a site distant to the target), whereby regression of non-irradiated distant metastases occurs, has been reported following treatment with radiotherapy (Mole, 1953; Rees and Ross, 1983; Ohba et al, 1998). Such reports are rare following treatment with radiotherapy alone and are largely confined to case reports, however, do suggest that radiotherapy can induce a systemic anti-cancer immune response. The potential for abscopal responses clinically was reported when radiotherapy was combined with ipilimumab (CTLA-4 inhibitor) in metastatic melanoma (Postow et

al, 2012). This phenomenon was also reported in a patient with treatment resistant metastatic lung adenocarcinoma treated with radiotherapy and ipilimumab, with regression of both tumour and distant metastases, and increased TILs and tumour marker normalisation observed; furthermore, the patient had no evidence of disease one year following treatment (Golden et al, 2013).

Clinical evidence exists in several tumour types for clinical benefit when immunotherapy is administered in combination with CRT. Durvalumab, a human PD-L1 blocking monoclonal antibody, resulted in improved progression free and overall survival in locally advanced unresectable non-small cell lung cancer following treatment with CRT (Antonia et al, 2018). Improved response and survival rates have also been demonstrated in metastatic melanoma, when ipilimumab is administered in combination with radiotherapy (Hiniker et al, 2016; Koller et al, 2017).

Similarly, interest has emerged in the setting of LARC to intensify neo-adjuvant treatment strategies with immunotherapy agents, with potential benefits including improved pathological response and reduced distant metastasis rates. The VOLTAGE-A study has investigated the use of nivolumab (PD-1 inhibition), in addition to CRT and radical surgery in T3/T4 stage disease; a 30% pCR rate was reported in MSS patients (n=37), with 60% pCR reported in MSI-H patients (n=5) (Yuki et al, 2020). In a randomised study investigating the addition of pembrolizumab (PD-1 inhibition) to a TNT regimen involving induction chemotherapy, CRT and radical surgery, no significant improvement in pCR (31.9% vs 29.4%, p=0.75) was observed with the addition of ICB (Rahma et al, 2021). However, it is worth noting that immunotherapy was preceded by bone marrow suppressing FOLFOX induction chemotherapy in this study, potentially negating any proposed immune-stimulatory effects of pembrolizumab. The AVANA study recently reported a 23% pCR and 60% major pathological response rate in patients (n=101) with resectable LARC receiving standard CRT plus 6 cycles of concurrent avelumab (PD-L1 human monoclonal antibody) (Salvatore et al, 2021). The AVERECTAL study assessed SCRT followed by 6 cycles of mFOLFOX plus avelumab (n=40), with a 37.5% pCR rate and further 30% achieving a near complete response (Shamseddine et al, 2021).

The early study of immune checkpoint blockade in combination with standard of care radiotherapy based neoadjuvant regimens in LARC, has yielded some promising results, albeit with most studies publishing only early results in abstract format. Several other clinical trials are underway to assess ICB in the neo-adjuvant setting for management of LARC, including PRIME-RT which is currently investigating the addition of durvalumab in two parallel arms to either SCRT or CRT (Hanna et al, 2021; Corrò et al, 2021; Bregni et al, 2021). The early studies described suggest promising results for immunotherapy in the neo-adjuvant management of LARC in a proportion of patients, however, biomarkers of response and resistance to these therapies would further aid the development of precision medicine approaches.

1.2.4 TGF-β Signalling

In addition to immune checkpoint blockade, interest has recently developed in targeting the transforming growth factor-beta (TGF-β) signalling pathway which is known to be highly expressed in CMS4, the molecular subtype of CRC with poorest prognosis (Calon et al, 2015). Under normal physiological circumstances, TGF-β is a regulatory cytokine regulating many signalling pathways involved in essential cellular processes including cell proliferation, differentiation, migration and survival, and functions to maintain tissue homeostasis and prevent tumorigenesis (Wu et al, 2009). Furthermore, TGF-β plays a crucial role in physiological processes such as embryological development, angiogenesis and wound healing. However, cancer cells have the ability to evade the suppressive influences of TGF-β signalling, with aberrant TGF-β signalling having the contrary effect of promoting tumour growth, immune evasion, epithelial-mesenchymal transition, cancer cell dissemination and metastasis (Massagué, 2008).

There are 32 members of the TGF-β superfamily of ligands, which are grouped into the TGF-β and bone morphogenetic protein (BMP) subfamilies, with each ligand binding to a specific type II TGF-β receptor (TGFBR) on the cell surface (David and Massagué, 2018). The TGF-β subfamily includes three TGF-β ligands (TGF-β1, TGF-β2 and TGF-β3), two activins (Activin A and B), Nodal, Myostatin and several growth and differentiation factors (GDF), while the BMP subfamily

includes 10 BMPs. The process of active TGF-ß release from latent complexes is a highly regulated process, achieved through both enzymatic and non-enzymatic processes within the extra-cellular space (Lawrence et al, 1984; Annes et al, 2004). All three TGF-ß isoforms are synthesised as latent complexes, with latency associated proteins (LAP) being cleaved from the mature TGF-ß dimer to enable TGF-ß bioactivity.

The TGF-ß pathway involves membrane to nucleus signalling through the receptor mediated activation of transcription factors. In the activated ligand form, TGF-ß ligand binds to two pairs of transmembrane serine/threonine protein kinases (TGFBR1 and 2), with TGFBR2 binding catalysing the phosphorylation of TGFBR1, with the resulting receptor activation leading to the phosphorylation of SMAD transcription factors (Wrana et al, 1992; Wrana et al, 1994). SMAD proteins act as signal transducers in the TGF-ß signalling pathway, and are structurally similar proteins consisting of a globular N-terminal MH1 domain (Mad Homology) and a C-terminal MH2 domain, with the domains functioning to bind DNA and to interact with other SMADs respectively (Shi and Massagué, 2003). In the normal inactivated basal state, SMAD proteins shuttle between the cytoplasm and nucleus (Inman et al, 2002). Upon phosphorylation, SMAD proteins enter the nucleus to activate or repress the expression of multiple genes, with continuous TGF-ß receptor activity required to maintain SMAD presence and activity within the nucleus (Figure 1.3).

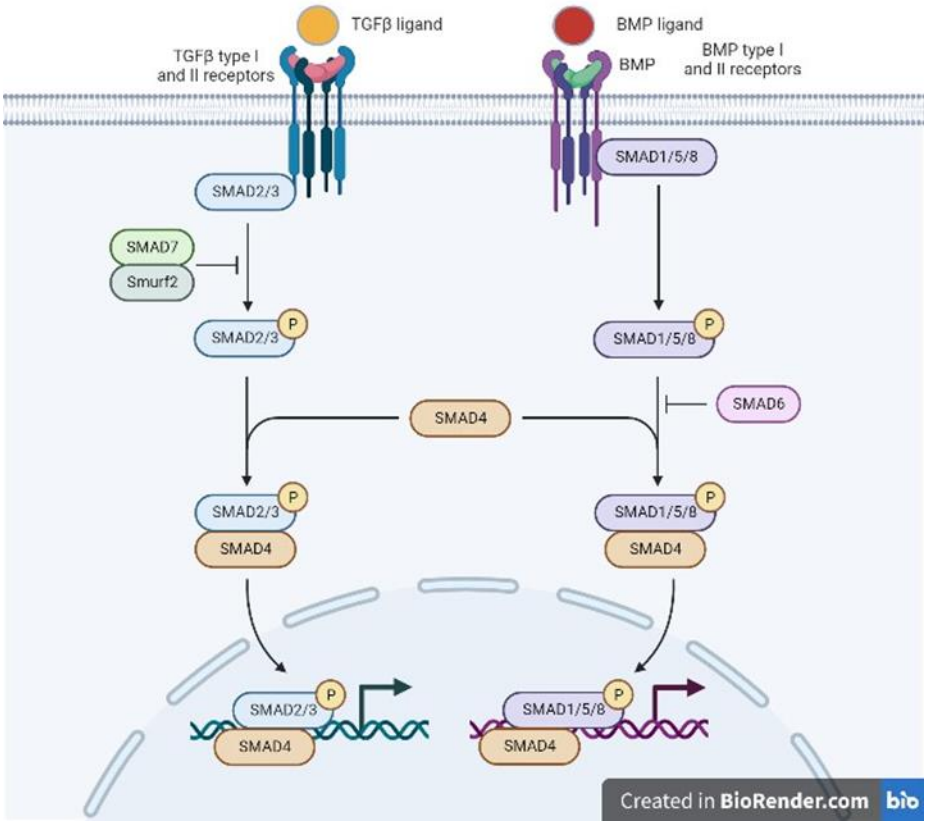

Figure 1.4: TGF-ß Signalling Pathway

Simplified schematic demonstrating the TGF-ß and BMP signalling pathways with SMAD dependent signalling cascade. Figure is adapted from Batlle and Massagué (2019).

Five members of the SMAD protein family act as receptor substrates (R-SMADs), with type I receptors for the TGF-ß ligand subfamily phosphorylating SMAD2 and SMAD3, while the type I receptors for the BMP ligand subfamily primarily phosphorylate SMADs 1, 5 and 8 (Heldin et al, 1997). Upon TGF-ß receptor activation, R-SMADs associate with co-SMADs (SMAD4 and SMAD10) in the cytoplasm to form heterotrimeric transcriptional complexes which translocate to the nucleus and ultimately trigger most TGF-ß induced gene responses (Shi and Massagué, 2003). Other SMAD proteins exert negative effects, with SMAD6 and SMAD7 having antagonistic roles which block activated SMAD1 and activated receptors respectively (Hayashi H et al, 1997; Massagué and Wotton, 2000).

1.2.5 Effects of TGF-β Signalling on the Immune Response

TGF-β is also a potent cytokine, playing a pivotal role in immune homeostasis and maintenance of immune tolerance via its regulation of lymphocyte proliferation, differentiation and survival. Furthermore, TGF-β controls inflammatory responses through regulation of chemotaxis and activation of various immune cells including natural killer (NK) cells, lymphocytes, dendritic cells, macrophages, mast cells and granulocytes (Wrzesinski et al, 2007). The effects of TGF-β on T-cells has been extensively studied, with Kehrl et al first reporting that TGF-β inhibited the proliferation of activated human T-cells in-vitro, through blocking the production of Interleukin-2 (IL-2), a cytokine which is known to regulate numerous immune cells including T-cells (Kehrl et al, 1986). In addition to suppressing T-cell proliferation, TGF-β has also been shown to have effects on T-cell function through inhibition of effector molecules such as IFN-γ and perforin (Mempel et al, 2006). Mempel et al demonstrated that TGF-β inhibits exocytosis of granules and the cytolytic function of CD8+ T cells; using intravital microscopy to image the lymph nodes of mice, CTLs were shown to have increased cytotoxicity in the absence of Treg cells or when CTLs refractory to TGF-β signalling were studied. Early pre-clinical studies using mice lacking TGF-β expression (TGFβ1-/-) demonstrated the development of multifocal inflammatory disease with increased cytokine production and an unrestrained adaptive T-cell response resulting in death shortly after birth, thus highlighting the role of normal TGF-β signalling in maintaining immune tolerance (Shull et al, 1992; Kulkarni et al, 1995).

Under normal physiological conditions, TGF-β acts as a tumour suppressor to induce apoptosis in pre-malignant cells and inhibit the proliferation of cancer cells. However, cancer cell clones can inactivate the TGF-β pathway to enable tumour progression, and under such circumstances tumour derived TGF-β can drive the development of an immune suppressive tumour micro-environment and induce a pro-metastatic niche (Batlle and Massagué, 2019). SMAD4 and TGFBR2 mutations are found in approximately 10% and 15% of sporadic CRC cases respectively, and are associated with disease progression from carcinoma to distant metastasis, thus making the TGF-β signalling pathway a potential therapeutic target in CRC (Markowitz et al, 1995; Koyama et al, 1999).

Evidence exists to suggest a role for a TGF-ß rich tumour micro-environment in suppressing anti-tumour T-cells responses, through inhibition of T-cell proliferation, differentiation and cytolytic function. In a study whereby a TGFBR2-/- mutation was specifically expressed in CD4+ cells of transgenic mice, eradication of tumours was demonstrated following tumour challenge with either the EL-4 thymoma or B16-F10 melanoma cell lines, both of which demonstrated expression of all three TGF-ß isoforms in-vitro (Gorelik and Flavell, 2001). These results showed that T-cell specific blockade of TGF-ß signalling was necessary for the generation and expansion of a CD8+ CTL tumour specific immune response, which was dependent on both CD4+ and CD8+ T-cell subsets. In a mouse model of prostate adenocarcinoma, T-cells from tumour draining lymph nodes were found to have heightened TGF-ß signalling when compared with TGFBR2-/- mutant T-cells, demonstrated through increased pSMAD2/3 expression in CD4+ and CD8+ T-cells (Donkor et al, 2011). Blockade of TGF-ß signalling in T-cells was associated with inhibition of tumour development, through enhanced tumour specific T-cell responses, with increased differentiation of effector CD8+ CTLs with increased cytolytic activity shown through increased expression of IFN-γ and granzyme B.

T regulatory cells (Tregs), which express CD4+ and CD25+, are known to suppress both the differentiation and function of effector T-cells, and function to maintain immune homeostasis under normal physiological circumstances (Suri-Payer et al, 1998). Tregs have been shown to utilise TGF-ß to suppress anti-tumour immune responses. In a CT26 murine CRC hindfoot transplant model, the presence or absence of adoptively transferred antigen specific Tregs did not affect the proliferation or activation of CD8+ CTLs, however, the presence of Tregs reduced the cytolytic activity of CD8+ CTLs and suppressed tumour growth (Chen et al, 2005). Treg suppression was demonstrated to be a TGF-ß dependent mechanism, as tumour specific CD8+ T-cells with TGFBR2-/- expression overcame suppression by Tregs and was associated with tumour rejection in this model. TGF-ß is known to have a role in the activation of Treg cells; in a murine Pan02 pancreatic cancer model expressing high levels of TGF-ß, adoptive transfer of naïve CD4+ cells resulted in the detection of higher populations of CD4+CD25+FoxP3+ve Treg cells, when compared with the low TGF-ß expressing Eso2 model (Moo-Young et al, 2009). Furthermore, T reg differentiation in the

Pan02 model was suppressed by systemic injection of a TGF-β antibody, highlighting the role of TGF-β in the induction of tumour immune suppressing Treg cells. In an in-vitro B16 melanoma tumour explant model, cytotoxic CD8+ T-cell function was also inhibited by Tregs, with anti-tumour effects observed when tumours explanted from Treg deficient mice were cultured, or when tumours were treated in-vivo with TGF-β neutralising antibodies (Budhu et al, 2017).

1.2.6 Clinical Application of TGF-β Inhibitors

The genetic or pharmacological ablation of the TGF-β pathway, particularly in CD4+ and CD8+ T cells, has demonstrated robust anti-tumour immune responses in pre-clinical models, leading to the development of several classes of TGF-β inhibitors for testing in clinical trials (Ciardiello et al, 2020). Multiple monoclonal antibodies against TGF-β have been developed, including Fresolimumab (GC1008), a human IgG4 monoclonal antibody with high affinity for all three TGF-β isoforms (Trachtman et al, 2009). In an early phase I trial in malignant melanoma and renal cell carcinoma patients (n=29), no dose limiting toxicity was observed, and one malignant melanoma patient achieved partial response with 6 patients exhibiting stable disease (Morris et al, 2014). A further small phase I study in malignant pleural mesothelioma showed modest results (n=13) with three patients showing stable disease following therapy (Stevenson et al, 2013).

Subsequent to the limited success observed with fresolimumab monotherapy, rationale for a combined therapeutic approach to combine TGF-β blockade with immune checkpoint inhibition was established. A large transcriptional dataset from metastatic urothelial cancers treated with the anti-PDL1 agent atezolimumab, demonstrated that lack of response to immune checkpoint blockade was associated with upregulation of genes involved in the TGF-β signalling pathway (Mariathasan et al, 2018). Mariathasan et al used the EMT6 mouse mammary cancer and MC38 CRC models, to demonstrate that dual immunotherapy with anti-PD-L1 and TGF-β inhibition resulted in significant increases in tumour infiltrating T-cells leading to tumour regression which did not occur with single agent treatment. Similarly, in a quadruple mutant (APC,

KRAS, TRP53, TGFBR2) mouse model of metastatic CRC, TGF-β inhibition led to increased tumour susceptibility to PD-1/PD-L1 inhibition, with TGF-β in the tumour micro-environment being identified as a mechanism of immune evasion by promoting T-cell exclusion and differentiation to an effector phenotype (Tauriello et al, 2018).

Bintrafusp alfa (M7824) is composed of an IgG1 monoclonal antibody targeting PD-L1 fused with two molecules on the extracellular domain of TGFBR2, acting as a 'trap' to sequester TGF-β in the tumour microenvironment (Lan et al, 2018; Lind et al, 2020). Bintrafusp alfa has shown tumour response in the pre-clinical setting, with inhibition of TGF-β mediated EMT, increased cytotoxicity of CD8+ T cells and NK cells, and suppression of Tregs. A phase I trial of bitrafusp alfa in patients with advanced solid tumours (n=19) showed limited efficacy with one complete response, two partial responses, one near partial response and two patients with stable disease (Strauss et al, 2018). Bintrafusp alfa demonstrated limited success in the context of heavily pre-treated advanced CRC (n=32), with only one patient demonstrating partial response, and one patient showing stable disease (Kopetz et al, 2018).

Another class of TGF-β targeting drugs are the small molecule receptor kinase inhibitors, which bind to TGF-β receptors to inhibit their kinase activity. Galunisertib (LY2157299) binds selectively to the TGFBR1 kinase domain, and has undergone initial phase I trials in unresectable hepatocellular carcinoma, advanced pancreatic cancer and advanced solid tumours with a limited number of patients showing stable disease following treatment (Ikeda et al, 2019; Ikeda et al, 2017; Fujiwara et al, 2015). A phase II trial of Galunisertib in combination with sorafenib (a protein kinase inhibitor) in patients with advanced hepatocellular carcinoma (n=47), demonstrated partial response (n=2) and stable disease (n=21) in some patients, with treatment responsive patients having an improved overall survival (22.8 vs 12 months; p=0.038) (Kelley RK et al, 2019). With the limited clinical benefits seen with TGF-β inhibition as monotherapy, current clinical trials are focused on combining other anti-cancer therapies including chemotherapy, radiotherapy or immunotherapy with TGF-β targeting drugs to improve efficacy and reduce resistance to therapy (Liu et al, 2021).

1.2.7 Targeting TGF-β Signalling in Combination with Radiotherapy in LARC

The recent ExiST study, a single arm phase II trial of galunisertib in combination with neo-adjuvant CRT in LARC, demonstrated a clinical complete response rate of 32% (n=38) with this treatment combination (Yamazaki et al, 2022). Although this study demonstrated an improvement in clinical response rate when compared with historical controls for standard of care neoadjuvant CRT, further assessment in randomised controlled trials is warranted. Interestingly, this study also included serial peripheral blood sampling before and during treatment, as well as endoscopic tumour biopsies obtained at day 0 and day 15 of treatment. Decreases in CXCR3+ (CXC Chemokine Receptor) expressing T cells and CD8+ memory T-cells were observed at day 15 in the peripheral blood of patients with a clinical complete response to CRT, with a corresponding increase in CXCR3+ CD8+ T-cells in the day 15 tumour biopsies of those patients seen. CXCR3 is responsible for leucocyte homing, therefore these results suggest a potential role of TGF-β inhibition in trafficking CD8+ T-cells to the tumour.

1.2.8 Research Priorities in Modern LARC Management

It is evident that our understanding of the molecular mechanisms underlying the tumour response to neoadjuvant therapy in LARC is incomplete and that further research is required to explain the heterogeneous responses seen in clinical practice. Analysis of tumour tissue whilst on treatment is one potential strategy to capture the evolving immunological changes which occur in the TME, given the relative accessibility of rectal tumours to endoscopic biopsy. Although feasible, this approach remains labour intensive posing a significant burden for patients. Translational data from ongoing clinical trials is paramount to determine the immunological factors associated with treatment response and failure. In addition, pre-clinical studies in models which recapitulate the histopathological, immunological and mutational profile of human disease, might serve to inform future clinical trials and investigate the mechanisms of recently discovered immunotherapy agents given in combination with radiotherapy.

1.3 Biomarkers of Response in Locally Advanced Rectal Cancer

Technological advances have enabled gene profiling to be undertaken at diagnosis, with potential delivery of a comprehensive genomic profile prior to therapy. Data from the Swedish Rectal Cancer Trial suggested that nuclear p53 staining, seen in 41% of tumours (n=163), was associated with local treatment failure following neo-adjuvant radiotherapy (Adell et al, 1999). Subsequent meta-analysis data also supported this observation, with low p53 expression or wild-type p53 status being associated with treatment response following neo-adjuvant radiotherapy-based treatment in LARC (Chen et al, 2012). However, evidence suggests that p53 mutations tend to accumulate throughout treatment with CRT, as demonstrated through DNA sequencing of pre- and post-treatment samples in non-responsive patients, highlighting a limitation of baseline p53 status as a predictive biomarker (Sakai et al, 2014). A recent study compared gene expression profiles in a small number of patients with complete or partial responses (n=8 per group), and found that mutations in four genes were associated with partial response: KDM6a, ABL1, DAXXZBTB22 and KRAS (Douglas et al, 2020). Other studies have revealed KRAS mutation to be an independent predictor of both poor response to CRT and locoregional recurrence (Chow et al, 2016; Iseas et al, 2021). However, conflicting evidence exists to suggest that KRAS mutations are associated with tumour response to CRT, albeit in retrospective studies with low numbers (Luna-Pérez et al, 2000). The study by Chow et al, includes a large patient cohort (n=229) of pre-treatment biopsies from the 'Timing Trial' whereby patients were treated with neoadjuvant CRT followed by increasing cycles of consolidation chemotherapy. Robust data is shown to suggest that KRAS mutations are associated with reduced pCR rates, even when treatment related variables are adjusted for; furthermore, the presence of p53 and KRAS mutation was associated with significantly lower rates of pCR (10%) and increased rates of lymph node metastasis. BRAF and SMAD4 mutations have also been shown as potential molecular markers to predict poor prognosis and resistance to neoadjuvant CRT in LARC, however, these mutations were only seen in a small number of patients within the study group (Jiang et al, 2019).

The 'immunoscore' initially described by Galon, measures the density of CD3+ and CD8+ lymphocytes in both the tumour core and invasive margin to give a

score (0-4), with high 'immunoscores' correlating with higher levels of immune cell recognition and being associated with improved relapse rates and disease-free recurrence in colonic cancer (Galon et al, 2006; Mlecnik et al, 2016). The 'immunoscore' has been assessed in rectal cancer patients (n=111) treated with surgery alone, with high CD3 and CD8 densities being associated with improved disease free and overall survival (Anitei et al, 2014). Further evidence exists from surgical resection specimens treated with neo-adjuvant CRT, to suggest that high post treatment CD4+ and CD8+ TILs (Tumour Infiltrating Lymphocytes), high PD-L1+ (Programmed Death Ligand 1) TILs, and low FOXP3+ TILs are associated with favourable response to CRT and that high CD8+TILs and low FOXP3+ TILs are associated with improved overall survival (Zhang et al, 2019).

When comparing pre- and post-treatment tumour samples, studies show that CRT is associated with increased densities of CD8+ and CD4+ TILs when post treatment samples are compared with pre-treatment biopsies (Teng et al, 2015). Furthermore, evidence suggests that tumours demonstrating high pre-treatment CD8+ and CD4+ densities are associated with increased treatment sensitivity and response to CRT (Yasuda et al, 2011; Anitei MG et al, 2014; Teng et al, 2015). A study comparing pre-treatment biopsies and post CRT resection specimens, showed that CRT is associated with increased stromal densities of CD8+ cells and stable FOXP3+ cells, and that high baseline intraepithelial CD8+ density and CD8+/FOXP3+ intraepithelial ratio is associated with favourable clinical outcome (Shinto et al, 2014). Pre-treatment PD-L1 expression has also been reported to have significant association with improved disease free and overall survival following treatment with neo-adjuvant CRT and surgical resection, in a study with 112 paired pre-treatment biopsy and surgical resection specimens (Chen et al, 2019).

FOXP3+ Treg cells have been shown to have an inhibitory role in the response to CRT in rectal cancer, with low stromal density of FOXP3+ cells being associated with pCR in post-surgical resection specimens (McCoy et al, 2015). Further evidence exists to suggest an immunosuppressive role for Treg cells in LARC, with a small study (n=8) of pre-treatment and post-treatment biopsies after 4 cycles of induction chemotherapy, showing that increases in FOXP3+ cells were associated with poor response to CRT, while decreased FOXP3+ cells were

associated with complete response in a small number of patients (Roxburgh et al, 2018).

Most studies to date aiming to identify biomarkers of response to neo-adjuvant therapy have detected correlations based upon immunohistochemistry, with limited conclusions upon which to stratify patients. A very recent study conducted genomic and transcriptomic analysis of 346 stage II/III rectal cancers which had undergone neo-adjuvant therapy, and identified over-expression of IGF2 (Insulin-like growth factor 2) and L1CAM (L1 cell adhesion molecule) genes as being associated with decreased response to neo-adjuvant therapy (Chatila et al, 2022). Furthermore, RNA sequencing identified a subset of MSS 'immune-hot' tumours with improved response rates. It is evident that gene expression data from tumour samples may prove informative in identifying reliable biomarkers, with the accessibility of rectal tumours also holding potential for temporal sampling throughout treatment to inform upon evolving changes in the tumour microenvironment.

Currently there is not sufficiently robust evidence upon which to base treatment response predictions according to both immunological and mutational parameters. Treatment response predictions are potentially challenging owing to intra-tumoral heterogeneity and so multiple biopsies must be acquired to account for this and to improve accuracy. Furthermore, methods to predict treatment response must be both time and cost effective to achieve clinical utility. The 'immunoscore' and other studies suggest that tumours densely infiltrated with favourable immune cell populations such as CD8+ TILs are more likely to exhibit a favourable response to therapy. Immunotherapy has recently emerged as a promising treatment modality to activate components of the immune system for therapeutic benefit.

1.4 Existing Pre-Clinical Models to Study LARC

1.4.1 Genetically Engineered Mouse Models of Colorectal Cancer

Significant developments in pre-clinical modelling of CRC have been achieved over the past three decades, with genetically engineered mouse models (GEMMs) becoming increasingly sophisticated (Jackstadt and Sansom, 2016). GEMMs are valuable tools to recapitulate human intestinal cancer, and have improved our

understanding of tumour biology and our ability to test novel therapies. The development of GEMMs of CRC began in the early 1990s, following the discovery of the APC tumour suppressor gene in ~80% of sporadic CRC (Fearon and Vogelstein, 1990). Early GEMMs focused on the mutation of APC, with the first *Apc* mutant mouse model being generated in 1990 by Moser et al, when introduction of the germ line mutagen N-ethyl-nitrosurea (ENU) resulted in a loss of function *Apc* gene mutation at codon 850 (Moser et al, 1990). In this model, spontaneous loss of a second *Apc* allele in adulthood resulted in the development of multiple small intestinal adenomas in mice, with this mutation subsequently being termed 'multiple intestinal neoplasia' or 'MIN.' When linkage analysis subsequently demonstrated that the murine homolog of the APC gene was linked to the MIN locus, this model was termed the $Apc^{Min/+}$ mouse (Su et al, 1992). The early $Apc^{Min/+}$ model mirrors the genetics of human FAP; however, significant limitations exist as polyps arise predominantly in the small intestine of $Apc^{Min/+}$ mice, whereas FAP patients develop colonic polyps with the potential to progress to invasive carcinoma.

The advent of Cre-Lox (Cre) technologies in the 1990s, enabled researchers to develop more sophisticated disease models with the ability to delete any gene in the correct tissue of interest (Nagy, 2000). Additionally, Cre-Lox technology has allowed the development of mouse models where mutations of interest are constitutively active or expressed selectively upon induction. The Cre-Lox system works through the Cre recombinase enzyme in bacteriophage P1, which causes recombination between pairs of LoxP gene recognition sites (Araki et al, 1997). Such LoxP gene recognition sites are inserted into the mouse genome to flank a particular genomic segment of interest; upon induction with Cre recombinase, deletion, inversion or translocation of the 'floxed' locus occurs in Cre expressing cells only. In the case of deletion, an essential exon of a gene can be 'floxed' so that upon recombination a gene knockout is created. Activation of an oncogene can also be induced using Cre-Lox technology whereby a LoxP flanked stop codon is inserted upstream of a transgene of interest, as is demonstrated in the case of $Kras^{G12D}$; in *Lox-Stop-Lox-*$Kras^{G12D/+}$ mice, oncogenic *Kras* expression is controlled by a removable stop codon (Jackson et al, 2001).

Ligand-dependent Cre-Recombinase systems have subsequently been developed through coupling of the Cre enzyme to ligands, most commonly the oestrogen

receptor, which enables Cre to be activated following administration of tamoxifen (Hayashi and McMahon, 2002; Feil et al, 2009). In the case of the digestive system, fusion of the oestrogen receptor to the Cre-recombinase expressing gut specific promotor 'Villin', enables recombination to occur specifically in the intestinal epithelium (el Marjou et al, 2004). Cre-Lox technology has significantly advanced pre-clinical modelling capabilities in CRC, by enabling manipulation of the mouse genome such that mutational combinations of interest can be induced in both a spatial and temporal manner.

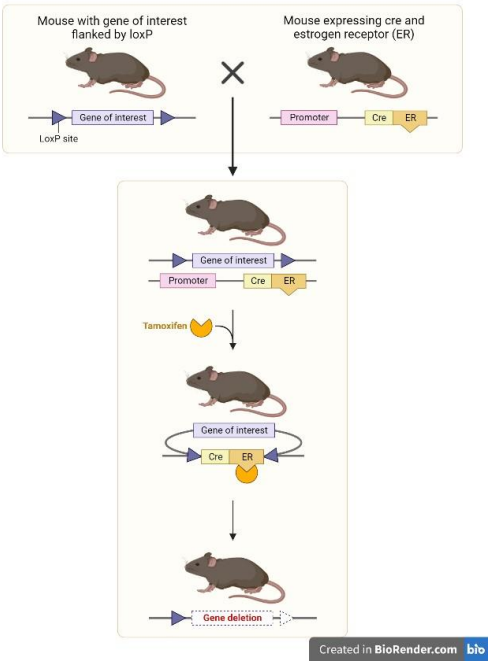

Figure 1.5: Ligand Dependent Cre-Recombinase System

Simplified schematic demonstrating a ligand dependent Cre-recombinase system. A gene of interest is flanked by two LoxP proteins. A cre-recombinase expressing tissue specific promotor is fused to the oestrogen receptor. Upon induction with tamoxifen, the gene of interest is deleted in a tissue specific manner. ER = oestrogen receptor. Figure is adapted from el Marjou et al (2004)

Using Cre-Lox technology, with delivery of Cre recombinase via an adenovirus vector (Adenovirus-Cre) to mice carrying a mutant $Apc^{508S/508S}$ allele, Shibata et al demonstrated colonic adenoma formation within 4 weeks following deletion of both allelic copies (Shibata et al, 1997). Inducible *Apc* models have provided valuable insight into the biological mechanisms of early tumorigenesis. For instance, an inducible Cre within the small intestine utilising AhCre (driven by the Cyp1a1 promotor and inducible by ß-naphthflavone and villinCreERT), has shown that acute homozygous *Apc* deletion has dramatic effects on intestinal

homeostasis (Sansom et al, 2004; Andreu et al, 2005). Acute models of homozygous *Apc* loss demonstrate that *Apc* loss in the small intestinal epithelium leads to enlargement of the crypt compartment and acute activation of Wnt signalling through nuclear beta-catenin accumulation, which consequently disrupts intestinal crypt cell differentiation, migration, proliferation and apoptosis.

To model more invasive disease, additional mutations in the adenoma-carcinoma sequence have been added to achieve more relevant and increasingly sophisticated CRC models. In the classical adenoma-carcinoma pathway, where APC loss is considered the initiating event, mutation of KRAS is observed in ~50% of CRC cases and is associated with the transition from early to intermediate adenoma (Fearon and Vogelstein, 1990). In CRC, KRAS mutations most commonly occur on codon 12, with the G12D variant being most prevalent (Muzny et al, 2012). KRAS is a member of the Ras protein family, which function as small GTPases and act as molecular switches, with signals being transduced from tyrosine kinases and G-protein coupled receptors at the cell surface to the nucleus. The KRAS gene encodes the Kirsten Rat Sarcoma 2 viral oncogene homolog (KRAS) protein, which is a guanine nucleotide binding protein and a member of the RAS protein family (Malumbres and Barbacid, 2003). After KRAS binds to guanosine 5'-triphosphate (GTP), it becomes activated and transduces signals across multiple molecular pathways including PI3-kinase and RAS-RAF-MAPK signalling, which regulate cell proliferation and differentiation (Meng et al, 2021). In the case of the G12D variant mutation, glycine is substituted with aspartic acid at codon 12 (G to D, in codon 12), resulting in an inability of KRAS to hydrolyse GTP, with its constantly active form able to aberrantly transduce signals which influence cell phenotype, proliferative capacity and survival (Tahir et al, 2021). Using a gene-targeting strategy, endogenous expression of $Kras^{G12D/+}$ has been demonstrated to be embryonically lethal, however, when conditional expression of the $Kras^{G12D/+}$ allele is induced in lung or gastrointestinal tissue, epithelial hyperplasia is observed (Tuveson et al, 2004).

In a Cre inducible model of CRC, expression of an oncogenic $Kras^{V12}$ allele in addition to *Apc* deletion was found to accelerate both intestinal adenoma formation and invasion, compared with $Apc^{fl/fl}$ allele expression alone (Sansom et al, 2006). Similarly, a compound mutant model expressing $Apc^{1638N/+}$;

Kras$^{V12G/+}$ showed increased tumour progression and multiplicity compared with single mutant animals, with malignant transformation felt to be due to synergistic activation of Wnt signalling and increased nuclear beta-catenin accumulation (Janssen et al, 2006). A further study by Haigis et al, showed that *Kras*$^{G12D/+}$ expression in the colonic epithelium stimulated hyperproliferation in a MEK-dependent manner, with *Kras*$^{G12S/+}$ mutant mice showing a hyperplastic crypt phenotype with increased proliferative progenitor cells and attenuated MAPK signalling (Haigis et al, 2008). Furthermore, colonic tumours from animals expressing conditional *Apc*$^{2lox14/+}$ and *Kras*$^{LSL-G12D/+}$ mutations demonstrated uniform high-grade dysplasia throughout, unlike tumours expressing wild-type *Kras*, suggesting that activated *Kras* accelerates progression to malignancy in colonic tumours. A propensity towards increased colonic tumour development rather than the small intestinal location classically observed in the *Apc*$^{Min/+}$ model, was observed in a conditional mutant *Kras* mouse model crossed with *Apc*$^{Min/+}$ mice and induced through ß-Naphthtoflavone treatment (Luo et al, 2009). Luo et al demonstrated a 1.5-fold increase in small intestinal adenomas, and a 5.7-fold increase in colonic adenomas when compound *Apc*$^{Min/+}$;*Kras*$^{Asp12/+}$ mutant mice were compared with *Apc*$^{Min/+}$ mice, with the markedly increased colonic adenoma prevalence being associated with increased expression of downstream target genes in the Wnt, AKT and MAPK signalling pathways.

A significant limitation of many Cre inducible models, is variability in the incidence, location and number of intestinal tumours which form; however, several methods exist which enable localised tumour induction (Shibata et al, 1997). A surgical method of adeno-cre delivery was described by Hung et al, which restricted recombination to a distinct region in the distal most 3cm of the murine colon (Hung et al, 2010). Following laparotomy, adeno-cre was delivered to the distal colon by enema, with application of surgical clips for 30 mins preventing adenoviral enema migration. Using this method, *Apc*$^{\Delta 580/+}$;*Kras*$^{tm4tyj/+}$ mice developed distal colonic invasive adenocarcinoma in 50% of mice analysed at 20 weeks, with a 20% liver metastasis rate demonstrated at 24 weeks. Development of a murine carbonic anhydrase1 promoter and cre recombinase (CAC) transgene construct, enabled exclusive transgene expression in the large intestine (Xue et al, 2010). In *CAC;Apc*$^{508S/+}$ mice, gross colonic tumours were apparent by 10 weeks of age which histologically resembled adenomas and

microadenomas. Tumorigenesis can also be restricted to the distal colon through tamoxifen dependent Cre recombinase driven by either the Villin (epithelial specific) or the Lgr5 (Leucine-rich repeat-containing G-protein coupled receptor 5) intestinal stem cell specific promotor (Roper et al, 2017). Roper et al describe the induction of distal colonic tumours following mucosal delivery of 4-hydroxytamoxifen (4-OHT), administered by colonoscopy guided needle injection in *VillinCreER;Apc$^{fl/fl}$* and *Lgr5CreER;Apc$^{fl/fl}$* mice, demonstrating CRC models in which tumorigenesis can be restricted to a specific site in the colon.

In order to develop invasive models of adenocarcinoma, multiple CRC driver mutations are required. When *Apc$^{Min/+}$* mice have a homozygous null allele of *p53* introduced (*Apc$^{Min/+}$;p53$^{-/-}$*), animals develop a significantly increased number of intestinal adenomas when compared with *Apc$^{Min/+}$* mice (Halberg et al, 2000). Furthermore, a significantly increased number of colonic tumours exhibiting features of carcinoma in-situ were observed in tumours from *Apc$^{Min/+}$;p53$^{-/-}$* mice when compared with *Apc$^{Min/+}$;p53$^{+/+}$* mice, suggesting that *p53* plays a crucial role in adenoma progression. Studies combining *Apc* mutation in mice with inactivation of various components of the TGF-ß signalling pathway, have demonstrated invasive adenocarcinoma. An early study investigated the role of *SMAD4* inactivation in *Apc* mutant mice, with homozygous inactivation of the *Dpc4(Smad4)* gene in *Apc^{Δ716}* mutant mice leading to adenomas which progressed to malignant and invasive adenocarcinomas (Takaku et al, 1998). A further study using *Apc^{Δ716};Smad4$^{+/-}$* mice, showed that loss of TGF-ß signalling in tumour epithelium leads to accumulation of immature myeloid cells at the invasive front, which promoted tumour invasion through expression of the chemokine receptor 1 (CCR1) and migration to the chemokine ligand 9 (CCL9) in the tumour epithelium (Kitamura et al, 2007).

Overall, it is observed in GEMMs of CRC that the addition of common CRC driver mutations to Apc mutation, provokes increased tumour progression, number and development of adenocarcinoma. A key aim of mouse models of cancer is to recapitulate the spectrum of human disease, including progression to distant metastasis, such that models can be used to test potential therapies and predict response in patients with advanced disease who have the greatest need for novel treatment strategies. GEMMs which display distant metastasis have been difficult to achieve, with the majority representing the alternative ‘serrated’ route,

characterised by initial KRAS or BRAF mutations and absence of initiating APC mutation, thus representing upto 30% of human cases (Jass, 2007; Rex et al, 2012). One APC driven GEMM of metastatic CRC has been described and termed the 'iKAP' model, whereby a doxycycline inducible oncogenic *Kras* allele was combined with conditional null alleles of *Apc* and *p53* (*VillinCreERT2;Apc*$^{fl/fl}$*;Kras*$^{Tet\text{-}G12D/+}$*;p53*$^{fl/fl}$), resulting in a 25% overall distant metastasis rate (Boutin et al, 2017).

A model of serrated CRC, whereby *VillinCre;Braf*$^{LSL\text{-}V637E/+}$ mice progress through a typical hyperplasia-dysplasia sequence, showed progression to carcinoma in only 13.8% of mice (Rad et al, 2013). When an additional *p53* mutation was introduced, *VillinCre;Braf*$^{LSL\text{-}V637E/+}$*;p53*$^{LSL\text{-}R172H/+}$ mice developed carcinoma at a much greater frequency of 56%, with 25% developing lymph node, pancreatic or lung metastasis. However, low penetrance and long latency was a limitation of this model. Another model of serrated CRC which demonstrated distant metastasis, was characterised by activation of KRAS plus additional inactivation of the tumour suppressor PTEN (phosphatase and tensin homologue) which has been identified in 5.8% of human CRC cases (Day et al, 2013). *VillinCreERT;Pten*$^{fl/fl}$*;Kras*$^{LSL/+}$ mice showed evidence of distant metastasis in 41% (11/27), most commonly to the liver; interestingly distant metastasis was not observed in *VillinCreERT;Apc*$^{fl/+}$*;Pten*$^{fl/fl}$*;Kras*$^{LSL/+}$ mice. Recently, a highly penetrant model of metastatic colorectal cancer was described by Jackstadt et al, demonstrating that activation of epithelial Notch-1 signalling in a *Kras*-driven serrated model, resulted in highly penetrant distant metastases (100%) predominantly to liver (Jackstadt et al, 2019).

Although significant advances have been described in the development of GEMMs of CRC, significant limitations exist in the application of such models to pre-clinical studies aimed at evaluating novel radiotherapy-immunotherapy treatment combinations in LARC. The majority of models described fail to recapitulate the anatomical location of rectal cancer, with tumours predominantly developing in the small intestine or colon. In the context of administering therapeutic targeted irradiation in an experimental setting, tumours located in the murine rectum are crucial if models are to accurately resemble human disease, and to enable targeting of irradiation to a fixed pelvic tumour. Furthermore, GEMMs are typically expensive with significant time

implications in the development and generation of adequate quantities of experimental animals to perform sufficiently powered treatment studies.

In this thesis, I aimed to develop an orthotopic model of LARC which recapitulates the anatomical and histological features of locally invasive disease. Furthermore, I sought to develop a model which is timely, cost-effective and reproducible, and which will enable generation of experimental animals for high throughput pre-clinical treatment studies. I aimed to utilise the ligand-dependent Cre-recombinase system, whereby the gut specific villin promotor is fused with the oestrogen receptor (*VillinCreERT2*), such that local delivery at the rectal location might induce orthotopic tumours. Roper et al described submucosal needle injection of tamoxifen under colonoscopic guidance at the distal colon in single *Apc* mutant mice, therefore, I anticipated that this strategy could be adapted to induce tumours at the rectal location in mice with increasingly complex mutational burdens (Roper et al, 2017).

1.4.2 Colitis Induced Models of CRC

Murine models of acute and chronic colitis can be established with the sulphated polysaccharide dextran sodium sulfate (DSS), which can be administered via drinking water (Okayasu et al, 1990). DSS exposure is toxic to the colonic epithelia, compromising epithelial barrier integrity and inducing inflammatory infiltration of the mucosa by luminal bacteria, resulting in ulceration and bloody diarrhoea, and pathology which is predominantly confined to the distal colon (Azuma et al, 2008; Chassaing et al, 2014). The induction of colitis with DSS is associated with progressive accumulation of neutrophils, macrophages, T helper cells, cytotoxic T cells and T reg cells within the colon, as well as colon length shortening, and progressive histological changes such as crypt destruction, loss of goblet cells and depletion of the epithelial barrier (Yan et al, 2009; Nunes et al, 2018). Colitis induced models have proven beneficial in the study of inflammatory bowel disease and colitis associated CRC, as well as having a role in the development of therapies which modulate inflammation in both cancer and inflammatory bowel disease (Low et al, 2013; Wang et al, 2015).

Colitis induction methods have been successfully used to model carcinoma development in mice with chronic colitis; administration of the carcinogen

azoxymethane (AOM), followed by repeated courses of DSS have been shown to induce colonic tumours ranging from low grade dysplasia to adenocarcinoma within 20 weeks of induction (Okayasu et al, 2002; Tanaka et al, 2003). A later study demonstrated induction of multiple colonic tumours within 10 weeks, following AOM administration and multiple cycles of DSS treatment (Neufert et al, 2007). Although the described studies demonstrate cost efficiency and reproducibility following AOM/DSS induction, effectiveness of this model can potentially be affected by numerous factors including dosage, cycle duration and number, DSS batch, mouse strain, sex and the microbial environment in which animals are housed. Colitis induced models of CRC are valuable tools to investigate the role of inflammation in colon carcinogenesis, as well as providing a platform to study potential chemo-preventative agents (De Robertis et al, 2011). Colitis induced models of CRC have enabled the identification of numerous potential targets in the setting of chronic inflammation and its association with carcinogenesis, including toll-like receptor 4 (TLR-4), IκB kinase (IKKβ) complex, and interleukin-6 (Fukata et al, 2007; Greten et al, 2004; Grivennikov et al, 2009).

Although DSS treatment in combination with AOM has proven useful for the investigation of colitis associated cancer, contributing to an expansion in knowledge of the immunological mechanisms underpinning inflammatory cancers, as well as the role of the gut mucosal immune response, intestinal microbiome and genetic susceptibility factors in the pathogenesis of colitis associated carcinogenesis (Sussman et al, 2012; Manicassamy et al, 2021). Colitis is associated with an increased risk of CRC development, with UC patients estimated to have an overall CRC prevalence of 3.7% (Eaden et al, 2001). However, inflammatory bowel disease only accounts for ~1% of colorectal cancers in Western populations, and so colitis induced models of CRC recapitulate only a minority of cases (Kuipers et al, 2015).

Colitis induced models are not the ideal setting to investigate most sporadic CRCs. Significant differences in the spectrum of genomic alterations exist when colitis-associated cancers are compared with sporadic CRCs; for instance, TP53 mutations are felt to be an early event in colitis associated cancers but are considered a later event in sporadic CRC, whereas WNT pathway alterations and APC mutations are more prevalent in sporadic CRC (Yaeger et al, 2016). It has

been shown that treatment with DSS significantly alters the colonic microenvironment, with markedly increased neutrophil infiltration, upregulation of inflammatory genes such as IL-1ß (Interleukin), IL-6, TNF-α (Tumour Necrosis Factor) and COX-2 (cyclooxygenase-2), as well as increased expression of TGF-ß related genes (Vidal-Lletjós et al, 2019). Although colitis induction methods might hold potential in the development of orthotopic rectal cancer models, owing to the propensity to develop distal colonic tumours, colitis associated CRC is not reflective of the molecular and histological features of sporadic CRCs which represent the majority of cases.

1.4.3 Cell-Line Transplant Models of Colorectal Cancer

Transplant models have been widely used in pre-clinical CRC research to model the adenoma-carcinoma-metastasis sequence, with the advantage of avoiding the cost, time constraints and complexities associated with GEMMs. An early study found that cell lines derived from primary human colonic cancers, when implanted in immunodeficient nude mice, yielded hepatic metastases when injected into the caecum or spleen, whereas human colon cancer cells injected subcutaneously did not yield metastasis, showing that the organ of implantation influences the metastatic phenotype (Fidler, 1991). The surgical implantation of intact human colorectal tumour fragments by suturing to the caecal wall serosa of immunodeficient mice has been described in other studies, with a small proportion exhibiting regional lymph node, liver metastases or peritoneal carcinomatosis (Fu et al, 1991; Jin et al, 2011). Injection of the human colon cancer cell line HT-29 below the renal capsule has also been described in early models (Tanaka et al, 1994).

Such early transplantation models are not truly orthotopic; at the caecal transplant site, cells are injected at the outer serosal layer, whereas direct splenic injection techniques bypass the molecular events which drive progression from primary tumour to distant metastasis. A later model involved a more refined technique of caecal wall implantation, with human CRC cell line suspensions being injected at laparotomy through microinjection between the caecal mucosa and muscularis propria layers in nude mice (Céspedes et al, 2007). Cespedes et al were able to demonstrate a ≥75% engraftment rate across

all cell lines implanted, with varying patterns of dissemination according to cell line, with metastatic sites including the retroperitoneal or mesenteric lymph nodes, lungs, liver and peritoneum.

It is important to note that different host backgrounds are used in studies involving xenograft transplant of both human and murine tumour derived cell lines, with varying degrees of immunodeficiency required in order to overcome xenograft rejection. Nude mice were the earliest immunodeficient mouse strain to be used in cancer research, with mutation in the forkhead box N1 gene (Foxn1nu) causing abnormal hair growth and defective thymic development (Pantelouris, 1968). As a result, nude mice are athymic, lack mature T-cells and suffer from a lack of cell-mediated immunity. Mice with increasing degrees of immunodeficiency have subsequently been developed, and the immunological features of mice strains commonly described in pre-clinical studies discussed in this thesis are summarised (Table 1.5)

	C57Bl/6	***CD1 Nude***	***BALB/c Nude***	***SCID***	***NOD SCID***	***NSG***
Mature B cells	Present	Present	Present	Absent	Absent	Absent
Mature T cells	Present	Absent	Absent	Absent	Absent	Absent
Dendritic cells	Present	Present	Present	Present	Defective	Defective
Macrophages	Present	Present	Present	Present	Defective	Defective
Natural killer cells	Present	Present	Present	Present	Defective	Absent

Table 1.5: Immune Features of Mouse Strains Commonly Used in Pre-Clinical Studies.

Table summarising the presence and absence of immune cells in mouse strains commonly used in pre-clinical studies. SCID = Severe Combined Immunodeficiency. NOD = Non-obese diabetic. NSG = NOD Scid Gamma. Table adapted from Charles River Europe (www.criver.com/immunodeficient)

Models have been described which specifically involve orthotopic transplant at the murine rectum. A rectal prolapse technique, with subsequent injection of murine CRC cell lines under direct vision to the rectal submucosa, yielded large rectal carcinomas and para-aortic lymph node metastasis in immunocompetent C57Bl/6 mice (Kashtan et al, 1992). A similar model described submucosal intra-

rectal injection taking place 1-2mm above the anal margin, yielding a 65% overall tumour engraftment rate when the CT-26 murine colon cancer cell line was injected into BALB/c immunocompetent albino mice, with poorly differentiated adenocarcinoma observed (Donigan et al, 2009). More recently, a rectal transplant model was described whereby rectal prolapse was induced using a haemostat clip and murine or human CRC tumour donor cells subsequently sutured to the mucosal layer (Enquist et al, 2014). Interestingly, when *Apc*$^{Min/+}$*;Kras*$^{LSL\text{-}G12D/+}$*;VillinCre* donor tumours were transplanted using this technique in C57Bl/6 immunocompetent mice, only 17.6% of tumours displayed malignant potential with tumour invasion through the colon wall, and subsequent lymph node and liver metastasis formation. In contrast, when the HCT-116 human CRC cell line was transplanted into NOD SCID (Non-Obese Diabetic; Severe Combined Immunodeficiency) mice, liver and lung metastases were typically observed at 7 weeks post implantation, a feature which was not demonstrated when donor tumours were implanted in the subcutaneous location.

Orthotopic models of CRC have been described by injecting the HT-29 human cancer cell line into the submucosa of the distal colon in NOD SCID mice, using colonoscopic guidance (Bettenworth et al, 2016). Although this model demonstrated rapid tumour growth resulting in colonic obstruction, as well as the development of both liver (28.6%) and peritoneal metastases (14.3%), tumours failed to engraft in immunocompromised nude mice when using this technique. Another intra-rectal submucosal injection model was described by Hite et al, whereby the HT-29 human cancer cell line was co-inoculated with lymph node stromal cells and subsequently injected by needle into the rectal submucosa of NOD SCID mice (Hite et al, 2018). This technique yielded rectal tumours in 100% (n=25), with liver (60%) and lung metastases (56%) observed in a significant proportion.

Orthotopic injection of 2D cell lines holds advantages over other heterotopic cell line transplant techniques, with instrument dilatation of the anus, rectal prolapse and colonoscopic guidance enabling needle injection under direct vision and avoiding the need for prolonged surgical intervention. However, cell line transplant models are limited as varying degrees of immunodeficiency are required to enable tumour uptake in the recipient host, and so important

immunological components which regulate tumorigenesis in the human condition are not recapitulated. Derivation of patient derived tumour xenografts into 2D cell lines involves extensive adaptation to in-vitro culture conditions, such that only rare clones are expanded and maintained over many passages, with the resulting cell lines failing to recapitulate the genetic composition of their original tumours. Furthermore, 2D cell lines lack a stromal compartment (Drost et al, 2018). The use of murine tumour derived cell lines has overcome some of these limitations, with engraftment successfully being achieved in immunocompetent murine hosts, as in the studies by Donigan and Enquist. However, these studies also involve the use of immortalised cell lines, which have undergone extensive in-vitro selection with indefinite division occurring as a result of aberrant gene expression, meaning these cell lines have significant limitations in their capacity to represent normal cell biology and human disease (Hynds et al, 2018). Clearly, the optimisation of experimental models is an important goal if clinically relevant data is to be generated from pre-clinical treatment studies. Although various methods have been described which enable the orthotopic transplant at the murine rectum, tumour xenografts must better recapitulate the molecular composition of human CRC.

1.4.4 Organoid Transplant Models of Colorectal Cancer

3D culture technology has recently developed to enable more physiologically accurate models of both normal tissue and cancer. Organoid technology has emerged as a valuable tool in stem cell and cancer biology research, whereby tissue derived mammalian stem cells are embedded into a 3D matrix and subsequently grow with high efficiency into self-organising 3D cell clusters which mimic the micro-anatomy of their originating tissue (Kretzschmar et al, 2014). Sato et al demonstrated that 3D epithelial organoids can be established from murine Lgr5+ intestinal stem cells, when embedded in a murine derived ex-vivo basement membrane substitute and cultured in serum free stem cell niche mimicking conditions (Sato et al, 2009). Subsequently, 3D organoid culture techniques have been developed and adapted to enable organoids to be derived from multiple murine and human epithelial tissues, including the long-term culture of human small intestinal and colonic tissue, murine Apc deficient adenomas and human CRC cells (Sato et al, 2011; Jung et al, 2011).

Organoids hold advantages over 2D cell lines, with greater retention of their original phenotypic and genetic features, an improved ability to study cancer progression, and the ability to have matched normal tissue derived control lines (Drost et al, 2018). Efforts have been made to generate biobanks consisting of human primary tumour derived organoids and matched healthy tissue derived organoids. A tumour organoid biobank from CRC patients was generated which consisted of 20 genetically diverse tumour organoid cultures with corresponding normal tissue derived organoids for most patients (van de Wetering et al, 2015). Histologically, tumour derived organoids resembled the tubular epithelial structures seen in their originating tumour, and genomic DNA analysed by whole exome sequencing correlated with large scale mutational analyses of CRC. The tumour organoids and their matched normal tissue derived organoids described by van de Wetering and colleagues, were amenable to high throughput drug screening, with one organoid culture showing sensitivity to a Wnt secretion inhibitor (the porcupine inhibitor LGK 974) in the presence of a mutation in RNF43 (Ring Finger Protein), a negative Wnt feedback regulator. This demonstrates the theoretical application of patient tumour derived organoids to in-vitro drug screens, to identify potential therapeutic targets associated with specific mutations. A further study by Fujii and colleagues, established an organoid library from 55 primary CRC patients, 41 of which had a corresponding normal tissue derived counterpart, and 6 with a corresponding metastasis derived organoid line (Fujii et al, 2016). This study also showed that tumour organoids recapitulated the histological features of their original tumour, and these features were importantly retained upon xenograft transplantation into the renal capsule of immunodeficient mice.

CRISPR/Cas9 technology has also been developed recently to allow specific genomic editing, whereby multiple RNA guide sequences are encoded into a single CRISPR (clustered regularly interspaced short palindromic repeat) array to enable editing of specific sites in the mammalian genome, with application to both murine models and in-vitro cell lines possible (Jinek et al, 2012; Hsu et al, 2014). CRISPR/Cas9 genome editing involves cell transfection with the Cas9 protein along with a guide RNA sequence to enable Cas9 nuclease localisation to a specific DNA sequence of interest. DSBs (double strand break) then occur in the DNA sequence of interest, with gene knockout or modification occurring due

to the error prone NHEJ (non-homologous end joining) repair process, or through HR (homologous repair) if a suitable template is provided. Following isolation of human intestinal stem cells as 3D organoids, CRISPR/Cas9 technology has been applied to engineer organoids which harbour mutations of interest, specifically APC, KRAS, Trp53 and SMAD4, with mutant organoids subsequently selected out by withdrawal of growth factors from cultured human intestinal stem cells (Drost et al, 2015). Upon subcutaneous flank xenograft transplantation in NOD Scid mice, tumours with features of invasive carcinoma were established. Matano and colleagues described a similar strategy, whereby CRISPR/Cas9 technology was used to introduce mutations in APC, KRAS, Trp53, SMAD4 and PIK3CA into human intestinal stem cells, which developed into organoids in-vitro independently of niche factors (Matano et al, 2015). Upon transplantation into the renal sub-capsule of NOD Scid mice, quadruple and quintuple mutant organoids developed tumours histologically representative of low-grade adenocarcinoma. Interestingly, upon splenic injection quadruple and quintuple mutant organoids developed only micro-metastatic lesions to the liver, whereas human adenoma derived organoids developed macroscopic liver metastasis upon splenic injection, suggesting that driver pathway mutations facilitate stem cell maintenance in the tumour microenvironment, with additional mutations being required for invasive behaviour.

The development of organoid lines which grow independently of stem cell niche factors, allows the growth of organoids at foreign sites lacking such factors, enabling the establishment of heterotopic xenograft transplant models. The models described efficiently recapitulate primary invasive tumours at their implantation site, however, failure to spontaneously metastasise likely relates to the lack of native microenvironment. Subsequent studies have utilised CRISPR/Cas9 editing of human derived intestinal stem cells, to establish quadruple mutant organoids (APC, KRAS, p53, SMAD4), which then reliably develop tumours which recapitulate well differentiated adenocarcinoma upon orthotopic injection at the caecal submucosa (Fumigalli et al, 2017; Fumigalli et al, 2018). Interestingly, quadruple mutant organoid transplantation yielded distant metastases at the liver in 44% (4/9), with distant spread rarely observed following transplantation of triple mutant organoids, indicating that disruption

of the Wnt, EGFR, p53 and TGF-β/BMP (Bone Morphogenetic Protein) signalling pathways are required for metastasis.

The differences in tumour growth and metastatic potential according to injection site were also demonstrated by de Sousa e Melo and colleagues, when murine small intestinal stem cell derived organoids carrying mutations in *Apc*, *Kras*, *Trp53* and *Smad4* were injected orthotopically at the distal colonic submucosa following rectal prolapse. Transplantation at the orthotopic site yielded progressive tumour growth and liver metastasis, whereas subcutaneous transplantation failed to demonstrate metastases (de Sousa e Melo et al, 2017). Interestingly, through *Lgr5*+ CSC ablation, this study showed that primary tumours are maintained by a proliferative *Lgr5*- CSC pool, however, *Lgr5*+ CSCs were essential for the formation and maintenance of liver metastasis. The application of the majority of described transplant models to date are limited by the use of immunocompromised mice, with the tumour micro-environment and host immune system failing to recapitulate the human condition. It is imperative that pre-clinical treatment studies are performed in the setting of an intact immune system if results are to be applied reliably to clinical studies.

Subsequently, orthotopic organoid transplant models in immunocompetent hosts have been described which recapitulate the entire adenoma-carcinoma-metastasis sequence. O'Rourke et al describe the establishment of *Apc*, *Kras*, *Trp53* mutant murine derived organoids through isolation of colonic stem cells from *LSL-Kras*$^{G12D/+}$/*p53*$^{fl/fl}$ mice in a C57Bl/6 immunocompetent background, followed by in-vitro induction of biallelic *Apc* mutation through CRISPR/Cas9 mediated editing (O'Rourke et al, 2017). C57Bl/6 syngeneic mice were then engrafted by enema pipette injection of organoids following colitis induction with 3% DSS; 62% engraftment was achieved following injection of *Apc*, *Kras*, *Trp53* mutant 3D organoids. In this model, adenocarcinoma was observed at 6 weeks, local dissemination at 11-12 weeks, and metastasis was also observed in a small number at >20 weeks (1/6). Similar mutant 3D organoids were established through infecting *Apc*$^{fl/fl}$;*Kras*$^{LSL-G12D/+}$;*p53*$^{fl/fl}$ murine colon organoids with adenoviral Cre (Ad5CMV::Cre), followed by selection in media lacking nutlin-3 and Wnt pathway agonists to generate 'AKP' tumour organoids. 'AKP' tumour organoids were then transplanted into the distal colonic submucosa through colonoscopy guided needle injection (Roper et al, 2017). In C57Bl/6

immunocompetent host recipients, a 95% engraftment rate was seen with tumours recapitulating invasive carcinomas with desmoplastic stromal reaction. Interestingly, distant metastasis was not observed in C57Bl/6 mice, however, liver metastasis was demonstrated in 33% when 'AKP' organoids were orthotopically injected in immunodeficient NOD Scid mice.

1.4.5 Orthotopic Modelling Techniques in Rectal Cancer

Colonoscopy guided submucosal injection is a technique which was first described by Zigmond and colleagues, who demonstrated 100% successful engraftment when the murine MC38 CRC cell line was injected into C57Bl/6 mice (Zigmond et al, 2011). Furthermore, the transduction of two distinct fluorescent reporter genes into the MC38 cell line, also highlighted the potential to monitor tumour burden through imaging. Injection of cell and organoid lines under colonoscopy guidance, represents an easily reproducible and high throughput method of orthotopic tumour implantation into the submucosal layer. Furthermore, this method of tumour transplantation avoids surgical intervention with animals requiring only a short general anaesthetic of 5-10 minutes. A significant limitation is that cells or organoids must be injected into the submucosal layer, so tumours do not originate from the mucosa in the manner observed in human carcinoma. Furthermore, potential exists for tumour seeding into the peritoneal cavity at the time of injection. Colonoscopy guided needle injection enables orthotopic transplant at the murine colon within the limits of a rigid veterinary endoscope, and so this technique has potential application for pre-clinical modelling of LARC.

Orthotopic injection at the rectal submucosa has been described through co-implantation of mouse tumour organoids and mouse colon fibroblasts in C57Bl/6 immunocompetent mice, following rectal mucosal prolapse with haemostats (Kasashima et al, 2021). Interestingly, Kasashima et al also describe co-implantation at the caecal subserosa following laparotomy; following rectal implantation, mice are reported to reach clinical endpoint sooner (4-5 weeks) when compared with caecal implantation (5-8 weeks), with this observation being the result of intraluminal growth of rectal tumours resulting in intestinal obstruction.

Several models of rectal cancer have been described whereby mucosal disruption prior to enema injection enables the engraftment of tumours. Kishimoto et al describe the chemical disruption of the mucosal layer using 4% acetic acid, followed by injection of the CT-26 murine CRC cell line in nude mice (Kishimoto et al, 2013). Rectal tumours originating in the mucosal layer with 100% successful engraftment was observed, with lymph node and lung metastasis observed at 4 weeks in >90% of animals. Mucosal disruption can also be achieved with induction of colitis using 3% DSS, with the CT-26 line being infused intra-rectally following DSS treatment in BALB/c mice (Takahashi et al, 2004). Takahashi et al successfully demonstrated isolated rectal tumours in >90% of animals injected at 2-4 weeks post implantation with tumour volume increasing over time.

A recently described method of mucosal disruption which avoids colitis inducing agents, involves the use of a small-calibre brush to gently injure the rectal mucosa, prior to enema injection of mutant murine rectal tissue derived organoids (*Apc*$^{fl/fl}$*;LSL-Kras*$^{G12D/+}$*;Trp53*$^{fl/fl}$) in C57Bl/6 immunocompetent mice (Kim et al, 2022). Interestingly, Kim et al were able to generate rectal tumours originating in the mucosal layer in immunocompetent hosts which microscopically resembled adenocarcinoma invading through the muscularis propria layer. However, the authors reported a procedural mortality of 17% owing to intestinal perforation, with an engraftment rate of 58% in surviving mice. Although the overall tumour engraftment rate presented in this model is low, this simple technique has potential to be highly reproducible, with a short anaesthesia time enabling high throughput; furthermore, the technique avoids the systemic inflammation and animal distress caused by induction of colitis.

Very recently, Nicolas et al described an orthotopic immunocompetent model of rectal cancer which allows study of the effects of local irradiation (Nicolas et al, 2022). Murine tumour organoids mutant for *Apc*, *Trp53*, *Tgfbr2* and *Kras*^{G12D} (termed APTK) or containing an additional mutation in myristoylated AKT (termed APTKA), were injected by enema into the rectum following a 5-day period of colitis induction with 4% DSS (Varga et al, 2020). Interestingly, APTK organoids led to the formation of single invasive tumours in the rectum with liver metastasis in 10%, whereas APTKA tumours led to rectal tumours displaying a more striking stromal response, more aggressive phenotype and a higher rate

of liver metastasis at ~60%. The method described by Nicolas et al reported a procedural time requirement of 5-10 minutes, with highly reproducible protocols for organoid preparation, tumour implantation and monitoring described (Nicolas et al, 2022). Some limitations exist in this study, with variable transplantation efficiency of 50-80% described; DSS batch, age of mouse at transplant and organoid viability are variables which are noted to influence engraftment rates. The studies described by Nicolas et al represent a significant advance in modelling of LARC, demonstrating a reproducible and efficient model which resembles the histopathological spectrum of human rectal cancer, with the use of genetically modified organoids highlighting a potential platform to recapitulate the diverse mutational genotypes seen in clinical practice.

1.4.6 In-Vitro Organoid Models of Rectal Cancer

Heterogenous responses to neoadjuvant CRT regimens are observed in LARC, with surveillance strategies demonstrating the potential to offer high rates of rectal preservation and pelvic tumour control amongst selected patients with complete clinical response to neoadjuvant therapy (Smith et al, 2019). More sophisticated modelling might enable prediction of response to standard therapies, and 3D organoid techniques have recently emerged as a potential tool to stratify patients. Initial efforts to derive human tumour derived organoid repositories have focused on colonic cancer, with rectal cancer organoid derivation remaining an unmet need until very recently (van de Wetering et al, 2015; Fujii et al, 2016). Co-clinical trials are likely to advance precision medicine approaches, whereby parallel studies are undertaken alongside clinical trials to match treatment responses in patients with corresponding pre-clinical models, with the aim of better understanding the molecular mechanisms underpinning treatment response and developing predictive tools (Byrne et al, 2017). Reliable co-clinical trial data which might enable response prediction in individual patients, is reliant upon pre-clinical models recapitulating the histopathological and molecular characteristics of the corresponding patient tumour.

A biobank of patient derived organoids (PDOs) from metastatic, pre-treated colorectal, gastro-oesophageal and cholangiocarcinoma obtained from numerous

phase I and II clinical trials was utilised to carry out high throughput drug screening (Vlachogiannis et al, 2018). Vlachogiannis et al achieved 70% success rate in culturing patient derived organoids (n=110), which showed 96% overlap in mutational profile when compared with their corresponding tumour sample; an 88% positive predictive value, and 100% negative predictive value was achieved in forecasting response to chemotherapy or targeted agents. Similar approaches have been used in other solid malignancies, including pancreatic ductal adenocarcinoma, with Tiriac et al generating pancreatic cancer patient derived organoids which recapitulated the mutational spectrum of human disease, and with therapeutic profiles mirroring that of the corresponding patient's tumour when PDOs were treated in-vitro with the chemotherapeutic agents gemcitabine, irinotecan, paclitaxel, 5-FU and oxaliplatin (Tiriac et al, 2018).

The first report of a rectal cancer specific organoid biobank by Ganesh et al, involved the generation of 65 patient derived rectal cancer organoid cultures, from primary, metastatic and recurrent disease, through adaptation of existing strategies for 3D ex-vivo tumour culture (Sato et al, 2011; Ganesh et al, 2019). From organoid derivation attempts (n=84), a success rate of 77% was achieved, with the majority of tumour biopsies obtained using 2.8mm endoscopic forceps. The established organoid cultures were found to recapitulate the histopathological features of their corresponding tumours, with correlation in features such as mucin pooling, nuclear stratification and degree of differentiation. Similar mutational profiles were noted between patient tumour and the derived organoid line with 92% concordance in expression of relevant oncogenic mutations. When tumour derived organoid lines were treated separately with 5-FU and FOLFOX chemotherapy ex-vivo, an 86% concordance rate with the corresponding patient's response was observed. Furthermore, rectal cancer derived organoids displayed heterogeneous sensitivity to ionising radiation ex-vivo, also corresponding with the response seen clinically. An orthotopic murine model was also developed in this study; following DSS colitis induction in NSG (NOD Scid Gamma) immunodeficient mice, human tumour derived organoid lines were injected intra-luminally, and adenocarcinoma subsequently developed at 16 weeks post injection and distant metastasis at 22 weeks, albeit with lung or liver metastases only observed in two animals.

Yao et al later generated a biobank of primary rectal cancer patient derived organoids solely from treatment naïve samples, in patients undergoing a phase III clinical trial to investigate the addition of oral capecitabine with or without irinotecan to neoadjuvant CRT in LARC (Zhu et al, 2017; Yao et al, 2019). From 112 endoscopically obtained rectal tumour samples, organoid lines were successfully established in 86% with 80 lines used in treatment validation studies. Similarly to the study by Ganesh et al, organoids recapitulated the histopathological features and mutational profiles of their corresponding tumour, with marker expression such as Ki67, ß-catenin and pan-cytokeratin also correlating. When organoids were treated in-vitro with the single agent 5-FU, irinotecan or irradiation, a high degree of accuracy (84.43%), sensitivity (78.01%) and specificity (91.97%) was observed between the organoid line and the corresponding patient as determined by tumour regression grade. Both studies demonstrate the potential to obtain informative data regarding potential treatment sensitivity in a period of approximately 6 weeks, with the process involving endoscopic acquisition of rectal tumour biopsies, subsequent culture into 3D organoid lines and the performing of in-vitro treatment assays.

These important studies by Ganesh et al and Yao et al represent a significant advance, and demonstrate the feasibility of using in-vitro 3D organoid cultures derived from patient tumour samples prior to initiation of neoadjuvant therapy, to predict the clinical and histopathological response of individual patients to CRT, and thus facilitate management decisions. One limitation of the study by Ganesh et al, is that most organoids (66%) were derived from patient tumours already undergoing treatment, and so histological and molecular changes may have been initiated prior to in-vitro testing. Yao et al show that in-vitro response to one agent is highly predictive of a clinical response to combination therapy, however, it remains unclear whether it is feasible for ineffective agents in-vitro to be omitted from the combination therapy regimens administered clinically (Kolahi et al, 2020). Furthermore, a small proportion of organoids tested in-vitro did not match the observed clinical response of its corresponding tumour counterpart, highlighting that treatment predictions are not yet robust enough to apply to the clinical setting, and that further prospective validation in the context of a clinical trial would be essential if PDOs were to be considered as a predictive tool. Particularly in the setting of studying radiation responses, the

in-vitro setting differs significantly from that in human tumours; the 3D culture settings described to date lack an immune component, and it is well established that radiotherapy generates a tumour immune response through the release of tumour antigens (Demaria et al, 2015). Nonetheless, advances in 3D organoid culturing technology have enabled the development of PDO systems which hold promise as a means of predicting therapeutic responses and performing high throughput drug screening.

1.4.7 Advantages and Limitations of Current Pre-Clinical Models

Early GEMMs such as the *Apc*$^{Min/+}$ model enabled functional testing of several genes and progressed our understanding of the underlying molecular mechanisms of CRC progression. However, early transgenic models have significant limitations as multiple small intestinal adenomas typically develop rather than colonic lesions, with models also failing to recapitulate late-stage disease (Table 1.4). Technological advances such as Cre-Lox technology have enabled the development of more clinically relevant CRC models, and site-specific expression of mutations is possible with the use of tissue specific promotors. Furthermore, GEMMs with multiple CRC driver mutations can be developed in both a time- and tissue- specific manner, meaning colonic tumours with more complex mutational burdens can be generated which closely model adenocarcinoma. However, GEMMs are limited in their capacity to model distant metastasis, remain expensive, and are a challenging method to achieve adequate throughput for pre-clinical treatment studies (Table 1.6). GEMMs which specifically model rectal cancer have been limited to date; however, the successful application of local tamoxifen injection under colonoscopy guidance to induce distal colon tumours holds promise in the context of generating anatomically relevant rectal cancer models (Roper et al, 2017).

Model System	*Advantages*	*Disadvantages*
Genetically Engineered Mouse Models		
Transgenic oncogene expression	- Allows mechanistic studies into mutations of interest	- Small intestinal adenomas - Long latency - Limited ability to model late disease
Cre-Lox Recombinase systems	- Multiple mutations - Time/tissue specific - Relevant site and layer of origin	- Limited metastasis - Low throughput - Expensive - Long latency
CRISPR/Cas-9 genome editing	- Manipulation of entire genome - Time/tissue specific - Relevant site and layer of origin - Can utilise ex-vivo - Lower cost than conventional GEMMs - Capacity to reverse mutations	- Limited metastasis - Long latency - Low throughput
Transplant Models		
Surgical Transplant	- Time efficient - Recapitulate invasiveness and metastasis	- Cell lines fail to recapitulate CRC histology - Not anatomically representative - Immunocompromised mice
Colonoscopy Guided injection of organoids	- Correct location - Immunocompetent - Reproducible - Short latency - High throughput	- Fail to arise in mucosa - Low penetrance of metastatic disease
Non-Animal Models		
Patient derived organoids	- Avoids animal studies - Tissue easily obtained - Time effective - Potential predictive tool and suitable for drug screens	- Lack of host stroma and immune system - Labour intensive

Table 1.6: Advantages and Disadvantages of Pre-Clinical Modelling Techniques.

Table summarising the key advantages and disadvantages of the modelling systems described. Table adapted from Gillespie et al (2021)

Early surgical transplant models have successfully recapitulated rectal cancer, however immunocompromised mice are commonly used to enable engraftment of cell lines. Such models hold advantages as they are reproducible, time-effective, and local and distant dissemination are reported in the literature. However, commercially available immortalised human and murine cancer cell lines are used in these studies, and it is known that extensive in-vitro selection can result in aneuploidy, and variation in both gene and microRNA expression between cell-lines and their originating tumour tissue (Pastor et al, 2010).

Development of organoid systems has significantly advanced pre-clinical modelling in CRC, with the ability to genetically engineer organoid lines to mimic tumours harbouring mutational combinations of interest; tumours can be cultured from GEMMs to generate organoid lines, and organoids can be genetically modified in-vitro through CRISPR/Cas9 genome editing techniques. Early heterotopic organoid transplant models have been described; however, these models fail to recapitulate the anatomy of colonic and rectal cancer. Recently, orthotopic transplant of organoids has successfully modelled both colonic and rectal cancer in C57Bl/6 immunocompetent mice. Enema pipette injection following induction of colitis or mucosal disruption, and needle injection under visualisation by colonoscopy are techniques which have been successfully applied to develop colon and rectal cancer models. Colonoscopy guided injection is a highly promising technique, which might enable the generation of immunocompetent orthotopic rectal cancer models without disrupting the host immune microenvironment, with the additional benefit of potentially being highly reproducible with the ability to generate sufficient experimental subjects. A key aim of this thesis will be to adapt the colonoscopy guided needle injection technique to generate organoid transplant and genetically engineered mouse models of rectal cancer, to recapitulate locally advanced disease and distant metastasis.

1.5 Understanding the Response to Radiotherapy

1.5.1 Clinical Application of Radiotherapy in Cancer

It is thought that around 50% of all cancer patients would potentially benefit from radiotherapy during the course of their treatment, to treat localised

disease, palliate symptoms or for local control (Atun et al, 2015; Barton et al, 2014; Delaney et al, 2005). Radiotherapy can be given alone, or in combination with other treatment modalities such as surgery and/or chemotherapy; it can be given with curative intent, to down-stage tumours, or for palliation of symptoms. UK data suggests that 40% of all rectal cancer patients will receive radiotherapy during their treatment, with only 3% of colon cancer patients receiving this treatment (NCRAS, 2017). Radiotherapy is a component of standard of care treatment in LARC, administered as SCPRT or CRT, to down-stage tumours prior to curative surgical resection.

To optimise therapeutic benefit, the aims of radiation therapy are to maximise the radiation dose to tumour tissue whilst minimising exposure to normal cells. Over the past 20 years, improvements in 3D treatment planning systems, coupled with advances in linear accelerators, have enabled the development of intensity-modulated radiotherapy (IMRT) techniques whereby the intensity of radiation beams can be matched to specific tumour contours to minimise damage to surrounding tissue (Schaue and McBride, 2015). Such technological advances have also enabled the development of stereotactic body radiation therapy (SBRT), where high precision delivery of large radiation doses in single or small numbers of fractions are administered (Blomgren et al, 1995; Lo et al, 2010). Despite advances in the delivery of radiotherapy, translating these into therapeutic benefit in the context of rectal cancer has been challenging. Fractionation regimens have not changed significantly over the past 20 years, with efforts to improve therapeutic efficacy being focused on developing various radio-sensitising agents.

Despite the potential therapeutic benefits from radiotherapy, adverse effects must be considered and minimised during treatment planning. Acute toxicity has been widely reported following pre-operative radiotherapy in rectal cancer, with wound healing, gastrointestinal, genitourinary and neurological issues commonly reported (Birgisson et al, 2005). Data from the Dutch 'total meso-rectal excision' Trial, showed that a significantly higher incidence of long-term faecal incontinence was associated with SCPRT when compared with patients undergoing surgery alone (62% v 38%; $p<0.001$) (Peeters et al, 2005). Long term data from the Swedish Trial also demonstrates a high proportion of patients without a stoma suffering from incontinence, with 49% reporting incontinence to

liquid stool, 44% reporting an inability to defer defecation, and these long-term complications are objectively shown to have a negative impact on quality of life (Bruheim K et al, 2010). Concerningly, a study of patients with cT2N0 undergoing CRT and local excision reported grade 3 or 4 complications in 43% of patients (Lynn et al, 2021).

Although clinical benefits are extensively reported in LARC following radiotherapy based neoadjuvant treatment strategies, adverse effects are experienced by a significant proportion of patients. Furthermore, many LARC patients fail to gain any clinical benefit from current radiotherapy and CRT regimens, and so early operative intervention or alternative neoadjuvant strategies would be more appropriate. Thus, it is important that a better understanding of the biological mechanisms underpinning the heterogeneous responses of tumours to radiotherapy is achieved. This might enable better prediction of treatment response, aid the development of immunomodulatory agents to prime the tumour immune microenvironment to a more responsive phenotype, and ultimately enable more individualised treatment plans to be devised in LARC.

1.5.2 Biological Mechanism of Radiotherapy Response

Radiotherapy typically utilises high-energy x-ray photons, with electrically charged particles depositing energy in the cells of tissues when passing through (Lomax et al, 2013). If radiation deposits sufficient energy, then DNA damage is induced, impairing the ability of cells to divide and proliferate (Baskar et al, 2012). When ionising radiation creates sufficient levels of clustered DNA damage, then tumour cell death can occur as a result of failure of DNA damage repair mechanisms.

Damage to cellular DNA occurs spontaneously during DNA metabolism, following exposure to physical and chemical environmental agents, and through exposure to endogenous reactive oxygen species (ROS) generated during normal cell metabolism. Ionising radiation delivered therapeutically as radiotherapy can induce oxidation of DNA bases, which leads to single-strand breaks (SSB) and double-strand breaks (DSB), resulting in genomic instability (Blanpain et al, 2011). 1Gy of conventional radiotherapy is thought to cause approximately 1 x

10^5 ionisation events per cell, resulting in 1000-2000 SSBs and 40 DSBs (Lewanski and Gullick, 2001). The most lethal DNA damaging lesion is the DSB, which represents a break in the phosphodiester backbone of both DNA strands, and is more likely to result in mutation and/or cell death. The effectiveness of radiation damage in killing cells is explained by linear energy transfer (LET), with high LET radiation resulting in a higher concentration of ionisation events and more complex DNA damage sites (Lomax et al, 2013). The majority of DSBs induced by low LET radiation are repaired within 30-60 minutes, however, as LET increases, so too does the complexity of the DSBs. If DNA damage is not sufficiently repaired, cell death can result through the generation of lethal chromosomal aberrations or direct induction of apoptosis. Furthermore, inaccurate repair of DSBs can lead to mutations in surviving cells, resulting in genomic instability and malignant cell transformation.

The success of conventional radiotherapy is classically thought of in terms of the '4Rs of Radiobiology', originally described by Withers (Withers, 1975). The outcome of radiotherapy is determined by the repair of DNA damage, repopulation of cells, redistribution of cells in the cell cycle, and the reoxygenation of hypoxic tumour areas.

Tumour cell death following ionising radiation is dependent upon irrepairable DNA damage being induced in the form of DSBs. However, many cells undergo sublethal DNA damage which is repaired through numerous DNA damage response (DDR) mechanisms (Pajonk et al, 2010). Fractionated radiotherapy is thought to allow the repair of sublethal DNA damage in slowly proliferating normal tissues, at the expense of tumours which might be less able to repair DNA damage. However, variation in the ability to repair DNA damage exists between tumour types and between tumours cells within the same tumour. Furthermore, the efficacy of radiotherapy is affected by the extent of DNA damage and the resulting DDR, as well as being influenced by various cancer associated mutations which impact upon DNA repair and the cell cycle.

Redistribution refers to the differences in radiosensitivity shown by cells during different phases of the cell cycle, whereby cells undergoing mitosis are most sensitive to DNA damaging stimuli with late S-phase being the most resistant phase (Pawlik and Keyomarski, 2004). Fractionated radiotherapy exploits cell cycle progression, as radio-resistant tumour cells in S-phase can move into a

more sensitive phase of the cell cycle between fractions, with more slowly cycling normal cells being more likely to survive repeated fractions. Therefore, the therapeutic efficacy of fractionated radiotherapy is dependent upon tumour tissue having a high proportion of rapidly cycling cells as opposed to slowly cycling CSCs, and normal tissue exhibiting a relatively smaller content of rapidly cycling cells. The role of chemotherapeutic agents in conjunction with radiotherapy can exploit the variation in radiosensitivity seen in different cell cycle phases. For instance, 5-FU is known to kill relatively radio-resistant S-phase cells as well as increasing the radiation sensitivity of cells which inappropriately progress through S-phase in the presence of drug (Lawrence et al, 2003). Radiation in combination with chemotherapeutic agents is utilised to exploit the cell cycle and checkpoints to enable synergistic tumoricidal effects.

Repopulation of tumours is considered a potential reason for failure of radiotherapy (Wang et al, 2019; Song et al, 2019). It is hypothesised that following radiotherapy depopulation of lineage committed cells occurs, and that subsequently surviving stem cells switch from asymmetric cell division which gives rise to a daughter stem cell and lineage-committed progenitor cell, to a symmetric form of cell division which produces two proliferative stem cells. In tumours, this phenomenon results in accelerated regrowth, whereby tumour regrowth after sublethal treatment exceeds the growth rate of untreated tumour tissue.

Tumour oxygenation is known to be a significant modifier of radiation sensitivity, with hypoxic cells thought to be more resistant to radiation (Gray et al, 1955; Bristow and Hill, 2008). Under hypoxic conditions, relatively decreased fixation of DNA DSBs occurs following exposure to free radicals induced by ionising radiation, with radiation sensitivity being reliant upon adequate oxygenation (Zhang et al, 1995). Fractionated radiotherapy partly overcomes this, with radio-resistant hypoxic cells potentially being reoxygenated between individual dose fractions, and the addition of pharmacological strategies to improve tumour oxygenation potentially improves radiosensitivity (Overgaard, 2007).

Subsequently, the 4Rs of radiobiology have been updated to include intrinsic radiosensitivity, with evidence that cells from different tumour types differ significantly in their inherent radiosensitivity (Steel et al, 1989). The differential radiosensitivity between different cancer cell lines has been extensively shown

in pre-clinical studies, with prediction of sensitivity demonstrated through gene expression profiling (Torres-Roca et al, 2005). However, in the context of rectal cancer surgery, predicting treatment response based on genomic profiling has not been possible to date. In order to fully exploit the therapeutic benefits of radiotherapy, improved understanding of how radiation influences both the cancer cell and the tumour microenvironment are required, with application of insights from translational studies required to improve treatment delivery and to exploit radio-sensitising agents (Harrington et al, 2007).

1.5.3 The DNA Damage Response

DNA damage threatens the ability of eukaryotes to transmit genetic information, and as a result cells have well developed DDR mechanisms to repair DNA and maintain genomic integrity. The DDR involves the activation of numerous complex signal transduction pathways, which modulate gene activity and control the multitude of cell responses to DNA damage through initiation of cell-cycle arrest, DNA repair mechanisms and apoptotic pathways (Ciccia and Elledge, 2010).

The DNA damage response (DDR) involves a complex signal transduction pathway to detect and repair DNA damage, and consists of sensors, transducers and effectors (Zhou and Elledge, 2000). Following radiation-induced DNA DSBs, the MRN 'sensor' complex (a trimer of MRE11-RAD50-NBS1 molecules) binds to the site of DNA damage recruiting the protein kinase ataxia telangiectasia mutated (ATM) protein. ATM acts as a 'transducer' by activating the DNA damage checkpoint signalling cascade, and controlling the phosphorylation of 'effector' proteins including checkpoint kinase 1 and 2 (CHK1 and CHK2) (Bakkenist and Kastan, 2003).

The effector responses which can result from this signalling cascade are cell growth arrest coupled with DNA damage repair and cell survival, or apoptosis to induce death in cells with irreparable DNA damage. Activation of ATM and CHK1/CHK2 ultimately leads to phosphorylation and activation of the tumour suppressor p53 protein, inducing its nuclear accumulation and upregulation of p53 target genes, which in turn mediate transient cell cycle arrest to allow time

for DNA damage repair or facilitate apoptosis in response to irreparable DNA damage (Fei and El-Deiry, 2003).

DDR mechanisms protect cells from the harmful effects of DSBs, with two main pathways mediating the repair of DSBs in mammalian cells, depending on the cell cycle status of the damaged cell: during the G0/G1 phase, DSBs are repaired by non-homologous end joining (NHEJ), while cells in the S-G2/M phase undergo homologous recombination (HR) (Khanna and Jackson, 2001; Willers et al, 2004). HR requires an undamaged template molecule with a homologous DNA sequence, and is an error-free DNA repair mechanism. During HR, the RAD52 protein binds to the DNA double-strand ends, which are then resected by nucleases in the 5' to 3' direction, with the resulting 3' single-stranded tails then invading the DNA double helix of a homologous, undamaged partner molecule; repair of the damaged region is then achieved through the action of DNA polymerase copying information and using the undamaged molecule as a template, with this process yielding two identical DNA molecules.

NHEJ involves the joining of two double stranded DNA ends without the requirement for an undamaged partner and is a more error prone process, due to the excision of damaged nucleotides at the DSB ends causing sequence alterations (Karran et al, 2000). The process involves a heterodimer of the Ku70 and Ku80 proteins binding to the DNA ends, which activates the catalytic subunit of DNA dependent protein kinase by stabilising its interaction with DNA ends. Re-joining then occurs through DNA ligase IV and XRCC4 (x-ray cross-complementing 4). NHEJ can introduce small sequence deletions, insertions, nucleotide changes, or chromosomal translocations due to the lack of an intact template, meaning this process is prone to error.

HR is the only mechanism of DNA repair which can restore the DNA sequence at the DSB site without error. The DNA repair mechanism employed by cells is dependent upon the type of DNA lesion induced, with radiation typically causing SSBs, DSBs and base damage (Jackson and Bartek, 2009). Complex DSBs induced by radiotherapy are often more reliant upon simple mechanisms such as alternative end-joining (alt-EJ) or single strand annealing (SSA), which restore genomic integrity but not sequence (Mladenov et al, 2016).

Rapid phosphorylation of histone H2AX (γ-H2AX) occurs in response to DNA DSBs and is thought to recruit repair enzymes involved in the repair processes (Olive and Banáth, 2004). Pre-clinical studies measuring γ-H2AX intensity in cultured cell lines, tumour xenografts and normal tissues, have shown that disappearance of γ-H2AX following irradiation is faster in radio-resistant cells tumour cells, representing a potential indicator of radio-sensitivity. A recent clinical study used primary peripheral blood lymphocytes from rectal cancer patients to study differences in DNA damage repair response capacity, with data showing that patients with poor responses to neo-adjuvant chemoradiotherapy had lower levels of γ-H2AX than complete responders (Arora et al, 2019). This data suggests that γH2AX and other DNA damage repair response markers may form the basis for predictive biomarkers.

1.5.4 The Effects of Radiotherapy on the Tumour Microenvironment

Previously the therapeutic efficacy of radiotherapy has focused on DNA damage induction and direct cytotoxic effects, however, it has become increasingly recognised that ionising radiation affects numerous cell types within the tumour microenvironment (TME). Although knowledge of the immunomodulatory effects of radiotherapy has improved, the effects on the tumour microenvironment remain incompletely understood. Radiotherapy can induce anti-tumour immune responses, and immunotherapy agents have the potential to enhance the therapeutic efficacy of irradiation (Weichselbaum et al, 2017; Colton et al, 2020). In contrast, profoundly immunosuppressive TMEs pose a greater clinical challenge, with RT potentially enhancing immunosuppression.

Irradiation triggers pro-inflammatory cytokine signalling such as IL-1β and TNF-α, and recruitment of immune cells through the intracellular actions of ROS (Lim et al, 2016). The resulting cellular stress generates damage-associated molecular patterns (DAMPs), or so called ‘eat me’ signals which stimulate an immune response (Schaue and McBride, 2010). DAMPs include those exposed on the surface of cells (i.e. calreticulin), which are recognised by dendritic cells (DCs) which promote phagocytosis. Other DAMPs are passively released (i.e. high-mobility-group box 1 (HMGB1) proteins), which enables DCs to process and cross present antigens through toll like receptor (TLR) 4 signalling. Following

radiotherapy, DAMP mediated responses lead to immunogenic cell death of cancer cells, resulting in an immune-stimulatory tumour micro-environment whereby activation and maturation of dendritic cells into effective antigen presenting cells occurs leading to the induction of effective T-cell mediated responses (Barker et al, 2015; Krysko et al, 2012; Kroemer et al, 2013).

Tumour antigen specific T-cell immunity following irradiation has been demonstrated in both in-vitro and in-vivo experiments as a result of interactions between HMBG1 released by dying tumour cells (a ‘danger’ signal) and toll-like receptor 4 (TLR4) expressed by DCs. Both TLR4 expression and the release of HMGB1 are essential for the efficient presentation of tumour antigens following radiation induced cell death (Apetoh et al, 2007). However, an effective immune response will only ensue when both 'eat me' and 'danger' signals are released by dying tumour cells then processed by dendritic cells. Calreticulin which is exposed on the surface of dying tumour cells, undergoes rapid translocation to the cell surface after exposure to DNA damaging agents (Obeid et al, 2007). Calreticulin is exclusively expressed on the surface of cells undergoing immunogenic cell death, with Obeid et al demonstrating that blockade or genetic knockdown of calreticulin in a CT26 murine flank xenograft model, suppressed the phagocytosis of tumour cells and that dendritic cells require this signal to stimulate immunogenicity. In addition, adenosine-5’-triphosphate (ATP) release from dying tumour cells acts on the purinergic P2RX7 receptor present on DCs, triggering the activation and secretion of pro-inflammatory cytokines, and subsequently priming interferon-γ (IFN-γ) producing CD8+ T-cells (Ma et al, 2010).

DCs cells are an important determinant of effector T-cell function following radiotherapy, as they act as APCs, in turn priming naïve T-cells into CD8+ cytotoxic T-cells with anti-tumour activity. Once mature, DCs migrate to tumour draining lymph nodes where naïve T-cells are primed to an effector phenotype (Lee et al, 2009; Takeshima et al, 2010; Gupta et al, 2012). Gupta et al demonstrated that following single fraction local irradiation (10Gy) in several murine xenograft tumour models, that DCs and CD8+ T cells are crucial to tumour response, whereas CD4+ T cells and macrophages are dispensable. In this study, DCs showed increased expression of the T-cell priming co-stimulatory molecules CD70 and CD86 at 2 days post irradiation, with increased CD8+ T-cells

seen in the tumour after 7 days. This demonstrated that radiotherapy initiates an inflammatory process which activates local dendritic cells, leading to the recruitment and activation of tumour specific CD8+ T-cells. Other pre-clinical studies support the observation that tumour response to radiotherapy is dependent upon effector T-cell and CD8+ lymphocyte responses (Lugade et al, 2005; Lee et al, 2009). Interestingly, Lugade et al show that favourable increases in tumour CD8+ T-cells are greater following a single 15Gy dose when compared with a 5 x 3Gy fractionated regimen. As well as its effects on priming cytotoxic T-cells, radiotherapy has also been shown to enhance infiltration of NK cells into tumour tissue which then exert cytotoxic effects (Ni et al, 2012).

Many immune suppressive mechanisms exist within the tumour microenvironment, which inhibit the anti-tumour activity of immune cells. Decreased immune activation is seen through inhibition of tumour-infiltrating lymphocytes (TILs), decreased antigen presenting capability of dendritic cells (DCs), upregulation of immune checkpoints, and through down regulation of recognition signals such as MHC (Munn and Bronte, 2016). Furthermore, increased Treg, tumour promoting M2 tumour associated macrophages (TAMs) and myeloid-derived suppressor cell (MDSC) activity are known to contribute to an immune suppressive tumour milieu (Gajewski et al, 2013).

As well as having immune-stimulatory effects, radiotherapy can induce immunosuppressive changes within the tumour microenvironment. Numerous changes in MDSCs are observed following radiotherapy, including effects on myeloid cell recruitment and removal, reorganisation of macrophages within tumours, repolarisation of TAMs to the M2 tumour promoting phenotype and re-presentation of tumour antigens (Vatner and Formenti, 2015). Pre-clinical evidence exists to show that radiotherapy results in the recruitment of bone marrow-derived CD11b+ myeloid cells, which express pro-angiogenic and chemoattractant molecules, resulting in restoration of tumour vasculature which stimulates tumour growth (Ahn et al, 2010). Upon CD11b+ antibody depletion, Ahn et al showed that radiation induced recruitment of myeloid cells was suppressed with a resulting inhibition of tumour regrowth. Further evidence shows that immunosuppressive CD11b+ myeloid cells are susceptible to killing by primed antigen-specific CTLs following radiotherapy (Wu et al, 2014). In a murine tumour model of prostate cancer, Xu et al show an increase in TAMs and

MDSCs at 7 days following 5 x 3Gy radiotherapy on consecutive days which correlated with increased serum concentration of colony stimulating factor 1 (CSF-1), a macrophage chemokine and growth factor (Xu et al, 2013). CSF-1 blockade prevented radiotherapy induced myeloid cell recruitment, highlighting a potential role of CSF1/CSF1R signalling in the recruitment of TAMs which limit the efficacy of radiotherapy.

Tregs suppress immunity through several distinct mechanisms, and have a role in inhibiting the early proliferation of naïve T-cells, as well as suppressing the effector functions of activated T-cells (von Boehmer, 2005). Furthermore, they maintain peripheral immune tolerance with immune inhibitory effects regulated by the local secretion of cytokines including TGF-ß and interleukins; expression of the TGF-ß receptor by CD8+ T-cells has been shown to be required for Tregs to exert an inhibitory effect, suggesting a specific role for TGF-ß signalling in the inhibition of immune-mediated cytotoxicity (Chen et al, 2005). Pre-clinical evidence shows that exposure to ionising radiation leads to the upregulation of MHC II expression on Langerhan's cells, which cause expansion of Treg cells upon migration to draining lymph nodes in a murine melanoma model (Price et al, 2015). Immediately following radiotherapy, Treg populations are thought to increase relative to other T-cells within the TME as they are more radioresistant that other lymphocytes (Kachikwu et al, 2011). Kachikwu et al were able to show that targeting Tregs in combination with radiotherapy, with anti-CD25 monoclonal antibody, led to increased tumour growth delay in a murine prostate cancer model.

It is evident that radiotherapy can have both immune-stimulatory and immune-suppressive effects, and understanding the heterogenous responses to radiotherapy is complex. Undoubtedly, the contexture of the TME determines the nature and extent of responses. However, response will also be influenced by dose, scheduling and fractionation, as well as the systemic response induced. In a T-cell rich TME, radiotherapy might drive the expansion and activation of T-cells with resulting upregulation of PD-L1 making tumours amenable to immune checkpoint inhibition. In contrast, a myeloid rich TME may be further expanded by radiotherapy and so immunotherapy agents which target myeloid cells or enhance T-cell priming may be beneficial. It is clear that immunotherapy agents can enhance the effects of radiotherapy, however, the heterogenous nature of

the TME and response to irradiation signify that agents which effect both the myeloid and lymphoid compartments require further study and investigation.

1.5.5 The Efficacy of Fractionated and Single Fraction Radiotherapy

Pre-clinical studies show that both single fraction high dose radiotherapy and low dose fractionated regimens can effectively transform the tumour microenvironment (Filatenkov et al, 2015; Arnold et al, 2018). In mice bearing subcutaneous murine CT26 colorectal tumours treated with single fraction irradiation (30Gy), Filatenkov et al demonstrated durable tumour remission, along with intense tumour infiltration by CD8+ T cells and reduced MDSCs, with peak cytotoxic T-cell infiltrate observed at 6 days post irradiation. These microenvironment changes were dependent upon antigen cross-presenting CD8+ DCs and IFN-γ secretion. Durable tumour remission and favourable CD8+ T cell tumour infiltrate were not observed when mice were treated with a 10 x 3Gy fractionated regimen, suggesting that repeat doses may adversely affect anti-tumour immune responses.

In contrast, other studies show that low dose fractionated radiotherapy (5 x 2Gy) results in T-cell infiltration at the irradiated site in subcutaneous CT26 colorectal tumour bearing mice (Dovedi et al, 2017). Dovedi et al show a decrease in infiltrating CD8+ T-cells at days 1 and 3 post radiotherapy, with an increase in tumour CD8+ T-cells occurring at day 7 when compared with non-irradiated controls. Furthermore, data demonstrated that tumour resident T-cells mediated local tumour control in a small proportion of mice (18.8%). Interestingly, similar rates of tumour regression were seen when a single 7Gy fraction was compared with a 3 x 4Gy fractionated regimen. Another study, using both subcutaneous breast and colorectal tumour models, showed comparable primary tumour growth delay when animals were treated with fractionated (3 x 8Gy or 5 x 6Gy) and single dose (20Gy) radiotherapy (Dewan et al, 2009). Comparison of single dose versus fractionated radiotherapy in an immunocompetent melanoma model, showed that tumour control improved with escalating single dose, however, optimal control and tumour immunity was achieved with fractionated radiation doses of 7.5Gy/fraction as measured by IFN-γ producing T-cells (Schaue et al, 2012).

Pre-clinical evidence from another prostate cancer model suggested that high dose single fraction radiotherapy (25Gy) and fractionated radiotherapy (15 x 4Gy) induces the TAM M2 phenotype associated genes ARG-1 and COX2, supported the repolarisation of macrophages to a pro-tumorigenic phenotype (Tsai et al, 2007). In contrast, low doses of irradiation (0.5 – 2Gy) in a human melanoma xenograft model resulted in repolarisation towards the M1 phenotype with increased production of iNOS, which facilitated improved tumour control through lymphocyte recruitment to tumours (Klug et al, 2013).

Fractionated dosing schedules affect tumours differently to single high dose treatments as shown in the discussed studies. Cell line studies comparing high dose and fractionated radiotherapy show significant differences in gene response depending on how radiation is delivered, with IFN-γ and TGF-ß associated genes being more robustly induced after fractionated radiotherapy (Tsai et al, 2007). Interestingly, gene expression profiles differed when cell lines were implanted in-vivo suggesting that the tumour micro-environment plays a crucial role in tumour responses, and it remains unclear how the tumour-host relationship is influenced by dose and scheduling.

1.5.6 Radiotherapy - Immunotherapy Combinations in Pre-Clinical Models

Interest in combining radiotherapy with immune-checkpoint inhibition to prime the immune system and optimise systemic anti-tumour immunity has developed both in pre-clinical models and the treatment of several solid cancers. Early pre-clinical findings demonstrated survival benefit with the addition of CTLA-4 inhibition to radiotherapy (12Gy as single or two fractions) in the subcutaneous 4T1 mammary cancer transplant model, in addition to delayed primary tumour growth and decreased lung metastasis being observed, with anti-metastatic effects being CD8+ T-cell dependent (Demaria et al, 2005). In both the TSA murine breast carcinoma and MC38 colon cancer bilateral subcutaneous injection models, treatment with single dose (20Gy) or fractionated radiotherapy in combination with CTLA-4 inhibition, led to enhanced primary tumour response in all radiotherapy regimens (Dewan et al, 2009). However, when combination therapy with CTLA-4 inhibition was studied, only animals treated with fractionated radiotherapy and CTLA-4 inhibition demonstrated a significant

growth inhibition in the tumour outside the radiotherapy field, with response being proportional to the frequency of CD8+ T-cells showing tumour specific IFN-γ production.

As well as inducing infiltration of tumour antigen specific T-cells, radiotherapy can also induce PD-L1 expression in the tumour microenvironment which suppresses immunity. In both the MC38 CRC and TUBO mammary cancer subcutaneous flank injection models, PD-L1 expression in tumour cells and DCs was found to be increased at 3 days post 12Gy single fraction radiotherapy, with tumour control subsequently being achieved when PD-L1 blockade was administered in combination with radiotherapy (Deng et al, 2014). A later pre-clinical study in both B16-OVA melanoma and RENCA renal cell carcinoma bilateral subcutaneous hindlimb transplant models, showed that a single 15Gy stereotactic radiotherapy dose induced anti-tumour immunity with out-of-field abscopal effects being restricted by PD-1 expression (Park et al, 2015). PD-1 knockout mice treated with radiotherapy showed improved survival and significantly increased reduction in growth of both the irradiated and non-irradiated secondary tumour, when compared with PD-1 wild-type mice. Treatment with radiotherapy and PD-1 blockade recapitulated the survival benefit, tumour regression and abscopal effects seen in PD-1 knockout mice, highlighting the potential for PD-1 blockade to synergise with radiotherapy to induce tumour specific CD8+ T-cell responses. In the B16 melanoma subcutaneous flank injection model expressing the ovalbumin (OVA) peptide, single dose 12Gy radiotherapy resulted in increased antigen specific T-cells and an increased proportion of CD25+ Treg cells, with the addition of PD-1 inhibition improving local tumour control, increasing the proportion of tumour specific CD8+ T-cells with memory phenotype and abrogating the increase in Tregs seen (Sharabi et al, 2015).

Radiotherapy has a role in upregulating tumour cell PD-L1 expression to drive treatment resistance in the context of low-dose fractionated RT. In the CT26 subcutaneous flank injection model of CRC, treatment with 5 x 2Gy fractionated radiotherapy resulted in increased expression of PD-L1 at days 1, 3 and 5 post last irradiation dose, further highlighting the PD-1/PD-L1 axis as a resistance mechanism (Dovedi et al, 2014). Using co-culture of CD8+ T-cells with CT26 tumour cells, Dovedi et al demonstrated that PD-L1 up-regulation was

dependent upon IFN-γ secreting CD8+ T-cells. Fractionated radiotherapy combined with PD-1/PD-L1 blockade led to significant reduction in tumour volume and survival extension when compared with fractionated RT alone. Furthermore, combined therapy was associated with induction of a tumour antigen-specific memory immune response, with mice able to completely reject tumours upon subsequent contralateral re-challenge. Dovedi et al later studied radiotherapy in the CT26 bilateral subcutaneous injection model of CRC, showing that neither ablative (10Gy single dose) nor fractionated radiotherapy (5 x 2Gy) was sufficient to induce out-of-field tumour responses (Dovedi et al, 2017). However, addition of PD-1 inhibition to fractionated radiotherapy led to complete regression of both irradiated and out-of-field tumours in >70% of mice. Addition of FTY-720 (a sphingosine 1-phosphate receptor agonist) which prohibits T-cell emigration from lymphoid tissue to combined radiotherapy/PD-1 inhibition, revealed a reduced therapeutic response highlighting that both tumour resident and tumour infiltrating T-cells are required for maximum local and systemic response.

TGF-β inhibition in combination with fractionated RT has also been assessed in the pre-clinical setting (Vanpouille-Box et al, 2015). In the 4T1 metastatic breast cancer bilateral subcutaneous transplant model, combination therapy with fractionated RT (5 x 6Gy) and TGF-β inhibition led to reduced primary tumour burden, with a reduction in lung metastasis and the non-irradiated tumour also seen. This effect was not seen following monotherapy, with the reduction of 'out of field' lesions suggesting systemic priming of tumour antigen specific T-cells. Combination therapy was associated with increased CD4+ and CD8+ T cell density, up regulation of IFN-γ signalling, and increased production of the chemokines and cytokines associated with CTL recruitment.

In a CT26 CRC heterotopic subcutaneous flank injection model of CRC, fractionated RT (5 x 5Gy or 15 x 2Gy) in combination with 5-FU and TGF-β inhibition with Galunisertib (small molecule inhibitor of ALK5), resulted in delayed tumour growth and improved survival compared with CRT alone (Gunderson et al, 2018). Improved clinical efficacy was dependent upon increased tumour infiltration of CD8+ T cells. CD8α specific deletion of TGFBR1 was found to enhance the expression of the chemokine CXCR3 on CD8+ T cells, resulting in increased CXCR3 dependent CD8+ T cell migration into tumours.

TGF-β was therefore proposed as an immunosuppressive mechanism through down-regulation of CD8+ T-cell expression of CXCR3, limiting the trafficking of CD8+ T-cells into the tumour. In another CT26 subcutaneous flank injection model of CRC, TGF-β inhibition was found to increase CD3+ and CD8+ T-cell density, while decreasing FOXP3+ T reg density in the tumour micro-environment (Young et al, 2014). Young et al demonstrated that TGF-β inhibition followed by a single 20Gy fraction, resulted in significantly improved tumour control and survival when compared with radiotherapy alone. Increased CD8+ T-cells were found to have a significant role in the therapeutic effects of TGF-β in combination with radiotherapy, with improved tumour control and survival being abrogated when combination therapy was administered in CD8+ depleted animals.

Although numerous pre-clinical studies have shown promising results with both single dose and fractionated radiotherapy regimens in combination with immune checkpoint blockade or TGF-β inhibition, numerous drawbacks exist with studies to date. The studies described utilise heterotopic models, which fail to recapitulate the anatomical location of colorectal cancer, whereby the subcutaneous tissue plane represents a different host microenvironment. Furthermore, irradiation methods typically do not deliver precise radiotherapy to the tumour alone, with whole body irradiators and shielding devices commonly utilised. Lastly, it remains unclear which radiotherapy dose and fractionation regimens offer optimal treatment synergy with immunotherapy agents, and this must be a focus of research to optimise translation of findings to the clinical setting.

Several issues must be addressed if robust data is to be derived from pre-clinical treatment studies to aid the development of novel radiotherapy-immunotherapy in LARC. It is important that immunocompetent orthotopic models of LARC are developed, which recapitulate both the histological and mutational characteristics of human disease. Furthermore, more precise methods of radiotherapy delivery must be developed, to minimise damage to adjacent tissues and to more accurately represent the treatment regimens which are delivered in the clinical setting.

A recent study using the subcutaneous CT26 colon cancer model was able to accurately assess different fractionation regimens using a SARRP (Small Animal

Radiation Research Platform) device which enables targeted radiotherapy to be delivered to murine tumours through in-built CT guided treatment planning systems (Grapin et al, 2019). In immunocompetent mice, different radiotherapy regimens induced different anti-tumour effects, with fractionated regimens (3 x 8Gy; 18 x 2Gy) resulting in delayed tumour growth when compared with a single 16.4Gy fraction. All regimens led to an increase in granzyme B secreting CD8+ T-cells at 7-days post treatment initiation, with the 3 x 8Gy regimen inducing the highest proportion of effector T-cells. Increased tumour infiltrating myeloid cells and a propensity towards an M2 tumour-associated macrophage phenotype was seen at 14-days post treatment initiation in the 18 x 2Gy treatment group. Addition of anti-PD-L1 was most effective when given in combination with 18 x 2Gy (8/12 complete response), when compared with the 3 x 8Gy regimen (3/10 complete response). This study highlights the importance of optimising radiotherapy fractionation regimens in association with immune checkpoint blockade, and also shows the feasibility of administering image-guided radiotherapy in the pre-clinical setting.

1.6 Thesis Aims

Heterogeneous responses to neoadjuvant radiotherapy-based treatment regimens exist in LARC. Pre-clinical and early clinical trial data suggest a potential role for immunotherapy in combination with radiotherapy in LARC, to improve rates of clinical response to neoadjuvant treatment. Pre-clinical studies have a role in testing novel radiotherapy immunotherapy-based treatment combinations, however, models must better recapitulate the anatomical, histological and mutational features of human rectal cancer. Early in this period of research I published a review article to outline the need to improve pre-clinical models specific to LARC, and to highlight the potential value which reliable pre-clinical studies hold in identifying and testing novel treatment targets, as well as informing upon optimal fractionation regimens and treatment scheduling (Gillespie et al, 2021).

In chapter 3, I aimed to develop orthotopic rectal cancer models which recapitulate the spectrum of human disease through the entire adenoma-carcinoma sequence, as well as developing models which histologically resemble

locally advanced disease and furthermore demonstrate distant metastasis. Furthermore, I aimed to develop a model which was both reproducible and with short latency, such to enable high throughput treatment experiments.

In chapter 4, I aimed to use a novel immunocompetent orthotopic identify model of rectal cancer to refine a protocol for administering fractionated radiotherapy. I then aimed to characterise the response of a newly developed model of LARC, to show the immunological changes which occur in the tumour immune microenvironment following radiotherapy. I then aimed to identify potential resistance mechanisms which could then be targeted in pre-clinical experiments to improve the response to radiotherapy.

In chapter 5, I aimed to test novel treatment combinations by combining radiotherapy with PD-1 inhibition or with TGF-β inhibition to identify and characterise responses to treatment. I aimed to identify potential treatment combinations which might have clinical efficacy and can then be tested further in the pre-clinical setting to assess their mechanism of action and to optimise dosing, fractionation and scheduling.

Chapter 2 – Materials and Methods

2.1 In-Vivo experiments

2.1.1 Animal Housing and Husbandry

All experiments undertaken on mice were carried out at the Biological Research Unit (BRU) within the CRUK Beatson Institute. All mice were handled, housed and monitored with strict adherence to UK Home Office regulations, and in accordance with the Animals (Scientific Procedures) Act 1986. This included a strict 12-hour light/dark cycle and access to standard diet and drinking water ad libitium. Mice were used in experiments once reaching a suitable age (>6 weeks) and weight (>20g). Animals were routinely monitored (at least three times weekly) for signs of ill health, and in accordance with refined protocols as detailed in the project licence, and adhering to the principles of the NC3Rs (National Centre for the Replacement, Refinement & Reduction of Animals in Research). Animals were culled using a schedule 1 method. Experiments were performed under UK Home Office personal licence (PIL I83707846) and project licence (PPL 7009112).

2.1.2 Genetically Engineered Mouse Model Systems and In-Vivo Induction

Cre-Lox technology is used in Chapter 3, to enable temporal and spatial control of genetic alleles within tissues.

2.1.2.1 *VillinCreERT2*

VillinCreERT2 mice are described in Chapter 3, often referred to as *VillinCreER*, and express Cre-recombinase specifically in the intestinal and colonic epithelium under the control of the Villin promotor (el Marjou et al, 2004). Cre expression was induced locally at the murine rectum through submucosal injection of tamoxifen under colonoscopy guidance, to enable recombination of alleles of interest.

2.1.2.2 Preparation of Tamoxifen for *In-Vivo* induction

Tamoxifen stock (Sigma #H7904) for in-vivo induction was prepared as follows: a concentration of 20mg/ml of tamoxifen was produced by dissolving 25mg of

tamoxifen stock powder in 1250µl of 100% ethanol, then diluted again in 100% ethanol to a final stock concentration of 5mM (stored at -20°C).

Prior to in-vivo induction 5mM stock was prepared as follows: 20µl of 5mM tamoxifen was diluted in 980µl of phosphate buffered solution (PBS) to give a working concentration of 100µM. Each animal received 70µl of 100µM tamoxifen, delivered as a submucosal injection at the rectal location under colonoscopy guidance (technique detailed in section 2.1.3.1).

2.1.2.3 Genetic Alleles

In the locally inducible models described in Chapter 3, combinations of the following alleles were used:

- $Apc^{fl/fl}$ (Shibata et al, 1997)
- *Lox-Stop-Lox* $Kras^{G12D/+}$ (Jackson et al, 2001)
- $p53^{fl/fl}$ (Jonkers et al, 2001)
- $Tgfbr1^{fl/fl}$ (Larson et al, 2001)
- $Smad4^{fl/fl}$ (Yang et al, 2002).

Genotyping was performed by Transnetyx (Cordova, Tennessee).

2.1.3 Orthotopic Transplant Models

For orthotopic organoid transplant models CD1-nude mice (Charles River, UK) and C57Bl/6 mice (Charles River, UK) were used. All animals were used for experimental procedures when >6 weeks and weighing >20g.

2.1.3.1 Colonoscopy-Guided Submucosal Injection

For administration of both tamoxifen and organoid fragments to the rectal submucosa, the same colonoscopy-guided injection technique was used. Mice were anaesthetised with inhalational sevoflurane, initially in an anaesthetic induction chamber, before being transferred to a heated surgical plate with temperature maintained at 37°C. Sevoflurane anaesthetic was maintained throughout the procedure through a nose cone at 2%, with mice in the supine

position. A rectal enema was then carried out using 10-20ml PBS delivered through a rat oral gavage needle attached to 20ml syringe.

The Karl Storz TELE PACK VET X LED endoscopic video unit and Karl Storz MINI Multi-Purpose Rigid Telescope (67030BA) were used, with following specifications: 9.5Fr with 3Fr working channel, and 14cm working length. A 100µl loading syringe (Hamilton 1710 RNR 100µl Syringe (22S/51/3)) was used to draw up 70µl of suspension to be injected. This was then attached to a custom-made injection needle (Hamilton RN Needle (33G/402mm/pst.4(45°bevel)) and passed through the endoscope working channel (Figure 1, top panel). The injection needle was then advanced under direct vision into the submucosal layer, at a distance of <1cm proximal to the anal verge, and the 70µl injection volume expelled to raise a submucosal bubble (Figure 1, bottom panel). Previous studies have regarded the distal-most 10mm of the murine colorectum to be classified as rectal (Siri et al, 2019) Animals were then monitored closely post procedure to ensure recovery from anaesthetic, and kept at 37°C in a warming cabinet for ~30 minutes. A health assessment including weight was performed daily for 7-days following the procedure.

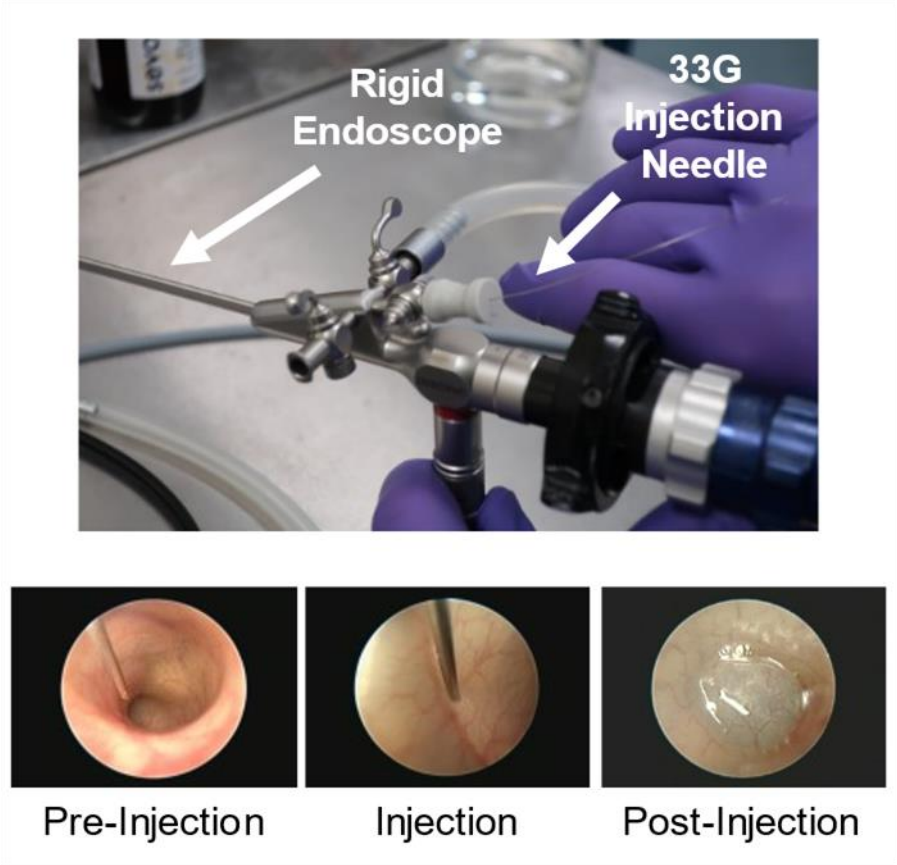

Figure 2.1: Colonoscopy-Guided Submucosal Injection Technique

Top – Diagram demonstrating set-up of rigid endoscope with injection needle. Bottom – Images to demonstrate appearance of rectal submucosa immediately prior (left), during (middle) and post (right) injection of organoid fragment suspension using 33G injection needle.

2.1.4 *In-Vivo* Drug Treatments

Alk5 inhibitor (AZ12601011) was stored as a powder at room temperature prior to preparation, and was made fresh on a weekly basis for use during experiments. During formulation, 0.5% hydroxypropyl methycellulose (HPMC) / 0.1% Tween was added to give a concentration of 12.5mg/ml. The drug was dissolved with a stirrer and kept at room temperature. Animals were treated with 50mg/kg twice daily by oral gavage. Vehicle treated animals were treated with 0.5% HPMC / 0.1% Tween given at 100µl twice daily by oral gavage.

Ultra-LEAFTM Purified anti-mouse CD279 clone RMP1-14 (Biolegend #114122) was used as PD-1 inhibitor. During formulation, the drug was dissolved in PBS to give a concentration of 1mg/ml, and stored at 4°C. Animals were treated with 10mg/kg twice weekly by intra-peritoneal injection. Ultra-LEAFTM Purified Rat IgG2a, κ Isotype Ctrl clone RTK2758 (Biolegend #400566) was used as PD1 isotype

control. During formulation the drug was dissolved in PBS to give a concentration of 1mg/ml, and stored at 4°C. Animals were treated with 10mg/kg twice weekly by intra-peritoneal injection.

2.1.5 *In-Vivo* Image-Guided Radiotherapy

Radiotherapy to rectal tumours was performed using a Small Animal Radiation Research Platform (SARRP; XStrahl), with animals anaesthetised using inhalational isoflurane maintained at 2% in medical air. A cone-beam computerised tomography (CBCT) image was acquired on the SARRP, at a tube voltage of 50kVp and 720 projections acquired over 360°. CBCT images were reconstructed using the SARRP's Muriplan treatment planning software, into 0.16mm isotropic voxels. The isocentre was determined based upon identification of the anal verge, with placement immediately proximal to the anus and adjacent to visible rectal luminal gas. Irradiation planning was based upon the isocentre, which was used to define the centre of rotation for either a static vertical beam, or a 280° continuous arc from -140° to +140°. Radiation was delivered through a 10mm square collimator, as either a single dose or as a fractionated regimen administered on Monday, Wednesday and Friday, with fractions ranging from 3-6Gy. No adjustment of absorbed radiation dose (Gray = joule of radiation energy/kilogram of mass) between human and mouse were made to account for potential differences in biodistribution between species, and doses were selected to recapitulate fractions given in short course RT regimens. Dosimetry studies were performed using a water-based phantom to confirm accuracy of the radiation doses administered in the mouse experiments described.

For subcutaneous tumours, the isocentre was placed over the centre of the tumour, which was readily identifiable on CBCT images, with radiation doses administered as 30° parallel opposed beams. For sham radiotherapy treatments, animals were anaesthetised by isoflurane anaesthetic, and maintained at 2% in medical air for 10 minutes in keeping with the time for one radiotherapy treatment session. Radiotherapy treatments with the SARRP were administered by Katrina Stevenson (SARRP Technician).

2.1.6 *In-Vivo* Imaging

Non-contrast CBCT imaging was performed as described in section 2.1.5, and was used for all irradiation treatments described in this thesis. Other imaging modalities used when refining irradiation strategies are described below.

2.1.6.1 CT Imaging with Intra-Peritoneal Contrast Enhancement

Omnipaque™ 300 (GE Healthcare #0407-1414-60) was diluted in 0.9% saline to a range of concentrations (20-40mg Iodine per ml), then 1ml of contrast solution administered by intra-peritoneal injections. Mice were then imaged at intervals of 5mins, 10mins or 15mins by CBCT acquired on the SARRP, at a tube voltage of 50kVp with 360 projections acquired over 360°. Animals were imaged under anaesthesia with inhalational isoflurane maintained at 2%.

2.1.6.2 MR Imaging

MRI scans were performed using a nanoScan PET/MRI scanner (Mediso Medical Imaging Systems, Hungary). During imaging, mice were anaesthetised with inhalational isoflurane (5% induction; 2% maintenance in medical air). T2 Fast Spin Echo (FSE) 3D axial sequences were used to acquire MRI scans (slice thickness 1mm, repetition time 2000msec, echo time 83.7msec, flip angle 90°).

2.1.7. Dosimetry Studies

Dosimetry studies and analysis was performed by Emer Curley (PhD Student, Dr David Lewis Lab, CRUK Beatson Institute). To calculate the dose rate of the SARRP a UNIDOS E Dosemeter (99-9208) ionisation chamber was used with radiochromic films (GafChromic™ EBT) exposed to ranges of doses upto 120% of the treatment dose to create a calibration curve. Experimental film was placed within a film-stack cubic water-based phantom composed of Plastic Water Diagnostic Therapy slabs (CIRS, Norfolk, VA). Dose calibration curves and gamma index analysis were performed using Radiochromic software (radiochromic.com).

2.2 Tissue sampling and fixation

Several methods of tissue fixation were employed to optimally prepare different tissue samples for further analyses. Sampling procedures and tissue fixation protocols are detailed below. Animals were euthanised by increasing concentration of CO_2 to enable extraction of blood to be carried out by cardiac puncture. ~300µl of blood was collected into a capillary EDTA tube. Where indicated for analysis of cell proliferation, animals underwent intra-peritoneal injection of 250µl bromodeoxyuridine (BrdU) cell proliferation labelling reagent (Amersham Bioscience, #RPN201) 2 hours prior to sampling.

2.2.1 Intestinal Tissue Fixation

Where the whole gut was required for analysis, predominantly to determine the effects of treatment on normal tissue, the colon, small intestine and caecum were dissected free and separated. They were then flushed with water and opened longitudinally prior to fixation. Intestinal sections were then pinned flat on wax plates with luminal side up, covered with 10% neutral buffered formalin (NBM) and kept at room temperature for 48-72hours. Subsequently, intestinal sections were then rolled by a 'swiss-roll' technique and for 'optimal fixation' were transferred to 70% ethanol for processing by the CRUK Beatson Histology Department.

2.2.2 Tumour Tissue Fixation

Where only tumour tissue was required for analysis, the rectum and adjacent 2-3cm of proximal colon was dissected, so that tumour sections with adjacent normal tissue could be easily cut for further analyses. The short intestinal section was flushed with water, opened longitudinally and placed luminal side up on Whatman paper. Tumour diameters were measured using calipers, and estimated volume subsequently calculated (Volume = (Length x $Width^2$)/2). Tumour samples were fixed in 10% NBM at room temperature for 48-72 hours before being transferred to 70% ethanol for processing.

Where tumour volume was sufficient a piece of tumour core was dissected (>2x2mm), placed in a 1.5ml Eppendorf tube submerged in RNA later (Sigma, #R0901), then stored at -80°C for later use.

2.2.3 Tissue Fixation for Evaluation of Metastases

Upon sampling of animals, tissue was dissected for analysis to determine presence of both local lymph node and distant organ metastasis. Lymph nodes were dissected from the colonic mesentery, and fixed separately in 10% NBM at room temperature. Liver, lungs, spleen and pancreas were dissected and fixed in 10% NBM. Any visible distant metastases were micro-dissected and fixed separately in 10% NBM. Tissue was kept in 10% NBM for 'long fix' and subsequent processing.

2.3 Tissue processing, Immuno-histochemistry and In-situ Hybridisation

Following tissue sampling and fixation, all samples were processed by the CRUK Beatson Histology Department using standard protocols. Tissues were first dehydrated and cleaned, then embedded in paraffin wax blocks. 4µm tissue sections were then cut using a microtome, floated in a water bath, then mounted onto glass slides for further use in a variety of staining procedures including Haematoxylin and Eosin (H+E), immunohistochemistry (IHC) and RNAscope.

2.3.1 In-Situ Hybridisation

In-situ hybridisation, or 'RNA scope' was performed by the CRUK Beatson Histology Department according to the manufacturer's protocol (RNAscope 2.0 High Definition – Brown, Advanced Cell Diagnostics). Key details of in-situ probes are listed in Table 2.1.

Target	Supplier	Catalogue Nō
PD-L1	Bio-Techne	#420508
Lgr5	Bio-Techne	#312178
SMAD7	Bio-Techne	#429418

Table 2.1: Probes used for in-situ Hybridisation

2.3.2 Immuno-histochemistry

All IHC stains were completed by the CRUK Beatson Histology Department using standard and optimised IHC protocols. Details and dilutions of all antibodies used for IHC stains are detailed in Table 2.2.

Target	Supplier	Catalogue Nō	Dilution
CD3	Abcam	#Ab16669	1:100
CD4	eBioscience	#14-9766-82	1:500
CD8	eBioscience	#14-0808-82	1:500
FOXP3	Cell Signalling	#12653	1:200
F4/80	Abcam	#Ab6640	1:100
Ly6G	Bioxcell	#BE0075-1	1:60000
S100A8	R&D Systems	#MAB3059	1:2000
S100A9	Santa Cruz	#sc-8115	1:1000
pSMAD3 (phospho S423 + S425)	Abcam	#Ab52903	1:50
IGFBP7	Sigma Aldrich	#HPA002196	1:100
CALD1	Sigma Aldrich	#HPA008066	1:500
BrdU	BD Biosciences	#347580	1:150
γH2AX	Cell Signalling	#9718	1:120
Cleaved Caspase3	Cell Signalling	#9661	1:500
SMAD2 (phospho S255)	Abcam	#Ab188334	1:50

Table 2.2: Antibodies used in Immunohistochemistry

2.3.3 Special Stain – Alcian Blue/Periodic Acid Schiff Staining

AB/PAS staining was performed by the CRUK Beatson Histology Department by a standard protocol, whereby all acidic mucins were first stained with Alcian blue solution (pH 2.5), then all mucins stained with 1% Periodic Acid solution and Schiffs Reagent (PAS) such that mucins are demonstrated in a contrasting manner.

2.3.4 Multiplex Immunofluorescence Staining

Multiplex immunofluorescence was performed and analysed by Dr Eoghan Mulholland (Professor Simon Leedham Lab, University of Oxford). Multiplex immunofluorescence was performed on 4µm thickness FFPE sections using the Opal™ protocol (Akoya Biosciences, Marlborough, MA) on the Leica BOND RXm autostainer (Leica Microsystems, Wetzlar, Germany). Six consecutive staining cycles were performed using the following primary antibody-Opal fluorophore pairs:

Target	Supplier	Catalogue Nō	Dilution	Fluorophore
Ly6G	BD Pharmingen	#551459	1:300	Opal 540
CD4	Abcam	#ab183685	1:500	Opal 520
CD8	Cell Signalling	#98941	1:800	Opal 570
CD68	Abcam	#ab125212	1:1200	Opal 620
FoxP3	Cell Signalling	#126553	1:400	Opal 650
E-cadherin	Cell Signalling	#3195	1:500	Opal 690

Table 2.3: Antibodies used in Multiplex Immunofluorescence

Whole-slide scans and multispectral images were obtained on the Akoya Bioscienes Ventra Polaris™. Batch analysis of multispectral images was performed with the inform 2.4.8 software provided, with images fused in HALO®

(Indica Labs) to produce a spectrally unmixed reconstructed whole-tissue image. Cell density analysis was performed for each cell of interest using HALO®.

2.4 Blood analysis

Blood was collected in EDTA columns post cardiac puncture, then analysed using an IDEXX Procyte Dx Haematology Analyser (IDEXX).

2.5 Scoring

Tumours were assessed by a Consultant Pathologist (Dr Noori Maka, Queen Elizabeth University Hospital) to determine tumour grading, and to identify histological features of response to radiotherapy.

2.5.1 Manual Scoring

Where manual scoring of IHC sections was performed, 10 representative areas 20X field of view regions were counted for positively staining cells per tumour. The mean value was then calculated to determine the number of positive cells per mm^2 of tumour.

2.5.2 Digital Pathology Analysis

Slides to be analysed digitally were scanned at a magnification of x20 using a Leica slide scanner, then exported to HALO® v2.0 software (Indica Labs). Using HALO® software, tumour sections were manually outlined then appropriate analysis algorithms used to detect positively stained cells. For most IHC stains, a CytoNuclear v2.0.9 algorithm was used with quantitative output shown as positively stained cells/μm^2 or as % of cells staining positively. For F4/80 and AB/PAS stains, an Area quantification v2.2.4 algorithm was used with quantitative output shown as % of tissue positive for the stain analysed. For ISH stains, an ISH v2.2 algorithm was used with output shown as total probes staining positively per μm^2.

2.6 Tissue Culture

'Supplemented Advanced DMEM/F12', 'ADF base' and 'Complete culture medium' are referred to throughout this section, and are made up as follows:

'Supplemented Advanced DMEM/F12' (Gibco, #12634-010)			
Supplement	**Supplier**	**Code**	**Concentration**
L-Glutamine	Gibco	25030-024	2mM
HEPES	Gibco	15630-056	10mM
Penicillin/Streptomycin	Gibco	15140-122	100U/ml
'ADF base' = Supplemented Advanced DMEM/F12 with growth factors			
Growth Factor	**Supplier**	**Code**	**Concentration**
N2	Gibco	17502-001	1X
B27	Gibco	125870-001	1X
'Complete Culture Medium' = ADF base with growth factors			
EGF	Peprotech	AF-100-15	50ng/ml
Noggin	Peprotech	AF-250-38	100ng/ml

Table 2.4: Components of Organoid Culture Media

2.6.1 Preparation of Organoids

Organoid lines were retrieved from -80° or liquid nitrogen storage, having been preserved in cell culture freezing medium (Gibco #12648010). The cryovial containing frozen organoids was thawed quickly in a waterbath at 37°C, transferred to pre-warmed supplemented Advanced DMEM/F12, and centrifuged at 1200rpm for 3 minutes. The cell pellet was then mechanically dissociated in 150µl ADF base, a further 5ml supplemented Advanced DMEM/F12 added, then centrifuged at 800rpm for 3 minutes. The cell pellet was then resuspended in 150µl growth factor reduced Matrigel® (Corning #356231), set on a 6-well plate with 2ml culture media added, and incubated at 37°C, 5% CO2, 21% O2.

Organoids were typically passaged and expanded at a ratio of 1:3, every 48-72 hours. Matrigel® domes were scraped out of wells by harsh mechanical pipetting to dissociate organoids from solidified Matrigel®. A 3-minute cycle of centrifugation at 1200rpm was carried out, with remnant Matrigel® aspirated

from the cell pellet. 150µl ADF base was then added to the cell pellet, and the suspension underwent vigorous manual pipetting with a P200 pipette; dissociation of organoids into fragments was confirmed by inspection under brightfield microscope. A further cycle of centrifugation was carried out at 800rpm for 3-minutes. Organoids were then re-plated in fresh Matrigel® on 6-well plates.

Prior to colonoscopy-guided injection, brightfield images were obtained at x4 magnification on an Olympus CKX41 microscope. 1ml of media was then aspirated from each well and 1ml of cold PBS added. Organoids were then dissociated from solidified Matrigel® by harsh manual pipetting. Centrifugation was then performed at 1400rpm for 3-minutes to clean dissociated organoids and to separate remnant Matrigel®. The cell pellet was then vigorously broken up using an aspirator and 1ml stripette with p200 pipette tip attached. PBS was then added and a further wash step carried out with centrifugation at 800rpm for 3 minutes. Cell pellets were then resuspended in PBS at 70µl per well, combined and divided into 1ml aliquots, and kept on ice prior to injection.

All organoid lines were routinely tested for mycoplasma prior to injection by qPCR (Minerva Biolabs #11-91250).

2.6.2 Derivation of Organoid Lines from Primary Tumours

For generation of primary organoid lines from locally induced rectal tumours, a tumour piece was dissected (at least 4x4mm) immediately following sacrifice and kept in cold PBS. The tumour was cut into small pieces in a 100mm dish, then washed in PBS three times. Tumour fragments were then incubated in 5ml 2.5% 10x Trypsin (Gibco #15090046) and 200U recombinant DNase I (Roche #04716728001) at 37°C for 30minutes. 5ml ADF base was then added and tumour fragments shaken vigorously to further dissociate, with this step repeated a further two times. Centrifugation at 1200rpm/3mins was performed, the cell pellet resuspended in 10ml ADF base, then passed through a 70µm cell strainer which was then washed with 5ml ADF base. Centrifugation was performed at 800rpm/3mins, and the cell pellet then resuspended in Matrigel® at a volume appropriate to the pellet volume. Organoids were cultured in complete culture medium at 37°C, 5% CO2, 21% O2. Organoids were typically passaged and

expanded every 48-72 hours, then frozen down in cell culture freezing medium (Gibco #12648010) once at a volume sufficient for a full 6-well plate.

2.6.3 Single Cell Suspension Seeding

For seeding of single cells suspension, AKPT organoids were cultured and passaged as previously described, until 3 wells of a standard 6 well plate were obtained. Organoids were manually scraped out of wells to dissociate organoids from Matrigel® and centrifuged at 1200rpm for 3-minutes. The cell pellet was then broken up by vigorous manual pipetting as previously described, then centrifuged at 800rpm for 3-minutes. The cell pellet was then incubated in 1ml 1X TrypLE Express (Gibco #12604013) and 2µl DNase (Roche #04716728001) at 37°C for 50minutes, with mixing performed every 10 minutes. 1ml ADF base was then added, mixed by pipetting, then passed through a 40µm cell strainer. The strainer was rinsed with 2ml ADF base, and the cell mix centrifuged at 1200rpm for 3-minutes. The cell pellet was then resuspended in 1ml complete culture medium, and cell counting performed by adding 20µl trypan blue (Invitrogen #T10282) to 20µl cell mix, then adding to a countess cell counting chamber slide (Invitrogen #C10228) for counting on a Countess II (Invitrogen, AMQAX1000). The number of live cells/ml was calculated by averaging two readings, then 4000 cells/ml suspended in the appropriate volume of complete cell culture medium. 2% Matrigel® was added to the cell mix to aid 2D layer seeding.

96 well plates were pre-coated with 10µl of Matrigel per well, then set at 37°C for 15 minutes. Following this, 150µl cell mixture (600 cells per well) was added to each well then incubated at 37°C, 5% CO2, 21% O2.

2.7 *In-Vitro* Irradiation Experiments

In-vitro treatment of organoids was performed at 72 hours post seeding as single cells in a 2D layer. 5 biological replicates were used for each experimental condition. Similar results were obtained from two independent experiments, with the second experiment presented in this thesis.

2.7.1 *In-Vitro* Irradiation

Irradiation of organoids was performed using the CellRad+ system (Precision Xray Irradiation). Doses of 2Gy, 4Gy, 6Gy, 8Gy and 10Gy were administered, with a 0Gy untreated plate maintained under the same conditions as a control.

2.7.2 *In-Vitro* Drug Treatment

Immediately prior to irradiation, organoids were treated with escalating concentrations of 5-FU or dimethyl sulfoxide (DMSO) in replenished complete culture medium. Solutions of 0.5μM, 1μM, 5μM, 10μM and 50μM 5-FU were prepared from stock solution by serial dilution in distilled water.

2.7.3 *In-Vitro* Imaging and Analysis

In-vitro imaging was performed using an Incucyte® Zoom System (Essen Bioscience), with images performed at 8-hour intervals over a period of 72-hours. Following a period of 72-hours, cell viability was assessed using the cell proliferation reagent WST-1 assay (Roche #05015944001). WST-1 reagent was added to each well at a dilution of 1:10, then returned to the incubator for 90 minutes to maintain dark conditions. Formazan dye formed was then quantified using an Infinite® 200 multi-well spectrophotometer ELISA reader (Tecan). Cell viability was then calculated by using the average of 5 replicate wells for each experimental condition, with % cell viability calculated by normalising values relative to the value obtained for the 0Gy/DMSO control condition.

2.8 RNA sequencing/Gene Expression Analysis

2.8.1 Isolation of RNA

RNA was isolated using the Qiagen RNeasy Minikit (Qiagen #74104) following the manufacturer's instructions. A maximum of 30mg of tumour tissue was placed in CK14 ceramic bead tubes (Precellys #P000912-LYSK0-A0), with 600μl RLT lysis buffer and 6μl β-mercaptoethanol (β-ME) and homogenised using a Precellys Evolution machine (Bertin Instruments) at 6800rpm for 3x20seconds cycles. Cell pellets were homogenised by adding 350μl buffer RLT with 3.5μl β-ME, and manually pipetting. Homogenised lysate was added to 700μl 70% ethanol, mixed by pipetting, then 700μl transferred to RNeasy Mini spin columns placed in a 2ml

collection tube, before centrifuging briefly for 15seconds at 8000g. The flow through was discarded, then this step repeated for the remaining tissue lysate. 350µl RW1 wash buffer was then added to the spin column and centrifuged briefly for 15 seconds at 8000g. DNase stock solution was prepared prior to RNA extraction using an RNase-Free DNase set (Qiagen #79254). 550µl RNase-free water was injected into the DNase I vial using an RNase-free needle and syringe, then mixed by gentle inversion, before dividing into aliquots and frozen at -20°C. For each sample, DNase solution was prepared by adding 10µl DNase stock solution to 70µl buffer RDD, then added to the spin column membrane and left at room temperature for 15minutes. A further 350µl RW1 wash buffer was added to each spin column, centrifuged at 8000g for 15 seconds, and the flow through discarded. Two washes with buffer RPE were performed, then the spin column centrifuged at 1300g for 1 minute to dry the membrane. 30µl of RNase free water was then added to each spin column, centrifuged at 8000g for 1 minute to elute the RNA. RNA concentration was then quantified using a NanoDrop 2000c Spectrophotometer (ThermoScientific).

2.8.2 RNA Sequencing and Bioinformatics Analysis

Quality of purified RNA was performed on 100µg/µl of each RNA sample on an Agilent 220 Tapestation using RNA screentape. Only samples with RNA Integrity Number (RIN) value ≥6.0, were considered for RNA sequencing. RNA sequencing and library preparation was performed by William Clark for data presented in chapters 3 and 4 (CRUK Beatson Institute Molecular Technologies Services) using an TruSeq RNA sample prep kit (Illumina). Samples were then run on an Illumina NextSeq 500 using the High Output 75 cycles kit (2 x 36 cycles, paired end reads, single index). RNA sequencing data presented in Chapter 6 was performed by Genewiz (Azenta Life Sciences).

Analysis of RNA sequencing data was performed by Dr Kathryn Gilroy (CRUK Beatson Institute) and Lily Hilson (University of Glasgow) or using the Molecular Subtyping Resource (MouSR) (https://mousr.qub.ac.uk/). The raw sequence quality was assessed using the FastQC algorithm version 0.11.9. Sequences were then trimmed to remove poor quality base calls and adaptor sequences, using the Trim Galore tool version 0.6.4. Trimmed sequences were aligned to the

mouse genome build GRCm38.98 (Church et al, 2011) using HISAT2 version 2.1.0, with raw counts per gene then determined using FeatureCounts version 1.6.4. Differential expression analysis was performed using the R package DESeq2 version 1.22.2. Gene Set Enrichment Analysis (GSEA) was carried out using R package fgsea version 1.8.0. Differential expression analysis and GSEA were performed by Dr Kathryn Gilroy (CRUK Beatson Institute).

Principal Component Analysis was conducted using the MouSR resource, with analysis performed through the prcomp function in the R stats package embedded in the resource (Ahmaderaghi et al, 2022). CMS analysis was performed through the human CMS template embedded in CMScaller, with conversion to mouse orthologues using biomaRT R stats package to remove remove intersected mouse genes embedded in the MouSR resource, with the nearest template prediction (NTP) method used to call mouse CMS. Microenvironment cell populations (mMCP) analysis was performed using the Murine MCP (mMCP) counter R package embedded in the MouSR resource (https://mousr.qub.ac.uk/).

2.9 Flow cytometry

At sampling, ~300µl of blood was obtained by cardiac puncture and kept in an EDTA tube, with ~20mg of mesenteric lymph node tissue and ~30mg tumour tissue harvested and exact weights recorded. Tissues and blood were kept on ice, then sample processing and staining was performed by Xabier Cortes-Lavaud (CRUK Beatson Institute). Tumour tissues were digested using the Mouse Tumour Dissociation Kit (Miltenyi Biotec, #130-096-730 and the GentleMACS Octo Dissociator with Heaters (Miltenyi Biotec, #130-096-427) using the 37_m_TDK_1 programme. Blood was processed by adding erythrocyte lysis buffer (20x volume) and incubating on ice for 10 minutes. Lymph node tissue was processed by adding 1ml RPMI 1640 (Gibco, #31870-025), Collagenase D (1.25mg/ml) and DNAse I (30µg/ml) and incubating at 37°C for 30 minutes. Cells were then passed through a 70µm cell strainer, and centrifuged at 400g for 5 minutes. 2 million cells were incubated in LIVE/DEAD fixable near-IR stain kit (ThermoFisher, #L10119) at 1:1000 dilution in 100µl PBS in the dark for 15 minutes at 4°C. Fc block was then performed to block CD16/32 activity, using TruStain FcX anti-

mouse CD16/32 (Biolegend, #101320) at 1:200 in PBS 1% BSA, and incubated for 10 minutes in the dark at 4°C. 25µl of antibody mix was then added per panel (lymphoid and myeloid), then incubated at 4°C in the dark for 30 minutes.

Target	Supplier	Catalogue Number	Dilution
CD44	Biolegend	#103032	1:100
CD4	Biolegend	#100510	1:100
PD1	Biolegend	#135225	1:100
NK1.1	Biolegend	#108745	1:200
Il-17	Biolegend	#108745	1:200
CD45	eBioscience	#63-0451-82	1:100
gdTCR	Biolegend	#118131	1:200
CD3	Biolegend	#100228	1:100
CD19	BD Biosciences	#749027	1:400
CD62L	BD Biosciences	#749027	1:200
CD8a	Biolegend	#301027	1:100
Granzyme B	Biolegend	#515406	1:100
IFN-γ	eBioscience	#25-7311-41	1:200
TCRb	Biolegend	#109239	1:400
CD69	Biolegend	#104508	1:100

Table 2.5: Details of Antibodies used for Lymphoid Panel

Target	Supplier	Catalogue Number	Dilution
MHCII	Biolegend	#114620	1:200
SiglecF	Biolegend	#155503	1:100
CD103	Biolegend	#121435	1:200
F4/80	Biolegend	#123149	1:100
CD45	eBioscience	#63-0451-82	1:100
CD11c	Biolegend	#117353	1:100
CD11b	BD Biosciences	#741934	1:200
Ly6G	BD Biosciences	#563978	1:50
Ly6C	Biolegend	#128024	1:100
CXCR2	Biolegend	#149604	1:50
CD48	Biolegend	#103424	1:200
CD64	Biolegend	#139319	1:100
CD101	eBioscience	#12-1011-82	1:100

Table 2.6: Details of Antibodies used for Myeloid Panel

For cell fixation, 50µl PBS with 4% paraformaldehyde was added to the cells, then incubated at room temperature for 15 minutes in the dark. The cells were then washed and resuspended in PBS. The cells were then washed in 10X Permeabilization buffer (Invitrogen, #00-8333-56), then washed and re-suspended in PBS for flow cytometry acquisition. Data was then acquired BD LSR Fortessa Flow Cytometer (BD Biosciences) and analysed with FlowJov10.4.2 (Performed by Xabier Cortes-Lavaud, CRUK Beatson Institute).

2.10 Data analysis and presentation

Graphs were generated using GraphPad Prism 9. Bar charts display mean +/- standard error of mean. Statistical significance was assessed by either one-tail or two-tail Mann-Whitney U-tests (for bar charts), or by Log Rank Mantel Cox test (for survival curves) with significance assumed at p values of <0.05. Details of experimental numbers, statistical test used and significance are denoted in each figure legend. Power calculations were performed using the NC3Rs Experimental

Design Assistant (https://eda.nc3rs.org.uk/eda). Group sizes were calculated to detect a 50% increase in survival based on a median untreated survival of 34 days in the AKPT organoid transplant model, with a type 1 error rate (α) of 5% and 95% power. Diagrams were generated using BioRender scientific image generation software (https://www.biorender.com/).

Chapter 3: Development and Characterisation of Orthotopic Models of Locally Advanced Rectal Cancer

3.1 Introduction

3.1.1 Orthotopic Models of Locally Advanced Rectal Cancer

Despite several decades of significant advances being achieved in the pre-clinical modelling of CRC, models which specifically recapitulate the anatomical characteristics of rectal cancer are lacking (Lannagan et al, 2021). Numerous surgical techniques have resulted in engraftment of tumours in the murine rectum. Submucosal needle injection of murine or human cancer cell lines following rectal prolapse induction has successfully established locally aggressive adenocarcinoma in immunocompetent hosts with high penetrance (Kashtan et al, 1991; Donigan et al, 2009; de Sousa e Melo et al, 2017). A similar rectal prolapse technique has also been employed, whereby donor murine colorectal tumour fragments are sutured to the rectal mucosa following prolapse induction with a haemostatic clip (Enquist et al, 2014).

Murine rectal tumour models can be generated following induction of colitis with orally administered dextran sulfate sodium (DSS), with a murine CRC cell suspension injected as an enema followed by temporary sealing of the anus with a small clamp to prevent spillage (Takahashi et al, 2004). Similarly, chemical induction of colitis can be achieved through intraluminal instillation of 4% acetic acid solution, with murine CRC cells also injected intra-luminally (Kishimoto et al, 2013). Both techniques report high penetrance of invasive adenocarcinoma within the murine rectum, with a short latency (~4 weeks) to tumorigenesis.

Recently, more sophisticated modelling strategies have been employed whereby murine derived organoids can be manipulated using CRISPR/Cas9 genome editing techniques, such that tumours express combinations of common CRC driver mutations. Following induction of colitis by DSS administration, pipette enema injection of *shApc/Kras*$^{G12D/+}$*/p53*$^{R127H/-}$ murine derived organoids successfully resulted in tumorigenesis at the rectum/distal colon with 62% success and a low incidence of distant metastasis (O'Rourke et al, 2017). DSS induction has been similarly employed to enable engraftment of organoids with more complex mutational burdens (*shApc/Trp53*$^{-/-}$*/Tgfbr2*$^{fl/fl}$*/K-ras*$^{G12D/+}$*/AKT*^{E17K}), successfully

modelling invasive adenocarcinoma with a high penetrance of distant metastasis in both distal colon and rectum (Varga et al, 2020; Nicolas et al, 2022).

The requirement for chemical colitis induction to achieve engraftment of tumour cell lines can be overcome by colonoscopy guided submucosal injection techniques. A rigid veterinary endoscope can be used to guide needle injection of organoids into the colonic submucosa under direct visualisation (Zigmond et al, 2011). Following the first description of this technique by Zigmond and colleagues, genomic editing strategies were utilised to inject *Apc*$^{fl/fl}$;*Kras*$^{LSL\text{-}G12D/+}$;*Trp53*$^{fl/fl}$ expressing tumour organoids into the distal colonic submucosa of NOD Scid Gamma (NSG) mice, resulting in invasive tumours at 12 weeks and liver metastasis in 33% of recipient mice (Roper et al, 2017). Similarly, organoid lines representative of serrated CRC engineered through CRISPR/Cas9 genome editing techniques, have been injected into the colonic submucosa of NSG mice modifying the technique initially described by Zigmond and colleagues (Lannagan TRM et al, 2019). Recent genome editing techniques now enable control over the mutational characteristics of murine tumour cell lines, with colonoscopy guided needle injection allowing orthotopic transplantation of tumours without the requirement for colitis induction or surgical intervention.

Orthotopic models of CRC can be generated without *the* transplant of human or murine cell lines, through ligand dependent and tissue specific Cre-recombinase systems. Cre recombination under the control of the intestinal specific Villin promotor (*VilCre-ERT2*) can be induced following tamoxifen injection, and allows temporal and tissue specific control over tumour formation (el Marjou et al, 2004; Feil et al, 2009). Colonoscopy guided submucosal needle injection can be utilised to deliver tamoxifen to a specific colonic site in Apc mutant mice (*Villin*^{creER}; *Apc*$^{fl/fl}$), with near 100% success with tumour induction, and may be a technique which could be applied to the rectal location (Roper et al, 2017).

3.1.2 Limitations of Orthotopic Models of Locally Advanced Rectal Cancer

The use of commercially available, immortalised cell lines limits their applicability to the pre-clinical development of treatment strategies in CRC (Hynds et al, 2018). It is only in retrospect that commonly used murine tumour derived cell lines, including CT26 and MC38 have undergone extensive molecular

characterisation. CT26 displays significant chromosomal aberration and extensive tri and tetraploidy. CT26 cells display *Kras*^{G12D} mutations, however, *Apc* and *Tp53* are not mutated (Castle et al, 2014). Characterisation of the MC38 cell line has shown this to be a valid model for investigating microsatellite unstable (MSI-H)/hypermutated CRC, which accounts for only ~1-2% of rectal cancer and furthermore represents a subset of patients with favourable prognosis and responsiveness to immune checkpoint blockade (Hutchins et al, 2011; Efremova et al, 2018).

Several studies using orthotopic colonic transplant models involve the use of human CRC derived cell lines, such as HCT116. Although Enquist et al reliably developed orthotopic rectal cancer models, invasive adenocarcinoma and a high penetrance of distant metastasis was achieved in an immunocompromised host (NOD scid gamma mice). Lack of host immune response significantly alters the tumour immune microenvironment, with the absence of mature T-cells limiting the utility of immunocompromised models in both mechanistic and treatment studies.

Chemical induction techniques confer significant advantages over other transplant models, as tumours establish in the mucosal layer in the same manner as human disease. However, colitis is required in these models to establish mucosal inflammation and a tumour promoting niche. The resulting microbiome and host immune response is significantly altered in comparison with normal conditions under which tumorigenesis arises. It is known that DSS colitis induction is associated with accumulation of immune cells within the colon microenvironment, including increased neutrophils, CTLs, T helper and Treg cells, as well histological changes such as crypt destruction, goblet cell loss and depletion of the epithelial barrier (Yan et al, 2009; Nunes et al, 2018).

The development of orthotopic rectal cancer models that accurately recapitulate the anatomical, histological and molecular characteristics of human disease remains an unmet need in the field of CRC research; in particular, models which represent poor prognosis and treatment resistant subtypes are lacking. Recent studies suggest that orthotopic transplant of murine tumour derived organoids, which can undergo additional genomic editing to express specific mutations of interest, is a feasible approach which could be adapted to the context of rectal cancer. Furthermore, Cre-recombinase systems permitting

local delivery of tamoxifen have the potential for simple modification to locally induce rectal tumours in genetically engineered mouse models.

3.1.3 Experimental Aims

The focus of this chapter was to develop experimental models of LARC which can be used in treatment studies to evaluate responses to radiotherapy, and to study novel radiotherapy-immunotherapy combinations. I aimed to overcome the drawbacks discussed with previously described orthotopic models of rectal cancer, to develop immunocompetent models which better recapitulate the anatomical and histological features of human disease, whilst also achieving reliable engraftment rates with rapid latency. I aimed to develop models which reflect the mutational burden observed in human disease, and furthermore recapitulate the poorest prognosis subtypes of disease, which are most in need of novel therapeutic strategies and a better understanding of the mechanisms underlying treatment resistance.

I aimed to model the commonest driver mutations of rectal cancer as described in the adenoma-carcinoma sequence, including APC, p53 and KRAS mutation (Fearon and Vogelstein, 1990). In addition, I aimed to model tumours with TGFβ activating mutations, to model poor prognosis subtypes with immunosuppressive tumour microenvironments. High expression of TGF-β has been found to be associated with worse overall and disease-free survival in patients who have undergone surgery for CRC (Chen et al, 2017). Furthermore, study of human organoid cultures shows that high TGF-β expression is associated with the development of the mesenchymal CMS4 subtype, and furthermore directs sessile serrated adenoma precursor lesions towards the CMS4 subtype (Fessler et al, 2016).

This chapter describes the development and characterisation of orthotopic models of LARC, and addressing the following aims:

- Development of novel orthotopic transplant and autochthonous models of LARC which recapitulate the anatomy of human disease while maintaining immune competence.

- Development of a model of LARC which is reproducible, with rapid latency and high engraftment rate.
- Characterisation of the histological features of newly developed models of LARC and their ability to model locally invasive disease and distant metastasis.
- Characterisation of the tumour immune microenvironment using immunohistochemistry and RNA sequencing to align developed models with molecular subtypes of human disease.

3.2 Results

3.2.1 Common CRC Driver Mutations are observed in a Rectal Cancer Subset

I characterised the mutational burden of human rectal cancer to establish any differences when compared with colonic cancer, and to guide the development of a suitable pre-clinical model. Data was analysed from a cohort of patient tumour samples (n=44) which had undergone mutational profiling by the Glasgow Precision Oncology Laboratory (GPOL) following curative surgical resection for rectal cancer. Rectal tumours of all T-stages (T1-4) were included in analysis. APC, TP53 and KRAS were the most commonly occurring mutations in this cohort, seen in 84%, 80% and 34% of patients respectively (Figure 3.1, upper panel). These results show similar concordance with mutational frequencies described in the literature for CRC (Cancer Genome Atlas Network, 2012). Furthermore, analysis of the publicly available TCGA (The Cancer Genome Atlas) database for the rectal cancer subgroup (n=82) revealed similarity with the data from our local patient cohort, with APC, TP53 and KRAS mutations showing 89%, 73% and 45% prevalence respectively (Figure 3.1, lower panel).

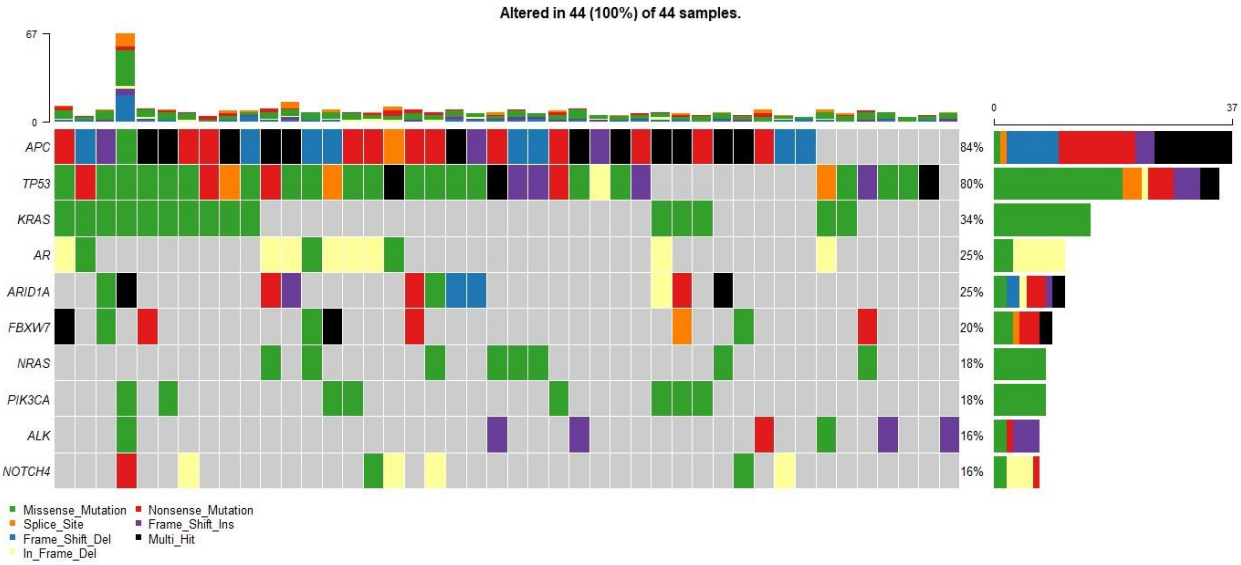

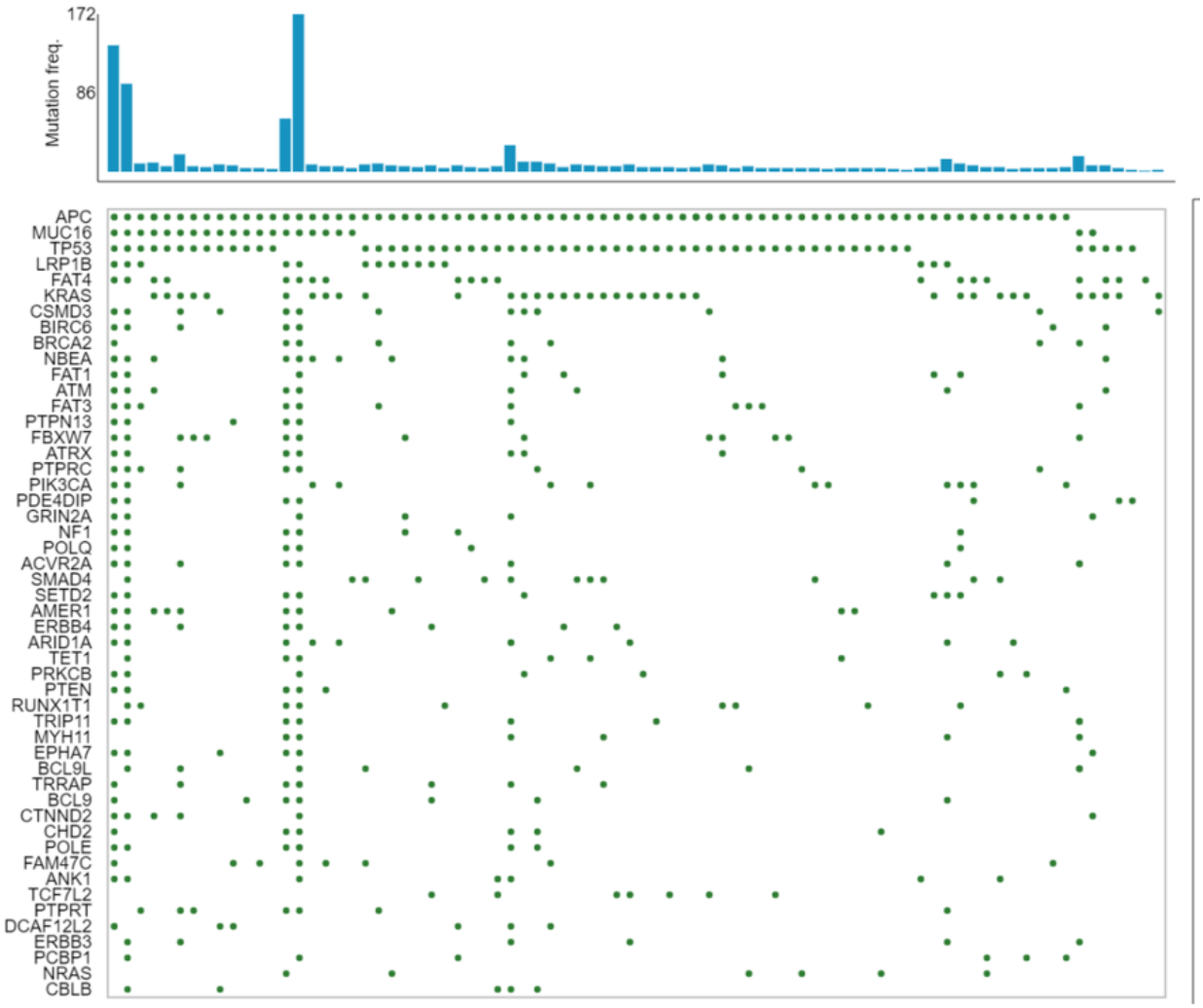

Figure 3.1: Mutational Profile in Human Rectal Cancer

Top - Oncoplot displaying the 10 most common mutations in a cohort of resected rectal cancer patients (n=44) analysed by mutational profiling performed using the Glasgow Precision Oncology Laboratory (GPOL) gene panel (See Appendix for full gene list). Bottom – Oncogrid displaying mutational frequency from rectal cancer profiles obtained through a publicly available data-set (The Cancer Genome Atlas). Top 50 most mutated genes shown (y-axis); individual patients displayed (x-axis).

3.2.2 Differences in Mutational Profile between Rectal and Colonic Cancer are observed

To determine the differences in mutational profiles between rectal cancer and colonic cancer, I compared the rectal cancer patient group with a corresponding cohort of colonic cancer patients who had undergone curative resection (n=166). Similarly, the most commonly observed mutations in colonic cancer were APC, TP53 and KRAS, seen in 73%, 58% and 51% respectively (Figure 3.2, upper panel). Comparative analysis demonstrated that TP53 mutations occur at a significantly

higher frequency in rectal cancer (p=0.0134) when compared with colonic cancer (Figure 3.2, lower panel). Interestingly, TGFBR2 (p=0.0198) and BRAF (p=0.0317) mutations were expressed in a significantly increased proportion of colonic cancer patients when compared with rectal cancer.

Mutations in the TGF-β signalling pathway were observed in a small proportion of patients in this cohort, with SMAD4 and TGFBR2 mutations detected in 14% and 2% of rectal cancer resection samples respectively (Figure 3.2, upper panel). Mutational inactivation of TGF-β signalling through somatic inactivation of TGFBR1/2 or mutation in downstream SMAD transcription factors, is thought to occur in 40-50% of colorectal cancer cases, driving progression from advanced adenoma to carcinoma (Markowitz et al, 2009; Grady et al, 1999). It has been well established that high TGF-β expression within tumours confers higher incidence of disease relapse in patients, with pre-clinical studies suggesting that TGF-β signalling is crucial in directing both mesenchymal subtype formation and the initiation of metastasis (Calon et al, 2012; Fessler et al, 2016). Furthermore, a recently developed radiosensitivity index showed in multiple patient cohorts that stromal TGF-β expressing fibroblasts and epithelial *APC* mutations are associated with radio-resistance to standard of care CRT in LARC (Domingo et al, 2021). Although TGF-β mutations were observed in a relatively low proportion of rectal tumours analysed, it is known that a significant proportion (27%) of rectal cancers align with the CMS4 subtype, which is associated with stromal TGF-β signalling, poor prognosis and treatment resistance (Loree et al, 2018).

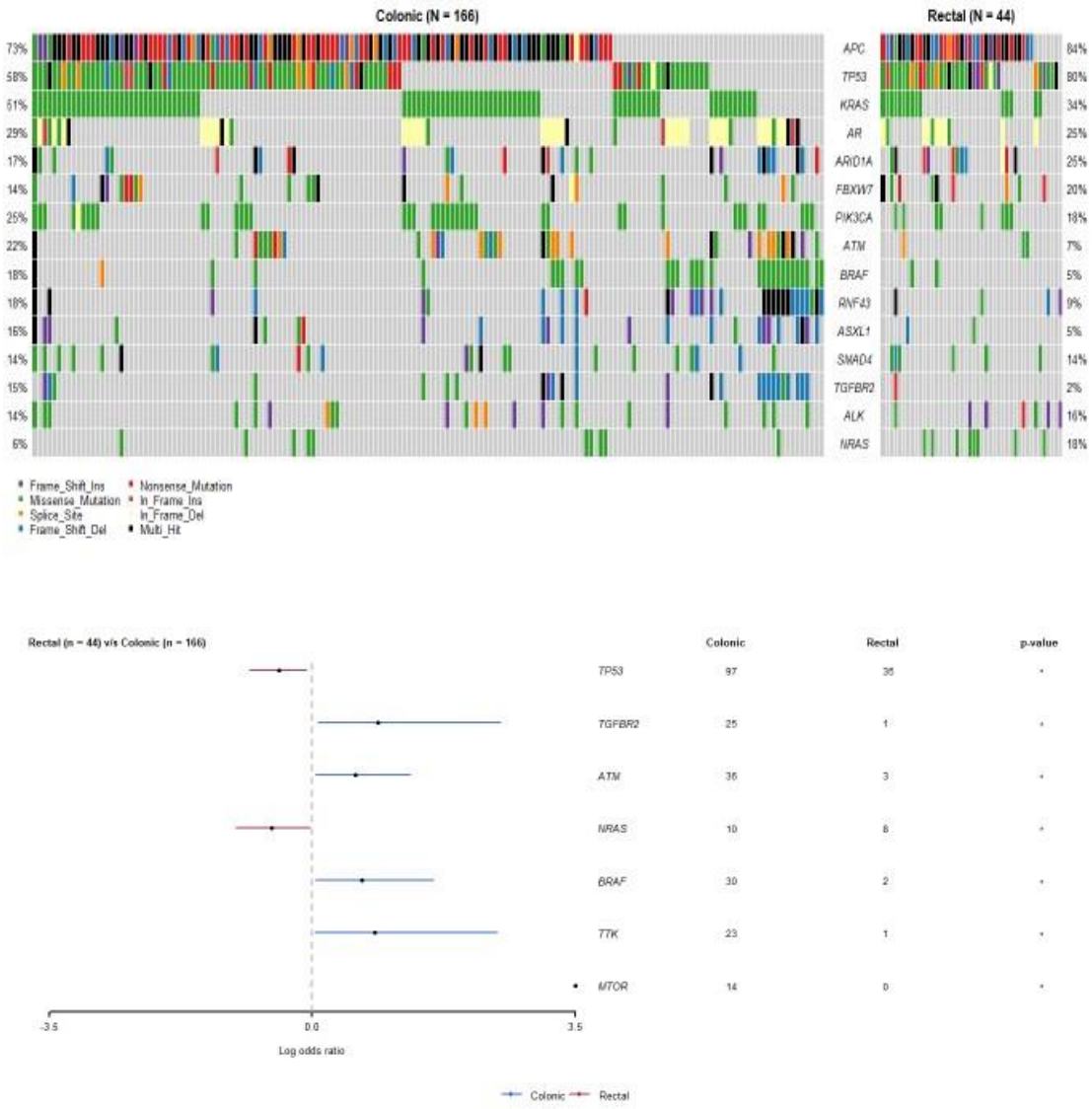

Figure 3.2: Mutational Comparison between Human Rectal and Colonic Cancer Specimens

Top – Oncoplot displaying the 15 most common mutations observed in resected colonic and rectal cancer patients. Lower – Forest plot displaying genes with significantly altered mutation frequency between rectal and colonic subgroups. Red lines represent genes with increased mutation frequency in rectal cancer. Blue lines represent genes with increased mutation frequency in colonic cancer. Significant p-value = <0.05. Confidence Intervals = 95%.

3.2.3 Modelling Common Driver Mutations of Rectal Cancer through Localised Submucosal Tamoxifen Injection

Locally inducible tumour models have previously been described using the tamoxifen dependent Cre recombinase (CreER) system (el Marjou et al, 2004). *CreER* driven by the epithelial specific promotor Villin, has been used to induce intestinal tumours in *Apc* mutant mice (*VillinCreER: Apc*$^{fl/fl}$) with *CreER* being

activated by mucosal delivery of 4-hydroxytamoxifen (4-OHT) under colonoscopic guidance (Roper et al, 2017). Through simple adaptation of the colonoscopy guided submucosal injection technique described by Roper et al, I aimed to generate rectal tumours through submucosal injection of tamoxifen to the most distal region of the mouse colon, similarly to previous studies which defined the rectum as being within 1cm of the anal margin (Siri et al, 2019). However, the presence of a murine rectum has been debated in the literature, with other studies describing only a distal colon (Freeling et al, 2016). Following submucosal injection of tamoxifen suspended in PBS (70µl total, concentration 100µM), Lox protein (*LoxP*) flanked alleles recombine to induce deletion of genes of interest, or oncogenic activation of an allele (in the case of $Kras^{G12D}$) through deletion of a stop codon (Fig 3.3, top panel). Initially, I developed rectal tumour models with *Apc* deletion and *Kras* activation (*VillinCreER:* $Apc^{fl/fl}$;$Kras^{G12D/+}$), and thereafter described as the 'AK' model. Similarly, a model with *Apc* deletion, *Kras* activation and *TP53* deletion was developed (*VillinCreER:* $Apc^{fl/fl}$;$Kras^{G12D/+}$;$p53^{fl/fl}$), and termed the 'AKP' model.

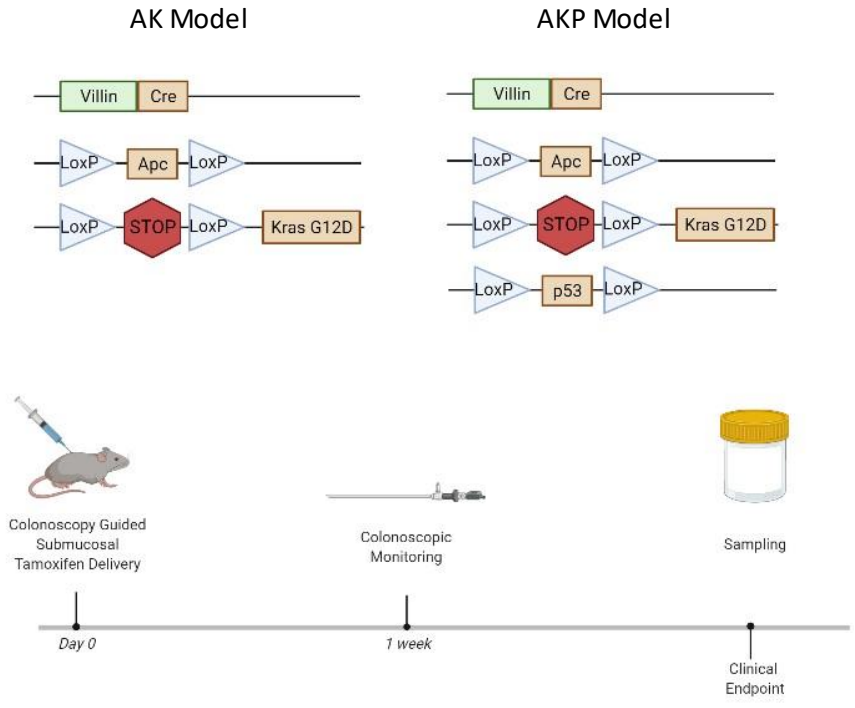

Figure 3.3: Modelling Common Driver Mutations of Rectal Cancer through Localised Submucosal Tamoxifen Injection

Top – Schematic demonstrating genetic modelling strategy for both 'AK' and 'AKP' models using the Cre-Lox recombinase system. Bottom – Schematic showing experimental timeline for model induction and monitoring.

Tumorigenesis was confirmed by colonoscopy at one week post induction (Figure 3.3, bottom panel). Following localised tamoxifen induction, a short latency to tumorigenesis was observed in both the AK and AKP models, with intra-luminal tumours establishing by 1-week post induction (Figure 3.4, top panel). Short survival was demonstrated in both AK and AKP genotypes, with median survival of 15 and 19.5 days respectively (Figure 3.4, bottom panel). No significant difference in survival was observed between locally inducible AK and AKP rectal models (Log Rank test p=0.8179). At clinical endpoint, animals typically demonstrated signs of weight loss, deteriorating body condition and often rectal prolapse. Interestingly, tumour burden was small at sampling with maximal tumour diameter typically measuring <5mm, with colonic obstruction not being frequently observed in either model. Evidently, homozygous deletion of the *Apc* gene resulted in rapid tumorigenesis, with tumours close to the anal verge frequently resulting in mucosal prolapse and a significant degree of distress and discomfort. In both models, animals typically showed evidence of clinical deterioration and distress at a short 2-3 week time-point, and as a result these models were not deemed to be suitable to utilise in later treatment experiments.

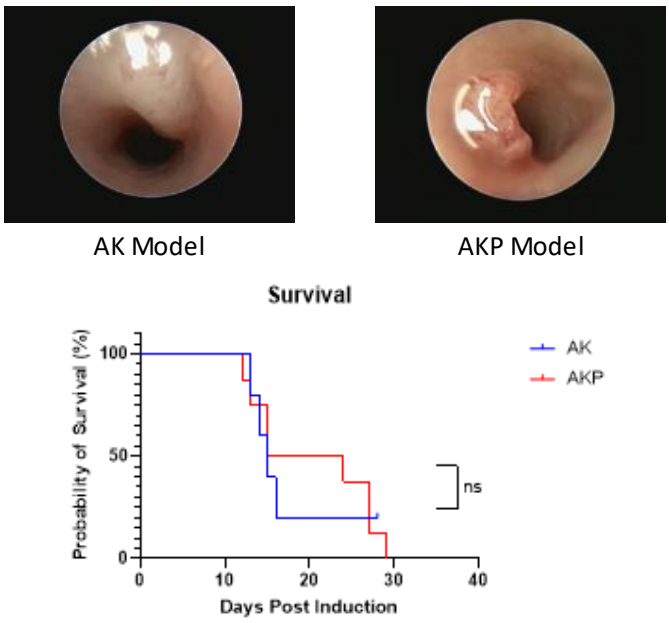

Figure 3.4: Tumour Latency and Survival in the AK and AKP Models.

Top – Representative colonoscopy images showing AK and AKP tumours at one week post induction. Bottom – Survival curve demonstrating ageing of the AK and AKP models. n=8-10. Censored subjects represent animals sacrificed at a planned time-point after irradiation. ns denotes non-significance (p≥0.05). Log Rank Test.

Tumour tissue from both ‘AK’ and ‘AKP’ models were stained for haematoxylin and eosin (H+E) to assess histological features. Non-invasive rectal tumours were observed which were confined to the mucosal layer (Figure 3.5, top panel). Cohesive epithelial structures were maintained throughout tumours, with epithelial cells demonstrating features of low-grade dysplasia (Figure 3.5, bottom panel). Uniformity of nuclei was maintained, with slight enlargement, elongation and hyperchromatism observed in keeping with early stages of the classical adenoma-carcinoma sequence. Invasion beyond the mucosal layer was not observed in either AK or AKP models, and furthermore, histological features were only consistent with low grade dysplasia. The characteristics described are likely to reflect the short clinical endpoint at which these tumours were sampled; with no features of invasion or carcinoma observed, these models are only representative of the earliest stage of the adenoma-carcinoma sequence. To model rectal adenocarcinoma and more advanced stages of disease, it was apparent that additional mutations beyond *Apc, Kras* and *TP53* would be required.

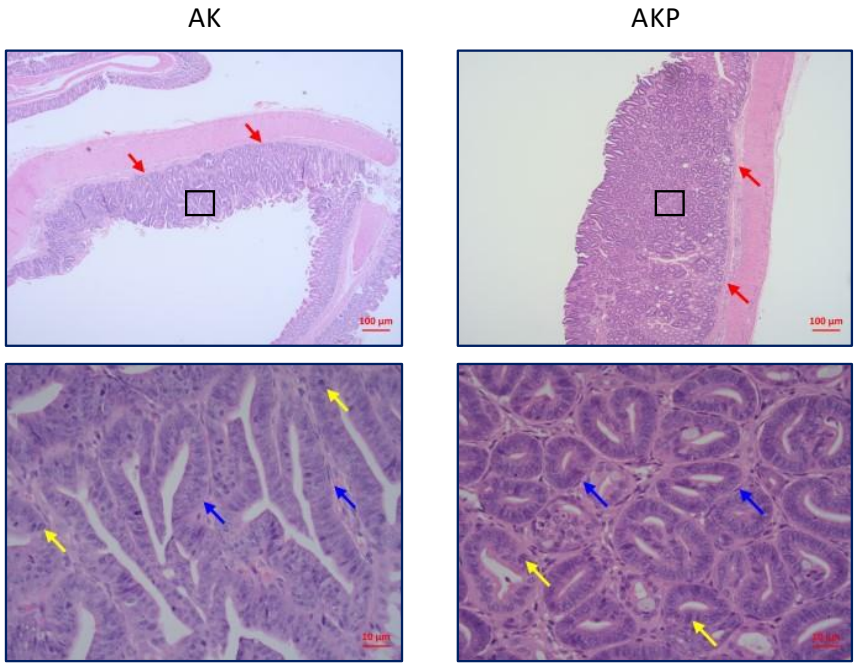

Figure 3.5: Histological Appearances of AK and AKP Rectal Tumours

Top – Representative overview images of AK rectal (Left) and AKP rectal (right) tumours, x4 magnification. Red arrows indicate muscularis mucosa with no invasion through this layer. Bottom – Representative images of tumour epithelium demonstrating features of low-grade dysplasia, x40 magnification. Blue arrows indicate well differentiated tumour epithelium. Yellow arrows indicate hyperchromatic nuclei. Scale bars = 100μm (top images) and 10μm (bottom images).

3.2.4 Adenocarcinoma Can be Modelled Through Additional TGF-ß Pathway Mutations

In addition to the induction of *Apc*, *Kras* and *TP53* mutations, I introduced additional deletion of genes involved in the TGF-ß signalling pathway by targeting the TGF-ß Receptor 1 (*Tgfbr1*) or *Smad4* genes. Similarly, tumours were induced by colonoscopy guided submucosal injection of tamoxifen at the rectal location to establish 'AKPS' and 'AKPT' orthotopic rectal cancer models (*VillinCreER: Apc$^{fl/+}$;Kras$^{G12D/+}$;p53$^{fl/fl}$;Smad4$^{fl/fl}$*) and (*VillinCreER: Apc$^{fl/+}$;Kras$^{G12D/+}$;p53$^{fl/fl}$;Tgfbr1$^{fl/fl}$*) respectively). I aimed to increase survival and the latency to tumorigenesis in these models, and so mice with one 'floxed' *Apc* allele were utilised, such that heterozygous *Apc* deletion would occur upon induction (Figure 3.6, top panel). As anticipated, animals displayed a longer latency to tumorigenesis, with tumours typically establishing at 8 weeks post induction (Figure 3.6, bottom panel).

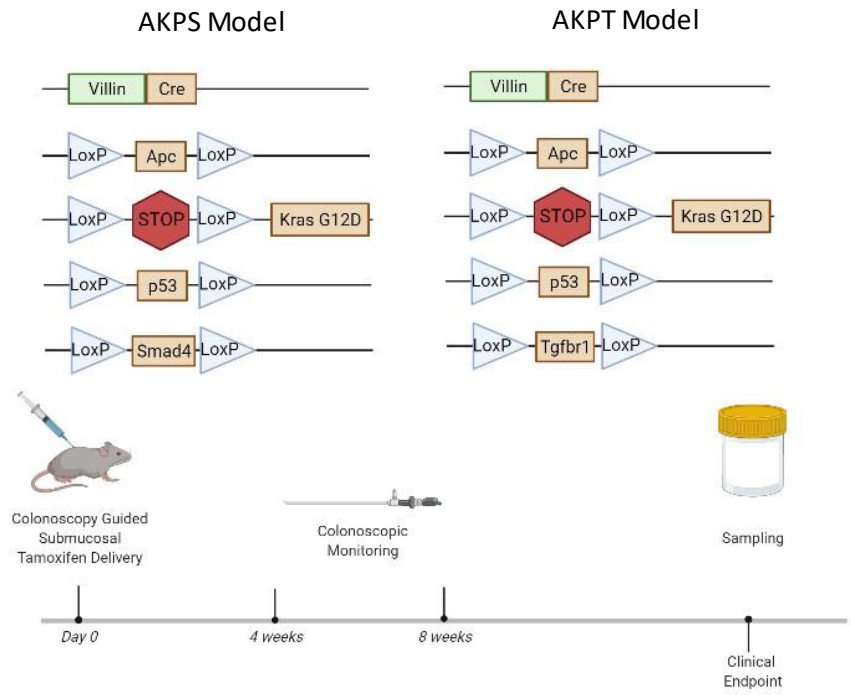

Figure 3.6: Modelling Adenocarcinoma through Localised Submucosal Tamoxifen Injection

Top – Schematic demonstrating genetic modelling strategy for both 'AKPS' and 'AKPT' models using the Cre-Lox recombinase system. Bottom – Schematic showing experimental timeline for model induction and monitoring strategy.

Following serial colonoscopy imaging, tumours typically became apparent at 8 weeks post induction, with flat lesions demonstrated in contrast to the intraluminal lesions observed in the AK and AKP models (Figure 3.7, top panel). Longer survival was also observed in both AKPS and AKPT genotypes, with median survival of 80 days and 71 days respectively and no significant difference seen between the two models (Figure 3.7, bottom panel). A range of signs were seen in the AKPS and AKPT models at clinical endpoint, including weight loss, deteriorating body condition and occasional rectal prolapse. Other signs suggestive of significant tumour burden were also observed, with animals displaying rectal bleeding and anaemia (noted through paling feet).

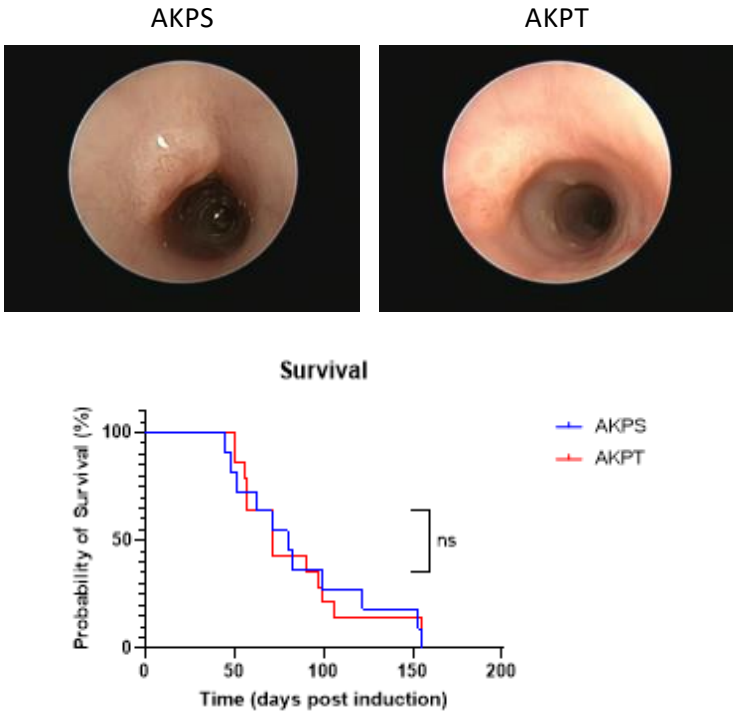

Figure 3.7: Tumour Latency and Survival in the AKPS and AKPT Models.

Top – Representative colonoscopy images showing AKPS and AKPT tumours at eight weeks post induction. Bottom – Survival curve demonstrating AKPS and AKPT ageing cohorts. n=11-14. Log Rank Test ($p=0.9751$). ns denotes non-significance ($p \geq 0.05$).

Tumour tissue from both AKPS and AKPT tumours were stained for H+E to assess histological features. Invasive adenocarcinoma was seen in both models with AKPS tumours showing invasion through the submucosal layer, while AKPT tumours invaded deeper through the muscularis propria and towards the serosa (Figure 3.8, top panel). Features of moderate differentiation were seen in both tumour epithelia with only some glandular structures maintained (Figure 3.8,

bottom panel). Features of adenocarcinoma were seen throughout tumours with nuclear enlargement and prominent nucleoli. A significant stromal reaction was seen, particularly in AKPT tumours, with dense immune and inflammatory infiltrate noted (Figure 3.8, bottom panel).

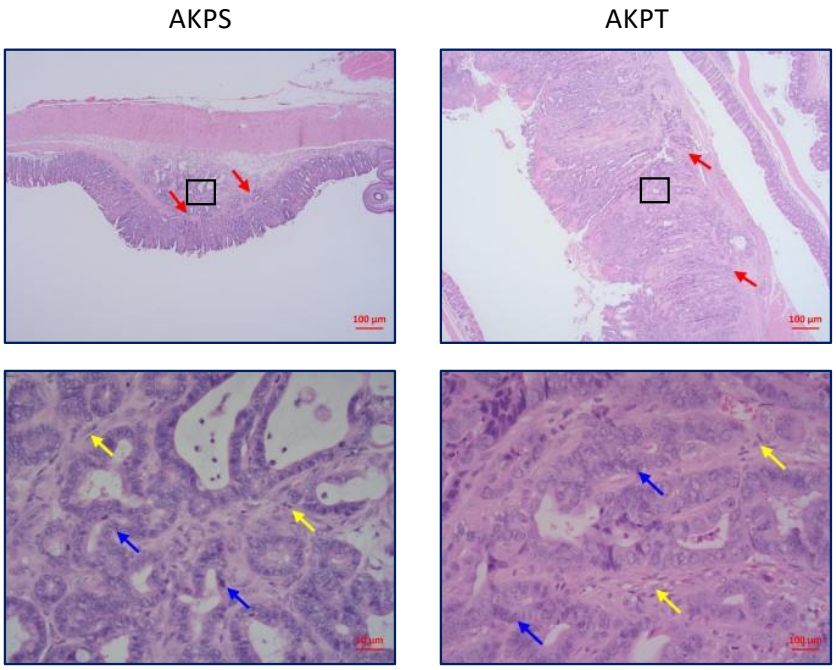

Figure 3.8: Histological Appearance of AKPS and AKPT Rectal Tumours

Top – Representative overview images (x4 magnification) of locally induced AKPS and AKPT rectal tumours. Red arrows indicate invasion through muscularis mucosa. Bottom – Representative images (x40 magnification) of AKPS and AKPT rectal tumours. Blue arrows demonstrate moderately differentiated tumour epithelium. Yellow arrows indicate infiltrated tumour stroma. Scale bars = 100μm (top images) and 10μm (bottom images).

Heterozygous *Apc* deletion successfully slowed tumour latency, increased survival, and enabled the development of progressive histological features in keeping with invasive adenocarcinoma, when compared with the AK and AKP models. A comparison between homozygous and heterozygous *Apc* deletion in both AK and AKP models would be required to further investigate the effect of heterozygous *Apc* deletion on tumour latency, survival, and whether more advanced histological features develop.

At clinical endpoint, mesenteric lymph nodes and relevant organs (lungs, liver, pancreas, and spleen) were harvested to assess local and distant tumour dissemination. Neither local lymph node dissemination nor distant metastasis were observed in the AKPS model; however, lung and liver metastases were seen

in the AKPT model (Figure 3.9, bottom panel). Although a small cohort of animals were induced for model development and characterisation, a distant metastasis rate of 14.3% was observed in the AKPT model (Figure 3.9, top panel).

	AKPS	AKPT
Total Number	11	14
Lymph Node Metastasis	0/11	0/14
Distant Metastasis	0/11	2/14
Liver	0/11	2/14
Lungs	0/11	1/14

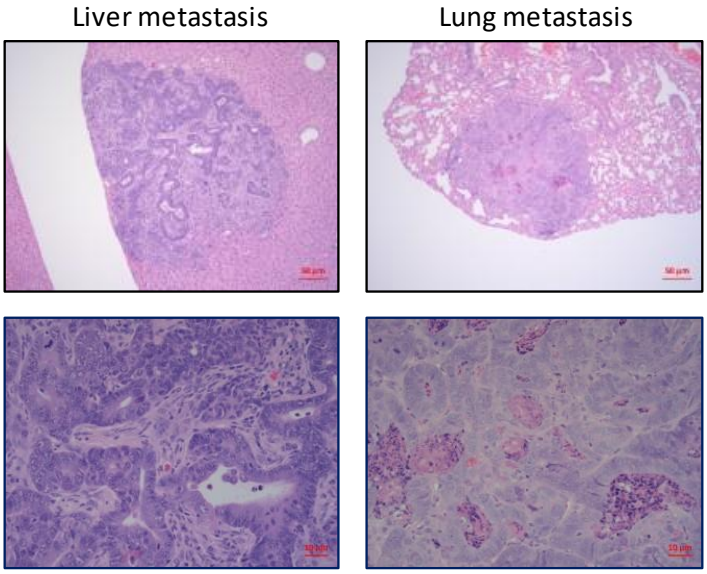

Figure 3.9: Evaluation of Metastasis in the AKPS and AKPT Models.

Top – Table depicting incidence of local and distant metastasis in both models. Middle and bottom – Representative images of liver and lung metastasis (x10 and x40 magnification). Scale bars 50μm (middle images) and 10μm (bottom images).

The locally inducible AKPS and AKPT models of LARC recapitulate locally aggressive rectal adenocarcinoma, and in addition the AKPT genotype distant metastasis with a low penetrance to the sites commonly observed in human rectal cancer. Significant limitations of these models, are the requirement for extensive in-house breeding, and the significant time and cost burden associated with generating sufficient quantities of animals to enable pre-clinical treatment studies. Both models show heterogeneous survival (AKPS range 45 – 155 days; AKPT range 50 – 155 days), with tumours typically becoming clinically detectable

between 4-8 weeks; further characterisation would be required to establish the optimum time-point post-induction to initiate treatment studies, through determining the time to develop sufficient tumour burden and histological features of invasion.

As well as utilising the locally induced AKPS and AKPT rectal cancer cohorts for model characterisation, tumour tissue was exploited to develop primary rectal tumour organoid lines in both genotypes (Figure 3.10). When significant tumour burden was encountered upon sampling, tumour pieces were harvested separately to generate tumour derived organoid lines (Figure 3.10, top panel). To assess the ability of primary rectal tumour derived organoid lines to establish orthotopic rectal tumours, I transplanted AKPS tumour derived organoids at the rectal submucosa of C57Bl/6 syngeneic mice (n=10) under colonoscopy guidance. Rectal tumours established in 100% of animals at one week post injection of organoids, as determined by colonoscopy monitoring (Figure 3.10, bottom panel).

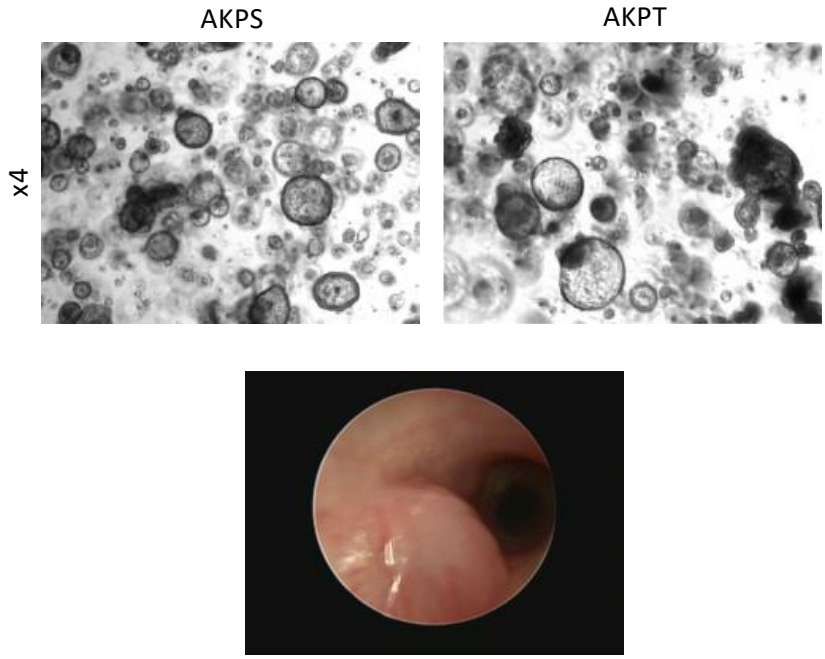

Figure 3.10: Development of Primary Rectal Tumour Derived Organoids

Top - Representative Brightfield images (x4) of both AKPS and AKPT rectal tumour derived organoids prior to cryopreservation. Bottom – Representative colonoscopic image of rectal tumour derived following submucosal injection of AKPS tumour derived organoids.

I have demonstrated the feasibility of establishing primary murine rectal tumour derived organoid lines harbouring mutational combinations of interest, which

can then be successfully transplanted under colonoscopy guidance to develop orthotopic transplant models of rectal cancer. Furthermore, this strategy might enable the rapid generation of experimental cohorts to perform time-point studies and adequately powered treatment studies.

3.2.5 An Orthotopic Model of Rectal Cancer Generated through Transplant of AKPT Organoids

I next aimed to develop an orthotopic transplant model of LARC, to enable rapid tumorigenesis and high experimental throughput. Consistent with the combination of mutations which established locally invasive rectal adenocarcinoma with low incidence of distant metastasis following localised tamoxifen induction, I utilised a previously established murine small intestinal tumour derived organoid line, expressing mutations in *Apc, Kras, Tp53* and *Tgfbr1* and herein referred to as 'AKPT'.

I sought to determine whether successful organoid engraftment is dependent upon host immune status, and so I initially undertook preliminary transplant experiments in small numbers of both C57Bl/6 immunocompetent and CD1 nude immunodeficient mice. Like the technique used during local tamoxifen induction, AKPT tumour derived organoid fragments were injected under colonoscopy guidance into the rectal submucosa, with the murine rectum defined as the most distal aspect of the colon within 1cm of the anal verge. Tumour monitoring was undertaken at 1 week post injection by colonoscopy (Figure 3.11, top panel). Comparable engraftment rates were observed following rectal injection in both C57Bl/6 and CD1 nude mice, with successful tumour engraftment in 67% and 60% respectively (Fig 3.11, middle panel). Rapid latency to tumorigenesis was observed, with large intra-luminal tumours typically being established in both groups at 1-week post-transplant (Figure 3.11, bottom panel).

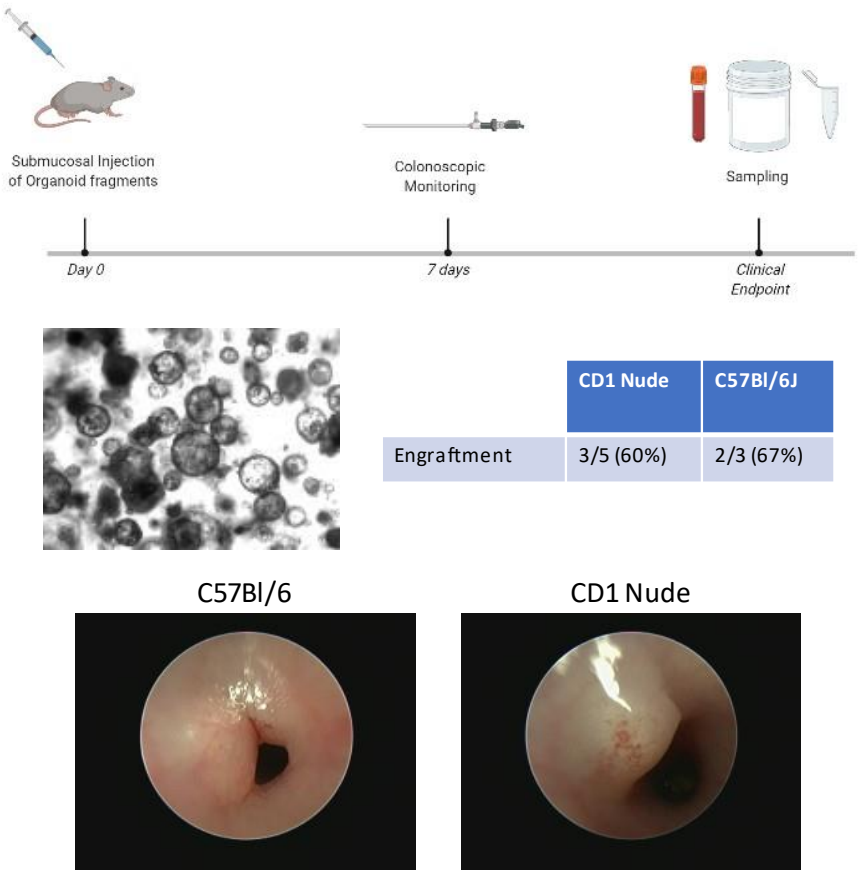

	CD1 Nude	C57Bl/6J
Engraftment	3/5 (60%)	2/3 (67%)

Figure 3.11: Establishing Tumours following Orthotopic Transplant of AKPT Organoids.

Top – Schematic depicting experimental timeline for orthotopic injection of AKPT organoid fragments. Middle – Representative images (Left) of AKPT tumour derived organoids prior to transplant (x4 magnification). Table (Right) depicting engraftment rates in both C57Bl/6 and CD1 nude mice. Bottom – Representative colonoscopy images of AKPT tumours in both C57Bl/6 and CD1 nude hosts at 1-week post injection.

Tumours which established following orthotopic transplant of AKPT organoid fragments, demonstrated several features of aggressive disease with rapid intramural tumour growth being observed. In both models, animals reached clinical endpoint at short time intervals post-transplant (Figure 3.12, top panel), with median survival of 20.5 days in C57Bl/6 mice and 43 days in CD1 nude mice observed. Significantly longer survival was demonstrated in the immunodeficient host, although only small cohorts were initially characterised. The clinical signs exhibited prior to endpoint were consistent with significant primary tumour burden, with animals showing weight loss, associated colonic obstruction, and visible external pelvic swelling in some animals. This organoid transplant model displayed a contrasting phenotype local tamoxifen induced model, which tended to show signs of chronic disease burden such as weight loss and anaemia at clinical endpoint.

Histological assessment was carried out by analysing H+E stained tumour sections with a pathologist. Tumour was found to infiltrate through the muscularis propria layer with an invasive front extending towards the serosa in both models, consistent with T3 disease (Figure 3.12, middle panel). Interestingly, in the C57Bl/6 host, tumours typically failed to invade into the mucosal layer due to its originating injection site being within the submucosal layer. However, in the immunodeficient CD1 nude host the mucosal layer was clearly infiltrated by malignant tumour cells, suggesting that differences in host tumour micro-environment exist which result in organoid derived tumours being unable to overcome components of the intestinal epithelial barrier when transplanted into an immunocompetent host (Figure 3.12, middle panel). Both tumour models demonstrate moderately differentiated adenocarcinoma, with a significant proportion of tumour consisting of stroma. As anticipated, the stromal compartment of C57Bl/6 host tumours show dense infiltration by immune and inflammatory cells, a feature which was not seen as abundantly in tumours in CD1 nude mice (Figure 3.12, bottom panel).

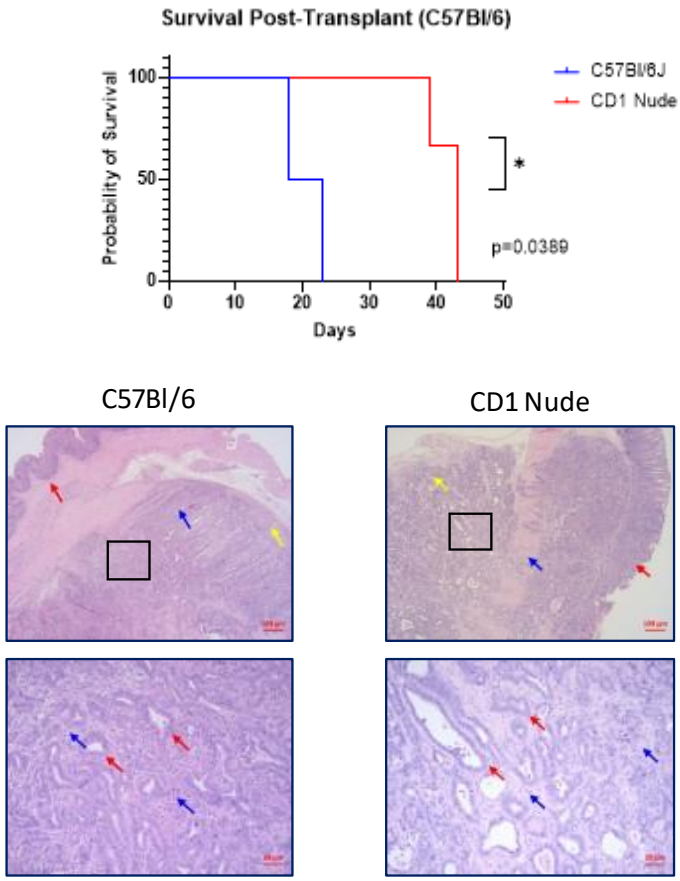

Figure 3.12: The AKPT Organoid Transplant Model is Characterised by Aggressive Disease.

Top – Survival curve demonstrating survival in the AKPT organoid transplant model in CD1 nude and C57Bl/6J hosts. n=2-3. Log Rank Test – p=0.0389. *denotes significant p-value ($p<0.05$). Middle – Representative H+E images of AKPT tumours (x4 magnification). Red arrows demonstrate mucosal layer. Blue arrows indicate invasion through muscularis propria. Yellow arrows indicate invasion towards serosa. Bottom – Representative H+E images of AKPT tumours (x20 magnification). Red arrows indicate moderately differentiated tumour epithelium. Blue arrows indicate tumour stroma. Scale bars 100μm (middle images) and 20μm (bottom images).

Local mesenteric lymph nodes and relevant organs (liver, lungs, pancreas and spleen) were harvested and analysed by H+E staining to determine presence of metastasis. Distant metastases were observed in both the CD1 nude immunodeficient and C57Bl/6 immunocompetent hosts, although experimental numbers were too small to characterise metastasis rates (Figure 3.13, top panel). Encouragingly, distant metastasis was observed in the lungs in the distribution attributed to mid- and low rectal cancers in humans, whereby pulmonary metastases are more frequently observed owing to the systemic venous drainage of the mid/lower rectum via the middle and inferior rectal veins (Figure 3.13, middle and bottom panels). Metastases were typically not evident on sampling, and were only visible when organs were examined by

microscopy. Preliminary experiments successfully demonstrated engraftment of AKPT tumour derived organoids in an immune competent host, resulting in a model of locally invasive adenocarcinoma, with the small cohort studied suggesting that distant metastasis might occur in a similar manner to low- and mid-rectal cancer clinically.

	C57Bl/6	CD1 Nude
Total Number	2	3
Lymph Node Metastasis	0/2	0/3
Distant Metastasis	1/2	3/3
Lungs	1/2	3/3

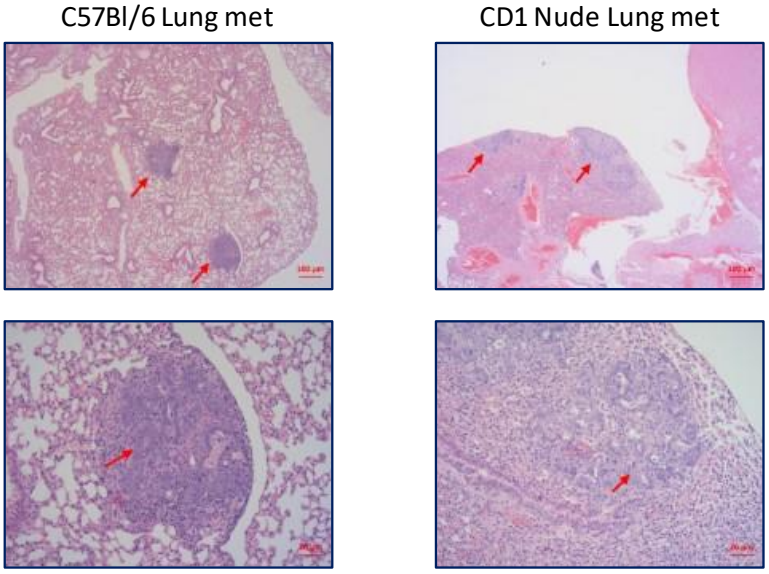

Figure 3.13: Metastatic Characterisation of the AKPT Organoid Transplant Model

Top – Table showing distribution of local and distant metastasis in the AKPT transplant model for both CD1 nude and C57Bl/6J host. Middle – Representative images of lung metastases in both C57Bl/6 and CD1 nude mice (x4 magnification). Bottom – Representative images of corresponding lung metastases (x20 magnification). Scale bars 100μm (middle images) and 20μm (bottom images). Red arrows depict micro-metastatic deposits.

To develop a pre-clinical model suitable for studying the biological mechanisms underlying tumour response to radiotherapy, and to investigate novel immunotherapy agents, an immunocompetent host is crucial to recapitulate the human condition. Therefore, I sought to further develop and characterise the AKPT organoid transplant model in C57Bl/6 mice, given that preliminary experiments were conducted in very limited cohorts. Following successful engraftment in preliminary experiments, subsequent experiments conducted in

expanded cohorts demonstrated tumour engraftment in 95% of animals (n=80, across 6 independent experiments). Short survival was again demonstrated in this model, with a median survival of 34 days observed when animals were untreated and aged until clinical endpoint (Figure 3.14).

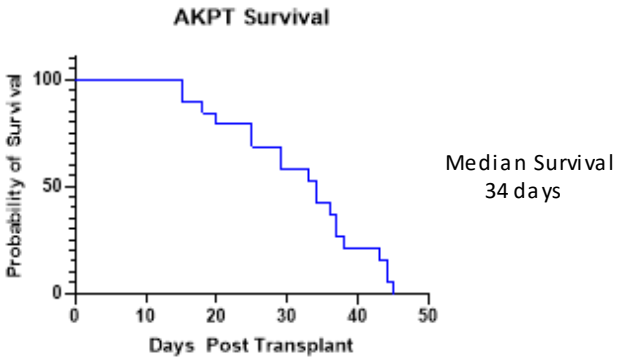

Figure 3.14: Survival in the Immunocompetent AKPT Organoid Transplant Model

Survival curve demonstrating time to clinical endpoint in the AKPT rectal organoid transplant model.

A more extensive characterisation of metastatic burden was carried out, through examination of mesenteric lymph nodes, lungs, liver, pancreas and spleen by H+E staining. An overall distant metastasis rate of 18% was observed in this model (n=91 total). A similar distribution was seen with metastases observed exclusively in the liver and/or lungs (Figure 3.15, middle panel). Although highly penetrant metastasis was not observed, this is likely to reflect the short survival seen in the model. Mice typically reached clinical endpoint due to primary tumour burden, typically displaying signs of weight loss, intestinal obstruction, or pelvic swelling secondary to an enlarging tumour mass. Interestingly, distant metastases showed high levels of Lgr5 stem cell marker expression, in keeping with findings in human CRC noting increased Lgr5 expression at the invasive tumour front and in distant metastases, with Lgr5 expression also being associated with treatment resistance (Uchida et al, 2012; Hsu et al, 2013).

	Total Number	Percentage
No Metastasis	75	82%
Distant Metastasis	16	18%

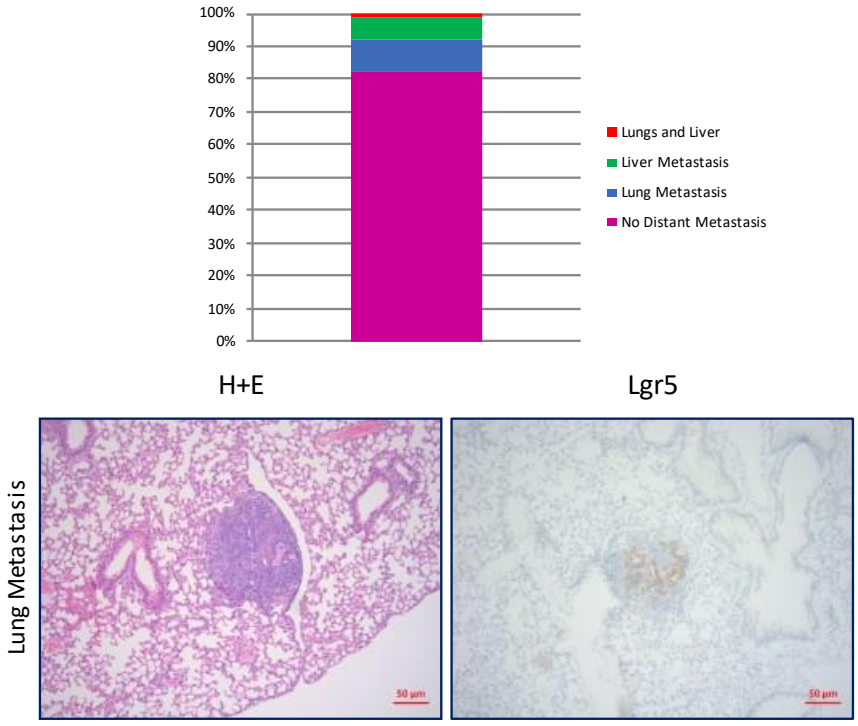

Figure 3.15: Characterisation of Metastasis in the AKPT Organoid Transplant Model.

Top – Table showing overall rate of distant metastasis (n=91 total). Middle - Graph depicting frequency and distribution of metastases. Bottom – representative H+E stain of lung metastasis (Left), and corresponding representative Lgr5 stain (x10 magnification). Scale bars 50µm.

3.2.6 Immune Characterisation of the Orthotopic AKPT Rectal Models

Having developed numerous orthotopic AKPT models of rectal cancer, through localised tamoxifen induction and transplant of tumour derived organoids in both immunocompetent and immune-deficient hosts, I sought to characterise the tumour immune microenvironment of these models. I aimed to identify differences which arise according to host immune status, and to determine whether tumour induction method influences the tumour microenvironment. It is well understood that the immune contexture of the tumour microenvironment is complex and heterogenous, and impacts upon responses to therapy; in the context of LARC, both increased CD4+ and CD8+ T-cell density and low T-reg cell density have been associated with pathological response to CRT (Yasuda et al, 2010; McCoy et al, 2015; Binnewies et al, 2018). Knowledge of the underlying

tumour immune microenvironment might enable prediction of the response to radiotherapy and/or immunotherapy in the models. It is known that the adaptive immune response and characteristics of tumour infiltrating immune cells are a valuable prognostic tool; a high 'immunoscore', calculated through the densities of cytotoxic and memory T cells at both the invasive margin and tumour core, is predictive of improved patient survival (Galon et al, 2006; Mlecnik et al, 2016).

The concept of immune infiltrated tumours whereby cytotoxic lymphocytes (CTLs) are excluded from the tumour core, suggests a mechanism of tumour immune escape (Spranger et al, 2016). I aimed to characterise the tumour microenvironment in the AKPT models, including tumours generated through local tamoxifen induction, and models generated through the injection of AKPT tumour derived organoids in both the C57Bl/6 and CD1 nude hosts. Immunohistochemistry was used to quantify common immune cell populations and to determine their location within tumours, with a combination of digital and manual scoring performed to quantify density of immune cells.

CD3+ staining was used as a pan T-cell marker, with a strikingly high expression identified in tumours derived following AKPT organoid transplant in C57Bl/6 hosts (Figure 3.16, top panel). In the immunocompetent AKPT organoid transplant model, CD3+ expressing cells were significantly more abundant when compared with both AKPT tumours derived following tamoxifen induction ($p=0.0079$) and following organoid transplant in the immunodeficient CD1 nude host ($p=0.0357$), when the whole tumour area was assessed (Figure 3.16, bottom panel). Of note, a small number of CD3+ expressing cells were seen in AKPT tumours transplanted in CD1 nude hosts, in contrast with what would be expected in a thymic deplete host (Pelleitier et al, 1975). CD1 nude mice possess a vestigial thymus which is incapable of producing mature T-cells, however, T-cell precursors in the bone marrow and immature T-cells express cytoplasmic CD3 (van Dongen et al, 1988).

When regional analysis was performed, it was observed that CD3+ cells are more densely clustered at the tumour invasive margin, particularly in the immunocompetent transplant model (Figure 3.16, top panel). Across all models, lymphocytic infiltration is observed to be spare within the tumour core, and suggestive of an immune-excluded phenotype whereby tumoricidal immune cell populations are unable to penetrate the tumour core (Figure 3.16, middle

panel). The concept of 'cold tumours,' characterised by lack of T-cell infiltration, is well known to correspond with lack of response to immune checkpoint inhibition, and it can be anticipated that these models may represent tumours resistant to immunotherapy (Bonaventura et al, 2019).

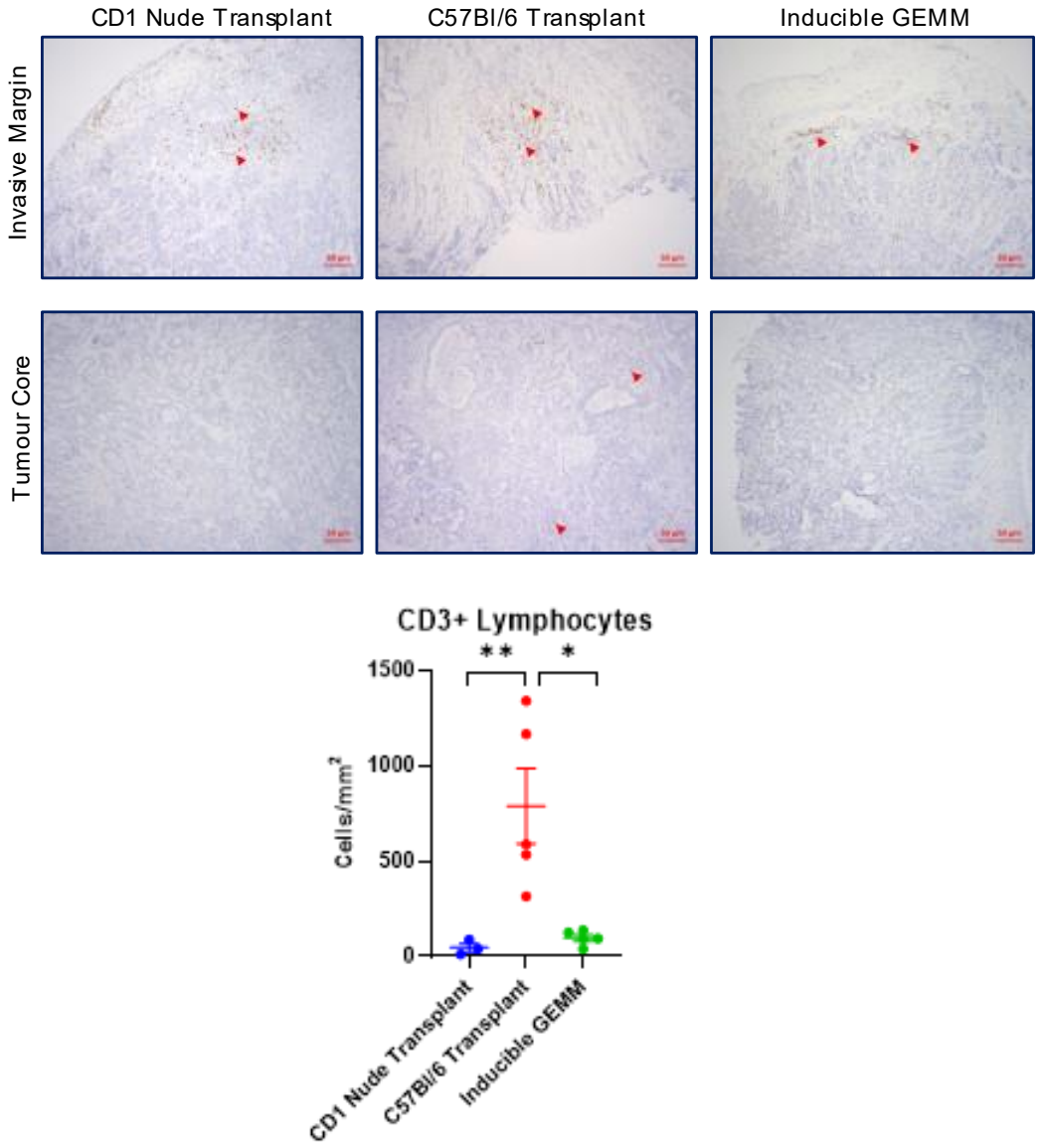

Figure 3.16: CD3+ Lymphocyte Infiltration in the AKPT Rectal Models

Top – Representative images of CD3 IHC staining (x10 magnification) in AKPT rectal models at the tumour invasive margin. Middle – Representative images of CD3 IHC staining (x10 magnification) at the tumour core. Bottom – Bar graph depicting whole tumour scoring of CD3+ lymphocytes. Scale bars 50µm. Red arrows depict CD3+ cells. * denotes p value <0.05. ** denotes p value <0.01. n=3-5. Mann Whitney U-test.

Having quantified all T-cells within whole tumour sections through CD3 staining, I aimed to quantify the presence of cytotoxic T-lymphocytes (CTLs) which are an important component of cell-mediated immunity against cancer. IHC was

performed to detect CD8+ expressing T-cells in the orthotopic AKPT rectal cancer models. Similarly, the majority of CD8+ CTLs were observed at the invasive margin of AKPT organoid transplant tumours in C57Bl/6 mice, with these cells very rarely detected in the CD1 nude host or in locally induced tumours (Figure 3.17, top panel). CD8+ expressing T-cells were seen very sparsely in the tumour core of all tumour models (Figure 3.17, middle panel). Due to background staining within tumour epithelium, these stains were scored manually by microscopy, with significantly elevated numbers seen in C57Bl/6 transplant tumours when compared with the CD1 nude ($p=0.0357$) and inducible GEMM ($p=0.0079$), when the whole tumour area was assessed (Figure 3.17, bottom panel).

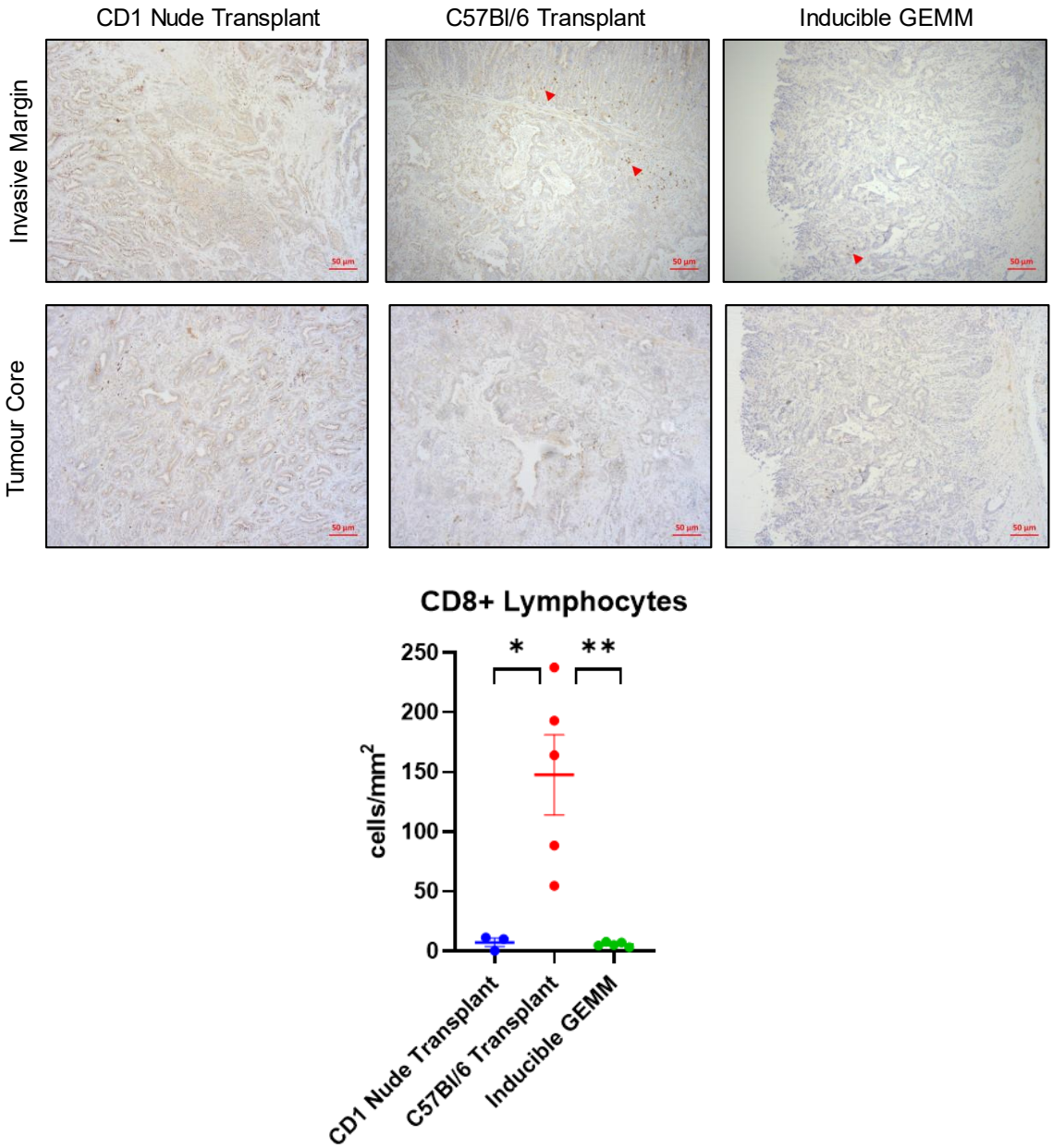

Figure 3.17: CD8+ Lymphocyte Infiltration in the AKPT Rectal Models

Top – Representative images of CD8 IHC staining (x10 magnification) in AKPT rectal models at the tumour invasive margin. Middle – Representative images of CD8 IHC staining (x10 magnification) in the tumour core. Bottom – Bar graph depicting manual scoring of CD8+ lymphocyte in whole tumour sections. 10 representative x20 FOV areas scored per tumour section, with mean values plotted as cells/mm^2. Scale bars 50µm. Red arrows depict CD8+ cells. * denotes p value <0.05. ** denotes p value <0.01. n=3-5. Mann Whitney U-test.

I next sought to characterise the myeloid cell component of the tumour immune microenvironment in the AKPT models, and first quantified macrophages through F4/80 staining. In all model types, dense macrophage populations were observed at the tumour invasive margin (Figure 3.18, top panel). In both organoid

transplant models, significant macrophage infiltration was seen in the stromal regions of the tumour core, with sparse numbers observed in the tumour stroma of locally induced tumours (Figure 3.18, middle panel). Macrophages were quantified using digital pathology to calculate the % of whole tumour area positively stained for F4/80 (Figure 3.18, bottom panel). When whole tumours were analysed, significantly increased macrophage populations were observed in organoid transplant tumours in immunocompetent C57Bl/6 mice, when compared with the CD1 nude immunodeficient host (p=0.0357) and with inducible GEMM tumours (p=0.0079).

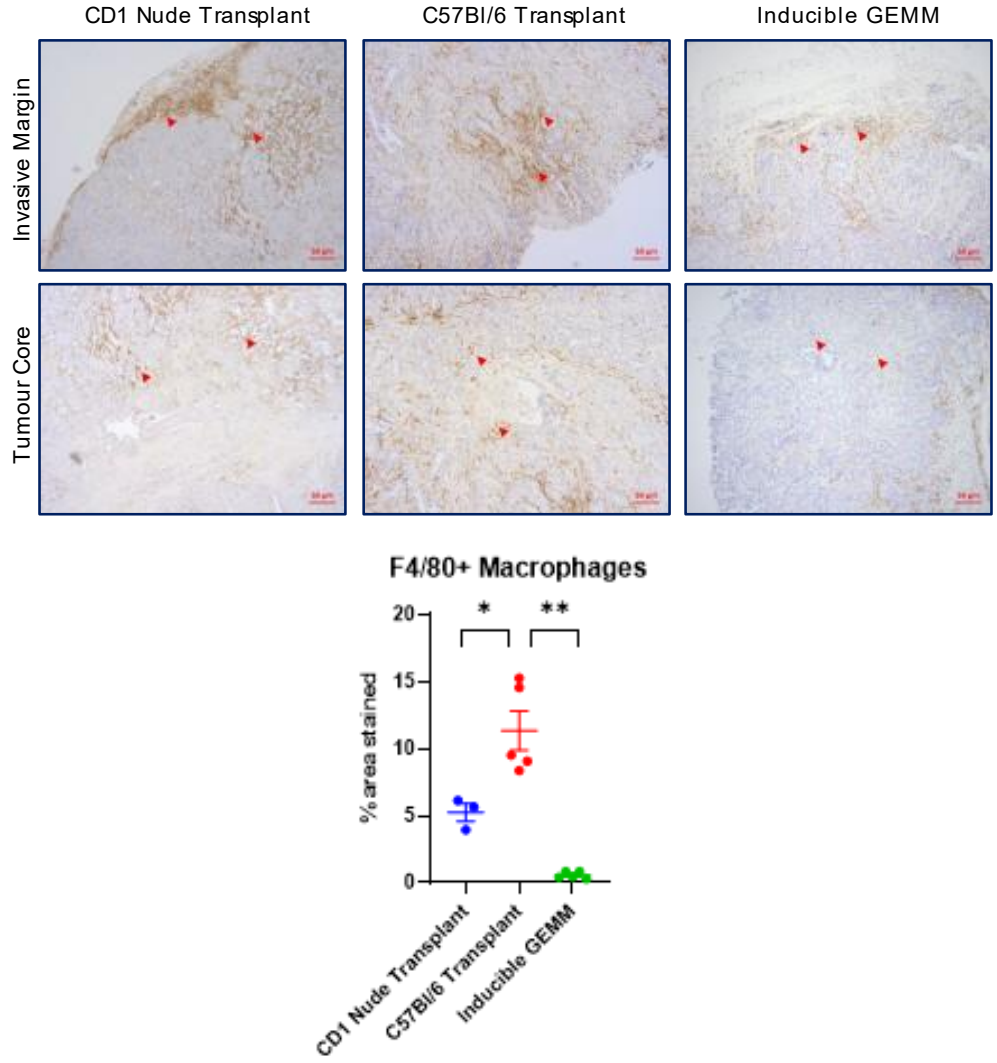

Figure 3.18: F4/80+ Macrophage Infiltration in the AKPT Rectal Models

Top – Representative images of F4/80 IHC staining (x10 magnification) in AKPT rectal models at the tumour invasive margin. Middle – Representative images of F4/80 IHC staining (x10 magnification) at the tumour core. Bottom – Bar graph depicting quantification of F4/80+ macrophages as % whole tumour area stained. Scale bars 50μm. Red arrows depict F4/80+ cells. * denotes p value <0.05. ** denotes p value <0.01. n=3-5. Mann Whitney U-test.

Macrophages have been identified as a potential mechanism of CD8+ CTL exclusion from tumour cell regions and prevention of their interaction with cancer cells, thus being an important determinant of the 'immune excluded' phenotype which plays a potential role in resistance to immunotherapy (Beatty et al, 2015; Peranzoni et al, 2018). Peranzoni et al show that macrophage interaction with CTLs, leads to reduced CD8+ cell motility and migration towards tumour cells. Similarly, Beatty et al demonstrate that Ly6C(low) F4/80(+) macrophages regulate infiltration of CTLs in a pancreatic ductal adenocarcinoma (PDAC) model.

Next, I assessed the presence of neutrophils within the tumour microenvironment using IHC staining for S100A9/Calgranulin B, a protein abundantly present in the cytoplasm of neutrophils (Sprenkeler et al, 2022). Interestingly, these cells were observed to densely cluster at the invasive margins of both the CD1 nude transplant model and inducible GEMM (Figure 3.19, top panel). Relatively smaller numbers were observed in both regions of tumour in the C57Bl/6 immunocompetent AKPT organoid transplant model (Figure 19, middle panel). When S100A9 expressing cells were scored across the whole tumour area, significantly less S100A9+ve cells were demonstrated in the C57Bl/6 transplant model ($p=0.0357$ versus CD1 nude; $p=0.0079$ versus inducible GEMM) (Figure 3.19, bottom panel). Indeed, S100A9/A8 protein is known to be expressed abundantly in both neutrophils and undifferentiated monocytes, with expression being lost upon monocyte differentiation and so the higher numbers observed in CD1 nude and inducible GEMM tumours may reflect immature myeloid lineages (Lagasse et al, 1992).

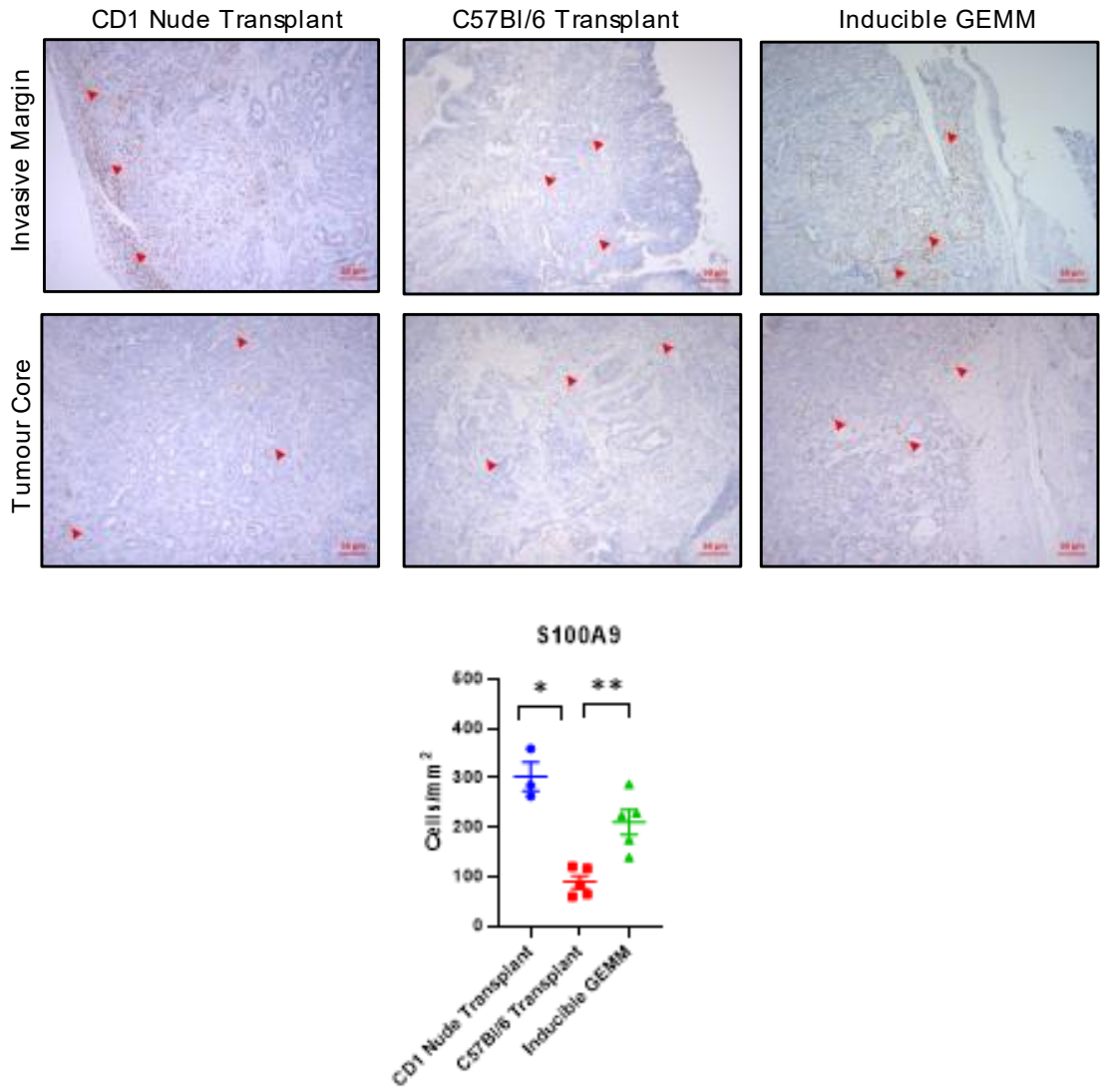

Figure 3.19: S100A9+ve Cell Quantification in the AKPT Rectal Models

Top – Representative images of S100A9 IHC staining (x10 magnification) in AKPT rectal models at the tumour invasive margin. Middle – Representative images of S100A9 IHC staining (x10 magnification) at the tumour core. Bottom – Bar graph depicting quantification of S100A9+ve cells in whole tumour sections. Scale bars 50μm. Red arrows depict S100A9+ cells. * denotes p value <0.05. ** denotes p value <0.01. n=3-5. Mann Whitney U-test.

I next aimed to quantify immunosuppressive T-regulatory cells (Tregs), which are known to play a role in limiting the activation of aberrant and over-reactive lymphocytes, thus preventing auto-immunity under normal physiological circumstances (Sakaguchi et al, 2008). However, Tregs can contribute to tumour development and progression by inhibiting components of anti-tumour immunity, with high levels of infiltration being associated with poor survival (Ohue and Nishikawa, 2019). Tregs were identified through IHC staining for FOXP3. Tregs are a differentiated T-cell population, and as anticipated were absent from tumours transplanted in CD1 nude mice. Populations were observed in the

tumour invasive margins in both the inducible GEMM and C57Bl/6 organoid transplant models, suggesting a potential mechanism of anti-tumour immunity at the invasive front (Figure 3.20, top panel). Significantly higher populations of Tregs were observed in the C57Bl/6 organoid transplant model (p=0.0357 versus CD1 nude; p=0.0317 versus inducible GEMM) when assessed across whole tumour sections (Figure 3.20, bottom panel).

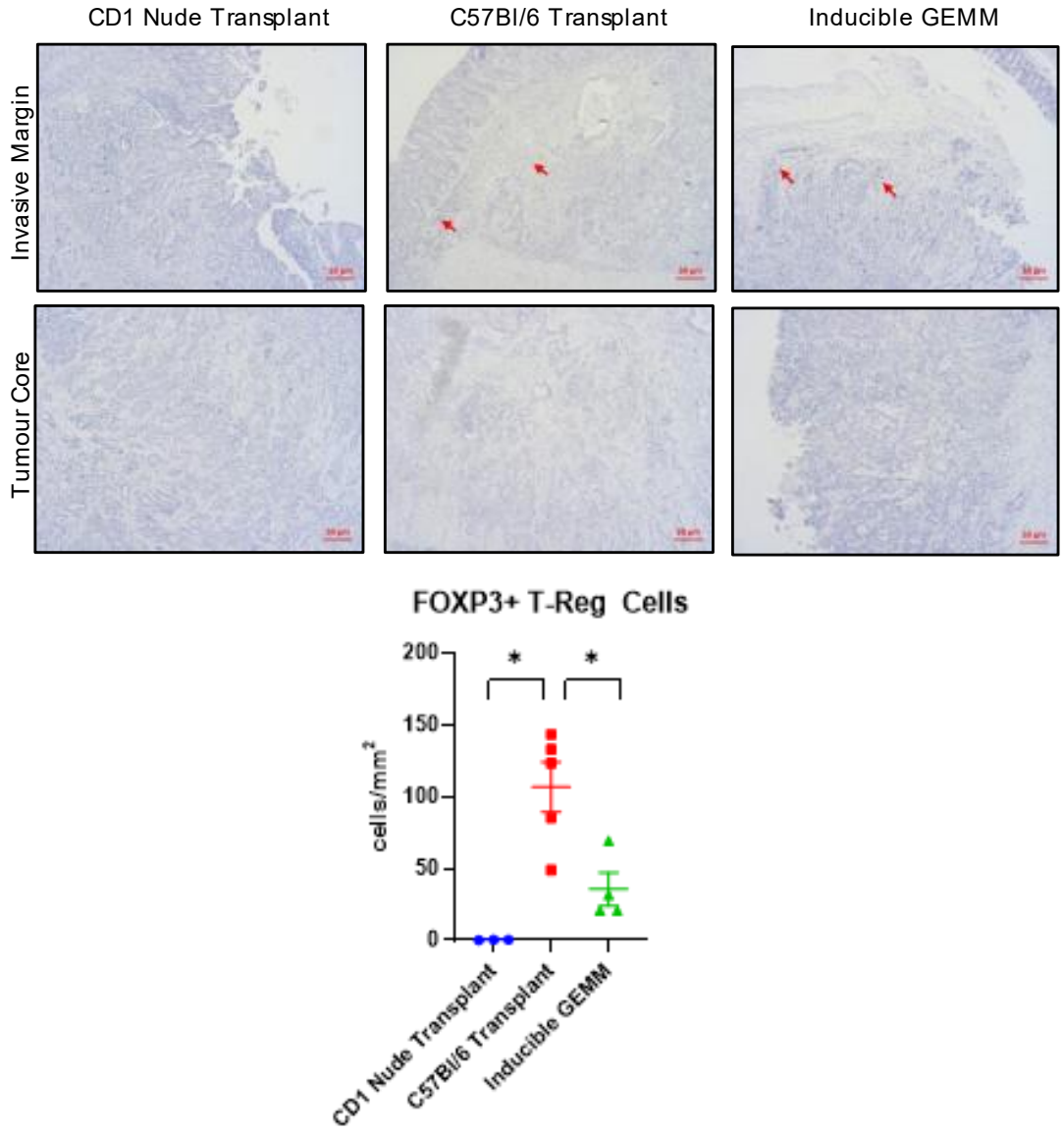

Figure 3.20: Quantification of FOXP3+ Cells in the AKPT Rectal Models

Top – Representative images of FOXP3 IHC staining (x10 magnification) in AKPT rectal models at the tumour invasive margin. Middle – Representative images of FOXP3 IHC staining (x10 magnification) at the tumour core. Bottom – Bar graph depicting quantification of FOXP3+ cells across whole tumour sections. Scale bars 50μm. Red arrows depict FOXP3+ cells. * denotes p value <0.05. n=3-5. Mann Whitney U-test.

3.2.7 TGF-ß Expression in the Orthotopic AKPT Rectal Models

I next sought to characterise the presence of TGF-ß signalling within the AKPT tumour models. Under normal conditions, TGF-ß is known to maintain tissue homeostasis through regulatory functions in cell proliferation, differentiation and survival, and prevents tumour progression under normal physiological circumstances. However, cancer cells can overcome these suppressive influences, and pathological tumour-derived TGF-ß signalling can modulate the tumour microenvironment to avert immune surveillance and promote tumour growth, invasion and metastasis (Massagué, 2008). Tumours with high levels of defective TGF-ß signalling may be more able to evade immune surveillance and create a pro-tumourigenic and pro-metastatic niche.

TGF-ß induces the association of type I and type II TGF-ß receptors, which are then activated to catalyse the phosphorylation of SMAD protein transcription factors including SMAD3, which in turn enter the nucleus to form complexes with SMAD4 which then subsequently induce transcriptional effects. IHC was therefore performed to detect the presence of phosphorylated SMAD3, to determine TGF-ß signalling activity within tumours. pSMAD3 was highly expressed in both the tumour epithelium and stroma of all three groups analysed (Figure 3.21, top panel). Furthermore, quantification reveals that the majority of cells within AKPT tumour models express nuclear pSMAD3 thus demonstrating high levels of TGF-ß signalling in these models (Figure 3.21, bottom panel). AKP murine rectal tumour derived organoids (*VillinCreER;Apc$^{fl/fl}$;Kras$^{G12D/+}$;Trp53$^{fl/fl}$*) without TGF-ß pathway mutation, and injected at the murine rectum were also analysed for comparison; although nuclear pSMAD3 expression appears less abundant in AKP organoid tumours, statistical significance was not reached and heterogeneity of nuclear pSMAD3 expression was noted upon quantification in AKP tumours (Figure 3.21, bottom panel).

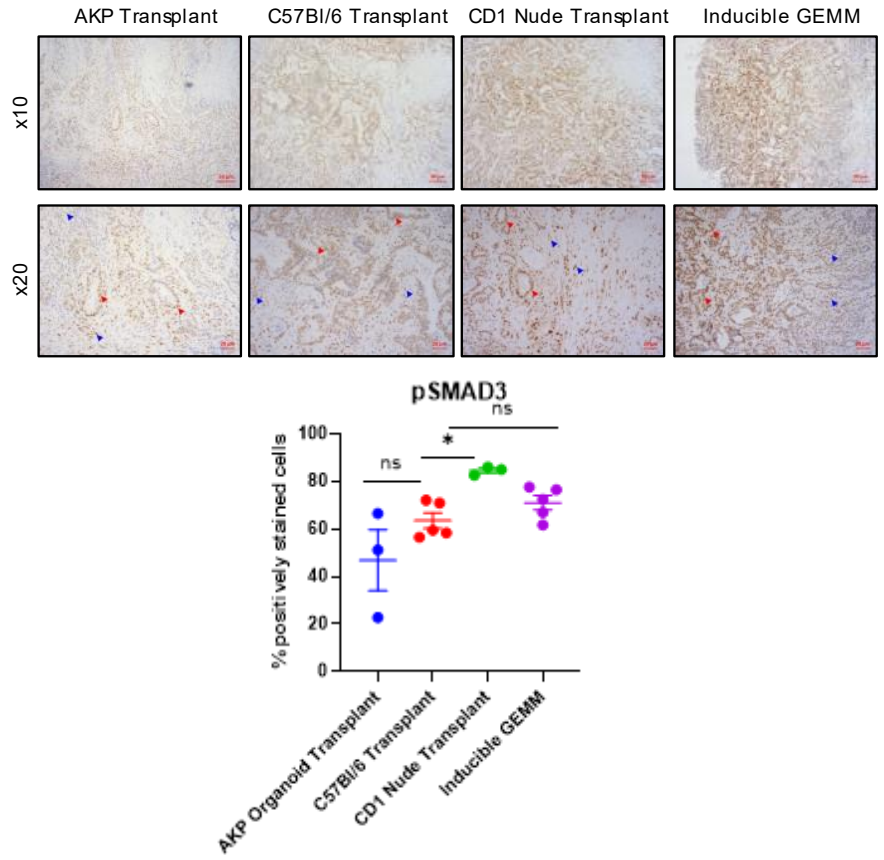

Figure 3.21: Quantification of Nuclear pSMAD3 Expression in the AKPT Rectal Models

Top – Representative images of pSMAD3 IHC staining (x10 magnification) in AKPT rectal models and AKP rectal organoid transplant model. Middle – Representative images of pSMAD3 IHC staining (x20 magnification) to demonstrate staining of both tumour epithelium and stroma. Red arrows show pSMAD3 expression in tumour epithelium. Blue arrows show pSMAD3 expression in stromal cells. Bottom – Bar graph depicting quantification of nuclear pSMAD3 expressing cells, with % of all cells positively stained being assessed. Scale bars 50μm. * denotes p value <0.05. ns denotes non-significance p≥0.05. n=3-5. Mann Whitney U-test.

AKPT organoid transplant and locally induced tumour models demonstrated highly abnormal and abundant TGF-β signalling, identifying a potential driver of the invasive properties displayed by the models. TGF-β expression by stromal cells potentially leads to excessive inflammation and promotion of tumour progression. Furthermore, TGF-β signalling by tumour epithelial cells is also likely to favour tumour progression through suppression of anti-tumour immune responses.

3.2.8 Transcriptomic Alignment of AKPT Rectal Cancer Models with Molecular Subtypes of Human CRC

I next aimed to characterise rectal tumours derived following AKPT tumour derived organoid transplantation into C57Bl/6 immunocompetent hosts, as this model will be used throughout subsequent experiments in this thesis. RNA sequencing data was analysed from tumour tissue of untreated AKPT tumours (n=5) to attempt to align this tumour model with the CMS (Consensus Molecular Subtypes) subtypes. The newly developed data analysis platform Molecular Subtyping Resource (MouSR) was used for interrogation of RNA sequencing data (Ahmaderaghi et al, 2022). Firstly, I conducted 2D Principal Component Analysis to assess basic characteristics of the samples and to identify inter-tumour heterogeneity (Figure 3.22). Samples are clearly demonstrated to cluster unevenly suggesting significant heterogeneity between tumour tissue samples.

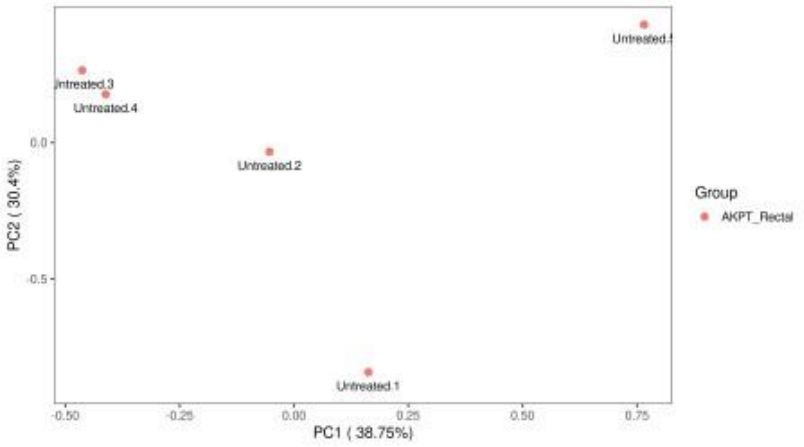

Figure 3.22: Inter-Tumour Heterogeneity between AKPT Rectal Tumour Samples

2D Principal Component Analysis (PCA) Plot of Rectal Tumour Samples derived from the Orthotopic AKPT Organoid Transplant Model. n=5, each sample plotted. Analysis performed through prcomp function in the R stats package, embedded in the MouSR resource (https://mousr.qub.ac.uk/).

I next sought to align the AKPT model with human CMS subtypes of CRC. Using the MouSR application, CMS classification in murine samples can be conducted through conversion of the human CMS template to mouse orthologues. Significant alignment with CMS4 is seen in two out of five samples, and correspond with the two samples which cluster closely together in 2D PCA (Figure 3.23). Alignment to each of the other subtypes is observed in only

individual samples, but in the case of the sample aligning to CMS2 statistical significance was not reached (Figure 3.23). This data gives an indication that this model may align with CMS4, however, results are likely to be confounded by sampling variability with heterogeneity potentially resulting from different regions of tumour being sampled. Furthermore, CMS alignment would need to conducted on a significantly larger sample size if any conclusions are to be drawn about whether the AKPT model conforms reliably to any subtype.

Similarly, molecular stratification in patients can be significantly confounded by stromal-derived intra-tumoural heterogeneity, with variability between sampled tumour regions affecting the ability of gene expression signatures to cluster samples (Dunne et al, 2016). Evidently, gene expression varies between different regions of tumour due to variation in the content of the tumour microenvironment, which potentially explains the inability to consistently align tumour samples to a particular CMS subtype. The CMS4 subtype is heavily reliant upon stromal gene expression, and is thus more susceptible to variation in gene expression profiling between tumour regions (Isella et al, 2015).

Sample	CMS Prediction	P-value
1	1	0.001
2	2	1
3	3	0.001
4	4	0.001
5	4	0.001

Figure 3.23: Consensus Molecular Subtyping (CMS) of AKPT Rectal Tumours

Table showing individual CMS predictions for individual samples, with corresponding p-value. n=5. Analysis performed through human CMS template embedded in CMScaller, with conversion to mouse orthologues using biomaRT R stats package to remove intersected mouse genes embedded in the MouSR resource, and nearest template prediction (NTP) method used to call mouse CMS (https://mousr.qub.ac.uk/).

I next aimed to estimate the abundance of various cell populations within the tumour micro-environment using RNA sequencing data. Notably, no individual

immune or stromal cell populations were universally expressed across tumour samples, highlighting the heterogenous nature of tumour tissue analysed (Figure 3.24). Only two samples were enriched for T-cell populations, with neutrophils and macrophage populations also enriched in a limited number of samples.

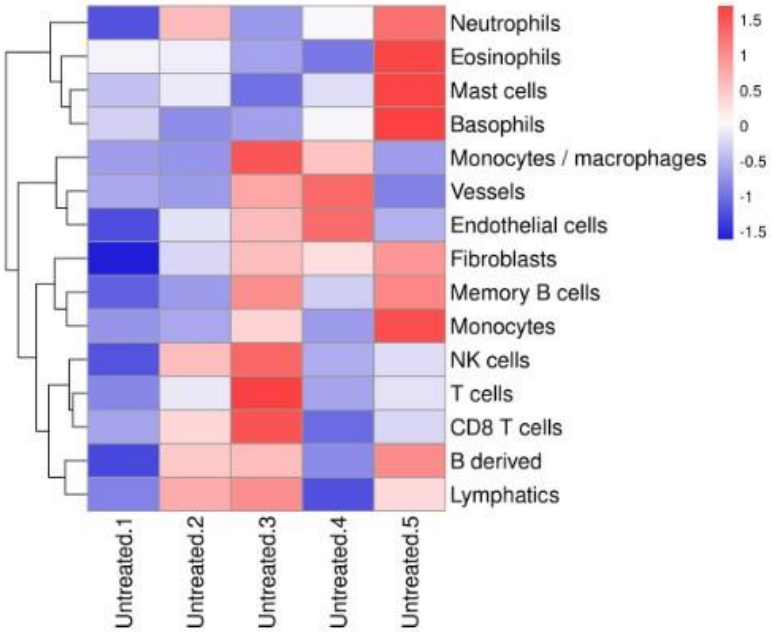

Figure 3.24: Microenvironment Cell Populations (mMCP) within AKPT Rectal Tumours

Heatmap to demonstrate estimated immune and stromal cell populations within individual AKPT rectal tumour samples. n=5, each sample represents one column of heatmap. Each row represents immune or stromal cell type as detailed on y-axis. Legend indicates z-score to indicate number of standard deviations above or below the mean. Murine MCP (mMCP) counter R package embedded in MouSR application used to perform analysis (https://mousr.qub.ac.uk/).

It is evident that alignment with transcriptomic subtypes of CRC is reliant upon consistent tumour biopsy sampling, to avoid intra-tumour variation in gene expression and tumour micro-environment composition. Sequencing data in this limited sample set suggests that the AKPT organoid transplant model may align with CMS4, the poor prognosis mesenchymal subtype, but given the potential for sampling variability this data should be interpreted cautiously. Furthermore, the inclusion of more tumour samples might enable more reliable alignment of transcriptomic features with human subtyping systems.

3.3 Discussion

Despite significant advances in genetic engineering strategies over the past few decades, and the achievement of advanced pre-clinical models of CRC, relatively few orthotopic models of rectal cancer exist in the literature. Previously described surgical techniques pose significant limitations with rectal tumours arising through the transplantation of commercially available cell lines, which have undergone extensive in-vitro selection and immortalisation, and furthermore fail to recapitulate the molecular characteristics of human disease. Colitis induction methods which result in distal colonic/rectal tumours also pose significant limitations, and were primarily developed to model inflammatory bowel disease (IBD) and colitis-associated CRC. Agents such as DSS result in severe acute colitis in animals, leading to epithelial injury and compromised barrier integrity, with a rapid inflammatory response following exposure of mucosal and submucosal immune cells to luminal antigens, thus creating a host niche which deviates significantly from the conditions under which the majority of CRC develops (Wirtz et al, 2017).

Ganesh et al recently described a murine rectal cancer model derived through the instillation of human rectal cancer derived organoids following colitis induction, which elegantly recapitulates the histological features and progression of human disease, and interestingly mimics the chemotherapy response observed in the corresponding patient (Ganesh et al, 2019). The models described by Ganesh et al, and recently described colonoscopy-guided organoid injection models, have relied upon immunocompromised recipient mice which lack several crucial components of the host immune system. However, immunocompetent orthotopic rectal cancer models following organoid injection post colitis induction have been described in recent literature, which have been utilised in pre-clinical treatment studies, and representing a significant advance in the modelling of LARC (Varga et al, 2020; Nicolas et al, 2022).

The aim of this chapter was to address the paucity of orthotopic rectal cancer models, through development of reproducible, immunocompetent models which recapitulate the human condition. In subsequent chapters in this thesis, I aimed to utilise developed models to study the immunological responses to radiotherapy, and to test novel radiotherapy-immunotherapy combinations.

This chapter successfully describes the development of rectal tumours through localised tamoxifen induction in a ligand-dependent site-specific Cre-recombinase system (*VillinCreER*). Such models are advantageous as they enable mutational combinations of interest to be studied, with site specific control over tumour induction. Tumours established in the mucosal layer in keeping with human disease, closely recapitulating the histology of human disease. Progressive histological changes were demonstrated in these inducible models in a manner consistent with the adenoma-carcinoma sequence, with 'AK' and 'AKP' models displaying early neoplastic changes consistent with low-grade dysplasia. The induction of localised rectal tumours in both AK (*VillinCreER:Apc*$^{fl/+}$*;Kras*$^{G12/D}$) and AKP (*VillinCreER:Apc*$^{fl/+}$*;Kras*$^{G12/D}$*;p53*$^{fl/fl}$) animals with heterozygous *Apc* deletion might slow tumour latency and prolong survival to enable the development of high grade dysplasia and early adenocarcinoma. However, it was is evident that in order to model locally invasive disease with aggressive histological features, that more complex mutational combinations were required.

More aggressive models of invasive adenocarcinoma were shown with additional TGF-ß pathway mutations (AKPS and AKPT). Although the AKPS and AKPT models successfully recapitulated locally invasive rectal adenocarcinoma, with tumours arising from the mucosal layer, they present several limitations in the context of pre-clinical treatment studies. The requirement for extensive animal breeding to generate experimental subjects and the significant latency period to tumourigenesis (≥8 weeks), pose significant limitations on the utility of this model in generating sufficient experimental animals to perform adequately powered pre-clinical treatment studies.

To develop a more reproducible, time-efficient and high throughput model, I established an organoid transplant model which gives rise to orthotopic rectal tumours following colonoscopy guided submucosal injection. A clinically relevant mutational burden of interest is expressed by the 'AKPT' organoid line used, with tumours successfully engrafting in both CD1 nude and C57Bl/6 host recipients. Given the successful engraftment in the immunocompetent host, this model was characterised further to identify key features of the tumour immune microenvironment which correspond with poor prognosis and treatment resistant disease. In the C57Bl/6 host, the high engraftment rate observed (95%) coupled

with the rapid latency to tumourigenesis (1 week) make this a highly reproducible model which is amenable to the rapid generation of experimental numbers.

Furthermore, this chapter sought to characterise the developed AKPT rectal cancer models, to determine their relevance to human disease. A distant metastasis rate of 18% was found, predominantly to the lungs which is in keeping with the pattern of spread observed in mid- and low rectal cancer. Development of a metastatic model of LARC was not a key aim of this thesis. To study the effects of radiotherapy on the primary tumour and to test novel neo-adjuvant treatment strategies in rectal cancer, it is of paramount importance to recapitulate locally invasive disease for which such treatment is offered clinically. I demonstrated that AKPT organoid transplant tumours were representative of locally aggressive disease, with invasive adenocarcinoma and abundant stromal infiltration shown. The observation of high tumour stroma proportion is associated with poor prognosis in CRC, further suggesting that this model recapitulates patients with the poorest outcomes (Park et al, 2014).

In this chapter, I analysed the tumour microenvironment of the immunocompetent AKPT organoid transplant model and compared with the corresponding tumours in CD1 nude hosts and those derived following localised tamoxifen induction. Vastly increased populations of CD3+ and CD8+ T-cells were observed in the immunocompetent transplant model, suggestive of a significant adaptive immune response following organoid transplant. These cells were noted to be present in higher abundances at the tumour invasive margin, with relative exclusion from the tumour core, suggesting that mechanisms of adaptive resistance exist within the tumour microenvironment of the AKPT transplant model (Ribas, 2015). This was further supported by the presence of macrophages at the tumour invasive margin, which are known to affect CTL motility and migration. Furthermore, the high expression of TGF-ß signalling in this tumour model is also suggestive of an immunosuppressive tumour microenvironment. In conclusion, although significant immune cell populations exist in the immunocompetent AKPT organoid transplant model, it is likely that an ‘immune excluded’ phenotype is observed, and that tumours will potentially demonstrate treatment resistance.

In this chapter, I have described the development and characterisation of a novel immunocompetent model of LARC which undergoes distant metastasis in a proportion of animals. Characterisation of the AKPT transplant model is highly suggestive of aggressive disease with an immunosuppressive tumour microenvironment. This model will be used throughout the remainder of this thesis, where I aim to study the effects of radiotherapy on the tumour immune microenvironment, to identify resistance mechanisms and to subsequently assess immunotherapy agents which might augment response to radiotherapy-based treatment strategies in LARC.

Chapter 4 – Characterising the Effects of Radiotherapy on the Tumour Immune Microenvironment in the AKPT Rectal Cancer Model

4.1 Introduction

4.1.1 Evaluating the Effects of Radiotherapy in Pre-Clinical Models

Until recently, conventional radiobiology studies in pre-clinical CRC models have typically been performed using broad irradiation fields from a fixed source, with lead shielding apparatus used to aid beam targeting and to protect non-tumour bearing tissue (Dewan et al, 2009; Filatenkov et al, 2015; Dovedi et al, 2017). Such approaches lack image guidance and treatment planning capability, with limited dosimetry and quality assurance data available (Verhaegen et al, 2011). Several novel small animal irradiation platforms have been developed which incorporate micro-CT devices, rotating gantries, and treatment planning systems, highlighting key technological advances which will improve the translational potential of pre-clinical radiobiology studies (Brown et al, 2022).

Two systems are now widely established worldwide in research laboratories; the Small Animal Radiation Research Platform (SARRP; Xstrahl Ltd) and the X-Rad small animal radiotherapy system (SmART; Precision X-Ray inc), developed in conjunction with John Hopkins University and Princess Margaret Hospital respectively (Wong et al, 2008; Clarkson et al, 2011). These systems incorporate cone-beam CT imaging and in-built treatment planning systems, to enable focused irradiation fields ranging from 0.5 – 10mm in diameter resulting in the delivery of clinically accurate radiotherapy. The initial aims of this chapter, were to develop an experimental protocol using the SARRP system to deliver precise image-guided radiotherapy to the orthotopic AKPT organoid transplant model of LARC, described previously in Chapter 3.

Since its initial description in 2008, the SARRP system has been applied in a limited number of studies involving CRC tumour models; for instance, different fractionation regimens were delivered using parallel opposed beams in a CT26 murine colon cancer subcutaneous xenograft model (Grapin et al, 2019). Treatment planning in the setting of orthotopic tumour models pose greater technical challenges, as tumours are not readily detectable on CT imaging in

contrast with clinically and radiologically apparent subcutaneous tumours. Furthermore, considerations must be made to limit toxicity to adjacent pelvic organs when delivering radiotherapy to tumours situated in the murine rectum, and small intestinal damage has been overcome in previous studies by treating animals in a head down position (Groselj et al, 2018).

In a very recent study, the SARRP system was used in the irradiation of an orthotopic rectal cancer model, with a radiopaque probe tip placed intra-luminally at the lower margin of the rectal tumour based on endoscopy measurements acquired before treatment (Nicolas et al, 2022). The combination of newly developed orthotopic models of LARC, and technological advances to allow delivery of precise radiotherapy to these models, provide an exciting opportunity to conduct pre-clinical research with greater translational potential.

Increasing evidence has emerged that radiotherapy does not solely affect tumour cells, but also triggers changes within the tumour microenvironment (TME), with the resulting biological interactions between the tumour and its surrounding stroma being critical in determining success to therapy (Barcellos-Hoff et al, 2000; Barker et al, 2015). An early pre-clinical study by Barcellos-Hoff et al, suggested that radiotherapy can induce changes in the extra-cellular matrix to facilitate tumorigenesis, as shown when mammary epithelial cells displayed increased neoplastic progression when implanted into irradiated mammary stroma.

The immune reactions within the irradiated TME are complex, and neither wholly immunosuppressive nor immunostimulatory. Immunogenic cell death (ICD) is known to occur following irradiation, with the generation of damage associated molecular patterns (DAMPs) such as calreticulin, HMGB1 and ATP, resulting in dendritic cell activation and effective anti-tumour T-cell mediated responses (Apetoh et al, 2007; Gupta et al, 2012; Krysko et al, 2012). In contrast, radiotherapy is reported to induce immunosuppressive mechanisms such as increased infiltration of Tregs and Myeloid Derived Suppressor Cells (MDSCs) to the TME, through an increase in tumour derived CCL2 chemokine production (Kalbasi et al, 2017; Mondini et al, 2019). The balance between immune-stimulatory and immunosuppressive effects is not fully understood, and likely varies according to several factors including the underlying TME and surrounding host stroma, tumour location and host immune status. In this

chapter, following the establishment of an experimental protocol to deliver image-guided radiotherapy to orthotopic rectal tumours, I aimed to investigate the response of the AKPT model to both single fraction and fractionated radiotherapy, to characterise the underlying effects on the TME and determine the sensitivity of the model to irradiation.

To date, the temporal and evolving immune changes in the TME following radiotherapy based neo-adjuvant treatment strategies in LARC have not been extensively studied. Dynamic changes in peripheral blood markers associated with CRT have been demonstrated, with lymphocytes decreasing throughout treatment, followed by an increase in both lymphocyte count and the CD8/CD4 ratio once CRT is completed (Lee et al, 2018). Furthermore, neutrophils and monocytes decrease during the first two weeks of CRT, with lower counts showing an association with pCR. In the context of rectal tumour tissue, pre-treatment biopsies with high infiltration of CD3+ and CD8+ lymphocytes, have been shown to be associated with downstaging of the tumour following CRT (Anitei et al, 2014). A further study analysing both pre-CRT biopsies and surgical resection specimens, reveal that both high CD8/FOXP3 intra-epithelial lymphocyte ratio before CRT, and high CD8+ stromal lymphocyte density after CRT, are associated with favourable outcomes (Shinto et al, 2014).

Clinical data characterising the effects of radiotherapy on the TME and the dynamic changes which occur throughout treatment is lacking in LARC. Owing to the relative accessibility of rectal tumours via endoscopy, serial on-treatment biopsy sampling is feasible. Additionally, pre-clinical models which accurately recapitulate human disease might also be a valuable and complementary tool to further study TME changes at specific time-points. In this chapter, I aimed to utilise the AKPT model to characterise changes in tumour infiltrating immune cells at different time-points following radiotherapy.

Previous pre-clinical studies show conflicting evidence regarding the differential efficacy of single fraction and fractionated radiotherapy. For instance, in the subcutaneous murine CT26 colorectal tumour model, high dose single 30Gy fraction radiotherapy induced durable tumour remission which was not observed with a 3x10Gy fractionated regimen (Filatenkov et al, 2015). However, a subsequent study in the same model demonstrated similar primary tumour growth delay when a single 7Gy fraction was compared with a 3x4Gy regimen

(Dovedi et al, 2017). In a further study using both a breast and CRC subcutaneous tumour model, fractionated regimens (3x8Gy and 5x6Gy) showed similar efficacy in delaying primary tumour growth when compared with a single 20Gy fraction (Dewan et al, 2009).

In addition to providing conflicting conclusions, such pre-clinical radiotherapy studies have limited translational potential; heterotopic tumour models fail to recapitulate the desired anatomical location, large ablative fractions are not used clinically in LARC (out-with palliative intent), and commonly used commercial cell lines have limited clinical relevance as previously discussed. A further aim of this chapter was to assess whether single fraction and fractionated radiotherapy regimens at clinically relevant doses, induce differential changes in the TME in the AKPT model.

4.1.2 Experimental Aims

In Chapter 3, I described the development of an orthotopic organoid transplant model of LARC, which recapitulates locally invasive and poor prognosis disease. In this chapter, I aimed to establish an experimental protocol for the delivery of radiotherapy to the AKPT organoid transplant model of LARC, using newly developed technology to enable treatment of pre-clinical tumour models with image-guided and precise radiotherapy. The following experimental aims are described in this chapter:

- The development and validation of image-guided radiotherapy in orthotopic LARC models.
- Characterisation of the temporal effects of single fraction radiotherapy on the tumour immune microenvironment in the AKPT model.
- Characterisation of the response of the AKPT model to fractionated radiotherapy.
- Identification of potential resistance mechanisms to radiotherapy in the AKPT model.
- Determining whether the radio-sensitivity of AKPT organoid derived tumours is affected by location.

4.2 Results

4.2.1 Orthotopic AKPT Rectal Tumours can be Targeted with Image-Guided Radiotherapy

To develop a protocol for image-guided irradiation, AKPT organoid fragments were implanted at the rectal submucosa by colonoscopy guided submucosal injection in immunocompetent C57Bl/6 mice. Following confirmation of successful tumorigenesis by colonoscopy at 1-week post implantation, animals were imaged by plain cone-beam computed tomography (CBCT) scan, which is integrated into the Small Animal Radiation Research Platform (SARRP; XStrahl). The SARRP allows image-guided radiotherapy to be delivered to small animals in the research setting, with in-built CT imaging and treatment planning software (Muriplan) enabling the delivery of clinically relevant radiotherapy treatment plans (Figure 4.1).

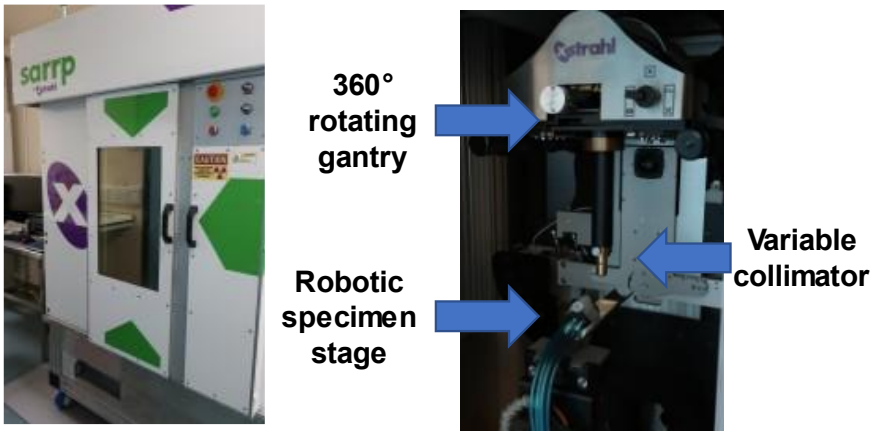

Figure 4.1: Small Animal Radiation Research Platform

Image of Small Animal Radiation Research Platform cabinet (Left). Image of SARRP system with key features indicated.

When imaged by non-contrast cone-beam CT scan, the anal verge was clearly detectable on sagittal plane images, but rectal tumours were not readily detectable. The presence of intra-luminal gas in the rectum and distal colon enabled placement of a beam isocentre at the predicted tumour location (Figure 4.2, top panel). A 10x10mm square collimator was then applied to ensure comprehensive coverage of the tumour location within the pelvis. Subsequently, treatment plans were then constructed using integrated Muriplan treatment planning software. Initially, rectal tumours were treated with a single static

beam of 4Gy with the gantry positioned directly above the animal at 0°. Subsequently, a continuous 280° rotating arc beam configuration was used, to recapitulate a more clinically relevant treatment configuration and potentially minimise irradiation of adjacent organs (Figure 4.2, bottom panel).

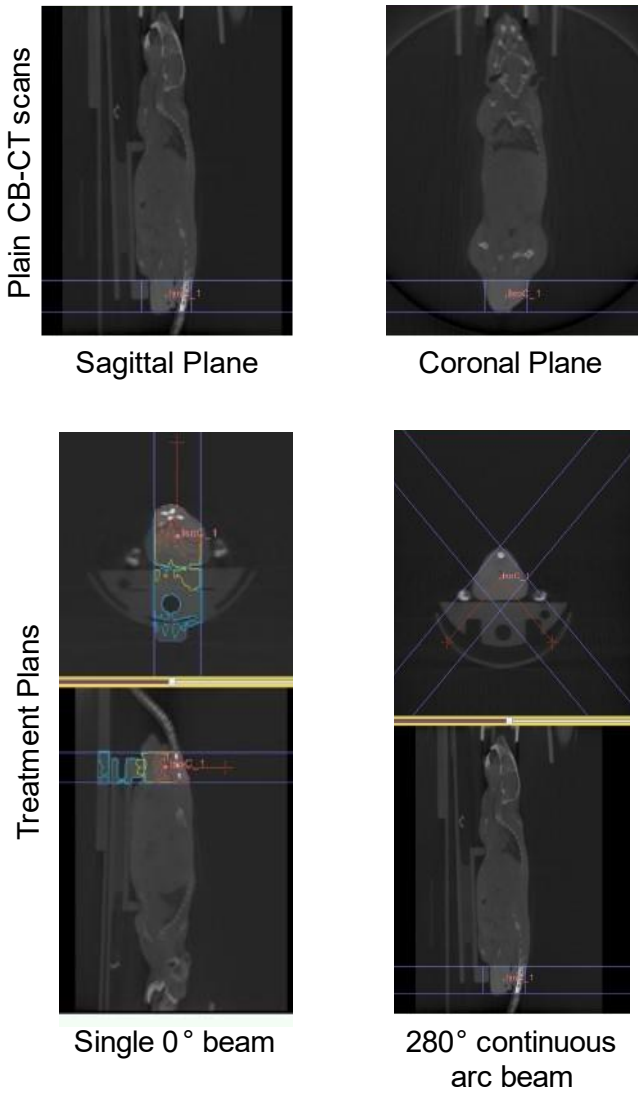

Figure 4.2: Radiotherapy Treatment Planning on the Small Animal Radiation Research Platform

Top – Plain CT images with 720 projections over 360° of one animal with an orthotopic rectal tumour in-situ. Sagittal (left) and coronal (right) plane images shown. Red dots depict beam isocentre placed adjacent to rectal gas. Blue lines depict prospective irradiation beam (diameter 10mm). Bottom – Treatment plans constructed using Muriplan to demonstrate 0° static beam configuration (left), and 280° continuous arc beam configuration (right). Blue lines depict irradiation beams. Red lines with cross depict start and end positions of irradiation beams (right).

I then sought to validate both treatment plans to ensure successful irradiation of rectal tumours. Following confirmation on colonoscopy of successful engraftment

of AKPT organoids, rectal tumours were irradiated with a single fraction of 4Gy at 2 weeks post-transplant (Figure 4.3, top panel). A dose of 4Gy was used to ensure biological effect, whilst maintaining clinical relevance and not causing myelosuppressive effects. Tumour tissue was harvested at 3hrs post irradiation and IHC staining performed to assess DNA damage through expression of γH2AX, which is known to increase immediately after ionising radiation; peak intensity has previously been demonstrated at ~1hr post irradiation, with levels gradually returning to normal at ~6hrs (Lee et al, 2019). Intense γH2AX staining in irradiated tumour tissue at 3hrs post irradiation was demonstrated when compared with time-matched untreated controls (Figure 4.3, bottom panel). Both tumour epithelial and associated stromal cells strongly expressed γH2AX following treatment with both beam configurations.

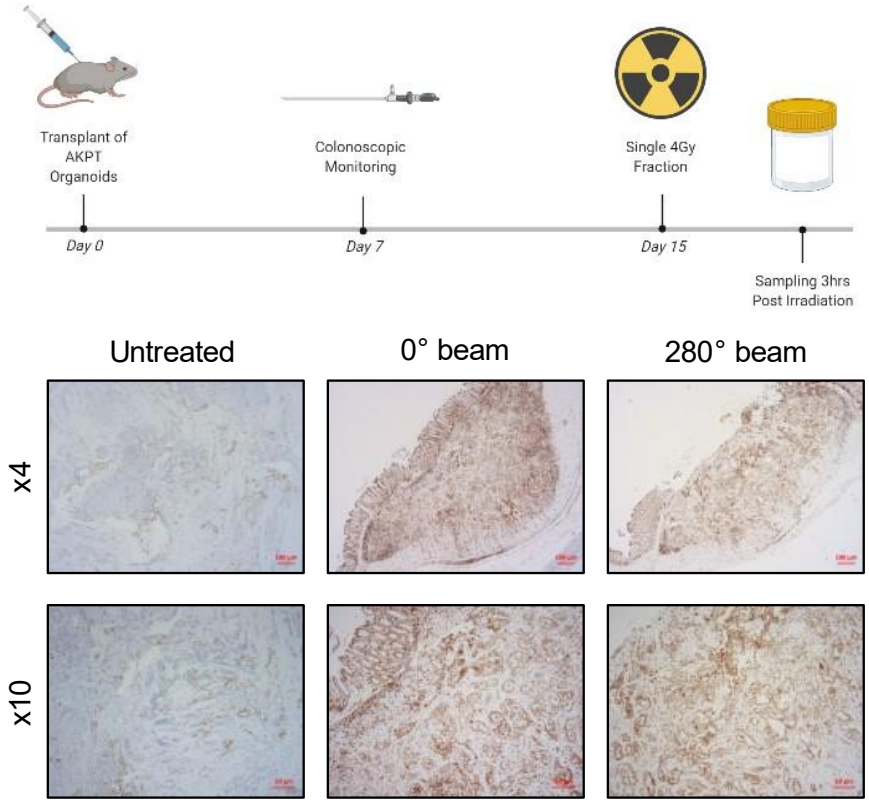

Figure 4.3: Radiotherapy Treatment Plans were validated through increased DNA Damage

Top – Schematic depicting experimental timeline for treatment validation. Bottom – γH2AX staining for untreated control samples, 4Gy delivered by 0° single beam and 4Gy delivered by 280° continuous arc beam. Scale bars 100μm (top images) and 50μm (bottom images).

Having validated the experimental approach with treatment planning aided by plain CBCT scanning, I sought to utilise different imaging techniques to improve

tumour detection. CBCT allows the prospective identification of orthotopic rectal tumours based on the identification of anatomical landmarks and prior knowledge of tumour location, however, tumours are not overtly visible using this imaging modality.

Rectal tumour bearing mice were imaged by MRI (Magnetic Resonance Imaging); with T2-weighted images in fast spin echo sequence (FSE), rectal tumours were clear (Figure 4.4, top panel). Tumour bearing mice were also scanned with a rectal temperature probe in-situ to confirm location of the rectal lumen, and further validate the visibility of tumours using this modality (Figure 4.4, bottom panel). Although MRI scanning generates reliable images upon which treatment plans could be constructed with greater confidence, there are multiple limitations in the experimental setting. Animals must undergo general anaesthetic for between 30-60 minutes to obtain images, causing significant distress and potential welfare considerations. Furthermore, the time and cost implications of performing MRI imaging in each experimental subject, would place considerable limitations on the potential cohort sizes which could be subjected to treatment experiments if conducted in this manner.

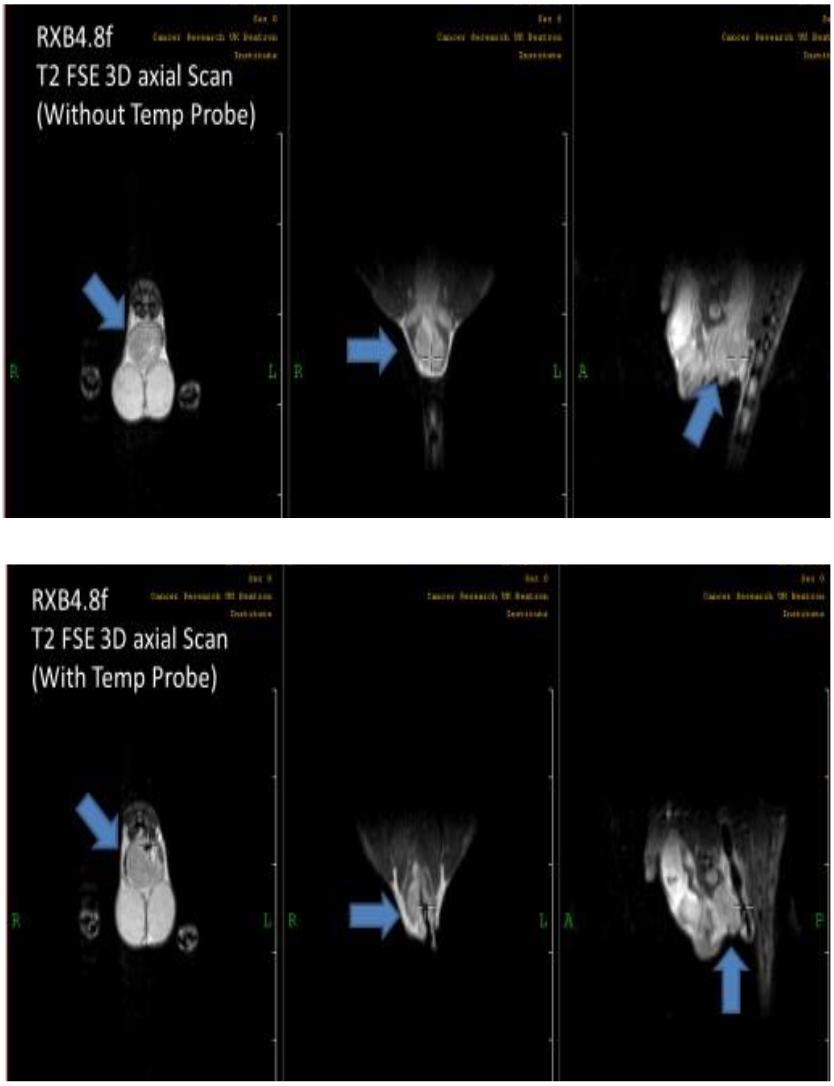

Figure 4.4: Visualisation of Orthotopic Rectal Tumours using Magnetic Resonance Imaging

Top – MRI T2-weighted images with FSE sequence of a rectal tumour bearing animal. Bottom – MRI T2-weighted images with FSE sequence of the same animal with a rectal temperature probe in-situ. Blue arrows depict rectal tumour.

I then sought to develop a reliable and time-efficient method of tumour identification on imaging, by determining whether administration of intra-peritoneal (i.p.) iodine-based contrast (Omnipaque™) would improve delineation of pelvic structures, as this method had previously been shown to be beneficial in abdominal tumour bearing mice (Aide et al, 2010). Following optimisation of iodine concentration and timings, contrast was administered i.p. (40mg/ml iodine) with rectal tumour bearing mice then scanned by plain CBCT at a 10-minute interval. Good delineation of abdominal organs was observed; however,

contrast did not sufficiently reach the pelvis to enable detection of rectal tumours (Figure 4.5).

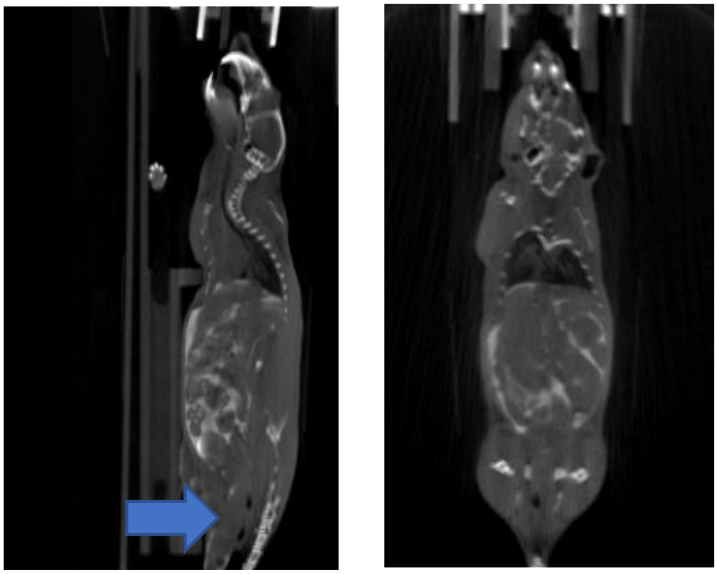

Figure 4.5: Intra-Peritoneal Contrast Enhanced CBCT Imaging fails to detect Rectal Tumours

CBCT images of rectal tumour bearing mouse at 10 minutes following intra-peritoneal administration of 1ml Omnipaque™ at 40mg/ml concentration. Sagittal (left) and coronal (right) planes shown. Blue arrow depicts tumour location based on luminal gas, with no migration of contrast to the murine pelvis.

Having successfully validated treatment plans based on identification of the predicted tumour location, using anatomical landmarks and prior knowledge of the location of tumour implantation, this technique will be used in the subsequent experiments described throughout this thesis. Acquisition of images, treatment planning and delivery can all be consistently administered within 15 minutes, limiting the adverse impact on animal welfare, and enabling the throughput of adequate cohort sizes in treatment studies.

To ensure accurate dose delivery during the developed treatment plans, dosimetry studies were performed. The dose rate of the SARRP was determined using an ionisation chamber and squares of radiochromic film were exposed to a range of doses up to 120% of the treatment dose to create a calibration curve that would allow us to determine the dose delivered to an experimental film. This experimental film was placed within a water-based phantom; after development, the dose calibration curve created earlier was used to create a dose plane from the film scan (Figure 4.6, top panel). Gamma index analysis was

then performed to compare the dose distribution generated from the film with that on the treatment planning system, to subsequently calculate the local (dose at each evaluated point) dose difference (%) and distance to agreement (mm) between both plans. The gamma passing rate (%) was calculated as the percentage of pixels which met the desired criteria and agreement between both plans. A gamma passing rate of 96.5% was achieved with parameters of 5%/4.5mm.

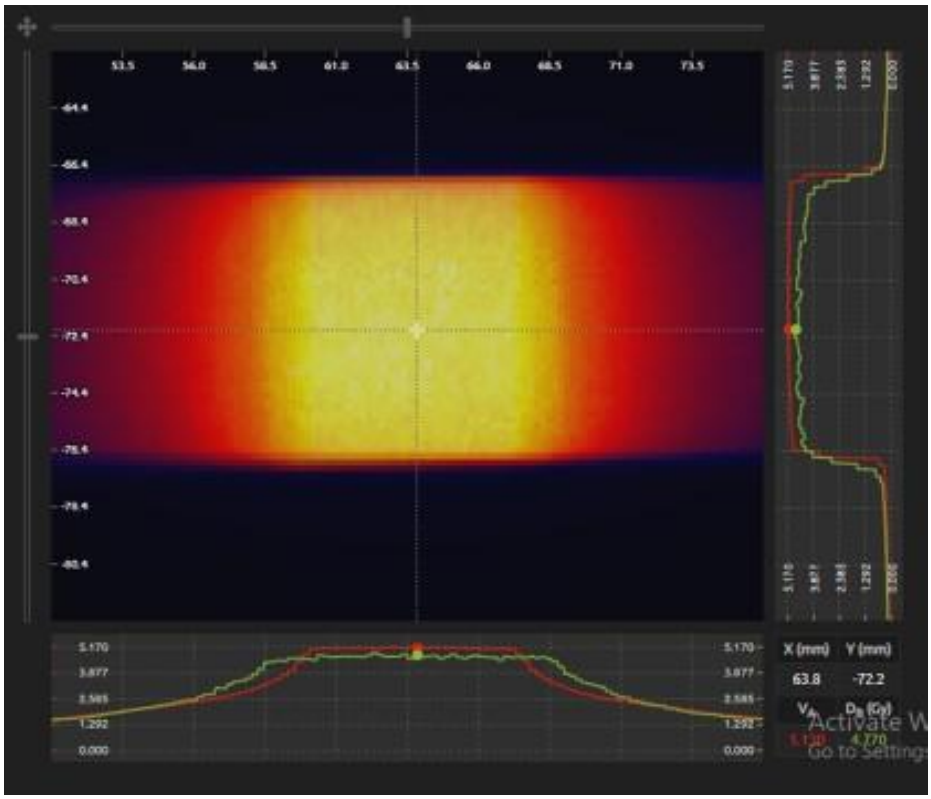

Gamma Index Analysis for 5Gy 280 degree Arc				
Aperture Size	**Dose Distribution Normalisation**	**Max Dose Difference (%)**	**Max Distance to Agreement (mm)**	**% Gamma Passing Rate**
10x10mm	Local	5	4.5	96.5

Figure 4.6: Validation of Treatment Plans through Dosimetry Studies

Top – Gamma index analysis for 5Gy delivered with a 280° arc using a 10x10mm collimator, with corresponding dose delivery curve. Bottom – Table showing values for the maximum dose difference (%), maximum distance to agreement (mm), and gamma passing rate (%) in the analysis. Dosimetry studies were performed by Emer Curley (PhD Student, Dr David Lewis Lab)

4.2.2 Determining the Effects of Single Fraction Radiotherapy on the Tumour Immune Micro-Environment

I next sought to determine the effect of single fraction radiotherapy on the orthotopic AKPT organoid transplant model of LARC, and to assess temporal changes arising within the tumour immune micro-environment. Rectal tumours were treated with a single 4Gy fraction of radiotherapy at 3-weeks post tumour implantation (Figure 4.7, top panel). A dose of 4Gy was used in keeping with validation experiments whereby short-term biological effects were demonstrated through increased DNA damage, and to closely align with doses applied clinically in LARC (5Gy per fraction in SCRT). Tumours were then harvested at 3-days or 7-days post irradiation and compared with tumours from time-matched untreated controls for each time-point. It was noted that the 3-day and 7-day time-points were performed as independent experiments, and so comparisons between groups must be interpreted cautiously.

Tumour measurements were performed at the time of sampling to calculate tumour volume, and no significant difference was seen between irradiated tumours and their corresponding untreated controls (Figure 4.7, bottom panel). Two experimental outliers were noted in the 3-day post treatment group, contributing to a higher mean tumour volume in this group when compared with its corresponding control group; however, this observed difference did not reach statistical significance ($p=0.0732$). Heterogeneity in tumour volume was observed between subjects within each experimental group, despite maintaining consistent experimental conditions and animals receiving injections derived from the same pooled suspension of organoid fragments. However, it was observed that some animals may not receive a full 70µl injection of organoid fragments into the submucosal layer, due to leakage of the suspension either intra-luminally or extra-luminally at the time of injection.

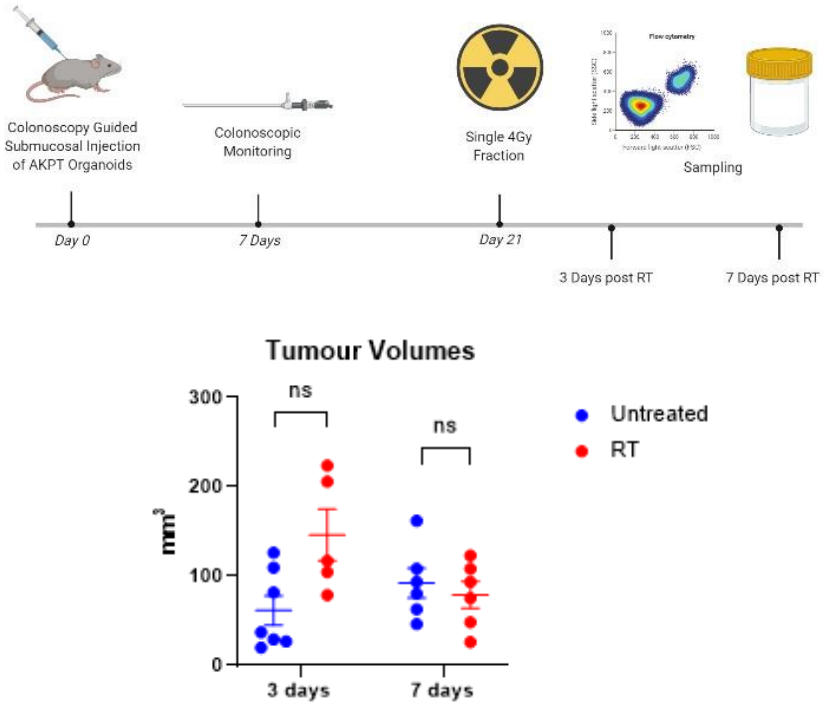

Figure 4.7: Single Fraction Radiotherapy fails to Reduce Tumour Volume

Top – Schematic depicting experimental protocol for delivery of single-fraction radiotherapy and time-point sampling. Bottom – Graph demonstrating tumour volume at 3-day and 7-day time-points for irradiated tumours and corresponding control groups. Each data point plotted. Error bars show mean and SEM. n=5-7 per group. Mann-Whitney U-test. ns denotes non-significance ($p=\geq 0.05$). 3-day and 7-day time-points performed as independent experiments.

Systemic blood counts were then analysed from animals at both 3-day and 7-day time-points post irradiation. No systemic response was seen following single fraction radiotherapy, with no significant change in any immune cell population observed at either time-point when compared with their corresponding time-matched control groups (Figure 4.8). Overall circulating white cell counts (WCC), as well as individual counts for lymphocytes, neutrophils and monocytes, were not altered following treatment with single fraction radiotherapy at both 3-days and 7-days.

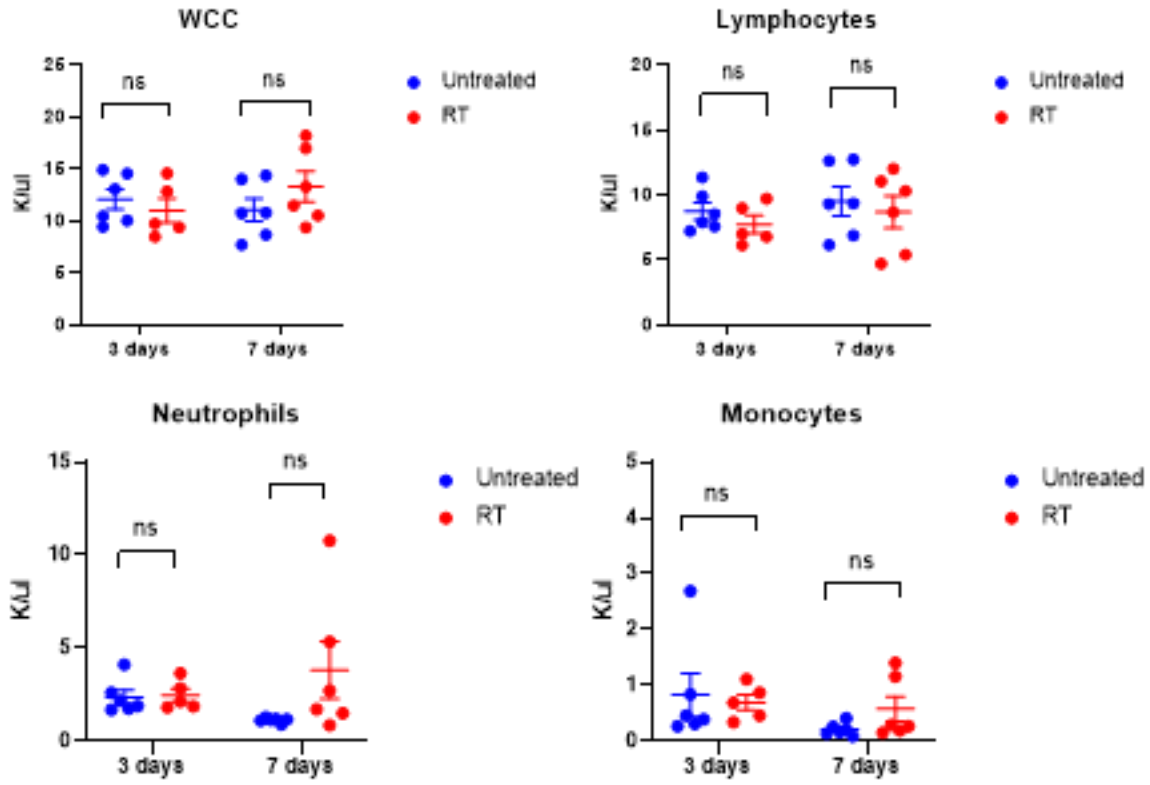

Figure 4.8: Changes in Systemic Blood Counts were not observed following Single Fraction Radiotherapy

Top – Bar graphs showing systemic blood counts for WCC and lymphocytes measured as 10^3 cells/µl (K/µl). Bottom – Bar graphs showing systemic blood counts for neutrophils and monocytes as K/µL. Each data point plotted. Error bars show mean and SEM. n=5-6 per group. Mann-Whitney U-test. ns denotes non-significance (p=≥0.05). 3-day and 7-day time-points performed as independent experiments.

Rectal tumours were then analysed by H+E staining to assess for histological evidence of tumour regression. Normal tumour epithelium was observed in tumour samples from both irradiated and control groups at both the 3-day and 7-day time-points, with no evidence of tumour regression noted (Figure 4.9). Furthermore, tumour stroma was also noted to contain immune cell infiltrate in all groups irrespective of treatment.

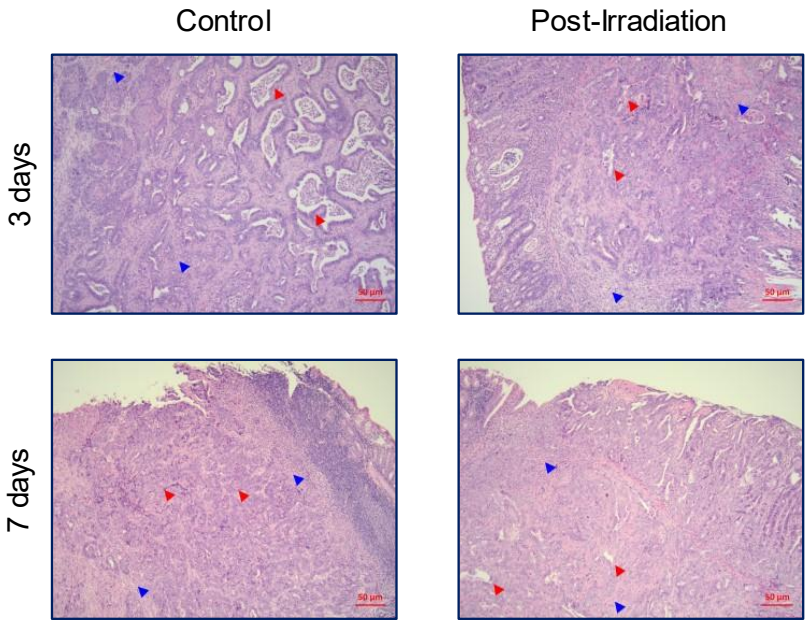

Figure 4.9: Effect of Single Fraction Radiotherapy on Tumour Histology

Top – Representative H+E stains for AKPT rectal tumours at 3-days post single fraction irradiation with corresponding time-matched control. Bottom – Representative H+E stains for AKPT rectal tumours at 7-days post single fraction irradiation with corresponding time-matched control. Scale bars = 50μm. Red arrows depict tumour epithelium. Blue arrows depict immune infiltrated stromal compartment.

IHC was then performed to assess whether changes in tumour immune cell infiltrate were observed at the 3-day and 7-day time-points following single-fraction radiotherapy. All T-cells were identified through CD3 staining. At the 3-day time-point, a decrease in mean cell density of CD3+ lymphocyte infiltration was observed following irradiation; however, this did not reach statistical significance (p=0.1000) (Figure 4.10, bottom panel). When the 7-day time-point was analysed, a significant change in CD3+ cell infiltration was not seen upon quantification. As in previous model characterisation described in Chapter 3, CD3+ve cells were noted to cluster more densely at the tumour invasive margin than in the tumour core.

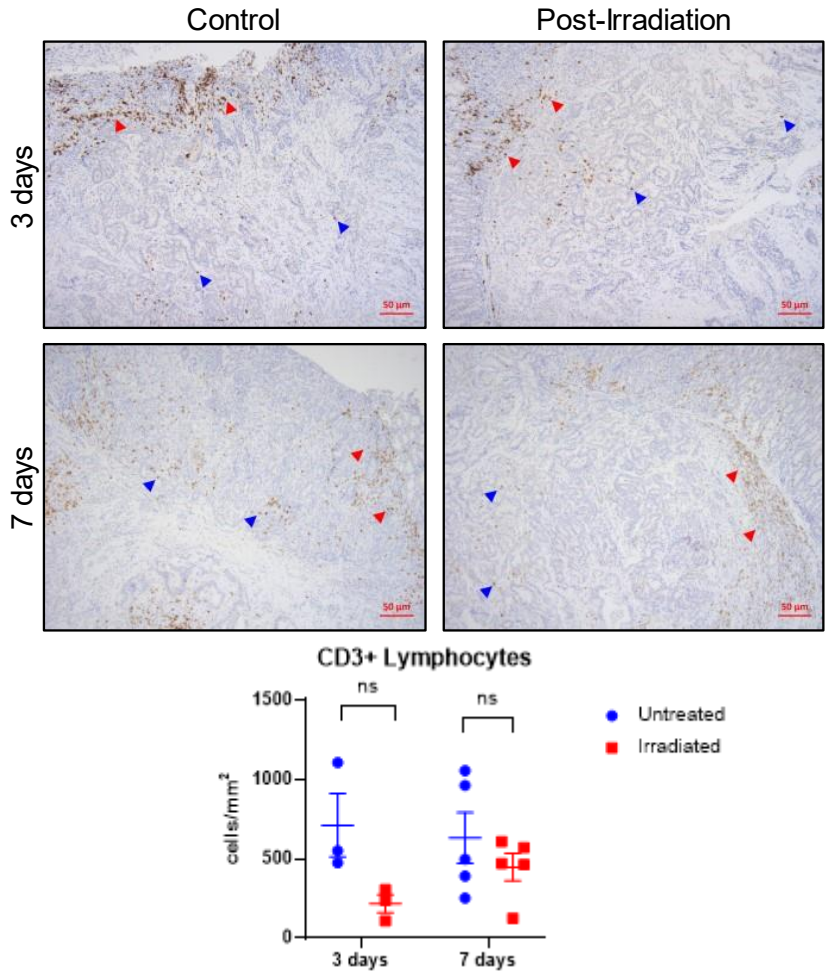

Figure 4.10: Effect of Single Fraction Radiotherapy on CD3+ Lymphocyte Infiltration

Top – Representative CD3 IHC stains for AKPT rectal tumours at 3-days post single fraction irradiation with corresponding time-matched control. Middle – Representative CD3 IHC stains for AKPT rectal tumours at 7-days post single fraction irradiation with corresponding time-matched control. Bottom panel – Bar graph showing CD3+ cell quantification by cells/mm^2. Error bars show mean and SEM, with each data point plotted. Mann-Whitney U-test. Group sizes n=3-5. ns denotes non-significance ($p \geq 0.05$). Scale bars 50µm. Red arrows depict positively stained cells at the tumour invasive margin. Blue arrows depict positively stained cells within the tumour core.

CD8 staining was performed to detect cytotoxic T-lymphocytes, with a non-significant decrease in mean cell density observed at 3-days following irradiation (p=0.1000). Cytotoxic T-lymphocytes were predominantly noted at the tumour invasive margin in both groups, with only sparse infiltration seen within the tumour core (Figure 4.11, top and middle panels). However, irrespective of whether tumours were irradiated, a lower mean cell density was observed between the 3-day and 7-day groups, and likely reflects each time-point being performed as independent experiments, making it difficult to draw definitive conclusions from this data (Figure 4.11, bottom panel).

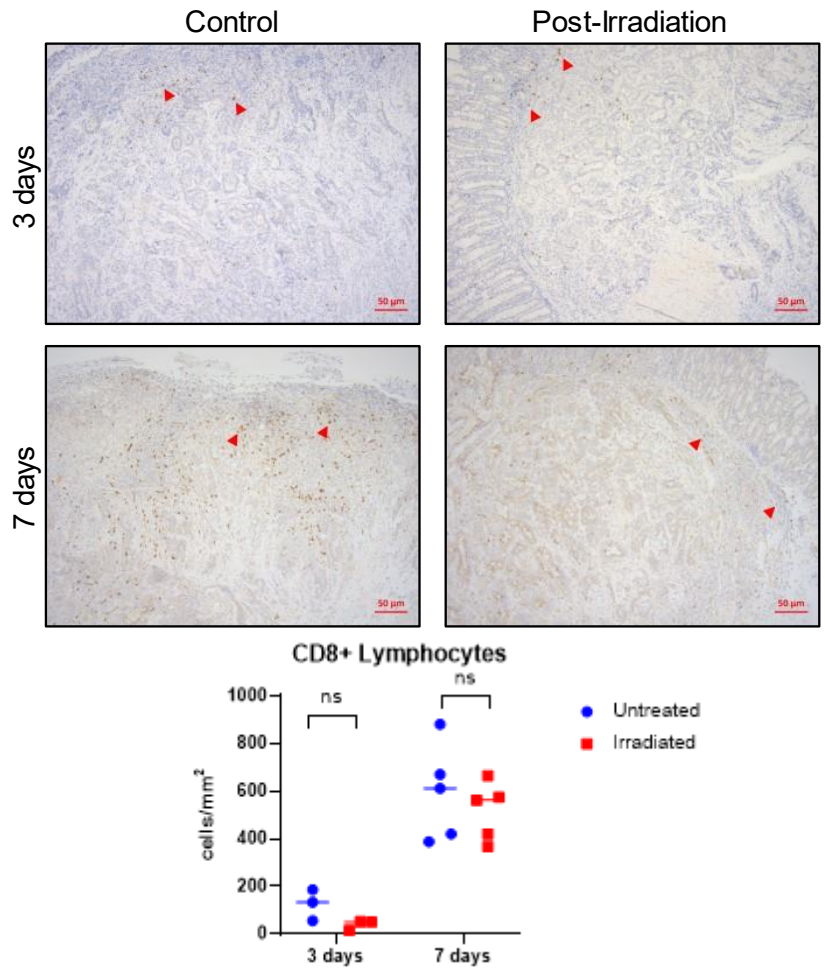

Figure 4.11: Effect of Single Fraction Radiotherapy on CD8+ Lymphocyte Infiltration

Top – Representative CD8+ IHC stains for AKPT rectal tumours at 3-days post single fraction irradiation with corresponding time-matched control. Middle – Representative CD8+ IHC stains for AKPT rectal tumours at 7-days post single fraction irradiation with corresponding time-matched control. Bottom panel – Bar graph showing CD8+ve cell quantification as cells/mm^2. Error bars show mean and SEM, with each data point plotted. Mann-Whitney U-test. Group sizes n=3-5. ns denotes non-significance ($p \geq 0.05$). Scale bars 50μm. Red arrows depict positively stained cells at the tumour invasive margin.

I next quantified changes in tumour neutrophil infiltration following single-fraction irradiation, through S100A9 IHC staining (Figure 4.12, top panel). An increase in mean cell density of S100A9 positive cells was observed at 3-days post irradiation when compared with its corresponding control group (Figure 4.12, bottom panel). However, this difference did not reach statistical significance ($p=0.7000$). Each of the 3-day cohorts contains one experimental outlier, and coupled with the small cohort size (n=3), it was not possible to conclude that increased neutrophil infiltration was observed at 3-days post irradiation.

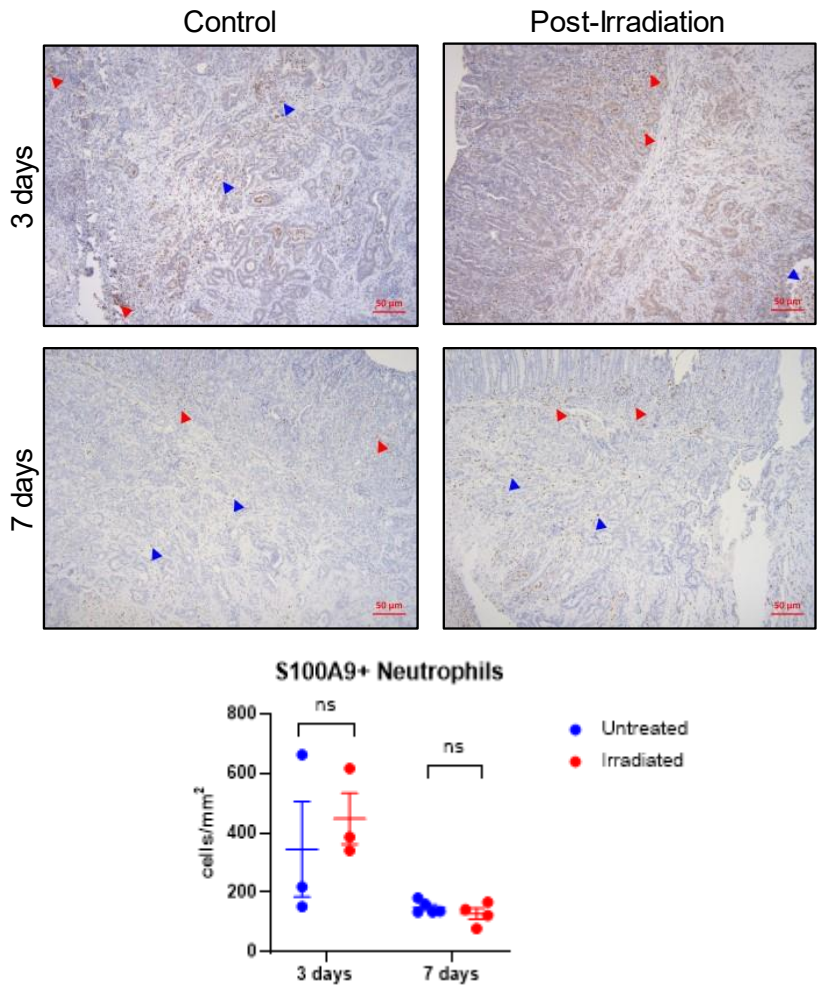

Figure 4.12: Effect of Single Fraction Radiotherapy on S100A9+ Neutrophil Infiltration

Top – Representative S100A9+ IHC stains for AKPT rectal tumours at 3-days post single fraction irradiation with corresponding time-matched control. Middle – Representative S100A9+ IHC stains for AKPT rectal tumours at 7-days post single fraction irradiation with corresponding time-matched control. Bottom panel – Bar graph showing S100A9+ cell quantification as cells/mm^2. Error bars show mean and SEM, with each data point plotted. Mann-Whitney U-test. Group sizes n=3-5. ns denotes non-significance ($p \geq 0.05$). Scale bars 50μm. Red arrows depict positively stained cells at the tumour invasive margin. Blue arrows depict positively stained cells within the tumour core.

Macrophage infiltration was then quantified using F4/80 IHC staining for both 3-day and 7-day time-points (Figure 4.13, top and middle panels). Similar to IHC performed to detect CD8+ lymphocytes, a significant variability was observed between the two experimental batches, with a lower density of macrophages seen in the 3-day time-point group irrespective of treatment, which can be appreciated both on microscopy images and upon quantification (Figure 4.13). Macrophages were noted to be densely clustered at the tumour invasive margin, with more sparsely concentrated populations seen in the stromal compartment and within the tumour core. A statistically significant decrease in macrophage density was observed following single-fraction radiotherapy at the 7-day time-

point when quantified as % of tumour area positively stained for F4/80 (p=0.0317), however, given the variability noted between untreated tumours according to experimental batch, this change again must be interpreted cautiously.

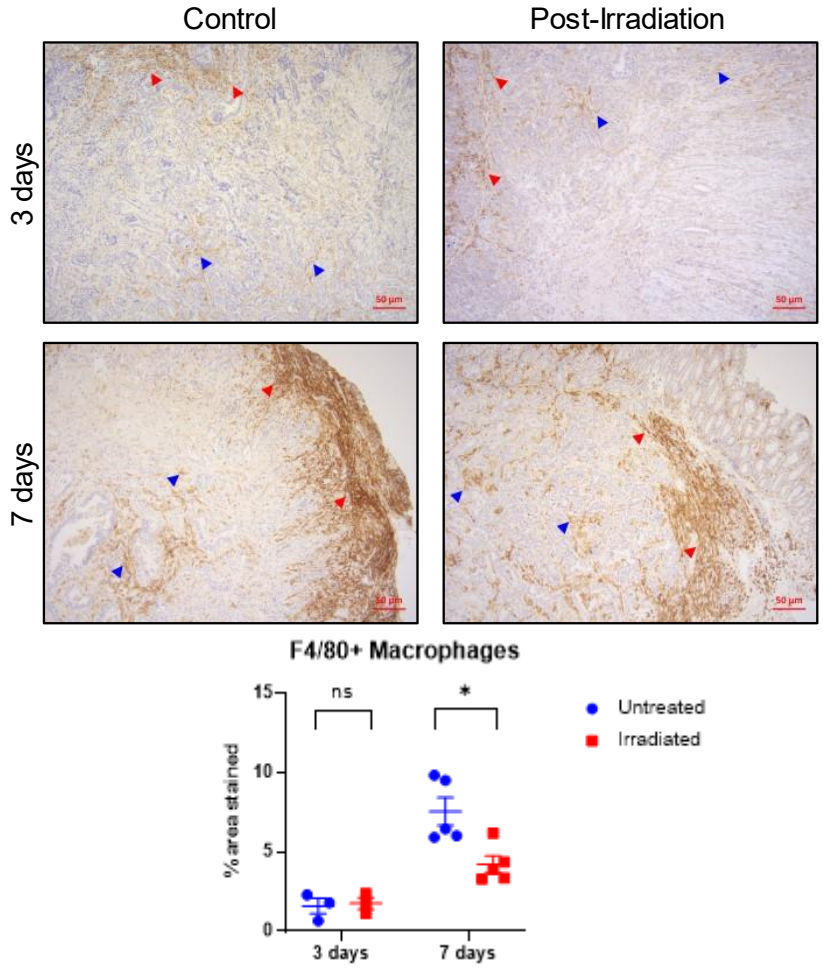

Figure 4.13: Effect of Single Fraction Radiotherapy on F4/80+ Macrophage Infiltration

Top – Representative F4/80 IHC stains for AKPT rectal tumours at 3-days post single fraction irradiation with corresponding time-matched control. Middle – Representative F4/80 IHC stains for AKPT rectal tumours at 7-days post single fraction irradiation with corresponding time-matched control. Bottom panel – Bar graph showing F4/80+ cell quantification as % of tumour area positively stained. Error bars show mean and SEM, with each data point plotted. Group sizes n=3-5. Mann-Whitney U-test. *denotes p-value <0.05. ns denotes non-significance (p≥0.05). Scale bars 50μm. Red arrows depict positively stained cells at tumour invasive margin. Blue arrows depict positively stained cells within the tumour core.

I then assessed nuclear pSMAD3 expression using IHC, to determine whether differences in TGF-β signalling were observed following single-fraction radiotherapy at both time-points (Figure 4.14, top and middle panels). Irrespective of treatment, a high proportion of both tumour epithelium and stromal cells expressed pSMAD3, highlighting that TGF-β signalling is abundantly

activated in this tumour model. An increase in nuclear pSMAD3 expression across all cell types was observed following single-fraction radiotherapy at the 7-day time-point upon quantification (p=0.0317), suggesting that irradiation potentially results in further upregulation of TGF-ß signalling in this model (Figure 4.414, bottom panel).

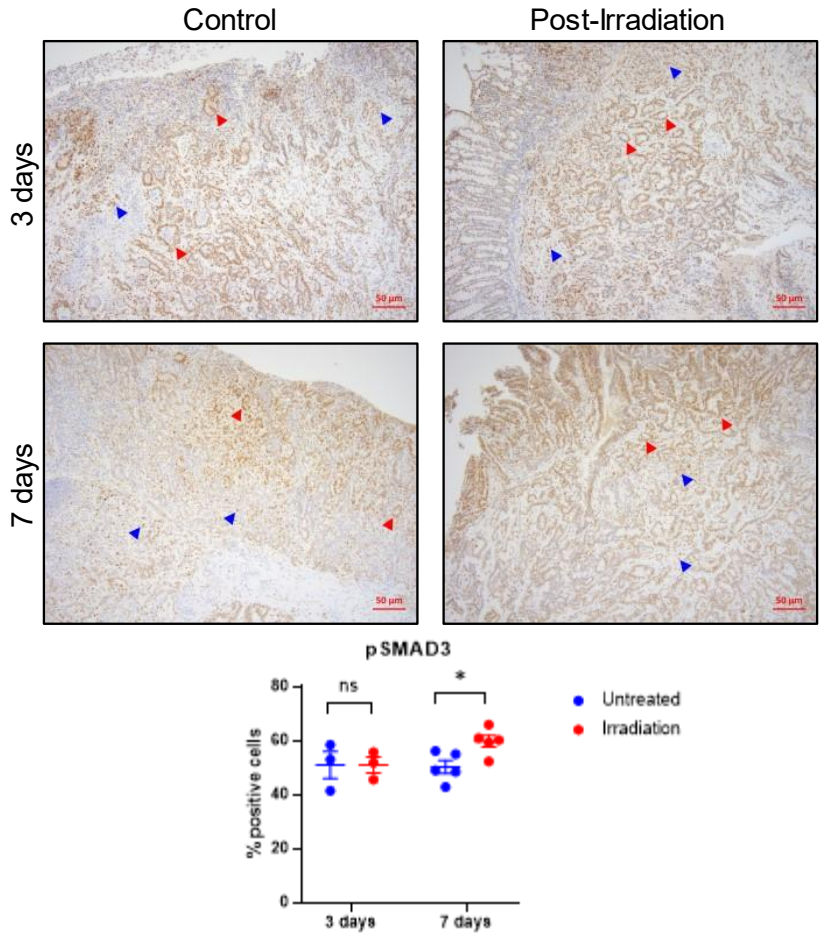

Figure 4.14: Effect of Single Fraction Radiotherapy on TGF-ß Signalling

Top – Representative nuclear pSMAD3 IHC stains for AKPT rectal tumours at 3-days post single fraction irradiation with corresponding time-matched control. Middle – Representative pSMAD3+ IHC stains for AKPT rectal tumours at 7-days post single fraction irradiation with corresponding time-matched control. Bottom panel – Bar graph showing pSMAD3+ cell quantification as % of positively staining cells. All cell types within tumour sections were included in analysis. Error bars show mean and SEM, with each data point plotted. Group sizes n=3-5. Mann-Whitney U-test. *denotes p-value <0.05. ns denotes non-significance (p≥0.05). Scale bars 50µm. Red arrows depict positively staining epithelial cells. Blue arrows depict positively staining stromal cells.

In addition to IHC, a piece of tumour core tissue was harvested from several animals in each experimental group for flow cytometry, along with tumour draining lymph nodes (obtained from the colonic mesentery) and circulating blood. Overall leucocyte counts were determined by gating all live cells

expressing the common leucocyte antigen CD45. In tumour tissue, no significant changes in overall leucocytes were observed at either time-point following irradiation (Figure 4.15, top panel). The presence of one experimental outlier in both the 3-day post-irradiation and 3-day control groups, coupled with low experimental numbers (n=3 per group), made it difficult to draw conclusions regarding tumour infiltration of leucocytes post-irradiation. However, data suggests that no clear difference in overall leucocyte infiltration occurred in AKPT tumours following single-fraction radiotherapy at 3-days and 7-days. Expanded cohorts performed in a single experimental batch would potentially overcome the effects of experimental outliers, and improve the likelihood of generating statistically significant results upon which to draw robust conclusions. Heterogeneity was noted to exist between tumours within the same experimental groups, and furthermore, intra-tumoral heterogeneity was also likely to be present, whereby different immune contextures exist within the same tumour, with results being influenced by the tumour region sampled.

Similarly, in circulating blood no differences in CD45 expressing cells were observed following irradiation at either time-point (Figure 4.15, top panel). Interestingly, in tumour draining lymph nodes, an increase in CD45 expressing cells was observed at 7-days post irradiation when compared with corresponding controls (mean treated = $4.53x10^5$ cells/mg versus untreated = $2.97x10^5$ cells/mg) (Figure 4.15, bottom panel). Although this increase in leucocytes failed to reach statistical significance (p=0.2000), results suggested that irradiation may induce a systemic inflammatory response in this tumour model, with accumulation of immune cells in local lymph nodes which subsequently fail to infiltrate tumours.

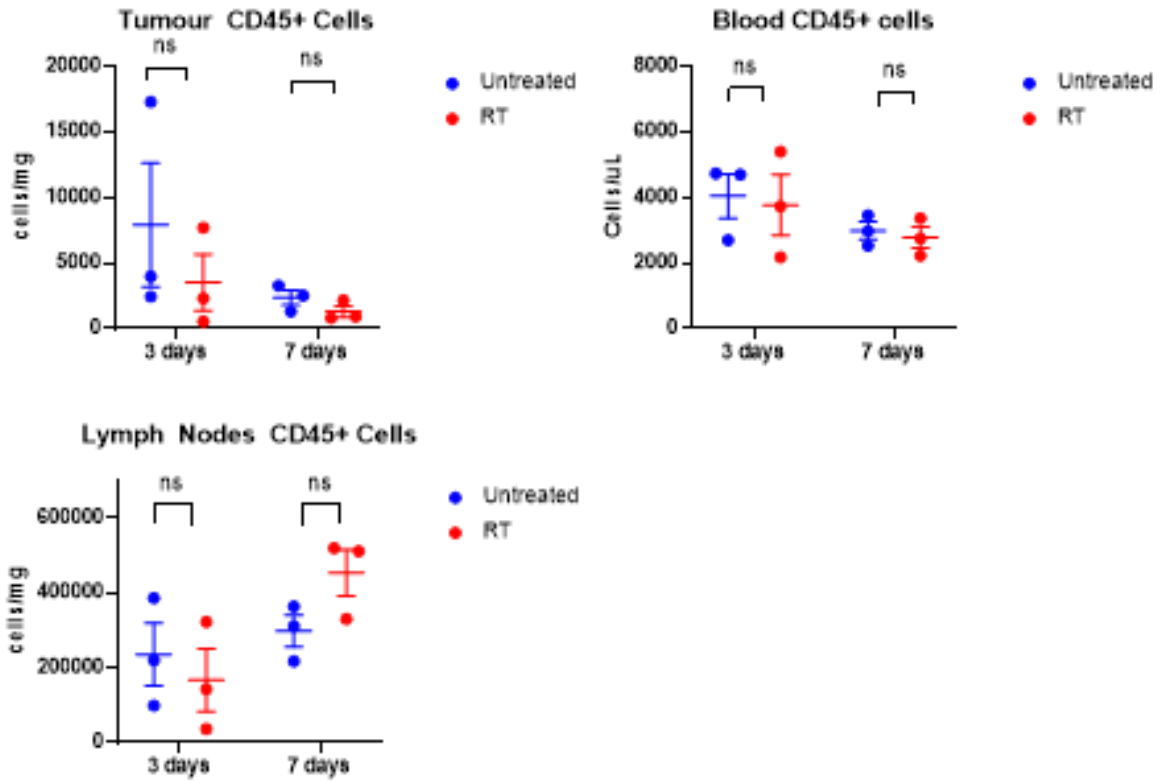

Figure 4.15: Quantification of Leucocytes by Flow Cytometry Following Single Fraction Radiotherapy

Top – Bar graphs showing quantification of CD45+ cells in tumour tissue (left) and circulating blood (right) measured as cells/mg and cells/µl respectively. Bottom – Bar graph showing quantification of CD45+ cells in tumour draining lymph nodes as cells/mg. Error bars show mean and SEM, with each data point plotted. n=3 per group. Mann Whitney U-test. ns denotes non-significance (p=≥0.05).

Using flow cytometry, the proportion and overall number of specific immune cell populations within tumour tissue were quantified. All CD45 expressing cells were gated for the CD19 antigen to differentiate B-cells, with CD19-ve cells then selected for expression of the CD3 antigen to identify all T-lymphocytes. CD19-ve, CD3-ve cells were gated to select for myeloid cell populations; subsequently, high expression of Ly6G was used to identify neutrophils. CD3-ve, CD19-ve, Ly6G-ve myeloid cells were gated for siglec-F expression to identify eosinophils. Subsequently, CD3-ve, CD19-ve, Ly6G-ve, siglec-F-ve cells were gated for either CD11b+ve, F4/80+ve, CD64+ve expression to identify macrophages, or MHC-II+ve, CD11c+ve expression to identify dendritic cells.

Again, changes in proportion and number of individual immune cell populations were difficult to interpret due to small group numbers (n=3 per condition), and due to variability within each experimental group. T-lymphocytes made up 5-15%

of the overall leucocyte populations in the majority of tumours, and a trend towards decreased T-cells following irradiation was observed at the 3-day time-point post irradiation, as quantified by % of all CD45+ve cells and by overall cell numbers (Figure 4.16, top panel). An obvious increase in neutrophils as a proportion of the overall leucocyte population was observed following radiotherapy at both time-points; however, this change was not reflected in overall neutrophil counts (Figure 4.16, upper middle panel). A clear decrease in both proportion and number of macrophages was observed at 7-days post radiotherapy when compared with the corresponding control group, however, this observation did not reach statistical significance (Figure 4.16, lower middle panel). A decrease in dendritic cells was observed at the 7-day time-point following irradiation, which failed to reach statistical significance (Figure 4.16, bottom panel). This data failed to demonstrate an obvious influx of any individual immune cell population to the TME following single fraction radiotherapy, however, conclusions should be made cautiously as experimental group numbers were low and subject to considerable variability within each group.

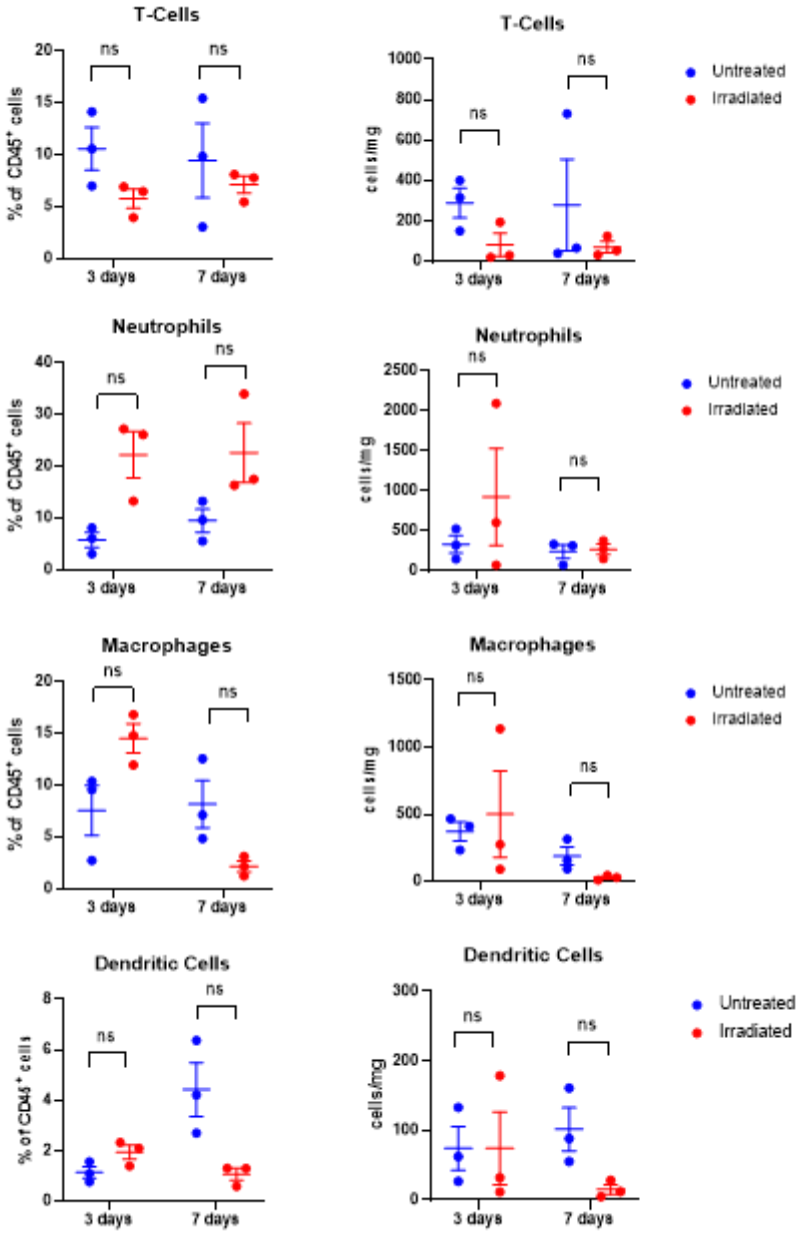

Figure 4.16: Quantification of Tumour Immune Cell Populations by Flow Cytometry

Top – Bar graphs showing T-cell quantification by flow cytometry following single fraction radiotherapy at 3-day and 7-day timepoints, quantified as % of all CD45+ve cells (left) and as cells/mg of tumour tissue (right). Upper middle – Bar graphs depicting neutrophil quantification. Lower middle – Bar graphs depicting macrophage quantification. Lower – Bar graphs depicting dendritic cell quantification. Error bars show mean and SEM, with each data point plotted. n=3 per group. Mann-Whitney U-test. ns denotes non-significance ($p \geq 0.05$).

Neutrophils identified from sorted tumour cells and circulating blood, were then analysed to identify phenotypic subtypes. CD101 is a negative co-stimulatory molecule expressed on subsets of lymphoid and myeloid cells, with CD101+ve cells known to reflect neutrophil maturity (Evrard et al, 2018). The majority of neutrophils in both circulating blood and in tumours across all experimental groups were found to express CD101 (Figure 4.17, top panel). In addition,

quantification of Ly6G expression can also reliably characterise neutrophil maturity with Ly6G^{int} neutrophils regarded as ‘immature’ with reduced migratory and regulatory capacity, and Ly6G^{Hi} neutrophils classified as ‘mature’ (Mackey et al, 2019). The majority of both blood and tumour neutrophils express high levels of Ly6G, confirming the predominance of a neutrophil mature phenotype within tumour and blood cells irrespective of experimental group (Figure 4.17, middle panel). CXC chemokine receptor 2 (CXCR2) is known to regulate neutrophil migration from bone marrow to blood, and subsequently promotes the migration of neutrophils to tumour sites (Han et al, 2019). A high proportion of neutrophils in the circulating blood expressed CXCR2+ve irrespective of treatment group, suggesting a migratory capability in the majority of circulating neutrophils (Figure 4.417, bottom panel). A low proportion of neutrophils in the tumour expressed CXCR2 irrespective of experimental group, likely reflecting rapid internalisation of the CXCR2 receptor following activation (Nasser et al, 2007).

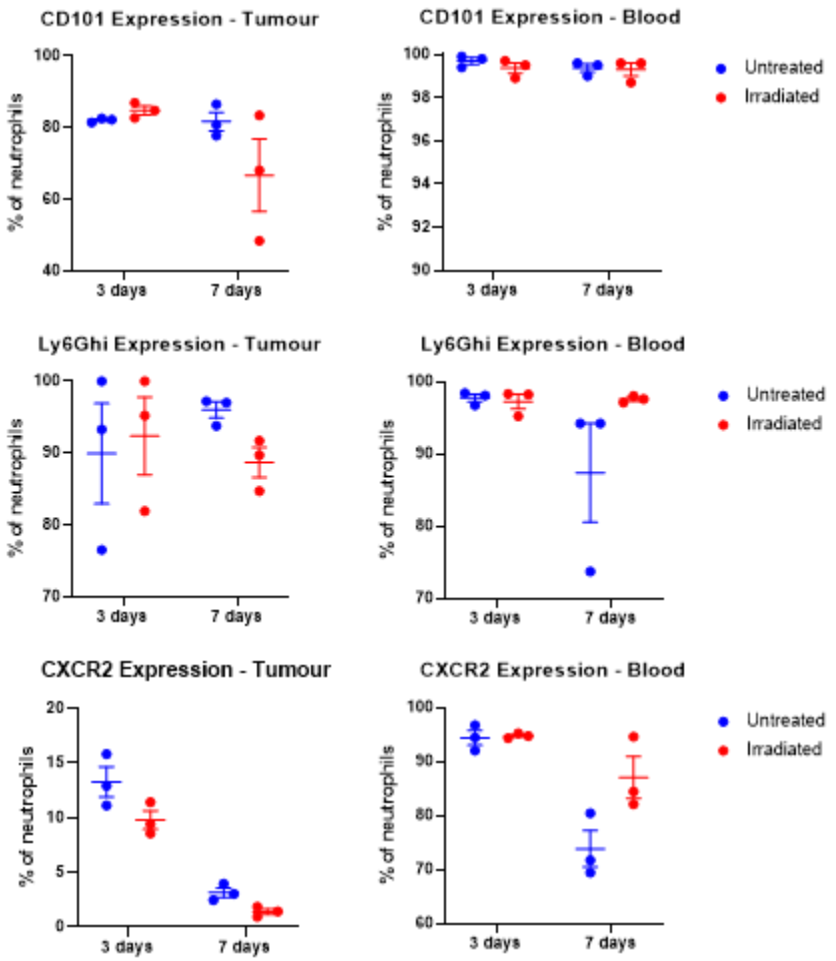

Figure 4.17: Flow Cytometry Characterisation of Neutrophil Phenotypes in Blood and Tumour

Top – Bar graphs showing CD101 expression on tumour (left) and blood neutrophils (right) by flow cytometry following single fraction radiotherapy at 3-day and 7-day timepoints, quantified by % of neutrophils. Middle – Bar graphs showing proportion of $Ly6G^{Hi}$ expression on neutrophils. Lower – Bar graphs showing CXCR2 expression on neutrophils. Error bars show mean and SEM, with each data point plotted. n=3 per group.

Subtyping of CD3+ve T-lymphocytes within tumour tissue was then carried out, using CD4 and CD8 expression to identify T-helper cells and cytotoxic T-lymphocytes respectively. The majority of CD3+ve T-cells were identified as CD4 expressing, indicating that a high proportion of T-lymphocytes can be categorised as T-helper cells (Figure 4.18). A smaller proportion of T-lymphocytes were shown to be cytotoxic T-cells (CD4-ve, CD8+ve). A small but statistically insignificant decrease in the proportion of cytotoxic T-lymphocytes was observed at 3-days following irradiation, consistent with data seen from IHC (Figure 4.18).

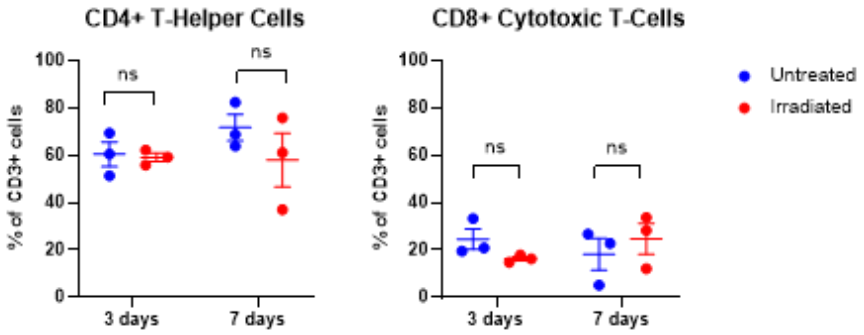

Figure 4.18: Tumour T-cell Compartment Phenotyping by Flow Cytometry

Top – Bar graphs showing expression of CD4+ve T-helper cells (left) and CD8+ve cytotoxic T-lymphocytes as % of CD3+ expressing T-cells. Error bars show mean and SEM, with each data point plotted. n=3 per group. Mann-Whitney U-test. ns denotes non-significance ($p \geq 0.05$).

Finally, inhibitory PD-1 receptor expression which is known to be suggestive of T-cell exhaustion and reduced effector function, was characterised by flow cytometry on all CD3+ve T-cells to determine whether radiation upregulates expression (Wherry et al, 2015). No significant change was identified following radiotherapy when compared with corresponding control groups at both 3-day and 7-day time-points (Figure 4.19, top panel). Expression of CD69, a marker of early lymphocyte activation was also quantified in all CD3+ve T-cells, with no significant change in expression observed following radiotherapy at both time-points studied (Figure 4.19, bottom panel).

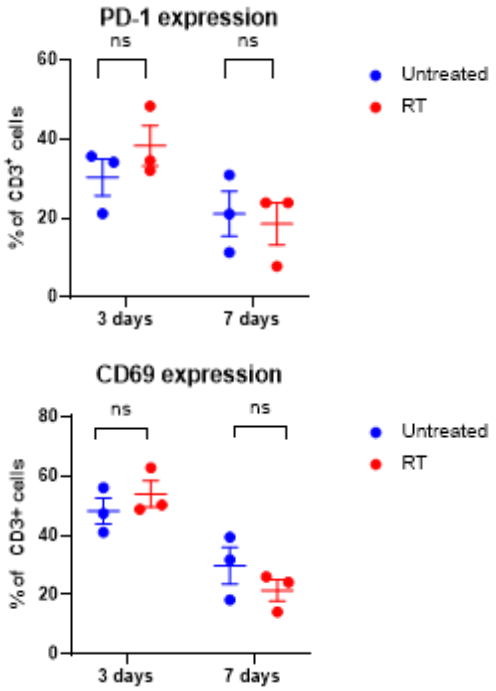

Figure 4.19: Quantification of PD-1 Receptor and CD69 Expression on T-Lymphocytes

Top – Bar graph showing expression of PD-1 receptor on CD3+ve lymphocytes as % of all CD3+ve T-lymphocytes. Bottom – Bar graph showing expression of CD69 on CD3+ve T-lymphocytes. Error bars show mean and SEM, with each data point plotted. n=3 per group. Mann Whitney U-test. ns denotes non-significance (p=≥0.05).

4.2.3 The Effects of Fractionated Radiotherapy on the Tumour Immune Micro-Environment of AKPT Rectal Tumours

Single fraction radiotherapy failed to elicit a reduction in tumour volume or any definitive changes in the tumour immune microenvironment of the orthotopic AKPT organoid transplant model of LARC. Therefore, I next sought to determine whether fractionated radiotherapy would induce any clinical, histological or immunological response. Fractionated radiotherapy regimens were designed to mimic SCRT which consists of 5 x 5Gy on consecutive days, and is a standard of care regimen used clinically in LARC. To account for potential differences in tissue responsiveness and tolerability between mice and humans, three preliminary regimens were adopted to recapitulate SCRT (5 x 5Gy; 5 x 3Gy; 3 x 5Gy). Furthermore, fractions were delivered on alternate days to ensure animals recovered sufficiently between fractions and their associated anaesthetic (Figure 4.20, top panel).

Following treatment at 3-weeks post tumour implantation, animals were aged until clinical endpoint (>10% weight loss, visible tumour burden or deteriorating

body condition) and then sampled. Fractionated radiotherapy failed to decrease tumour burden when compared with an unirradiated control group which underwent sham radiotherapy (Figure 4.20, middle panel). Conversely, reduced tumour volume was observed in the untreated group, which likely reflected the short survival seen in this small cohort. Aside from one subject in the 3 x 5Gy cohort, a marked extension in survival was not observed following fractionated radiotherapy. A statistically significant extension in survival was observed ($p=0.0389$) when the 5 x 3Gy group was compared with the untreated cohort. However, considering each treatment cohort consisted of low numbers ($n=3$), it was not possible to conclude that fractionated radiotherapy extended survival in the AKPT model, and expanded cohorts were subsequently studied to assess this. Serial colonoscopy images demonstrated that intra-luminal tumour burden failed to regress despite treatment with fractionated radiotherapy (Figure 4.20, bottom panel).

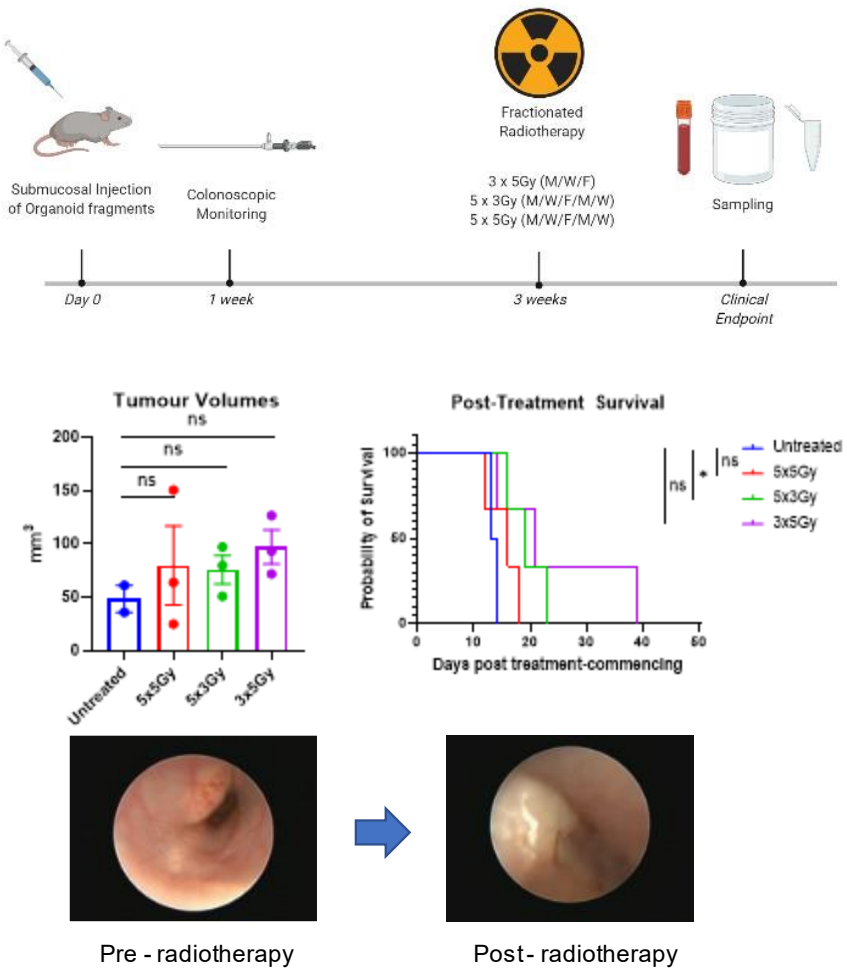

Figure 4.20: Development of Short-Course Fractionated Radiotherapy Regimens

Top – Schematic demonstrating the experimental timeline for delivery of fractionated radiotherapy regimens. Middle – Bar graph showing tumour volumes for each treatment group from tumours sampled at clinical endpoint (left). Survival curve demonstrating survival post treatment commencement for fractionated radiotherapy (right). Bottom – Representative colonoscopy images of an AKPT tumour pre-treatment and 1-week post fractionated radiotherapy. Error bars show mean and SEM, with each data point plotted. n=2-3 per group. Mann-Whitney U-test (bar graph). Log-rank Mantel-Cox test (survival curve). ns denotes non-significance (p-value ≥0.05). * denotes p-value <0.05.

As no clear therapeutic efficacy was demonstrated with any fractionated radiotherapy regimen, the 3 x 5Gy regimen was utilised in further experiments to minimise the number of treatment sessions and exposure to anaesthetic which animals were subjected to. When a larger cohort of animals were treated at an earlier timepoint (2-weeks post tumour implantation) when tumour burden was less established, a small extension in survival was observed when compared with a sham radiotherapy control group. However, this extension did not reach statistical significance (p=0.2752) (Figure 4.21, bottom panel). Furthermore, no

change in tumour volume was observed between groups (Figure 4.21, bottom panel).

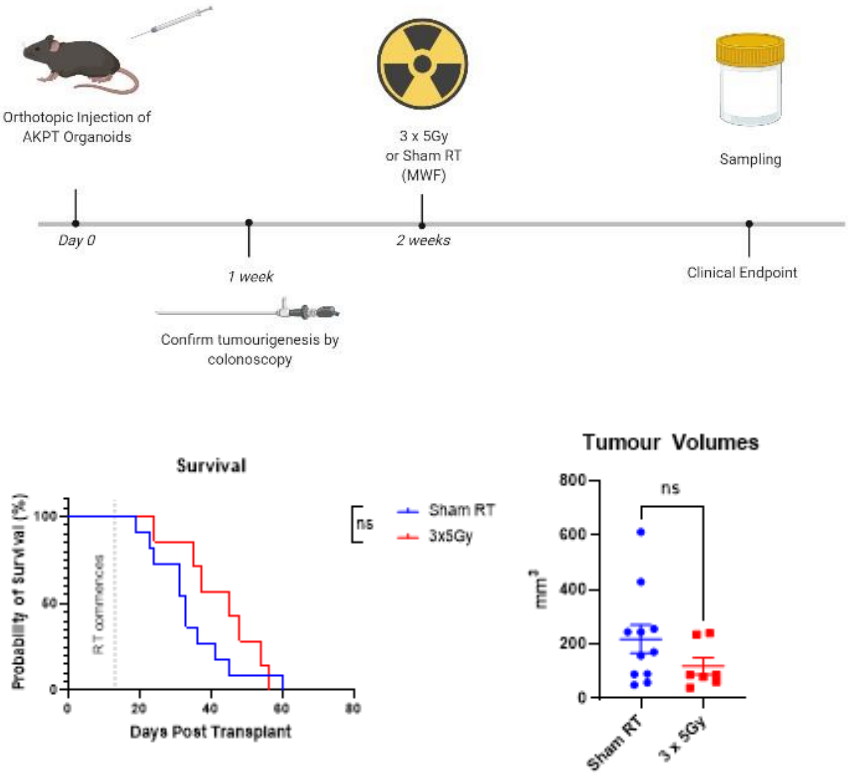

Figure 4.21: Improved Survival and Tumour Volume Reduction was not demonstrated following Fractionated Radiotherapy

Top – Schematic demonstrating the experimental timeline for delivery of 3x5Gy fractionated radiotherapy. Bottom – Survival curve showing post-transplant survival compared with sham radiotherapy (left). Bar graph showing tumour volumes for each treatment group at clinical endpoint (right). Error bars show mean and SEM, each data point plotted. n=7 fractionated radiotherapy group, n=11 sham radiotherapy group. Log-rank Mantel-Cox test (survival curve). Mann-Whitney U-test (bar graph). ns denotes non-significance (p-value ≥0.05).

Systemic blood was analysed from animals at clinical endpoint following fractionated radiotherapy (all regimens described) and compared with age-matched untreated controls, to determine changes in circulating immune cell populations (Figure 4.22). A significant increase in systemic white cell counts were seen following fractionated radiotherapy (p=0.0041). Furthermore, a significant increase in lymphocyte counts were observed in the fractionated radiotherapy group (p=0.0346), whilst non-significant elevations in neutrophil, monocyte and eosinophil counts were seen. The observed changes are suggestive that fractionated radiotherapy induced a durable systemic inflammatory response, which was not observed at short-time intervals (3- and 7-days) following single fraction radiotherapy.

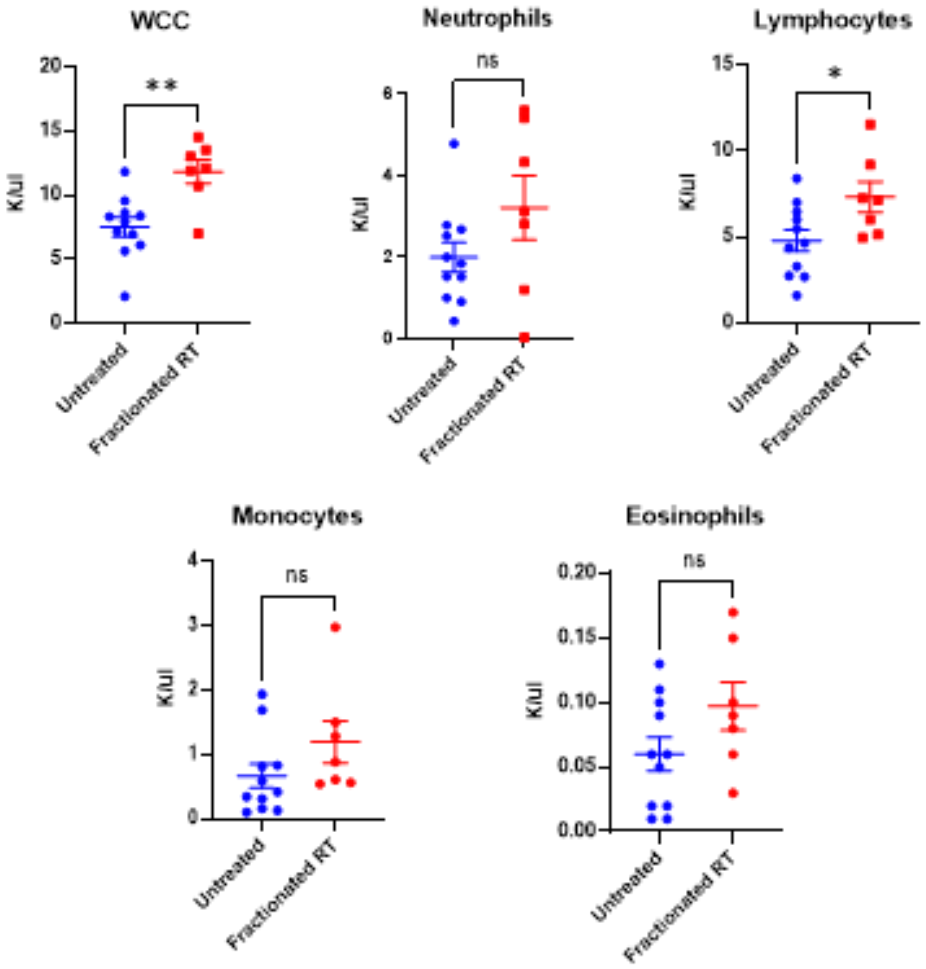

Figure 4.22: Fractionated Radiotherapy affects Circulating Blood Markers

Top – Bar graphs showing white cell, neutrophil and lymphocyte counts following fractionated radiotherapy, compared with age-matched controls. Bottom – Bar graphs showing monocyte and eosinophil counts. All cell types measured as 10^3 cells per µl (K/µl). Error bars show mean and SEM, with each data point plotted. n=7-11 per group. Mann-Whitney U-test. ns denotes non-significance (p-value ≥0.05). * denotes p-value <0.05. ** denotes p-value <0.01.

In the absence of tumour volume reduction, H+E stains were analysed to assess histological changes associated with radiation (Figure 4.23, top panel). Numerous tumour regression grading (TRG) systems exist in clinical practice to assess therapeutic response to radiotherapy and CRT, including the modified Dworak and the American Joint Committee on Cancer (AJCC) systems (Dworak et al, 1997; Kim et al, 2016). Such classification systems classify the degree of tumour regression by assessing the proportion of tumour occupied by fibrosis relative to viable tumour cells. However, significant areas of fibrosis were not observed in post fractionated radiotherapy samples, and so this measure was not used as a surrogate marker for therapy response (Figure 4.23).

High grade inflammatory cell response, particularly at the invasive margin is associated with improved survival outcomes in CRC patients (Klintrup et al, 2005). Several clinical studies show that an improved recurrence free survival rate is associated with both increased inflammatory cells within fibrotic stroma, and the presence of surface ulceration (Shia et al, 2004; Nagtegaal et al 2001). On assessing H+E sections, areas of immune cell infiltrate and acute necrosis were observed following fractionated radiotherapy, suggesting some tumour regions undergo an inflammatory reaction following fractionated radiotherapy (Figure 4.23, top panel).

Presence of mucin pools lacking neoplastic epithelium, is regarded as a feature of treatment response, but is not associated with improved recurrence free survival in rectal cancer patients who have undergone neo-adjuvant therapy (Shia et al, 2011). Areas of mucin pooling were observed in AKPT tumours treated with fractionated radiotherapy which were not obvious upon analysis of tumour sections from untreated controls (Figure 4.23, top panel). In order to quantify these changes, tumour tissue was stained using the Alcian Blue/periodic-acid Schiff (AB/PAS) sequence to assess mucin secretion by adenocarcinoma cells. A significant increase in AB/PAS staining was observed in post-fractionated radiotherapy tumour samples, when quantified as % of tumour area positively stained ($p=0.0159$) (Figure 4.23, lower panel). Areas of mucin pooling were observed in only some regions of irradiated tumours, suggesting that expulsion of mucin from tumour cells occurred in isolated tumour regions with some tumour areas being less affected by irradiation. Although tumour volume regression and clear survival extension were not observed following fractionated radiotherapy in the AKPT model, histological changes were demonstrated to suggest that tumours undergo a more subtle response to therapy.

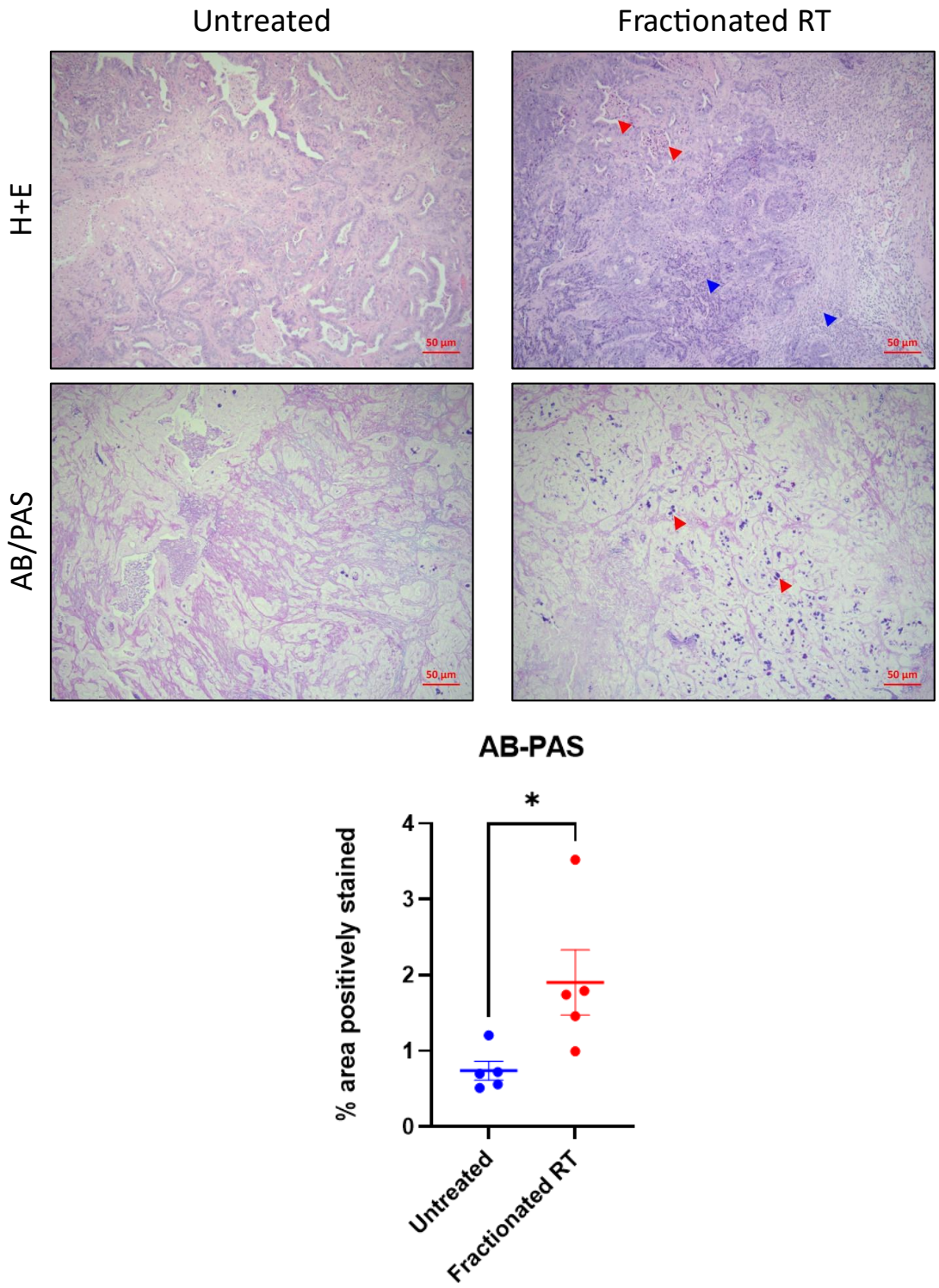

Figure 4.23: Histological Changes are seen following Fractionated Radiotherapy

Top – Representative H+E staining of untreated and post fractionated radiotherapy AKPT rectal tumour samples. Middle – Representative AB/PAS staining from the corresponding AKPT tumours. Bottom - Bar graph showing AB/PAS quantification as % of tumour area stained. Error bars show mean and SEM, with each data point plotted. n=5 per group. Mann-Whitney U-test. * denotes p-value <0.05. Scale bars 50µm. Red arrows depict areas of mucin pooling. Blue arrows indicate acute necrosis/inflammatory infiltrate.

Immunohistochemistry was then performed to assess whether changes in infiltration of common immune cell groups could be observed following fractionated radiotherapy, with tumour samples from clinical endpoint analysed. Clusters of T-lymphocytes (CD3+ve cells) and cytotoxic T-lymphocytes (CD8+ve cells) were observed at the invasive margins of both untreated AKPT tumours and at clinical endpoint following treatment with fractionated radiotherapy (Figure 4.24, top and middle panels). Less abundant and patchy infiltration of CD3+ve and CD8+ve lymphocytes were observed within the tumour core of both treated and control tumour samples. Upon quantification, no significant changes in lymphocyte infiltration were observed following treatment with fractionated radiotherapy (Figure 4.24, lower panel).

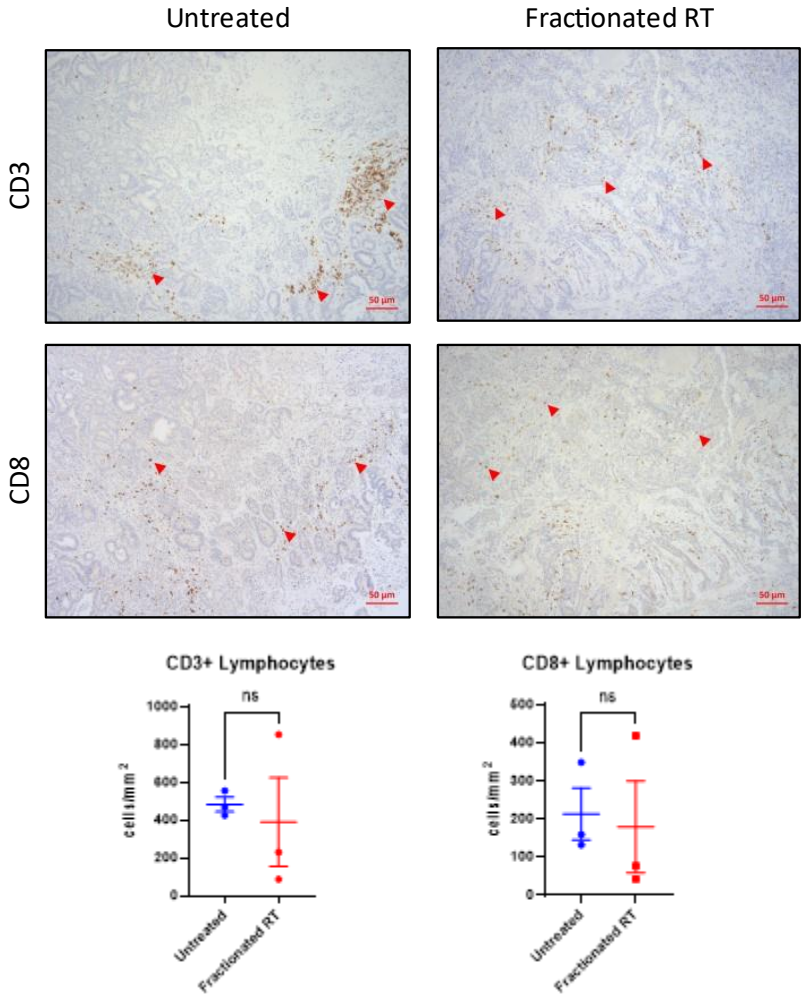

Figure 4.24: Tumour Infiltrating Lymphocytes are unchanged Following Fractionated Radiotherapy

Top – Representative CD3 staining in untreated and post fractionated radiotherapy AKPT rectal tumours. Middle – Representative CD8 staining. Lower – Bar graphs showing expression of CD3 and CD8 as cells per mm^2. Error bars show mean and SEM, with each data point plotted. n=3 per group. Mann-Whitney U-test. ns denotes non-significance (p-value ≥0.05). Scale bars = 50µm. Red arrows depict positively stained cells.

S100A9 expression was quantified to assess for changes in tumour infiltrating neutrophils, with no significant change between groups observed (Figure 4.25, top panel). Furthermore, no significant effect on macrophage populations were observed following fractionated radiotherapy through quantification of F4/80 expression, although an apparent increase in mean % of area staining positively for F4/80 was seen in the fractionated radiotherapy group (Figure 4.25, middle panel). For both S100A9 expressing neutrophils and F4/80+ve macrophages, populations appeared to be more evenly distributed throughout tumours, with myeloid cells infiltrating the tumour core irrespective of treatment with fractionated radiotherapy.

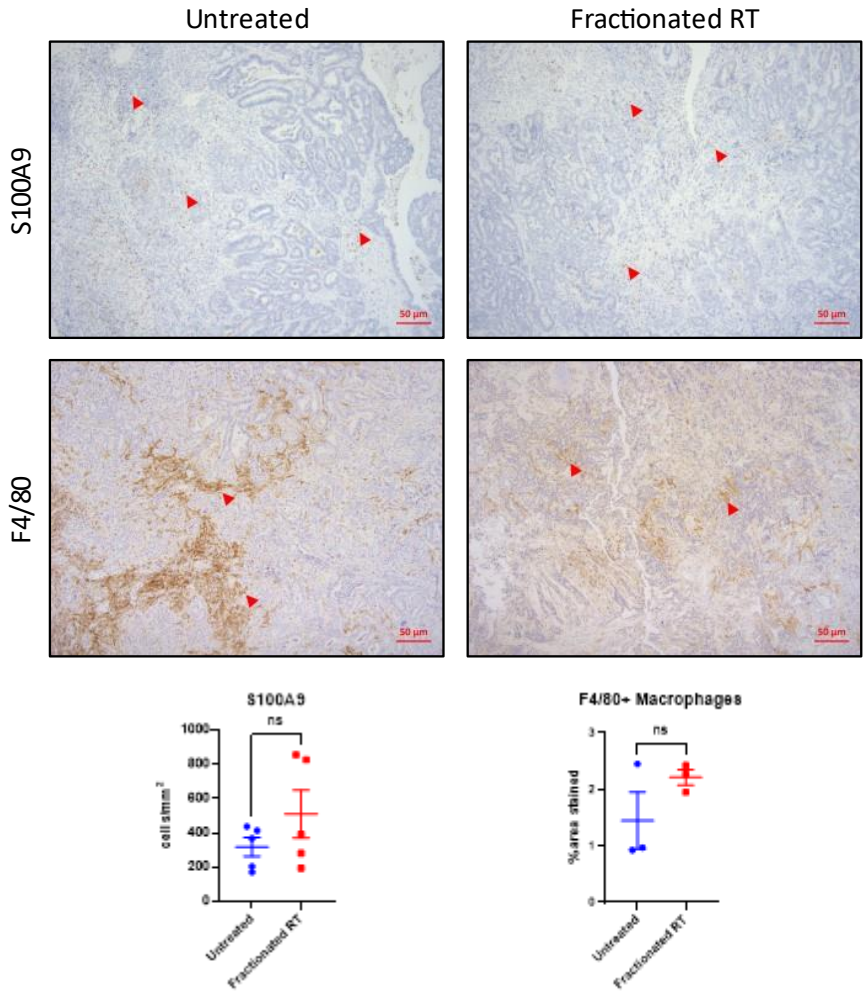

Figure 4.25: Changes in Tumour Infiltrating Myeloid Cells were not observed following Fractionated Radiotherapy

Top – Representative S100A9 staining in untreated and post fractionated radiotherapy AKPT rectal tumour samples. Middle – Representative F4/80 staining. Lower – Bar graphs showing S100A9 and F4/80 quantification, as cells per mm^2 and % of tumour area positively stained respectively. Error bars show mean and SEM, with each data point plotted. n=3-5 per group. Mann-Whitney U-test. ns denotes non-significance (p-value ≥0.05). Scale bars = 50µm. Red arrows depict positively stained cells.

Despite the observation of small regions of necrosis on H+E sections following fractionated radiotherapy, IHC data suggests that fractionated radiotherapy failed to induce a clear change in immune cell infiltrate when whole tumours were assessed at clinical endpoint. To identify potential mechanisms of treatment resistance and drivers of an immunosuppressive tumour microenvironment, TGF-ß signalling was assessed through pSMAD3 staining of post fractionated radiotherapy tumour samples. Having previously shown abundant levels of TGF-ß signalling in the AKPT organoid transplant model, extensive pSMAD3 expression was observed in tumour epithelial cells at clinical endpoint following fractionated radiotherapy (Figure 4.26, top panel). Upon quantification, no significant change in expression was observed following treatment, with the TGF-ß signalling pathway known to be highly activated at baseline in this model (Figure 4.26, lower panel).

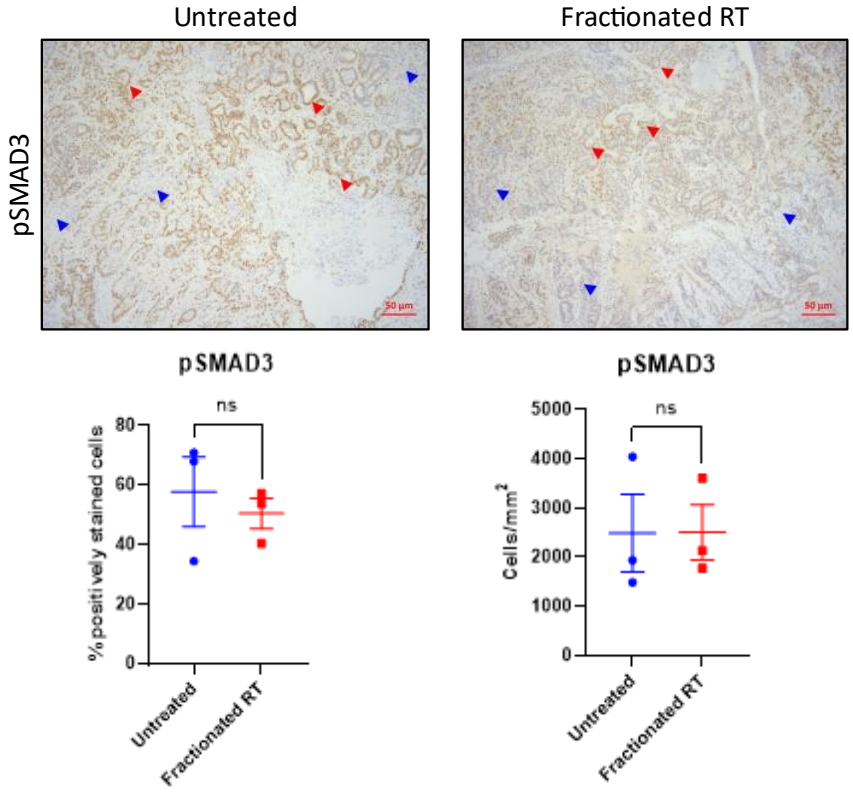

Figure 4.26: Changes in TGF-ß Signalling Following Fractionated Radiotherapy are not observed

Top – Representative pSMAD3 staining in untreated and post fractionated radiotherapy AKPT rectal tumour samples. Lower - Bar graphs quantifying pSMAD3 staining by % of pSMAD3 expressing cells and by positively stained cells/mm^2. Error bars show mean and SEM, with each data point plotted. n=3 per group. Mann-Whitney U-test. ns denotes non-significance (p-value ≥0.05). Scale bars = 50µm. Red arrows depict pSMAD3 expressing epithelial cells. Blue arrows depict pSMAD3 expressing stromal cells.

Multiplex IHC was performed to characterise the spatial relationships between different immune cell populations in both untreated and post-fractionated radiotherapy samples from tumours at clinical endpoint. CD4+ve T-helper cells, CD8+ve CTLs, CD68+ve macrophages, Ly6G expressing neutrophils, and Treg cells (FOXP3 expression) were included in the panel. Images show a predominance of myeloid cells (CD68 and Ly6G) at the tumour edge of untreated samples, with an infiltration of CD4+ve and CD8+ve lymphocytes seen in this area following fractionated radiotherapy (Figure 4.27, top panel). When the tumour core was examined, sparse immune infiltrate was observed in untreated samples with scattered populations of lymphocyte and myeloid cells seen. In contrast, following fractionated radiotherapy the tumour core appeared to be infiltrated with CD68 expressing macrophages (Figure 4.27, middle panel). No statistically significant difference in any of the noted immune cell markers was noted, however, only a small number of samples (n=3 per group) were analysed (Figure 4.27, bottom panel).

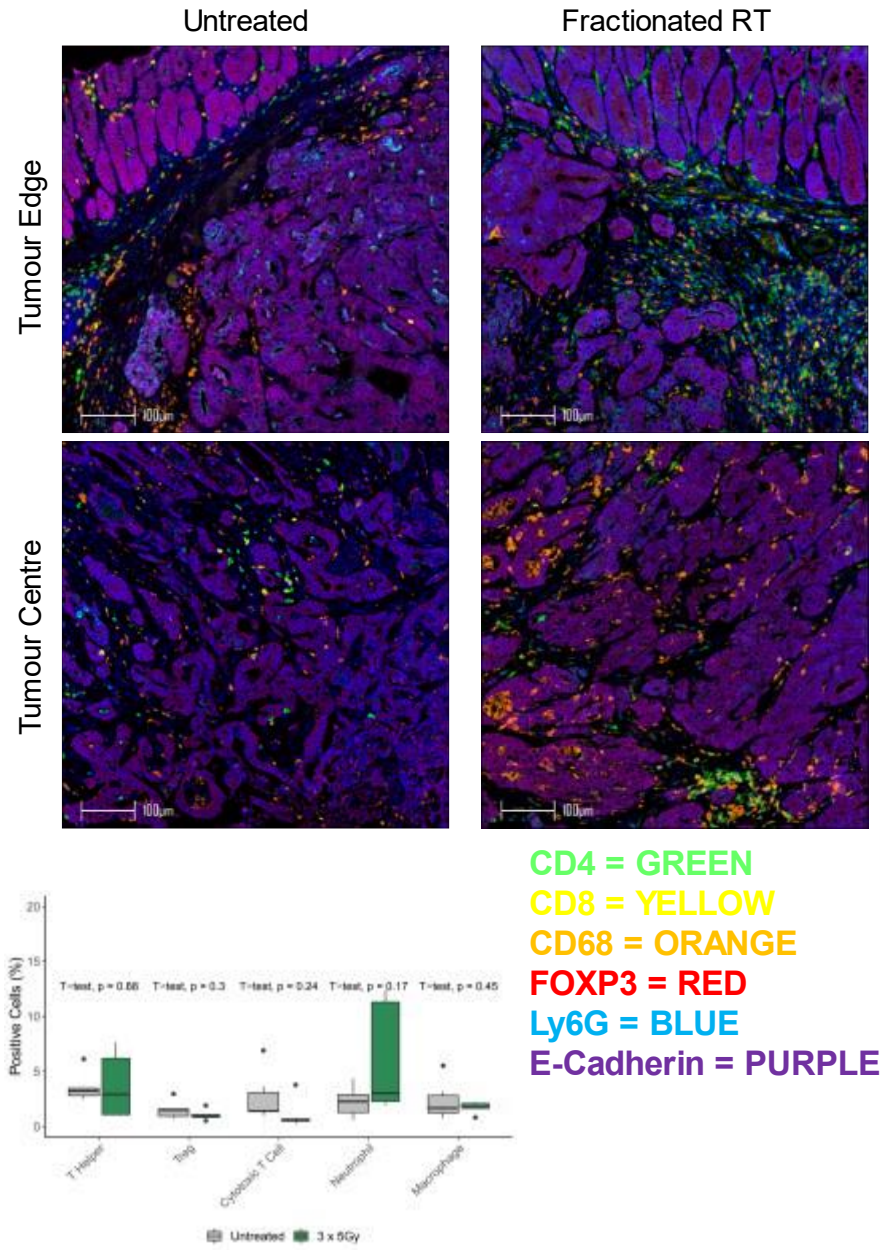

Figure 4.27: Multiplex IHC demonstrates a Radioresistant Tumour Immune Microenvironment

Top – Representative multiplex IHC images for untreated and irradiated tumour edges. Bottom – Representative multiplex IHC images for untreated and irradiated tumour core. Lower - Bar graphs quantifying immune markers as % of positively expressing cells. Scale bars 100μm. n=3 per group. Bars show mean and SEM, with each data point plotted. Mann-Whitney U-test. p-values stated. Legend to depict immune cell marker staining by fluorophore colour. Multiplex staining and analysis performed by Dr Eoghan Mulholland (University of Oxford).

In the limited number of samples analysed, data was suggestive of a tumour immune microenvironment which demonstrates resistance to fractionated radiotherapy in the orthotopic AKPT rectal cancer model. Systemic blood analysis showed clear increases in overall leucocyte, lymphocyte and neutrophil counts following fractionated radiotherapy, however, no significant change in

any immune cell population was observed on IHC following treatment. No benefit in survival or tumour burden were observed upon treatment with 3 x 5Gy in expanded cohorts. F4/80 staining and multiplex IHC were suggestive that macrophages may infiltrate the tumour core following fractionated radiotherapy, however, higher numbers and repeat experiments would be required to substantiate this conclusion.

4.2.4 Transcriptomic Changes following Radiotherapy in the AKPT Model

I next performed bulk RNA sequencing on AKPT rectal tumour samples treated with both single-fraction and fractionated radiotherapy. Tumours treated with a single 4Gy fraction and sampled at 3-day, 7-day and 14-day time-points, were analysed as described previously. Tumours subjected to fractionated radiotherapy (5 x 5Gy, 5 x 3Gy or 3 x 5Gy) were sampled at clinical endpoint, with a cohort of untreated clinical endpoint samples included as a control group.

Principal Component Analysis (PCA) was performed for all samples, to detect the degree of similarity in gene expression values between samples and groups (Figure 4.28). In PCA, the dimensionality of a large data set is reduced by transforming a large set of variables into a smaller set, whilst still consisting of most of the information within the original data. Linear combinations of the original data are used to define a new set of variables (principal components), which enables the visualisation of closely correlated samples by the degree of clustering, and also allowing identification of outliers. Within PCA, axes are ranked in order of importance, with differences in dimension 1 (x-axis) being more important than differences in dimension 2 (y-axis). No obvious patterns of clustering were observed upon PCA, illustrating that these samples exhibit a significant degree of molecular heterogeneity.

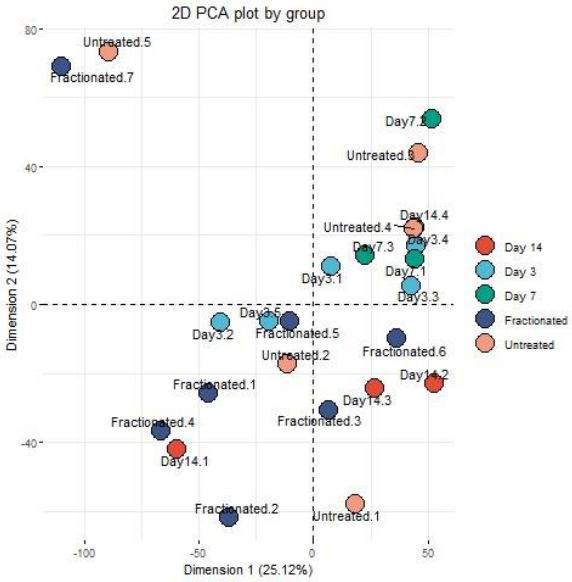

Figure 4.28: 2D Principal Component Analysis of AKPT Rectal Tumour Samples Post Radiotherapy

2D PCA generated from RNA sequencing data of AKPT rectal tumours (untreated, post single 4Gy fraction at 3-day, 7-day and 14-day time-points, and post fractionated radiotherapy). Each data point plotted, with sample groups indicated by key. Dimension 1 plotted on x-axis, dimension 2 on y-axis. n=3-7 per group. Data analysis performed by Dr Kathryn Gilroy (CRUK Beatson Institute).

Gene-set variation analysis (GSVA) was conducted to determine expression of hallmark gene-sets of interest across each experimental group. Hallmark gene-sets of interest included those associated with the immune response, including interferon-alpha (IFN-α), interferon gamma (IFN-γ), interleukin-6 mediated janus kinase/signal transducer and activator of transcription 3 signalling (IL-6 JAK/STAT3) and inflammatory response. An up-regulation in IFN-γ, IFN-α, IL-6 JAK/STAT3 signalling and inflammatory response was observed at short time-points post single fraction radiotherapy (3-days and 7-days), with this response not observed at the 14-day time-point and in tumours analysed at clinical endpoint following fractionated radiotherapy (Figure 29). Up-regulation in expression of the TGF-ß hallmark gene-set was observed at all time-points studied following single fraction radiotherapy and following fractionated radiotherapy, when compared with untreated control group samples (Figure 4.29).

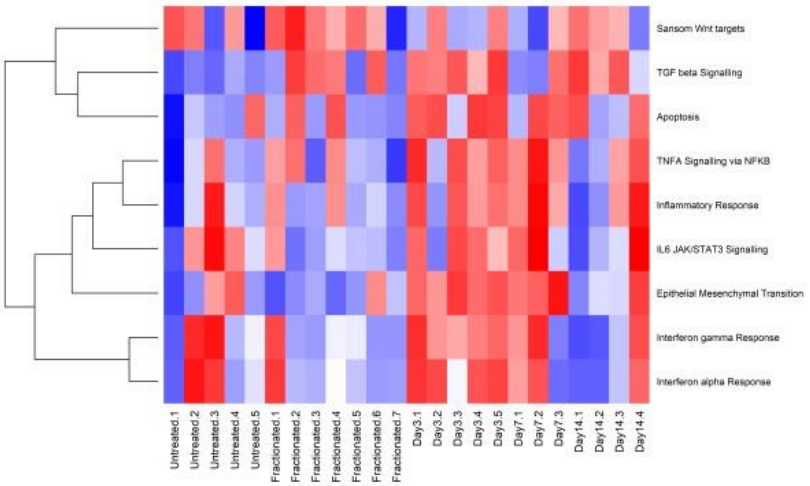

Figure 4.29: Upregulation of Hallmark Gene-sets is observed following Radiotherapy

Heatmap demonstrating hallmark gene-sets with significant up-regulation shown in red, and significant down regulation in blue. Each individual sample plotted along bottom x-axis. Each hallmark gene-set described on right y-axis. n=3-7 per group. Data analysis performed by Dr Kathryn Gilroy (CRUK Beatson Institute).

Following the observation of up-regulation of the TGF-β hallmark gene-set in all treatment groups, individual genes were then analysed for significant up-regulation in expression with comparison made from each individual treatment groups with the untreated control cohort. No individual genes were found to display differentially altered expression (defined as adjusted p value < 0.05 and log2 fold change >1), when compared with the untreated control cohort. When mean expression of individual genes were displayed as a heatmap, no obvious pattern of upregulation in SMAD protein (Smad1, 3, 6 or 7) or TGF-β receptor (Tgfbr1) related genes were observed in any treatment group.

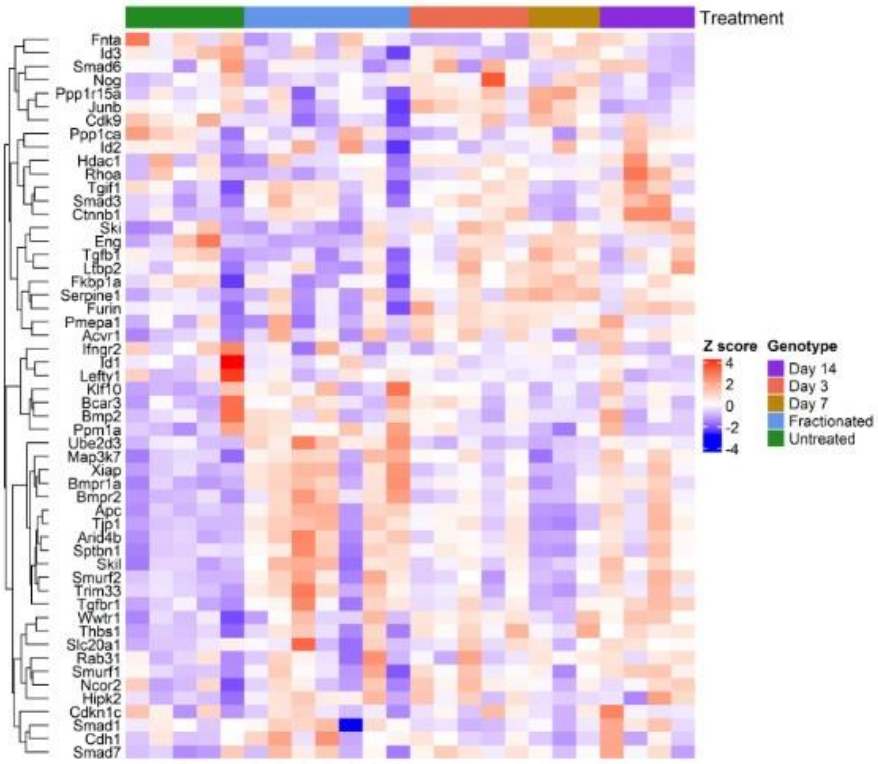

Figure 4.30: No Significantly Up-regulated Genes are Demonstrated in the TGF-ß Hallmark Gene-Set

Heatmap demonstrating normalised transcript reads for individual genes within the TGF-ß hallmark gene-set. Each individual sample plotted along upper x-axis. Individual genes shown on left y-axis. Key shows individual treatment groups. z-score indicating up-regulation in gene expression plotted in red with down-regulation plotted in blue, with numerical value representing number of standard deviations away from the mean expression of all samples plotted. n=3-7 per group. Data analysis performed by Dr Kathryn Gilroy (CRUK Beatson Institute).

Individual treatment groups were then compared with untreated control samples, to identify significant changes when differential gene expression was performed across all genes and then within gene-sets of interest. Following fractionated radiotherapy, many genes were significantly up- or down-regulated when compared with untreated controls, showing that fractionated radiotherapy induced durable transcriptomic changes in the AKPT rectal tumour model (Figure 4.31).

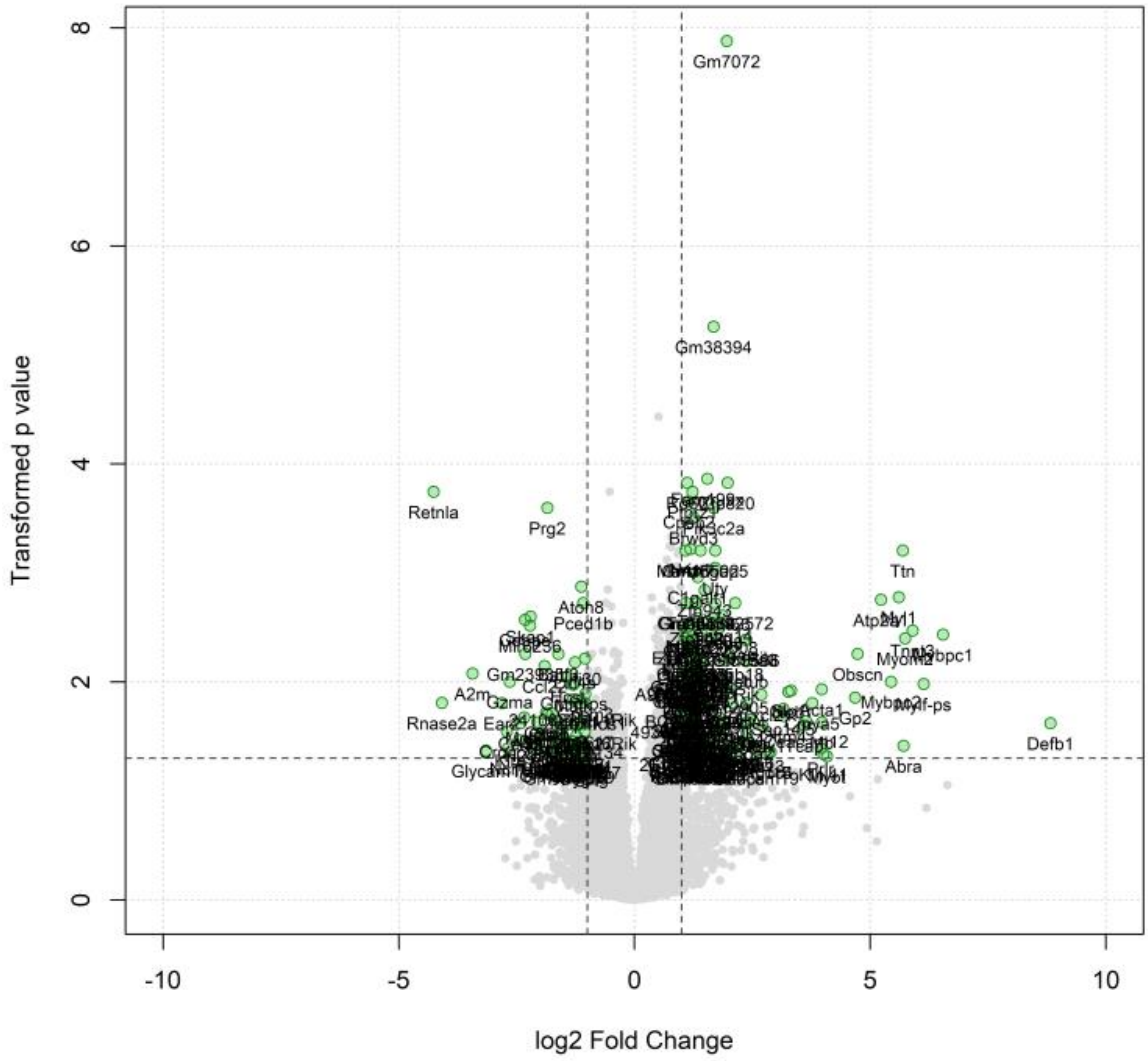

Figure 4.31: Altered Expression of Genes was Demonstrated Following Fractionated Radiotherapy

Volcano plot demonstrating differential expression across all genes when post fractionated radiotherapy tumours were compared with untreated controls. Significant gene changes plotted in green with label. x-axis shows log2 fold change, with >1 depicting significantly up-regulated genes, and <1 depicting significantly down-regulated genes. y-axis shows transformed p-value (-$\log_{10}$ of p-value), with $p<0.05$ depicting significance. Non-significantly altered genes plotted as grey dots. Data analysis performed by Dr Kathryn Gilroy (CRUK Beatson Institute).

Differential gene expression analysis was then performed for hallmark gene-sets associated with immune response and inflammation (IFN-γ, IFN-α, IL-6 JAK/STAT3 signalling and inflammatory response). Upon probing for specific genes of interest demonstrating differential expression following fractionated radiotherapy, up-regulation of the Ptgs2 (Prostaglandin-endoperoxide synthase 2) gene within the interferon-γ hallmark gene-set was noted to be up-regulated following fractionated radiotherapy (Figure 4.32).

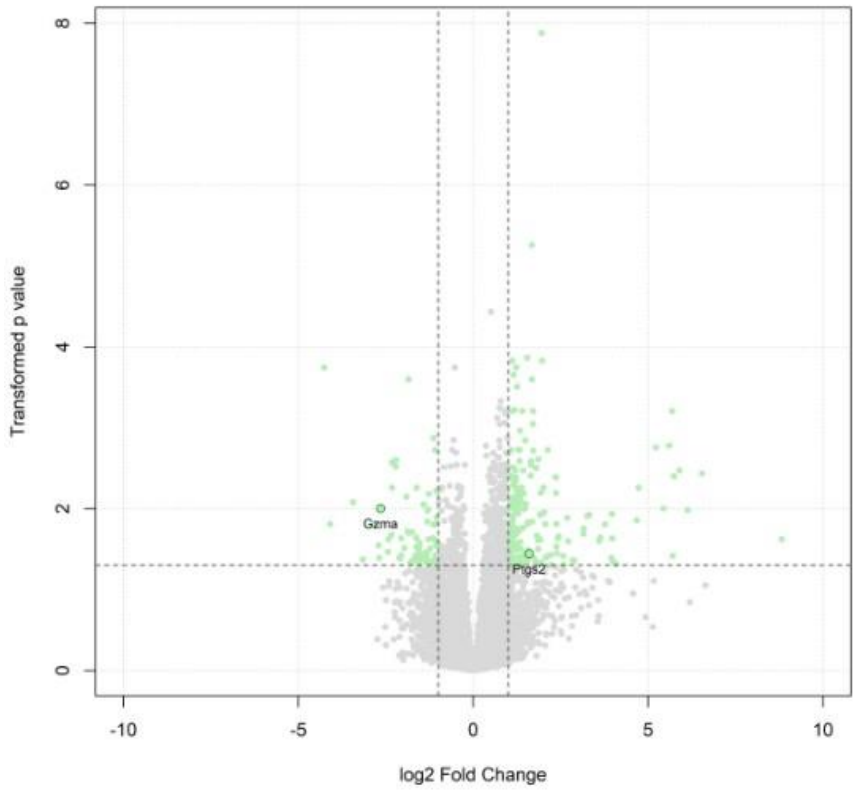

Figure 4.32: Upregulation of Ptgs2 is Demonstrated Following Fractionated Radiotherapy

Volcano plot demonstrating differential expression of individual genes within the INF-γ hallmark gene-set. Significant gene changes plotted in green with only IFN-γ associated genes labelled. x-axis shows log2 fold change, with >1 depicting significantly up-regulated genes, and <1 depicting significantly down-regulated genes. y-axis shows transformed p-value ($-\log_{10}$ of p-value), with $p<0.05$ depicting significance. Non-significantly altered genes plotted as grey dots. Data analysis performed by Dr Kathryn Gilroy (CRUK Beatson Institute).

When differential expression of individual genes within the IFN-γ hallmark gene-set was plotted for the single fraction time-point treatment groups, the Ptgs2 gene was noted to be upregulated at both the 3-day and 7-day time-points post single fraction radiotherapy (Figure 4.33, upper and lower panels respectively). Prostaglandin-endoperoxide synthase 2 (Ptsg2), also known as cyclooxygenase 2 (COX-2), is involved in the conversion of arachidonic acid to various prostaglandins, and is a key mediator of inflammation and known to be upregulated in response to cytokines (Portanova et al, 1996). The COX-2 derived prostaglandin PGE2 is known to promote tumour growth, through activating signalling pathways involved with cell proliferation, migration, apoptosis and angiogenesis, and by suppressing immune responses (Wang and Dubois, 2006).

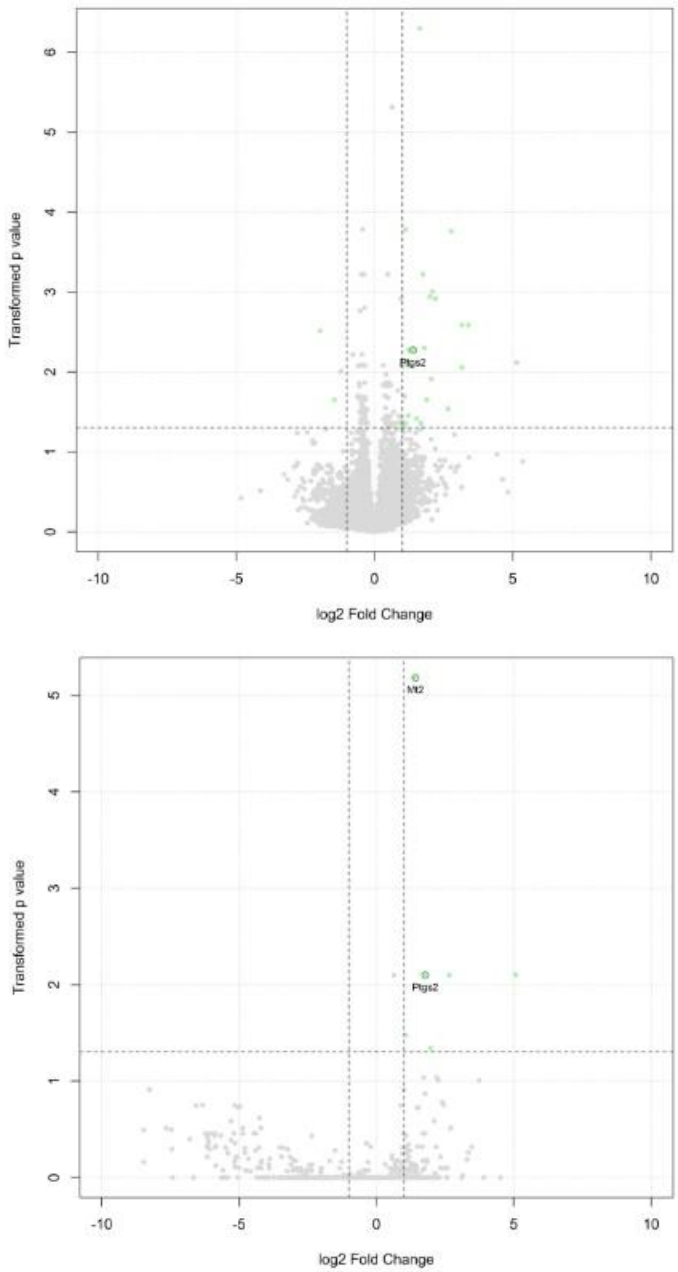

Figure 4.33: Ptgs2 is Upregulated Following Single Fraction Radiotherapy

Volcano plots demonstrating differential expression of individual genes with INF-γ hallmark gene-set. Top – demonstrates 3-day timepoint group post single fraction radiotherapy. Bottom – demonstrates 7-day timepoint group following single fraction radiotherapy. Significant gene changes plotted in green with only IFN-γ associated genes labelled. x-axis shows log2 fold change, with >1 depicting significantly up-regulated genes, and <1 depicting significantly down-regulated genes. y-axis shows transformed p-value ($-\log_{10}$ of p-value), with $p<0.05$ depicting significance. Non-significantly altered genes plotted as grey dots. Data analysis performed by Dr Kathryn Gilroy (CRUK Beatson Institute).

4.2.5 AKPT Organoids Demonstrate Responsiveness to Irradiation *In-vitro*

Having demonstrated resistance to radiotherapy in the orthotopic AKPT organoid transplant model of rectal cancer, I sought to determine whether AKPT organoids would demonstrate responsiveness to irradiation *in-vitro*, in the absence of a host immune system. AKPT organoids were cultured, dissociated into single cells, then seeded in 2D conditions to allow serial imaging of organoid growth. At 3-days post seeding, organoids were treated with a single fraction of radiotherapy at a range of doses (0, 2, 4, 6, 8 and 10Gy) (Figure 4.34, top panel). Furthermore, media was treated with increasing concentrations of 5-FU chemotherapy (or dimethyl sulfoxide (DMSO) as vehicle), a known radio-sensitising agent given in standard of care CRT in rectal cancer.

At 72 hours post irradiation, cell viability was assessed using WST-1 assay, which measures mitochondrial dehydrogenase activity through quantification of formazan dye formed by viable cells. Data for % of cell viability was normalised to the readouts obtained for wells treated with 0Gy irradiation and DMSO vehicle. An increasing response was seen following radiotherapy, with 19.9% cell viability observed in the 10Gy plus DMSO treatment condition at 72 hours (Figure 4.34, bottom panel). In the absence of irradiation, AKPT organoids responded similarly to escalating concentrations of 5-FU, with the 0Gy plus 50μM 5-FU treatment condition demonstrating 20.5% cell viability (Figure 4.34, bottom panel). This data demonstrates that maximal therapeutic effect *in-vitro* was achieved with fractions of 8-10Gy, with no synergistic effect demonstrated following the addition of 5-FU. However, in the absence of irradiation, this maximal therapeutic effect was also achieved with the maximal concentration of 5-FU (50μM) studied. In the absence of a host stroma and infiltrating immune cells, AKPT organoids demonstrated increasing sensitivity to both irradiation and 5-FU chemotherapy *in-vitro*.

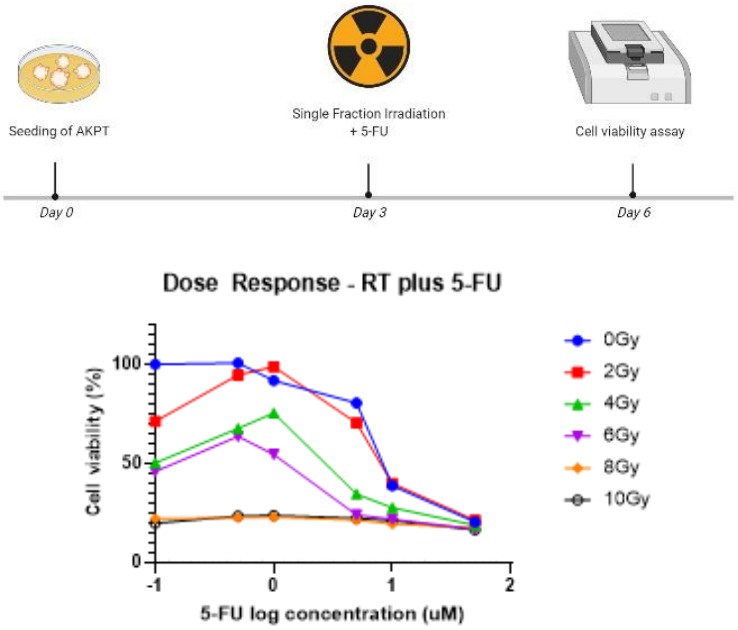

Figure 4.34: AKPT Organoids Demonstrate Sensitivity to Irradiation and 5-FU *In-Vitro*

Top – Schematic showing experimental timeline for seeding of AKPT single cells and treatment *in-vitro*. Bottom – Dose response curve demonstrating % cell viability as normalised to 0Gy and DMSO-treated media. Treatment with escalating dose of radiotherapy (0Gy, 2Gy, 4Gy, 6Gy, 8Gy and 10Gy), and media treated with escalating concentrations of 5-FU (DMSO, 0.5μM, 1μM, 5μM, 10μM and 50μM). y-axis shows % cell viability. x-axis shows 5-FU concentration converted to logarithmic form. 5 replicates per experimental condition. Experiment performed on two occasions, with second dataset presented.

In addition, immediately following initiation of treatment, growth of established organoids were monitored through serial imaging (8 hourly intervals) using an Incucyte® imaging system. When analysing organoids treated with radiotherapy and DMSO-treated media, longitudinal continuous growth of organoids can be seen following 0Gy and with lower 2Gy or 4Gy fractions of radiotherapy (Figure 4.35). At the higher 8Gy and 10Gy radiotherapy fractions, limited organoid growth was detected upon serial imaging, with evidence of organoid rupture demonstrated at 48-72 hours (Figure 4.35).

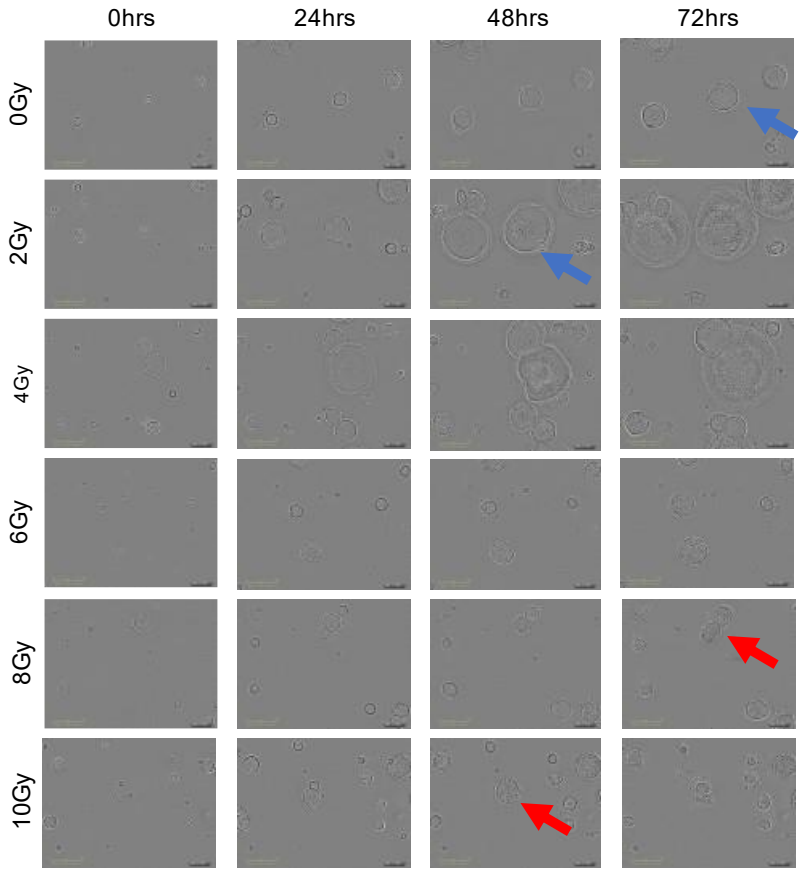

Figure 4.35: AKPT Organoids Demonstrate Sensitivity to Irradiation In-Vitro

Representative serial images of organoids treated with escalating fractions of radiotherapy (with DMSO vehicle treated media) at baseline, 24hrs, 48hrs and 72hrs. Images obtained from incucyte. Blue arrows depict healthy and expanding organoids. Red arrows depict ruptured organoids.

Cell confluence was then assessed using Incucyte® images, to determine the % of area per well occupied by single cells and organoids. Serial values were then plotted to determine whether escalating doses of radiotherapy (with DMSO treated media) resulted in less cell growth over time (Figure 4.36). Different starting % cell confluences were observed between different treatment groups, with subsequent gradients of cell growth appearing to be similar over 72 hours post irradiation. The lower % of cell confluence seen in the higher radiotherapy fraction groups (6Gy, 8Gy and 10Gy) at 72 hours, when compared with smaller fractions, likely reflects the lower starting cell confluence and so limited conclusions can be drawn regarding the effect of escalating radiation dose upon cell and organoid growth when measured in this manner.

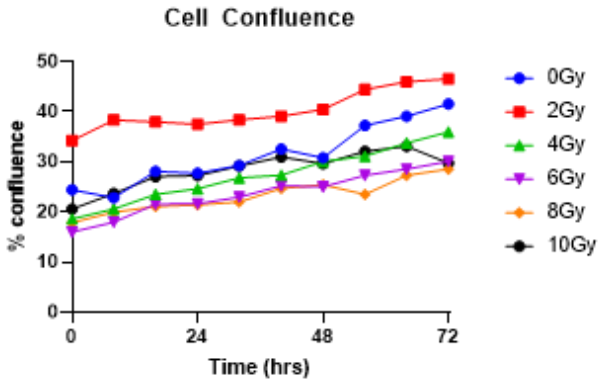

Figure 4.36: AKPT Cell and Organoids Growth is Slowed with Escalating Irradiation

Graph to show serial growth of AKPT cells and organoids over time, demonstrated as % confluence of imaged wells. Data points plotted at 8 hourly time intervals for each radiotherapy fraction. Each data point represents the mean value of 5 experimental replicates.

4.2.6 The AKPT Subcutaneous Xenograft Model Demonstrates Responsiveness to Fractionated Radiotherapy

I then sought to determine whether AKPT organoid derived tumours would be more responsive *in-vivo* when injected subcutaneously at the flank region, to assess whether changes in tumour infiltrating immune cells differ according to tumour site. AKPT organoid fragments were injected unilaterally in the subcutaneous flank region of immunocompetent C57Bl/6 mice, and were treated with a 3 x 6Gy fractionated radiotherapy regimen at 2 weeks post tumour implantation (Figure 4.37, top panel). Mice were sampled at clinical endpoint, defined as tumour diameter ≥15mm in one dimension, deteriorating body condition, or the presence of skin ulceration. An extension in survival was observed in the cohort subjected to fractionated radiotherapy, however, this did not reach statistical significance (p=0.1163) (Figure 4.37, middle panel).

Serial tumour measurements were carried out 3 times weekly (Mon/Wed/Fri), by measuring maximum diameter and the corresponding perpendicular width; these values were then used to calculate estimated tumour volume and to chart tumour growth (Figure 4.37, bottom panel). A transient tumour volume reduction was observed in several treated tumours at 10-14 days post commencement of treatment, whereas all untreated subjects displayed continuous tumour growth (Figure 4.37, bottom panel). Irradiated tumours (n=2) which did not exhibit transient tumour volume regression had reached clinical endpoint prior to 10

days post treatment initiation, as a result of skin ulceration or maximal tumour diameter being reached.

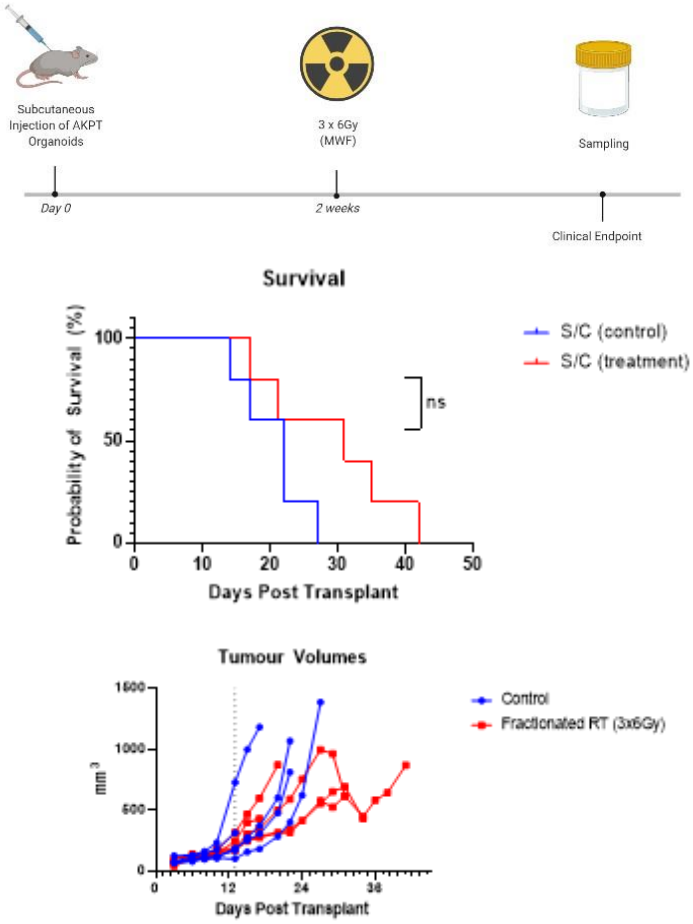

Figure 4.37: AKPT Subcutaneous Xenografts Demonstrate Transient Response to Fractionated Radiotherapy

Top – Schematic demonstrating experimental timeline for irradiation of AKPT subcutaneous xenografts. Middle – Survival curve demonstrating survival of irradiated and untreated tumours. Bottom – Graph showing serial tumour volume measurements demonstrating tumour growth or regression. Dotted line indicates treatment start. Log Rank Mantel-Cox test. ns denotes non-significance ($p \geq 0.05$). n=5 per group.

Histological analysis of subcutaneous AKPT tumours following fractionated radiotherapy by H+E staining, revealed a reduction in tumour epithelium when compared with the control cohort, and most notably in animals which had undergone a transient tumour volume reduction (Figure 4.38). Although large tumour volumes were observed at clinical endpoint following fractionated radiotherapy, significant areas of fibrosis and regression were seen within tumours (Figure 4.38, top panel). Dense populations of immune cells were observed at the tumour invasive edge and throughout the stromal compartment

in both untreated and irradiated tumour samples (Figure 4.38, bottom panel). However, immune cell populations appear to be relatively sparse in the regions of treated tumours which had undergone regression and replaced by fibrosis.

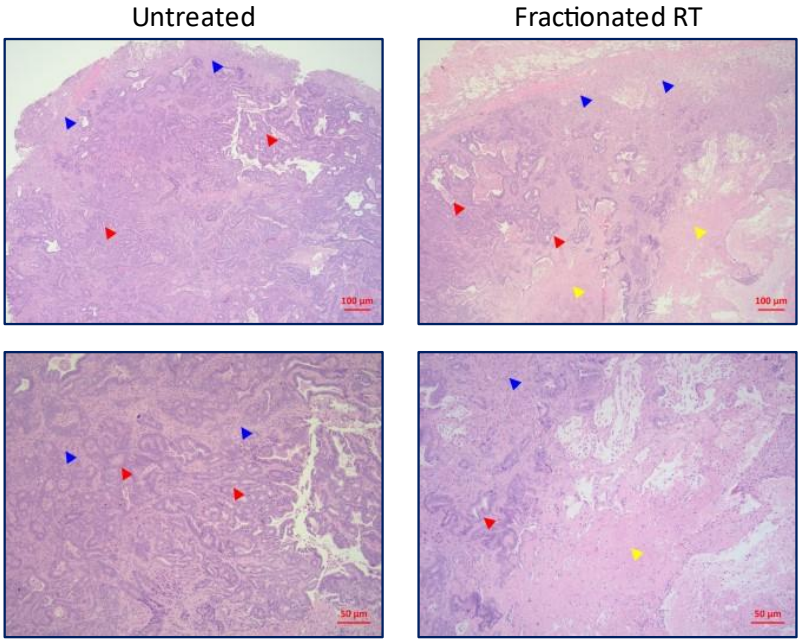

Figure 4.38: AKPT Subcutaneous Xenografts Demonstrate Histological Evidence of Tumour Regression Following Fractionated Radiotherapy

Top – Representative H+E stains (x4) from untreated and post fractionated radiotherapy AKPT subcutaneous xenograft tumours. Bottom – Corresponding H+Es at higher magnification (x10). Red arrows depict tumour epithelium. Blue arrows depict areas of immune/inflammatory infiltrate. Yellow arrows depict areas of tumour regression/fibrosis. Scale bars = 100µm and 50µm.

As a surrogate marker of tumour response, I quantified mucin pooling in tumours through AB/PAS staining. Large areas of mucin pooling were noted in tumours at clinical endpoint following radiotherapy (Figure 4.39, top and middle panels). Quantification revealed a significantly increased level of AB/PAS staining following fractionated radiotherapy when measured by % of tumour area positively stained ($p=0.0079$), further demonstrating that subcutaneous tumours underwent irradiation induced histological changes (Figure 4.39, bottom panel).

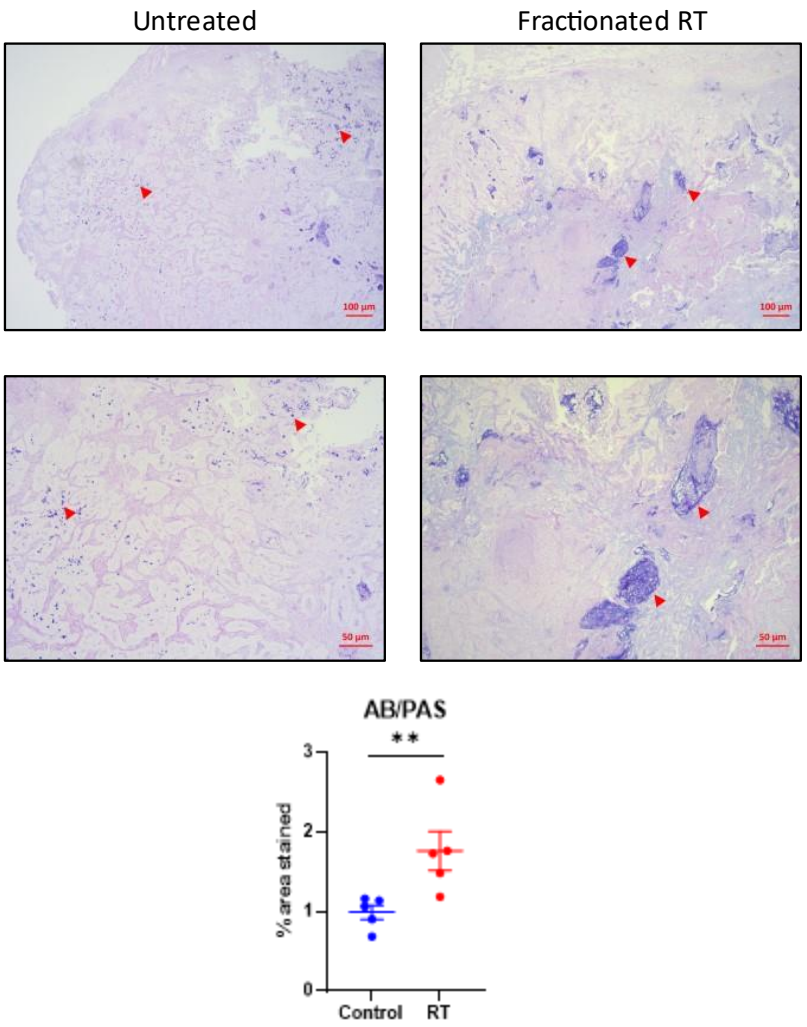

Figure 4.39: AKPT Subcutaneous Xenografts Demonstrate Increased Mucin Pooling Following Fractionated Radiotherapy

Top - Representative AB/PAS stains (x4) from untreated and post fractionated radiotherapy AKPT subcutaneous xenograft tumours. Middle – Corresponding AB/PAS stains at higher magnification (x10). Bottom – Bar graph demonstrating % tumour area stained for AB/PAS in untreated and post fractionated radiotherapy samples. n=5 per group. Error bars show mean and SEM. Each data point plotted. Mann-Whitney U-test. **denotes p-value ≤0.01. Scale bars 100µm and 50µm. Red arrows depict regions staining positively for mucin.

I next analysed common immune cell markers to assess changes in immune infiltrate in AKPT subcutaneous xenograft tumours following treatment with fractionated radiotherapy at clinical endpoint. T-lymphocyte populations were assessed by staining for CD3, CD8 and FOXP3 T-regulatory cells. In both untreated and post irradiated tumours, abundant populations of both CD3+ lymphocytes and CD8+ cytotoxic T-lymphocytes were observed at the tumour invasive margin with these cells less densely populated in the stromal compartment within the tumour core (Figure 4.40, top and upper middle panels). FOXP3+ T-regulatory cells were seen in low densities at the tumour

invasive margin in both untreated and treated tumours, and were relatively absent from the tumour core (Figure 4.40, lower middle panel). Upon quantification, significantly lower populations of CD3+, CD8+ and FOXP3+ cells were seen following fractionated radiotherapy, likely reflecting the relative absence of lymphocytic infiltrate from regions of irradiated tumour which had undergone regression and replacement by fibrotic tissue (Figure 4.40, bottom panel).

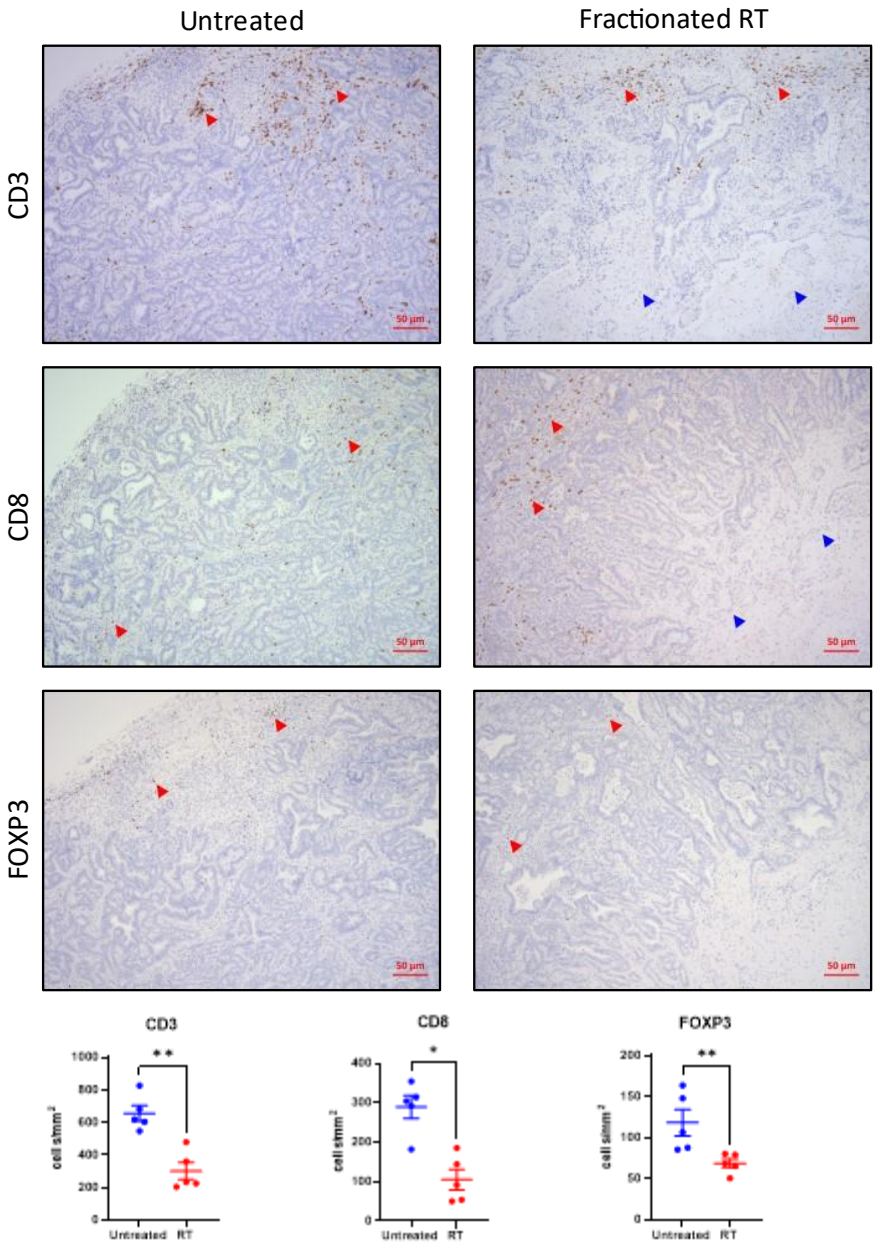

Figure 4.40: Overall Lymphocytic Infiltrate in AKPT Subcutaneous Xenograft Tumours is decreased following Fractionated Radiotherapy

Top - Representative CD3 stains (x10) from untreated and post fractionated radiotherapy AKPT subcutaneous xenograft tumours. Top middle – Representative CD8 stains (x10) from the corresponding tumour. Bottom middle – Representative FOXP3 stains (x10) from the corresponding tumour. Bottom - Bar graphs depicting CD3, CD8 and FOXP3 quantification as cells/mm^2. Error bars show mean and SEM. Each data point plotted. n=5 per group. Mann-Whitney U-test. *denotes p-value ≤0.05. **denotes p-value ≤0.01. Scale bars 50µm. Red arrows depict positively staining cells. Blue arrows depict regions with absence of immune cell of interest.

I next analysed infiltrating myeloid cell populations, firstly through staining for S100A9 expression to detect neutrophils. S100A9 positive neutrophil cell populations were seen at the tumour invasive margin in both untreated and

irradiated tumour samples, while relatively sparse numbers were seen in the tumour core (Figure 4.41, top panel). Neutrophil populations were observed in regions of treated tumours which had undergone regression, likely reflecting recruitment to these areas with subsequent phagocytosis of tumour cells. This observation is likely to reflect the significantly higher number of S100A9 expressing cells seen in tumours post fractionated radiotherapy (Figure 4.41, bottom panel). Dense regions of macrophage infiltration in the tumour invasive margins were detected through F4/80 staining (Figure 4.41, middle panel), with significant populations maintained in the stromal compartment throughout the tumour core in both untreated and irradiated tumours, with no significant differences observed upon quantification (Figure 4.41, bottom panel).

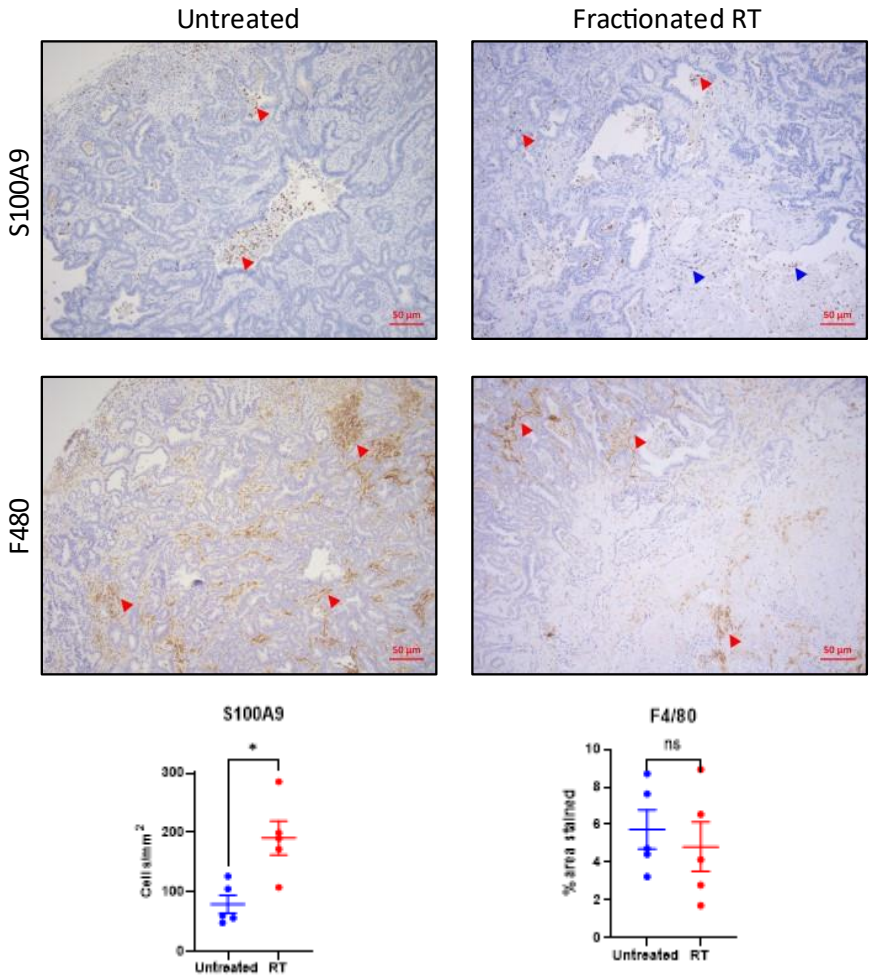

Figure 4.41: Neutrophil Infiltration is increased in the AKPT Subcutaneous Xenograft Model Following Fractionated Radiotherapy

Top – Representative S100A9 staining (x10) from untreated and treated AKPT subcutaneous xenograft tumours. Middle – Representative F4/80 staining (x10) from corresponding tumours. Bottom – Bar graphs depicting S100A9 and F4/80 quantification, as cells/mm^2 or % area positively stained respectively. Error bars show mean and SEM. Each data point plotted. n=5 per group. Mann-Whitney U-test. *denotes p-value ≤0.05. ns denotes no-significance. Scale bars 50μm. Red arrows depict positively staining cells. Blue arrows depict S100A9 positive cells within regions of tumour regression.

Data from serial tumour volume calculations, tumour histology and immune cell quantification suggest that AKPT tumours were more sensitive to radiotherapy when implanted at the heterotopic subcutaneous flank region when compared with the orthotopic rectal location. It must be noted that subcutaneous tumours were subjected to slightly higher radiotherapy fractions (3 x 6Gy), which may account for the transient clinical response described. However, AKPT rectal tumours subjected to 3 x 6Gy fractionated radiotherapy failed to demonstrate survival extension or tumour volume reduction (data not presented).

Nonetheless, a potential difference in tumour immune micro-environment between the subcutaneous flank and rectal locations is highlighted, with the microbiome potentially creating a more immunosuppressive tumour milieu.

4.3 Discussion

4.3.1 Targeting Orthotopic Rectal Cancer Models with Radiotherapy

This chapter has described the development of an experimental protocol for the delivery of image-guided precision radiotherapy to the orthotopic AKPT organoid transplant model of LARC, representing a significant advancement in the ability to conduct clinically translatable pre-clinical irradiation studies. The successful delivery of image-guided radiotherapy to orthotopic pre-clinical models of rectal cancer has only recently been described in the literature, with Nicolas and colleagues describing the delivery of a 5 x 2Gy fractionated radiotherapy regimen using a SARRP (Nicolas et al, 2022). The approach described in this chapter was validated through the demonstration of DNA damage induction at 3 hours post irradiation, as shown by increased expression of γH2AX on IHC (Figure 4.3). Repeated experiments have demonstrated the reproducibility of the irradiation protocol described, with increased γH2AX expression consistently shown at short time-points (3-6 hours).

Despite a failure to visualise rectal tumours during treatment planning, it was evident that non-contrast CBCT image acquisition enabled identification of the tumour location in relation to anatomical landmarks (anal margin and distal colonic gas). In developing a protocol for irradiating pre-clinical rectal tumours, it was evident that improving tumour detection through MRI would result in a significantly increased experimental time of ~60 minutes per treatment, compared with ~15 minutes when CBCT is used for planning. Contrast agents delivered as a rectal enema is a strategy employed clinically to evaluate rectal tumours, and might prove to be a time efficient method of improving tumour detection in the pre-clinical setting, and could potentially be employed to further refine irradiation protocols (Murai et al, 2022). Having demonstrated successful tumour targeting, it remains unlikely that improved tumour detection through refined imaging protocols would alter experimental outputs. However, improved tumour detection might enable radiotherapy to be administered with a

smaller beam diameter to minimise normal tissue effects, and could be a useful tool to monitor tumour response to treatment.

A large increase in the number of published studies reporting the use of small animal irradiators has been observed over the past 10 years, with the majority consisting of biology contributions which evaluate either tumour or normal tissue responses to irradiation (Brown et al, 2022). Technological advances in image-guided small animal irradiation, which have undergone rigorous dosimetric evaluation, highlight exciting opportunities within the laboratory to conduct pre-clinical irradiation studies with greater potential to support translation to the clinical setting (Ghita et al, 2017). Although the ability to replicate modern clinical radiotherapy systems in the laboratory has recently been realised, it is crucial that pre-clinical irradiation studies in CRC also progress beyond heterotopic xenograft models which continue to be reported in the literature (Grapin et al, 2019). The delivery of image-guided radiotherapy to orthotopic models of rectal cancer has only recently been described, and the results presented in this thesis so far highlight the recent advances made in both accurate modelling of LARC, and in the ability to deliver radiotherapy to small animals in a manner which closely mimics the clinical scenario.

4.3.2 The AKPT Orthotopic Rectal Cancer Model Demonstrates Resistance to Radiotherapy

In this chapter, I then utilised the developed model of LARC and irradiation protocol to evaluate tumour responses to a single 4Gy fraction of radiotherapy, with analyses performed at 3-days and 7-days post treatment. At these short-term time-points, tumour volume reduction and histological tumour regression were not observed at this dose (Figures 4.7 and 4.9). Pre-clinical reports of tumour remission following single fraction radiotherapy have been described in CRC models, however, these involve ablative fractions as high as 30Gy, with intense CD8+ T-cell infiltrate demonstrated within the TME (Filatkenov et al, 2015). Although stereotactic ablative radiotherapy (SABR) has shown clinical efficacy in multiple solid cancers with oligometastatic disease, including CRC with lung metastases, the use of fractions >5Gy has not been routinely used in the treatment of primary LARC (Olson et al, 2020; Nicosia et al 2022). With this

rationale, I sought to evaluate the effects of clinically relevant radiotherapy fractions on the TME, with the aim of identifying immunological changes with the potential to be augmented pharmacologically in combination with irradiation.

Upon analysis of the tumour immune microenvironment following single fraction radiotherapy, IHC and flow cytometry both demonstrated an observed reduction in T-cell infiltration in AKPT tumours at 3-days post irradiation, with no changes being observed at the 7-day time-point (Figures 4.10 and 4.16). Studies from both murine blood and tissue show that T-cells demonstrate a relatively radio-sensitive phenotype, and so the observation of a transient decline in T-cell populations in the AKPT model is consistent with previously published data (Heylmann et al, 2014). An increase in leucocytes was observed in tumour draining lymph nodes at 7-days post irradiation, suggesting that a local inflammatory response was induced following a single 4Gy fraction (Figure 4.16). However, definitive conclusions cannot be drawn from these observations due to the low cohort numbers included in each analysis (n=3-5). Furthermore, different TME compositions were seen in the 3-day and 7-day control cohorts, with much lower densities of CD8+ve CTLs and F4/80+ve macrophages noted in the 3-day group; as each time-points were performed as independent experiments, this highlights that significant heterogeneity in TME composition existed between individual experimental batches. Repeating this experiment with larger cohorts performed at the same time, might help to confirm the observation that irradiation transiently decreases populations of infiltrating lymphocytes. T-cell immune responses are likely to develop at 7-days following RT owing to initial radio-sensitivity, with earlier time-points likely to detect innate immune cell responses; more extensive time-course analyses such as 1-day, 3-days, 7-days and 10-days would help to characterise the timeline of T-cell mediated immune responses to RT.

When AKPT rectal tumours were treated with fractionated radiotherapy regimens mimicking SCRT, therapy resistance was again demonstrated with no tumour volume reduction or survival extension demonstrated (Figure 4.21). However, evidence of histological change was demonstrated through the presence of mucin pooling and patches of acute necrosis in clinical endpoint tumours (Figure 4.23). In the absence of a clinical response assessed through

gross parameters, I adopted a surrogate marker of histological response, with fractionated radiotherapy being associated with a significant increase in mucin pooling when quantified by AB/PAS staining (Figure 4.23). The presence of 'acellular' mucin in patient tumours following neo-adjuvant radiotherapy is a recognised phenomenon and typically correlates with 'good response,' however, reports in the literature conflict as to whether the presence of mucin pooling is associated with improved patient outcome (Shia et al, 2011; Kang et al, 2016; Reynolds et al, 2018). As a surrogate marker solely to detect histological response, quantification of mucin pooling was utilised as a simple method to demonstrate the biological effect of fractionated radiotherapy in the absence of obvious changes in tumour volume. In the clinical setting, change in tumour cell density (TCD) between pre-treatment biopsies and surgical resection specimens has shown correlation with response to neo-adjuvant therapy, with decreased TCD associated with good responses; quantification of the proportion of tumour occupied by epithelium represents an alternative means to assess histological response (Wilkins et al, 2021).

Although a small number of tumours were analysed to assess changes in TME following fractionated radiotherapy in clinical endpoint tumours, no obvious changes in common immune cell populations were detected (Figures 4.24 and 4.25). Several clinical studies have shown that CD3+ve and CD8+ve cell densities are increased in surgical resection specimens of patients who have received CRT, when compared with pre-treatment biopsies (Shinto et al 2014; Teng et al, 2015). In the pre-clinical setting, Frey and colleagues describe the irradiation of CT26 colon cancer subcutaneous xenografts with 2 x 5Gy, resulting in delayed tumour growth (Frey et al, 2017). Interestingly, this study describes a time-course analysis of immune infiltrate, with animals sacrificed for flow cytometry analysis at daily intervals for a 14-day time course post irradiation. A transient increase in macrophages (CD11b+ve, F4/80+ve) and antigen presenting cells (MHCII+ve) was observed between 5-10 days, with an increase in CD8+ve cells observed between 7-9 days. This data highlights that any changes in immune cell infiltrate in the AKPT rectal model are unlikely to be observed at clinical endpoint. A further experiment to analyse tumours subjected to fractionated radiotherapy and sampled at planned time-points (e.g., 7 days post irradiation),

would help to inform upon any transient changes in immune cell infiltrate in the AKPT model.

4.3.3 Potential Resistance Mechanisms in the AKPT Model

High levels of TGF-ß signalling were demonstrated in the AKPT model, with no change in pSMAD3 expression seen following fractionated radiotherapy (Figure 4.26). It is known that many solid cancers can evade normal growth regulation and increase TGF-ß production, in turn suppressing immune surveillance and contributing to a pro-tumourigenic micro-environment (Saunier and Akhurst, 2006). Pre-clinical studies have shown a potential role for TGF-ß blocking agents in combination with radiotherapy, with tumour growth delay and reduced metastases observed in breast cancer models (Biswas et al, 2007; Bouquet et al, 2011). Bulk transcriptomic data in treated AKPT tumour samples indicated an upregulation of the TGF-ß hallmark gene-set, following both single fraction and fractionated radiotherapy; however, no individual TGF-ß related genes were found to be upregulated when individual treatment groups were compared with control samples. Nonetheless, abundant TGF-ß signalling in the AKPT model which is further up-regulated following irradiation, represents a potential mechanism of treatment resistance in the model which merits further investigation with pharmacological inhibition.

Despite failing to observe changes in immune infiltrate following fractionated radiotherapy in tumours sampled at clinical endpoint, transcriptomic analysis through bulk RNA sequencing of tumour samples treated with a single 4Gy fraction of radiotherapy, showed up-regulation of immune and inflammation related signalling pathways. Up-regulation of hallmark gene-sets associated with interferon-α, interferon-γ, inflammation, IL-6 JAK/STAT3 signalling, epithelial-mesenchymal transition and TNF-α signalling via NF-κB were demonstrated at 3-days and 7-days post single fraction radiotherapy, but not at a later time-point or at clinical endpoint following fractionated regimens (Figure 4.29). These observations correlate with the transient changes in immune cell composition demonstrated by Frey and colleagues at 5-10 days post irradiation. Furthermore, Dovedi et al show in the CT26 murine CRC subcutaneous xenograft model, that fractionated radiotherapy with 5 x 2Gy results in a transient up-regulation of PD-

L1 expression on tumour cells driven by IFN-γ secretion by CD8+ve T-cells (Dovedi et al, 2014).

The JAK/STAT3 pathway has several inter-cellular signalling functions between tumour cells and the immune micro-environment, with activation being reported to be pro-tumourigenic with a role in mediating resistance to therapy and to irradiation (Sabaawy et al, 2021). The JAK/STAT3 pathway is known to be associated with colorectal cancer, both through independent effects on risk and through the modifying effect by lifestyle factors such as smoking (Slattery et al, 2013). The inflammatory response induced by irradiation (and other cytotoxic agents) leads to activation of STAT3, with the resulting up-regulation of chemokines and cytokines promoting therapy resistance (Spitzner et al, 2014). Furthermore, PD-L1 is known to be a STAT3 target gene with PD-L1 up-regulation being associated with STAT3 activation in other cancers (Song et al, 2018). This observation highlights JAK/STAT signalling as a potential mechanism of resistance to radiotherapy in the AKPT model, and a further potential treatment target.

Interferon-γ signalling was also up-regulated at short time-points following radiotherapy in the AKPT model, and is a known potent activator of JAK/STAT signalling (Ivashkiv, 2018). When the IFN-γ hallmark gene-set was analysed, up-regulation of the Ptgs2 gene was identified at the 3-day and 7-day time-points, as well as in tumours subjected to fractionated radiotherapy (Figures 4.32 and 4.433). The Ptgs2 gene is synonymous with COX2, one of two prostaglandin endoperoxide synthases (COX1 and COX2), enzymes which convert arachidonic acid into prostaglandins. COX1 is expressed constitutively, however, COX2 is induced by cytokines during inflammation with its activation resulting in production of prostaglandin E2 (PGE2) which acts on numerous cell signalling pathways potentiating tumour progression, including tumour cell proliferation, apoptosis, invasion, angiogenesis and immunosuppression (Wang and Dubois, 2006).

PTGS2 upregulation is common in CRC and some evidence exists to suggest association with PTGS2 expression and increased risk of tumour recurrence and worse CRC specific survival, though it is unclear whether an independent association with prognosis exists (Eberhart et al, 1994; Kunzmann et al, 2013). Early evidence in FAP patients and in $Apc^{\Delta 716}$, Ptgs2 knock-out mice, suggest that

COX-2 plays a key role in CRC tumourigenesis with both gene knockdown or pharmacological inhibition of COX-2 reducing polyp numbers in both humans and mice (Giardiello FM et al, 1993; Oshima M et al, 1996). Randomised controlled trial data has provided strong evidence that selective COX-2 inhibition with celecoxib reduces colorectal adenoma recurrence in patients who have had previous adenoma removal, however cardiovascular events preclude routine use of this agent (Bertagnolli et al, 2006). Furthermore, RCT data shows that long-term aspirin use (>2 years) results in a long-term reduction in CRC incidence in Lynch syndrome patients, and current NICE guidelines recommends consideration of aspirin in these patients (Burn et al, 2020). Pre-clinical data has shown a radio-sensitising effect of celecoxib in both cell lines and *in-vivo* models, further demonstrating COX-2 inhibition as a potential target in the AKPT rectal cancer model (Yang et al, 2014; Xu et al, 2017).

4.3.4 Radiosensitivity is Determined by Location in the AKPT Organoid Transplant Model of Rectal Cancer

In-vitro data highlights a dose dependent response to irradiation when AKPT organoids were seeded as single cells in 2-D, with a marked reduction in cell viability when 8Gy and 10Gy fractions were administered in the absence of 5-FU (Figure 4.34). Although *in-vitro* culture conditions fail to replicate the orthotopic *in-vivo* setting, with a lack of infiltrating immune cells and TME, data suggests that greater sensitivity to irradiation might be realised at higher fractions in the orthotopic setting. Further experiments with a higher dose per fraction or increased fraction number, might elicit a clinical response in the AKPT orthotopic rectal cancer model. However, in the context of this thesis, I aimed to develop a fractionated regimen which mimicked clinical treatment and did not induce a complete tumour response, such that pharmacological agents could be administered in combination with radiotherapy to develop novel strategies.

When transplanted in the subcutaneous flank region, AKPT organoid derived tumours demonstrated a transient tumour volume reduction following fractionated radiotherapy, with increased mucin pooling observed following treatment (Figures 4.37 and 4.39). Significant changes in immune infiltrate were observed; decreased lymphocyte density likely reflected the increased areas of

tumour epithelium replaced by fibrosis, with increased neutrophil populations in treated tumours resulting from infiltration to areas of tumour regression. The clinical responses and associated changes in immune infiltrate demonstrated in the heterotopic model at clinical endpoint, were not observed following orthotopic injection, suggesting a more immunosuppressive tumour microenvironment at the rectal location. Transcriptomic analysis of subcutaneous tumours might elicit differential expression of immune response pathways when compared with rectal tumours, and microenvironment cell population counter (MCP) methods might quantify tissue infiltrating immune and stromal cells more accurately.

Subcutaneous tumour models in immunocompromised hosts have been used extensively in the literature to evaluate novel therapeutic strategies involving radiotherapy, potentially leading to incorrect conclusions upon which to base clinical translation. Pre-clinical evaluation of radiotherapy-based treatment strategies should be performed in a microenvironment which closely recapitulates the physiological conditions of human disease, thus should comprise an intact host immune system, tumour stroma and relevant surrounding normal tissue. Differences in tumour model responsiveness according to location has been reported previously; Tran Chau et al show that Lewis lung carcinoma (LL2) subcutaneous tumours respond to the DNA damage response inhibitor Olaparib plus ionising irradiation, whereas a very narrow therapeutic window is observed in the LL2 lung orthotopic model with minimal additional anti-tumour effect seen compared with radiotherapy alone (Tran Chau et al, 2020).

Studies in a pre-clinical melanoma model, with tumours induced at either the subcutaneous or lung location, showed that different TAM subsets were resident in tumours growing at the different environments, with $Ly6C^{High}$ monocytes recruited through the CCL2-CCR2 axis being crucial for response to immunotherapy in skin tumours, whereas lung tumours required colony stimulating factor 2 (CSF2) dependent macrophages to enable immunotherapy (Lehmann et al, 2017). Zhao et al directly compared CT26 and MC38 murine colon cancer cell lines transplanted at both the subcutaneous and colonic locations, with significantly different immune compositions and response to immune checkpoint blockade demonstrated (Zhao et al, 2017). In the orthotopic

model, increased tumour infiltrating T-cells and expression of inflammatory cytokines were observed, alongside decreased MDSC infiltration and an improved response to immunotherapy. Although this conflicts with data presented in this chapter, whereby the orthotopic location demonstrated greater treatment resistance, the study highlights that identical cell-lines are likely to result in significantly different tumours and therapy response depending upon location.

Although previous literature reports on the efficacy of fractionated radiotherapy and immunotherapy combinations in subcutaneous models of CRC, as discussed previously in this thesis, translation of such promising results are unlikely to achieve translation to the clinical setting. Future research and pre-clinical development of radiotherapy-based treatment combinations must utilise orthotopic treatment resistant models, reflective of the challenges faced in the clinical scenario whereby patients with poorest prognosis demonstrate a complex TME with numerous potential resistance mechanisms. The remainder of this thesis will use the orthotopic organoid transplant model AKPT model of LARC, along with the developed irradiation protocols described, to assess radiotherapy – immunotherapy combinations which might overcome the therapy resistance which has been demonstrated when irradiation alone is delivered to the AKPT model of LARC.

Chapter 5: Evaluating Radiotherapy – Immunotherapy Combinations in the Orthotopic AKPT Transplant Model of Locally Advanced Rectal Cancer

5.1 Introduction

5.1.1 Targeting TGF-ß Signalling in Pre-Clinical Cancer Models

TGF-ß signalling in the tumour micro-environment (TME) has been associated with poor prognosis, and is one of the processes enriched in poor prognosis molecular subtypes of CRC, particularly CMS4 (De Sousa E Melo et al, 2013; Marisa et al, 2013; Sadanandam et al, 2013; Calon et al, 2015). Gene signatures upregulated by TGF-ß in stromal cells have been shown to be associated with cancer recurrence and metastasis in cohorts of CRC patients (Calon et al, 2012). The TGF-ß stromal gene response signature associated with CRC recurrence, included several genes associated with bone metastasis in breast cancer such as IL-11 and JAG1, highlighting TGF-ß signalling as a promising therapeutic target in advanced CRC (Kang et al, 2003; Sethi et al, 2011).

TGF-ß signalling and its effects on the immune system have been described previously in sections 1.2.4 and 1.2.5 of this thesis. TGF-ß signalling normally slows proliferation of epithelial CRC cells and does not trigger epithelial-mesenchymal transition; however, some tumours evade the normal physiological actions of TGF-ß signalling through reduced sensitivity and acquired resistance to its normal growth inhibitory mechanisms (Shi et al, 2020). This can occur through mutations to inactivate TGF-ß receptors or SMAD signal transducers, or through loss of downstream gene responses. Dysfunction of the TGF-ß cytokine can contribute to tumour progression through loss of growth inhibitory control, increasing metastatic potential, and through evasion of immune surveillance. Meanwhile, in CAFs, TGF-ß boosts tumour initiating capacity with a resulting increase in metastatic potential and the enabling of treatment resistance.

The role of TGF-ß inhibition in overcoming the immune evasion induced by tumour secreted TGF-ß has been shown in pre-clinical CRC models. Quadruple mutant murine tumour derived organoids (*Apc$^{fl/fl}$; Kras$^{LSL\text{-}G12D/+}$; Tgfbr2$^{fl/fl}$; Trp53$^{fl/fl}$; Lgr5$^{eGFP\text{-}creERT2}$*) harbouring *Apc, Kras, Trp53* and *Tgfbr2* mutations in ISCs, demonstrated invasive colonic tumours and liver metastases (in 40% of

engrafted tumours) when implanted in the caecal wall. Primary tumours showed increased TGF-ß activity and T-cell exclusion, with cancer-associated fibroblasts (CAFs) being the most prominent source of TGF-ß (Tauriello et al, 2018). When tumour derived organoids were injected into the portal circulation, treatment with galunisertib (a small molecule inhibitor of TGFBRI) led to a marked decrease in metastatic burden. In the CT-26 subcutaneous flank injection model of CRC, treatment with galunisertib led to a reduction in mean tumour volume when compared with controls, with this effect being dependent upon the presence of CD8+ T-cells (Holmgaard et al, 2018).

Data from pre-clinical models is suggestive of an enhanced role for TGF-ß inhibition when administered in combination with PD-1/PD-L1 axis inhibition. Resistance to immune checkpoint inhibition has been attributed to several factors; in a large cohort of metastatic urothelial cancer patients, response to anti PD-L1 (atezolizumab) was associated with an increased presence of a CD8+ effector T-cell phenotype and high tumour mutational burden, while lack of response was associated with TGF-ß signalling in CAFs (Mariathasan et al, 2018). Mariathasan et al then demonstrated significant tumour reduction in both the EMT6 mammary cancer and MC38 CRC models when TGF-ß inhibition was administered in combination with anti PD-L1 therapy, with limited tumour response seen when TGF-ß inhibition or PD-L1 inhibition were administered as monotherapy. This effect was shown to be CD8+ T-cell dependent, with increased abundance of TILs seen, an increased CD8+ T-cell effector gene signature, and a greater distribution of TILs towards the tumour centre.

Although Tauriello et al showed reduced liver metastases following treatment with TGF-ß inhibition, few complete remissions were observed and treatment resistance was associated with T-cell surface expression of PD-1 and the recruitment of stromal PD-L1+ cells to metastatic tissue (Tauriello et al, 2018). Dual therapy in this model with the addition of an anti PD-L1 monoclonal antibody produced a pronounced immune response with increased GzmB production in CTLs and the eradication of most metastases. In the CT-26 CRC heterotopic transplant model described by Holmgaard et al, enhanced anti-tumour activity was demonstrated with the combination of anti-PD-L1 therapy and galunisertib, with 9/14 animals showing complete response and all exhibiting a marked reduction in tumour volume (Holmgaard et al, 2018).

Translational studies and pre-clinical data highlight a potential therapeutic role for TGF-ß inhibition; however, it is likely that significant clinical benefit can only be achieved through further evaluation of combination therapies.

5.1.2 Therapeutic Strategies to Target TGF-ß Signalling

Molecular targeting of the TGF-ß pathway is based on the premise that TGF-ß has strong immunosuppressive effects on tumours, and that blockade of TGF-ß might restore the cytotoxic effects of the immune system. Several strategies have been described to target the TGF-ß signalling pathway pharmacologically (Huang et al, 2021). The pathway can be inhibited at the translational level using anti-sense oligonucleotides (ASOs), which act as artificial short single strand RNAs which are complementary to chosen segments of TGF-ß mRNA and result in mRNA degradation. Some limitations exist with this approach, including unpredictable RNA-binding affinity, technically challenging sequence design, and difficulty in delivering large molecules which are impermeable to the plasma membrane (Teicher, 2020).

Another strategy employed is TGF-ß ligand traps using monoclonal neutralizing antibodies, which act through inhibiting the binding of the TGF-ß ligand to TGFBRII. Fresolimumab (GC1008) acts as a pan-specific monoclonal antibody which binds to all three TGF-ß isoforms, reducing their biological activity. Fresolimumab has been used clinically in early phase 1 trials in advanced malignant melanoma and renal cell carcinoma (Morris et al, 2014).

A more attractive approach has been small molecule inhibitors of TGF-ß receptor kinase, owing to economic advantages, ease of production and ability to administer orally (Teicher, 2020). TGF-ß receptor kinase inhibitors are ATP mimetics which specifically inhibit R-SMAD phosphorylation through potent binding to the kinase domain of the TGF-ß receptor ATP binding sites. Such small molecule inhibitors effectively decrease TGF-ß responsiveness; however, evidence suggests that in the long-term cancer cells acquire resistance to monotherapy, suggesting that TGF-ß inhibition should be administered in combination with other therapeutic agents (Connelly et al, 2011).

5.1.3 Targeting TGF-β Signalling in Combination with Radiotherapy

Radiotherapy has been shown both clinically and in pre-clinical models to have the potential to induce an anti-tumour immune response in the irradiated tumour (Formenti and Demaria, 2005). Despite this, cancer cells and the TME can promote mechanisms which impede anti-tumour immunity such as exhaustion of CD8+ T lymphocytes and NK cells (Mortezaee and Najafi, 2021). The activation of TGF-β has also been suggested as a potential mechanism by which radiotherapy can impede the generation of tumour antigen specific immune responses. ROS induced by radiotherapy have previously been shown to result in the release of active TGF-β from its inactive form whereby it is bound to a latency-associated peptide complex (Barcellos-Hoff et al, 1994). Activated TGF-β has been shown to reduce the radiosensitivity of cancer cells through activation of DNA damage response mechanisms (Bouquet et al, 2011; Barcellos-Hoff et al, 2014).

Evidence from pre-clinical studies has suggested a potential role for TGF-β inhibition in combination with fractionated radiotherapy as described previously in this thesis (Young et al, 2014; Vanpouille-Box et al, 2015; Gunderson et al, 2020). In these studies, combination therapy is associated with increased CD3+, CD4+ and CD8+ T-cell density, up regulation of gene signatures associated with IFN-γ signalling, and increased production of chemokines and cytokines associated with CTL recruitment.

Focal irradiation has been combined with TGF-β inhibition in a small clinical trial, with acceptable toxicity and tolerance to therapy observed. Metastatic breast cancer patients with at least three distant metastatic lesions, and refractory to at least one form of systemic therapy, were treated with fractionated radiotherapy (3 x 7.5Gy) to one metastatic lesion in combination with fresolimumab, a human monoclonal antibody which neutralises all three TGF-β isoforms (Formenti et al, 2018). Although limited clinical and abscopal responses were seen, extended survival was seen in the group treated with the higher dose of fresolimumab (1mg/kg versus 10mg/kg), with the higher dose group having a median survival of 16.0 months, compared with 7.6 months in the lower dose group. The higher dose was also associated with a favourable increase in memory CD8+ T-cells, as well as an increase in T reg cells.

Although promising therapeutic effects have been demonstrated in heterotopic tumour models following treatment with TGF-ß inhibition and fractionated radiotherapy, further pre-clinical studies should aim to assess treatment combinations in more clinically relevant orthotopic models, to better understand the immunological effects of this treatment combination and to optimise treatment scheduling.

5.1.4 Targeting the PD-1 Immune Checkpoint in Cancer

It is well established that the PD-1/PD-L1 immune checkpoint pathway can have suppressive effects on anti-tumour immunity (Zou et al, 2016). PD-L1+ tumour cells and APCs engage with the PD-1 receptor on T-cells to induce T-cell apoptosis, functional exhaustion, anergy and release of immunosuppressive cytokines such as IL-10. PD-1/PD-L1 blockade has resulted in clinical benefit in several malignancies including Hodgkin's Lymphoma, renal cell carcinoma, NSCLC and advanced melanoma (Ansell et al, 2015; Brahmer et al, 2012; Hamid et al, 2013). In CRC, a limited clinical benefit has been observed in patients with progressive metastatic carcinoma, with poor response seen in patients with pMMR status (Le et al, 2015).

The higher somatic mutation and tumour neo-antigen burden seen in dMMR tumours are recognised by the patient's immune system, with blockade of the PD-1/PD-L1 pathway enabling an immune response which results in tumour cell destruction (Segal et al, 2008). It is hypothesised that 'immunogenic' tumours respond more readily to immune-checkpoint blockade, owing to high levels of CD8+ T-cells, high tumour neo-antigen burden and PD-L1 expression, as well as low levels of immunosuppressive T regs and MDSCs. It is thought that pre-treatment PD-L1 expression on tumour cells reflects an immune-activated tumour microenvironment, and has been shown to be a potential predictive biomarker for response to PD-1 pathway inhibition (Taube et al, 2014). In the context of CRC, it has previously been shown that in the dMMR subset which is predictive for response to immune checkpoint blockade, that tumours are characterised by high Th1 T-cell and CD8+ T-cell infiltration, with high PD-L1 and PD-1 expression also observed (Llosa et al, 2019; Le et al, 2015).

However, the promising results and responses observed in clinical practice are only seen in select patient cohorts with favourable immune characteristics, and most patients undergoing treatment with immune checkpoint inhibition fail to respond (Haslam and Prasad, 2019; Cercek et al, 2022). It is likely that immunotherapy must be administered in combination with other therapeutic agents, including chemotherapy and radiotherapy, in order to achieve synergistic effects and improve clinical efficacy (Pardoll and Drake, 2012).

5.1.5 Targeting the PD-1 Immune Checkpoint in Combination with Radiotherapy in Pre-Clinical Models

It is known that radiotherapy can induce numerous adaptive immune responses including the priming of T-cells in tumour draining lymph nodes, induction of type 1 IFN-γ, modulation of suppressive T regs, and differentiation of pro-inflammatory M1 macrophages (Lee et al, 2009; Wei et al, 2013; Klug et al, 2013). However, tumours often fail to respond to radiotherapy and local relapses often occur following initial response, with persistence of cytokines induced by radiation having a potential role in promoting carcinogenesis such as TGF-ß, EGF and fibroblast growth factor (Barcellos-Hoff et al, 2005).

Pre-clinical data has supported the concept that radiotherapy can simultaneously induce a local tumour inflammatory response with the infiltration of tumour antigen specific T-cells, as well as inducing PD-L1 expression in the tumour microenvironment which might suppress anti-tumour immunity (Deng et al, 2014). Deng et al demonstrated with flow cytometry that PD-L1 expression was significantly increased in tumour cells and DCs at 3-days post 12Gy single fraction radiotherapy. In both the TUBO mammary tumour and MC38 CRC flank injection models in BALB/c mice described by Deng et al, tumour growth was slowed slightly with 12Gy radiotherapy alone; however, control of tumour growth was achieved with radiotherapy and anti PD-L1 antibody treatment. Antibody depletion demonstrated that the benefit of combination therapy in this model was dependent upon CD8+ T-cell activation, an effect which has a negative impact upon the accumulation of TNF induced MDSC accumulation.

In a bilateral B16-F10 subcutaneous flank injection model of metastatic melanoma treated concurrently with 20Gy radiotherapy and CTLA-4 inhibition,

only 17% of mice showed response to dual therapy with responses being CD8+ T-cell dependent (Twyman-Saint Victor et al, 2015). Twyman-Saint Victor et al derived cell lines from resistant murine B16-F10 tumours to identify that a lack of increase in the CD8/Treg ratio was strongly associated with treatment resistance; furthermore, transcriptomic profiling revealed that PD-L1 gene expression was strongly upregulated in resistant tumours. Tumour response was significantly increased to 80% in this model with the addition of PD-L1 inhibition. This study suggested that irradiation improves the T-cell repertoire and diversity of clonotypes, that CTLA-4 inhibition functions to reduce T reg cells, and that PD-1 axis inhibition overcomes treatment resistance which is conferred by PD-L1 upregulation and its role in T-cell exhaustion.

The role of irradiation in upregulating PD-L1 expression on tumour cells to drive resistance to radiotherapy was also demonstrated in the context of low-dose fractionated radiotherapy in the CT-26 subcutaneous flank injection model of CRC (Dovedi et al, 2014). Dovedi et al also demonstrated through co-culture of CD8+ T-cells with CT-26 tumour cells, that tumour cell up-regulation of PD-L1 was dependent upon IFN-γ secreting CD8+ T-cells. In this study, combined therapy with fractionated radiotherapy and PD-1/PD-L1 blockade led to significant reduction in tumour volume and survival extension when compared with fractionated radiotherapy alone.

Limited benefits have been observed in the clinical setting to date with radiotherapy and immunotherapy combinations, with favourable responses typically seen in immunogenic subtypes such as CRC with deficient MMR status. However, numerous pre-clinical studies have described promising results with combinations of radiotherapy, and inhibition of PD-1/PD-L1, CTLA-4 and TGF-β. The majority of pre-clinical studies discussed describe heterotopic transplant models using immortalised commercial cell lines which fail to recapitulate the heterogeneity of human disease and the inherent molecular complexity of tumours which confer treatment resistance. In order to improve the translational potential of pre-clinical studies it is imperative that more sophisticated models which represent the anatomical, histological and molecular features of human disease are utilised. The AKPT orthotopic transplant model of LARC more closely reflects histologically aggressive rectal cancer with resistance to radiotherapy alone, and this chapter aims to assess fractionated radiotherapy in combination

with TGF-β inhibition or PD-1 inhibition to determine whether the model responds to combination therapy and to demonstrate the feasibility of testing fractionated radiotherapy in combination with immunotherapy in orthotopic models of LARC.

5.1.6. Experimental Aims

In Chapter 4, the orthotopic AKPT model of LARC demonstrated resistance to both single fraction and fractionated radiotherapy. I next sought to evaluate the effects of immunotherapy agents in combination with fractionated radiotherapy, to determine whether response to fractionated radiotherapy can be augmented. The following experimental aims are addressed in this results chapter:

- Demonstrate the feasibility of administering immunotherapy in combination with fractionated radiotherapy in the AKPT model.
- Evaluating the effects of TGF-β inhibition in combination with fractionated radiotherapy
- Evaluating the effects of PD-1 inhibition in combination with fractionated radiotherapy
- Assessing the changes in tumour immune microenvironment following treatment with PD-1 inhibition and fractionated radiotherapy

5.2 Results

5.2.1. TGF-β Inhibition in Combination with Fractionated Radiotherapy

Initially, I sought to investigate whether pharmacological inhibition of TGF-β signalling in combination with fractionated radiotherapy would induce TME changes or tumour volume reduction in the orthotopic AKPT tumour derived organoid transplant model of LARC. Immunocompetent C57Bl/6 mice were injected with AKPT organoid fragments at the rectal location, with tumorigenesis confirmed by colonoscopy at 1-week post implantation. Animals were then treated with an activin receptor like kinase 5 inhibitor (ALK5 inhibitor), which inhibits TGF-β type 1 receptor kinase activity. ALK5 inhibition was then commenced three days prior to the delivery of fractionated radiotherapy (3 x 5Gy on alternate days), with drug treatment continued until experimental endpoint (Figure 5.1, top panel). Animals were sacrificed at 2-weeks post radiotherapy initiation to assess tolerability of the treatment combination and to identify short-term markers of treatment response. ALK5 inhibitor was selected to specifically inhibit the effects of active TGF-β on the TGF-β transmembrane receptor complex, and subsequently inhibit the phosphorylation of the pSMAD2/3 complex and the resulting transcription of TGF-β responsive genes (Higashiyama et al, 2007). Following treatment with fractionated radiotherapy and ALK5 inhibition, no reduction in tumour volume was observed at the 2-week time-point when compared with fractionated radiotherapy alone and age-matched untreated controls (Figure 5.1, bottom panel).

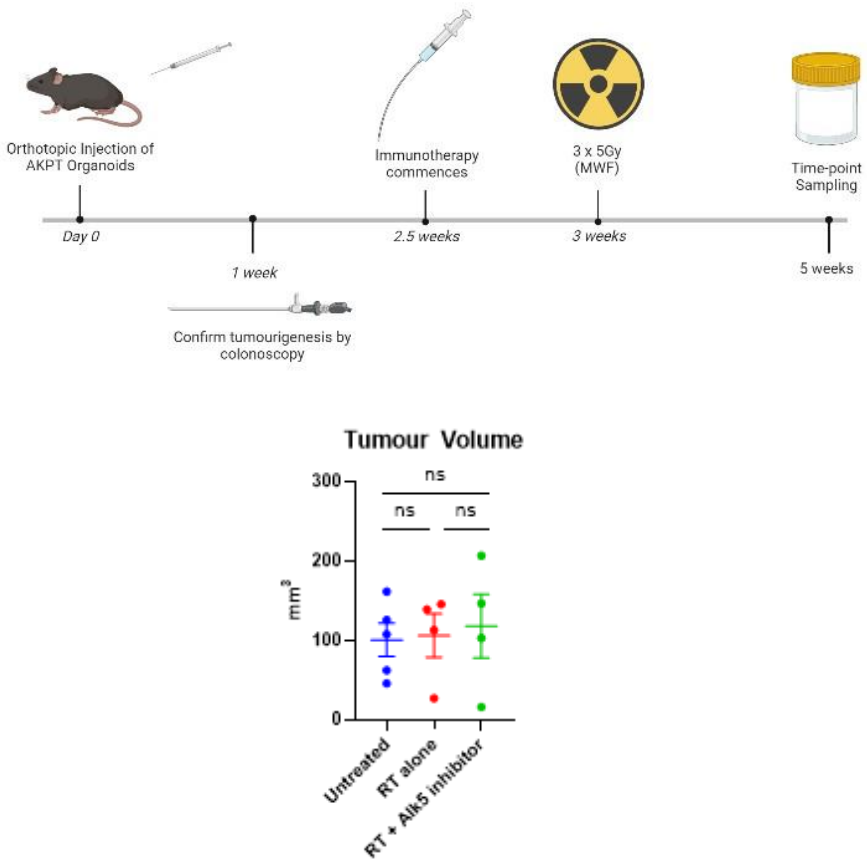

Figure 5.1: Fractionated Radiotherapy in Combination with ALK5 Inhibition Fails to Induce Tumour Volume Reduction at the 2-week Time-point.

Top – Schematic depicting the experimental timeline for fractionated radiotherapy treatment in combination with ALK5 inhibition. Bottom – Bar graph showing tumour volumes for each treatment group (mm^3) when sampled at 2-weeks post initiation of fractionated radiotherapy. Error bars show mean and SEM, with each data point plotted. Group sizes n=4-5. Mann-Whitney U-test. ns denotes non-significance ($p \geq 0.05$).

H+E staining of sampled rectal tumours was performed to determine whether histological changes were apparent at the 2-week timepoint following treatment with fractionated radiotherapy and ALK5 inhibition. Across all experimental groups, isolated tumour regions with absent tumour epithelium were observed, with no obvious features of tumour regression seen following fractionated radiotherapy and ALK5 inhibition (Figure 5.2). As previously demonstrated in AKPT rectal tumours, the stromal compartment was densely occupied by immune infiltrate with no clear differences seen following fractionated radiotherapy and ALK5 inhibition.

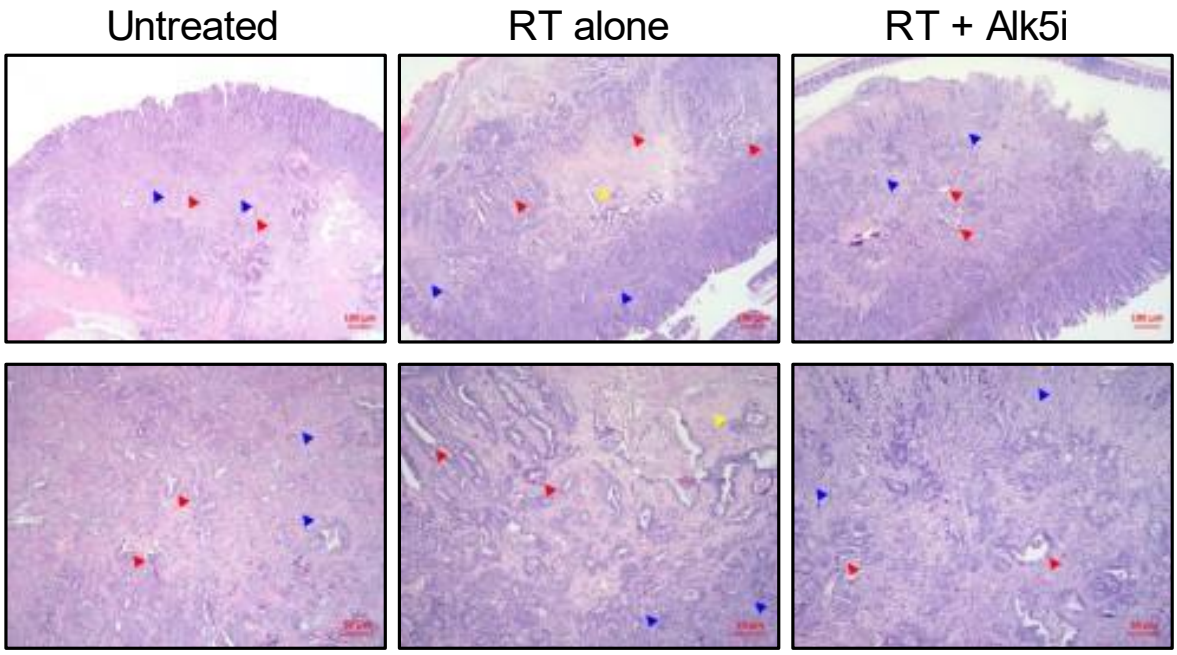

Figure 5.2: Histological Evidence of Tumour Regression is not observed at a 2-week Timepoint

Representative H+E images of tumours from each treatment group at 2-weeks post RT initiation. Top panel represents x4 magnification, bottom panel represents x10 magnification. Red arrows depict tumour epithelium. Blue arrows depict tumour stroma. Yellow arrows depict regions of absent tumour epithelium. Scale bars = 100μm and 50μm.

In the absence of tumour regression on H+E staining following combination treatment, I then sought to determine whether differences in tumour cell apoptosis were observed at 2-weeks post initiation of radiotherapy. IHC staining of tumour samples for cleaved caspase 3 was performed (Figure 5.3, top panel). It was hypothesised that treatment with fractionated radiotherapy would result in increased tumour cell apoptosis when compared with untreated controls, and that addition of ALK5 inhibition to fractionated radiotherapy would result in a further increase in the expression of apoptosis markers. A low percentage of apoptotic cells were present across all experimental groups, with no increase in tumour cell apoptosis observed following treatment with fractionated radiotherapy, or fractionated radiotherapy in combination with ALK5 inhibition at the 2-week time-point (Figure 5.3, bottom panel).

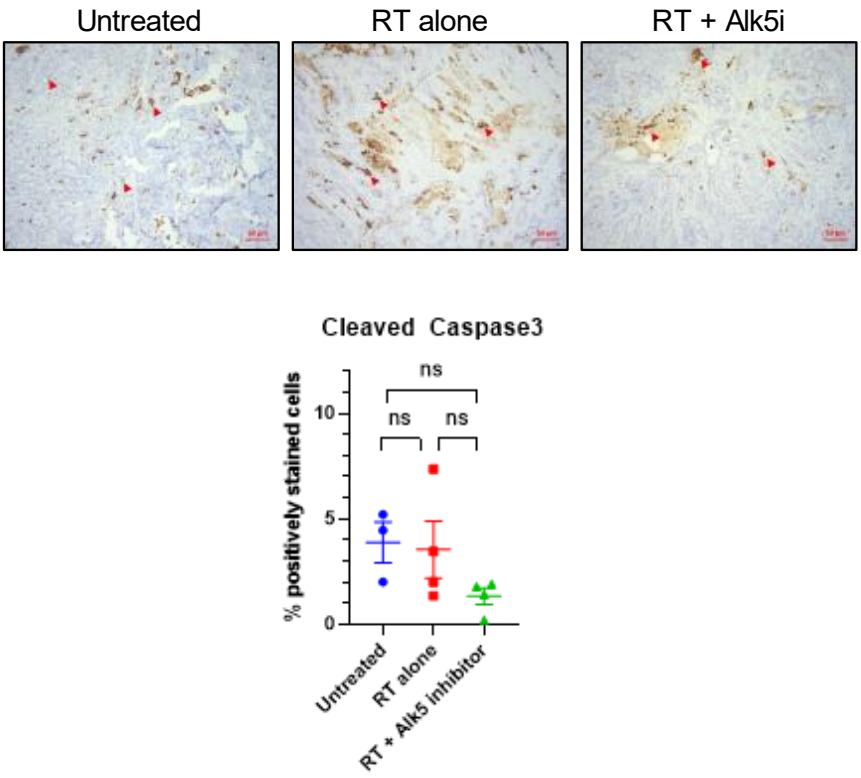

Figure 5.3: Increased Apoptosis is not Observed Following Treatment with Fractionated Radiotherapy and ALK5 Inhibition

Top – Cleaved Caspase 3 IHC staining for each treatment group (x10 magnification). Bottom – Bar graph showing quantification of cleaved caspase 3 by % cells positively stained. Red arrows cells positively staining for cleaved caspase 3. Error bars show mean and SEM, with each data point plotted. Group sizes n=4. Mann-Whitney U-test. ns denotes non-significance ($p \geq 0.05$). Scale bars = 50µm.

I next analysed cell proliferation in AKPT rectal tumours following treatment with fractionated radiotherapy and ALK5 inhibition through IHC staining for 5'-bromo-2'doxyuridine (BrdU), to determine whether this treatment combination impacted tumour cell proliferation (Figure 5.4, top panel). BrdU is incorporated into cells during the S-phase and serves as a marker for DNA replication and actively proliferating cells. It was hypothesised that treatment would have a deleterious effect on tumour cell proliferation, when compared with untreated age-matched tumours. No significant effect on tumour cell proliferation was observed in either treatment group when compared with untreated controls (Figure 5.4, bottom panel).

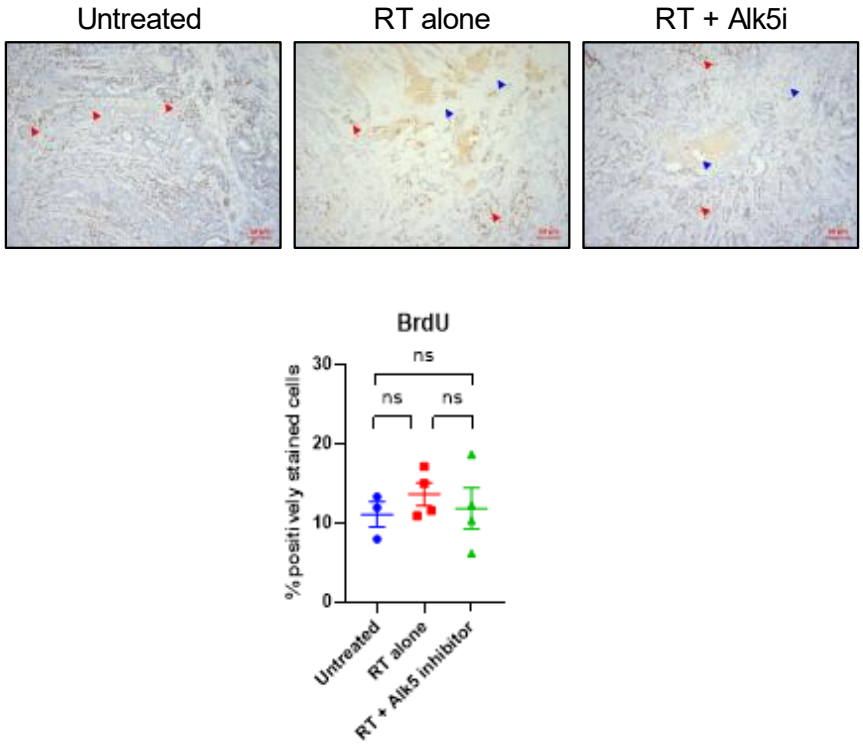

Figure 5.4: Tumour Cell Proliferation is not Affected by Fractionated Radiotherapy and ALK5 Inhibition

Top – BrdU IHC for each treatment group (x10 magnification). Bottom – Bar graph showing quantification of BrdU by % cells positively stained. Red arrows depict cells positively staining for BrdU. Blue arrows depict tumour regions with absence of proliferating cells. Error bars show mean and SEM, with each data point plotted. Group sizes n=4. Mann-Whitney U-test. ns denotes non-significance ($p \geq 0.05$). Scale bars = 50μm.

At the short-term time-point of 2-weeks post initiation of fractionated radiotherapy, no significant clinical benefit was observed when tumour volume was used as a treatment outcome measure. When tumour histology was assessed using H+E staining, no obvious tumour regression was observed in either treatment group when compared with time-matched controls. Furthermore, treatment with fractionated radiotherapy and ALK5 inhibition failed to induce any demonstrable intrinsic effects on tumour cells, with no significant change in the proportion of apoptotic or proliferating cells observed between experimental cohorts.

The negative findings from tumour analysis at 2-weeks post-treatment suggest that the AKPT rectal tumour model is resistant to treatment with fractionated radiotherapy in combination with ALK5 inhibition. Furthermore, the absence of effect on tumour volume, tumour cell apoptosis and proliferation at the 2-week time-point post-treatment, suggest that this pharmacological approach to

targeting TGF-β signalling may be ineffective. Therefore, I sought to determine whether the TGF-β signalling pathway is adequately targeted with ALK5 inhibition in the AKPT rectal tumour model. ALK5 inhibition should inhibit the effects of active TGF-β on TGF-β receptor 1 situated on the cell membrane, with subsequent inactivation of SMAD2/3 protein complex phosphorylation. IHC staining to assess nuclear pSMAD3 expression was performed, with high levels of expression observed in all cell types within AKPT rectal tumours across all treatment groups at the 2-week time-point (Figure 5.5). Although a trend towards increased pSMAD3 expression is observed when sham irradiated control tumours were compared with fractionated radiotherapy plus ALK5 inhibition, this did not achieve statistical significance (p=0.0714) (Figure 5.5, bottom panel).

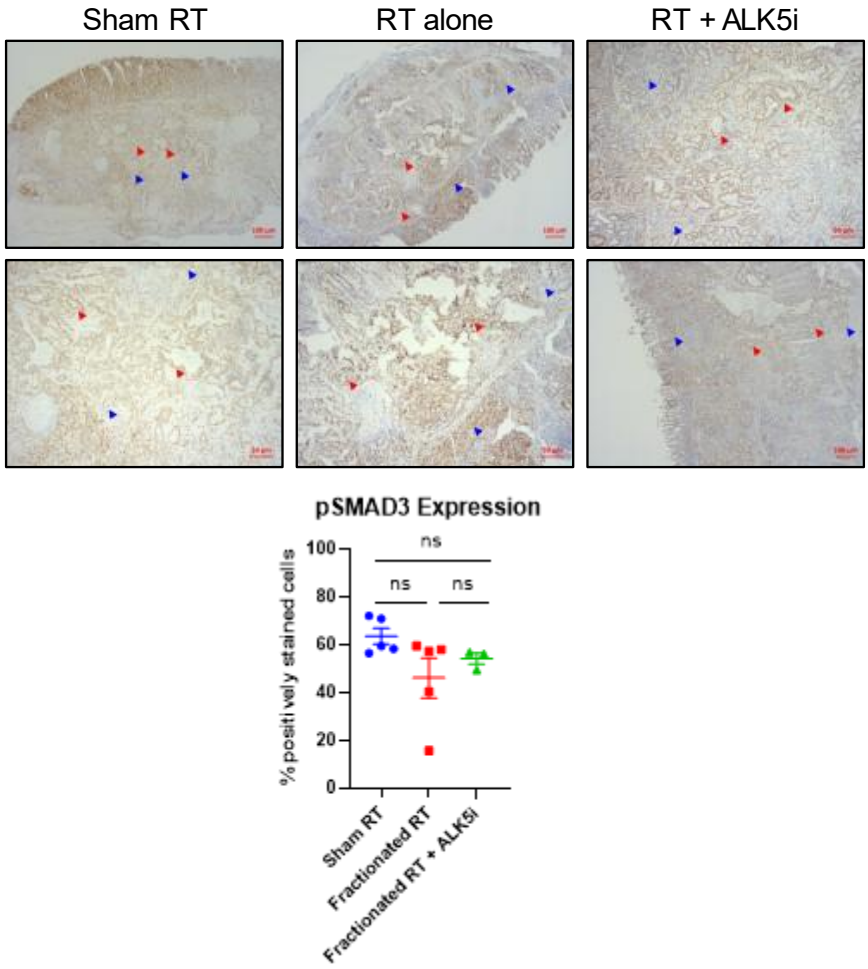

Figure 5.5: Nuclear pSMAD3 Expression is not Affected by Fractionated Radiotherapy and ALK5 Inhibition

Top – pSMAD3 IHC staining for each experimental group (x4 magnification). Middle – pSMAD3 IHC staining for each experimental group (x10 magnification). Bottom – Bar graph showing quantification of nuclear pSMAD3 by % cells positively stained. Red arrows depict positively staining epithelial cells. Blue arrows depict positively staining stromal cells. Error bars show mean and SEM, with each data point plotted. Group sizes n=4. Mann-Whitney U-test. ns denotes non-significance (p≥0.05). Scale bars = 100μm and 50μm.

To further substantiate the lack of TGF-β signalling pathway inhibition in the AKPT rectal tumour model following treatment, I assessed expression of downstream effector genes which are known to be regulated by TGF-β. Insulin-like growth factor binding protein 7 (IGFBP7) is known to be upregulated in the presence of TGF-β, so tumours were stained with this marker to determine whether expression decreases following treatment with fractionated radiotherapy and ALK5 inhibition (Jin et al, 2020). Similarly, high expression of Caldesmon 1 (CALD1) is associated with TGF-β signalling, with up-regulation of CALD1 being associated with the CMS4 group of CRC patients (Zheng et al, 2021). I assessed whether expression of these markers was impacted by treatment with fractionated radiotherapy in combination with ALK5 inhibition (Figure 5.6). Similar levels of CALD1 and IGFBP7 expression were observed across all experimental groups, with no significant differences seen when % of positive cells were quantified (Figure 5.6, bottom panel).

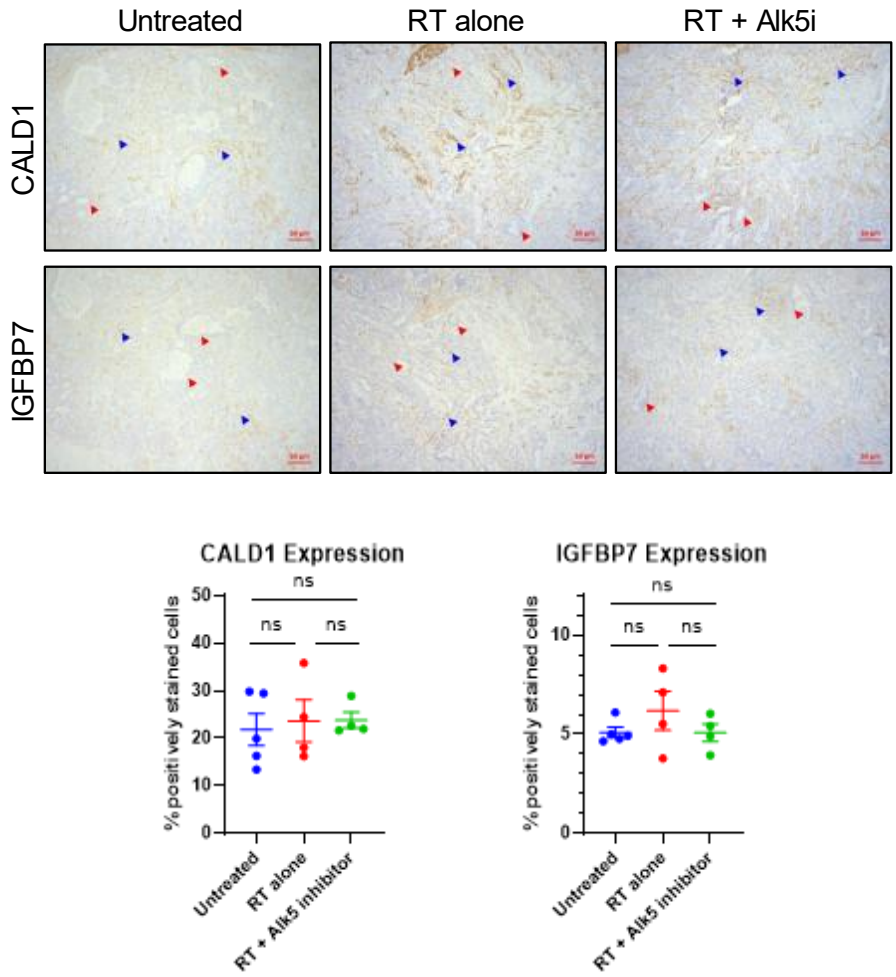

Figure 5.6: TGF-β Signalling Pathway Effectors are not Down-Regulated Following Fractionated Radiotherapy and ALK5 Inhibition

Top – CALD1 immunohistochemistry staining for each treatment group (x10 magnification). Middle – IGFBP7 immunohistochemistry staining for each treatment group (x10 magnification). Bottom - Bar graphs showing quantification of CALD1 and IGFBP7 expression by % cells positively stained. Red arrows depict tumour epithelium. Blue arrows depict stromal compartment. Error bars show mean and SEM, with each data point plotted. Group sizes n=4-5. Mann-Whitney U-test. ns denotes non-significance ($p \geq 0.05$). Scale bars = 50μm.

To further assess the TGF-β signalling pathway in response to ALK5 inhibition in the AKPT rectal cancer model, IHC was performed to quantify nuclear SMAD2, the first SMAD protein which undergoes phosphorylation following TGFBR1 activation (Figure 5.7). IHC images show high expression of nuclear SMAD2 in the tumour epithelial cells within each treatment group, with no obvious effect on SMAD2 expression following treatment with Alk5 inhibition demonstrated. Upon quantification, there appears to be a small decrease in the % of all cells positively staining for nuclear SMAD2 following treatment with ALK5 inhibition and/or fractionated radiotherapy; however, this did not reach statistical significance and quantification of phosphorylated SMAD2 would have been more

informative in detecting any TGFBR mediated effects on SMAD signalling. The lack of effect on the SMAD signalling cascade and on expression of downstream effector targets, suggests that the AKPT model is resistant to TGF-ß inhibition using the ALK5 inhibitor.

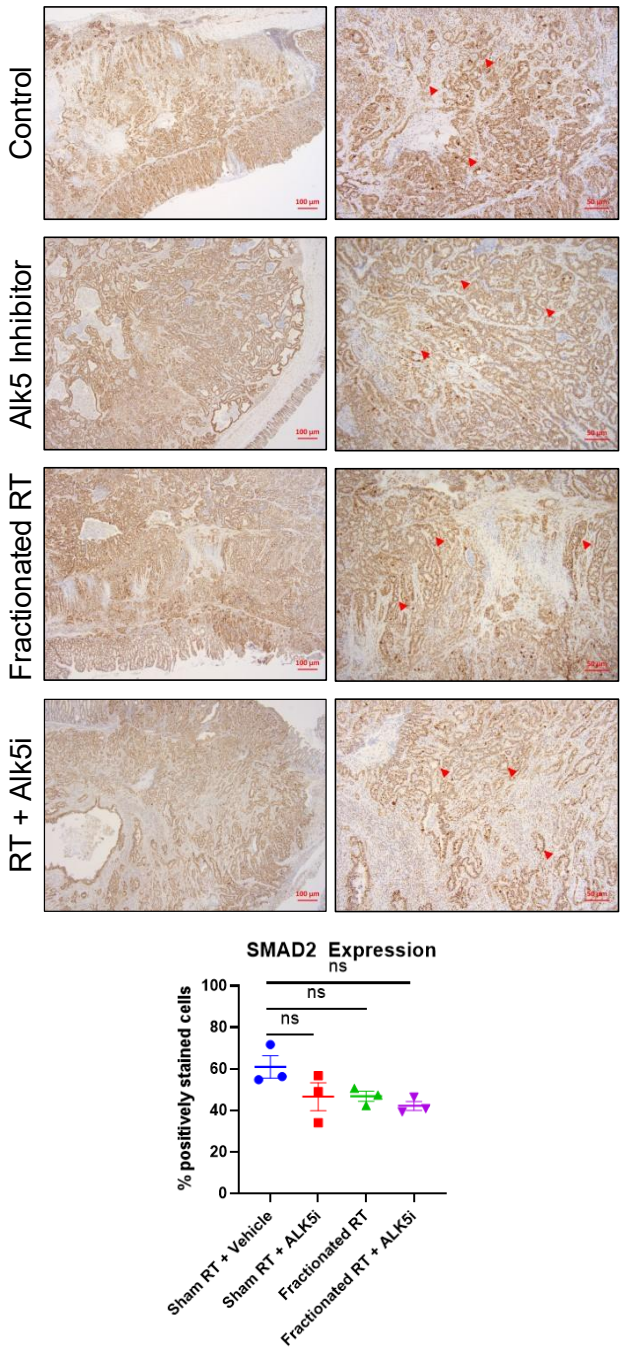

Figure 5.7: SMAD2 phosphorylation is not Significantly Decreased Following Fractionated Radiotherapy and ALK5 Inhibition

Top – SMAD2 immunohistochemistry staining for each treatment group (as labelled) with x4 magnification (left images) and x10 magnification (right images). Bottom - Bar graph showing quantification of nuclear SMAD2 expression by % cells positively stained, with all cell types analysed. Red arrows depict positively staining tumour epithelial cells. Error bars show mean and SEM, with each data point plotted. Group sizes n=3. Mann-Whitney U-test. ns denotes non-significance ($p \geq 0.05$). Scale bars = 100µm and 50µm.

To further investigate the effects of fractionated radiotherapy in combination with ALK5 inhibition, ageing cohorts were established. Immunocompetent C57Bl/6 mice were injected with AKPT organoid fragments then treated with fractionated radiotherapy (3 x 5Gy on alternate days) at 2-weeks post-implantation with ALK5 inhibition administered 3 days prior to radiotherapy commencing (Figure 5.8, top panel). ALK5 inhibition was continued until animals reached clinical endpoint. Treatment with ALK5 inhibitor with or without fractionated radiotherapy failed to improve survival of animals when compared with a control cohort treated with sham radiotherapy and vehicle (Figure 5.8, middle panel). When tumour volume was calculated using tumour measurements recorded at clinical endpoint, no significant difference was observed between treatment groups (Figure 5.8, bottom panel). Results from these ageing cohorts are suggestive that treatment with fractionated radiotherapy in combination with ALK5 inhibitor does not result in clinical benefit in the AKPT rectal cancer model, with survival benefit and tumour volume reduction not observed.

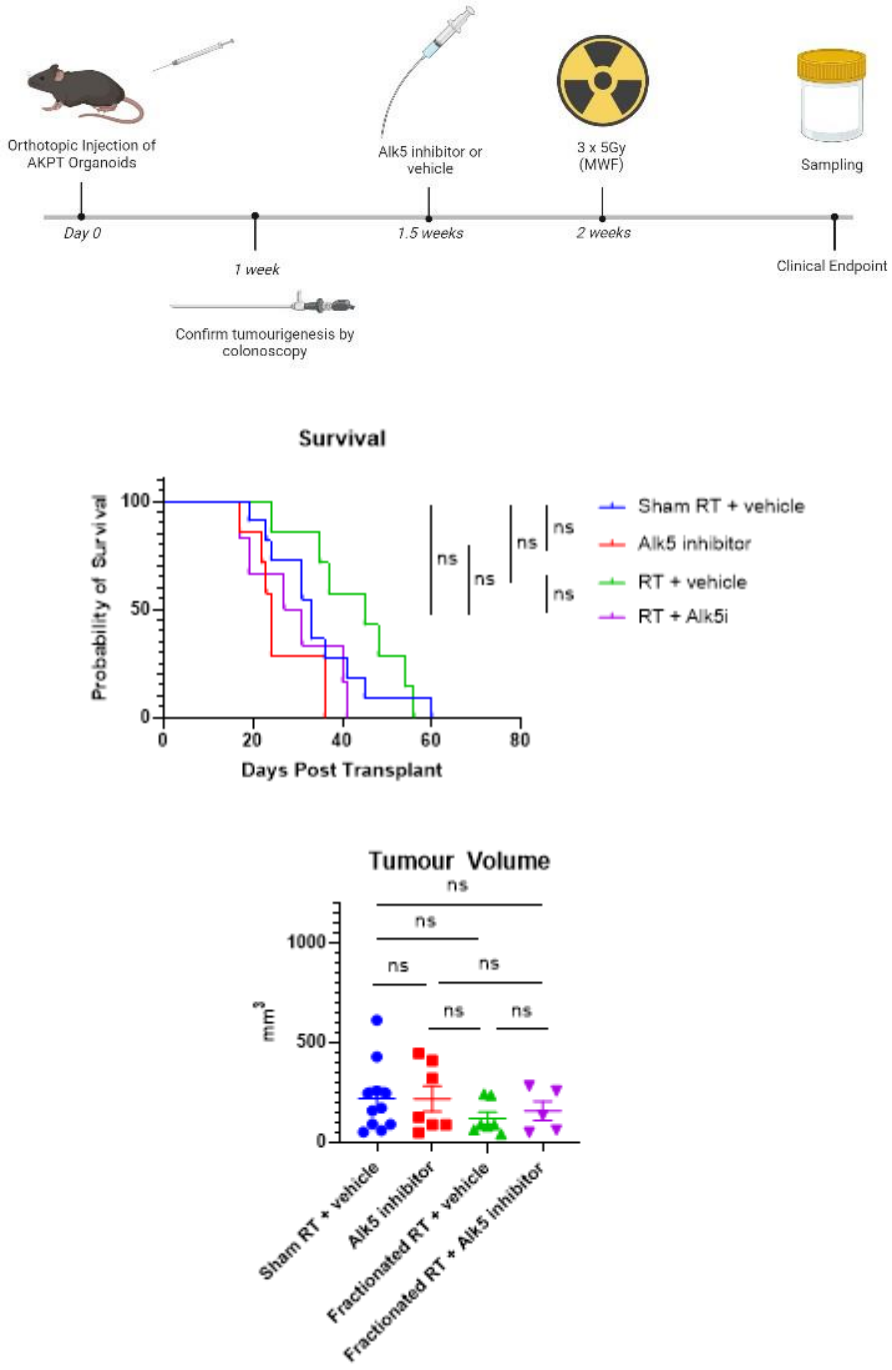

Figure 5.8: Fractionated Radiotherapy and ALK5 Inhibition Fails to Improve Survival or Tumour Burden

Top – Schematic depicting experimental timeline for treatment with fractionated radiotherapy in combination with ALK5 inhibition. Middle – Survival curve demonstrating post-transplant survival in each treatment group, with each subject plotted. Bottom - Bar graph showing tumour volumes (mm^3) at clinical endpoint in each treatment group. Error bars show mean and SEM, with each data point plotted. Group sizes n=5-11. Mann-Whitney U-test (tumour volume), Log Rank Mantel-Cox test (survival). ns denotes non-significance ($p \geq 0.05$).

5.2.2 Evaluating the Clinical Response to Fractionated Radiotherapy and PD-1 Inhibition

I next aimed to assess PD-1 inhibition in combination with fractionated radiotherapy, to determine whether this treatment combination would result in survival extension and tumour regression in the orthotopic AKPT tumour derived organoid transplant model of LARC. C57Bl/6 immunocompetent mice were injected with AKPT organoid fragments at the rectal location under colonoscopy guidance, with tumour engraftment confirmed at one week post implantation by colonoscopy. PD-1 inhibition was then administered at 1.5 weeks post tumour implantation with fractionated radiotherapy (3 x 5Gy on alternate days) commenced 3 days later (Figure 5.9, top panel). PD-1 inhibition was administered twice weekly by intra-peritoneal injection, and continued until clinical endpoint. Animals were euthanised at clinical endpoint (deteriorating body condition, ≥10% weight loss, visible tumour burden), with tumour dimensions recorded at sampling to enable calculation of tumour volume. No statistically significant difference in tumour volume was observed between any of the treatment groups at clinical endpoint (Figure 5.9, bottom panel).

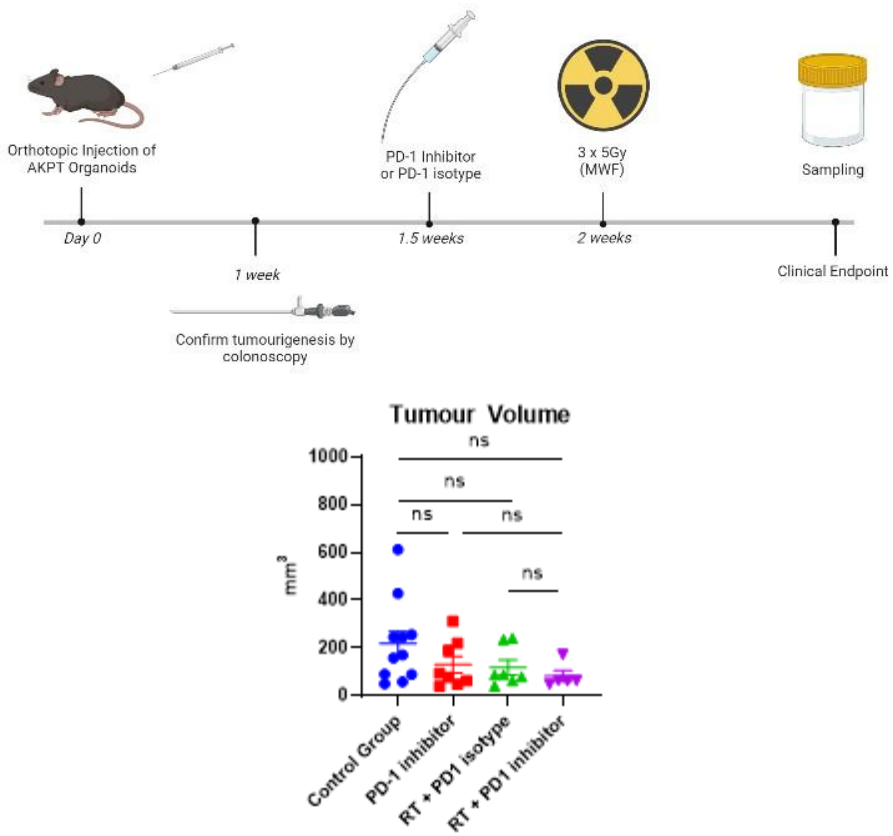

Figure 5.9: Fractionated Radiotherapy and PD-1 Inhibition Fails to Reduce Tumour Volume

Top – Schematic depicting experimental timeline for treatment with fractionated radiotherapy in combination with PD-1 inhibition. Bottom - Bar graph showing tumour volumes (mm^3) at clinical endpoint in each treatment group. Error bars show mean and SEM, with each data point plotted. Group sizes n=6-11. Mann-Whitney U-test (tumour volume). ns denotes non-significance ($p \geq 0.05$).

Following treatment with fractionated radiotherapy and PD-1 inhibition, one experimental subject showed complete response to treatment, with no tumour evident at 12-weeks post tumour implantation on colonoscopy visualisation (Figure 5.10, top panel). A significant extension in survival was demonstrated following fractionated radiotherapy and PD-1 inhibition, when compared with radiotherapy and PD-1 isotype (p=0.0252) and when compared with the control group (p=0.0127). Although a trend towards increased survival was demonstrated when the radiotherapy plus PD-1 inhibition group was compared with PD-1 inhibition alone, statistical significance was not achieved (p=0.0792).

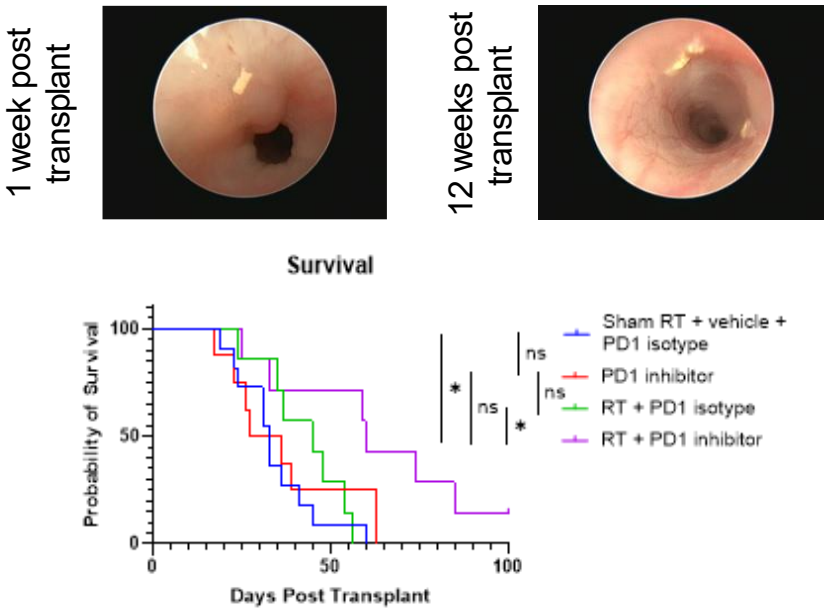

Figure 5.10: Fractionated Radiotherapy and PD-1 Inhibition Improves Survival

Top – Colonoscopy images demonstrating a complete tumour response to fractionated radiotherapy and PD-1 inhibition, with images showing tumour at 1-week post implantation (Left) followed by complete tumour response at 12 weeks (Right). Bottom – Survival curve demonstrating post-transplant survival in each treatment group, with each subject plotted. Censor point denotes subject with complete tumour response. Group sizes n=7-11. Log Rank Mantel-Cox test. ns denotes non-significance ($p \geq 0.05$). * denotes p-value <0.05.

Histological features were then analysed through H+E staining of tumours sampled at clinical endpoint following treatment. Tumours from the control group displayed similar histological features to previous experiments, with tumour invasion through the muscularis propria and densely infiltrated stromal compartments observed (Figure 5.11, top panel). No obvious histological changes were demonstrated in tumours following treatment with PD-1 inhibition alone, with the tumour core regions demonstrating infiltration of immune cells (Figure 5.11, top middle panel). In tumours treated with fractionated radiotherapy or with fractionated radiotherapy and PD-1 inhibition, regions of tumour regression are demonstrated within the tumour cores with tumour epithelium occasionally being replaced by fibrosis (Figure 5.11, lower middle and bottom panels).

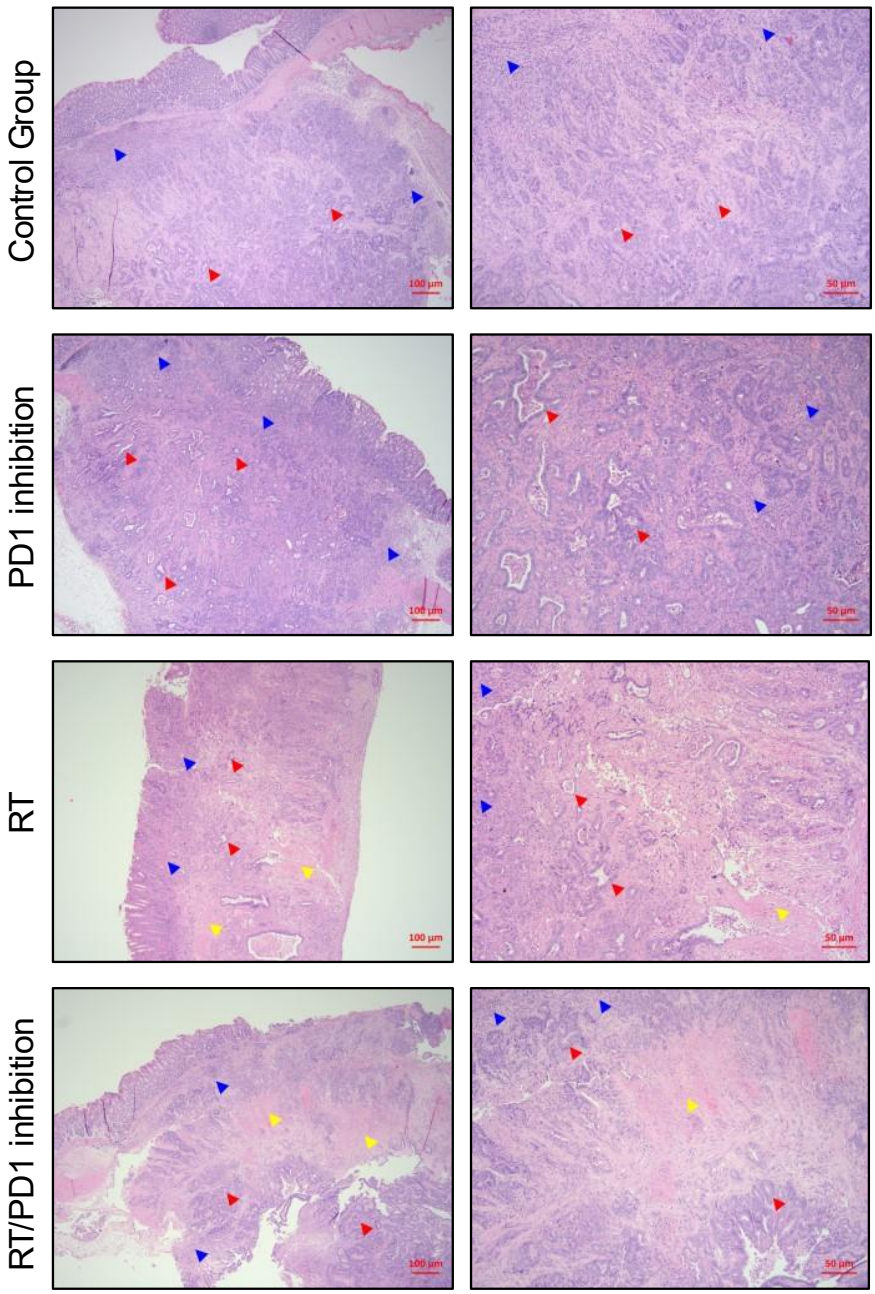

Figure 5.11: Fractionated Radiotherapy and PD-1 Inhibition Induces Histological Changes

Top – Representative H+E images (x4 and x10) of AKPT rectal tumours treated with sham radiotherapy, vehicle and PD-1 isotype. Top middle – Representative H+E images (x4 and x10) of AKPT rectal tumours treated with PD-1 inhibition. Bottom middle – Representative H+E images (x4 and x10) of AKPT rectal tumours treated with fractionated radiotherapy. Bottom – Representative H+E images (x4 and x10) of AKPT rectal tumours treated with fractionated radiotherapy and PD-1 inhibition. Red arrows depict tumour epithelium. Blue arrows depict tumour stroma. Yellow arrows depict regions of fibrosis. Scale bars = 100μm (left images) and 50μm (right images).

Histological changes associated with treatment were then assessed further through special staining for the AB/PAS sequence to quantify mucin pooling

(Figure 5.12, top and middle panels). Across all treatment groups only small regions of AB/PAS positivity were observed, with no significant difference in percentage of area positively stained observed between groups (Figure 5.12, bottom panel). Interestingly, in the regions of tumour demonstrating fibrosis following treatment with fractionated radiotherapy or fractionated radiotherapy plus PD-1 inhibition, there is complete absence of mucin pooling, suggesting that mucin pooling may not be a useful surrogate measure of tumour response at clinical endpoint.

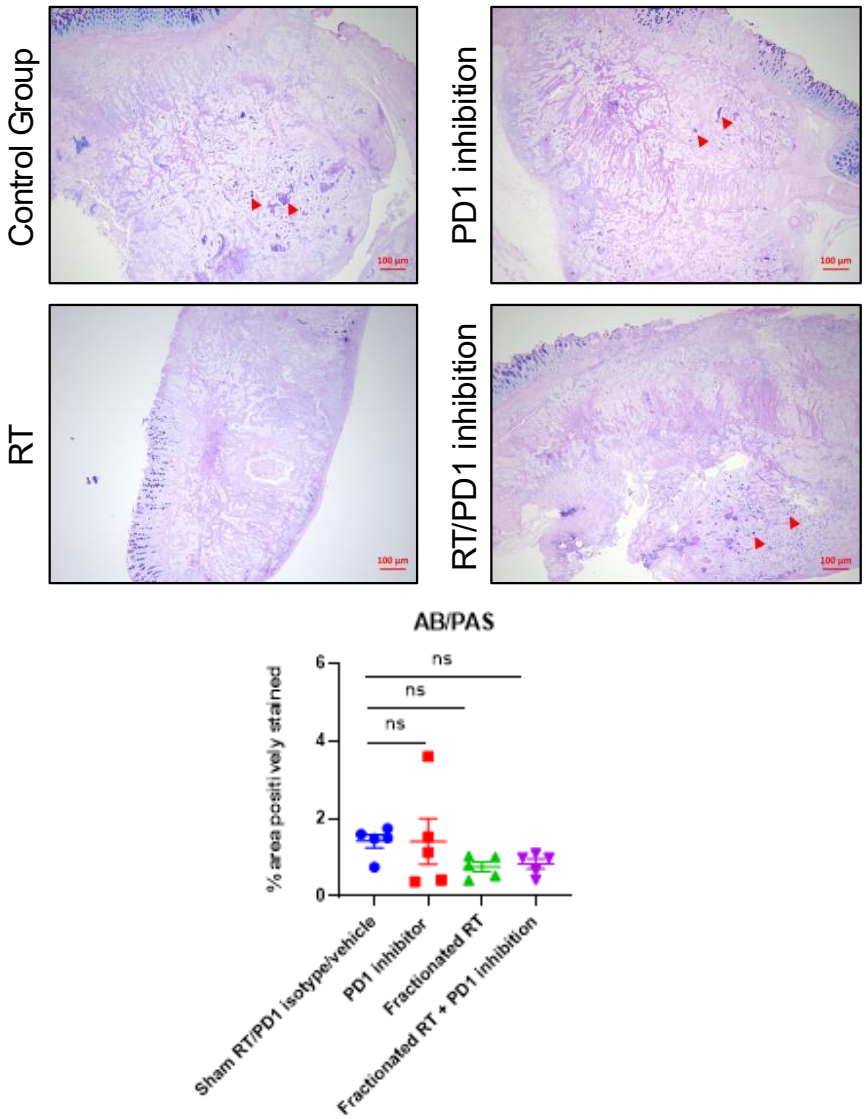

Figure 5.12: Increased Mucin Pooling is not Demonstrated Following Fractionated Radiotherapy and PD-1 Inhibition

Top – Representative AB/PAS special stain images (x4) of AKPT rectal tumours treated with sham radiotherapy, vehicle and PD-1 isotype (left), and PD-1 inhibition (right). Middle – Representative AB/PAS special stain images (x4) of AKPT rectal tumours treated with fractionated radiotherapy (left) and fractionated radiotherapy plus PD-1 inhibition (right). Bottom - Bar graph showing % of area positively stained for AB/PAS in each treatment group. Error bars show mean and SEM, with each data point plotted. Group sizes n=5. Mann-Whitney U-test. ns denotes non-significance ($p \geq 0.05$). Scale bars = 100μm.

5.2.3 Assessing the Immune Response to Fractionated Radiotherapy and PD1 Inhibition

Following the absence of immune cell changes demonstrated in the tumour micro-environment following treatment with fractionated radiotherapy alone in previous experiments undertaken in the AKPT rectal transplant model, I next sought to determine whether the addition of PD-1 inhibition would induce

immunological changes in the TME. Similarly to previous experiments, IHC staining for the pan T-cell marker CD3 revealed abundant lymphocyte clustering at the tumour invasive margins with a relative paucity of CD3+ cells in the tumour core of control group samples. CD3+ T-cell quantification (cells per mm^2) revealed a trend towards increased CD3+ T-cell densities in both the PD-1 inhibition alone and fractionated radiotherapy plus PD1 inhibition groups, when compared with both control and fractionated radiotherapy groups (Figure 5.13, bottom panel). However, no statistically significant differences in CD3+ T-lymphocyte density were observed between any treatment groups.

Interestingly, it was observed that tumours treated with PD-1 inhibition (with or without fractionated radiotherapy) displayed more CD3+ cells within the tumour core, suggesting that PD-1 inhibition might enable the migration of effector T-cells into the tumour core (Figure 5.13, top and middle panels). Quantification of CD3+ T-cell density within the whole tumour may not accurately quantify the intra-tumoral immune response following fractionated radiotherapy and PD-1 inhibition; areas of fibrosis which display absent immune cell infiltrate are observed following combination treatment, and so effects on CD3+ T-cell infiltration may be under-estimated (Figure 5.11).

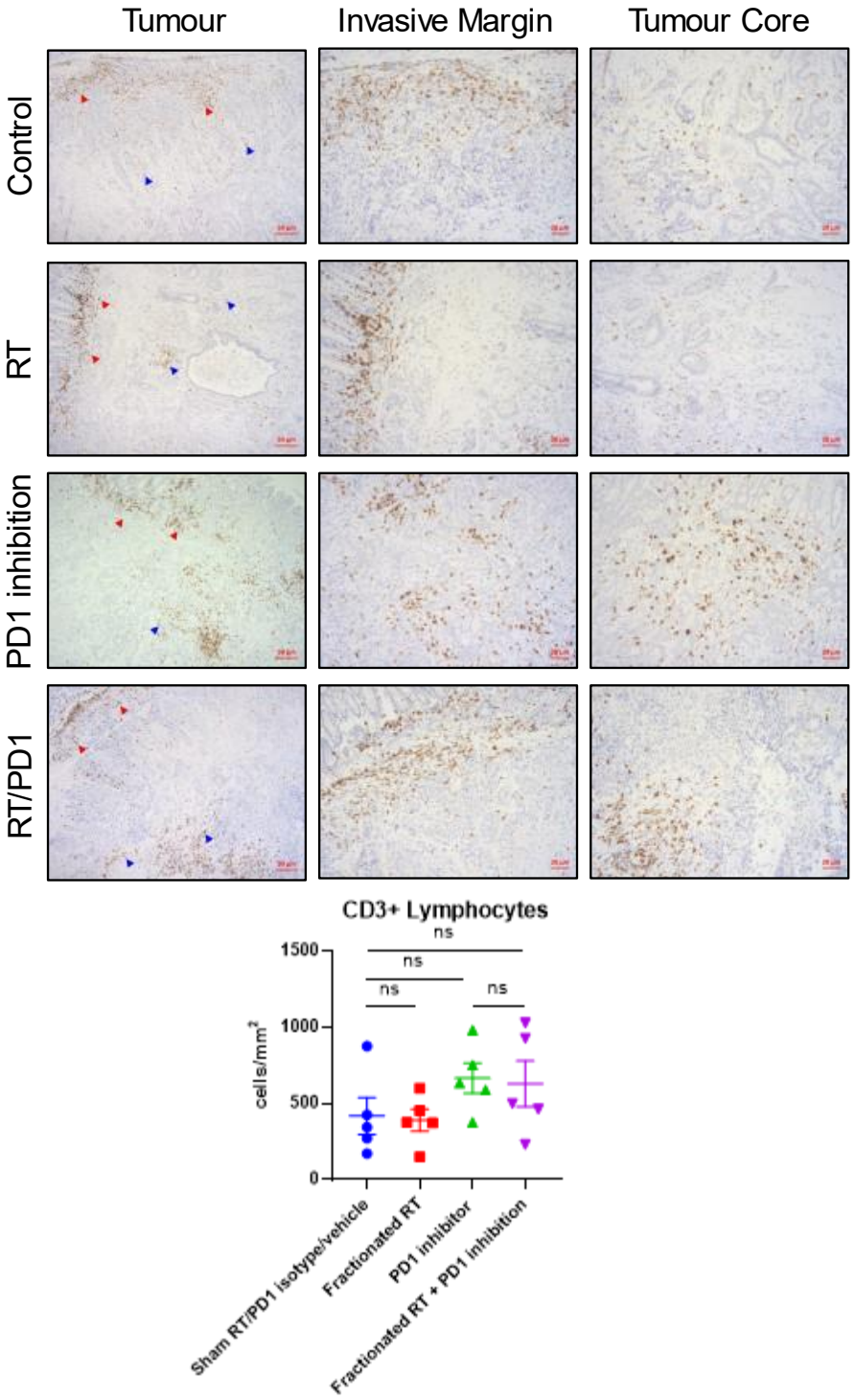

Figure 5.13: Increased CD3+ Lymphocyte Density is not Demonstrated Following Fractionated Radiotherapy and PD-1 Inhibition

Top – Representative CD3+ IHC images (x10) of AKPT rectal tumours from each treatment group (left column). Representative CD3+ IHC images (x20) of invasive margin region from AKPT rectal tumours (middle column). Representative CD3+ IHC images (x20) of tumour core region from AKPT rectal tumours (right column). Bottom - Bar graph showing quantification of CD3+ lymphocytes (cells/mm^2) for whole tumour area. Error bars show mean and SEM, with each data point plotted. Group sizes n=5 scored per group. Mann-Whitney U-test. ns denotes non-significance ($p \geq 0.05$). Red arrows depict invasive margin. Blue arrows depict tumour core. Scale bars = 50μm and 20μm.

To further investigate changes in T-cell populations following treatment with fractionated radiotherapy and PD-1 inhibition, IHC was performed on tumour samples to identify T-helper cells through CD4+ marker staining (Figure 5.14, top and middle panels). Similarly, dense CD4+ T-cell clustering was observed at the tumour invasive margin in all experimental groups. A trend towards increased CD4+ T-cell density across whole tumour sections was observed following treatment with PD-1 inhibition or fractionated radiotherapy plus PD-1 inhibition, when compared with the control and fractionated radiotherapy groups (Figure 5.14, bottom panel). A statistically significant difference was observed in CD4+ T-cell density between the control and fractionated radiotherapy plus PD-1 inhibition groups ($p=0.0159$), further suggesting that PD-1 inhibition enhances T-cell infiltration in this model. The previous observation that more abundant CD3+ lymphocytes are seen in the tumour core following PD-1 inhibition with or without fractionated radiotherapy, was not observed for CD4+ lymphocytes.

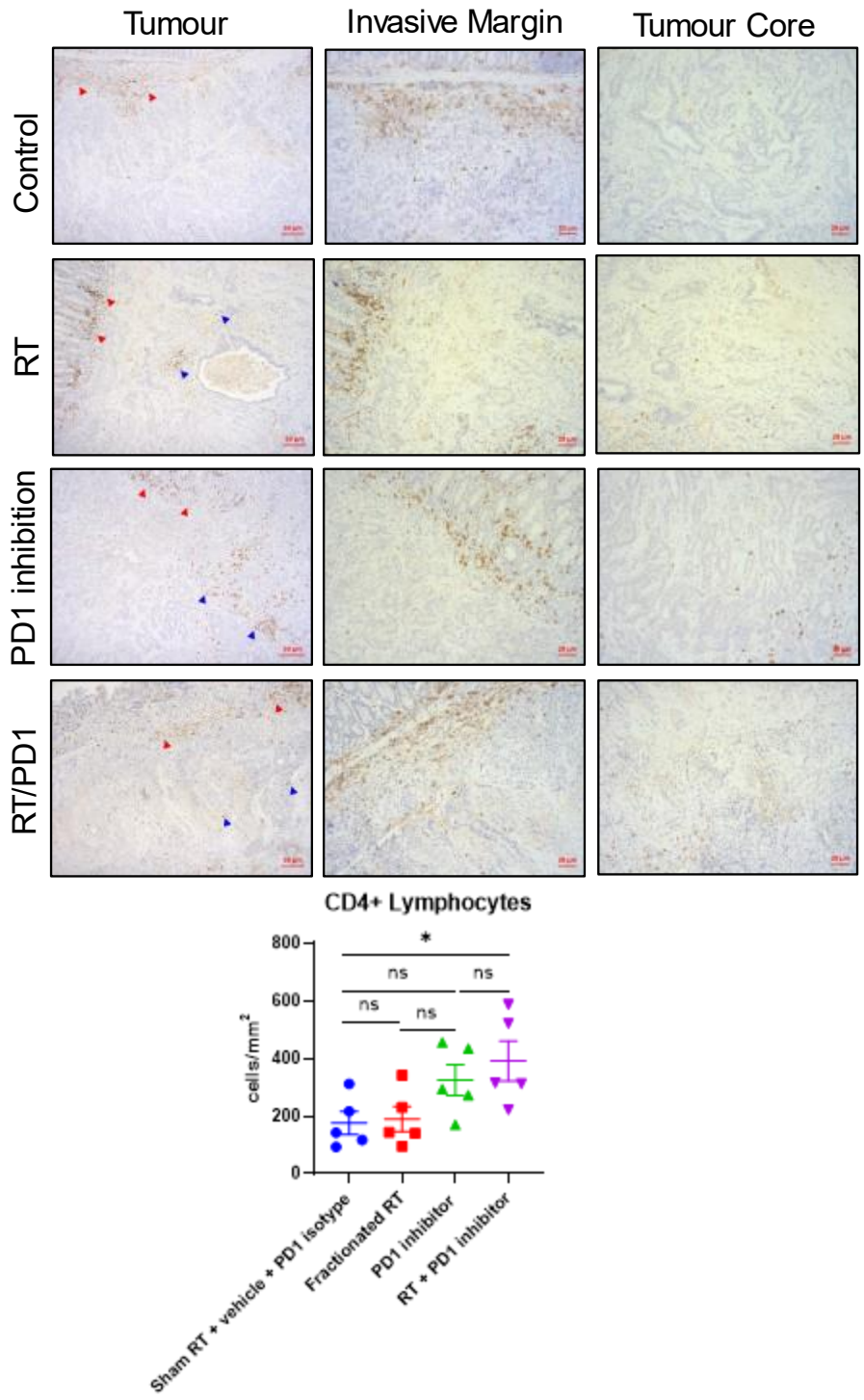

Figure 5.14: Increased CD4+ Lymphocyte Density is Demonstrated Following Fractionated Radiotherapy and PD-1 Inhibition

Top – Representative CD4+ IHC images (x10) of AKPT rectal tumours from each treatment group (left column). Representative CD4+ IHC images (x20) of invasive margin region from AKPT rectal tumours (middle column). Representative CD4+ IHC images (x20) of tumour core region from AKPT rectal tumours (right column). Bottom - Bar graph showing quantification of CD4+ lymphocytes (cells/mm2) for whole tumour area. Error bars show mean and SEM, with each data point plotted. Group sizes n=5 scored per group. Mann-Whitney U-test. ns denotes non-significance ($p \geq 0.05$). * denotes statistical significance ($p < 0.05$). Red arrows depict invasive margin. Blue arrows depict tumour core. Scale bars = 50μm and 20μm.

IHC staining was performed for the CD8 marker to analyse whether treatment with fractionated radiotherapy and PD-1 inhibition induced changes in cytotoxic T-lymphocytes. Abundant CD8+ T-cells were observed at the tumour invasive margin in all experimental groups, with increased CD8+ T-cell numbers in the tumour core of the PD-1 inhibition and fractionated radiotherapy plus PD-1 inhibition groups being observed on IHC (Figure 5.15, top and middle panels). A wide heterogeneity in CD8+ T-cell density was observed in the PD-1 inhibition group, making it difficult to interpret whether PD-1 inhibition affects CD8+ T-cell infiltration in this experimental group, suggesting some AKPT tumours may be resistant to treatment with PD-1 inhibition. Although a difference in CD8+ T-cell density between the fractionated radiotherapy and fractionated radiotherapy plus PD-1 inhibition groups was noted, this did not reach statistical significance ($p=0.0556$) (Figure 5.15, bottom panel). The trend towards increased CD8+ T-cell infiltration in PD-1 treated groups, as well as higher densities being observed within the tumour core, is seen in other pre-clinical studies where it is suggested that PD-1 inhibition enhances T-cell migration through increased expression of IFN-γ and CXCL10 which improves T-cell migration to tumour sites (Peng et al, 2012).

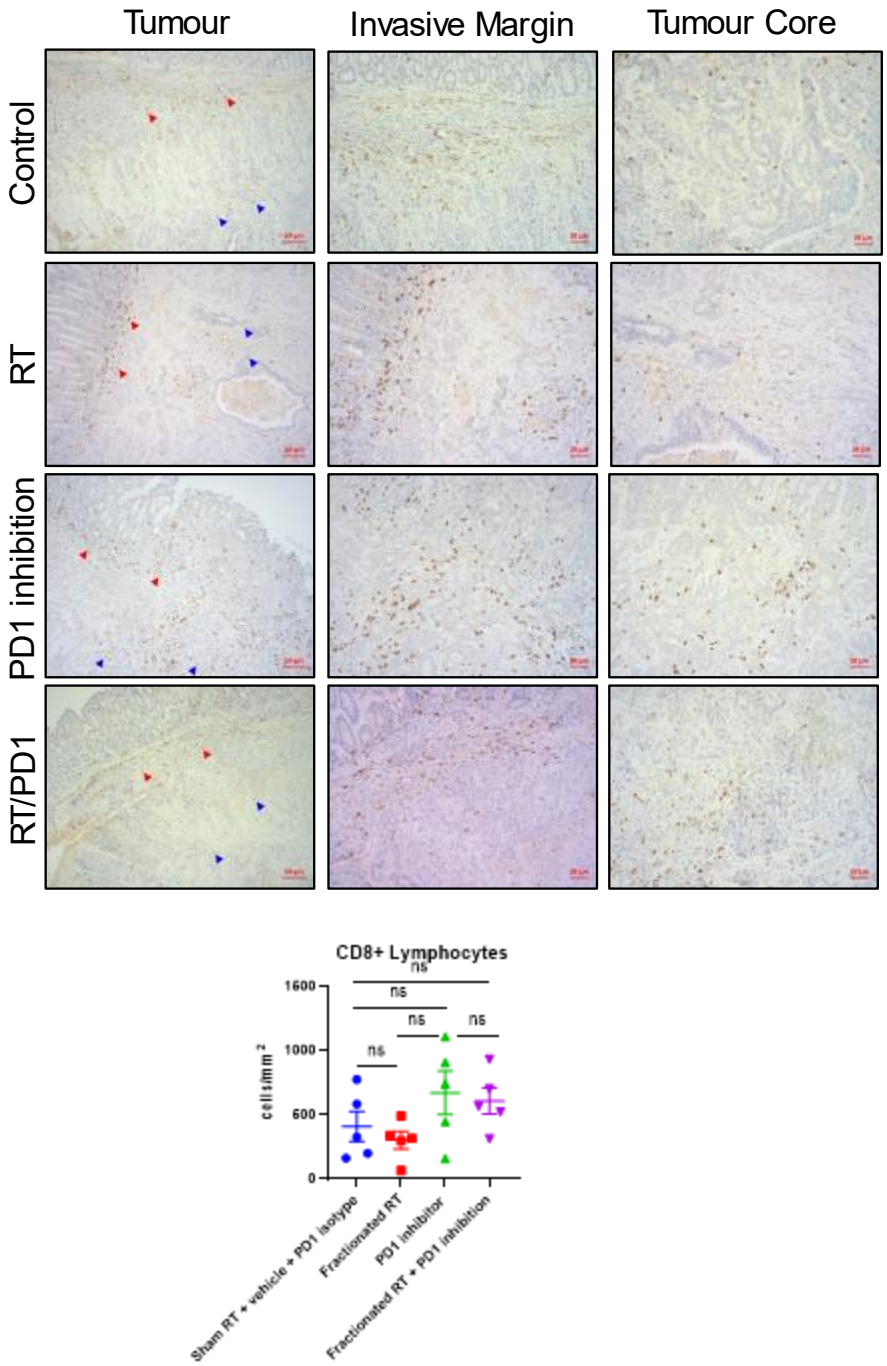

Figure 5.15: Increased CD8+ Lymphocyte Density is not Demonstrated Following Fractionated Radiotherapy and PD-1 Inhibition

Top – Representative CD8+ IHC images (x10) of AKPT rectal tumours from each treatment group (left column). Representative CD8+ IHC images (x20) of invasive margin region from AKPT rectal tumours (middle column). Representative CD8+ IHC images (x20) of tumour core region from AKPT rectal tumours (right column). Bottom - Bar graph showing quantification of CD8+ lymphocytes (cells/mm2) for whole tumour area. Error bars show mean and SEM, with each data point plotted. Group sizes n=5 scored per group. Mann-Whitney U-test. ns denotes non-significance ($p \geq 0.05$). Red arrows depict positive cells at the invasive margin. Blue arrows depict positive cells within the tumour core. Scale bars = 50μm and 20μm.

I then analysed the effects of fractionated radiotherapy and PD-1 inhibition on FOXP3+ T regulatory cell infiltration, given their known role in tumour development through the inhibition of anti-tumour immunity (Zhulai and Oleinik, 2021). Conflicting evidence exists for the role of PD-1 inhibition in the function of T regs, with some pre-clinical studies showing that PD-1 blockade promotes the proliferation and immunosuppressive function of T regs, while other studies suggest PD-1 inhibition might induce terminal differentiation and apoptosis of T regs (Kamada et al, 2019; Asano et al, 2017). IHC staining for the FOXP3 marker was used to determine whether treatment with PD-1 inhibition, fractionated radiotherapy or fractionated radiotherapy and PD-1 inhibition induced any changes in T reg populations within AKPT tumours (Figure 5.16).

Similarly to other immune cells, T reg cells were predominantly observed at the tumour invasive margins in all treatment groups, with a paucity of T reg cells within the tumour core (Figure 5.16, top and middle panels). Interestingly, a significant increase ($p=0.0317$) in T reg cell density in the whole tumour was observed when fractionated radiotherapy and PD-1 inhibition was compared with fractionated radiotherapy alone, suggesting a role for this treatment combination in enhancing T reg cell infiltration (Figure 5.16, bottom panel). However, no significant difference was observed when any treatment group was compared with the control group, with fractionated radiotherapy alone not being shown to induce T reg infiltration.

This finding conflicts with data from the B16-OVA melanoma flank injection model described by Sharabi et al, whereby single fraction stereotactic 12Gy irradiation resulted in increased T reg infiltration, with this effect being abrogated following the addition of PD-1 inhibition (Sharabi et al, 2015). However, it was noted in untreated B16-OVA tumours that immune infiltrate was sparse with absence of CD4 and CD8+ T-cells, highlighting that different underlying TME immune compositions will result in a heterogeneity of response to treatment across different pre-clinical tumour models.

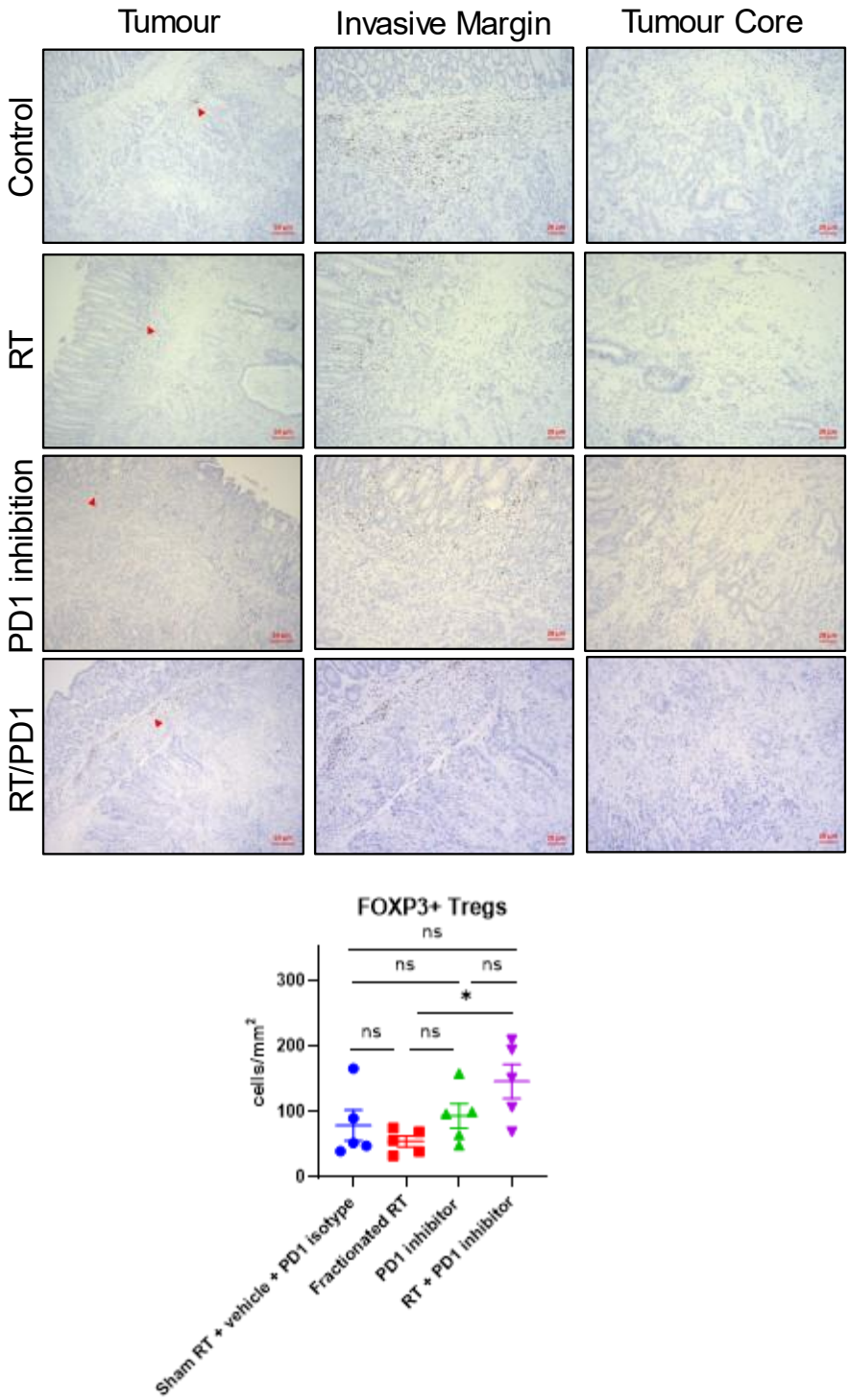

Figure 5.16: Increased FOXP3+ T regulatory Cell Density is Demonstrated when PD-1 Inhibition is administered in Combination with Fractionated Radiotherapy

Top – Representative FOXP3+ IHC images (x10) of AKPT rectal tumours from each treatment group (left column). Representative FOXP3+ IHC images (x20) of invasive margin region from AKPT rectal tumours (middle column). Representative FOXP3+ IHC images (x20) of tumour core region from AKPT rectal tumours (right column). Bottom - Bar graph showing quantification of FOXP3+ Treg cells (cells/mm2) for whole tumour area. Error bars show mean and SEM, with each data point plotted. Group sizes n=5 scored per group. Mann-Whitney U-test. ns denotes non-significance ($p \geq 0.05$). *denotes p-value <0.05. Red arrows depict positive cells. Scale bars = 50μm and 20μm.

I next analysed the effects of fractionated radiotherapy and PD-1 inhibition on macrophage infiltration by performing IHC staining for the F4/80 marker on tumour samples at clinical endpoint. Similarly to lymphoid cell infiltrate, macrophages are observed to cluster densely at the tumour invasive margin (Figure 5.17, top and middle panels). A decrease in macrophage cell density (calculated as % of total tumour area positively stained) was observed following treatment with fractionated radiotherapy alone when compared with the control group, however, statistical significance was not reached (p=0.0952) (Figure 5.17, bottom panel). When PD-1 inhibition alone was compared with the fractionated radiotherapy group, a significant increase in macrophage infiltration was observed in the PD-1 inhibition group (p=0.0317), however, no significant change in macrophage density was observed in the fractionated radiotherapy plus PD-1 inhibition group (Figure 5.17, bottom panel).

Macrophages are a potential therapeutic target in cancer therapy, and they are known to have effects in mediating tumour cytotoxicity and phagocytosis of tumour cells (Mantovani et al, 2022). Immunosuppressive tumour associated macrophages have high expression of immune checkpoint molecules including PD-1, and may therefore contribute to inducing T-cell exhaustion. High macrophage infiltration at the tumour invasive margin has been shown to be associated with improved survival in colonic (but not rectal) cancers, with *in-vivo* experiments suggesting that macrophage contact with tumour cells influences the balance between the pro- and anti-tumorigenic effects of macrophages (Forsell et al, 2007). Interestingly, using the MC38 colon cancer cell line, a recent study by Tang et al suggested that PD-L1 expression on tumour cells is not essential for the response to PD-L1 blockade (Tang et al, 2018). Using CRISPR/Cas9 technology, knockout tumour cells lacking PD-L1 were generated which responded similarly to PD-L1 blockade when compared with wild type cells; levels of PD-L1 expression on myeloid cells including macrophages were similar between tumours, suggesting that myeloid cells may have a role in mediating the response to immune checkpoint blockade through the regulation of T-cell function. Further analysis would have to be performed in the AKPT model to determine the phenotypic characteristics of the macrophage populations seen, and whether immune checkpoint blockade induces anti-tumour effects in macrophage populations.

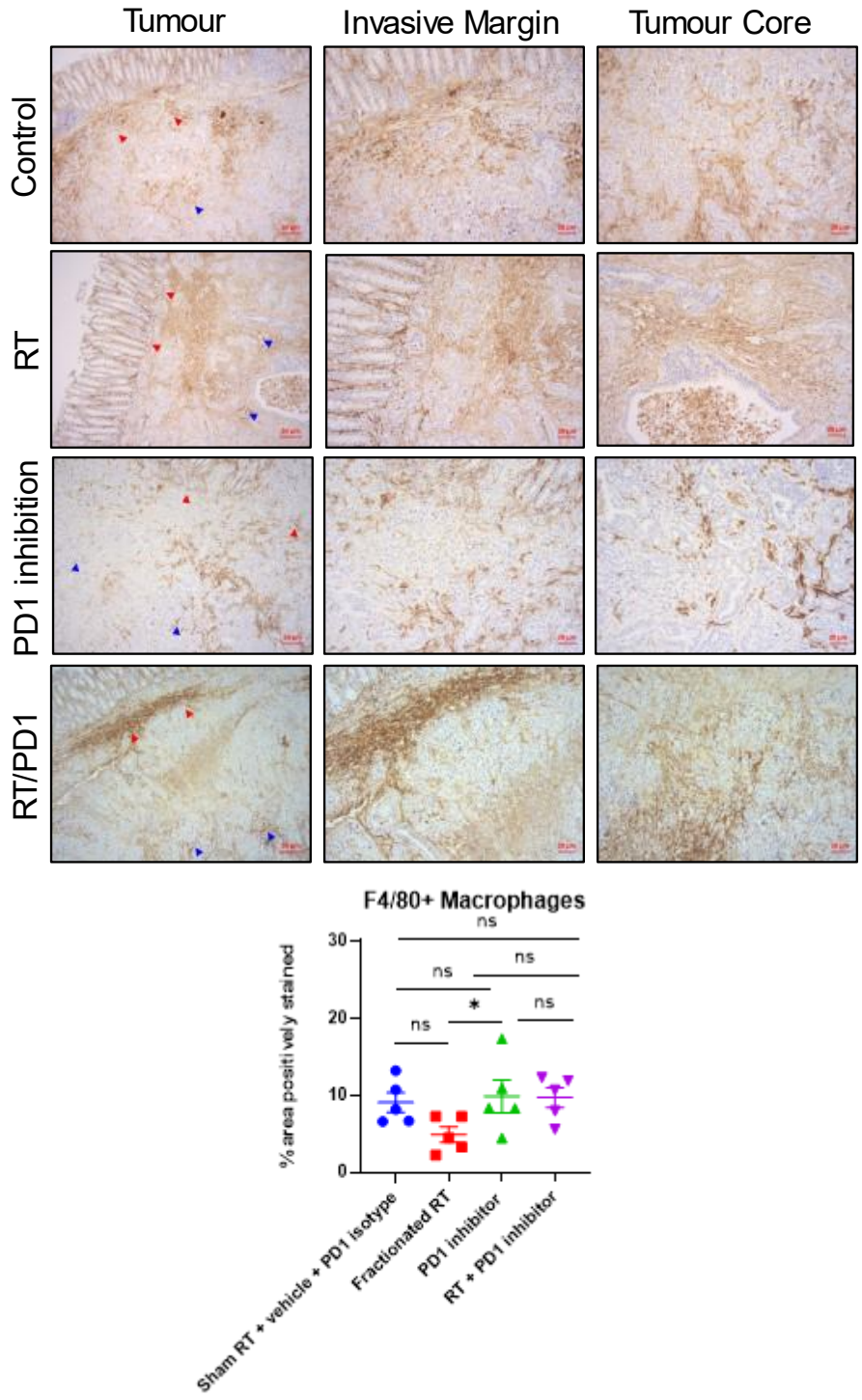

Figure 5.17: Increased F4/80+ Macrophage Density is not Demonstrated when PD-1 Inhibition is administered in Combination with Fractionated Radiotherapy

Top – Representative F4/80+ IHC images (x10) of AKPT rectal tumours from each treatment group (left column). Representative F4/80+ IHC images (x20) of invasive margin region from AKPT rectal tumours (middle column). Representative F4/80+ IHC images (x20) of tumour core region from AKPT rectal tumours (right column). Bottom - Bar graph showing quantification of F4/80+ Macrophages (% of area positively stained) for whole tumour area. Error bars show mean and SEM, with each data point plotted. Group sizes n=5 scored per group. Mann-Whitney U-test. ns denotes non-significance ($p \geq 0.05$). *denotes p-value <0.05. Red arrows depict positive cells at invasive margin. Blue arrows depict positive cells within the tumour core. Scale bars = 50μm and 20μm.

Neutrophil infiltration following fractionated radiotherapy and PD-1 inhibition through IHC staining for S100A8 was performed. A trend towards increased neutrophils following fractionated radiotherapy or fractionated radiotherapy plus PD-1 inhibition was observed when compared with the control group or PD-1 inhibition alone, although statistical significance was not reached (Figure 5.18, bottom panel). Across all treatment groups, neutrophils do not appear to cluster more densely at the tumour invasive margin (Figure 5.18, top and middle panels). In the tumours which have undergone fractionated radiotherapy, abundant neutrophils appear to be present in regions with absent tumour epithelium and cellular debris, suggesting that neutrophils may undergo trafficking into discrete tumour regions following radiotherapy with resulting phagocytosis of tumour epithelium (Figure 5.18, top and bottom panels).

Although no statistically significant difference in neutrophil density was observed following treatment, a trend towards increased neutrophil infiltration was noted following fractionated radiotherapy with or without PD-1 inhibition. These findings conflict with results in the literature, with Deng et al demonstrating in the TUBO breast tumour model that irradiation and anti-PD-L1 therapy led to a significant reduction in MDSCs in the tumour microenvironment (Deng et al, 2014). However, other studies suggest that radiotherapy induces neutrophil infiltration with a peak being observed at 24 hours post radiotherapy as demonstrated by Liu et al in a Lewis lung carcinoma tumour bearing immunocompetent model following 3 x 8Gy fractions (Liu et al, 2021). The heterogenous responses of neutrophils following radiotherapy-based treatment regimens likely reflects underlying differences in the tumour micro-environment across model systems, and highlights the importance of understanding the range of neutrophil phenotypes and subtypes which exist.

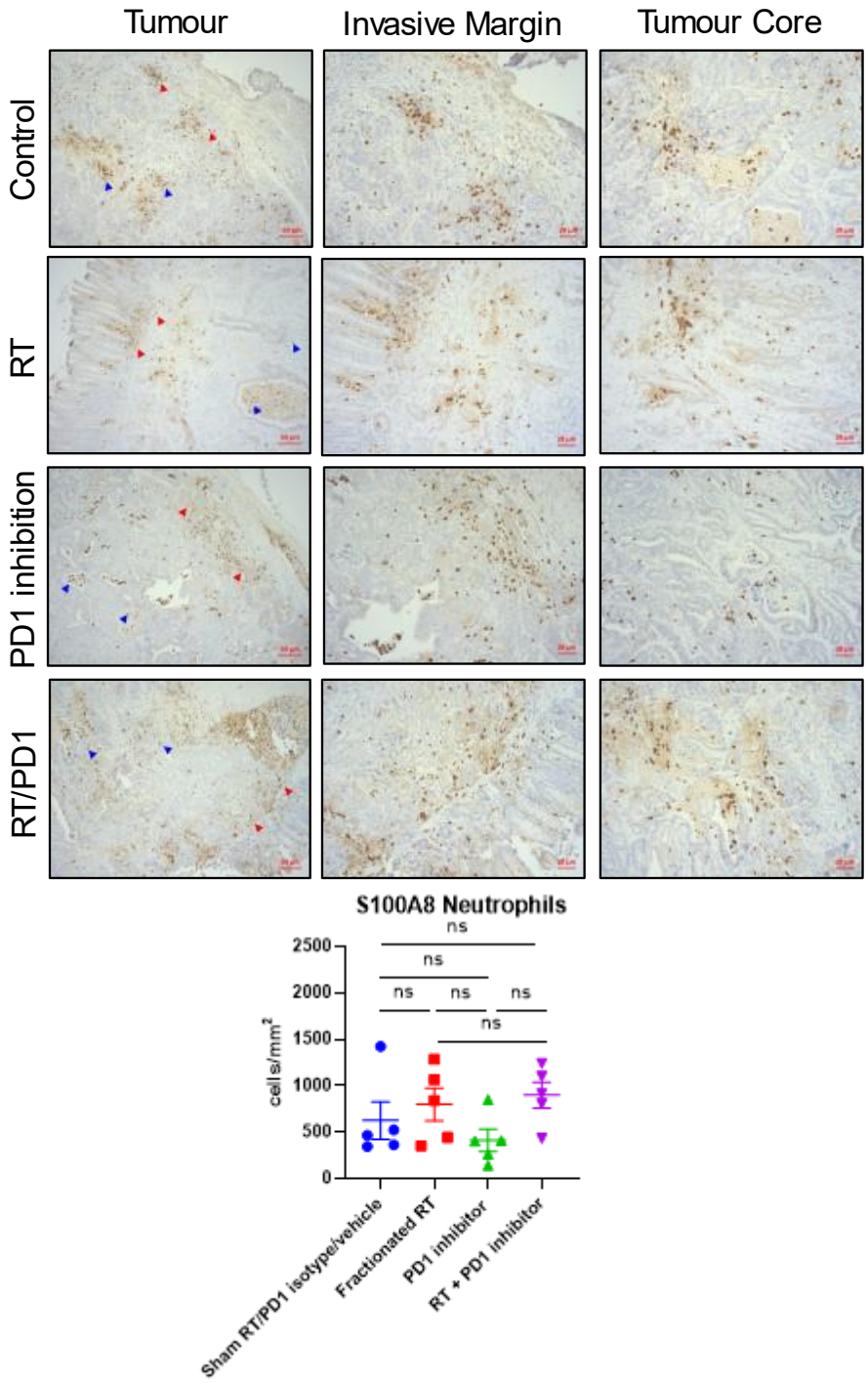

Figure 5.18: Changes in S100A8 Expressing Neutrophil Infiltration is not Demonstrated Following Treatment with Fractionated Radiotherapy and PD-1 Inhibition

Top – Representative S100A8 IHC images (x10) of AKPT rectal tumours from each treatment group (left column). Representative S100A8+ IHC images (x20) of invasive margin region from AKPT rectal tumours (middle column). Representative S100A8+ IHC images (x20) of tumour core region from AKPT rectal tumours (right column). Bottom - Bar graph showing quantification of S100A+ Neutrophils (cells/mm^2) for whole tumour area. Error bars show mean and SEM, with each data point plotted. Group sizes n=5 scored per group. Mann-Whitney U-test. ns denotes non-significance ($p \geq 0.05$). Red arrows depict positive cells at invasive margin. Blue arrows depict positive cells within the tumour core. Scale bars = 50μm and 20μm.

I next attempted to assess whether treatment with radiotherapy and/or PD-1 inhibition in this model had any effect on PD-L1 expression within tumour tissue. Previous studies in human rectal cancer tissue suggests that neo-adjuvant radiotherapy-based treatment regimens leads to an up-regulation of PD-L1 expression, with the suggestion that high tumour PD-L1 expression is associated with better response to immune checkpoint inhibition (Hecht et al, 2016; Boustani J et al, 2020). Tumour tissue from clinical endpoint underwent RNAscope to detect the presence of PD-L1 expression (Figure 5.19). No statistically significant changes in PD-L1 expression were observed between any treatment group when tumour sections were analysed. Two tumours analysed in the fractionated radiotherapy plus PD-1 inhibition group appear to demonstrate higher PD-L1 expression, suggesting a potential heterogeneity of response to this treatment combination.

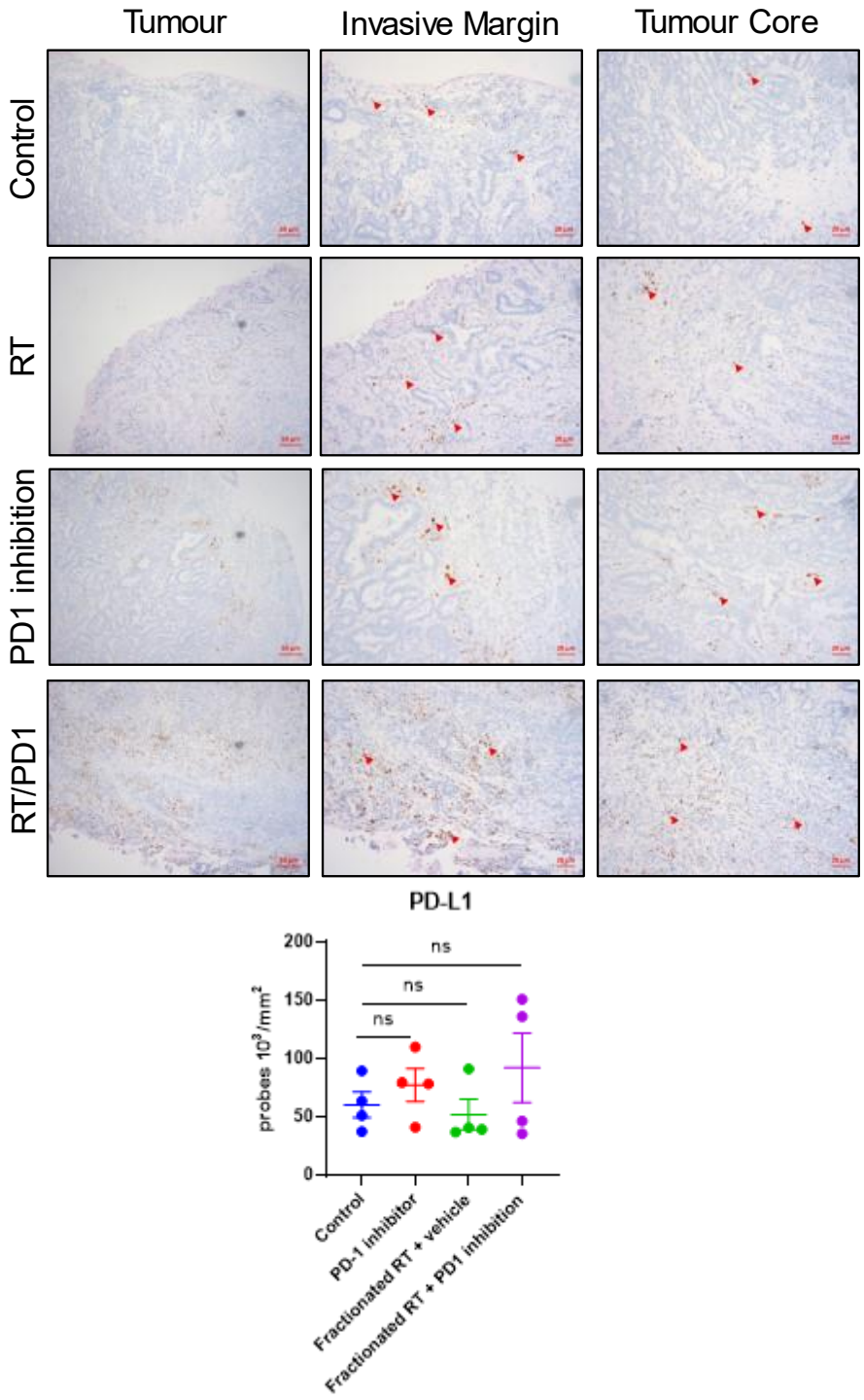

Figure 5.19: Changes in PD-L1 Expression are not Demonstrated Following Treatment with Fractionated Radiotherapy and PD-1 Inhibition

Top – Representative S100A8 IHC images (x10) of AKPT rectal tumours from each treatment group (left column). Representative S100A8+ IHC images (x20) of invasive margin region from AKPT rectal tumours (middle column). Representative S100A8+ IHC images (x20) of tumour core region from AKPT rectal tumours (right column). Bottom - Bar graph showing quantification of S100A+ Neutrophils (cells/mm2) for whole tumour area. Error bars show mean and SEM, with each data point plotted. Group sizes n=5 scored per group. Mann-Whitney U-test. ns denotes non-significance ($p \geq 0.05$). Red arrows depict positive cells at invasive margin. Blue arrows depict positive cells within the tumour core. Scale bars = 50μm and 20μm.

IHC and RNAscope failed to demonstrate any clear changes in the tumour immune microenvironment when analysed at clinical endpoint. Tumour tissue sampled from the tumour core at clinical endpoint in these treatment cohorts were also analysed using bulk RNA sequencing. The untreated control, fractionated radiotherapy alone, and fractionated radiotherapy plus PD-1 inhibition groups were compared to identify transcriptomic changes associated with treatment. Principal Component Analysis revealed inter-tumoral heterogeneity, with variation in gene expression demonstrated within each treatment group (Figure 5.20). However, within each treatment group a proportion of samples (n=2-3) appeared to cluster closely, suggesting that a proportion of tumours within each group responded similarly.

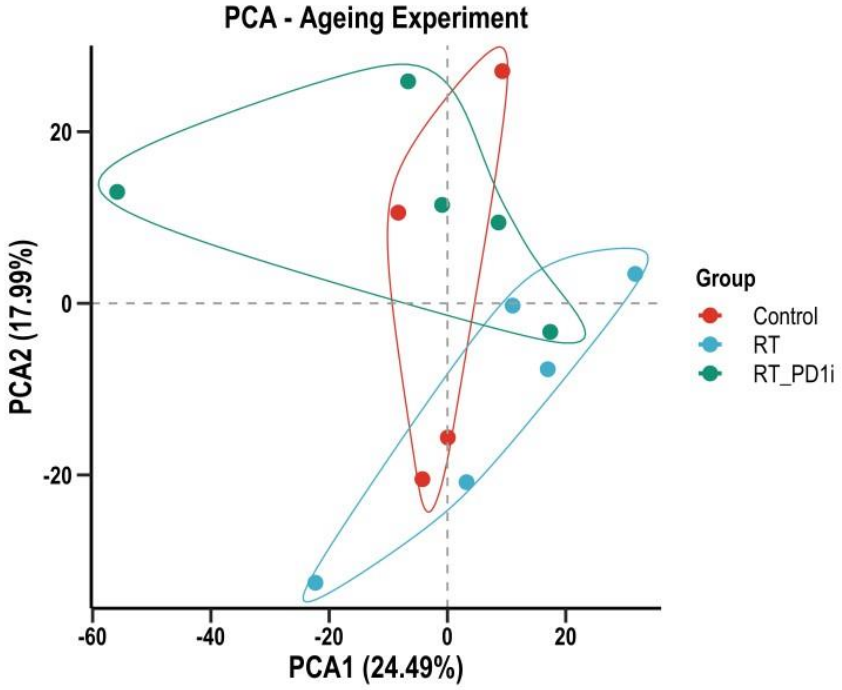

Figure 5.20: 2D Principal Component Analysis Reveals Inter-Tumoral Heterogeneity of Transcriptomic Change following Treatment

2D PCA generated from RNA sequencing data of AKPT rectal tumours (control, fractionated radiotherapy, fractionated radiotherapy plus PD-1 inhibition). Each data point plotted, with sample groups indicated by key. Dimension 1 plotted on x-axis, dimension 2 on y-axis. n=4-5 per group. Data analysis performed by Lily Hillson (Institute of Cancer Sciences, University of Glasgow).

Gene-set enrichment analysis was then performed to conduct pair-wise comparisons between control, fractionated radiotherapy, and fractionated radiotherapy plus PD-1 inhibition groups (Figure 5.21). The Molecular Signatures Database (MSigDB), a resource with thousands of annotated gene-sets was used

to identify altered expression of hallmark gene signatures associated with inflammation and infective processes. When fractionated radiotherapy was compared with control group samples, significant up-regulation in gene expression signatures for IFN-α, IFN-γ, IL-6 JAK-STAT3 signalling, inflammatory response and TNF-α signalling were observed. Interestingly, when fractionated radiotherapy alone was compared with fractionated radiotherapy plus PD-1 inhibition a further up-regulation in these gene expression signatures were observed.

IL-6/JAK/STAT3 signalling pathway activation is associated with promotion of tumour cell activation, invasiveness, and metastasis, with negative regulatory effects on effector T cells (Johnson et al, 2018). Similarly, activation of TNF-α signalling via NF-κß is associated with the upregulation of pro-inflammatory gene expression (Slattery et al, 2018). Although, potential activation of immunosuppressive pathways were identified following treatment with fractionated radiotherapy with or without PD-1 inhibition, the activation of IFN-γ signalling represents a potential driver of anti-tumour immunity. Tumour infiltrating CD8+ cells are known to produce IFN-γ with subsequent anti-tumour effects, and so the increase in IFN-γ signalling demonstrated following the addition of PD-1 inhibition to fractionated radiotherapy may explain the improved survival benefit seen in the AKPT model (Du et al, 2021).

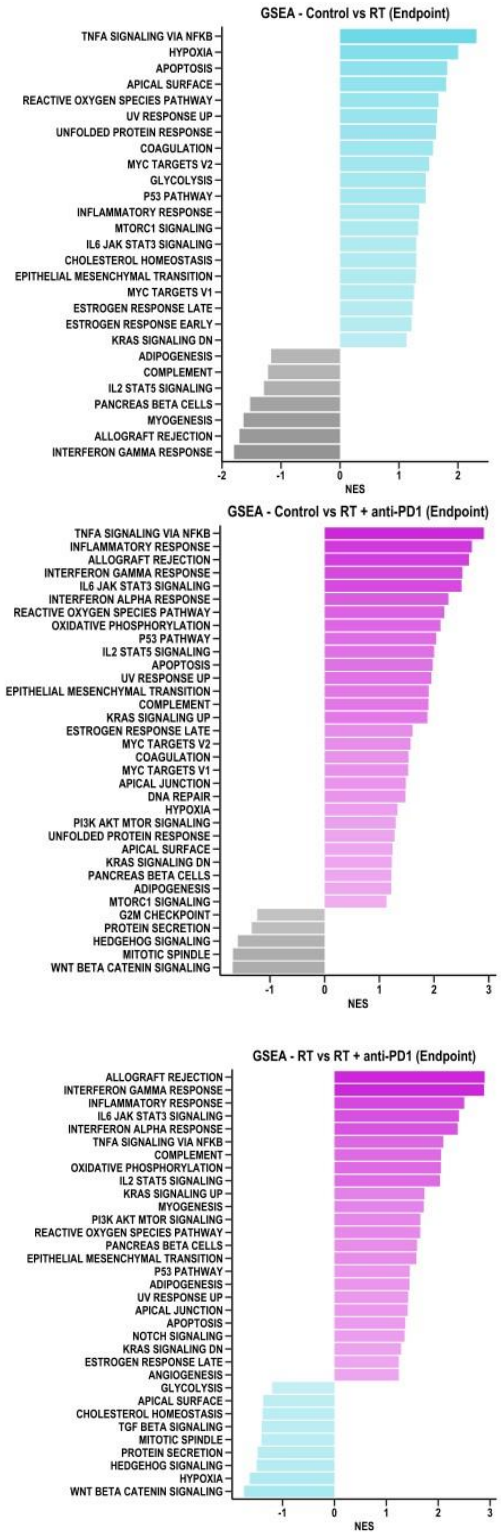

Figure 5.21: Gene Set Enrichment Analysis Reveals Up-Regulation of Hallmark Genesets associated with Inflammation and Immune Related Signalling Pathways

Gene Set Enrichment Analysis performed using MSigDB (Molecular Signatures Database) to identify positively enriched hallmark genesets. Top panel – Graph showing control versus fractionated radiotherapy alone. Middle panel – Graph showing control versus fractionated radiotherapy plus PD-1 inhibition. Bottom panel – Graph showing fractionated radiotherapy alone versus fractionated radiotherapy plus PD-1 inhibition. X-axis depicts enrichment score value. Y-axis depicts hallmark geneset. n=4-5 per group. Data analysis performed by Lily Hillson (Institute of Cancer Sciences, University of Glasgow).

Microenvironment Cell Population (MCP) counter analysis was then performed to identify significant up-regulation of genes associated with individual immune cell populations (Figure 5.22). Significant heterogeneity was observed between samples within each treatment group. However, up-regulation of both T-cells and CD8+ cells were noted in the majority of tumours within the fractionated radiotherapy plus PD-1 inhibition group (Figure 5.22). Interestingly, neutrophils, fibroblasts and monocytes were up-regulated in some of the tumours treated with fractionated radiotherapy plus PD-1 inhibition. Although heterogeneity was observed between tumours, gene expression data from tumour samples at clinical endpoint does reveal that some tumours undergo changes in the tumour immune microenvironment following treatment with fractionated radiotherapy and PD-1 inhibition.

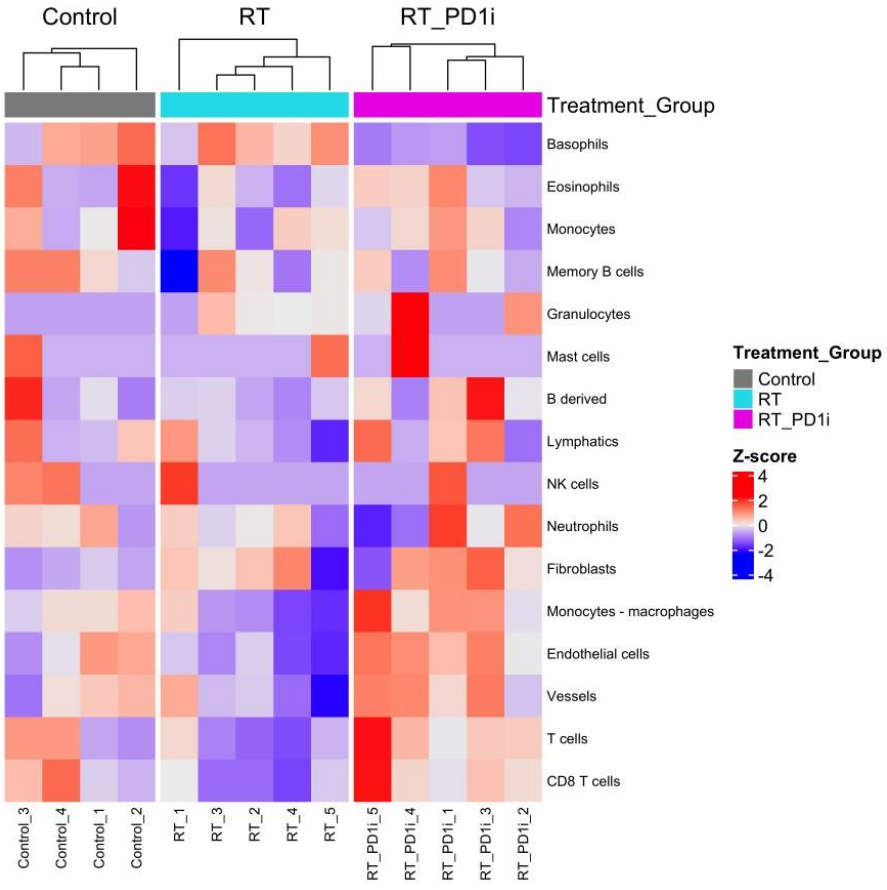

Figure 5.22: Microenvironment Cell Population Counter Reveals Increased T-Cell Populations Following Fractionated Radiotherapy and PD-1 Inhibition

Heatmap to demonstrate estimated immune and stromal cell populations within individual AKPT rectal tumour samples (control, fractionated radiotherapy, fractionated radiotherapy plus PD-1 inhibition). n=4-5, each sample represents one column of heatmap. Each row represents immune or stromal cell type as detailed on y-axis. Legend indicates z-score to indicate number of standard deviations above or below the mean. Murine MCP (mMCP) counter R package used to perform analysis. Data analysis performed by Lily Hillson (Institute of Cancer Sciences, University of Glasgow).

5.3. Discussion

5.3.1 The AKPT Model of LARC Fails to Respond to Fractionated Radiotherapy and TGF-β Inhibition

This thesis has demonstrated that the AKPT organoid transplant model is resistant to regimens of fractionated radiotherapy which mimic SCPRT given in the clinical setting (5 x 5Gy), with no improvement in survival or tumour volume seen following treatment. The responses to fractionated radiotherapy alone in recent published studies using CRC models are heterogenous; in the CT-26 bilateral flank transplant model a small proportion of tumours (2/7) completely responded to 3 x 4Gy, with the remainder showing a transient reduction in tumour volume (Dovedi et al, 2014). However, in the MC38 heterotopic CRC model, no tumour regression or survival benefit was observed following a 3 x 8Gy regimen (Rodriguez-Ruiz et al, 2019). Pre-clinical studies consistently demonstrate improved clinical effects when fractionated radiotherapy is administered in combination with immunotherapy agents, suggesting that combination therapy might be required to achieve treatment response in the AKPT model.

The AKPT model demonstrates abundant TGF-β expression and so I hypothesised that fractionated radiotherapy in combination with TGF-β inhibition would result in tumour regression and improved survival. It is known that irradiation can upregulate TGF-β signalling by releasing TGF-β from its latent isoform, with radiotherapy also inducing EMT which can increase the stemness of cancer cells and promote radio-resistance (Farhood et al, 2020; Zhong et al, 2019). By reducing the inhibitory effects of the pleiotropic TGF-β cytokine on CD4+ and CD8+ effector T-cell activation, I anticipated that reduced TGF-β signalling would enable fractionated radiotherapy to induce tumour antigen specific immune responses. In an ageing experiment, treatment with fractionated radiotherapy and TGF-β inhibition failed to improve survival or tumour burden (Figure 5.8), demonstrating resistance to this treatment combination. Furthermore, IHC analysis of apoptosis and proliferation markers at a 2-week time-point showed no effect on tumour cell survival following combination therapy (Figures 5.1, 5.3 and 5.4).

Previous clinical studies have suggested that TGF-β activated stroma plays a key role in treatment resistance, with lack of response to PD-1/PD-L1 blockade being associated with a fibroblast-specific TGF-β gene expression signature (Mariathasan et al, 2018). In metastatic urothelial cancers, Mariathasan et al showed that 'immune excluded' tumours, where T-cells are located within peri-tumoral desmoplastic stroma, were associated with lack of response to immune checkpoint blockade which also correlated with upregulated TGF-β associated gene expression in CAFs. Other pan-cancer analyses have linked upregulation of extra-cellular matrix genes and activated TGF-β signalling in fibroblasts with a lack of response to immunotherapy in immunologically active tumours, signifying a role for CAF associated TGF-β signalling in tumour immune evasion (Chakravarthy et al, 2018).

It remains unclear in the AKPT tumour model whether tumour cells, stromal cells or CAFs mediate TGF-β signalling in the model. TGF-β is known to be a potent mediator of EMT which is a crucial driver of tumour cell dissemination (Brunen et al, 2013). TGF-β plays an important role in the development of fibrosis, by up-regulating many extra cellular matrix (ECM) proteins and inducing the conversion of resident fibroblasts into myofibroblasts with the overall effect of distorting the ECM (Nakatsukasa et al, 1990; Hecker et al 2009; Caja et al, 2018). The ECM subsequently becomes stiffer following a desmoplastic stromal response, with CAFs being shown to secrete matrix proteins, with the resulting modification of the ECM conferring a more aggressive tumour phenotype (Deville and Cordes, 2019). CAF associated TGF-β signalling is known to enhance ECM remodelling, thus favouring tumour cell invasion through an increasingly permeable basement membrane (Broders-Bondon et al, 2018). In the experiments described, TGF-β inhibition was commenced at 10- or 17-days post tumour implantation in the AKPT model, with radiotherapy commenced 3-days later; it is likely that significant ECM modification has taken place by this time, with an aggressive tumour phenotype and extensive proliferation and dissemination of cancer stem cells already being displayed.

Furthermore, it has been proposed that radiotherapy impedes CAF mobility by increasing expression of integrins, which mediate attachments between cancer cells, stromal cells and the surrounding ECM (Barker et al, 2015). Pre-clinical studies have implicated β1-integrin expression with pronounced desmoplastic

reactions which facilitate CAF survival and promote radio-resistance (Park et al, 2008). Pre-clinical *in-vitro* studies have shown heterogeneity in tumour cell morphology and motility, with both single cell and collective movement of tumour cells possible; inhibition of TGF-ß signalling prevents cells from moving singly *in-vivo*, however doesn't prevent the collective motility of cells which remain capable of lymphatic invasion (Giampieri et al, 2009). It remains possible that initiation of TGF-ß inhibition was too late in these experiments, with formation of fibrotic networks which impede tissue penetration of immune cells already being established by the time therapy was commenced. Further work could be done in this model to characterise whether resistance to radiotherapy is driven by CAF associated TGF-ß; isolation of fibroblasts from tumour samples would enable *in-vitro* studies, whilst single cell sequencing would enable specific gene expression patterns from individual cell types to be analysed (Wu et al, 2021).

With an aggressive tumour phenotype already existing at 10-14 days post implantation, it is likely that pre-existing therapy resistance contributes to the lack of response in the AKPT model (Friedman, 2016). Resistance to TGF-ß inhibition may result from pre-existing or rapidly acquired mutations which alter the active domain of the target protein to prevent binding of the drug (Schmitt et al, 2016). Furthermore, the AKPT organoid suspensions utilised in experiments are likely to contain a high density of cancer stem cells (CSCs) with malignant potential; following multiple *in-vitro* passages, the most aggressive and treatment resistant sub-clones are likely to have been selected (Nowell, 1976). The organoids used in these experiments have survived extensive *in-vitro* selection, and likely represent selected cancer stem cell sub-clones with treatment resistant characteristics (Clevers, 2011). The AKPT organoid line has shown several key hallmarks of cancer, including the ability to evade apoptosis, limitless replicative potential and the ability for tissue invasion and metastasis (Hanahan and Weinberg, 2000).

TGF-ß signalling has been recognised as a significant determining factor contributing to the lack of response to PD-1/PD-L1 inhibition (Ganesh and Massagué, 2018). In a the MC38 heterotopic transplant model of CRC, combination therapy with a TGFBR1 kinase inhibitor (LY364947) and anti-PDL1 monoclonal antibody, demonstrated improved overall long-term survival when

compared with PD-1/PD-L1 axis blockade alone (Sow et al, 2019). The improved effects were found to correlate with increased influx of CD3+ lymphocytes following combination therapy, which was largely the result of increased CD8+ influx. These results were seen in the immunogenic MC38 cell line, and were not replicated in the less immunogenic KPC1 model of pancreatic cancer highlighting that a heterogeneity of response to therapy will be observed based upon the underlying TME.

It is possible that alternative pharmacological approaches to TGF-ß inhibition might prove more effective. The ALK5 inhibitor used in this thesis acts by binding to the TGF-ß receptor kinase domain to decrease tumour responsiveness to TGF-ß. TGF-ß ligand trapping agents may offer more clinical benefit, which act by mimicking the extra cellular ligand binding domain of TGFBRII, and competitively binding TGF-ß ligands with high affinity, reducing levels of latent TGF-ß ligand in the TME and reducing SMAD2/SMAD3 signalling (Kim et al, 2021). The bifunctional agent bintrafusp alfa consists of an IgG1 anti-PDL1 antibody fused to two TGFBRII molecules, thus targeting both the immunosuppressive PD-1/PD-L1 axis and 'trapping' TGF-ß in the TME (Lind et al, 2020). MC7824, a novel bifunctional checkpoint inhibitor which comprises of the extracellular domain of TGFBRII linked to human anti-PD-L1, was studied in the MC38 CRC subcutaneous flank injection model; decreased tumour burden, improved overall survival and 30% overall cure rate were seen following treatment which was dependent upon enhanced CD8+ and NK cell activity (Knudson et al, 2018). This study highlights the potential benefits of TGF-ß ligand trapping agents to decrease TGF-ß induced signalling in the TME, and furthermore suggests that dual targeting agents may be more efficacious in promoting CD8+ anti-tumour responses.

5.3.2 The AKPT Model of LARC Demonstrates Heterogenous Response to Fractionated Radiotherapy and PD-1 Inhibition

When the AKPT model of LARC was treated with fractionated radiotherapy and PD-1 inhibition, a significant improvement in survival was demonstrated when compared with radiotherapy alone and with the control group (Figure 5.10). Although extension of median survival was observed (60 days vs 33 days; radiotherapy plus PD1 versus control), tumour control was only achieved in a

minority of animals (1/7) with only one subject achieving complete tumour response, and no significant reduction in tumour volume at clinical endpoint being observed between groups (Figure 5.9). This differs from the results published by Dovedi et al, whereby tumour control was achieved in the majority receiving radiotherapy and PD-1 inhibition or radiotherapy and PD-L1 inhibition (80% and 66% respectively) (Dovedi et al, 2014). In a study of both the TUBO mammary and MC38 colon cancer subcutaneous flank transplant models, tumour control was achieved in all experimental subjects as demonstrated by serial tumour volume measurements following a 12Gy single fraction of radiotherapy and PD-1 inhibition (Deng et al, 2014). Contrasting results were observed in another study using the MC38 colon cancer subcutaneous flank injection model to study fractionated radiotherapy (3 x 8Gy) in combination with immunotherapy agents; despite demonstrating a significant delay in tumour growth with fractionated radiotherapy and anti-PD-1 therapy, complete cure and survival extension was not demonstrated (Rodriguez-Ruiz et al, 2016).

In the AKPT orthotopic model of LARC, it has been challenging to assess tumour response to therapy. In subcutaneous flank injection models previously published, researchers have been able to monitor tumour volume changes with regular calliper measurements. However, orthotopic rectal tumours are not easily amenable to frequent tumour measurements due to the invasiveness of repeated colonoscopy procedures. Furthermore, although regular calculation of tumour growth might be possible through measuring the luminal percentage occupied by tumour, this method is potentially inaccurate and would fail to account for extra-luminal tumour growth. As demonstrated in Chapter 4, CT based imaging would be inadequate to accurately measure rectal tumours; although we have demonstrated that MRI would enable accurate tumour measurements, this modality poses unrealistic time and cost burdens, as well as being potentially detrimental to animal welfare owing to prolonged anaesthesia. The treatment combination experiments described in this thesis have significant limitations, as analysis has all been performed at clinical endpoint so any transient reduction in tumour volume, or dynamic changes in the tumour immune microenvironment will not have been appreciated.

Although the orthotopic AKPT model of LARC recapitulates the heterogeneity of response seen in clinical practice, this finding is challenging to explain given the

control of potential experimental variables. Consistency was maintained as best as possible for experimental conditions including *in-vitro* culture technique, organoid passage number and transplantation technique. However, this experiment was performed in batches with subjects distributed evenly amongst groups, with experimental numbers per batch being limited by the time required to perform a single irradiation treatment (~15 mins per treatment). Consequently, tumour characteristics may vary between batches due to different organoid vials being used for individual batches, variation of experimental conditions during harvesting and injection sessions, and potential differences between commercially purchased cohorts of host C57Bl/6 recipients.

Other immune checkpoint inhibitors have been studied in pre-clinical models of CRC. In the CT-26 subcutaneous transplant model of CRC, a complete response to the immune checkpoint agent CTLA-4 followed by single fraction 20Gy irradiation was observed in 100% of experimental animals (Young et al, 2016). Young et al demonstrate more heterogeneous responses to therapy when CTLA-4 inhibition is administered concurrently or sequentially with radiotherapy (50%), highlighting the importance of scheduling when immune checkpoint inhibition is combined with radiotherapy. In a B16-F10 bilateral subcutaneous flank injection model of melanoma, only a 17% complete response to 20Gy single fraction radiotherapy and CTLA-4 blockade was observed, however, greater tumour volume reduction and survival extension occurred when CTLA-4 was administered either before or concurrently with radiotherapy (Twyman-Saint Victor et al, 2016).

The study by Twyman-Saint Victor et al goes on to demonstrate improved response rates of 80% when anti-PD-1 or anti-PD-L1 is administered in combination with radiotherapy and CTLA-4 inhibition, suggesting that dual checkpoint blockade may be required in treatment resistant tumours. Twyman-Saint Victor et al show that CTLA-4 inhibition inhibits Tregs and increases the CD8/Treg ratio, whilst radiotherapy enhances the T-cell receptor repertoire of intra-tumoral T-cells; however, resistance correlates with up-regulation of PD-L1 on tumour cells which is associated with T-cell exhaustion, and this can be overcome with the addition of anti-PD-1/PD-L1 therapy. Pre-clinical data appears to support the administration of immune checkpoint blockade either before or concurrently with radiotherapy, with Dovedi et al showing optimal

efficacy when PD-1 inhibition is commenced on day 1 or day 5 of the fractionated radiotherapy schedule (Dovedi et al, 2014). Dovedi et al show that PD-L1 is upregulated on tumour cells, peaking at 72 hours post irradiation, and declining significantly thereafter. This supports a rationale for administering ICB throughout treatment with radiotherapy, with pre-treatment not being required and sequential therapy likely to be ineffective. Furthermore, previous studies only describe cycles of PD-1 inhibition over a 2- or 3-week period suggesting that the indefinite therapy used in this study is not necessary.

The experiments discussed in this chapter demonstrate that it is feasible to test novel radiotherapy-immunotherapy treatment combinations in an orthotopic pre-clinical model of LARC. Future experiments in this model would help to inform upon the sequencing of PD-1/PD-L1 scheduling in relation to radiotherapy, with experimental arms to include PD-1 inhibition commencing concurrently with fractionated radiotherapy as well as sequentially, in addition to the 'pre-treatment' cohort used in this thesis. Limited courses of PD-1 inhibition should also be used in future experiments to refine treatment regimens and to rationalise costs of experiments.

IHC from tumour samples at clinical endpoint suggest that immune changes may occur following treatment with PD-1 inhibition with or without fractionated radiotherapy. A trend towards increasing tumour lymphocyte populations in the groups receiving PD-1 inhibition is demonstrated, with the observation of infiltration being denser within the tumour core following treatment. Although experiments are suggestive of immune changes, further work is required to confirm whether immunological changes are observed following fractionated radiotherapy and PD-1 inhibition in this model. Tumour sampling at short-term time-points following treatment to conduct flow cytometry, would provide informative data to assess immune changes observed following treatment with fractionated radiotherapy and PD-1 inhibition; more detailed phenotypic analysis should be performed, and would allow the quantification of markers of T-cell activation, cytotoxicity and exhaustion to better assess the immunological effects of fractionated radiotherapy and immune checkpoint inhibition.

Chapter 6 – Discussion

6.1. The Development of Clinically Relevant Models of Locally Advanced Rectal Cancer

Within this body of work, I addressed the need to develop pre-clinical models of LARC which more accurately recapitulate the anatomical, histological, and transcriptomic features of human disease. Previous chapters have discussed the various limitations of both heterotopic and immunocompromised models, and so this work focused on the development of models whereby tumours arise within the murine rectum in an immunocompetent host. In chapter 3, I described the development of genetically engineered mouse models (GEMMs) of rectal cancer expressing common driver mutations of CRC. The administration of submucosal tamoxifen in mice expressing the intestinal-specific Villin promotor fused to the oestrogen receptor, enabled the induction of site-specific rectal tumours arising from the mucosal layer. These models recapitulated both early and late stages of the adenoma-carcinoma sequence, with the inducible AKPT model (*VillinCre^{ER}: Apc$^{fl/+}$;Kras$^{G12D/+}$;Trp53$^{fl/fl}$;Tgfbr1$^{fl/fl}$*) demonstrating locally invasive adenocarcinoma invading through the muscularis propria.

Previous studies have described similar local induction methods, with a tamoxifen enema being administered to induce distal colon tumours in the 'iKAP' model described by Boutin and colleagues (*VillinCre^{ERT2};Tet-Kras$^{G12/D/+}$;Apc$^{fl/fl}$;Trp53$^{fl/fl}$*), whereby *Apc* and *Trp53* mutations were induced in combination with a doxycycline inducible *Kras^{G12D}* transgene (Boutin et al, 2017). The 'iKAP' model revealed T2-4 disease in 38% of animals (23/60) and 25% exhibited local or distant metastasis, with this model demonstrating a role for oncogenic *Kras* in driving disease progression and metastases when compared with the 'iAP' model (*VillinCre^{ERT2};Apc$^{fl/fl}$;Trp53$^{fl/fl}$*). The delivery of tamoxifen to the distal colon using a colonoscopy-guided needle technique was described prior to the work in this thesis; however, only early adenomas harbouring *Apc* mutation alone (*VillinCre^{ER};Apc$^{fl/fl}$*) were described (Roper et al, 2017).

In Chapter 3, I demonstrated the feasibility of applying a colonoscopy-guided needle injection technique to administer tamoxifen at the rectal location of GEMMs with multiple CRC driver mutations, and was able to recapitulate locally

invasive disease in the 'AKPT' genotype (*VillinCre^{ER};Apc$^{fl/+}$;Kras$^{G12D/+}$;p53$^{fl/fl}$;Tgfbr1$^{fl/fl}$*), with distant metastasis seen in a small proportion (14%). In this body of work, other histological stages of disease including high-grade dysplasia and early adenocarcinoma were not established; in Chapter 3, short survival was noted in both the 'AK' and 'AKP' genotypes when homozygous *Apc* deletion was induced, with only non-invasive low-grade dysplasia observed on histological analysis. Animals typically exhibited acute weight loss and/or intestinal obstruction at ~2 weeks post-induction, and it was evident that homozygous *Apc* deletion induced an acute phenotype with tumours unable to undergo histological progression.

In the 'iKAP' model described by Boutin et al, the majority of tumours (65%) exhibited T1 disease or higher with the induction of a heterozygous *Apc* (*Apc$^{\Delta 580/+}$*) allele. Previous studies also show that homozygous *Apc* knock-out results in embryonic lethality, with heterozygosity leading to a tumour predisposition phenotype (Kuraguchi et al, 2006). Acute homozygous loss of *Apc* in intestinal tissue is known to result in acute activation of Wnt signalling, with subsequent disruption of normal crypt differentiation, migration, proliferation, and apoptosis, with animals becoming unwell at only 5 days (Sansom et al, 2004). Previous studies coupled with the short survival demonstrated in the AK and AKP genotypes presented in Chapter 3, suggest that acute homozygous *Apc* deletion fails to model adenocarcinoma due to the acute phenotypic features demonstrated.

This thesis describes a novel autochthonous model of LARC, with heterozygous *Apc* deletion in the inducible AKPT model displaying histological features consistent with locally invasive T3 adenocarcinoma. Despite the numerous limitations previously discussed with the inducible autochthonous models described, a reproducible technique to generate GEMMs of LARC with mutational combinations of interest has been developed. This technique could be applied to future experiments using other mutational combinations of interest; for instance, it would be interesting to ascertain whether an 'AKP' model with heterozygous *Apc* deletion (*VillinCre^{ER};Apc$^{fl/+}$;Kras$^{G12D/+}$;p53$^{fl/fl}$*) might enable the development of high-grade dysplasia or an early adenocarcinoma model.

CRC displays significant genotypic and phenotypic heterogeneity, and it remains challenging to comprehensively model this complexity in the pre-clinical setting,

with most human tumours not conforming to a set of pre-defined mutational combinations. Furthermore, it is likely that variable efficiencies exist during cre-mediated recombination with the possibility of mosaic expression of mutated alleles existing within tumours (Wong et al, 2000). The R26R locus has been exploited in the past to introduce reporter genes such as LacZ, with reporter expression then analysed to assess recombination activity (Soriano, 1999). If the autochthonous models described in this thesis were to be used further in treatment studies, then lineage tracing studies should be performed to assess the reliability and efficiency of the recombination of each allele being induced.

A key objective of this thesis was to develop a pre-clinical model of LARC which was reproducible, time-effective, and suitable for the generation of sufficient experimental animals to conduct adequately powered treatment studies. The development of the 'AKPT' organoid transplant model of LARC described in Chapter 3, represents a highly efficient model with numerous advantageous features; a 95% engraftment rate was achieved, tumourigenesis typically occurred at 1-week post transplantation, immunocompetence was maintained, and tumours recapitulated locally invasive disease with distant metastasis. The workflow to expand and prepare organoids, undertake colonoscopy-guided needle injection, then subsequently perform both health monitoring and tumour monitoring by colonoscopy is highly reproducible and can be feasibly applied to experimental batches of 40 animals.

The transplantation of 'AKP' murine colon derived organoids in C57Bl/6 mice to establish locally invasive tumours was previously described, however only small numbers (n=6) were generated, with tumours failing to reproduce the glandular architecture of human tumours (Roper et al, 2017). The work presented in this thesis developed existing methodology further, and demonstrated the feasibility of applying this technique in high numbers of experimental animals to recapitulate tumours displaying locally invasive disease and a desmoplastic stromal reaction, features consistent with treatment resistant and poor prognosis disease subtypes. The application of colonoscopy guided needle injection of organoids to the rectal location and the development of the orthotopic 'AKPT' model of LARC, represents a significant contribution in the field of pre-clinical modelling of rectal cancer. The high engraftment rate and time efficiency of generating experimental animals has not been replicated in

other immunocompetent orthotopic models of rectal cancer described in the literature, and is a technique which is accessible and feasible to learn by other research groups.

Several studies utilising colonoscopy-guided submucosal injection techniques have required immunodeficient NSG (NOD scid gamma) mice to achieve the successful engraftment of human derived cancer cell lines or genetically-modified murine organoids respectively, and it is of critical importance that pre-clinical studies are conducted in hosts with a functionally intact immune system (Bettenworth et al, 2016; Lannagan et al, 2019). Studies previously discussed which achieved successful engraftment in immunocompetent C57Bl/6 mice following colonoscopy-guided transplantation of the MC38 murine colon cancer cell line have several drawbacks (Zigmond et al, 2011). Commercially available murine tumour-derived cells lines have typically been used for over 40 years in pre-clinical research, demonstrate high tumour mutational burdens, and have undergone extensive in-vitro selection (Corbett et al, 1975). Recent longitudinal immune characterisation of the commonly used syngeneic models CT-26, MC38 and 4T1, highlight that pre-clinical studies which have published promising results for immune checkpoint blockade, have often been conducted in models known to have strong cytolytic T-cell responses following tumour implantation and thus represent models with susceptibility to immunotherapy (Taylor et al, 2019). Furthermore, immortalised cell lines are prone to inconsistency across studies with distinct sub-lines showing that different immunogenic, transcriptomic and genomic features can develop over time (Schrörs et al, 2023). Commonly used murine tumour cell lines fail to represent the mutational burden of human CRC; the CT-26 model does not have mutations in *Apc* or *Trp53*, whilst the MC38 model does not have mutation in *Apc* or *Kras* (Zhong et al, 2020). The AKPT organoid transplant model described in this thesis, successfully overcomes several limitations of previously described models, as immunocompetence is maintained and tumours recapitulating the commonest mutations observed in CRC.

In Chapter 3, I then describe the characterisation of the AKPT organoid transplant model, with both dense lymphoid and myeloid immune infiltration being demonstrated. Conducting a longitudinal immune characterisation would have been interesting to further characterise the AKPT immunocompetent

transplant model, as tumours characterised at clinical endpoint are likely to represent an immunosuppressive phenotype with any anti-tumour immune responses likely to have been suppressed. Characterisation of the tumour immune microenvironment at early time-points following tumour implantation might reveal a different immune contexture. In a study by Taylor et al, flow cytometry revealed that the CT-26 colon cancer model underwent early expansion of cytolytic T-cells (granzyme B, PD-1 expressing CD8+ T-cells) at day-3 and -7 post tumour implantation, with more immunosuppressive features becoming apparent at day-14 with increased myeloid cells and M2 tumour promoting macrophages (Taylor et al, 2019).

As previously discussed, a recent advance in pre-clinical modelling of rectal cancer was described in the literature by Nicolas et al, with orthotopic transplantation of 'APTKA' organoids (*Apc, Trp53, Kras^{G12D}, Tgfbr1* and *myristoylated AKT*) successfully modelling locally invasive distal colonic tumours (Nicolas et al, 2022). However, a significant advantage of the AKPT model described in this thesis, is the avoidance of colitis induction; it is known that chronic inflammation alters the immune system, with elevated lymphocytes, plasma cells and macrophages infiltrating at the site of injury, as well as increased pro-inflammatory components such as NF-κB, JAK/STAT3 signalling, TNF-α and IL-6 (Snider et al, 2016).

A significant limitation of the colonoscopy-guided needle injection model described in this thesis, is the establishment of tumours within the submucosal layer, resulting in tumours which do not fully recapitulate the typical histological progression seen in the adenoma-carcinoma sequence. Furthermore, the 'AKPT' organoid line has undergone *in-vitro* selection whereby only malignant tumour clones withstanding multiple passages have survived, therefore tumours are representative of aggressive cancers exhibiting a pronounced desmoplastic reaction. A recent model of LARC which avoids both colitis induction and tumour initiation in the submucosal layer, describes a 'mucosal brush' technique, whereby 'AKP' (*Apc$^{-/-}$, Kras$^{G12D/+}$, Tp53$^{-/-}$*) organoids can be instilled intra-luminally following disruption of the rectal mucosa with a small-calibre brush (Kim et al, 2022). Although this method limits the systemic inflammatory response, considerable concerns exist with the reproducibility of this model; 17%

of animals died following intestinal perforation using this technique, and among the surviving animals only a 58% engraftment rate was achieved.

Chapter 3 previously discussed the transcriptomic characterisation of the AKPT organoid transplant model, and the challenges associated with aligning pre-clinical models to a particular CMS of human disease. Bulk RNA sequencing is susceptible to regional differences and intra-tumoural heterogeneity, despite efforts to consistently sample tissue from within the tumour core. To better characterise gene expression profiles and to align the AKPT model more accurately to a molecular subtype of human disease, bulk RNA sequencing would need to be undertaken on a significantly larger sample size with consideration made for the time at which tumours are sampled post implantation.

Further work should endeavour to address the development of a suite of organoid transplant models which recapitulate molecular subtypes of human disease reliably and comprehensively. Previous studies have demonstrated the feasibility and accuracy of aligning CRC cell line and patient derived xenograft models with the CMS classification system; 43 CRC models were subtyped based on publicly available expression datasets, with cell lines representing all CMS subtypes in similar distribution to human disease, and 66% concordance for alignment observed when multiple classifiers were applied (Linnekamp et al, 2018). *In-vitro* testing of characterised cell lines demonstrated a sensitivity to 5-FU and oxaliplatin in CMS2 aligned models, with chemo-resistance demonstrated in CMS4 models. This study demonstrated the potential application of CMS aligned murine models to identify patterns of response according to molecular subtype, to potentially aid the development of novel treatment strategies and precision medicine-based approaches in CRC. *In-vitro* drug screening of organoid/cell lines which have undergone accurate molecular characterisation, represents a potential strategy to identify treatment targets which can be developed further in the in-vivo setting.

However, limitations exist in the stratification of cell-line and patient-derived xenograft models to molecular subtypes of disease, as the tumour microenvironment is known to make a significant contribution to gene expression profiles in bulk tumour tissue (Isella et al, 2015). The development of adapted CMS classifiers can overcome this drawback, with Sveen and colleagues describing the development of an optimized classifier enriching for cancer-cell

intrinsic gene expression signals, to align a panel of 48 cell-lines and 32 patient-derived xenograft models to CMS groups (Sveen et al, 2018). Sveen et al were able to demonstrate sensitivity to 5-FU and HSP-90 inhibition (Heat Shock Protein) in CMS4 aligned models, highlighting a potential treatment combination which might overcome chemoresistance in this phenotype.

The complexity of accurately aligning whole tumours to broad molecular subtypes has been appreciated in previous studies, with distinct differences in gene expression profiles within the same tumour being identified dependent upon sample location, with stromal derived genes having the potential to preferentially stratify tumours into the CMS4 subtype (Dunne et al, 2016). Intra-tumoral heterogeneity of gene expression profiling suggests that CMS stratification through bulk RNA sequencing in both clinical and pre-clinical samples may not be representative of the whole tumour, and that accurate profiling must account for tissue morphology and sample origin. Data from murine derived tissue must also be analysed with caution, as computational methods must ensure that the divergence between murine and human orthologs is accounted for (Petitprez et al, 2020).

6.2. Improving Irradiation of Pre-Clinical Models of Locally Advanced Rectal Cancer

In Chapter 4, I described the development and validation of a precise image-guided radiotherapy protocol to administer clinically relevant fractions to murine rectal tumours. A single radiotherapy fraction can be administered in approximately 15 minutes, including the induction of anaesthesia, CT imaging, treatment planning and dose administration, ensuring the feasibility of treating sufficiently powered experimental cohorts. Accurate targeting of tumours was confirmed by demonstrating increased expression of the DNA damage marker γ-H2AX at 3-hours post irradiation when compared with untreated tumour tissue, successfully validating the methodology used throughout this thesis.

The experimental protocol described in Chapter 4 has significant benefits over previous pre-clinical studies demonstrating clinical efficacy with combining radiotherapy with immune-checkpoint blockade (Demaria et al, 2005; Dewan et

al, 2009; Deng et al, 2014; Dovedi et al, 2017). These studies used whole-body irradiation devices, resulting in the delivery of much broader fields of irradiation with a greater potential for adverse off-target effects. More clinically precise delivery of radiotherapy has recently been adopted in pre-clinical CRC research, with various recent studies investigating fractionated radiotherapy in combination with immunotherapy agents with radiotherapy delivered using the Small Animal Radiation Research Platform (SARRP), or linear accelerator devices with small diameter (10-15mm) collimators (Vanpouille-Box et al, 2015; Grapin et al, 2019; Rodriguez-Ruiz et al, 2019).

Early irradiation studies in pre-clinical models of CRC using the SARRP did not encounter difficulties with tumour targeting and treatment planning, owing to the subcutaneous implantation of tumours. Technical challenges have therefore emerged with the use of orthotopic models of rectal cancer, which are not externally visible and clinically obvious on non-contrast imaging modalities. Although rectal tumours were not reliably detected upon plain CT imaging, I was able to adopt anatomical landmarks to successfully target rectal tumours; organoid fragments were consistently injected within 1cm of the anal verge, and so this landmark coupled with the identification of luminal gas on CT imaging, enabled the placement of a dose isocentre at the known tumour location. As discussed in Chapter 4, experiments conducted to improve tumour targeting proved either ineffective (intra-peritoneal contrast administration) or conferred unacceptable time and cost constraints (MRI scanning). In future experiments, rectal contrast administration may prove both time-efficient and effective in delineating rectal tumours more confidently on the CT imaging system in-built within the SARRP, however, this technique was not included in the Home Office project licence under which the research in this thesis was conducted.

In the recent study by Nicolas et al, rectal tumours were targeted with a radio-opaque probe inserted intra-luminally to the distal aspect of the rectal tumour based upon endoscopically determined measurements (Nicolas et al, 2022). It is unclear whether this technique would offer improved accuracy of tumour targeting when compared with the methods described in this thesis; both endoscopic measurements and placement of the rectal probe are likely susceptible to variability and inaccuracy, particularly in the context of small sub-centimetre tumours. Although Nicolas et al were able to apply a smaller 5mm

diameter collimator, the AKPT tumours described in this thesis predominantly exceed 5mm in diameter and therefore use of a 10mm collimator ensures delivery of radiation to the whole tumour is optimised.

In the orthotopic LARC model described by Kim et al, an irradiation technique was also described and highlighted the cost implications to researchers in acquiring sophisticated small animal irradiation devices such as the SARRP (Kim et al, 2022). Kim et al describe the use of a customised cerrobend apparatus, enabling the use of cheaper and more accessible whole-body irradiation devices to be used in pre-clinical experiments, with the additional advantage that 5 animals can be treated in each device. Despite the cost and accessibility advantages described, this technique exposes the whole murine pelvis and lower limbs to irradiation, with greater potential for off target treatment effects. However, the technique described by Kim et al offers significant advantages in terms of cost and reproducibility, and may on balance offer sufficiently accurate radiotherapy delivery upon which to translate experimental findings to the clinical setting.

Accurate longitudinal tumour monitoring was not demonstrated in the orthotopic AKPT transplant model of LARC. Colonoscopy imaging was utilised to confirm tumorigenesis and successful engraftment, and enabled the detection of suspected tumour regression. Serial colonoscopic tumour measurement (as a % of lumen occupied by tumour) could be applied to monitor tumour growth/regression in future experiments, however this method is likely to be prone to inaccuracy owing to the variability in luminal distension which occurs upon insufflation during colonoscopy; furthermore, luminal measurements would fail to account for extra-luminal tumour growth. Bioluminescence is a potential technique which could be applied to monitor tumour response to treatment and to detect distant metastasis. For instance, the light-emitting properties of luciferase mediated oxidation of luciferin, enables the detection of luciferase transduced cancer lines *in-vivo* (Contag et al, 2000). The labelling of cells of interest with fluorescent proteins such as green fluorescent protein (GFP) or red fluorescent protein (RFP), also enables the efficacy of anti-tumour agents to be determined *in-vivo* (Hoffman, 2015). Although bioluminescence techniques hold potential to study specific cell interactions, in the context of monitoring tumour growth such imaging is qualitative and attempts to quantify bioluminescence

signal are confounded by numerous factors including anaesthetic technique, luciferin exposure, and depth of the tissue of interest, and would likely not be amenable to the accurate monitoring of tumour growth (Sinha et al, 2018).

This thesis has described the development of methodology to deliver clinically precise radiotherapy fractions to orthotopic models of LARC, with many previous studies being undertaken in heterotopic models. The adoption of orthotopic models in radiotherapy-based treatment studies in LARC is in its relative infancy, and this thesis describes the successful delivery of RT to orthotopic LARC models through increased γH2AX expression. The use of non-contrast CT imaging with anatomical landmarks is reproducible and time-efficient; delivery of a single RT fraction is feasible within ~15 minutes, and could be applied by other research groups to enable high throughput treatment studies.

Experiments described in this thesis were dependent upon gross clinical parameters to detect treatment efficacy, including survival, tumour volume at clinical endpoint, and histological and immunological analyses. Serial tumour measurements in future treatment studies utilising orthotopic models of LARC are unlikely to be feasible, and treatment response should be assessed through survival data, and the histological, transcriptomic and immunological analysis of tumours at pre-determined time-points.

6.3. Characterising the Response of the Orthotopic AKPT Transplant Model of LARC to Radiotherapy

Initial irradiation experiments failed to demonstrate significant response in orthotopic AKPT tumours following a single 4Gy fraction of radiotherapy. A single fraction of 4Gy was administered in these experiments to maintain consistency with fractions which are used clinically in LARC (1.8Gy or 5Gy), and data presented in Chapter 4 suggests that a single 4Gy fraction was insufficient to induce tumour regression or an immunological response. Early pre-clinical studies highlighting the immune priming role of radiotherapy, demonstrated significant changes in CD8+ T cell tumour immune infiltration when large stereotactic doses were delivered (Apetoh et al, 2007; Lee et al, 2009). When comparing a stereotactic dose (15Gy) with fractionated radiotherapy (5 x 3Gy) in

the B16 melanoma transplant model, a greater slowing of tumour growth was demonstrated following 15Gy; increased antigen presenting capability and IFN-γ secreting T-cells within tumour draining lymph nodes, with subsequent increases in CD45+ leucocyte infiltration to the tumour site were observed (Lugade et al, 2005). Future experiments in the AKPT model using a much larger stereotactic dose of radiotherapy, such as 15Gy, might demonstrate a different immunological response to radiotherapy and further highlight that clinical response to radiotherapy is dependent upon dosage and fractionation.

It is crucial that future time-point analyses of tumour immune infiltration are not limited to simple IHC analysis, which is only representative of one tumour section and offers limited information regarding immune cell phenotypes and spatial interactions. Infiltration of effector T-cells could have been analysed, to determine significant changes in activated T-cells with anti-tumour efficacy following irradiation; enzyme linked immunosorbent spot (ELISpot) assays could be utilised to determine the quantity of IFN-γ secreting CD8+ T-cells. A time-point experiment utilising flow cytometry in larger cohort numbers to compare a clinically relevant 5Gy fraction of radiotherapy with a larger stereotactic dose would be highly informative to characterise the immunological response to different radiotherapy doses in the AKPT orthotopic rectal cancer model.

In Chapter 4, 3 x 5Gy fractionated radiotherapy did not result in extended survival or tumour volume reduction when compared with a sham radiotherapy treated control group. Furthermore, IHC and multiplex IHC performed on tumour tissue sampled at clinical endpoint failed to demonstrate any significant changes in immune cell infiltrates following fractionated radiotherapy. In keeping with previous studies which suggest that significant immune cell infiltration occurs at 7-days post radiotherapy, analysis of immune infiltrate in tumour samples at the 7-day time-point post commencement of fractionated radiotherapy would have been beneficial (Filatenkov et al, 2015). It is possible that repair of sub-lethal DNA damage occurs between fractions when low radiation doses are administered, and that relatively radio-sensitive tumour infiltrating T-cells are killed due to repeated doses.

RNA sequencing data presented in Chapter 4 suggests that transcriptomic changes occur at short time-points following single fraction radiotherapy, with up-regulation of several hallmark gene-sets being observed at 3- and 7-day time-

points (IFN-γ, IFN-α, IL-6/JAK/STAT3 signalling, inflammation, and TNFα via NF-κB), with these changes in gene expression not seen at 14-days or tumours sampled at clinical endpoint following fractionated radiotherapy. Similarly, a transient response to radiotherapy was seen in the subcutaneous AKPT transplant model, with a reduction in tumour volume detected at 10-14 days post fractionated radiotherapy, with rebound growth subsequently being observed. It remains unclear whether the colonic/rectal or subcutaneous region represents the more immunosuppressive tumour microenvironment, however, orthotopic models better recapitulate the human condition and must be used if translation of pre-clinical studies is to be achieved. The characterisation of an orthotopic model of LARC which demonstrates resistance to radiotherapy alone represents a significant tool in pre-clinical rectal cancer research, as it provides an ideal model in which immune modulating therapies can be tested in combination with radiotherapy.

Interestingly, similar models described in the literature do not demonstrate similar radio-resistance; when Nicolas et al treated APTK (*Apc, Trp53, Tgfbr2 and* $Kras^{G12D}$ mutant) organoid derived rectal tumours with 5 x 2Gy radiotherapy, a massive reduction in tumour size was demonstrated at 21-days post initiation of therapy (Nicolas et al, 2022). When additional expression of myristoylated AKT was added to 'APTK' tumours, rectal tumours then demonstrated complete resistance to fractionated radiotherapy, with increased invasion and higher frequency of liver metastases. In the AKP ($Apc^{fl/fl}$;*LSL-*$Kras^{G12D/+}$:$Tp53^{-/-}$) organoid transplant model described by Kim et al following mucosal brush disruption, single dose 15Gy pelvic irradiation resulted in delayed endoluminal tumour growth (% of luminal involvement) and improved overall survival (Kim et al, 2022).

Ideally, models of LARC should exhibit a limited response to fractionated radiotherapy alone, to enable the study of underlying mechanisms of radiotherapy resistance to be studied and to allow addition of immunotherapy agents to augment responses to radiotherapy. Further work is required in the AKPT transplant model of LARC to fully understand the mechanism of resistance to radiotherapy. Importantly, better utilisation of patient tumour samples following neo-adjuvant radiotherapy-based treatment strategies are essential if

the mechanisms underlying the heterogenous responses to therapy are to be fully understood.

6.4. Assessing TGF-β Inhibition in Combination with Fractionated Radiotherapy in the Orthotopic AKPT Transplant Model of LARC

TGF-β is demonstrated to be abundantly expressed in AKPT tumours, and its known immunosuppressive effects and induction of cancer associated fibroblasts (CAFs) have been previously discussed (Vanpouille-Box et al, 2015; Farhood et al, 2020; Frangogiannis, 2020). The abundant expression of TGF-β demonstrated within AKPT tumours may confer a highly fibrogenic phenotype impeding the infiltration of immune cells, and further work to characterise the presence of fibrosis within tissues (e.g. detection of collagen markers, α-SMA and fibronectin), and to assess markers of CAFs such as FAP (Fibroblast Activation Protein), PDGFR (Platelet Derived Growth Factor Receptor) and vimentin is required (Chen and Song, 2019).

Chapter 5 describes a profound treatment resistance in the AKPT model when fractionated radiotherapy is administered in combination with ALK5 inhibition. Further work in the AKPT model would be required to better understand the contribution of TGF-β signalling to the profound treatment resistance observed. Although the high abundance of pSMAD3 expression observed in AKPT tumours is suggestive of highly activated TGF-β signalling, it remains unclear which cells are exhibiting over-expression and/or defective signalling of this pathway. It is known that numerous cells including fibroblasts, T-cells, platelets and macrophages are potential sources of TGF-β with a multitude of possible resulting effects and interactions with other components of the TME (Chung et al, 2018). Although the immunosuppressive effects of TGF-β on lymphocytes are well described in the literature, including the down-regulation of T-helper cells, and enhancing of T reg function, it remains unclear how TGF-β is exerting its effects in the AKPT model (Gorelik et al, 2002). One previously described method to identify the predominant sources of TGF-β production within tumours is to analyse relative mRNA expression of cell sorted populations, demonstrated by Tauriello et al in identifying CAFs as the major source of TGF-β in both murine and human tumour samples (Tauriello et al, 2018).

Contrasting results with other pre-clinical studies described in the literature are demonstrated when fractionated radiotherapy is administered in combination with TGF-ß inhibition. Gunderson et al show that pre-treatment with galunisertib followed by 15 x 2Gy fractionated radiotherapy and 5-FU chemotherapy, resulted in slowed tumour growth and improved survival in a CT-26 subcutaneous transplant model (Gunderson et al, 2020). In this study, numerous differences exist with the experiments in this thesis, including use of the heterotopic CT-26 injection model, a more prolonged course of radiotherapy, and the addition of chemotherapy to the treatment regimen. Another CT-26 subcutaneous injection model treated with SM16, a small molecule TGFBR1 kinase inhibitor, demonstrated favourable immune changes with flow cytometry showing increased CD3+ T-cells, increased early activated CD8+ T-cells, and reduced T regs at day 7 post initiation of TGF-ß inhibition (Young et al, 2014). Young et al showed reduced tumour volume and improved survival when TGF-ß inhibition was administered in combination with a single 20Gy dose of radiotherapy. Again, significant differences in the tumour model used and the radiotherapy regimen administered are noted between this study and the experiments in this thesis, however, pre-clinical evidence in the literature consistently demonstrates treatment responses to TGF-ß inhibition with or without radiotherapy.

6.5. Assessing PD-1 Inhibition in Combination with Fractionated Radiotherapy in the Orthotopic AKPT Transplant Model of LARC

Previous pre-clinical evidence in heterotopic models of CRC demonstrate clinical efficacy when fractionated radiotherapy is administered in combination with PD-1 inhibition (Deng et al, 2014; Dovedi et al, 2014). Fractionated radiotherapy and PD-1 inhibition also led to significantly improved survival in the orthotopic AKPT model of LARC. However, heterogeneity of response was demonstrated with one instance of complete tumour regression noted and several tumours failing to demonstrate tumour volume reduction at clinical endpoint. Although such heterogeneity of response may reflect the scenario seen following neo-adjuvant radiotherapy-based treatment regimens in LARC, it is challenging to explain this phenomenon in the context of consistent experimental conditions. However, heterogeneity of response is observed in other published pre-clinical

experiments, and potential variability exists between experimental subjects at the tumour implantation stage, administration of radiotherapy fractions, and in the immune composition of host C57Bl/6 animals.

Further work is required in this model to understand the underlying immunological mechanism of response to fractionated radiotherapy and PD-1 inhibition. IHC analysis of tumours sampled at clinical endpoint revealed a significant increase in CD4+ T-helper cells following treatment with fractionated radiotherapy and PD-1 inhibition when compared with the control group, with non-significant trends towards increased CD3+ and CD8+ T-cells being observed within the tumour core. Although these findings might suggest a role for PD-1 inhibition in the activation of effector T-cells in this model, more detailed characterisation would be required to confirm such observations (Sharpe et al, 2018).

Ideally, further treatment experiments should be performed to confirm the extension in survival seen in the AKPT model following fractionated radiotherapy and PD-1 inhibition. In the CT-26 CRC subcutaneous transplant model, Dovedi et al demonstrated that extended treatment with PD-1 axis blockade (3 weeks total) compared with only 1 week of therapy coinciding with fractionated radiotherapy, did not confer any additional survival benefit. This is suggestive that continuous therapy with PD-1 inhibition is both unnecessary and costly, and that further experiments in the AKPT model should only administer PD-1 inhibition during the fractionated radiotherapy course. Furthermore, in the experiments described by Dovedi et al, sequential administration of PD-1 inhibition following fractionated radiotherapy did not result in any clinical benefit, supporting the strategy of administering concurrent PD-1 inhibition; radiotherapy potentially has an anergic and deleterious effect on T-cells, suggesting that PD-1 inhibition must coincide with fractionated radiotherapy for its anti-tumour effects to occur.

Time-point studies would prove essential in analysing the effects of fractionated radiotherapy and PD-1 inhibition on the tumour immune microenvironment, with short time-point sampling (upto 7 days post completion of radiotherapy) likely to be more informative than clinical endpoint analysis. Endpoint tumour samples were analysed for PD-L1 expression by RNAscope to determine whether the PD-1/PD-L1 axis had been successfully targeted by this treatment, however, no

significant differences in probe numbers were observed when comparing groups. In the study by Dovedi et al, increased PD-1 expression was observed on CD4+ and CD8+ cells at 24 hours after the last radiotherapy dose, however, at 7 days levels were either unchanged or reduced respectively (Dovedi et al, 2014). This highlights the limitations of performing immunological analysis of treatment effects at clinical endpoint. It is critical that short time-point analyses using flow cytometry, IHC and RNA sequencing are performed in the AKPT model at 1-7 days after fractionated radiotherapy has been completed, to elucidate the underlying mechanisms of the survival extension observed with this treatment combination.

Although fractionated radiotherapy and PD-1/PD-L1 inhibition has been previously studied in pre-clinical models of CRC, this treatment combination has not been assessed in clinically relevant orthotopic models specific to LARC. This thesis demonstrates the feasibility of studying fractionated radiotherapy in combination with immunotherapy in immunocompetent rectal cancer models. The AKPT orthotopic rectal cancer model does not respond as promisingly as previously described heterotopic models of CRC, likely reflecting variation in radiosensitivity between cell/organoid lines used, disparate phenotypes of the tumour microenvironment according to transplant location, and different radiotherapy fractionation schedules. It is essential that ongoing work to understand the immunological mechanisms underpinning responses to radiotherapy and PD-1/PD-L1 blockade is undertaken in more clinically relevant orthotopic models, if pre-clinical data relating to fractionation and scheduling can be translated to inform clinical trials.

6.6. Future Directions in Rectal Cancer Research

As previously highlighted, 10-20% of patients with LARC demonstrate a complete pathological response to neoadjuvant therapy, and the development of tools and biomarkers to predict individual patient response to therapy remains an unmet need. DNA mismatch repair status has been established as a biomarker in colorectal cancer, however, its role in the rectal cancer subset is less clear. Meta-analysis data suggests there is no significant difference in pCR rates between microsatellite stable and microsatellite unstable rectal tumours

following CRT (O'Connell et al, 2020). Encouragingly, complete clinical response in mismatch repair deficient LARC following single agent PD-1 blockade has been demonstrated recently, highlighting the potential for MMR status as a biomarker (Cercek et al, 2022). However, mismatch repair deficiency is a feature in <10% of rectal cancers, therefore further research must focus on other biomarkers to enable stratification of patients to effective treatment regimens.

The role of immune cells and inflammation has been extensively investigated in pre- and post-treatment samples, with both raised C-reactive protein (CRP) and decreased tumour infiltrating lymphocyte densities being associated with non-response to CRT (Yasuda et al, 2011; Dreyer et al, 2017; Matsutani et al, 2018). Many other biomarkers associated with response and non-response have been identified in the literature, however, studies to date have demonstrated associations with no robust findings upon which to guide individual treatment stratification (Alkan et al, 2021). Further evaluation on the role of circulating tumour DNA (ctDNA) to guide patient treatment stratification is required; studies have shown association between disease recurrence and post treatment presence of ct-DNA, as well as a negative correlation between response to CRT in pre-treatment ct-DNA samples showing APC and p53 mutation (Tie et al, 2019; Yang et al, 2019). Identification of novel biomarkers of response to neo-adjuvant radiotherapy and CRT in LARC are required, if precision medicine-based treatment approaches are to be achieved.

Future experiments to identify genes associated with sensitivity to neo-adjuvant radiotherapy-based treatment regimens in LARC, could utilise CRISPR screening methods. The RNA-guided CRISPR-Cas9 nuclease system is an effective means to introduce loss of function mutations at specific genomic sites, with large scale oligonucleotide library synthesis enabling genome wide functional screening (Cong et al, 2013). CRISPR knockout screens have been utilised previously in model systems to functionally interrogate genes and specific biological processes, to aid in the identification of novel therapeutic targets (Shalem et al, 2014; Ungricht et al, 2022). Whole genome CRISPR-Cas9 knockout screening was described in a human head and neck cancer cell line (FaDu) treated with ionising radiation, to show that STING (stimulator of interferon genes) regulates the generation of reactive oxygen species, with STING loss reducing DNA damage and resulting in therapeutic resistance (Hayman et al, 2021).

With sufficient resources, a genome wide CRISPR-Cas9 knockout screen in multiple pre-treatment human rectal cancer derived cell lines representative of the spectrum of clinical responses, could be conducted to identify both biomarkers of response and novel therapeutic targets. Correlation of pre-treatment tumour derived cell lines with the corresponding patient response to therapy would enable the testing of both treatment sensitive and treatment resistant cell lines. Rectal tumour derived cell lines could then be challenged with *in-vitro* radiation, with next generation sequencing then performed on surviving cells in both treated and control groups to enable the identification of enriched or depleted gene expression associated with treatment response; such an approach might aid in the development of novel therapeutic candidates to test in the pre-clinical setting, using both *in-vitro* organoid models and newly described orthotopic *in-vivo* models which recapitulate LARC.

A further approach to identify novel therapeutic candidates would be to conduct drug screening studies, whereby patient tumour derived cells are treated against a large drug library. The feasibility of conducting high throughput drug screens in patient derived organoid cultures has previously been described in CRC, demonstrating the potential to combine genetic and drug sensitivity data to guide individualised treatment regimens (van de Wetering et al, 2015). Recent studies developing human rectal cancer derived organoids demonstrate molecular concordance with their corresponding tumours, thus highlighting tumour derived organoids as an attractive model system with potential scalability for high throughput drug screening (Ganesh et al, 2019; Yao et al, 2020).

Recent attempts in a prospective trial to utilise treatment refractory metastatic CRC patient derived organoids, which were then subjected to a targeted drug screen, failed to demonstrate objective clinical response to the recommended treatments in the corresponding patients (Ooft et al, 2021). A further small study whereby tumour derived organoids at multiple stages in the disease course of a single patient with metastatic rectal cancer were derived, then subjected to a screening panel of 33 drugs, with sensitivity to the SMAC (second mitochondria-derived activator of caspase) mimetic LCL161 being demonstrated, showing the feasibility of PDOs to identify experimental therapies (Kryeziu et al, 2021). Several pre-treatment rectal tumour derived organoids (n=26) were obtained in

a recent study, with an *in-vitro* assay described to test fractionated RT in combination with 5-FU, and responses of patient derived tumour organoids correlated with those of the corresponding patient (Janakiraman et al, 2020). Furthermore, the addition of cetuximab to the chemoradiotherapy regimen enhanced treatment sensitivity in KRAS wild-type organoids, highlighting the potential for tumour derived organoids in developing individualised treatment combinations.

If adequate resources were available, then performing high throughput *in-vitro* drug screening on clinically relevant pre-treatment patient tumour derived organoid cell lines, particularly from patients who go on to demonstrate treatment resistance, might yield several novel therapeutic targets. Patients who fail to respond to current neo-adjuvant chemoradiotherapy strategies, represent a group with unmet clinical need and future research must focus on better understanding the molecular mechanisms underlying treatment resistance, with the aim of identifying therapeutic strategies to overcome this.

6.7. Concluding Remarks

Numerous trials have recently investigated PD-1 axis inhibition in addition to current standard of care neo-adjuvant treatment regimens in LARC. The recent VOLTAGE trial (NCT02948348) demonstrated 30% (MSS) and 60% (MSI) pCR rates following sequential CRT and nivolumab (Bando et al, 2022). A 48.1% overall pCR rate was found in a recent clinical trial (NCT04231552) evaluating SCRT followed by CAPOX and camrelizumab (Lin et al, 2021). The recent TORCH trial (NCT04518280) evaluated induction CAPOX and toripalimab followed by SCRT or SCRT followed by 6 cycles of CAPOX and toripalimab; an overall 46.8% complete pathological response rate was observed (Wang et al, 2023). In a further study assessing the concurrent addition of tislelizumab to neo-adjuvant CRT, a 50% pCR was observed (Gao et al, 2023). Early clinical trials have shown highly promising results when additional PD-1/PD-L1 inhibition is given alongside neo-adjuvant CRT, with numerous other similar studies also ongoing. Similarly promising results have been published for both concurrent and sequential administration of immune checkpoint blockade relative to fractionated radiotherapy, and further

randomised controlled trials are essential to determine optimal scheduling of therapy.

Early pre-clinical studies have limited translational value owing to the lack of anatomical relevance of the models, and it is essential that future pre-clinical studies more faithfully recapitulate the anatomical, histological, and molecular characteristics of human disease. The orthotopic AKPT organoid transplant model described in this thesis more closely represents locally invasive rectal cancer, and the technique of colonoscopy-guided organoid injection is both reproducible and amenable to a range of genotypes of interest. Further experiments are essential in this model to investigate the underlying mechanism of response to this treatment combination, and to further refine effective fractionation regimens.

Sufficiently powered and robustly designed treatment experiments in reliable pre-clinical models of LARC, hold promise to inform future clinical trial design; for instance, pre-clinical treatment studies are the ideal setting to investigate unanswered questions regarding treatment scheduling in the context of PD-1/PD-L1 inhibition. In addition, it is crucial that improved understanding of the heterogenous responses to neo-adjuvant treatment strategies better utilises clinical samples. Owing to the anatomical location of rectal tumours, sequential on-treatment biopsies are a feasible strategy to obtain invaluable information on the evolving changes within the tumour microenvironment, which can be incorporated into clinical trial design (Hanna et al, 2021).

In the design of future clinical trials and discovery of novel therapeutic targets, it is essential that pre-clinical research is combined with clinical findings to enable optimal clinical translation. The recent study by Nicolas et al demonstrates this principal in the context of LARC, whereby inflammatory cancer-associated fibroblasts were found to be associated with poor response to CRT in patients, with polarisation to the inflammatory phenotype driven by IL-1α (Nicolas et al, 2022). IL-1 signalling was subsequently identified as an attractive treatment target to overcome resistance to CRT in LARC, and a clinical trial has recently been initiated to test CRT with recombinant IL-1RA (anakinra) in rectal cancer (NCT04942626). As described, understanding of the mechanisms underpinning responses to radiotherapy and the discovery of new therapeutic targets, might benefit from both high throughput drug and CRISPR-Cas9

screening in patient derived tumour cell lines to identify novel biomarkers and personalised therapies.

This thesis describes the development of more relevant pre-clinical orthotopic models which better recapitulate clinical and molecular features of LARC, and will be easily reproducible by other researchers in the pre-clinical setting. Furthermore, a platform upon which to perform experimental treatment studies involving radiotherapy and immune-modulating agents is described, and will be applicable to investigating both scheduling of immune checkpoint blockade and the testing of novel therapeutic agents with the aim of augmenting treatment responses in patients resistant to current standard of care neoadjuvant regimens.

Bibliography

Adell, G., Sun, X.F., Stål, O., Klintenberg, C., Sjödahl, R. and Nordenskjöld, B. (1999). p53 status: an indicator for the effect of preoperative radiotherapy of rectal cancer. Radiotherapy and oncology: journal of the European Society for Therapeutic Radiology and Oncology, 51(2), 169–174. doi:10.1016/s0167-8140(99)00041-9

Ahmaderaghi, B., Amirkhah, R., Jackson, J., Lannagan, T.R.M., Gilroy, K., Malla, S.B., Redmond, K.L., Quinn, G., McDade, S.S., ACRCelerate Consortium, Maughan, T., Leedham, S., Campbell, A.S.D., Sansom, O.J., Lawler, M. and Dunne, P.D. (2022). Molecular Subtyping Resource: a user-friendly tool for rapid biological discovery from transcriptional data. Disease models & mechanisms, 15(3), dmm049257. doi:10.1242/dmm.049257

Ahn, G.O., Tseng, D., Liao, C.H., Dorie, M.J., Czechowicz, A. and Brown, J.M. (2010). Inhibition of Mac-1 (CD11b/CD18) enhances tumor response to radiation by reducing myeloid cell recruitment. Proceedings of the National Academy of Sciences of the United States of America, 107(18), 8363–8368. doi:10.1073/pnas.0911378107

Aide, N., Kinross, K., Beauregard, J.M., Neels, O., Potdevin, T., Roselt, P., Dorow, D., Cullinane, C. and Hicks, R.J. (2011). A dual radiologic contrast agent protocol for 18F-FDG and 18F-FLT PET/CT imaging of mice bearing abdominal tumors. Molecular imaging and biology, 13(3), 518–525. doi:10.1007/s11307-010-0378-x

Albert, M.L., Sauter, B. and Bhardwaj, N. (1998). Dendritic cells acquire antigen from apoptotic cells and induce class I-restricted CTLs. Nature, 392(6671), 86–89. doi:10.1038/32183

Alexandrov, L.B., Nik-Zainal, S., Wedge, D.C., Aparicio, S.A., Behjati, S., Biankin, A.V., Bignell, G.R., Bolli, N., Borg, A., Børresen-Dale, A.L., Boyault, S., Burkhardt, B., Butler, A.P., Caldas, C., Davies, H.R., Desmedt, C., Eils, R., Eyfjörd, J.E., Foekens, J.A., Greaves, M., … Stratton, M.R. (2013). Signatures of mutational processes in human cancer. Nature, 500(7463), 415–421. doi:10.1038/nature12477

Alkan, A., Hofving, T., Angenete, E. and Yrlid, U. (2021). Biomarkers and cell-based models to predict the outcome of neoadjuvant therapy for rectal cancer patients. Biomarker research, 9(1), 60. doi:10.1186/s40364-021-00313-9

Amado, R.G., Wolf, M., Peeters, M., Van Cutsem, E., Siena, S., Freeman, D.J., Juan, T., Sikorski, R., Suggs, S., Radinsky, R., Patterson, S.D. and Chang, D.D. (2008). Wild-Type KRAS Is Required for Panitumumab Efficacy in Patients With Metastatic Colorectal Cancer. Journal of Clinical Oncology, 26(10), pp.1626–1634. doi:10.1200/jco.2007.14.7116.

André, T., Boni, C., Navarro, M., Tabernero, J., Hickish, T., Topham, C., Bonetti, A., Clingan, P., Bridgewater, J., Rivera, F. and de Gramont, A. (2009). Improved overall survival with oxaliplatin, fluorouracil, and leucovorin as adjuvant treatment in stage II or III colon cancer in the MOSAIC trial. Journal of clinical oncology, 27(19), 3109–3116. doi:10.1200/JCO.2008.20.6771

Andreu, P., Colnot, S., Godard, C., Gad, S., Chafey, P., Niwa-Kawakita, M., Laurent-Puig, P., Kahn, A., Robine, S., Perret, C. and Romagnolo, B. (2005).

Crypt-restricted proliferation and commitment to the Paneth cell lineage following Apc loss in the mouse intestine. Development, 132(6), 1443–1451. doi:10.1242/dev.01700

Anitei, M.G., Zeitoun, G., Mlecnik, B., Marliot, F., Haicheur, N., Todosi, A.M., Kirilovsky, A., Lagorce, C., Bindea, G., Ferariu, D., Danciu, M., Bruneval, P., Scripcariu, V., Chevallier, J. M., Zinzindohoué, F., Berger, A., Galon, J. and Pagès, F. (2014). Prognostic and predictive values of the immunoscore in patients with rectal cancer. Clinical cancer research, 20(7), 1891–1899. doi:10.1158/1078-0432.CCR-13-2830

Annes, J.P., Chen, Y., Munger, J.S. and Rifkin, D.B. (2004). Integrin alphaVbeta6-mediated activation of latent TGF-beta requires the latent TGF-beta binding protein-1. The Journal of cell biology, 165(5), 723–734. doi:10.1083/jcb.200312172

Ansell, S.M., Lesokhin, A.M., Borrello, I., Halwani, A., Scott, E.C., Gutierrez, M., Schuster, S.J., Millenson, M.M., Cattry, D., Freeman, G.J., Rodig, S.J., Chapuy, B., Ligon, A.H., Zhu, L., Grosso, J.F., Kim, S.Y., Timmerman, J.M., Shipp, M.A. and Armand, P. (2015). PD-1 blockade with nivolumab in relapsed or refractory Hodgkin's lymphoma. The New England journal of medicine, 372(4), 311–319. doi:10.1056/NEJMoa1411087

Antonia, S.J., Villegas, A., Daniel, D., Vicente, D., Murakami, S., Hui, R., Kurata, T., Chiappori, A., Lee, K.H., de Wit, M., Cho, B.C., Bourhaba, M., Quantin, X., Tokito, T., Mekhail, T., Planchard, D., Kim, Y.C., Karapetis, C.S., Hiret, S., Ostoros, G., … PACIFIC Investigators (2018). Overall Survival with Durvalumab after Chemoradiotherapy in Stage III NSCLC. The New England journal of medicine, 379(24), 2342–2350. doi:10.1056/NEJMoa1809697

Apetoh, L., Ghiringhelli, F., Tesniere, A., Obeid, M., Ortiz, C., Criollo, A., Mignot, G., Maiuri, M.C., Ullrich, E., Saulnier, P., Yang, H., Amigorena, S., Ryffel, B., Barrat, F.J., Saftig, P., Levi, F., Lidereau, R., Nogues, C., Mira, J.P., Chompret, A., … Zitvogel, L. (2007). Toll-like receptor 4-dependent contribution of the immune system to anticancer chemotherapy and radiotherapy. Nature medicine, 13(9), 1050–1059. doi:10.1038/nm1622

Araki, K., Imaizumi, T., Okuyama, K., Oike, Y. and Yamamura, K. (1997). Efficiency of recombination by Cre transient expression in embryonic stem cells: comparison of various promoters. Journal of biochemistry, 122(5), 977–982. doi:10.1093/oxfordjournals.jbchem.a021860

Arnold, K.M., Flynn, N.J., Raben, A., Romak, L., Yu, Y., Dicker, A.P., Mourtada, F. and Sims-Mourtada, J. (2018). The Impact of Radiation on the Tumor Microenvironment: Effect of Dose and Fractionation Schedules. Cancer growth and metastasis, 11, 1179064418761639. doi:10.1177/1179064418761639

Arnold, M., Sierra, M.S., Laversanne, M., Soerjomataram, I., Jemal, A. and Bray, F. (2016). Global patterns and trends in colorectal cancer incidence and mortality. Gut, 66(4), pp.683–691. doi:10.1136/gutjnl-2015-310912.

Arora, S., Demidova, E., Avkshtol, V., Lesh, R., Browne, A.J., Handorf, E.A., Golemis, E. and Meyer, J.E. Correlation of peripheral blood markers of DNA damage and immune response with chemoradiation response in patients with locally advanced rectal cancer. (2019). Journal of Clinical Oncology, 37(15_suppl), e15109. doi:10.1200/JCO.2019.37.15_suppl.e15109

Asano, T., Meguri, Y., Yoshioka, T., Kishi, Y., Iwamoto, M., Nakamura, M., Sando, Y., Yagita, H., Koreth, J., Kim, H.T., Alyea, E.P., Armand, P., Cutler, C. S., Ho, V.T., Antin, J.H., Soiffer, R.J., Maeda, Y., Tanimoto, M., Ritz, J. and Matsuoka, K.I. (2017). PD-1 modulates regulatory T-cell homeostasis during low-dose interleukin-2 therapy. Blood, 129(15), 2186–2197. doi:10.1182/blood-2016-09-741629

Atun, R., Jaffray, D.A., Barton, M.B., Bray, F., Baumann, M., Vikram, B., Hanna, T.P., Knaul, F.M., Lievens, Y., Lui, T.Y., Milosevic, M., O'Sullivan, B., Rodin, D. L., Rosenblatt, E., Van Dyk, J., Yap, M.L., Zubizarreta, E. and Gospodarowicz, M. (2015). Expanding global access to radiotherapy. The Lancet. Oncology, 16(10), 1153–1186. doi:10.1016/S1470-2045(15)00222-3

Azuma, Y.T., Hagi, K., Shintani, N., Kuwamura, M., Nakajima, H., Hashimoto, H., Baba, A. and Takeuchi, T. (2008). PACAP provides colonic protection against dextran sodium sulfate induced colitis. Journal of cellular physiology, 216(1), 111–119. doi:10.1002/jcp.21381

Bach, S P., Gilbert, A., Brock, K., Korsgen, S., Geh, I., Hill, J., Gill, T., Hainsworth, P., Tutton, M.G., Khan, J., Robinson, J., Steward, M., Cunningham, C., Levy, B., Beveridge, A., Handley, K., Kaur, M., Marchevsky, N., Magill, L., Russell, A., … TREC collaborators (2021). Radical surgery versus organ preservation via short-course radiotherapy followed by transanal endoscopic microsurgery for early-stage rectal cancer (TREC): a randomised, open-label feasibility study. The lancet. Gastroenterology & hepatology, 6(2), 92–105. doi:10.1016/S2468-1253(20)30333-2

Bagshaw, P.F., Allardyce, R.A., Frampton, C.M., Frizelle, F.A., Hewett, P.J., McMurrick, P.J., Rieger, N.A., Smith, J.S., Solomon, M.J., Stevenson, A.R. and Australasian Laparoscopic Colon Cancer Study Group (2012). Long-term outcomes of the australasian randomized clinical trial comparing laparoscopic and conventional open surgical treatments for colon cancer: the Australasian Laparoscopic Colon Cancer Study trial. Annals of surgery, 256(6), 915–919. doi:10.1097/SLA.0b013e3182765ff8

Bahadoer, R.R., Dijkstra, E.A., van Etten, B., Marijnen, C.A.M., Putter, H., Kranenbarg, E.M., Roodvoets, A.G.H., Nagtegaal, I.D., Beets-Tan, R.G.H., Blomqvist, L.K., Fokstuen, T., Ten Tije, A.J., Capdevila, J., Hendriks, M.P., Edhemovic, I., Cervantes, A., Nilsson, P.J., Glimelius, B., van de Velde, C.J.H., Hospers, G.A.P., … RAPIDO collaborative investigators. (2021). Short-course radiotherapy followed by chemotherapy before total mesorectal excision (TME) versus preoperative chemoradiotherapy, TME, and optional adjuvant chemotherapy in locally advanced rectal cancer (RAPIDO): a randomised, open-label, phase 3 trial. The Lancet Oncology, 22(1), 29–42. doi:10.1016/S1470-2045(20)30555-6

Baker, S.J., Preisinger, A.C., Jessup, J.M., Paraskeva, C., Markowitz, S., Willson, J.K., Hamilton, S. and Vogelstein, B. (1990). p53 gene mutations occur in combination with 17p allelic deletions as late events in colorectal tumorigenesis. Cancer Research, 50(23), pp. 7717–7722.

Bakkenist, C.J. and Kastan, M.B. (2003). DNA damage activates ATM through intermolecular autophosphorylation and dimer dissociation. Nature, 421(6922), 499–506. doi:10.1038/nature01368

Bando, H., Tsukada, Y., Inamori, K., Togashi, Y., Koyama, S., Kotani, D., Fukuoka, S., Yuki, S., Komatsu, Y., Homma, S., Taketomi, A., Uemura, M., Kato, T., Fukui, M., Wakabayashi, M., Nakamura, N., Kojima, M., Kawachi, H., Kirsch, R., Yoshida, T. and Yoshino, T. (2022). Preoperative Chemoradiotherapy plus Nivolumab before Surgery in Patients with Microsatellite Stable and Microsatellite Instability-High Locally Advanced Rectal Cancer. Clinical cancer research, 28(6), 1136–1146. doi:10.1158/1078-0432.CCR-21-3213

Barcellos-Hoff, M.H., Derynck, R., Tsang, M.L. and Weatherbee, J. A. (1994). Transforming growth factor-beta activation in irradiated murine mammary gland. The Journal of clinical investigation, 93(2), 892–899. doi:10.1172/JCI117045

Barcellos-Hoff, M.H. and Ravani, S.A. (2000). Irradiated mammary gland stroma promotes the expression of tumorigenic potential by unirradiated epithelial cells. Cancer research, 60(5), 1254–1260.

Barcellos-Hoff, M.H., Park, C. and Wright, E.G. (2005). Radiation and the microenvironment - tumorigenesis and therapy. Nature reviews. Cancer, 5(11), 867–875. doi:10.1038/nrc1735

Barcellos-Hoff, M.H. and Cucinotta, F.A. (2014). New tricks for an old fox: impact of TGFβ on the DNA damage response and genomic stability. Science signaling, 7(341), re5. doi:10.1126/scisignal.2005474

Barker, H.E., Paget, J.T., Khan, A.A. and Harrington, K.J. (2015). The tumour microenvironment after radiotherapy: mechanisms of resistance and recurrence. Nature reviews. Cancer, 15(7), 409–425. doi:10.1038/nrc3958

Barton, M.B., Jacob, S., Shafiq, J., Wong, K., Thompson, S.R., Hanna, T.P. and Delaney, G. P. (2014). Estimating the demand for radiotherapy from the evidence: a review of changes from 2003 to 2012. Radiotherapy and oncology: journal of the European Society for Therapeutic Radiology and Oncology, 112(1), 140–144. doi:10.1016/j.radonc.2014.03.024

Baskar, R., Lee, K.A., Yeo, R. and Yeoh, K.W. (2012). Cancer and radiation therapy: current advances and future directions. International journal of medical sciences, 9(3), 193–199. doi:10.7150/ijms.3635

Batlle, E. and Massagué, J. (2019). Transforming Growth Factor-β Signaling in Immunity and Cancer. Immunity, 50(4), 924–940. doi:10.1016/j.immuni.2019.03.024

Beatty, G.L., Winograd, R., Evans, R.A., Long, K.B., Luque, S.L., Lee, J.W., Clendenin, C., Gladney, W.L., Knoblock, D.M., Guirnalda, P.D. and Vonderheide, R.H. (2015). Exclusion of T Cells From Pancreatic Carcinomas in Mice Is Regulated by Ly6C(low) F4/80(+) Extratumoral Macrophages. Gastroenterology, 149(1), 201–210. doi:10.1053/j.gastro.2015.04.010

Becker, C., Fantini, M.C., Schramm, C., Lehr, H.A., Wirtz, S., Nikolaev, A., Burg, J., Strand, S., Kiesslich, R., Huber, S., Ito, H., Nishimoto, N., Yoshizaki, K., Kishimoto, T., Galle, P.R., Blessing, M., Rose-John, S. and Neurath, M. F. (2004). TGF-beta suppresses tumor progression in colon cancer by inhibition of IL-6 trans-signaling. Immunity, 21(4), 491–501. doi:10.1016/j.immuni.2004.07.020

Benson, A.B., Venook, A.P., Al-Hawary, M.M., Cederquist, L., Chen, Y.J., Ciombor, K.K., Cohen, S., Cooper, H.S., Deming, D., Engstrom, P F., Grem, J. L., Grothey, A., Hochster, H.S., Hoffe, S., Hunt, S., Kamel, A., Kirilcuk, N., Krishnamurthi, S., Messersmith, W.A., Meyerhardt, J., … Freedman-Cass, D.A. (2018). Rectal Cancer, Version 2.2018, NCCN Clinical Practice Guidelines in Oncology. Journal of the National Comprehensive Cancer Network: JNCCN, 16(7), 874–901. doi:10.6004/jnccn.2018.0061

Bernier, L., Balyasnikova, S., Tait, D. and Brown, G. (2018). Watch-and-Wait as a Therapeutic Strategy in Rectal Cancer. Current colorectal cancer reports, 14(2), 37–55. doi:10.1007/s11888-018-0398-5

Bertagnolli, M.M., Eagle, C.J., Zauber, A.G., Redston, M., Solomon, S.D., Kim, K., Tang, J., Rosenstein, R.B., Wittes, J., Corle, D., Hess, T.M., Woloj, G.M., Boisserie, F., Anderson, W.F., Viner, J.L., Bagheri, D., Burn, J., Chung, D.C., Dewar, T., Foley, T.R., … APC Study Investigators (2006). Celecoxib for the prevention of sporadic colorectal adenomas. The New England journal of medicine, 355(9), 873–884. doi:10.1056/NEJMoa061355

Bettenworth, D., Mücke, M.M., Schwegmann, K., Faust, A., Poremba, C., Schäfers, M., Domagk, D. and Lenz, P. (2016). Endoscopy-guided orthotopic implantation of colorectal cancer cells results in metastatic colorectal cancer in mice. Clinical & experimental metastasis, 33(6), 551–562. doi:10.1007/s10585-016-9797-7

Binnewies, M., Roberts, E.W., Kersten, K., Chan, V., Fearon, D.F., Merad, M., Coussens, L.M., Gabrilovich, D.I., Ostrand-Rosenberg, S., Hedrick, C.C., Vonderheide, R.H., Pittet, M.J., Jain, R.K., Zou, W., Howcroft, T.K., Woodhouse, E.C., Weinberg, R.A. and Krummel, M.F. (2018). Understanding the tumor immune microenvironment (TIME) for effective therapy. Nature medicine, 24(5), 541–550. doi:10.1038/s41591-018-0014-x

Birgisson, H., Påhlman, L., Gunnarsson, U., Glimelius, B. and Swedish Rectal Cancer Trial Group (2005). Adverse effects of preoperative radiation therapy for rectal cancer: long-term follow-up of the Swedish Rectal Cancer Trial. Journal of clinical oncology, 23(34), 8697–8705. doi:10.1200/JCO.2005.02.9017

Biswas, S., Guix, M., Rinehart, C., Dugger, T.C., Chytil, A., Moses, H.L., Freeman, M.L. and Arteaga, C.L. (2007). Inhibition of TGF-beta with neutralizing antibodies prevents radiation-induced acceleration of metastatic cancer progression. The Journal of clinical investigation, 117(5), 1305–1313. doi:10.1172/JCI30740

Blanpain, C., Mohrin, M., Sotiropoulou, P.A. and Passegué, E. (2011). DNA-damage response in tissue-specific and cancer stem cells. Cell stem cell, 8(1), 16–29. doi:10.1016/j.stem.2010.12.012

Blomgren, H., Lax, I., Näslund, I. and Svanström, R. (1995). Stereotactic high dose fraction radiation therapy of extracranial tumors using an accelerator. Clinical experience of the first thirty-one patients. Acta oncologica, 34(6), 861–870. doi:10.3109/02841869509127197

Blomqvist, L. and Glimelius, B. (2008). The 'good', the 'bad', and the 'ugly' rectal cancers. Acta oncologica, 47(1), 5–8. doi:10.1080/02841860701802585

von Boehmer H. (2005). Mechanisms of suppression by suppressor T cells. Nature immunology, 6(4), 338–344. doi:10.1038/ni1180

Boland, C.R., Thibodeau, S.N., Hamilton, S.R., Sidransky, D., Eshleman, J.R., Burt, R.W., Meltzer, S.J., Rodriguez-Bigas, M.A., Fodde, R., Ranzani, G.N. and Srivastava, S. (1998). A National Cancer Institute Workshop on Microsatellite Instability for cancer detection and familial predisposition: development of international criteria for the determination of microsatellite instability in colorectal cancer. Cancer research, 58(22), 5248–5257.

Bonaventura, P., Shekarian, T., Alcazer, V., Valladeau-Guilemond, J., Valsesia-Wittmann, S., Amigorena, S., Caux, C. and Depil, S. (2019). Cold Tumors: A Therapeutic Challenge for Immunotherapy. Frontiers in immunology, 10, 168. doi:10.3389/fimmu.2019.00168

Bonjer, H.J., Deijen, C.L., Haglind, E. and COLOR II Study Group. (2015). A Randomized Trial of Laparoscopic versus Open Surgery for Rectal Cancer. The New England journal of medicine, 373(2), 194. doi:10.1056/NEJMc1505367

Bosset, J.F., Calais, G., Mineur, L., Maingon, P., Stojanovic-Rundic, S., Bensadoun, R.J., Bardet, E., Beny, A., Ollier, J.C., Bolla, M., Marchal, D., Van Laethem, J.L., Klein, V., Giralt, J., Clavère, P., Glanzmann, C., Cellier, P., Collette, L. and EORTC Radiation Oncology Group (2014). Fluorouracil-based adjuvant chemotherapy after preoperative chemoradiotherapy in rectal cancer: long-term results of the EORTC 22921 randomised study. The Lancet Oncology, 15(2), 184–190. doi:10.1016/S1470-2045(13)70599-0

Botteri, E., Iodice, S., Bagnardi, V., Raimondi, S., Lowenfels, A.B. and Maisonneuve, P. (2008). Smoking and colorectal cancer: a meta-analysis. JAMA, 300(23), pp.2765–78. doi:10.1001/jama.2008.839.

Bouquet, F., Pal, A., Pilones, K.A., Demaria, S., Hann, B., Akhurst, R.J., Babb, J.S., Lonning, S.M., DeWyngaert, J.K., Formenti, S.C. and Barcellos-Hoff, M.H. (2011). TGFβ1 inhibition increases the radiosensitivity of breast cancer cells in vitro and promotes tumor control by radiation in vivo. Clinical cancer research, 17(21), 6754–6765. doi:10.1158/1078-0432.CCR-11-0544

Boustani, J., Derangère, V., Bertaut, A., Adotevi, O., Morgand, V., Charon-Barra, C., Ghiringhelli, F. and Mirjolet, C. (2020). Radiotherapy Scheme Effect on PD-L1 Expression for Locally Advanced Rectal Cancer. Cells, 9(9), 2071. doi:10.3390/cells9092071

Boutin, A.T., Liao, W.T., Wang, M., Hwang, S.S., Karpinets, T.V., Cheung, H., Chu, G.C., Jiang, S., Hu, J., Chang, K., Vilar, E., Song, X., Zhang, J., Kopetz, S., Futreal, A., Wang, Y.A., Kwong, L.N. and DePinho, R.A. (2017). Oncogenic Kras drives invasion and maintains metastases in colorectal cancer. Genes & development, 31(4), 370–382. doi:10.1101/gad.293449.116

Boutros, C., Tarhini, A., Routier, E., Lambotte, O., Ladurie, F.L., Carbonnel, F., Izzeddine, H., Marabelle, A., Champiat, S., Berdelou, A., Lanoy, E., Texier, M., Libenciuc, C., Eggermont, A.M., Soria, J.C., Mateus, C. and Robert, C. (2016). Safety profiles of anti-CTLA-4 and anti-PD-1 antibodies alone and in combination. Nature Reviews Clinical oncology, 13(8), 473–486. doi:10.1038/nrclinonc.2016.58

Brahmer, J.R., Tykodi, S.S., Chow, L.Q., Hwu, W.J., Topalian, S.L., Hwu, P., Drake, C.G., Camacho, L.H., Kauh, J., Odunsi, K., Pitot, H.C., Hamid, O., Bhatia, S., Martins, R., Eaton, K., Chen, S., Salay, T.M., Alaparthy, S., Grosso, J.F., Korman, A.J., … Wigginton, J.M. (2012). Safety and activity of anti-PD-L1 antibody in patients with advanced cancer. The New England journal of medicine, 366(26), 2455–2465. doi:10.1056/NEJMoa1200694

Brahmer, J., Reckamp, K.L., Baas, P., Crinò, L., Eberhardt, W.E., Poddubskaya, E., Antonia, S., Pluzanski, A., Vokes, E.E., Holgado, E., Waterhouse, D., Ready, N., Gainor, J., Arén Frontera, O., Havel, L., Steins, M., Garassino, M.C., Aerts, J.G., Domine, M., Paz-Ares, L., … Spigel, D.R. (2015). Nivolumab versus Docetaxel in Advanced Squamous-Cell Non-Small-Cell Lung Cancer. The New England journal of medicine, 373(2), 123–135. doi:10.1056/NEJMoa1504627

Bray, F., Ferlay, J., Soerjomataram, I., Siegel, R.L., Torre, L.A. and Jemal, A. (2018). Global cancer statistics 2018: GLOBOCAN estimates of incidence and mortality worldwide for 36 cancers in 185 countries. CA: A Cancer Journal for Clinicians, 68(6), pp.394–424. doi:10.3322/caac.21492.

Bregni, G., Vandeputte, C., Pretta, A., Senti, C., Trevisi, E., Acedo Reina, E., Kehagias, P., Liberale, G., Moretti, L., Bali, M.A., Demetter, P., Flamen, P., Carrasco, J., D'Hondt, L., Geboes, K., Gokburun, Y., Peeters, M., Van den Eynde, M., Van Laethem, J.L., Vergauwe, P., … Sclafani, F. (2021). Rationale and design of REGINA, a phase II trial of neoadjuvant regorafenib, nivolumab, and short-course radiotherapy in stage II and III rectal cancer. Acta oncologica, 60(4), 549–553. doi:10.1080/0284186X.2020.1871067

Breugom, A.J., Swets, M., Bosset, J.F., Collette, L., Sainato, A., Cionini, L., Glynne-Jones, R., Counsell, N., Bastiaannet, E., van den Broek, C.B., Liefers, G. J., Putter, H. and van de Velde, C.J. (2015). Adjuvant chemotherapy after preoperative (chemo)radiotherapy and surgery for patients with rectal cancer: a systematic review and meta-analysis of individual patient data. The Lancet Oncology, 16(2), 200–207. doi:10.1016/S1470-2045(14)71199-4

Bristow, R.G. and Hill, R.P. (2008). Hypoxia and metabolism. Hypoxia, DNA repair and genetic instability. Nature reviews. Cancer, 8(3), 180–192. doi:10.1038/nrc2344

Broders-Bondon F, Ho-Bouldoires THN, Fernandez-Sanchez M-E, Farge E. Mechanotransduction in tumor progression: the dark side of the force. J Cell Biol. (2018) 217:1571–87. doi:10.1083/jcb.201701039

Bronner, C. E., Baker, S. M., Morrison, P. T., Warren, G., Smith, L. G., Lescoe, M. K., Kane, M., Earabino, C., Lipford, J. and Lindblom, A. (1994). Mutation in the DNA mismatch repair gene homologue hMLH1 is associated with hereditary non-polyposis colon cancer. Nature, 368(6468), 258–261. doi:10.1038/368258a0

Brown, K.H., Ghita, M., Dubois, L.J., de Ruysscher, D., Prise, K.M., Verhaegen, F. and Butterworth, K.T. (2022). A scoping review of small animal image-guided radiotherapy research: Advances, impact and future opportunities in translational radiobiology. Clinical and translational radiation oncology, 34, 112–119. doi:10.1016/j.ctro.2022.04.004

Bruheim, K., Guren, M.G., Skovlund, E., Hjermstad, M.J., Dahl, O., Frykholm, G., Carlsen, E. and Tveit, K.M. (2010). Late side effects and quality of life after

radiotherapy for rectal cancer. International journal of radiation oncology, biology, physics, 76(4), 1005–1011. doi:10.1016/j.ijrobp.2009.03.010

Brunen, D., Willems, S., Kellner, U., Midgley, R., Simon, I., and Bernards, R. (2013). TGF-ß: An Emerging Player in Drug Resistance. Cell Cycle 12, 2960–2968. doi:10.4161/cc.26034

Budhu, S., Schaer, D.A., Li, Y., Toledo-Crow, R., Panageas, K., Yang, X., Zhong, H., Houghton, A.N., Silverstein, S.C., Merghoub, T. and Wolchok, J.D. (2017). Blockade of surface-bound TGF-ß on regulatory T cells abrogates suppression of effector T cell function in the tumor microenvironment. Science signaling, 10(494), eaak9702. doi:10.1126/scisignal.aak9702

Bujko, K., Nowacki, M.P., Nasierowska-Guttmejer, A., Michalski, W., Bebenek, M. and Kryj, M. (2006). Long-term results of a randomized trial comparing preoperative short-course radiotherapy with preoperative conventionally fractionated chemoradiation for rectal cancer. The British journal of surgery, 93(10), 1215–1223. doi:10.1002/bjs.5506

Bujko, K., Wyrwicz, L., Rutkowski, A., Malinowska, M., Pietrzak, L., Kryński, J., Michalski, W., Olędzki, J., Kuśnierz, J., Zając, L., Bednarczyk, M., Szczepkowski, M., Tarnowski, W., Kosakowska, E., Zwoliński, J., Winiarek, M., Wiśniowska, K., Partycki, M., Bęczkowska, K., Polkowski, W., … Polish Colorectal Study Group. (2016). Long-course oxaliplatin-based preoperative chemoradiation versus 5 × 5 Gy and consolidation chemotherapy for cT4 or fixed cT3 rectal cancer: results of a randomized phase III study. Annals of oncology, 27(5), 834–842. doi:10.1093/annonc/mdw062

Burn, J., Sheth, H., Elliott, F., Reed, L., Macrae, F., Mecklin, J.P., Möslein, G., McRonald, F.E., Bertario, L., Evans, D.G., Gerdes, A.M., Ho, J.W.C., Lindblom, A., Morrison, P.J., Rashbass, J., Ramesar, R., Seppälä, T., Thomas, H.J.W., Pylvänäinen, K., Borthwick, G.M., … CAPP2 Investigators (2020). Cancer prevention with aspirin in hereditary colorectal cancer (Lynch syndrome), 10-year follow-up and registry-based 20-year data in the CAPP2 study: a double-blind, randomised, placebo-controlled trial. Lancet, 395(10240), 1855–1863. doi:10.1016/S0140-6736(20)30366-4

Byrne, A.T., Alférez, D.G., Amant, F., Annibali, D., Arribas, J., Biankin, A.V., Bruna, A., Budinská, E., Caldas, C., Chang, D.K., Clarke, R.B., Clevers, H., Coukos, G., Dangles-Marie, V., Eckhardt, S.G., Gonzalez-Suarez, E., Hermans, E., Hidalgo, M., Jarzabek, M.A., de Jong, S., … Trusolino, L. (2017). Interrogating open issues in cancer precision medicine with patient-derived xenografts. Nature reviews. Cancer, 17(4), 254–268. doi:10.1038/nrc.2016.140

Byrne, R.M. and Tsikitis, V.L. (2017). Colorectal polyposis and inherited colorectal cancer syndromes. Ann Gastroenterol, 31(1), pp.24-34. doi: 10.20524/aog.2017.0218.

Cai, S., Li, Y., Ding, Y., Chen, K. and Jin, M. (2014). Alcohol drinking and the risk of colorectal cancer death. European Journal of Cancer Prevention, 23(6), pp.532–539. doi:10.1097/cej.0000000000000076.

Caja, L., Dituri, F., Mancarella, S., Caballero-Diaz, D., Moustakas, A., Giannelli, G. and Fabregat, I. (2018). TGF-ß and the Tissue Microenvironment: Relevance in Fibrosis and Cancer. International journal of molecular sciences, 19(5), 1294. doi:10.3390/ijms19051294

Calon, A., Espinet, E., Palomo-Ponce, S., Tauriello, D.V., Iglesias, M., Céspedes, M.V., Sevillano, M., Nadal, C., Jung, P., Zhang, X.H., Byrom, D., Riera, A., Rossell, D., Mangues, R., Massagué, J., Sancho, E. and Batlle, E. (2012). Dependency of colorectal cancer on a TGF-ß-driven program in stromal cells for metastasis initiation. Cancer cell, 22(5), 571–584. doi:10.1016/j.ccr.2012.08.013

Calon, A., Lonardo, E., Berenguer-Llergo, A., Espinet, E., Hernando-Momblona, X., Iglesias, M., Sevillano, M., Palomo-Ponce, S., Tauriello, D.V., Byrom, D., Cortina, C., Morral, C., Barceló, C., Tosi, S., Riera, A., Attolini, C.S., Rossell, D., Sancho, E. and Batlle, E. (2015). Stromal gene expression defines poor-prognosis subtypes in colorectal cancer. Nature genetics, 47(4), 320–329. doi:10.1038/ng.3225

Cammà, C., Giunta, M., Fiorica, F., Pagliaro, L., Craxì, A. and Cottone, M. (2000). Preoperative radiotherapy for resectable rectal cancer: A meta-analysis. JAMA, 284(8), 1008–1015. doi:10.1001/jama.284.8.1008

Cancer Genome Atlas Network (2012). Comprehensive molecular characterization of human colon and rectal cancer. Nature, 487(7407), 330–337. doi:10.1038/nature11252

Cancer Research UK. (2015). Bowel cancer incidence statistics. [online] Available at: https://www.cancerresearchuk.org/health-professional/cancer-statistics/statistics-by-cancer-type/bowel-cancer/incidence#ref-4. [Accessed 9 Jul. 2020].

Carethers, J.M. and Jung, B.H. (2015). Genetics and Genetic Biomarkers in Sporadic Colorectal Cancer. Gastroenterology, 149(5), pp.1177-1190.e3. doi:10.1053/j.gastro.2015.06.047.

Castle, J.C., Loewer, M., Boegel, S., de Graaf, J., Bender, C., Tadmor, A.D., Boisguerin, V., Bukur, T., Sorn, P., Paret, C., Diken, M., Kreiter, S., Türeci, Ö. and Sahin, U. (2014). Immunomic, genomic and transcriptomic characterization of CT26 colorectal carcinoma. BMC genomics, 15(1), 190. doi:10.1186/1471-2164-15-190

Cercek, A., Roxburgh, C.S.D., Strombom, P., Smith, J.J., Temple, L.K.F., Nash, G.M., Guillem, J.G., Paty, P.B., Yaeger, R., Stadler, Z.K., Seier, K., Gonen, M., Segal, N.H., Reidy, D.L., Varghese, A., Shia, J., Vakiani, E., Wu, A.J., Crane, C. H., Gollub, M.J., … Weiser, M.R. (2018). Adoption of Total Neoadjuvant Therapy for Locally Advanced Rectal Cancer. JAMA oncology, 4(6), e180071. doi:10.1001/jamaoncol.2018.0071

Cercek, A., Dos Santos Fernandes, G., Roxburgh, C. S., Ganesh, K., Ng, S., Sanchez-Vega, F., Yaeger, R., Segal, N. H., Reidy-Lagunes, D. L., Varghese, A. M., Markowitz, A., Wu, C., Szeglin, B., Sauvé, C. G., Salo-Mullen, E., Tran, C., Patel, Z., Krishnan, A., Tkachuk, K., Nash, G. M., … Stadler, Z. K. (2020). Mismatch Repair-Deficient Rectal Cancer and Resistance to Neoadjuvant Chemotherapy. Clin Cancer Res, 26(13), 3271–3279. doi:10.1158/1078-0432.CCR-19-3728

Cercek, A., Lumish, M., Sinopoli, J., Weiss, J., Shia, J., Lamendola-Essel, M., El Dika, I.H., Segal, N., Shcherba, M., Sugarman, R., Stadler, Z., Yaeger, R., Smith, J.J., Rousseau, B., Argiles, G., Patel, M., Desai, A., Saltz, L.B., Widmar, M., Iyer, K., … Diaz Jr, L.A. (2022). PD-1 Blockade in Mismatch Repair-Deficient,

Locally Advanced Rectal Cancer. The New England journal of medicine, 386(25), 2363–2376. doi:10.1056/NEJMoa2201445

Céspedes, M.V., Espina, C., García-Cabezas, M.A., Trias, M., Boluda, A., Gómez del Pulgar, M.T., Sancho, F.J., Nistal, M., Lacal, J.C. and Mangues, R. (2007). Orthotopic microinjection of human colon cancer cells in nude mice induces tumor foci in all clinically relevant metastatic sites. The American journal of pathology, 170(3), 1077–1085. doi:10.2353/ajpath.2007.06077

Chakravarthy, A., Khan, L., Bensler, N.P., Bose, P. and De Carvalho, D.D. (2018). TGF-β-associated extracellular matrix genes link cancer-associated fibroblasts to immune evasion and immunotherapy failure. Nature communications, 9(1), 4692. doi:10.1038/s41467-018-06654-8

Chalabi, M., Fanchi, L.F., Dijkstra, K.K., Van den Berg, J.G., Aalbers, A.G., Sikorska, K., Lopez-Yurda, M., Grootscholten, C., Beets, G.L., Snaebjornsson, P., Maas, M., Mertz, M., Veninga, V., Bounova, G., Broeks, A., Beets-Tan, R.., de Wijkerslooth, T.R., van Lent, A.U., Marsman, H.A., Nuijten, E., … Haanen, J.B. (2020). Neoadjuvant immunotherapy leads to pathological responses in MMR-proficient and MMR-deficient early-stage colon cancers. Nature medicine, 26(4), 566–576. doi:10.1038/s41591-020-0805-8

Chan, D.S.M., Lau, R., Aune, D., Vieira, R., Greenwood, D.C., Kampman, E. and Norat, T. (2011). Red and Processed Meat and Colorectal Cancer Incidence: Meta-Analysis of Prospective Studies. PLoS ONE, 6(6), p.e20456. doi:10.1371/journal.pone.0020456.

Chassaing, B., Aitken, J.D., Malleshappa, M. and Vijay-Kumar, M. (2014). Dextran sulfate sodium (DSS)-induced colitis in mice. Current protocols in immunology, 104, 15.25.1–15.25.14. doi:10.1002/0471142735.im1525s104

Chatila, W.K., Kim, J.K., Walch, H., Marco, M.R., Chen, C.T., Wu, F., Omer, D. M., Khalil, D.N., Ganesh, K., Qu, X., Luthra, A., Choi, S.H., Ho, Y.J., Kundra, R., Groves, K.I., Chow, O.S., Cercek, A., Weiser, M.R., Widmar, M., Wei, I.H., … Garcia-Aguilar, J. (2022). Genomic and transcriptomic determinants of response to neoadjuvant therapy in rectal cancer. Nature medicine, 28(8), 1646–1655. doi:10.1038/s41591-022-01930-z

Chen, E.X., Jonker, D.J., Loree, J.M., Kennecke, H.F., Berry, S.R., Couture, F., Ahmad, C.E., Goffin, J.R., Kavan, P., Harb, M., Colwell, B., Samimi, S., Samson, B., Abbas, T., Aucoin, N., Aubin, F., Koski, S.L., Wei, A.C., Magoski, N.M., Tu, D., … O'Callaghan, C.J. (2020). Effect of Combined Immune Checkpoint Inhibition vs Best Supportive Care Alone in Patients With Advanced Colorectal Cancer: The Canadian Cancer Trials Group CO.26 Study. JAMA oncology, 6(6), 831–838. doi:10.1001/jamaoncol.2020.0910

Chen, M.B., Wu, X.Y., Yu, R., Li, C., Wang, L.Q., Shen, W. and Lu, P.H. (2012). P53 status as a predictive biomarker for patients receiving neoadjuvant radiation-based treatment: a meta-analysis in rectal cancer. PloS one, 7(9), e45388. doi:10.1371/journal.pone.0045388

Chen, M.L., Pittet, M.J., Gorelik, L., Flavell, R.A., Weissleder, R., von Boehmer, H. and Khazaie, K. (2005). Regulatory T cells suppress tumor-specific CD8 T cell cytotoxicity through TGF-beta signals in vivo. Proceedings of the National Academy of Sciences of the United States of America, 102(2), 419–424. doi:10.1073/pnas.0408197102

Chen, T.W., Huang, K.C., Chiang, S.F., Chen, W.T., Ke, T.W. and Chao, K.S.C. (2019). Prognostic relevance of programmed cell death-ligand 1 expression and CD8+ TILs in rectal cancer patients before and after neoadjuvant chemoradiotherapy. Journal of cancer research and clinical oncology, 145(4), 1043–1053. doi:10.1007/s00432-019-02874-7

Chen, X. and Song, E. (2019). Turning foes to friends: targeting cancer-associated fibroblasts. Nat Rev Drug Disc, 18(2), 99–115. https://doi.org/10.1038/s41573-018-0004-1

Chen, X.L., Chen, Z.Q., Zhu, S.L., Liu, T.W., Wen, Y., Su, Y.S., Xi, X.J., Hu, Y., Lian, L. and Liu, F.B. (2017). Prognostic value of transforming growth factor-beta in patients with colorectal cancer who undergo surgery: a meta-analysis. BMC cancer, 17(1), 240. doi:10.1186/s12885-017-3215-7

Chow, O.S., Kuk, D., Keskin, M., Smith, J.J., Camacho, N., Pelossof, R., Chen, C.T., Chen, Z., Avila, K., Weiser, M.R., Berger, M.F., Patil, S., Bergsland, E. and Garcia-Aguilar, J. (2016). KRAS and Combined KRAS/TP53 Mutations in Locally Advanced Rectal Cancer are Independently Associated with Decreased Response to Neoadjuvant Therapy. Annals of surgical oncology, 23(8), 2548–2555. doi:10.1245/s10434-016-5205-4

Chung, S., Overstreet, J.M., Li, Y., Wang, Y., Niu, A., Wang, S., Fan, X., Sasaki, K., Jin, G.N., Khodo, S.N., Gewin, L., Zhang, M.Z. and Harris, R.C. (2018). TGF-β promotes fibrosis after severe acute kidney injury by enhancing renal macrophage infiltration. JCI insight, 3(21), e123563. doi:10.1172/jci.insight.123563

Church, D.M., Schneider, V.A., Graves, T., Auger, K., Cunningham, F., Bouk, N., Chen, H.C., Agarwala, R., McLaren, W.M., Ritchie, G.R., Albracht, D., Kremitzki, M., Rock, S., Kotkiewicz, H., Kremitzki, C., Wollam, A., Trani, L., Fulton, L., Fulton, R., Matthews, L. and Hubbard, T. (2011). Modernizing reference genome assemblies. PLoS biology, 9(7), e1001091. doi:10.1371/journal.pbio.1001091

Ciardiello, D., Elez, E., Tabernero, J. and Seoane, J. (2020). Clinical development of therapies targeting TGFβ: current knowledge and future perspectives. Annals of oncology: official journal of the European Society for Medical Oncology, 31(10), 1336–1349. doi:10.1016/j.annonc.2020.07.009

Ciccia, A. and Elledge, S.J. (2010). The DNA damage response: making it safe to play with knives. Molecular cell, 40(2), 179–204. doi:10.1016/j.molcel.2010.09.019

Clark, S., Cuthill, V., Hawkins, J., Hyer, W., Latchford, A., Sinha, A., Din, F., Beggs, A., Desai, A., Morton, D., Hitchen, D., Hill, J., Lalloo, F., Newton, K., Pugh, S., Dolwani, S., Hargest, R., Horwood, J., Ramaraj, R., Rogers, M., Collins, P., McNichol, F., Beck, N., Side, L. and McDermott, F. (2023). Hereditary gastrointestinal polyposis syndromes Rare Disease Collaborative Network consensus statement agreed at the RDCN meeting Birmingham 17th February 2022. BJC Reports, 1(10), doi:10.1038/s44276-023-00011-z

Clarkson, R., Lindsay, P.E., Ansell, S., Wilson, G., Jelveh, S., Hill, R.P. and Jaffray, D.A. (2011). Characterization of image quality and image-guidance performance of a preclinical microirradiator. Medical physics, 38(2), 845–856. doi:10.1118/1.3533947

Clevers H. (2006). Wnt/ß-Catenin Signaling in Development and Disease. Cell, 127(3), 469-80. doi:10.1016/j.cell.2006.10.018

Clevers H. (2011). The cancer stem cell: premises, promises and challenges. Nature medicine, 17(3), 313–319. doi:10.1038/nm.2304

Cohen, R., Rousseau, B., Vidal, J., Colle, R., Diaz Jr, L.A. and André, T. (2020). Immune Checkpoint Inhibition in Colorectal Cancer: Microsatellite Instability and Beyond. Targeted oncology, 15(1), 11–24. doi:10.1007/s11523-019-00690-0

Colton, M., Cheadle, E.J., Honeychurch, J. and Illidge, T.M. (2020). Reprogramming the tumour microenvironment by radiotherapy: implications for radiotherapy and immunotherapy combinations. Radiation oncology, 15(1), 254. doi:10.1186/s13014-020-01678-1

Cong, L., Ran F, A., Cox, D., Lin, S., Barretto, R., Habib, N., Hsu, P.D., Wu, X., Jiang, W., Marraffini, L.A. and Zhang, F. (2013). Multiplex genome engineering using CRISPR/Cas systems. Science, 339, 819–823. doi:10.1126/science.1231143

Connolly, E.C., Saunier, E.F., Quigley, D., Luu, M.T., De Sapio, A., Hann, B., Yingling, J.M. and Akhurst, R.J. (2011). Outgrowth of drug-resistant carcinomas expressing markers of tumor aggression after long-term TβRI/II kinase inhibition with LY2109761. Cancer research, 71(6), 2339–2349. doi:10.1158/0008-5472.CAN-10-2941

Conroy, T., Bosset, J.F., Etienne, P.L., Rio, E., François, É., Mesgouez-Nebout, N., Vendrely, V., Artignan, X., Bouché, O., Gargot, D., Boige, V., Bonichon-Lamichhane, N., Louvet, C., Morand, C., de la Fouchardière, C., Lamfichekh, N., Juzyna, B., Jouffroy-Zeller, C., Rullier, E., Marchal, F., … Unicancer Gastrointestinal Group and Partenariat de Recherche en Oncologie Digestive (PRODIGE) Group. (2021). Neoadjuvant chemotherapy with FOLFIRINOX and preoperative chemoradiotherapy for patients with locally advanced rectal cancer (UNICANCER-PRODIGE 23): a multicentre, randomised, open-label, phase 3 trial. The Lancet Oncology, 22(5), 702–715. doi:10.1016/S1470-2045(21)00079-6

Contag, C.H., Jenkins, D., Contag, P.R. and Negrin, R.S. (2000). Use of reporter genes for optical measurements of neoplastic disease in vivo. Neoplasia, 2(1-2), 41–52. doi:10.1038/sj.neo.7900079

Corbett, T.H., Griswold, D.P., Jr, Roberts, B.J., Peckham, J.C. and Schabel, F. M., Jr (1975). Tumor induction relationships in development of transplantable cancers of the colon in mice for chemotherapy assays, with a note on carcinogen structure. Cancer research, 35(9), 2434–2439.

Corrò, C., Dutoit, V. and Koessler, T. (2021). Emerging Trends for Radio-Immunotherapy in Rectal Cancer. Cancers, 13(6), 1374. doi:10.3390/cancers13061374

Cunningham, D., Humblet, Y., Siena, S., Khayat, D., Bleiberg, H., Santoro, A., Bets, D., Mueser, M., Harstrick, A., Verslype, C., Chau, I. and Van Cutsem, E. (2004). Cetuximab Monotherapy and Cetuximab plus Irinotecan in Irinotecan-Refractory Metastatic Colorectal Cancer. New England Journal of Medicine, 351(4), pp.337–345. doi:10.1056/nejmoa033025.

Dattani, M., Heald, R.J., Goussous, G., Broadhurst, J., São Julião, G.P., Habr-Gama, A., Perez, R.O. and Moran, B.J. (2018). Oncological and Survival Outcomes in Watch and Wait Patients With a Clinical Complete Response After Neoadjuvant Chemoradiotherapy for Rectal Cancer: A Systematic Review and Pooled Analysis. Annals of surgery, 268(6), 955–967. doi:10.1097/SLA.0000000000002761

David, C.J. and Massagué, J. (2018). Contextual determinants of TGFβ action in development, immunity and cancer. Nature reviews. Molecular cell biology, 19(7), 419–435. doi:10.1038/s41580-018-0007-0

Davies, H., Bignell, G. R., Cox, C., Stephens, P., Edkins, S., Clegg, S., Teague, J., Woffendin, H., Garnett, M. J., Bottomley, W., Davis, N., Dicks, E., Ewing, R., Floyd, Y., Gray, K., Hall, S., Hawes, R., Hughes, J., Kosmidou, V., Menzies, A., … Futreal, P. A. (2002). Mutations of the BRAF gene in human cancer. Nature, 417(6892), pp. 949–954. doi:10.1038/nature00766.

Day, F.L., Jorissen, R.N., Lipton, L., Mouradov, D., Sakthianandeswaren, A., Christie, M., Li, S., Tsui, C., Tie, J., Desai, J., Xu, Z.Z., Molloy, P., Whitehall, V., Leggett, B.A., Jones, I.T., McLaughlin, S., Ward, R.L., Hawkins, N.J., Ruszkiewicz, A.R., Moore, J., … Sieber, O.M. (2013). PIK3CA and PTEN gene and exon mutation-specific clinicopathologic and molecular associations in colorectal cancer. Clinical cancer research, 19(12), 3285–3296. doi:10.1158/1078-0432.CCR-12-3614

De Robertis, M., Massi, E., Poeta, M.L., Carotti, S., Morini, S., Cecchetelli, L., Signori, E. and Fazio, V.M. (2011). The AOM/DSS murine model for the study of colon carcinogenesis: From pathways to diagnosis and therapy studies. Journal of carcinogenesis, 10, 9. doi:10.4103/1477-3163.78279

Dekker, E., Tanis, P.J., Vleugels, J.L.A., Kasi, P.M. and Wallace, M.B. (2019). Colorectal cancer. The Lancet, 394(10207), pp.1467–1480. doi:10.1016/s0140-6736(19)32319-0.

Delaney, G., Jacob, S., Featherstone, C. and Barton, M. (2005). The role of radiotherapy in cancer treatment: estimating optimal utilization from a review of evidence-based clinical guidelines. Cancer, 104(6), 1129–1137. doi:10.1002/cncr.21324

Demaria, S., Kawashima, N., Yang, A.M., Devitt, M.L., Babb, J.S., Allison, J.P. and Formenti, S.C. (2005). Immune-mediated inhibition of metastases after treatment with local radiation and CTLA-4 blockade in a mouse model of breast cancer. Clinical cancer research, 11(2 Pt 1), 728–734.

Demaria, S., Golden, E.B. and Formenti, S.C. (2015). Role of Local Radiation Therapy in Cancer Immunotherapy. JAMA oncology, 1(9), 1325–1332. doi:10.1001/jamaoncol.2015.2756

Deng, L., Liang, H., Burnette, B., Beckett, M., Darga, T., Weichselbaum, R.R. and Fu, Y.X. (2014). Irradiation and anti-PD-L1 treatment synergistically promote antitumor immunity in mice. The Journal of clinical investigation, 124(2), 687–695. doi:10.1172/JCI67313

Deville, S.S. and Cordes, N. (2019). The Extracellular, Cellular, and Nuclear Stiffness, a Trinity in the Cancer Resistome-A Review. Frontiers in oncology, 9, 1376. doi:10.3389/fonc.2019.01376

Dewan, M.Z., Galloway, A.E., Kawashima, N., Dewyngaert, J.K., Babb, J.S., Formenti, S.C. and Demaria, S. (2009). Fractionated but not single-dose radiotherapy induces an immune-mediated abscopal effect when combined with anti-CTLA-4 antibody. Clinical cancer research, 15(17), 5379–5388. doi:10.1158/1078-0432.CCR-09-0265

Diamandis, M., White, N.M.A. and Yousef, G.M. (2010). Personalized Medicine: Marking a New Epoch in Cancer Patient Management. Molecular Cancer Research, 8(9), pp.1175–1187. doi:10.1158/1541-7786.MCR-10-0264.

Domingo, E., Rathee, S., Blake, A., Samuel, L., Murray, G., Sebag-Montefiore, D., Gollins, S., West, N., Begum, R., Duggan, M., White, L., Hassanieh, S., Richman, S., Quirke, P., Robineau, J., Redmond, K., Chatzipli, A., McDermott, U., Koelzer, V., Leedham, S., Tomlinson, I., Dunne, P., Buffa, F. and Maughan, T. (2021). The immune infiltrate, TGFb signalling and APC mutation determine complete response to radiation in rectal cancer. NCRI Cancer Conference (Abstract).

Dong, H., Strome, S.E., Salomao, D.R., Tamura, H., Hirano, F., Flies, D.B., Roche, P.C., Lu, J., Zhu, G., Tamada, K., Lennon, V.A., Celis, E. and Chen, L. (2002). Tumor-associated B7-H1 promotes T-cell apoptosis: a potential mechanism of immune evasion. Nature medicine, 8(8), 793–800. doi:10.1038/nm730

van Dongen, J.J., Krissansen, G.W., Wolvers-Tettero, I.L., Comans-Bitter, W.M., Adriaansen, H.J., Hooijkaas, H., van Wering, E.R. and Terhorst, C. (1988). Cytoplasmic expression of the CD3 antigen as a diagnostic marker for immature T-cell malignancies. Blood, 71(3), 603–612.

Donigan, M., Norcross, L.S., Aversa, J., Colon, J., Smith, J., Madero-Visbal, R., Li, S., McCollum, N., Ferrara, A., Gallagher, J.T. and Baker, C.H. (2009). Novel murine model for colon cancer: non-operative trans-anal rectal injection. The Journal of surgical research, 154(2), 299–303. doi:10.1016/j.jss.2008.05.028

Donkor, M.K., Sarkar, A., Savage, P.A., Franklin, R.A., Johnson, L.K., Jungbluth, A.A., Allison, J.P. and Li, M.O. (2011). T cell surveillance of oncogene-induced prostate cancer is impeded by T cell-derived TGF-β1 cytokine. Immunity, 35(1), 123–134. doi:10.1016/j.immuni.2011.04.019

Douglas, J.K., Callahan, R.E., Hothem, Z.A., Cousineau, C.S., Kawak, S., Thibodeau, B.J., Bergeron, S., Li, W., Peeples, C.E. and Wasvary, H.J. (2020). Genomic variation as a marker of response to neoadjuvant therapy in locally advanced rectal cancer. Molecular & cellular oncology, 7(3), 1716618. doi:10.1080/23723556.2020.1716618

Dovedi, S.J., Adlard, A.L., Lipowska-Bhalla, G., McKenna, C., Jones, S., Cheadle, E.J., Stratford, I.J., Poon, E., Morrow, M., Stewart, R., Jones, H., Wilkinson, R.W., Honeychurch, J. and Illidge, T.M. (2014). Acquired resistance to fractionated radiotherapy can be overcome by concurrent PD-L1 blockade. Cancer research, 74(19), 5458–5468. doi:10.1158/0008-5472.CAN-14-1258

Dovedi, S.J., Cheadle, E.J., Popple, A.L., Poon, E., Morrow, M., Stewart, R., Yusko, E.C., Sanders, C.M., Vignali, M., Emerson, R.O., Robins, H.S., Wilkinson, R.W., Honeychurch, J. and Illidge, T.M. (2017). Fractionated Radiation Therapy Stimulates Antitumor Immunity Mediated by Both Resident and Infiltrating

Polyclonal T-cell Populations when Combined with PD-1 Blockade. Clinical cancer research, 23(18), 5514–5526. doi:10.1158/1078-0432.CCR-16-1673

Downing, A., Glaser, A.W., Finan, P.J., Wright, P., Thomas, J.D., Gilbert, A., Corner, J., Richards, M., Morris, E.J.A. and Sebag-Montefiore, D. (2019). Functional Outcomes and Health-Related Quality of Life After Curative Treatment for Rectal Cancer: A Population-Level Study in England. International journal of radiation oncology, biology, physics, 103(5), 1132–1142. doi:10.1016/j.ijrobp.2018.12.005

Dreyer, S.B., Powell, A.G., McSorley, S.T., Waterston, A., Going, J.J., Edwards, J., McMillan, D.C. and Horgan, P.G. (2017). The Pretreatment Systemic Inflammatory Response is an Important Determinant of Poor Pathologic Response for Patients Undergoing Neoadjuvant Therapy for Rectal Cancer. Annals of surgical oncology, 24(5), 1295–1303. doi:10.1245/s10434-016-5684-3

Drost, J., van Jaarsveld, R.H., Ponsioen, B., Zimberlin, C., van Boxtel, R., Buijs, A., Sachs, N., Overmeer, R.M., Offerhaus, G.J., Begthel, H., Korving, J., van de Wetering, M., Schwank, G., Logtenberg, M., Cuppen, E., Snippert, H.J., Medema, J.P., Kops, G.J. and Clevers, H. (2015). Sequential cancer mutations in cultured human intestinal stem cells. Nature, 521(7550), 43–47. doi:10.1038/nature14415

Drost, J. and Clevers, H. (2018). Organoids in cancer research. Nature reviews. Cancer, 18(7), 407–418. doi:10.1038/s41568-018-0007-6

Dunn, G.P., Old, L.J. and Schreiber, R.D. (2004). The three Es of cancer immunoediting. Annual review of immunology, 22, 329–360. doi:10.1146/annurev.immunol.22.012703.104803

Dunne, P.D., McArt, D.G., Bradley, C.A., O'Reilly, P.G., Barrett, H.L., Cummins, R., O'Grady, T., Arthur, K., Loughrey, M.B., Allen, W.L., McDade, S.S., Waugh, D.J., Hamilton, P.W., Longley, D.B., Kay, E.W., Johnston, P.G., Lawler, M., Salto-Tellez, M. and Van Schaeybroeck, S. (2016). Challenging the Cancer Molecular Stratification Dogma: Intratumoral Heterogeneity Undermines Consensus Molecular Subtypes and Potential Diagnostic Value in Colorectal Cancer. Clinical cancer research, 22(16), 4095–4104. doi:10.1158/1078-0432.CCR-16-0032

Dworak, O., Keilholz, L. and Hoffmann, A. (1997). Pathological features of rectal cancer after preoperative radiochemotherapy. International journal of colorectal disease, 12(1), 19–23. doi:10.1007/s003840050072

Eaden, J.A., Abrams, K.R. and Mayberry, J.F. (2001). The risk of colorectal cancer in ulcerative colitis: a meta-analysis. Gut, 48(4), 526–535. doi:10.1136/gut.48.4.526

Eberhart, C.E., Coffey, R.J., Radhika, A., Giardiello, F.M., Ferrenbach, S. and DuBois, R.N. (1994). Up-regulation of cyclooxygenase 2 gene expression in human colorectal adenomas and adenocarcinomas. Gastroenterology, 107(4), 1183–1188. doi:10.1016/0016-5085(94)90246-1

Efremova, M., Rieder, D., Klepsch, V., Charoentong, P., Finotello, F., Hackl, H., Hermann-Kleiter, N., Löwer, M., Baier, G., Krogsdam, A. and Trajanoski, Z. (2018). Targeting immune checkpoints potentiates immunoediting and changes

the dynamics of tumor evolution. Nature communications, 9(1), 32. doi:10.1038/s41467-017-02424-0

Eggermont, A.M., Chiarion-Sileni, V., Grob, J.J., Dummer, R., Wolchok, J.D., Schmidt, H., Hamid, O., Robert, C., Ascierto, P.A., Richards, J.M., Lebbé, C., Ferraresi, V., Smylie, M., Weber, J.S., Maio, M., Bastholt, L., Mortier, L., Thomas, L., Tahir, S., Hauschild, A., … Testori, A. (2016). Prolonged Survival in Stage III Melanoma with Ipilimumab Adjuvant Therapy. The New England journal of medicine, 375(19), 1845–1855. doi:10.1056/NEJMoa1611299

Emmertsen, K.J. and Laurberg, S. (2012). Low anterior resection syndrome score: development and validation of a symptom-based scoring system for bowel dysfunction after low anterior resection for rectal cancer. Annals of surgery, 255(5), 922–928. doi:10.1097/SLA.0b013e31824f1c21

Enquist, I.B., Good, Z., Jubb, A.M., Fuh, G., Wang, X., Junttila, M.R., Jackson, E.L. and Leong, K.G. (2014). Lymph node-independent liver metastasis in a model of metastatic colorectal cancer. Nature communications, 5, 3530. doi:10.1038/ncomms4530

Erlandsson, J., Lörinc, E., Ahlberg, M., Pettersson, D., Holm, T., Glimelius, B. and Martling, A. (2019). Tumour regression after radiotherapy for rectal cancer - Results from the randomised Stockholm III trial. Radiotherapy and oncology : journal of the European Society for Therapeutic Radiology and Oncology, 135, 178–186. doi:10.1016/j.radonc.2019.03.016

Evrard, M., Kwok, I.W.H., Chong, S.Z., Teng, K.W.W., Becht, E., Chen, J., Sieow, J.L., Penny, H.L., Ching, G.C., Devi, S., Adrover, J.M., Li, J.L.Y., Liong, K.H., Tan, L., Poon, Z., Foo, S., Chua, J.W., Su, I.H., Balabanian, K., Bachelerie, F.… Ng, L. G. (2018). Developmental Analysis of Bone Marrow Neutrophils Reveals Populations Specialized in Expansion, Trafficking, and Effector Functions. Immunity, 48(2), 364–379.e8. doi:10.1016/j.immuni.2018.02.002

Fabrizio, D.A., George Jr, T.J., Dunne, R.F., Frampton, G., Sun, J., Gowen, K., Kennedy, M., Greenbowe, J., Schrock, A.B., Hezel, A.F., Ross, J.S., Stephens, P.J., Ali, S.M., Miller, V.A., Fakih, M. and Klempner, S.J. (2018). Beyond microsatellite testing: assessment of tumor mutational burden identifies subsets of colorectal cancer who may respond to immune checkpoint inhibition. Journal of gastrointestinal oncology, 9(4), 610–617. doi:10.21037/jgo.2018.05.06

Farhood, B., Khodamoradi, E., Hoseini-Ghahfarokhi, M., Motevaseli, E., Mirtavoos-Mahyari, H., Eleojo Musa, A. and Najafi, M. (2020). TGF-β in radiotherapy: Mechanisms of tumor resistance and normal tissues injury. Pharmacological research, 155, 104745. doi:10.1016/j.phrs.2020.104745

Fearnhead, N.S., Britton, M.P. and Bodmer, W.F. (2001). The ABC of APC. Human Molecular Genetics, 10(7), pp. 721–733. doi:10.1093/hmg/10.7.721.

Fearon, E.R. and Vogelstein, B. (1990). A genetic model for colorectal tumorigenesis. Cell, 61(5), pp. 759–767. doi:10.1016/0092-8674(90)90186-i.

Fearon, E.R., Cho, K.R., Nigro, J.M., Kern, S.E., Simons, J.W., Ruppert, J.M., Hamilton, S.R., Preisinger, A.C., Thomas, G., Kinzler, K.W. and Vogelstein, B. (1990). Identification of a Chromosome 18q Gene that Is Altered in Colorectal Cancers. Science, 247(4938), pp. 49–56. doi:10.1126/science.2294591.

Fedirko, V., Tramacere, I., Bagnardi, V., Rota, M., Scotti, L., Islami, F., Negri, E., Straif, K., Romieu, I., La Vecchia, C., Boffetta, P., & Jenab, M. (2011). Alcohol drinking and colorectal cancer risk: an overall and dose-response meta-analysis of published studies. Annals of oncology, 22(9), 1958–1972. doi:10.1093/annonc/mdq653

Fei, P. and El-Deiry, W.S. (2003). P53 and radiation responses. Oncogene, 22(37), 5774–5783. doi:10.1038/sj.onc.1206677

Feil, S., Valtcheva, N. and Feil, R. (2009). Inducible Cre mice. Methods in molecular biology, 530, 343–363. doi:10.1007/978-1-59745-471-1_18

Fernandez-Martos, C., Garcia-Albeniz, X., Pericay, C., Maurel, J., Aparicio, J., Montagut, C., Safont, M.J., Salud, A., Vera, R., Massuti, B., Escudero, P., Alonso, V., Bosch, C., Martin, M. and Minsky, B.D. (2015). Chemoradiation, surgery and adjuvant chemotherapy versus induction chemotherapy followed by chemoradiation and surgery: long-term results of the Spanish GCR-3 phase II randomized trial†. Annals of oncology, 26(8), 1722–1728. doi:10.1093/annonc/mdv223

Fernebro, E., Halvarsson, B., Baldetorp, B. and Nilbert, M. (2002). Predominance of CIN versus MSI in the development of rectal cancer at young age. BMC cancer, 2, 25. doi:10.1186/1471-2407-2-25

Fessler, E., Drost, J., van Hooff, S.R., Linnekamp, J.F., Wang, X., Jansen, M., De Sousa E Melo, F., Prasetyanti, P.R., IJspeert, J.E., Franitza, M., Nürnberg, P., van Noesel, C.J., Dekker, E., Vermeulen, L., Clevers, H. and Medema, J.P. (2016). TGFβ signaling directs serrated adenomas to the mesenchymal colorectal cancer subtype. EMBO molecular medicine, 8(7), 745–760. doi:10.15252/emmm.201606184

Fidler I.J. (1991). Orthotopic implantation of human colon carcinomas into nude mice provides a valuable model for the biology and therapy of metastasis. Cancer metastasis reviews, 10(3), 229–243. doi:10.1007/BF00050794

Filatenkov, A., Baker, J., Mueller, A.M., Kenkel, J., Ahn, G.O., Dutt, S., Zhang, N., Kohrt, H., Jensen, K., Dejbakhsh-Jones, S., Shizuru, J.A., Negrin, R.N., Engleman, E.G. and Strober, S. (2015). Ablative Tumor Radiation Can Change the Tumor Immune Cell Microenvironment to Induce Durable Complete Remissions. Clinical cancer research, 21(16), 3727–3739. doi:10.1158/1078-0432.CCR-14-2824

Fleshman, J., Sargent, D.J., Green, E., Anvari, M., Stryker, S.J., Beart, R.W., Jr, Hellinger, M., Flanagan, R., Jr, Peters, W., Nelson, H. and Clinical Outcomes of Surgical Therapy Study Group (2007). Laparoscopic colectomy for cancer is not inferior to open surgery based on 5-year data from the COST Study Group trial. Annals of surgery, 246(4), 655–664. doi:10.1097/SLA.0b013e318155a762

Fleshman, J., Branda, M., Sargent, D.J., Boller, A.M., George, V., Abbas, M., Peters, W.R., Jr, Maun, D., Chang, G., Herline, A., Fichera, A., Mutch, M., Wexner, S., Whiteford, M., Marks, J., Birnbaum, E., Margolin, D., Larson, D., Marcello, P., Posner, M., … Nelson, H. (2015). Effect of Laparoscopic-Assisted Resection vs Open Resection of Stage II or III Rectal Cancer on Pathologic Outcomes: The ACOSOG Z6051 Randomized Clinical Trial. JAMA, 314(13), 1346–1355. doi:10.1001/jama.2015.10529

Fokas, E., Liersch, T., Fietkau, R., Hohenberger, W., Beissbarth, T., Hess, C., Becker, H., Ghadimi, M., Mrak, K., Merkel, S., Raab, H.R., Sauer, R., Wittekind, C. and Rödel, C. (2014). Tumor regression grading after preoperative chemoradiotherapy for locally advanced rectal carcinoma revisited: updated results of the CAO/ARO/AIO-94 trial. Journal of clinical oncology, 32(15), 1554–1562. doi:10.1200/JCO.2013.54.3769

Fokas, E., Allgäuer, M., Polat, B., Klautke, G., Grabenbauer, G.G., Fietkau, R., Kuhnt, T., Staib, L., Brunner, T., Grosu, A.L., Schmiegel, W., Jacobasch, L., Weitz, J., Folprecht, G., Schlenska-Lange, A., Flentje, M., Germer, C.T., Grützmann, R., Schwarzbach, M., Paolucci, V., … German Rectal Cancer Study Group. (2019). Randomized Phase II Trial of Chemoradiotherapy Plus Induction or Consolidation Chemotherapy as Total Neoadjuvant Therapy for Locally Advanced Rectal Cancer: CAO/ARO/AIO-12. Journal of clinical oncology, 37(34), 3212–3222. doi:10.1200/JCO.19.00308

Folkesson, J., Birgisson, H., Pahlman, L., Cedermark, B., Glimelius, B. and Gunnarsson, U. (2005). Swedish Rectal Cancer Trial: long lasting benefits from radiotherapy on survival and local recurrence rate. Journal of clinical oncology, 23(24), 5644–5650. doi:10.1200/JCO.2005.08.144

Formenti, S.C. and Demaria, S. (2012). Radiation therapy to convert the tumor into an in situ vaccine. International journal of radiation oncology, biology, physics, 84(4), 879–880. doi:10.1016/j.ijrobp.2012.06.020

Formenti, S. C. and Demaria, S. (2013). Combining radiotherapy and cancer immunotherapy: a paradigm shift. Journal of the National Cancer Institute, 105(4), 256–265. doi:10.1093/jnci/djs629

Formenti SC, Lee P, Adams S, Goldberg JD, Li X, Xie MW, Ratikan JA, Felix C, Hwang L, Faull KF, Sayre JW, Hurvitz S, Glaspy JA, Comin-Anduix B, Demaria S, Schaue D, McBride WH. (2018). Focal Irradiation and Systemic TGFß Blockade in Metastatic Breast Cancer. Clin Cancer Res, 24(11), 2493-2504. doi: 10.1158/1078-0432.CCR-17-3322

Forrester, K., Almoguera, C., Han, K., Grizzle, W.E. and Perucho, M. (1987). Detection of high incidence of K-ras oncogenes during human colon tumorigenesis. Nature, 327(6120), pp. 298–303. doi:10.1038/327298a0.

Forssell, J., Oberg, A., Henriksson, M.L., Stenling, R., Jung, A. and Palmqvist, R. (2007). High macrophage infiltration along the tumor front correlates with improved survival in colon cancer. Clinical cancer research: an official journal of the American Association for Cancer Research, 13(5), 1472–1479. doi:10.1158/1078-0432.CCR-06-2073

Frangogiannis N. (2020). Transforming growth factor-ß in tissue fibrosis. The Journal of experimental medicine, 217(3), e20190103. doi:10.1084/jem.20190103

Freeling, J.L. and Rezvani, K. (2016). Assessment of murine colorectal cancer by micro-ultrasound using three dimensional reconstruction and non-linear contrast imaging. Molecular therapy. Methods & clinical development, 5, 16070. doi:10.1038/mtm.2016.70

Frey, B., Rückert, M., Weber, J., Mayr, X., Derer, A., Lotter, M., Bert, C., Rödel, F., Fietkau, R. and Gaipl, U.S. (2017). Hypofractionated Irradiation Has Immune

Stimulatory Potential and Induces a Timely Restricted Infiltration of Immune Cells in Colon Cancer Tumors. Frontiers in immunology, 8, 231. doi:10.3389/fimmu.2017.00231

Friedman, A.A., Letai, A., Fisher, D.E. and Flaherty, K.T. (2015). Precision medicine for cancer with next-generation functional diagnostics. Nature reviews. Cancer, 15(12), 747–756. doi:10.1038/nrc4015

Friedman R. (2016). Drug resistance in cancer: molecular evolution and compensatory proliferation. Oncotarget, 7(11), 11746–11755. doi:10.18632/oncotarget.7459

Frykholm, G.J., Glimelius, B. and Påhlman, L. (1993). Preoperative or postoperative irradiation in adenocarcinoma of the rectum: final treatment results of a randomized trial and an evaluation of late secondary effects. Diseases of the colon and rectum, 36(6), 564–572. doi:10.1007/BF02049863

Fu, X.Y., Besterman, J.M., Monosov, A. and Hoffman, R.M. (1991). Models of human metastatic colon cancer in nude mice orthotopically constructed by using histologically intact patient specimens. Proceedings of the National Academy of Sciences of the United States of America, 88(20), 9345–9349. doi:10.1073/pnas.88.20.9345

Fujii, M., Shimokawa, M., Date, S., Takano, A., Matano, M., Nanki, K., Ohta, Y., Toshimitsu, K., Nakazato, Y., Kawasaki, K., Uraoka, T., Watanabe, T., Kanai, T. and Sato, T. (2016). A Colorectal Tumor Organoid Library Demonstrates Progressive Loss of Niche Factor Requirements during Tumorigenesis. Cell stem cell, 18(6), 827–838. doi:10.1016/j.stem.2016.04.003

Fujiwara, Y., Nokihara, H., Yamada, Y., Yamamoto, N., Sunami, K., Utsumi, H., Asou, H., TakahashI, O., Ogasawara, K., Gueorguieva, I. and Tamura, T. (2015). Phase 1 study of galunisertib, a TGF-beta receptor I kinase inhibitor, in Japanese patients with advanced solid tumors. Cancer chemotherapy and pharmacology, 76(6), 1143–1152. doi:10.1007/s00280-015-2895-4

Fukata, M., Chen, A., Vamadevan, A.S., Cohen, J., Breglio, K., Krishnareddy, S., Hsu, D., Xu, R., Harpaz, N., Dannenberg, A.J., Subbaramaiah, K., Cooper, H.S., Itzkowitz, S.H. and Abreu, M.T. (2007). Toll-like receptor-4 promotes the development of colitis-associated colorectal tumors. Gastroenterology, 133(6), 1869–1881. doi:10.1053/j.gastro.2007.09.008

Fumagalli, A., Drost, J., Suijkerbuijk, S.J., van Boxtel, R., de Ligt, J., Offerhaus, G.J., Begthel, H., Beerling, E., Tan, E.H., Sansom, O.J., Cuppen, E., Clevers, H. and van Rheenen, J. (2017). Genetic dissection of colorectal cancer progression by orthotopic transplantation of engineered cancer organoids. Proceedings of the National Academy of Sciences of the United States of America, 114(12), E2357–E2364. doi:10.1073/pnas.1701219114

Fumagalli, A., Suijkerbuijk, S.J.E., Begthel, H., Beerling, E., Oost, K.C., Snippert, H.J., van Rheenen, J. and Drost, J. (2018). A surgical orthotopic organoid transplantation approach in mice to visualize and study colorectal cancer progression. Nature protocols, 13(2), 235–247. doi:10.1038/nprot.2017.137

Gajewski, T.F., Schreiber, H. and Fu, Y.X. (2013). Innate and adaptive immune cells in the tumor microenvironment. Nature immunology, 14(10), 1014–1022. doi:10.1038/ni.2703

Galiatsatos, P. and Foulkes, W.D. (2006). Familial Adenomatous Polyposis. The American Journal of Gastroenterology, 101(2), pp.385–398. doi:10.1111/j.1572-0241.2006.00375.x.

Galon, J., Costes, A., Sanchez-Cabo, F., Kirilovsky, A., Mlecnik, B., Lagorce-Pagès, C., Tosolini, M., Camus, M., Berger, A., Wind, P., Zinzindohoué, F., Bruneval, P., Cugnenc, P.H., Trajanoski, Z., Fridman, W.H. and Pagès, F. (2006). Type, density, and location of immune cells within human colorectal tumors predict clinical outcome. Science, 313(5795), 1960–1964. doi:10.1126/science.1129139

Ganesh, K. and Massagué, J. (2018). TGF-ß Inhibition and Immunotherapy: Checkmate. Immunity, 48(4), 626–628. doi:10.1016/j.immuni.2018.03.037

Ganesh, K., Stadler, Z.K., Cercek, A., Mendelsohn, R.B., Shia, J., Segal, N.H. and Diaz Jr, L. (2019). Immunotherapy in colorectal cancer: rationale, challenges and potential. Nature reviews Gastroenterology & hepatology, 16(6), 361–375. doi:10.1038/s41575-019-0126-x

Ganesh, K., Wu, C., O'Rourke, K.P., Szeglin, B.C., Zheng, Y., Sauvé, C.G., Adileh, M., Wasserman, I., Marco, M.R., Kim, A.S., Shady, M., Sanchez-Vega, F., Karthaus, W.R., Won, H.H., Choi, S.H., Pelossof, R., Barlas, A., Ntiamoah, P., Pappou, E., Elghouayel, A., … Smith, J. J. (2019). A rectal cancer organoid platform to study individual responses to chemoradiation. Nature medicine, 25(10), 1607–1614. doi:10.1038/s41591-019-0584-2

Gao, J., Zhang, X., Yang, Z., Zhang, J., Bai, Z., Deng, W., Chen, G., Xu, R., Wei, Q., Liu, Y., Han, J., Li, A., Liu, G., Sun, Y., Kong, D., Yao, H. and Zhang, Z. (2023). Interim result of phase II, prospective, single-arm trial of long-course chemoradiotherapy combined with concurrent tislelizumab in locally advanced rectal cancer. Frontiers in oncology, 13, 1057947. doi:10.3389/fonc.2023.1057947

Garcia-Aguilar, J., Chow, O.S., Smith, D.D., Marcet, J.E., Cataldo, P.A., Varma, M.G., Kumar, A.S., Oommen, S., Coutsoftides, T., Hunt, S.R., Stamos, M.J., Ternent, C.A., Herzig, D.O., Fichera, A., Polite, B.N., Dietz, D.W., Patil, S., Avila, K. and Timing of Rectal Cancer Response to Chemoradiation Consortium (2015). Effect of adding mFOLFOX6 after neoadjuvant chemoradiation in locally advanced rectal cancer: a multicentre, phase 2 trial. The Lancet Oncology, 16(8), 957–966. doi:10.1016/S1470-2045(15)00004-2

Garcia-Aguilar, J., Renfro, L.A., Chow, O.S., Shi, Q., Carrero, X.W., Lynn, P.B., Thomas, C.R., Jr, Chan, E., Cataldo, P.A., Marcet, J.E., Medich, D.S., Johnson, C.S., Oommen, S.C., Wolff, B.G., Pigazzi, A., McNevin, S.M., Pons, R.K. and Bleday, R. (2015). Organ preservation for clinical T2N0 distal rectal cancer using neoadjuvant chemoradiotherapy and local excision (ACOSOG Z6041): results of an open-label, single-arm, multi-institutional, phase 2 trial. The Lancet. Oncology, 16(15), 1537–1546. doi:10.1016/S1470-2045(15)00215-6

Garcia-Aguilar, J., Patil, S., Gollub, M.J., Kim, J.K., Yuval, J.B., Thompson, H. M., Verheij, F.S., Omer, D.M., Lee, M., Dunne, R.F., Marcet, J., Cataldo, P., Polite, B., Herzig, D.O., Liska, D., Oommen, S., Friel, C.M., Ternent, C.,

Coveler, A.L., Hunt, S., … Saltz, L.B. (2022). Organ Preservation in Patients With Rectal Adenocarcinoma Treated With Total Neoadjuvant Therapy. Journal of clinical oncology, 40(23), 2546–2556. doi:10.1200/JCO.22.00032

Gavaruzzi, T., Lotto, L., Giandomenico, F., Perin, A. and Pucciarelli, S. (2014). Patient-reported outcomes after neoadjuvant therapy for rectal cancer: a systematic review. Expert review of anticancer therapy, 14(8), 901–918. doi:10.1586/14737140.2014.911090

George Jr, T.J., Allegra, C.J. and Yothers, G. (2015). Neoadjuvant Rectal (NAR) Score: a New Surrogate Endpoint in Rectal Cancer Clinical Trials. Current colorectal cancer reports, 11(5), 275–280. doi:10.1007/s11888-015-0285-2

Gérard, J.P., Conroy, T., Bonnetain, F., Bouché, O., Chapet, O., Closon-Dejardin, M.T., Untereiner, M., Leduc, B., Francois, E., Maurel, J., Seitz, J.F., Buecher, B., Mackiewicz, R., Ducreux, M. and Bedenne, L. (2006). Preoperative radiotherapy with or without concurrent fluorouracil and leucovorin in T3-4 rectal cancers: results of FFCD 9203. Journal of clinical oncology, 24(28), 4620–4625. doi:10.1200/JCO.2006.06.7629

Ghita, M., McMahon, S.J., Thompson, H.F., McGarry, C.K., King, R., Osman, S. O.S., Kane, J.L., Tulk, A., Schettino, G., Butterworth, K.T., Hounsell, A.R. and Prise, K.M. (2017). Small field dosimetry for the small animal radiotherapy research platform (SARRP). Radiation oncology, 12(1), 204. doi:10.1186/s13014-017-0936-3

Giampieri, S., Manning, C., Hooper, S., Jones, L., Hill, C.S. and Sahai, E. (2009). Localized and reversible TGFbeta signalling switches breast cancer cells from cohesive to single cell motility. Nature cell biology, 11(11), 1287–1296. doi:10.1038/ncb1973

Giardiello, F.M., Hamilton, S.R., Krush, A.J., Piantadosi, S., Hylind, L.M., Celano, P., Booker, S.V., Robinson, C.R. and Offerhaus, G.J. (1993). Treatment of colonic and rectal adenomas with sulindac in familial adenomatous polyposis. The New England journal of medicine, 328(18), 1313–1316. doi:10.1056/NEJM199305063281805

Giglia, M.D. and Stein, S.L. (2019). Overlooked Long-Term Complications of Colorectal Surgery. Clinics in colon and rectal surgery, 32(3), 204–211. doi:10.1055/s-0038-1677027

van Gijn, W., Marijnen, C.A., Nagtegaal, I.D., Kranenbarg, E.M., Putter, H., Wiggers, T., Rutten, H.J., Påhlman, L., Glimelius, B., van de Velde, C. . and Dutch Colorectal Cancer Group. (2011). Preoperative radiotherapy combined with total mesorectal excision for resectable rectal cancer: 12-year follow-up of the multicentre, randomised controlled TME trial. The Lancet Oncology, 12(6), 575–582. doi:10.1016/S1470-2045(11)70097-3

Gillespie, M.A., Steele, C.W., Lannagan, T.R.M., Sansom, O.J. and Roxburgh, C.S.D. (2021). Pre-clinical modelling of rectal cancer to develop novel radiotherapy-based treatment strategies. Oncology reviews, 15(1), 511. doi:10.4081/oncol.2021.511

Glynne-Jones, R., Wyrwicz, L., Tiret, E., Brown, G., Rödel, C., Cervantes, A., Arnold, D. and ESMO Guidelines Committee (2017). Rectal cancer: ESMO Clinical Practice Guidelines for diagnosis, treatment and follow-up. Annals of oncology:

official journal of the European Society for Medical Oncology, 28(suppl_4), iv22–iv40. doi:10.1093/annonc/mdx224

Golden, E.B., Demaria, S., Schiff, P.B., Chachoua, A. and Formenti, S.C. (2013). An abscopal response to radiation and ipilimumab in a patient with metastatic non-small cell lung cancer. Cancer immunology research, 1(6), 365–372. doi:10.1158/2326-6066.CIR-13-0115

Gorelik, L. and Flavell, R.A. (2001). Immune-mediated eradication of tumors through the blockade of transforming growth factor-beta signaling in T cells. Nature medicine, 7(10), 1118–1122. doi:10.1038/nm1001-1118

Gorelik, L., Constant, S. and Flavell, R. A. (2002). Mechanism of transforming growth factor beta-induced inhibition of T helper type 1 differentiation. The Journal of experimental medicine, 195(11), 1499–1505. doi:10.1084/jem.20012076

Gorelik, L. and Flavell, R. A. (2002). Transforming growth factor-beta in T-cell biology. Nature reviews. Immunology, 2(1), 46–53. doi:10.1038/nri704

Grady, W.M., Myeroff, L.L., Swinler, S.E., Rajput, A., Thiagalingam, S., Lutterbaugh, J.D., Neumann, A., Brattain, M.G., Chang, J., Kim, S.J., Kinzler, K. W., Vogelstein, B., Willson, J.K. and Markowitz, S. (1999). Mutational inactivation of transforming growth factor beta receptor type II in microsatellite stable colon cancers. Cancer research, 59(2), 320–324.

Grapin, M., Richard, C., Limagne, E., Boidot, R., Morgand, V., Bertaut, A., Derangere, V., Laurent, P.A., Thibaudin, M., Fumet, J.D., Crehange, G., Ghiringhelli, F. and Mirjolet, C. (2019). Optimized fractionated radiotherapy with anti-PD-L1 and anti-TIGIT: a promising new combination. Journal for immunotherapy of cancer, 7(1), 160. doi:10.1186/s40425-019-0634-9

Gray, L.H., Conger, A.D., Ebert, M., Hornsey, S. and Scott, O.C. (1953). The concentration of oxygen dissolved in tissues at the time of irradiation as a factor in radiotherapy. The British journal of radiology, 26(312), 638–648. doi:10.1259/0007-1285-26-312-638

Greten, F.R., Eckmann, L., Greten, T.F., Park, J.M., Li, Z.W., Egan, L.J., Kagnoff, M.F. and Karin, M. (2004). IKKbeta links inflammation and tumorigenesis in a mouse model of colitis-associated cancer. Cell, 118(3), 285–296. doi:10.1016/j.cell.2004.07.013

Grivennikov, S., Karin, E., Terzic, J., Mucida, D., Yu, G.Y., Vallabhapurapu, S., Scheller, J., Rose-John, S., Cheroutre, H., Eckmann, L. and Karin, M. (2009). IL-6 and Stat3 are required for survival of intestinal epithelial cells and development of colitis-associated cancer. Cancer cell, 15(2), 103–113. doi:10.1016/j.ccr.2009.01.001

Groden, J., Thliveris, A., Samowitz, W., Carlson, M., Gelbert, L., Albertsen, H., Joslyn, G., Stevens, J., Spirio, L. and Robertson, M. (1991). Identification and characterization of the familial adenomatous polyposis coli gene. Cell, 66(3), 589–600. doi:10.1016/0092-8674(81)90021-0

Groselj, B., Ruan, J. L., Scott, H., Gorrill, J., Nicholson, J., Kelly, J., Anbalagan, S., Thompson, J., Stratford, M.R.L., Jevons, S.J., Hammond, E.M., Scudamore, C.L., Kerr, M. and Kiltie, A.E. (2018). Radiosensitization In Vivo by Histone

Deacetylase Inhibition with No Increase in Early Normal Tissue Radiation Toxicity. Molecular cancer therapeutics, 17(2), 381–392. doi:10.1158/1535-7163.MCT-17-0011

Guinney, J., Dienstmann, R., Wang, X., de Reyniès, A., Schlicker, A., Soneson, C., Marisa, L., Roepman, P., Nyamundanda, G., Angelino, P., Bot, B. M., Morris, J. S., Simon, I. M., Gerster, S., Fessler, E., De Sousa E Melo, F., Missiaglia, E., Ramay, H., Barras, D., Homicsko, K., … Tejpar, S. (2015). The consensus molecular subtypes of colorectal cancer. Nature medicine, 21(11), 1350–1356. doi:10.1038/nm.3967

Gunderson, A.J., Yamazaki, T., McCarty, K., Fox, N., Phillips, M., Alice, A., Blair, T., Whiteford, M., O'Brien, D., Ahmad, R., Kiely, M.X., Hayman, A., Crocenzi, T., Gough, M.J., Crittenden, M.R. and Young, K.H. (2020). TGFβ suppresses CD8+ T cell expression of CXCR3 and tumor trafficking. Nature communications, 11(1), 1749. doi:10.1038/s41467-020-15404-8

Gupta, A., Probst, H.C., Vuong, V., Landshammer, A., Muth, S., Yagita, H., Schwendener, R., Pruschy, M., Knuth, A. and van den Broek, M. (2012). Radiotherapy promotes tumor-specific effector CD8+ T cells via dendritic cell activation. Journal of immunology, 189(2), 558–566. doi:10.4049/jimmunol.1200563

Habr-Gama, A., Perez, R.O., Nadalin, W., Sabbaga, J., Ribeiro, U., Silva e Sousa, A.H., Campos, F.G., Kiss, D.R. and Gama-Rodrigues, J. (2004). Operative Versus Nonoperative Treatment for Stage 0 Distal Rectal Cancer Following Chemoradiation Therapy. Annals of Surgery, 240(4), pp.711–718. doi:10.1097/01.sla.0000141194.27992.32.

Haigis, K.M., Kendall, K.R., Wang, Y., Cheung, A., Haigis, M.C., Glickman, J.N., Niwa-Kawakita, M., Sweet-Cordero, A., Sebolt-Leopold, J., Shannon, K.M., Settleman, J., Giovannini, M. and Jacks, T. (2008). Differential effects of oncogenic K-Ras and N-Ras on proliferation, differentiation and tumor progression in the colon. Nature genetics, 40(5), 600–608. doi:10.1038/ng.115

Halberg, R.B., Katzung, D.S., Hoff, P.D., Moser, A.R., Cole, C.E., Lubet, R.A., Donehower, L.A., Jacoby, R.F. and Dove, W.F. (2000). Tumorigenesis in the multiple intestinal neoplasia mouse: redundancy of negative regulators and specificity of modifiers. Proceedings of the National Academy of Sciences of the United States of America, 97(7), 3461–3466. doi:10.1073/pnas.97.7.3461

Hamid, O., Robert, C., Daud, A., Hodi, F.S., Hwu, W.J., Kefford, R., Wolchok, J. D., Hersey, P., Joseph, R.W., Weber, J.S., Dronca, R., Gangadhar, T.C., Patnaik, A., Zarour, H., Joshua, A.M., Gergich, K., Elassaiss-Schaap, J., Algazi, A., Mateus, C., Boasberg, P., … Ribas, A. (2013). Safety and tumor responses with lambrolizumab (anti-PD-1) in melanoma. The New England journal of medicine, 369(2), 134–144. doi:10.1056/NEJMoa1305133

Han, X., Shi, H., Sun, Y., Shang, C., Luan, T., Wang, D., Ba, X. and Zeng, X. (2019). CXCR2 expression on granulocyte and macrophage progenitors under tumor conditions contributes to mo-MDSC generation via SAP18/ERK/STAT3. Cell death & disease, 10(8), 598. doi:10.1038/s41419-019-1837-1

Hanahan, D. and Weinberg, R.A. (2000). The hallmarks of cancer. Cell, 100(1), 57–70. doi:10.1016/s0092-8674(00)81683-9

Hanahan, D. and Weinberg, R.A. (2011). Hallmarks of cancer: the next generation. Cell, 144(5), 646–674. doi:10.1016/j.cell.2011.02.013

Hanna, C.R., O'Cathail, S.M., Graham, J.S., Saunders, M., Samuel, L., Harrison, M., Devlin, L., Edwards, J., Gaya, D.R., Kelly, C.A., Lewsley, L.A., Maka, N., Morrison, P., Dinnett, L., Dillon, S., Gourlay, J., Platt, J.J., Thomson, F., Adams, R.A. and Roxburgh, C.S.D. (2021). Durvalumab (MEDI 4736) in combination with extended neoadjuvant regimens in rectal cancer: a study protocol of a randomised phase II trial (PRIME-RT). Radiation oncology, 16(1), 163. doi:10.1186/s13014-021-01888-1

Harrington, K., Jankowska, P. and Hingorani, M. (2007). Molecular biology for the radiation oncologist: the 5Rs of radiobiology meet the hallmarks of cancer. Clinical oncology, 19(8), 561–571. doi:10.1016/j.clon.2007.04.009

Haslam, A. and Prasad, V. (2019). Estimation of the Percentage of US Patients With Cancer Who Are Eligible for and Respond to Checkpoint Inhibitor Immunotherapy Drugs. JAMA network open, 2(5), e192535. doi:10.1001/jamanetworkopen.2019.2535

Havel, J.J., Chowell, D. and Chan, T.A. (2019). The evolving landscape of biomarkers for checkpoint inhibitor immunotherapy. Nature Reviews Cancer, 19(3), 133–150. doi:10.1038/s41568-019-0116-x

Hawkins, N.J. and Ward, R.L. (2001). Sporadic Colorectal Cancers With Microsatellite Instability and Their Possible Origin in Hyperplastic Polyps and Serrated Adenomas. JNCI Journal of the National Cancer Institute, 93(17), pp. 1307–1313. doi:10.1093/jnci/93.17.1307.

Hayashi, H., Abdollah, S., Qiu, Y., Cai, J., Xu, Y.Y., Grinnell, B.W., Richardson, M.A., Topper, J.N., Gimbrone, M.A., Jr, Wrana, J.L. and Falb, D. (1997). The MAD-related protein Smad7 associates with the TGFbeta receptor and functions as an antagonist of TGFbeta signaling. Cell, 89(7), 1165–1173. doi:10.1016/s0092-8674(00)80303-7

Hayashi, S. and McMahon, A.P. (2002). Efficient recombination in diverse tissues by a tamoxifen-inducible form of Cre: a tool for temporally regulated gene activation/inactivation in the mouse. Developmental biology, 244(2), 305–318. doi:10.1006/dbio.2002.0597

Haydon A. (2003). Adjuvant chemotherapy in colon cancer: what is the evidence? Internal medicine journal, 33(3), 119–124. doi:10.1046/j.1445-5994.2003.00324.x

Hayman, T.J., Baro, M., MacNeil, T., Phoomak, C., Aung, T.N., Cui, W., Leach, K., Iyer, R., Challa, S., Sandoval-Schaefer, T., Burtness, B.A., Rimm, D.L. and Contessa, J.N. (2021). STING enhances cell death through regulation of reactive oxygen species and DNA damage. Nature communications, 12(1), 2327. doi:10.1038/s41467-021-22572-8

He, T.C., Sparks, A.B., Rago, C., Hermeking, H., Zawel, L., da Costa, L.T., Morin, P.J., Vogelstein, B. and Kinzler, K.W. (1998). Identification of c-MYC as a target of the APC pathway. Science, 281(5382), 1509–1512. doi:10.1126/science.281.5382.1509

Heald, R. J. and Ryall, R. D. (1986). Recurrence and survival after total mesorectal excision for rectal cancer. Lancet, 1(8496), 1479–1482. doi:10.1016/s0140-6736(86)91510-2

Hecht, M., Büttner-Herold, M., Erlenbach-Wünsch, K., Haderlein, M., Croner, R., Grützmann, R., Hartmann, A., Fietkau, R. and Distel, L.V. (2016). PD-L1 is upregulated by radiochemotherapy in rectal adenocarcinoma patients and associated with a favourable prognosis. European journal of cancer, 65, 52–60. doi:10.1016/j.ejca.2016.06.015

Hecker, L., Vittal, R., Jones, T., Jagirdar, R., Luckhardt, T.R., Horowitz, J.C., Pennathur, S., Martinez, F.J. and Thannickal, V.J. (2009). NADPH oxidase-4 mediates myofibroblast activation and fibrogenic responses to lung injury. Nature medicine, 15(9), 1077–1081. doi:10.1038/nm.2005

Heldin, C.H., Miyazono, K. and ten Dijke, P. (1997). TGF-beta signalling from cell membrane to nucleus through SMAD proteins. Nature, 390(6659), 465–471. doi:10.1038/37284

Henrikson, N.B., Webber, E.M., Goddard, K.A., Scrol, A., Piper, M., Williams, M.S., Zallen, D.T., Calonge, N., Ganiats, T.G., Janssens, A.C.J.W., Zauber, A., Lansdorp-Vogelaar, I., van Ballegooijen, M. and Whitlock, E.P. (2015). Family history and the natural history of colorectal cancer: systematic review. Genetics in Medicine, 17(9), pp.702–712. doi:10.1038/gim.2014.188.

Herman, J.G., Umar, A., Polyak, K., Graff, J.R., Ahuja, N., Issa, J.P., Markowitz, S., Willson, J.K., Hamilton, S.R., Kinzler, K.W., Kane, M.F., Kolodner, R.D., Vogelstein, B., Kunkel, T.A. and Baylin, S.B. (1998). Incidence and functional consequences of hMLH1 promoter hypermethylation in colorectal carcinoma. Proceedings of the National Academy of Sciences of the United States of America, 95(12), 6870–6875. doi:10.1073/pnas.95.12.6870

Heylmann, D., Rödel, F., Kindler, T. and Kaina, B. (2014). Radiation sensitivity of human and murine peripheral blood lymphocytes, stem and progenitor cells. Biochimica et biophysica acta, 1846(1), 121–129. doi:10.1016/j.bbcan.2014.04.009

Higashiyama, H., Yoshimoto, D., Kaise, T., Matsubara, S., Fujiwara, M., Kikkawa, H., Asano, S. and Kinoshita, M. (2007). Inhibition of activin receptor-like kinase 5 attenuates bleomycin-induced pulmonary fibrosis. Experimental and molecular pathology, 83(1), 39–46. doi:10.1016/j.yexmp.2006.12.003

Hiniker, S.M., Reddy, S.A., Maecker, H.T., Subrahmanyam, P.B., Rosenberg-Hasson, Y., Swetter, S.M., Saha, S., Shura, L. and Knox, S.J. (2016). A Prospective Clinical Trial Combining Radiation Therapy With Systemic Immunotherapy in Metastatic Melanoma. International journal of radiation oncology, biology, physics, 96(3), 578–588. doi:10.1016/j.ijrobp.2016.07.005

Hino, R., Kabashima, K., Kato, Y., Yagi, H., Nakamura, M., Honjo, T., Okazaki, T. and Tokura, Y. (2010). Tumor cell expression of programmed cell death-1 ligand 1 is a prognostic factor for malignant melanoma. Cancer, 116(7), 1757–1766. doi:10.1002/cncr.24899

Hite, N., Klinger, A., Hellmers, L., Maresh, G.A., Miller, P.E., Zhang, X., Li, L. and Margolin, D.A. (2018). An Optimal Orthotopic Mouse Model for Human

Colorectal Cancer Primary Tumor Growth and Spontaneous Metastasis. Diseases of the colon and rectum, 61(6), 698–705. doi:10.1097/DCR.0000000000001096

Hodi, F.S., O'Day, S.J., McDermott, D.F., Weber, R.W., Sosman, J.A., Haanen, J.B., Gonzalez, R., Robert, C., Schadendorf, D., Hassel, J.C., Akerley, W., van den Eertwegh, A.J., Lutzky, J., Lorigan, P., Vaubel, J.M., Linette, G.P., Hogg, D., Ottensmeier, C.H., Lebbé, C., Peschel, C., … Urba, W.J. (2010). Improved survival with ipilimumab in patients with metastatic melanoma. The New England journal of medicine, 363(8), 711–723. doi:10.1056/NEJMoa1003466

Hoffman R.M. (2015). Application of GFP imaging in cancer. Laboratory investigation, 95(4), 432–452. doi:10.1038/labinvest.2014.154

Holmgaard, R.B., Schaer, D.A., Li, Y., Castaneda, S.P., Murphy, M.Y., Xu, X., Inigo, I., Dobkin, J., Manro, J.R., Iversen, P.W., Surguladze, D., Hall, G.E., Novosiadly, R.D., Benhadji, K.A., Plowman, G.D., Kalos, M. and Driscoll, K.E. (2018). Targeting the TGFß pathway with galunisertib, a TGFßRI small molecule inhibitor, promotes anti-tumor immunity leading to durable, complete responses, as monotherapy and in combination with checkpoint blockade. Journal for immunotherapy of cancer, 6(1), 47. doi:10.1186/s40425-018-0356-4

Hsu, H.C., Liu, Y.S., Tseng, K.C., Hsu, C.L., Liang, Y., Yang, T.S., Chen, J.S., Tang, R.P., Chen, S.J. and Chen, H.C. (2013). Overexpression of Lgr5 correlates with resistance to 5-FU-based chemotherapy in colorectal cancer. International journal of colorectal disease, 28(11), 1535–1546. doi:10.1007/s00384-013-1721-x

Hsu, P.D., Lander, E.S. and Zhang, F. (2014). Development and applications of CRISPR-Cas9 for genome engineering. Cell, 157(6), 1262–1278. doi:10.1016/j.cell.2014.05.010

Huang, C.Y., Chung, C.L., Hu, T.H., Chen, J.J., Liu, P.F. and Chen, C.L. (2021). Recent progress in TGF-ß inhibitors for cancer therapy. Biomedicine & pharmacotherapy, 134, 111046. doi:10.1016/j.biopha.2020.111046

Hung, K.E., Maricevich, M.A., Richard, L.G., Chen, W.Y., Richardson, M.P., Kunin, A., Bronson, R.T., Mahmood, U. and Kucherlapati, R. (2010). Development of a mouse model for sporadic and metastatic colon tumors and its use in assessing drug treatment. Proceedings of the National Academy of Sciences of the United States of America, 107(4), 1565–1570. doi:10.1073/pnas.0908682107

Hutchins, G., Southward, K., Handley, K., Magill, L., Beaumont, C., Stahlschmidt, J., Richman, S., Chambers, P., Seymour, M., Kerr, D., Gray, R. and Quirke, P. (2011). Value of mismatch repair, KRAS, and BRAF mutations in predicting recurrence and benefits from chemotherapy in colorectal cancer. Journal of Clinical Oncology, 29(10), 1261–1270. doi:10.1200/JCO.2010.30.1366

Hynds, R.E., Vladimirou, E. and Janes, S.M. (2018). The secret lives of cancer cell lines. Disease models & mechanisms, 11(11), dmm037366. doi:10.1242/dmm.037366

Ikeda, M., Takahashi, H., Kondo, S., Lahn, M.M.F., Ogasawara, K., Benhadji, K. A., Fujii, H. and Ueno, H. (2017). Phase 1b study of galunisertib in combination with gemcitabine in Japanese patients with metastatic or locally advanced pancreatic cancer. Cancer chemotherapy and pharmacology, 79(6), 1169–1177. doi:10.1007/s00280-017-3313-x

Ikeda, M., Morimoto, M., Tajimi, M., Inoue, K., Benhadji, K.A., Lahn, M.M.F. and Sakai, D. (2019). A phase 1b study of transforming growth factor-beta receptor I inhibitor galunisertib in combination with sorafenib in Japanese patients with unresectable hepatocellular carcinoma. Investigational new drugs, 37(1), 118–126. doi:10.1007/s10637-018-0636-3

Inman, G.J., Nicolás, F.J. and Hill, C.S. (2002). Nucleocytoplasmic shuttling of Smads 2, 3, and 4 permits sensing of TGF-beta receptor activity. Molecular cell, 10(2), 283–294. doi:10.1016/s1097-2765(02)00585-3

Iseas, S., Sendoya, J.M., Robbio, J., Coraglio, M., Kujaruk, M., Mikolaitis, V., Rizzolo, M., Cabanne, A., Ruiz, G., Salanova, R., Gualdrini, U., Méndez, G., Antelo, M., Carballido, M., Rotondaro, C., Viglino, J., Eleta, M., Di Sibio, A., Podhajcer, O.L., Roca, E., … Abba, M.C. (2022). Prognostic Impact of An Integrative Landscape of Clinical, Immune, and Molecular Features in Non-Metastatic Rectal Cancer. Frontiers in oncology, 11, 801880. doi:10.3389/fonc.2021.801880

Isella, C., Terrasi, A., Bellomo, S.E., Petti, C., Galatola, G., Muratore, A., Mellano, A., Senetta, R., Cassenti, A., Sonetto, C., Inghirami, G., Trusolino, L., Fekete, Z., De Ridder, M., Cassoni, P., Storme, G., Bertotti, A. and Medico, E. (2015). Stromal contribution to the colorectal cancer transcriptome. Nature genetics, 47(4), 312–319. doi:10.1038/ng.3224

Ishida, Y., Agata, Y., Shibahara, K. and Honjo, T. (1992). Induced expression of PD-1, a novel member of the immunoglobulin gene superfamily, upon programmed cell death. The EMBO journal, 11(11), 3887–3895. doi:10.1002/j.1460-2075.1992.tb05481.x

Ivashkiv L.B. (2018). IFNγ: signalling, epigenetics and roles in immunity, metabolism, disease and cancer immunotherapy. Nature reviews. Immunology, 18(9), 545–558. doi:10.1038/s41577-018-0029-z

Jackson, E.L., Willis, N., Mercer, K., Bronson, R.T., Crowley, D., Montoya, R., Jacks, T. and Tuveson, D.A. (2001). Analysis of lung tumor initiation and progression using conditional expression of oncogenic K-ras. Genes & development, 15(24), 3243–3248. doi:10.1101/gad.943001

Jackson, S.P. and Bartek, J. (2009). The DNA-damage response in human biology and disease. Nature, 461(7267), 1071–1078. doi:10.1038/nature08467

Jackstadt, R. and Sansom, O.J. (2016). Mouse models of intestinal cancer. The Journal of pathology, 238(2), 141–151. doi:10.1002/path.4645

Jackstadt, R., van Hooff, S. R., Leach, J.D., Cortes-Lavaud, X., Lohuis, J.O., Ridgway, R.A., Wouters, V.M., Roper, J., Kendall, T.J., Roxburgh, C.S., Horgan, P.G., Nixon, C., Nourse, C., Gunzer, M., Clark, W., Hedley, A., Yilmaz, O.H., Rashid, M., Bailey, P., Biankin, A.V., … Sansom, O.J. (2019). Epithelial NOTCH Signaling Rewires the Tumor Microenvironment of Colorectal Cancer to Drive Poor-Prognosis Subtypes and Metastasis. Cancer cell, 36(3), 319–336.e7. doi:10.1016/j.ccell.2019.08.003

Janakiraman, H., Zhu, Y., Becker, S.A., Wang, C., Cross, A., Curl, E., Lewin, D., Hoffman, B.J., Warren, G.W., Hill, E.G., Timmers, C., Findlay, V.J. and Camp, E.R. (2020). Modeling rectal cancer to advance neoadjuvant precision therapy. International journal of cancer, 147(5), 1405–1418. doi:10.1002/ijc.32876

Janssen, K.P., Alberici, P., Fsihi, H., Gaspar, C., Breukel, C., Franken, P., Rosty, C., Abal, M., El Marjou, F., Smits, R., Louvard, D., Fodde, R. and Robine, S. (2006). APC and oncogenic KRAS are synergistic in enhancing Wnt signaling in intestinal tumor formation and progression. Gastroenterology, 131(4), 1096–1109. doi:10.1053/j.gastro.2006.08.011

Jass, J.R. (2007). Classification of colorectal cancer based on correlation of clinical, morphological and molecular features. Histopathology, 50(1), pp. 113–130. doi:10.1111/j.1365-2559.2006.02549.x.

Jayne, D.G., Guillou, P.J., Thorpe, H., Quirke, P., Copeland, J., Smith, A.M., Heath, R.M., Brown, J.M. and UK MRC CLASICC Trial Group (2007). Randomized trial of laparoscopic-assisted resection of colorectal carcinoma: 3-year results of the UK MRC CLASICC Trial Group. Journal of clinical oncology, 25(21), 3061–3068. doi:10.1200/JCO.2006.09.7758

Jayne, D.G, Pigazzi, A., Marshall, H., Croft, J., Corrigan, N., Copeland, J., Quirke, P., West, N., Rautio, T., Thomassen, N., Tilney, H., Gudgeon, M., Bianchi, P.P., Edlin, R., Hulme, C. and Brown, J. (2017). Effect of Robotic-Assisted vs Conventional Laparoscopic Surgery on Risk of Conversion to Open Laparotomy Among Patients Undergoing Resection for Rectal Cancer: The ROLARR Randomized Clinical Trial. JAMA, 318(16), 1569–1580. doi:10.1001/jama.2017.7219

Jeong, S.Y., Park, J.W., Nam, B.H., Kim, S., Kang, S.B., Lim, S.B., Choi, H.S., Kim, D.W., Chang, H.J., Kim, D.Y., Jung, K.H., Kim, T.Y., Kang, G.H., Chie, E. K., Kim, S.Y., Sohn, D.K., Kim, D.H., Kim, J.S., Lee, H.S., Kim, J.H., … Oh, J.H. (2014). Open versus laparoscopic surgery for mid-rectal or low-rectal cancer after neoadjuvant chemoradiotherapy (COREAN trial): survival outcomes of an open-label, non-inferiority, randomised controlled trial. The Lancet Oncology, 15(7), 767–774. doi:10.1016/S1470-2045(14)70205-0

Jiang, D., Wang, X., Wang, Y., Philips, D., Meng, W., Xiong, M., Zhao, J., Sun, L., He, D. and Li, K. (2019). Mutation in BRAF and SMAD4 associated with resistance to neoadjuvant chemoradiation therapy in locally advanced rectal cancer. Virchows Archiv: an international journal of pathology, 475(1), 39–47. doi:10.1007/s00428-019-02576-y

Jin, H., Yang, Z., Wang, J., Zhang, S., Sun, Y. and Ding, Y. (2011). A superficial colon tumor model involving subcutaneous colon translocation and orthotopic transplantation of green fluorescent protein-expressing human colon tumor. Tumour biology, 32(2), 391–397. doi:10.1007/s13277-010-0132-7

Jin, L., Shen, F., Weinfeld, M. and Sergi, C. (2020). Insulin Growth Factor Binding Protein 7 (IGFBP7)-Related Cancer and IGFBP3 and IGFBP7 Crosstalk. Frontiers in oncology, 10, 727. doi:10.3389/fonc.2020.00727

Jinek, M., Chylinski, K., Fonfara, I., Hauer, M., Doudna, J.A. and Charpentier, E. (2012). A programmable dual-RNA-guided DNA endonuclease in adaptive bacterial immunity. Science, 337(6096), 816–821. doi:10.1126/science.1225829

Johnson, D.E., O'Keefe, R.A. and Grandis, J.R. (2018). Targeting the IL-6/JAK/STAT3 signalling axis in cancer. Nature reviews. Clinical oncology, 15(4), 234–248. doi:10.1038/nrclinonc.2018.8

Jonkers, J., Meuwissen, R., van der Gulden, H., Peterse, H., van der Valk, M. and Berns, A. (2001). Synergistic tumor suppressor activity of BRCA2 and p53 in a conditional mouse model for breast cancer. Nature genetics, 29(4), 418–425. doi:10.1038/ng747

Jonkers J, Meuwissen R, van der Gulden H, Peterse H, van der Valk M, Berns A. Synergistic tumor suppressor activity of BRCA2 and p53 in a conditional mouse model for breast cancer. Nat Genet. 2001 Dec;29(4):418-25. doi: 10.1038/ng747.

Jung, P., Sato, T., Merlos-Suárez, A., Barriga, F.M., Iglesias, M., Rossell, D., Auer, H., Gallardo, M., Blasco, M.A., Sancho, E., Clevers, H. and Batlle, E. (2011). Isolation and in vitro expansion of human colonic stem cells. Nature medicine, 17(10), 1225–1227. doi:10.1038/nm.2470

Juul, T., Ahlberg, M., Biondo, S., Espin, E., Jimenez, L.M., Matzel, K.E., Palmer, G.J., Sauermann, A., Trenti, L., Zhang, W., Laurberg, S. and Christensen, P. (2014). Low anterior resection syndrome and quality of life: an international multicenter study. Diseases of the colon and rectum, 57(5), 585–591. doi:10.1097/DCR.0000000000000116

Kachikwu, E.L., Iwamoto, K.S., Liao, Y.P., DeMarco, J.J., Agazaryan, N., Economou, J.S., McBride, W.H. and Schaue, D. (2011). Radiation enhances regulatory T cell representation. International journal of radiation oncology, biology, physics, 81(4), 1128–1135. doi:10.1016/j.ijrobp.2010.09.034

Kalbasi, A., Komar, C., Tooker, G.M., Liu, M., Lee, J.W., Gladney, W.L., Ben-Josef, E. and Beatty, G.L. (2017). Tumor-Derived CCL2 Mediates Resistance to Radiotherapy in Pancreatic Ductal Adenocarcinoma. Clinical cancer research : an official journal of the American Association for Cancer Research, 23(1), 137–148. doi:10.1158/1078-0432.CCR-16-0870

Kamada, T., Togashi, Y., Tay, C., Ha, D., Sasaki, A., Nakamura, Y., Sato, E., Fukuoka, S., Tada, Y., Tanaka, A., Morikawa, H., Kawazoe, A., Kinoshita, T., Shitara, K., Sakaguchi, S. and Nishikawa, H. (2019). PD-1+ regulatory T cells amplified by PD-1 blockade promote hyperprogression of cancer. Proceedings of the National Academy of Sciences of the United States of America, 116(20), 9999–10008. doi:10.1073/pnas.1822001116

Kamal, Y., Schmit, S.L., Hoehn, H.J., Amos, C.I. and Fromst, H.R. (2019). Transcriptomic Differences between Primary Colorectal Adenocarcinomas and Distant Metastases Reveal Metastatic Colorectal Cancer Subtypes. Cancer Research, 79(16), 4227-4241. doi:10.1158/0008-5472.CAN-18-3945

Kambara, T., Simms, L.A., Whitehall, V.L., Spring, K.J., Wynter, C.V., Walsh, M. D., Barker, M.A., Arnold, S., McGivern, A., Matsubara, N., Tanaka, N., Higuchi, T., Young, J., Jass, J.R. and Leggett, B.A. (2004). BRAF mutation is associated with DNA methylation in serrated polyps and cancers of the colorectum. Gut, 53(8), 1137–1144. doi:10.1136/gut.2003.037671

Kang, C.M., Lim, S.B., Hong, S.M., Yu, C.S., Hong, Y.S., Kim, T.W., Park, J.H., Kim, J.H. and Kim, J.C. (2016). Prevalence and clinical significance of cellular and acellular mucin in patients with locally advanced mucinous rectal cancer who underwent preoperative chemoradiotherapy followed by radical surgery. Colorectal disease, 18(1), O10–O16. doi:10.1111/codi.13169

Kang, S.B., Park, J.W., Jeong, S.Y., Nam, B.H., Choi, H.S., Kim, D.W., Lim, S. B., Lee, T.G., Kim, D.Y., Kim, J.S., Chang, H.J., Lee, H.S., Kim, S.Y., Jung, K.H., Hong, Y.S., Kim, J.H., Sohn, D.K., Kim, D.H. and Oh, J.H. (2010). Open versus laparoscopic surgery for mid or low rectal cancer after neoadjuvant chemoradiotherapy (COREAN trial): short-term outcomes of an open-label randomised controlled trial. The Lancet Oncology, 11(7), 637–645. doi:10.1016/S1470-2045(10)70131-5

Kang, Y., Siegel, P.M., Shu, W., Drobnjak, M., Kakonen, S.M., Cordón-Cardo, C., Guise, T.A. and Massagué, J. (2003). A multigenic program mediating breast cancer metastasis to bone. Cancer cell, 3(6), 537–549. doi:10.1016/s1535-6108(03)00132-6

Kapiteijn, E., Liefers, G.J., Los, L.C., Kranenbarg, E.K., Hermans, J., Tollenaar, R.A., Moriya, Y., van de Velde, C.J. and van Krieken, J.H. (2001). Mechanisms of oncogenesis in colon versus rectal cancer. The Journal of pathology, 195(2), 171–178. doi:10.1002/path.918

Kapiteijn, E., Marijnen, C.A., Nagtegaal, I.D., Putter, H., Steup, W.H., Wiggers, T., Rutten, H.J., Pahlman, L., Glimelius, B., van Krieken, J.H., Leer, J.W., van de Velde, C.J. and Dutch Colorectal Cancer Group (2001). Preoperative radiotherapy combined with total mesorectal excision for resectable rectal cancer. The New England journal of medicine, 345(9), 638–646. doi:10.1056/NEJMoa010580

Kapiteijn, E., Putter, H., van de Velde, C. J. and Cooperative investigators of the Dutch ColoRectal Cancer Group (2002). Impact of the introduction and training of total mesorectal excision on recurrence and survival in rectal cancer in The Netherlands. The British journal of surgery, 89(9), 1142–1149. doi:10.1046/j.1365-2168.2002.02196.x

Karapetis, C.S., Khambata-Ford, S., Jonker, D.J., O'Callaghan, C.J., Tu, D., Tebbutt, N.C., Simes, R.J., Chalchal, H., Shapiro, J.D., Robitaille, S., Price, T.J., Shepherd, L., Au, H.-J., Langer, C., Moore, M.J. and Zalcberg, J.R. (2008). K-ras mutations and benefit from cetuximab in advanced colorectal cancer. The New England journal of medicine, 359(17), pp.1757–65. doi:10.1056/NEJMoa0804385.

Kasashima, H., Duran, A., Cid-Diaz, T., Muta, Y., Kinoshita, H., Batlle, E., Diaz-Meco, M.T. and Moscat, J. (2021). Mouse model of colorectal cancer: orthotopic co-implantation of tumor and stroma cells in cecum and rectum. STAR protocols, 2(1), 100297. doi:10.1016/j.xpro.2021.100297

Kashtan, H., Rabau, M., Mullen, J.B., Wong, A.H., Roder, J.C., Shpitz, B., Stern, H.S. and Gallinger, S. (1992). Intra-rectal injection of tumour cells: a novel animal model of rectal cancer. Surgical oncology, 1(3), 251–256. doi:10.1016/0960-7404(92)90072-s

Kasi, P.M., Shahjehan, F., Cochuyt, J.J., Li, Z., Colibaseanu, D.T. and Merchea, A. (2019). Rising Proportion of Young Individuals With Rectal and Colon Cancer. Clinical Colorectal Cancer, 18(1), pp.e87–e95. doi:10.1016/j.clcc.2018.10.002.

Kehrl, J.H., Wakefield, L.M., Roberts, A.B., Jakowlew, S., Alvarez-Mon, M., Derynck, R., Sporn, M.B. and Fauci, A.S. (1986). Production of transforming growth factor beta by human T lymphocytes and its potential role in the

regulation of T cell growth. The Journal of experimental medicine, 163(5), 1037–1050. doi:10.1084/jem.163.5.1037

Kelley, R.K., Gane, E., Assenat, E., Siebler, J., Galle, P.R., Merle, P., Hourmand, I.O., Cleverly, A., Zhao, Y., Gueorguieva, I., Lahn, M., Faivre, S., Benhadji, K.A. and Giannelli, G. (2019). A Phase 2 Study of Galunisertib (TGF-ß1 Receptor Type I Inhibitor) and Sorafenib in Patients With Advanced Hepatocellular Carcinoma. Clinical and translational gastroenterology, 10(7), e00056. doi:10.14309/ctg.0000000000000056

Khanna, K.K. and Jackson, S.P. (2001). DNA double-strand breaks: signaling, repair and the cancer connection. Nature genetics, 27(3), 247–254. doi:10.1038/85798

Kim, B.G., Li, C., Qiao, W., Mamura, M., Kasprzak, B., Anver, M., Wolfraim, L., Hong, S., Mushinski, E., Potter, M., Kim, S.J., Fu, X.Y., Deng, C. and Letterio, J.J. (2006). Smad4 signalling in T cells is required for suppression of gastrointestinal cancer. Nature, 441(7096), 1015–1019. doi:10.1038/nature04846

Kim, B.G., Malek, E., Choi, S.H., Ignatz-Hoover, J.J. and Driscoll, J.J. (2021). Novel therapies emerging in oncology to target the TGF-ß pathway. Journal of hematology & oncology, 14(1), 55. D oi:10.1186/s13045-021-01053-x

Kim, J.K., Wu, C., Del Latto, M., Gao, Y., Choi, S.H., Kierstead, M., Gabriel Sauvé, C.E., Firat, C., Perez, A.C., Sillanpaa, J., Chen, C.T., Lawrence, K.E., Paty, P.B., Barriga, F.M., Wilkinson, J.E., Shia, J., Sawyers, C.L., Lowe, S.W., García-Aguilar, J., Romesser, P.B., … Smith, J.J. (2022). An immunocompetent rectal cancer model to study radiation therapy. Cell reports methods, 2(12), 100353. doi:10.1016/j.crmeth.2022.100353

Kim, S.H., Chang, H.J., Kim, D.Y., Park, J.W., Baek, J.Y., Kim, S.Y., Park, S.C., Oh, J.H., Yu, A. and Nam, B.H. (2016). What Is the Ideal Tumor Regression Grading System in Rectal Cancer Patients after Preoperative Chemoradiotherapy?. Cancer research and treatment, 48(3), 998–1009. doi:10.4143/crt.2015.254

Kinzler, K.W., Nilbert, M.C., Su, L.K., Vogelstein, B., Bryan, T.M., Levy, D.B., Smith, K.J., Preisinger, A.C., Hedge, P. and McKechnie, D. (1991). Identification of FAP locus genes from chromosome 5q21. Science, 253(5020), pp.661–665. doi:10.1126/science.1651562.

Kishimoto, H., Momiyama, M., Aki, R., Kimura, H., Suetsugu, A., Bouvet, M., Fujiwara, T. and Hoffman, R.M. (2013). Development of a clinically-precise mouse model of rectal cancer. PloS one, 8(11), e79453. doi:10.1371/journal.pone.0079453

Kitamura, T., Kometani, K., Hashida, H., Matsunaga, A., Miyoshi, H., Hosogi, H., Aoki, M., Oshima, M., Hattori, M., Takabayashi, A., Minato, N. and Taketo, M. M. (2007). SMAD4-deficient intestinal tumors recruit CCR1+ myeloid cells that promote invasion. Nature genetics, 39(4), 467–475. doi:10.1038/ng1997

Klintrup, K., Mäkinen, J.M., Kauppila, S., Väre, P.O., Melkko, J., Tuominen, H., Tuppurainen, K., Mäkelä, J., Karttunen, T.J. and Mäkinen, M.J. (2005). Inflammation and prognosis in colorectal cancer. European journal of cancer (Oxford, England : 1990), 41(17), 2645–2654. doi:10.1016/j.ejca.2005.07.017

Klug, F., Prakash, H., Huber, P.E., Seibel, T., Bender, N., Halama, N., Pfirschke, C., Voss, R.H., Timke, C., Umansky, L., Klapproth, K., Schäkel, K., Garbi, N., Jäger, D., Weitz, J., Schmitz-Winnenthal, H., Hämmerling, G. J. and Beckhove, P. (2013). Low-dose irradiation programs macrophage differentiation to an iNOS^{+}/M1 phenotype that orchestrates effective T cell immunotherapy. Cancer cell, 24(5), 589–602. doi:10.1016/j.ccr.2013.09.014

Knudson, K.M., Hicks, K.C., Luo, X., Chen, J.Q., Schlom, J. and Gameiro, S.R. (2018). M7824, a novel bifunctional anti-PD-L1/TGFβ Trap fusion protein, promotes anti-tumor efficacy as monotherapy and in combination with vaccine. Oncoimmunology, 7(5), e1426519. doi:10.1080/2162402X.2018.1426519

Koebel, C.M., Vermi, W., Swann, J.B., Zerafa, N., Rodig, S.J., Old, L.J., Smyth, M. J. and Schreiber, R.D. (2007). Adaptive immunity maintains occult cancer in an equilibrium state. Nature, 450(7171), 903–907. doi:10.1038/nature06309

Kolahi, K.S., Nakano, M. and Kuo, C.J. (2020). Organoids as Oracles for Precision Medicine in Rectal Cancer. Cell stem cell, 26(1), 4–6. doi:10.1016/j.stem.2019.12.003

Koller, K.M., Mackley, H.B., Liu, J., Wagner, H., Talamo, G., Schell, T.D., Pameijer, C., Neves, R.I., Anderson, B., Kokolus, K.M., Mallon, C.A. and Drabick, J.J. (2017). Improved survival and complete response rates in patients with advanced melanoma treated with concurrent ipilimumab and radiotherapy versus ipilimumab alone. Cancer biology & therapy, 18(1), 36–42. doi:10.1080/15384047.2016.1264543

Kopetz, S., Spira, A.I., Wertheim, M., Kim, E., Tan, B.R., Lenz, H., Niklinakos, P., Rich, P., Smith, D.A., Helwig, C., Dussault, I., Ojalva, L. and Gullet, J.L. (2018). M7824 (MSB0011359C), a bifunctional fusion protein targeting PD-L1 and TGF-β, in patients with heavily pretreated CRC: Preliminary results from a phase I trial. Journal of Clinical Oncology, 36(4_suppl), 764.

Koyama, M., Ito, M., Nagai, H., Emi, M. and Moriyama, Y. (1999). Inactivation of both alleles of the DPC4/SMAD4 gene in advanced colorectal cancers: identification of seven novel somatic mutations in tumors from Japanese patients. Mutation research, 406(2-4), 71–77. doi:10.1016/s1383-5726(99)00003-5

Kretzschmar, K. and Clevers, H. (2016). Organoids: Modeling Development and the Stem Cell Niche in a Dish. Developmental cell, 38(6), 590–600. doi:10.1016/j.devcel.2016.08.014

Kroemer, G., Galluzzi, L., Kepp, O. and Zitvogel, L. (2013). Immunogenic cell death in cancer therapy. Annual review of immunology, 31, 51–72. doi:10.1146/annurev-immunol-032712-100008

Kryeziu, K., Moosavi, S.H., Bergsland, C.H., Guren, M.G., Eide, P.W., Totland, M.Z., Lassen, K., Abildgaard, A., Nesbakken, A., Sveen, A. and Lothe, R.A. (2021). Increased sensitivity to SMAC mimetic LCL161 identified by longitudinal ex vivo pharmacogenomics of recurrent, KRAS mutated rectal cancer liver metastases. Journal of translational medicine, 19(1), 384. doi:10.1186/s12967-021-03062-3

Krysko, D.V., Garg, A.D., Kaczmarek, A., Krysko, O., Agostinis, P. and Vandenabeele, P. (2012). Immunogenic cell death and DAMPs in cancer therapy. Nature reviews. Cancer, 12(12), 860–875. doi:10.1038/nrc3380

Kuipers, E.J., Grady, W.M., Lieberman, D., Seufferlein, T., Sung, J.J., Boelens, P.G., van de Velde, C.J. and Watanabe, T. (2015). Colorectal cancer. Nature reviews, 1, 15065. doi:10.1038/nrdp.2015.65

Kulkarni, A.B., Ward, J.M., Yaswen, L., Mackall, C.L., Bauer, S.R., Huh, C.G., Gress, R.E. and Karlsson, S. (1995). Transforming growth factor-beta 1 null mice. An animal model for inflammatory disorders. The American journal of pathology, 146(1), 264–275.

Kunzmann, A.T., Murray, L.J., Cardwell, C.R., McShane, C.M., McMenamin, U. C. and Cantwell, M. M. (2013). PTGS2 (Cyclooxygenase-2) expression and survival among colorectal cancer patients: a systematic review. Cancer epidemiology, biomarkers & prevention, 22(9), 1490–1497. doi:10.1158/1055-9965.EPI-13-0263

Kuraguchi, M., Wang, X.P., Bronson, R.T., Rothenberg, R., Ohene-Baah, N.Y., Lund, J.J., Kucherlapati, M., Maas, R.L. and Kucherlapati, R. (2006). Adenomatous polyposis coli (APC) is required for normal development of skin and thymus. PLoS genetics, 2(9), e146. doi:10.1371/journal.pgen.0020146

Kyrgiou, M., Kalliala, I., Markozannes, G., Gunter, M.J., Paraskevaidis, E., Gabra, H., Martin-Hirsch, P. and Tsilidis, K.K. (2017). Adiposity and cancer at major anatomical sites: umbrella review of the literature. BMJ, p.j477. doi:10.1136/bmj.j477.

Lagasse, E. and Weissman, I.L. (1992). Mouse MRP8 and MRP14, two intracellular calcium-binding proteins associated with the development of the myeloid lineage. Blood, 79(8), 1907–1915.

Lamlum, H., Ilyas, M., Rowan, A., Clark, S., Johnson, V., Bell, J., Frayling, I., Efstathiou, J., Pack, K., Payne, S., Roylance, R., Gorman, P., Sheer, D., Neale, K., Phillips, R., Talbot, I., Bodmer, W. and Tomlinson, I. (1999). The type of somatic mutation at APC in familial adenomatous polyposis is determined by the site of the germline mutation: a new facet to Knudson's 'two-hit' hypothesis. Nature Medicine, 5(9), pp.1071–1075. doi:10.1038/12511.

Lan, Y., Zhang, D., Xu, C., Hance, K.W., Marelli, B., Qi, J., Yu, H., Qin, G., Sircar, A., Hernández, V.M., Jenkins, M.H., Fontana, R.E., Deshpande, A., Locke, G., Sabzevari, H., Radvanyi, L. and Lo, K.M. (2018). Enhanced preclinical antitumor activity of M7824, a bifunctional fusion protein simultaneously targeting PD-L1 and TGF-β. Science translational medicine, 10(424), eaan5488. doi:10.1126/scitranslmed.aan5488

Lannagan, T.R.M., Lee, Y.K., Wang, T., Roper, J., Bettington, M.L., Fennell, L., Vrbanac, L., Jonavicius, L., Somashekar, R., Gieniec, K., Yang, M., Ng, J. Q., Suzuki, N., Ichinose, M., Wright, J. A., Kobayashi, H., Putoczki, T. L., Hayakawa, Y., Leedham, S.J., Abud, H.E. and Woods, S. L. (2019). Genetic editing of colonic organoids provides a molecularly distinct and orthotopic preclinical model of serrated carcinogenesis. Gut, 68(4), 684–692. doi:10.1136/gutjnl-2017-315920

Lannagan, T.R.M., Jackstadt, R., Leedham, S.J. and Sansom, O.J. (2021). Advances in colon cancer research: in vitro and animal models. Current opinion in genetics & development, 66, 50–56. doi:10.1016/j.gde.2020.12.003

Larsson, J., Goumans, M.J., Sjöstrand, L.J., van Rooijen, M.A., Ward, D., Levéen, P., Xu, X., ten Dijke, P., Mummery, C.L. and Karlsson, S. (2001). Abnormal angiogenesis but intact hematopoietic potential in TGF-beta type I receptor-deficient mice. The EMBO journal, 20(7), 1663–1673. doi:10.1093/emboj/20.7.1663

Law, W. L. and Chu, K. W. (2004). Anterior resection for rectal cancer with mesorectal excision: a prospective evaluation of 622 patients. Annals of surgery, 240(2), 260–268. doi:10.1097/01.sla.0000133185.23514.32

Lawrence, D.A., Pircher, R., Krycève-Martinerie, C. and Jullien, P. (1984). Normal embryo fibroblasts release transforming growth factors in a latent form. Journal of cellular physiology, 121(1), 184–188. doi:10.1002/jcp.1041210123

Lawrence, T.S., Blackstock, A.W. and McGinn, C. (2003). The mechanism of action of radiosensitization of conventional chemotherapeutic agents. Seminars in radiation oncology, 13(1), 13–21. doi:10.1053/srao.2003.50002

Le, D.T., Uram, J.N., Wang, H., Bartlett, B.R., Kemberling, H., Eyring, A.D., Skora, A.D., Luber, B.S., Azad, N.S., Laheru, D., Biedrzycki, B., Donehower, R. C., Zaheer, A., Fisher, G.A., Crocenzi, T.S., Lee, J.J., Duffy, S.M., Goldberg, R. M., de la Chapelle, A., Koshiji, M., … Diaz, L.A., Jr (2015). PD-1 Blockade in Tumors with Mismatch-Repair Deficiency. The New England journal of medicine, 372(26), 2509–2520. doi:10.1056/NEJMoa1500596

Leach, D.R., Krummel, M.F. and Allison, J.P. (1996). Enhancement of antitumor immunity by CTLA-4 blockade. Science, 271(5256), 1734–1736. doi:10.1126/science.271.5256.1734

Lee, Y., Auh, S.L., Wang, Y., Burnette, B., Wang, Y., Meng, Y., Beckett, M., Sharma, R., Chin, R., Tu, T., Weichselbaum, R.R. and Fu, Y.X. (2009). Therapeutic effects of ablative radiation on local tumor require CD8+ T cells: changing strategies for cancer treatment. Blood, 114(3), 589–595. doi:10.1182/blood-2009-02-206870

Lee, Y., Wang, Q., Shuryak, I., Brenner, D.J. and Turner, H.C. (2019). Development of a high-throughput γ-H2AX assay based on imaging flow cytometry. Radiation oncology (London, England), 14(1), 150. doi:10.1186/s13014-019-1344-7

Lee, Y.J., Lee, S.B., Beak, S.K., Han, Y.D., Cho, M.S., Hur, H., Lee, K.Y., Kim, N.K. and Min, B.S. (2018). Temporal changes in immune cell composition and cytokines in response to chemoradiation in rectal cancer. Scientific reports, 8(1), 7565. doi:10.1038/s41598-018-25970-z

Lehmann, B., Biburger, M., Brückner, C., Ipsen-Escobedo, A., Gordan, S., Lehmann, C., Voehringer, D., Winkler, T., Schaft, N., Dudziak, D., Sirbu, H., Weber, G. F. and Nimmerjahn, F. (2017). Tumor location determines tissue-specific recruitment of tumor-associated macrophages and antibody-dependent immunotherapy response. Science immunology, 2(7), eaah6413. doi:10.1126/sciimmunol.aah6413

Lenz, H.J., Ou, F.S., Venook, A.P., Hochster, H.S., Niedzwiecki, D., Goldberg, R. M., Mayer, R.J., Bertagnolli, M.M., Blanke, C.D., Zemla, T., Qu, X., Wirapati, P., Tejpar, S., Innocenti, F. and Kabbarah, O. (2019). Impact of Consensus Molecular Subtype on Survival in Patients With Metastatic Colorectal Cancer: Results From CALGB/SWOG 80405 (Alliance). Journal of clinical oncology, 37(22), 1876–1885. doi:10.1200/JCO.18.02258

Lenz, H.J., Van Cutsem, E., Luisa Limon, M., Wong, K.Y.M., Hendlisz, A., Aglietta, M., García-Alfonso, P., Neyns, B., Luppi, G., Cardin, D.B., Dragovich, T., Shah, U., Abdullaev, S., Gricar, J., Ledeine, J.M., Overman, M.J. and Lonardi, S. (2022). First-Line Nivolumab Plus Low-Dose Ipilimumab for Microsatellite Instability-High/Mismatch Repair-Deficient Metastatic Colorectal Cancer: The Phase II CheckMate 142 Study. Journal of clinical oncology, 40(2), 161–170. doi:10.1200/JCO.21.01015

Lewanski, C.R. and Gullick, W.J. (2001). Radiotherapy and cellular signalling. The Lancet. Oncology, 2(6), 366–370. doi:10.1016/S1470-2045(00)00391-0

Li, M.O., Sanjabi, S. and Flavell, R.A. (2006). Transforming growth factor-beta controls development, homeostasis, and tolerance of T cells by regulatory T cell-dependent and -independent mechanisms. Immunity, 25(3), 455–471. doi:10.1016/j.immuni.2006.07.011

Lim, S., Ko, E.J., Kang, Y.J., Baek, K.W., Ock, M.S., Song, K.S., Kang, H.J., Keum, Y.S., Hyun, J.W., Kwon, T.K., Nam, S.Y., Cha, H.J. and Choi, Y.H. Effect of irradiation on cytokine secretion and nitric oxide production by inflammatory macrophages. (2016). Genes Genom, 38, 717–722. doi:10.1007/s13258-016-0416-4

Lin, Z., Cai, M., Zhang, P., Li, G., Liu, T., Li, X., Cai, K., Nie, X., Wang, J., Liu, J., Liu, H., Zhang, W., Gao, J., Wu, C., Wang, L., Fan, J., Zhang, L., Wang, Z., Hou, Z., Ma, C. and Zhang, T. (2021). Phase II, single-arm trial of preoperative short-course radiotherapy followed by chemotherapy and camrelizumab in locally advanced rectal cancer. Journal for immunotherapy of cancer, 9(11), e003554. doi:10.1136/jitc-2021-003554

Lind, H., Gameiro, S.R., Jochems, C., Donahue, R.N., Strauss, J., Gulley, J.L., Palena, C. and Schlom, J. (2020). Dual targeting of TGF-β and PD-L1 via a bifunctional anti-PD-L1/TGF-βRII agent: status of preclinical and clinical advances. Journal for immunotherapy of cancer, 8(1), e000433. doi:10.1136/jitc-2019-000433

Linnekamp, J.F., Hooff, S.R.V., Prasetyanti, P.R., Kandimalla, R., Buikhuisen, J. Y., Fessler, E., Ramesh, P., Lee, K.A.S.T., Bochove, G.G.W., de Jong, J.H., Cameron, K., Leersum, R.V., Rodermond, H.M., Franitza, M., Nürnberg, P., Mangiapane, L.R., Wang, X., Clevers, H., Vermeulen, L., Stassi, G., … Medema, J.P. (2018). Consensus molecular subtypes of colorectal cancer are recapitulated in in vitro and in vivo models. Cell death and differentiation, 25(3), 616–633. doi:10.1038/s41418-017-0011-5

Liu, Q., Hao, Y., Du, R., Hu, D., Xie, J., Zhang, J., Deng, G., Liang, N., Tian, T., Käsmann, L., Rades, D., Rim, C. H., Hu, P. and Zhang, J. (2021). Radiotherapy programs neutrophils to an antitumor phenotype by inducing mesenchymal-epithelial transition. Translational lung cancer research, 10(3), 1424–1443. doi:10.21037/tlcr-21-152

Liu, S., Ren, J. and Ten Dijke, P. (2021). Targeting TGFß signal transduction for cancer therapy. Signal transduction and targeted therapy, 6(1), 8. doi:10.1038/s41392-020-00436-9

Llosa, N.J., Cruise, M., Tam, A., Wicks, E.C., Hechenbleikner, E.M., Taube, J. M., Blosser, R.L., Fan, H., Wang, H., Luber, B.S., Zhang, M., Papadopoulos, N., Kinzler, K.W., Vogelstein, B., Sears, C.L., Anders, R.A., Pardoll, D.M. and Housseau, F. (2015). The vigorous immune microenvironment of microsatellite instable colon cancer is balanced by multiple counter-inhibitory checkpoints. Cancer discovery, 5(1), 43–51. doi:10.1158/2159-8290.CD-14-0863

Llosa, N.J., Luber, B., Siegel, N., Awan, A.H., Oke, T., Zhu, Q., Bartlett, B.R., Aulakh, L.K., Thompson, E.D., Jaffee, E.M., Durham, J.N., Sears, C.L., Le, D.T., Diaz, L.A., Jr, Pardoll, D.M., Wang, H., Housseau, F. and Anders, R.A. (2019). Immunopathologic Stratification of Colorectal Cancer for Checkpoint Blockade Immunotherapy. Cancer immunology research, 7(10), 1574–1579. doi:10.1158/2326-6066.CIR-18-0927

Lo, S.S., Fakiris, A.J., Chang, E.L., Mayr, N.A., Wang, J.Z., Papiez, L., Teh, B. S., McGarry, R.C., Cardenes, H.R. and Timmerman, R.D. (2010). Stereotactic body radiation therapy: a novel treatment modality. Nature reviews. Clinical oncology, 7(1), 44–54. doi:10.1038/nrclinonc.2009.188

Logan, C.Y. and Nusse, R. (2004). The Wnt signaling pathway in development and disease. Annual review of cell and developmental biology, 20, 781–810. doi:10.1146/annurev.cellbio.20.010403.113126

Lomax, M.E., Folkes, L.K. and O'Neill, P. (2013). Biological consequences of radiation-induced DNA damage: relevance to radiotherapy. Clinical oncology, 25(10), 578–585. doi:10.1016/j.clon.2013.06.007

Longley, D.B., Harkin, D.P. and Johnston, P.G. (2003). 5-fluorouracil: mechanisms of action and clinical strategies. Nat Rev Cancer, 3(5), 330–338. doi:10.1038/nrc1074

Lopez-Kostner, F., Lavery, I.C., Hool, G.R., Rybicki, L.A. and Fazio, V.W. (1998). Total mesorectal excision is not necessary for cancers of the upper rectum. Surgery, 124(4), 612–618. doi:10.1067/msy.1998.91361

Loree, J.M., Pereira, A.A.L., Lam, M., Willauer, A.N., Raghav, K., Dasari, A., Morris, V.K., Advani, S., Menter, D.G., Eng, C., Shaw, K., Broaddus, R., Routbort, M.J., Liu, Y., Morris, J.S., Luthra, R., Meric-Bernstam, F., Overman, M.J., Maru, D. and Kopetz, S. (2018). Classifying Colorectal Cancer by Tumor Location Rather than Sidedness Highlights a Continuum in Mutation Profiles and Consensus Molecular Subtypes. Clinical cancer research, 24(5), 1062–1072. doi:10.1158/1078-0432.CCR-17-2484

Low, D., Nguyen, D.D. and Mizoguchi, E. (2013). Animal models of ulcerative colitis and their application in drug research. Drug design, development and therapy, 7, 1341–1357. doi:10.2147/DDDT.S40107

Ludmir, E.B., Palta, M., Willett, C.G. and Czito, B.G. (2017). Total neoadjuvant therapy for rectal cancer: An emerging option. Cancer, 123(9), 1497–1506. doi:10.1002/cncr.30600

Lugade, A.A., Moran, J.P., Gerber, S.A., Rose, R.C., Frelinger, J.G. and Lord, E.M. (2005). Local radiation therapy of B16 melanoma tumors increases the generation of tumor antigen-specific effector cells that traffic to the tumor. Journal of immunology, 174(12), 7516–7523. doi:10.4049/jimmunol.174.12.7516

Luna-Pérez, P., Segura, J., Alvarado, I., Labastida, S., Santiago-Payán, H. and Quintero, A. (2000). Specific c-K-ras gene mutations as a tumor-response marker in locally advanced rectal cancer treated with preoperative chemoradiotherapy. Annals of surgical oncology, 7(10), 727–731. doi:10.1007/s10434-000-0727-0

Luo, F., Brooks, D.G., Ye, H., Hamoudi, R., Poulogiannis, G., Patek, C.E., Winton, D.J. and Arends, M.J. (2009). Mutated K-ras(Asp12) promotes tumourigenesis in Apc(Min) mice more in the large than the small intestines, with synergistic effects between K-ras and Wnt pathways. International journal of experimental pathology, 90(5), 558–574. doi:10.1111/j.1365-2613.2009.00667.x

Lynch, T.J., Bondarenko, I., Luft, A., Serwatowski, P., Barlesi, F., Chacko, R., Sebastian, M., Neal, J., Lu, H., Cuillerot, J.M. and Reck, M. (2012). Ipilimumab in combination with paclitaxel and carboplatin as first-line treatment in stage IIIB/IV non-small-cell lung cancer: results from a randomized, double-blind, multicenter phase II study. Journal of clinical oncology, 30(17), 2046–2054. doi:10.1200/JCO.2011.38.4032

Lynn, P.B., Van der Valk, M., Claassen, Y.H.M., Shi, Q., Widmar, M., Bastiaannet, E., Van de Velde, C. and Garcia-Aguilar, J. (2021). Chemoradiation and Local Excision versus Total Mesorectal Excision for T2N0 Rectal Cancer: Comparison of Short- and Long-Term Outcomes from Two Prospective Studies. Annals of surgery, published online 2021. doi:10.1097/SLA.0000000000005052

Ma, Y., Kepp, O., Ghiringhelli, F., Apetoh, L., Aymeric, L., Locher, C., Tesniere, A., Martins, I., Ly, A., Haynes, N.M., Smyth, M.J., Kroemer, G. and Zitvogel, L. (2010). Chemotherapy and radiotherapy: cryptic anticancer vaccines. Seminars in immunology, 22(3), 113–124. doi:10.1016/j.smim.2010.03.001

Maas, M., Nelemans, P.J., Valentini, V., Das, P., Rödel, C., Kuo, L.J., Calvo, F. A., García-Aguilar, J., Glynne-Jones, R., Haustermans, K., Mohiuddin, M., Pucciarelli, S., Small, W., Jr, Suárez, J., Theodoropoulos, G., Biondo, S., Beets-Tan, R.G. and Beets, G.L. (2010). Long-term outcome in patients with a pathological complete response after chemoradiation for rectal cancer: a pooled analysis of individual patient data. The Lancet Oncology, 11(9), 835–844. doi:10.1016/S1470-2045(10)70172-8

Mackey, J.B.G., Coffelt, S.B. and Carlin, L.M. (2019). Neutrophil Maturity in Cancer. Frontiers in immunology, 10, 1912. doi:10.3389/fimmu.2019.01912

Malumbres, M. and Barbacid, M. (2003). RAS oncogenes: the first 30 years. Nature reviews. Cancer, 3(6), 459–465. doi:10.1038/nrc1097

Mandard, A.M., Dalibard, F., Mandard, J.C., Marnay, J., Henry-Amar, M., Petiot, J.F., Roussel, A., Jacob, J.H., Segol, P. and Samama, G. (1994). Pathologic assessment of tumor regression after preoperative chemoradiotherapy of esophageal carcinoma. Clinicopathologic correlations. Cancer, 73(11), 2680–2686. doi:10.1002/1097-0142(19940601)73:11<2680::aid-cncr2820731105>3.0.co;2-c

Manicassamy, S., Prasad, P.D. and Swafford, D. (2021). Mouse Models of Colitis-Associated Colon Cancer. Methods in molecular biology, 2224, 133–146. doi:10.1007/978-1-0716-1008-4_10

Mariathasan, S., Turley, S.J., Nickles, D., Castiglioni, A., Yuen, K., Wang, Y., Kadel III, E.E., Koeppen, H., Astarita, J.L., Cubas, R., Jhunjhunwala, S., Banchereau, R., Yang, Y., Guan, Y., Chalouni, C., Ziai, J., Şenbabaoğlu, Y., Santoro, S., Sheinson, D., Hung, J., … Powles, T. (2018). TGFβ attenuates tumour response to PD-L1 blockade by contributing to exclusion of T cells. Nature, 554(7693), 544–548. doi:10.1038/nature25501

Marisa, L., de Reyniès, A., Duval, A., Selves, J., Gaub, M.P., Vescovo, L., Etienne-Grimaldi, M.C., Schiappa, R., Guenot, D., Ayadi, M., Kirzin, S., Chazal, M., Fléjou, J.F., Benchimol, D., Berger, A., Lagarde, A., Pencreach, E., Piard, F., Elias, D., Parc, Y., … Boige, V. (2013). Gene expression classification of colon cancer into molecular subtypes: characterization, validation, and prognostic value. PLoS medicine, 10(5), e1001453. doi:10.1371/journal.pmed.1001453

el Marjou, F., Janssen, K.P., Chang, B.H., Li, M., Hindie, V., Chan, L., Louvard, D., Chambon, P., Metzger, D. and Robine, S. (2004). Tissue-specific and inducible Cre-mediated recombination in the gut epithelium. Genesis, 39(3), 186–193. doi:10.1002/gene.20042

Markowitz, S., Wang, J., Myeroff, L., Parsons, R., Sun, L., Lutterbaugh, J., Fan, R. S., Zborowska, E., Kinzler, K.W. and Vogelstein, B. (1995). Inactivation of the type II TGF-beta receptor in colon cancer cells with microsatellite instability. Science, 268(5215), 1336–1338. doi:10.1126/science.7761852

Markowitz, S.D. and Bertagnolli, M.M. (2009). Molecular Basis of Colorectal Cancer. New England Journal of Medicine, 361(25), pp. 2449–2460. doi:10.1056/nejmra0804588.

Martling, A. L., Holm, T., Rutqvist, L. E., Moran, B. J., Heald, R. J. and Cedemark, B. (2000). Effect of a surgical training programme on outcome of rectal cancer in the County of Stockholm. Stockholm Colorectal Cancer Study Group, Basingstoke Bowel Cancer Research Project. Lancet, 356(9224), 93–96. doi:10.1016/s0140-6736(00)02469-7

Massagué, J. and Wotton, D. (2000). Transcriptional control by the TGF-beta/Smad signaling system. The EMBO journal, 19(8), 1745–1754. doi:10.1093/emboj/19.8.1745

Massagué J. (2008). TGFbeta in Cancer. Cell, 134(2), 215–230. doi:10.1016/j.cell.2008.07.001

Matano, M., Date, S., Shimokawa, M., Takano, A., Fujii, M., Ohta, Y., Watanabe, T., Kanai, T. and Sato, T. (2015). Modeling colorectal cancer using CRISPR-Cas9-mediated engineering of human intestinal organoids. Nature medicine, 21(3), 256–262. doi:10.1038/nm.3802

Matsutani, S., Shibutani, M., Maeda, K., Nagahara, H., Fukuoka, T., Nakao, S., Hirakawa, K. and Ohira, M. (2018). Significance of tumor-infiltrating lymphocytes before and after neoadjuvant therapy for rectal cancer. Cancer science, 109(4), 966–979. doi:10.1111/cas.13542

McCoy, M.J., Hemmings, C., Miller, T.J., Austin, S.J., Bulsara, M.K., Zeps, N., Nowak, A.K., Lake, R.A. and Platell, C.F. (2015). Low stromal Foxp3+ regulatory T-cell density is associated with complete response to neoadjuvant chemoradiotherapy in rectal cancer. British journal of cancer, 113(12), 1677–1686. doi:10.1038/bjc.2015.427

McDermott, F.D., Heeney, A., Kelly, M.E., Steele, R.J., Carlson, G.L. and Winter, D.C. (2015). Systematic review of preoperative, intraoperative and postoperative risk factors for colorectal anastomotic leaks. The British journal of surgery, 102(5), 462–479. doi:10.1002/bjs.9697

Mehlen, P. and Fearon, E.R. (2004). Role of the Dependence Receptor DCC in Colorectal Cancer Pathogenesis. Journal of Clinical Oncology, 22(16), pp. 3420–3428. doi:10.1200/jco.2004.02.019.

Mellman, I., Coukos, G. and Dranoff, G. (2011). Cancer immunotherapy comes of age. Nature, 480(7378), 480–489. doi:10.1038/nature10673

Mempel, T.R., Pittet, M.J., Khazaie, K., Weninger, W., Weissleder, R., von Boehmer, H. and von Andrian, U.H. (2006). Regulatory T cells reversibly suppress cytotoxic T cell function independent of effector differentiation. Immunity, 25(1), 129–141. doi:10.1016/j.immuni.2006.04.015

Meng, M., Zhong, K., Jiang, T., Liu, Z., Kwan, H. Y., & Su, T. (2021). The current understanding on the impact of KRAS on colorectal cancer. Biomedicine & pharmacotherapy, 140, 111717. doi:10.1016/j.biopha.2021.111717

Mladenov, E., Magin, S., Soni, A. and Iliakis, G. (2016). DNA double-strand-break repair in higher eukaryotes and its role in genomic instability and cancer: Cell cycle and proliferation-dependent regulation. Seminars in cancer biology, 37-38, 51–64. doi:10.1016/j.semcancer.2016.03.003

Mlecnik, B., Bindea, G., Angell, H.K., Maby, P., Angelova, M., Tougeron, D., Church, S.E., Lafontaine, L., Fischer, M., Fredriksen, T., Sasso, M., Bilocq, A. M., Kirilovsky, A., Obenauf, A.C., Hamieh, M., Berger, A., Bruneval, P., Tuech, J.J., Sabourin, J.C., Le Pessot, F., … Galon, J. (2016). Integrative Analyses of Colorectal Cancer Show Immunoscore Is a Stronger Predictor of Patient Survival Than Microsatellite Instability. Immunity, 44(3), 698–711. doi:10.1016/j.immuni.2016.02.025

Mole, R.H. (1953). Whole body irradiation; radiobiology or medicine?. The British journal of radiology, 26(305), 234–241. doi:10.1259/0007-1285-26-305-234

Mondini, M., Loyher, P.L., Hamon, P., Gerbé de Thoré, M., Laviron, M., Berthelot, K., Clémenson, C., Salomon, B.L., Combadière, C., Deutsch, E. and Boissonnas, A. (2019). CCR2-Dependent Recruitment of Tregs and Monocytes Following Radiotherapy Is Associated with TNFα-Mediated Resistance. Cancer immunology research, 7(3), 376–387. doi:10.1158/2326-6066.CIR-18-0633

Moo-Young, T.A., Larson, J.W., Belt, B.A., Tan, M.C., Hawkins, W.G., Eberlein, T.J., Goedegebuure, P.S. and Linehan, D.C. (2009). Tumor-derived TGF-beta mediates conversion of CD4+Foxp3+ regulatory T cells in a murine model of pancreas cancer. Journal of immunotherapy, 32(1), 12–21. doi:10.1097/CJI.0b013e318189f13c

Moorcraft, S.Y., Smyth, E.C. and Cunningham, D. (2013). The role of personalized medicine in metastatic colorectal cancer: an evolving landscape. Therapeutic Advances in Gastroenterology, 6(5), pp.381–395. doi:10.1177/1756283x13491797.

Morris, E.J.A., Finan, P.J., Spencer, K., Geh, I., Crellin, A., Quirke, P., Thomas, J.D., Lawton, S., Adams, R. and Sebag-Montefiore, D. (2016). Wide Variation in the Use of Radiotherapy in the Management of Surgically Treated Rectal Cancer Across the English National Health Service. Clinical oncology (Royal College of Radiologists (Great Britain)), 28(8), 522–531. doi:10.1016/j.clon.2016.02.002

Morris, J.C., Tan, A.R., Olencki, T.E., Shapiro, G.I., Dezube, B.J., Reiss, M., Hsu, F.J., Berzofsky, J.A. and Lawrence, D.P. (2014). Phase I study of GC1008 (fresolimumab): a human anti-transforming growth factor-beta (TGFß) monoclonal antibody in patients with advanced malignant melanoma or renal cell carcinoma. PloS one, 9(3), e90353. doi:10.1371/journal.pone.0090353

Mortezaee, K. and Najafi, M. (2021). Immune system in cancer radiotherapy: Resistance mechanisms and therapy perspectives. Critical reviews in oncology/hematology, 157, 103180. doi:10.1016/j.critrevonc.2020.103180

Moser, A.R., Pitot, H.C. and Dove, W.F. (1990). A dominant mutation that predisposes to multiple intestinal neoplasia in the mouse. Science, 247(4940), 322–324. doi:10.1126/science.2296722

Munn, D.H. and Bronte, V. (2016). Immune suppressive mechanisms in the tumor microenvironment. Current opinion in immunology, 39, 1–6. doi:10.1016/j.coi.2015.10.009

Murai, S., Kawai, K., Sonoda, H., Nozawa, H., Sasaki, K., Murono, K., Emoto, S., Yokoyama, Y., Anzai, H. and Ishihara, S. (2022). Computed tomographic colonography versus double-contrast barium enema for the preoperative evaluation of rectal cancer. Surgery today, 52(5), 755–762. doi:10.1007/s00595-021-02411-5

Nagtegaal, I.D., Marijnen, C.A., Kranenbarg, E.K., Mulder-Stapel, A., Hermans, J., van de Velde, C.J. and van Krieken, J.H. (2001). Local and distant recurrences in rectal cancer patients are predicted by the nonspecific immune response; specific immune response has only a systemic effect--a histopathological and immunohistochemical study. BMC cancer, 1, 7. doi:10.1186/1471-2407-1-7

Nagy A. (2000). Cre recombinase: the universal reagent for genome tailoring. Genesis, 26(2), 99–109.

Nakatsukasa, H., Nagy, P., Evarts, R.P., Hsia, C.C., Marsden, E. and Thorgeirsson, S.S. (1990). Cellular distribution of transforming growth factor-beta 1 and procollagen types I, III, and IV transcripts in carbon tetrachloride-induced rat liver fibrosis. The Journal of clinical investigation, 85(6), 1833–1843. doi:10.1172/JCI114643

Nassar, D. and Blanpain, C. (2016). Cancer Stem Cells: Basic Concepts and Therapeutic Implications. Annual Review of Pathology: Mechanisms of Disease, 11(1), pp. 47–76. doi:10.1146/annurev-pathol-012615-044438.

Nasser, M.W., Raghuwanshi, S.K., Malloy, K.M., Gangavarapu, P., Shim, J.Y., Rajarathnam, K. and Richardson, R.M. (2007). CXCR1 and CXCR2 activation and regulation. Role of aspartate 199 of the second extracellular loop of CXCR2 in CXCL8-mediated rapid receptor internalization. The Journal of biological chemistry, 282(9), 6906–6915. doi:10.1074/jbc.M610289200

National Cancer Registration & Analysis Service and Cancer Research UK. Chemotherapy, Radiotherapy and Tumour Resections in England: 2013-2014. NCRAS; 2017. Accessed Jan 2023: https://www.cancerdata.nhs.uk/treatments

Neufert, C., Becker, C. and Neurath, M.F. (2007). An inducible mouse model of colon carcinogenesis for the analysis of sporadic and inflammation-driven tumor progression. Nature protocols, 2(8), 1998–2004. doi:10.1038/nprot.2007.279

Ngan, S.Y., Burmeister, B., Fisher, R.J., Solomon, M., Goldstein, D., Joseph, D., Ackland, S.P., Schache, D., McClure, B., McLachlan, S.A., McKendrick, J., Leong, T., Hartopeanu, C., Zalcberg, J. and Mackay, J. (2012). Randomized trial of short-course radiotherapy versus long-course chemoradiation comparing rates of local recurrence in patients with T3 rectal cancer: Trans-Tasman Radiation Oncology Group trial 01.04. Journal of clinical oncology, 30(31), 3827–3833. doi:10.1200/JCO.2012.42.9597

Ni, J., Miller, M., Stojanovic, A., Garbi, N. and Cerwenka, A. (2012). Sustained effector function of IL-12/15/18-preactivated NK cells against established tumors. The Journal of experimental medicine, 209(13), 2351–2365. doi:10.1084/jem.20120944

NICE (2020). Colorectal cancer. Available at: https://www.nice.org.uk/guidance/ng151. [Accessed 9 Jul. 2020].

Nicolas, A.M., Pesic, M., Engel, E., Ziegler, P.K., Diefenhardt, M., Kennel, K.B., Buettner, F., Conche, C., Petrocelli, V., Elwakeel, E., Weigert, A., Zinoveva, A., Fleischmann, M., Häupl, B., Karakütük, C., Bohnenberger, H., Mosa, M.H., Kaderali, L., Gaedcke, J., Ghadimi, M., … Greten, F.R. (2022). Inflammatory fibroblasts mediate resistance to neoadjuvant therapy in rectal cancer. Cancer cell, 40(2), 168–184.e13. doi:10.1016/j.ccell.2022.01.004

Nicolas, A.M., Pesic, M., Rödel, F., Fokas, E. and Greten, F.R. (2022). Image-guided radiotherapy in an orthotopic mouse model of rectal cancer. STAR protocols, 3(4), 101749. doi:10.1016/j.xpro.2022.101749

Nicosia, L., Franceschini, D., Perrone-Congedi, F., Casamassima, F., Gerardi, M. A., Rigo, M., Mazzola, R., Perna, M., Scotti, V., Fodor, A., Iurato, A., Pasqualetti, F., Gadducci, G., Chiesa, S., Niespolo, R.M., Bruni, A., Alicino, G., Frassinelli, L., Borghetti, P., Di Marzo, A., … Alongi, F. (2022). A multicenter LArge retrospectIve daTabase on the personalization of stereotactic ABlative radiotherapy use in lung metastases from colon-rectal cancer: The LaIT-SABR study. Radiotherapy and oncology, 166, 92–99. doi:10.1016/j.radonc.2021.10.023

Niemi, V., Gaskarth, D. and Kemp, R. A. (2020). Extensive variability in the composition of immune infiltrate in different mouse models of cancer. Laboratory animal research, 36(1), 43. doi:10.1186/s42826-020-00075-9

Nowell P.C. (1976). The clonal evolution of tumor cell populations. Science (New York, N.Y.), 194(4260), 23–28. doi:10.1126/science.959840

Nunes, N.S., Kim, S., Sundby, M., Chandran, P., Burks, S.R., Paz, A.H. and Frank, J.A. (2018). Temporal clinical, proteomic, histological and cellular immune responses of dextran sulfate sodium-induced acute colitis. World journal of gastroenterology, 24(38), 4341–4355. doi:10.3748/wjg.v24.i38.4341

Nusse, R. and Clevers, H. (2017). Wnt/β-Catenin Signaling, Disease, and Emerging Therapeutic Modalities. Cell, 169(6), 985–999. doi:10.1016/j.cell.2017.05.016

Nymann, T., Jess, P. and Christiansen, J. (1995). Rate and treatment of pelvic recurrence after abdominoperineal resection and low anterior resection for rectal cancer. Diseases of the colon and rectum, 38(8), 799–802. doi:10.1007/BF02049834

Obeid, M., Tesniere, A., Ghiringhelli, F., Fimia, G.M., Apetoh, L., Perfettini, J. L., Castedo, M., Mignot, G., Panaretakis, T., Casares, N., Métivier, D., Larochette, N., van Endert, P., Ciccosanti, F., Piacentini, M., Zitvogel, L. and Kroemer, G. (2007). Calreticulin exposure dictates the immunogenicity of cancer cell death. Nature medicine, 13(1), 54–61. doi:10.1038/nm1523

O'Connell, E., Reynolds, I.S., McNamara, D.A., Prehn, J.H.M. and Burke, J.P. (2020). Microsatellite instability and response to neoadjuvant chemoradiotherapy in rectal cancer: A systematic review and meta-analysis. Surgical oncology, 34, 57–62. doi:10.1016/j.suronc.2020.03.009

Ohba, K., Omagari, K., Nakamura, T., Ikuno, N., Saeki, S., Matsuo, I., Kinoshita, H., Masuda, J., Hazama, H., Sakamoto, I. and Kohno, S. (1998). Abscopal regression of hepatocellular carcinoma after radiotherapy for bone metastasis. Gut, 43(4), 575–577. doi:10.1136/gut.43.4.575

Ohue, Y. and Nishikawa, H. (2019). Regulatory T (Treg) cells in cancer: Can Treg cells be a new therapeutic target?. Cancer science, 110(7), 2080–2089. https://doi.org/10.1111/cas.14069

Ojima, E., Inoue, Y., Watanabe, H., Hiro, J., Toiyama, Y., Miki, C. and Kusunoki, M. (2006). The optimal schedule for 5-fluorouracil radiosensitization in colon cancer cell lines. Oncology reports, 16(5), 1085–1091.

Okayasu, I., Hatakeyama, S., Yamada, M., Ohkusa, T., Inagaki, Y. and Nakaya, R. (1990). A novel method in the induction of reliable experimental acute and chronic ulcerative colitis in mice. Gastroenterology, 98(3), 694–702. doi:10.1016/0016-5085(90)90290-h

Okayasu, I., Yamada, M., Mikami, T., Yoshida, T., Kanno, J. and Ohkusa, T. (2002). Dysplasia and carcinoma development in a repeated dextran sulfate sodium-induced colitis model. Journal of gastroenterology and hepatology, 17(10), 1078–1083. doi:10.1046/j.1440-1746.2002.02853.x

Olive, P.L. and Banáth, J.P. (2004). Phosphorylation of histone H2AX as a measure of radiosensitivity. International journal of radiation oncology, biology, physics, 58(2), 331–335. doi:10.1016/j.ijrobp.2003.09.028

Olson, R., Mathews, L., Liu, M., Schellenberg, D., Mou, B., Berrang, T., Harrow, S., Correa, R.J.M., Bhat, V., Pai, H., Mohamed, I., Miller, S., Schneiders, F., Laba, J., Wilke, D., Senthi, S., Louie, A.V., Swaminath, A., Chalmers, A., Gaede, S., … Palma, D.A. (2020). Stereotactic ablative radiotherapy for the

comprehensive treatment of 1-3 Oligometastatic tumors (SABR-COMET-3): study protocol for a randomized phase III trial. BMC cancer, 20(1), 380. doi:10.1186/s12885-020-06876-4

Ooft, S.N., Weeber, F., Schipper, L., Dijkstra, K.K., McLean, C.M., Kaing, S., van de Haar, J., Prevoo, W., van Werkhoven, E., Snaebjornsson, P., Hoes, L.R., Chalabi, M., van der Velden, D., van Leerdam, M., Boot, H., Grootscholten, C., Huitema, A.D.R., Bloemendal, H.J., Cuppen, E. and Voest, E.E. (2021). Prospective experimental treatment of colorectal cancer patients based on organoid drug responses. ESMO open, 6(3), 100103. doi:10.1016/j.esmoop.2021.100103

O'Rourke, K.P., Loizou, E., Livshits, G., Schatoff, E.M., Baslan, T., Manchado, E., Simon, J., Romesser, P.B., Leach, B., Han, T., Pauli, C., Beltran, H., Rubin, M. A., Dow, L.E. and Lowe, S.W. (2017). Transplantation of engineered organoids enables rapid generation of metastatic mouse models of colorectal cancer. Nature biotechnology, 35(6), 577–582. doi:10.1038/nbt.3837

Oshima, M., Dinchuk, J.E., Kargman, S.L., Oshima, H., Hancock, B., Kwong, E., Trzaskos, J.M., Evans, J.F. and Taketo, M.M. (1996). Suppression of intestinal polyposis in Apc delta716 knockout mice by inhibition of cyclooxygenase 2 (COX-2). Cell, 87(5), 803–809. doi:10.1016/s0092-8674(00)81988-1

Overgaard, J. (2007). Hypoxic radiosensitization: adored and ignored. Journal of clinical oncology, 25(26), 4066–4074. doi:10.1200/JCO.2007.12.7878

Overman, M.J., McDermott, R., Leach, J.L., Lonardi, S., Lenz, H.J., Morse, M. A., Desai, J., Hill, A., Axelson, M., Moss, R.A., Goldberg, M.V., Cao, Z.A., Ledeine, J.M., Maglinte, G.A., Kopetz, S. and André, T. (2017). Nivolumab in patients with metastatic DNA mismatch repair-deficient or microsatellite instability-high colorectal cancer (CheckMate 142): an open-label, multicentre, phase 2 study. The Lancet Oncology, 18(9), 1182–1191. doi:10.1016/S1470-2045(17)30422-9

Pajonk, F., Vlashi, E. and McBride, W.H. (2010). Radiation resistance of cancer stem cells: the 4 R's of radiobiology revisited. Stem cells, 28(4), 639–648. doi:10.1002/stem.318

Pantelouris E. M. (1968). Absence of thymus in a mouse mutant. Nature, 217(5126), 370–371. doi:10.1038/217370a0

Pardoll D.M. (2012). The blockade of immune checkpoints in cancer immunotherapy. Nature Reviews Cancer, 12(4), 252–264. doi:10.1038/nrc3239

Pardoll, D. and Drake, C. (2012) Immunotherapy earns its spot in the ranks of cancer therapy. The Journal of Experimental Medicine, 209(2), 201-209. doi:10.1084/jem.20112275.

Park, C.C., Zhang, H.J., Yao, E.S., Park, C.J. and Bissell, M.J. (2008). Beta1 integrin inhibition dramatically enhances radiotherapy efficacy in human breast cancer xenografts. Cancer research, 68(11), 4398–4405. doi:10.1158/0008-5472.CAN-07-6390

Park, J.H., Richards, C.H., McMillan, D.C., Horgan, P.G. and Roxburgh, C.S.D. (2014). The relationship between tumour stroma percentage, the tumour

microenvironment and survival in patients with primary operable colorectal cancer. Annals of oncology, 25(3), 644–651. doi:10.1093/annonc/mdt593

Park, S.S., Dong, H., Liu, X., Harrington, S.M., Krco, C.J., Grams, M.P., Mansfield, A.S., Furutani, K.M., Olivier, K.R. and Kwon, E.D. (2015). PD-1 Restrains Radiotherapy-Induced Abscopal Effect. Cancer immunology research, 3(6), 610–619. doi:10.1158/2326-6066.CIR-14-0138

Pastor, D.M., Poritz, L.S., Olson, T.L., Kline, C.L., Harris, L.R., Koltun, W.A., Chinchilli, V.M. and Irby, R.B. (2010). Primary cell lines: false representation or model system? a comparison of four human colorectal tumors and their coordinately established cell lines. International journal of clinical and experimental medicine, 3(1), 69–83. PMID: 20369042

Pawlik, T.M. and Keyomarsi, K. (2004). Role of cell cycle in mediating sensitivity to radiotherapy. International journal of radiation oncology, biology, physics, 59(4), 928–942. doi:10.1016/j.ijrobp.2004.03.005

Peeters, K.C., van de Velde, C.J., Leer, J.W., Martijn, H., Junggeburt, J.M., Kranenbarg, E.K., Steup, W.H., Wiggers, T., Rutten, H.J. and Marijnen, C.A. (2005). Late side effects of short-course preoperative radiotherapy combined with total mesorectal excision for rectal cancer: increased bowel dysfunction in irradiated patients - a Dutch colorectal cancer group study. Journal of clinical oncology, 23(25), 6199–6206. doi:10.1200/JCO.2005.14.779

Pelleitier, M. and Montplaisir, S. (1975). The nude mouse: a model of deficient T-cell function. Methods and achievements in experimental pathology, 7, 149–166.

Peltomäki, P. and Vasen, H. (2004). Mutations Associated with HNPCC Predisposition — Update of ICG-HNPCC/INSiGHT Mutation Database. Disease Markers, 20(4-5), pp.269–276. doi:10.1155/2004/305058.

Peng, W., Liu, C., Xu, C., Lou, Y., Chen, J., Yang, Y., Yagita, H., Overwijk, W.W., Lizée, G., Radvanyi, L. and Hwu, P. (2012). PD-1 blockade enhances T-cell migration to tumors by elevating IFN-γ inducible chemokines. Cancer research, 72(20), 5209–5218. doi:10.1158/0008-5472.CAN-12-1187

Peranzoni, E., Lemoine, J., Vimeux, L., Feuillet, V., Barrin, S., Kantari-Mimoun, C., Bercovici, N., Guérin, M., Biton, J., Ouakrim, H., Régnier, F., Lupo, A., Alifano, M., Damotte, D. and Donnadieu, E. (2018). Macrophages impede CD8 T cells from reaching tumor cells and limit the efficacy of anti-PD-1 treatment. Proceedings of the National Academy of Sciences of the United States of America, 115(17), E4041–E4050. doi:10.1073/pnas.1720948115

Petitprez, F., Levy, S., Sun, C.M., Meylan, M., Linhard, C., Becht, E., Elarouci, N., Tavel, D., Roumenina, L.T., Ayadi, M., Sautès-Fridman, C., Fridman, W.H. and de Reyniès, A. (2020). The murine Microenvironment Cell Population counter method to estimate abundance of tissue-infiltrating immune and stromal cell populations in murine samples using gene expression. Genome medicine, 12(1), 86. doi:10.1186/s13073-020-00783-w

Plawski, A., Banasiewicz, T., Borun, P., Kubaszewski, L., Krokowicz, P., Skrzypczak-Zielinska, M. and Lubinski, J. (2013). Familial adenomatous polyposis of the colon. Hereditary Cancer in Clinical Practice, 11(1). doi:10.1186/1897-4287-11-15.

Portanova, J.P., Zhang, Y., Anderson, G.D., Hauser, S.D., Masferrer, J.L., Seibert, K., Gregory, S.A. and Isakson, P.C. (1996). Selective neutralization of prostaglandin E2 blocks inflammation, hyperalgesia, and interleukin 6 production in vivo. The Journal of experimental medicine, 184(3), 883–891. doi:10.1084/jem.184.3.883

Postow, M.A., Callahan, M.K., Barker, C.A., Yamada, Y., Yuan, J., Kitano, S., Mu, Z., Rasalan, T., Adamow, M., Ritter, E., Sedrak, C., Jungbluth, A.A., Chua, R., Yang, A.S., Roman, R.A., Rosner, S., Benson, B., Allison, J.P., Lesokhin, A. M., Gnjatic, S., … Wolchok, J.D. (2012). Immunologic correlates of the abscopal effect in a patient with melanoma. The New England journal of medicine, 366(10), 925–931. doi:10.1056/NEJMoa1112824

Prete, F.P., Pezzolla, A., Prete, F., Testini, M., Marzaioli, R., Patriti, A., Jimenez-Rodriguez, R.M., Gurrado, A. and Strippoli, G.F.M. (2018). Robotic Versus Laparoscopic Minimally Invasive Surgery for Rectal Cancer: A Systematic Review and Meta-analysis of Randomized Controlled Trials. Annals of surgery, 267(6), 1034–1046. doi:10.1097/SLA.0000000000002523

Price, J.G., Idoyaga, J., Salmon, H., Hogstad, B., Bigarella, C.L., Ghaffari, S., Leboeuf, M. and Merad, M. (2015). CDKN1A regulates Langerhans cell survival and promotes Treg cell generation upon exposure to ionizing irradiation. Nature immunology, 16(10), 1060–1068. doi:10.1038/ni.3270

Prins, R.M., Incardona, F., Lau, R., Lee, P., Claus, S., Zhang, W., Black, K.L. and Wheeler, C.J. (2004). Characterization of defective CD4-CD8- T cells in murine tumors generated independent of antigen specificity. Journal of immunology, 172(3), 1602–1611. doi:10.4049/jimmunol.172.3.1602

Public Health Scotland (2017). Bowel screening [online]. Available at: http://www.healthscotland.scot/health-topics/screening/bowel-screening. [Accessed Jan 2022].

Public Health Scotland (2021). Detect cancer early staging data - Detect cancer early staging data - Publications - Public Health Scotland [online]. Available at: https://publichealthscotland.scot/publications/detect-cancer-early-staging-data/detect-cancer-early-staging-data-year-9-1-january-2019-to-31-december-2020/. [Accessed Jun 2022].

Quah, H.M., Chou, J.F., Gonen, M., Shia, J., Schrag, D., Saltz, L.B., Goodman, K. A., Minsky, B.D., Wong, W.D., & Weiser, M.R. (2008). Pathologic stage is most prognostic of disease-free survival in locally advanced rectal cancer patients after preoperative chemoradiation. Cancer, 113(1), 57–64. doi:10.1002/cncr.23516

Rad, R., Cadiñanos, J., Rad, L., Varela, I., Strong, A., Kriegl, L., Constantino-Casas, F., Eser, S., Hieber, M., Seidler, B., Price, S., Fraga, M. F., Calvanese, V., Hoffman, G., Ponstingl, H., Schneider, G., Yusa, K., Grove, C., Schmid, R.M., Wang, W., … Bradley, A. (2013). A genetic progression model of Braf(V600E)-induced intestinal tumorigenesis reveals targets for therapeutic intervention. Cancer cell, 24(1), 15–29. doi:10.1016/j.ccr.2013.05.014

Rahma, O.E., Yothers, G., Hong, T.S., Russell, M.M., You, Y.N., Parker, W., Jacobs, S.A., Colangelo, L.H., Lucas, P.C., Gollub, M.J., Hall, W.A., Kachnic, L. A., Vijayvergia, N., O'Rourke, M.A., Faller, B.A., Valicenti, R.K., Schefter, T.E., George, S., Kainthla, R., Stella, P.J., … George, T.J. (2021). Use of Total

Neoadjuvant Therapy for Locally Advanced Rectal Cancer: Initial Results From the Pembrolizumab Arm of a Phase 2 Randomized Clinical Trial. JAMA oncology, 7(8), 1225–1230. doi:10.1001/jamaoncol.2021.1683

Rajagopalan, H., Bardelli, A., Lengauer, C., Kinzler, K.W., Vogelstein, B. and Velculescu, V.E. (2002). RAF/RAS oncogenes and mismatch-repair status. Nature, 418(6901), pp. 934–934. doi:10.1038/418934a.

Reck, M., Rodríguez-Abreu, D., Robinson, A.G., Hui, R., Csőszi, T., Fülöp, A., Gottfried, M., Peled, N., Tafreshi, A., Cuffe, S., O'Brien, M., Rao, S., Hotta, K., Leiby, M.A., Lubiniecki, G.M., Shentu, Y., Rangwala, R., Brahmer, J.R. and KEYNOTE-024 Investigators. (2016). Pembrolizumab versus Chemotherapy for PD-L1-Positive Non-Small-Cell Lung Cancer. The New England journal of medicine, 375(19), 1823–1833. doi:10.1056/NEJMoa1606774

Rees, G.J. and Ross, C.M. (1983). Abscopal regression following radiotherapy for adenocarcinoma. The British journal of radiology, 56(661), 63–66. doi:10.1259/0007-1285-56-661-63

Renehan, A.G., Malcomson, L., Emsley, R., Gollins, S., Maw, A., Myint, A.S., Rooney, P.S., Susnerwala, S., Blower, A., Saunders, M.P., Wilson, M.S., Scott, N. and O'Dwyer, S.T. (2016). Watch-and-wait approach versus surgical resection after chemoradiotherapy for patients with rectal cancer (the OnCoRe project): a propensity-score matched cohort analysis. The Lancet Oncology, 17(2), 174–183. doi:10.1016/S1470-2045(15)00467-2

Rex, D.K., Baron, J.A., Batts, K.P., Burke, C.A., Burt, R.W., Goldblum, J.R., Guillem, J.R., Kahi, C.J., Kalady, M.F., O'Brien, M.J., Odze, R.D., Ogino, S., Parry, S., Snover, D.C., Torlakovic, E.E., Wise, P.E., Young, J., Church, J. (2012). Serrated Lesions of the Colorectum: Review and Recommendations From an Expert Panel. American Journal of Gastroenterology, 107(9), pp. 1315–1329. doi:10.1038/ajg.2012.161.

Reynolds, I.S., McNamara, D.A., Kay, E.W., O'Neill, B., Deasy, J. and Burke, J.P. (2018). The significance of mucin pools following neoadjuvant chemoradiotherapy for locally advanced rectal cancer. Journal of surgical oncology, 118(7), 1129–1134. doi:10.1002/jso.25247

Ribas A. (2015). Adaptive Immune Resistance: How Cancer Protects from Immune Attack. Cancer discovery, 5(9), 915–919. doi:10.1158/2159-8290.CD-15-0563

Rodriguez-Ruiz, M.E., Rodriguez, I., Garasa, S., Barbes, B., Solorzano, J.L., Perez-Gracia, J.L., Labiano, S., Sanmamed, M.F., Azpilikueta, A., Bolaños, E., Sanchez-Paulete, A.R., Aznar, M.A., Rouzaut, A., Schalper, K.A., Jure-Kunkel, M. and Melero, I. (2016). Abscopal Effects of Radiotherapy Are Enhanced by Combined Immunostimulatory mAbs and Are Dependent on CD8 T Cells and Crosspriming. Cancer research, 76(20), 5994–6005. doi:10.1158/0008-5472.CAN-16-0549

Rodríguez-Ruiz, M. E., Rodríguez, I., Mayorga, L., Labiano, T., Barbes, B., Etxeberria, I., Ponz-Sarvise, M., Azpilikueta, A., Bolaños, E., Sanmamed, M. F., Berraondo, P., Calvo, F. A., Barcelos-Hoff, M. H., Perez-Gracia, J. L., & Melero, I. (2019). TGFβ Blockade Enhances Radiotherapy Abscopal Efficacy Effects in Combination with Anti-PD1 and Anti-CD137 Immunostimulatory Monoclonal Antibodies. Molecular cancer therapeutics, 18(3), 621–631. https://doi.org/10.1158/1535-7163.MCT-18-0558

Roper, J., Tammela, T., Cetinbas, N.M., Akkad, A., Roghanian, A., Rickelt, S., Almeqdadi, M., Wu, K., Oberli, M.A., Sánchez-Rivera, F.J., Park, Y.K., Liang, X., Eng, G., Taylor, M.S., Azimi, R., Kedrin, D., Neupane, R., Beyaz, S., Sicinska, E. T., Suarez, Y., … Yilmaz, Ö.H. (2017). In vivo genome editing and organoid transplantation models of colorectal cancer and metastasis. Nature biotechnology, 35(6), 569–576. doi:10.1038/nbt.3836

Rowshanravan, B., Halliday, N. and Sansom, D.M. (2018). CTLA-4: a moving target in immunotherapy. Blood, 131(1), 58–67. doi:10.1182/blood-2017-06-741033

Roxburgh, C.S., Shia, J., Vakiani, E., Daniel, T. and Weiser, M.R. (2018). Potential immune priming of the tumor microenvironment with FOLFOX chemotherapy in locally advanced rectal cancer. Oncoimmunology, 7(6), e1435227. doi:10.1080/2162402X.2018.1435227

Rullier, E., Rouanet, P., Tuech, J.J., Valverde, A., Lelong, B., Rivoire, M., Faucheron, J.L., Jafari, M., Portier, G., Meunier, B., Sileznieff, I., Prudhomme, M., Marchal, F., Pocard, M., Pezet, D., Rullier, A., Vendrely, V., Denost, Q., Asselineau, J. and Doussau, A. (2017). Organ preservation for rectal cancer (GRECCAR 2): a prospective, randomised, open-label, multicentre, phase 3 trial. Lancet (London, England), 390(10093), 469–479. doi:10.1016/S0140-6736(17)31056-5

Sabaawy, H.E., Ryan, B.M., Khiabanian, H. and Pine, S.R. (2021). JAK/STAT of all trades: linking inflammation with cancer development, tumor progression and therapy resistance. Carcinogenesis, 42(12), 1411–1419. doi:10.1093/carcin/bgab075

Sadanandam, A., Lyssiotis, C.A., Homicsko, K., Collisson, E.A., Gibb, W.J., Wullschleger, S., Ostos, L.C., Lannon, W.A., Grotzinger, C., Del Rio, M., Lhermitte, B., Olshen, A.B., Wiedenmann, B., Cantley, L.C., Gray, J.W. and Hanahan, D. (2013). A colorectal cancer classification system that associates cellular phenotype and responses to therapy. Nature medicine, 19(5), 619–625. doi:10.1038/nm.3175

Sakaguchi, S., Yamaguchi, T., Nomura, T. and Ono, M. (2008). Regulatory T cells and immune tolerance. Cell, 133(5), 775–787. doi:10.1016/j.cell.2008.05.009

Sakai, K., Kazama, S., Nagai, Y., Murono, K., Tanaka, T., Ishihara, S., Sunami, E., Tomida, S., Nishio, K. and Watanabe, T. (2014). Chemoradiation provides a physiological selective pressure that increases the expansion of aberrant TP53 tumor variants in residual rectal cancerous regions. Oncotarget, 5(20), 9641–9649. doi:10.18632/oncotarget.2438

Saltz, L.B., Meropol, N.J., Loehrer, P.J., Needle, M.N., Kopit, J. and Mayer, R.J. (2004). Phase II Trial of Cetuximab in Patients With Refractory Colorectal Cancer That Expresses the Epidermal Growth Factor Receptor. Journal of Clinical Oncology, 22(7), pp.1201–1208. doi:10.1200/jco.2004.10.182.

Salvatore, L., Bensi, M., Corallo, S., Bergamo, F., Pellegrini, I., Rasola, C., Borelli, B., Tamburini, E., Randon, G., Galuppo, S., Boccaccino, A., Viola, M.G., Auriemma, A., Fea, E., Barbara, C., Bustreo, S., Smiroldo, V., Barbaro, B., Gambacorta, M.A. and Tortora, G. (2021). Phase II study of preoperative chemoradiotherapy plus avelumab in patients with locally advanced rectal

cancer: the AVANA study. J Clin Oncol, 39(suppl_15), pp3511. doi:10.1200/JCO.2021.39.15_suppl.3511

Sansom, O.J., Reed, K.R., Hayes, A.J., Ireland, H., Brinkmann, H., Newton, I.P., Batlle, E., Simon-Assmann, P., Clevers, H., Nathke, I.S., Clarke, A.R. and Winton, D.J. (2004). Loss of Apc in vivo immediately perturbs Wnt signaling, differentiation, and migration. Genes & Development, 18(12), pp.1385–1390. doi:10.1101/gad.287404.

Sansom, O.J., Meniel, V., Wilkins, J.A., Cole, A.M., Oien, K.A., Marsh, V., Jamieson, T.J., Guerra, C., Ashton, G.H., Barbacid, M. and Clarke, A.R. (2006). Loss of Apc allows phenotypic manifestation of the transforming properties of an endogenous K-ras oncogene in vivo. Proceedings of the National Academy of Sciences of the United States of America, 103(38), 14122–14127. doi:10.1073/pnas.0604130103

Sato, T., Vries, R.G., Snippert, H.J., van de Wetering, M., Barker, N., Stange, D. E., van Es, J.H., Abo, A., Kujala, P., Peters, P.J. and Clevers, H. (2009). Single Lgr5 stem cells build crypt-villus structures in vitro without a mesenchymal niche. Nature, 459(7244), 262–265. doi:10.1038/nature07935

Sato, T., Stange, D.E., Ferrante, M., Vries, R.G., Van Es, J.H., Van den Brink, S., Van Houdt, W.J., Pronk, A., Van Gorp, J., Siersema, P.D. and Clevers, H. (2011). Long-term expansion of epithelial organoids from human colon, adenoma, adenocarcinoma, and Barrett's epithelium. Gastroenterology, 141(5), 1762–1772. doi:10.1053/j.gastro.2011.07.050

Sauer, R., Becker, H., Hohenberger, W., Rödel, C., Wittekind, C., Fietkau, R., Martus, P., Tschmelitsch, J., Hager, E., Hess, C.F., Karstens, J.H., Liersch, T., Schmidberger, H., Raab, R. and German Rectal Cancer Study Group (2004). Preoperative versus postoperative chemoradiotherapy for rectal cancer. The New England journal of medicine, 351(17), 1731–1740. doi:10.1056/NEJMoa040694

Sauer, R., Liersch, T., Merkel, S., Fietkau, R., Hohenberger, W., Hess, C., Becker, H., Raab, H.R., Villanueva, M.T., Witzigmann, H., Wittekind, C., Beissbarth, T. and Rödel, C. (2012). Preoperative versus postoperative chemoradiotherapy for locally advanced rectal cancer: results of the German CAO/ARO/AIO-94 randomized phase III trial after a median follow-up of 11 years. Journal of clinical oncology, 30(16), 1926–1933. doi:10.1200/JCO.2011.40.1836

Saunier, E.F. and Akhurst, R.J. (2006). TGF beta inhibition for cancer therapy. Curr Cancer Drug Targets, 6(7), 565-578. doi:10.2174/156800906778742460

Sawayama, H., Miyamoto, Y., Ogawa, K., Yoshida, N. and Baba, H. (2020). Investigation of colorectal cancer in accordance with consensus molecular subtype classification. Annals of gastroenterological surgery, 4(5), 528–539. doi:10.1002/ags3.12362

Schaue, D. and McBride, W.H. (2010). Links between innate immunity and normal tissue radiobiology. Radiation research, 173(4), 406–417. doi:10.1667/RR1931.1

Schaue, D., Ratikan, J.A., Iwamoto, K.S. and McBride, W.H. (2012). Maximizing tumor immunity with fractionated radiation. International journal of radiation oncology, biology, physics, 83(4), 1306–1310. doi:10.1016/j.ijrobp.2011.09.049

Schaue, D. and McBride, W.H. (2015). Opportunities and challenges of radiotherapy for treating cancer. Nature reviews. Clinical oncology, 12(9), 527–540. doi:10.1038/nrclinonc.2015.120

Schmitt, M.W., Loeb, L.A. and Salk, J.J. (2016). The influence of subclonal resistance mutations on targeted cancer therapy. Nature reviews. Clinical oncology, 13(6), 335–347. doi:10.1038/nrclinonc.2015.175

Schmitt, M. and Greten, F.R. (2021). The inflammatory pathogenesis of colorectal cancer. Nature Reviews Immunology, 21(10), pp. 653–667. doi:10.1038/s41577-021-00534-x.

Schreiber, R.D., Old, L.J. and Smyth, M.J. (2011). Cancer immunoediting: integrating immunity's roles in cancer suppression and promotion. Science, 331(6024), 1565–1570. doi:10.1126/science.1203486

Schrörs, B., Hos, B.J., Yildiz, I.G., Löwer, M., Lang, F., Holtsträter, C., Becker, J., Vormehr, M., Sahin, U., Ossendorp, F. and Diken, M. (2023). MC38 colorectal tumor cell lines from two different sources display substantial differences in transcriptome, mutanome and neoantigen expression. Frontiers in immunology, 14, 1102282. doi:10.3389/fimmu.2023.1102282

Schwartz R.H. (1992). Costimulation of T lymphocytes: the role of CD28, CTLA-4, and B7/BB1 in interleukin-2 production and immunotherapy. Cell, 71(7), 1065–1068. doi:10.1016/s0092-8674(05)80055-8

Scott, N. and Quirke, P. (1993). Molecular biology of colorectal neoplasia. Gut, 34(3), pp. 289–292. doi:10.1136/gut.34.3.289.

Sebag-Montefiore, D., Stephens, R.J., Steele, R., Monson, J., Grieve, R., Khanna, S., Quirke, P., Couture, J., de Metz, C., Myint, A.S., Bessell, E., Griffiths, G., Thompson, L.C. and Parmar, M. (2009). Preoperative radiotherapy versus selective postoperative chemoradiotherapy in patients with rectal cancer (MRC CR07 and NCIC-CTG C016): a multicentre, randomised trial. Lancet, 373(9666), 811–820. doi:10.1016/S0140-6736(09)60484-0

Segal, N.H., Parsons, D.W., Peggs, K.S., Velculescu, V., Kinzler, K.W., Vogelstein, B. and Allison, J.P. (2008). Epitope landscape in breast and colorectal cancer. Cancer research, 68(3), 889–892. doi:10.1158/0008-5472.CAN-07-3095

Sethi, N., Dai, X., Winter, C.G. and Kang, Y. (2011). Tumor-derived JAGGED1 promotes osteolytic bone metastasis of breast cancer by engaging notch signaling in bone cells. Cancer cell, 19(2), 192–205. doi:10.1016/j.ccr.2010.12.022

Shalem, O., Sanjana, N.E., Hartenian, E., Shi, X., Scott, D.A., Mikkelson, T., Heckl, D., Ebert, B.L., Root, D.E., Doench, J.G. and Zhang, F. (2014). Genome-scale CRISPR-Cas9 knockout screening in human cells. Science, 343(6166), 84–87. doi:10.1126/science.1247005

Shamseddine, A., Zeidan, Y., Bouferra, Y., Turfa, R., Kattan, J., Mukherji, D., Temraz, S., Alqasem, K., Amarin, R., Al Awabdeh, A., Deeba, S., Doughan, S., Mohamed, I., Elkhaldi, M., Daoud, F., Al Masri, M., Dabous, A., Hushki, A., Charafeddine, M., Al Darazi, M. and Geara, F. (2021). SO-30 Efficacy and safety of neoadjuvant short-course radiation followed by mFOLFOX-6 plus avelumab for

locally-advanced rectal adenocarcinoma: averectal study. Ann Oncol,32(3):S215. doi:10.1016/j.annonc.2021.05.054

Sharabi, A.B., Nirschl, C.J., Kochel, C.M., Nirschl, T.R., Francica, B.J., Velarde, E., Deweese, T.L. and Drake, C.G. (2015). Stereotactic Radiation Therapy Augments Antigen-Specific PD-1-Mediated Antitumor Immune Responses via Cross-Presentation of Tumor Antigen. Cancer immunology research, 3(4), 345–355. doi:10.1158/2326-6066.CIR-14-0196

Sharpe, A.H. and Pauken, K.E. (2018). The diverse functions of the PD1 inhibitory pathway. Nature reviews. Immunology, 18(3), 153–167. doi:10.1038/nri.2017.108

Shen, L., Toyota, M., Kondo, Y., Lin, E., Zhang, L., Guo, Y., Hernandez, N.S., Chen, X., Ahmed, S., Konishi, K., Hamilton, S.R. and Issa, J.P. (2007). Integrated genetic and epigenetic analysis identifies three different subclasses of colon cancer. Proceedings of the National Academy of Sciences of the United States of America, 104(47), 18654–18659. doi:10.1073/pnas.0704652104

Shi, X., Young, C.D., Zhou, H. and Wang, X. (2020). Transforming Growth Factor-β Signaling in Fibrotic Diseases and Cancer-Associated Fibroblasts. Biomolecules, 10(12), 1666. doi:10.3390/biom10121666

Shi, Y. and Massagué, J. (2003). Mechanisms of TGF-beta signaling from cell membrane to the nucleus. Cell, 113(6), 685–700. doi:10.1016/s0092-8674(03)00432-x

Shia, J., Guillem, J.G., Moore, H.G., Tickoo, S.K., Qin, J., Ruo, L., Suriawinata, A., Paty, P.B., Minsky, B.D., Weiser, M.R., Temple, L.K., Wong, W.D. and Klimstra, D.S. (2004). Patterns of morphologic alteration in residual rectal carcinoma following preoperative chemoradiation and their association with long-term outcome. The American journal of surgical pathology, 28(2), 215–223. doi:10.1097/00000478-200402000-00009

Shia, J., McManus, M., Guillem, J.G., Leibold, T., Zhou, Q., Tang, L.H., Riedel, E.R., Weiser, M.R., Paty, P.B., Temple, L.K., Nash, G., Kolosov, K., Minsky, B. D., Wong, W.D. and Klimstra, D.S. (2011). Significance of acellular mucin pools in rectal carcinoma after neoadjuvant chemoradiotherapy. The American journal of surgical pathology, 35(1), 127–134. doi:10.1097/PAS.0b013e318200cf78

Shibata, H., Toyama, K., Shioya, H., Ito, M., Hirota, M., Hasegawa, S., Matsumoto, H., Takano, H., Akiyama, T., Toyoshima, K., Kanamaru, R., Kanegae, Y., Saito, I., Nakamura, Y., Shiba, K. and Noda, T. (1997). Rapid colorectal adenoma formation initiated by conditional targeting of the Apc gene. Science, 278(5335), 120–123. doi:10.1126/science.278.5335.120

Shinto, E., Hase, K., Hashiguchi, Y., Sekizawa, A., Ueno, H., Shikina, A., Kajiwara, Y., Kobayashi, H., Ishiguro, M. and Yamamoto, J. (2014). CD8+ and FOXP3+ tumor-infiltrating T cells before and after chemoradiotherapy for rectal cancer. Annals of surgical oncology, 21(Suppl 3), S414–S421. doi:10.1245/s10434-014-3584-y

Shtutman, M., Zhurinsky, J., Simcha, I., Albanese, C., D'Amico, M., Pestell, R. and Ben-Ze'ev, A. (1999). The cyclin D1 gene is a target of the beta-catenin/LEF-1 pathway. Proceedings of the National Academy of Sciences of the United States of America, 96(10), 5522–5527. doi:10.1073/pnas.96.10.5522

Shull, M.M., Ormsby, I., Kier, A.B., Pawlowski, S., Diebold, R.J., Yin, M., Allen, R., Sidman, C., Proetzel, G. and Calvin, D. (1992). Targeted disruption of the mouse transforming growth factor-beta 1 gene results in multifocal inflammatory disease. Nature, 359(6397), 693–699. doi:10.1038/359693a0

Sinha, D., Pieterse, Z. and Kaur, P. (2018). Qualitative in vivo bioluminescence imaging. Bio-protocol, 8(18), e3020. doi:10.21769/BioProtoc.3020

Siri, S., Maier, F., Santos, S., Pierce, D. M. and Feng, B. (2019). Load-bearing function of the colorectal submucosa and its relevance to visceral nociception elicited by mechanical stretch. American journal of physiology. Gastrointestinal and liver physiology, 317(3), 349–358. doi:10.1152/ajpgi.00127.2019

Slattery, M.L., Lundgreen, A., Kadlubar, S.A., Bondurant, K.L. and Wolff, R.K. (2013). JAK/STAT/SOCS-signaling pathway and colon and rectal cancer. Molecular carcinogenesis, 52(2), 155–166. doi:10.1002/mc.21841

Slattery, M.L, Mullany, L.E., Sakoda, L., Samowitz, W.S., Wolff, R.K., Stevens, J. R. and Herrick, J.S. (2018). The NF-κB signalling pathway in colorectal cancer: associations between dysregulated gene and miRNA expression. Journal of cancer research and clinical oncology, 144(2), 269–283. doi:10.1007/s00432-017-2548-6

Slone, H.B., Peters, L.J. and Milas, L. (1979). Effect of host immune capability on radiocurability and subsequent transplantability of a murine fibrosarcoma. Journal of the National Cancer Institute, 63(5), 1229–1235.

Smith, J.J. and Garcia-Aguilar, J. (2015). Advances and Challenges in Treatment of Locally Advanced Rectal Cancer. Journal of Clinical Oncology, 33(16), pp.1797–1808. doi:10.1200/jco.2014.60.1054.

Smith, J.J., Strombom, P., Chow, O.S., Roxburgh, C.S., Lynn, P., Eaton, A., Widmar, M., Ganesh, K., Yaeger, R., Cercek, A., Weiser, M.R., Nash, G.M., Guillem, J.G., Temple, L.K.F., Chalasani, S.B., Fuqua, J.L., Petkovska, I., Wu, A.J., Reyngold, M., Vakiani, E., … Paty, P.B. (2019). Assessment of a Watch-and-Wait Strategy for Rectal Cancer in Patients With a Complete Response After Neoadjuvant Therapy. JAMA oncology, 5(4), e185896. doi:10.1001/jamaoncol.2018.5896

Snider, A.J., Bialkowska, A.B., Ghaleb, A.M., Yang, V.W., Obeid, L.M. and Hannun, Y.A. (2016). Murine Model for Colitis-Associated Cancer of the Colon. Methods in molecular biology, 1438, 245–254. doi:10.1007/978-1-4939-3661-8_14

Snyder, A., Makarov, V., Merghoub, T., Yuan, J., Zaretsky, J.M., Desrichard, A., Walsh, L.A., Postow, M.A., Wong, P., Ho, T.S., Hollmann, T.J., Bruggeman, C., Kannan, K., Li, Y., Elipenahli, C., Liu, C., Harbison, C.T., Wang, L., Ribas, A., Wolchok, J. D., … Chan, T.A. (2014). Genetic basis for clinical response to CTLA-4 blockade in melanoma. The New England journal of medicine, 371(23), 2189–2199. doi:10.1056/NEJMoa1406498

Son, J., Lyssiotis, C.A., Ying, H., Wang, X., Hua, S., Ligorio, M., Perera, R.M., Ferrone, C.R., Mullarky, E., Shyh-Chang, N., Kang, Y., Fleming, J.B., Bardeesy, N., Asara, J.M., Haigis, M.C., DePinho, R.A., Cantley, L.C. and Kimmelman, A.C. (2013). Glutamine supports pancreatic cancer growth through a KRAS-regulated metabolic pathway. Nature, 496(7443), 101–105. doi:10.1038/nature12040

Song, C.W., Griffin, R.J., Lee, Y.J., Cho, H., Seo, J., Park, I., Kim, H.K., Kim, D. H., Kim, M.S., Dusenbery, K.E. and Cho, L.C. (2019). Reoxygenation and Repopulation of Tumor Cells after Ablative Hypofractionated Radiotherapy (SBRT and SRS) in Murine Tumors. Radiation research, 192(2), 159–168. doi:10.1667/RR15346.1

Song, T.L., Nairismägi, M.L., Laurensia, Y., Lim, J.Q., Tan, J., Li, Z.M., Pang, W. L., Kizhakeyil, A., Wijaya, G.C., Huang, D.C., Nagarajan, S., Chia, B.K., Cheah, D., Liu, Y.H., Zhang, F., Rao, H.L., Tang, T., Wong, E.K., Bei, J.X., Iqbal, J., … Ong, C.K. (2018). Oncogenic activation of the STAT3 pathway drives PD-L1 expression in natural killer/T-cell lymphoma. Blood, 132(11), 1146–1158. doi:10.1182/blood-2018-01-829424

Soriano P. (1999). Generalized lacZ expression with the ROSA26 Cre reporter strain. Nature genetics, 21(1), 70–71. doi:10.1038/5007

de Sousa E Melo, F., Wang, X., Jansen, M., Fessler, E., Trinh, A., de Rooij, L.P., de Jong, J.H., de Boer, O.J., van Leersum, R., Bijlsma, M.F., Rodermond, H., van der Heijden, M., van Noesel, C.J., Tuynman, J.B., Dekker, E., Markowetz, F., Medema, J.P. and Vermeulen, L. (2013). Poor-prognosis colon cancer is defined by a molecularly distinct subtype and develops from serrated precursor lesions. Nature medicine, 19(5), 614–618. doi:10.1038/nm.3174

de Sousa e Melo, F., Kurtova, A.V., Harnoss, J.M., Kljavin, N., Hoeck, J.D., Hung, J., Anderson, J.E., Storm, E.E., Modrusan, Z., Koeppen, H., Dijkgraaf, G. J., Piskol, R. and de Sauvage, F.J. (2017). A distinct role for Lgr5+ stem cells in primary and metastatic colon cancer. Nature, 543(7647), 676–680. doi:10.1038/nature21713

Sow, H., Ren, J., Camps, M., Ossendorp, F., and Ten Dijke, P. (2019). Combined Inhibition of TGF-β Signaling and the PD-L1 Immune Checkpoint Is Differentially Effective in Tumor Models. Cells 8, 320. doi:10.3390/cells8040320

Spitzner, M., Ebner, R., Wolff, H.A., Ghadimi, B.M., Wienands, J. and Grade, M. (2014). STAT3: A Novel Molecular Mediator of Resistance to Chemoradiotherapy. Cancers, 6(4), 1986–2011. doi:10.3390/cancers6041986

Spranger S. (2016). Mechanisms of tumor escape in the context of the T-cell-inflamed and the non-T-cell-inflamed tumor microenvironment. International immunology, 28(8), 383–391. doi:10.1093/intimm/dxw014

Sprenkeler, E.G.G., Zandstra, J., van Kleef, N.D., Goetschalckx, I., Verstegen, B., Aarts, C.E.M., Janssen, H., Tool, A.T.J., van Mierlo, G., van Bruggen, R., Jongerius, I. and Kuijpers, T.W. (2022). S100A8/A9 Is a Marker for the Release of Neutrophil Extracellular Traps and Induces Neutrophil Activation. Cells, 11(2), 236. doi:10.3390/cells11020236

Steel, G.G., McMillan, T.J. and Peacock, J.H. (1989). The 5Rs of radiobiology. International journal of radiation biology, 56(6), 1045–1048. doi:10.1080/09553008914552491

Stevenson, A.R., Solomon, M.J., Lumley, J.W., Hewett, P., Clouston, A.D., Gebski, V.J., Davies, L., Wilson, K., Hague, W., Simes, J. and ALaCaRT Investigators (2015). Effect of Laparoscopic-Assisted Resection vs Open Resection on Pathological Outcomes in Rectal Cancer: The ALaCaRT Randomized Clinical Trial. JAMA, 314(13), 1356–1363. doi:10.1001/jama.2015.12009

Stevenson, J.P., Kindler, H.L., Papasavvas, E., Sun, J., Jacobs-Small, M., Hull, J., Schwed, D., Ranganathan, A., Newick, K., Heitjan, D.F., Langer, C.J., McPherson, J.M., Montaner, L.J. and Albelda, S.M. (2013). Immunological effects of the TGFβ-blocking antibody GC1008 in malignant pleural mesothelioma patients. Oncoimmunology, 2(8), e26218. doi:10.4161/onci.26218

Stijns, R.C.H., de Graaf, E.J.R., Punt, C.J.A., Nagtegaal, I.D., Nuyttens, J.J.M. E., van Meerten, E., Tanis, P.J., de Hingh, I.H.J.T., van der Schelling, G.P., Acherman, Y., Leijtens, J.W.A., Bremers, A.J.A., Beets, G.L., Hoff, C., Verhoef, C., Marijnen, C.A.M., de Wilt, J.H.W. and CARTS Study Group (2019). Long-term Oncological and Functional Outcomes of Chemoradiotherapy Followed by Organ-Sparing Transanal Endoscopic Microsurgery for Distal Rectal Cancer: The CARTS Study. JAMA surgery, 154(1), 47–54. doi:10.1001/jamasurg.2018.3752

Stintzing, S., Wirapati, P., Lenz, H.J., Neureiter, D., Fischer von Weikersthal, L., Decker, T., Kiani, A., Kaiser, F., Al-Batran, S., Heintges, T., Lerchenmüller, C., Kahl, C., Seipelt, G., Kullmann, F., Moehler, M., Scheithauer, W., Held, S., Modest, D.P., Jung, A., Kirchner, T., … Heinemann, V. (2019). Consensus molecular subgroups (CMS) of colorectal cancer (CRC) and first-line efficacy of FOLFIRI plus cetuximab or bevacizumab in the FIRE3 (AIO KRK-0306) trial. Annals of oncology : official journal of the European Society for Medical Oncology, 30(11), 1796–1803. doi:10.1093/annonc/mdz387

Stoffel, E., Mukherjee, B., Raymond, V.M., Tayob, N., Kastrinos, F., Sparr, J., Wang, F., Bandipalliam, P., Syngal, S. and Gruber, S.B. (2009). Calculation of Risk of Colorectal and Endometrial Cancer Among Patients With Lynch Syndrome. Gastroenterology, 137(5), pp.1621–1627. doi:10.1053/j.gastro.2009.07.039.

Strauss, J., Heery, C.R., Schlom, J., Madan, R.A., Cao, L., Kang, Z., Lamping, E., Marté, J.L., Donahue, R.N., Grenga, I., Cordes, L., Christensen, O., Mahnke, L., Helwig, C. and Gulley, J.L. (2018). Phase I Trial of M7824 (MSB0011359C), a Bifunctional Fusion Protein Targeting PD-L1 and TGFβ, in Advanced Solid Tumors. Clinical cancer research, 24(6), 1287–1295. doi:10.1158/1078-0432.CCR-17-2653

Street, S.E., Cretney, E. and Smyth, M.J. (2001). Perforin and interferon-gamma activities independently control tumor initiation, growth, and metastasis. Blood, 97(1), 192–197. doi:10.1182/blood.v97.1.192

Su, L.K., Kinzler, K.W., Vogelstein, B., Preisinger, A.C., Moser, A.R., Luongo, C., Gould, K.A. and Dove, W.F. (1992). Multiple intestinal neoplasia caused by a mutation in the murine homolog of the APC gene. Science, 256(5057), 668–670. doi:10.1126/science.1350108

Suri-Payer, E., Amar, A.Z., Thornton, A.M. and Shevach, E. M. (1998). CD4+CD25+ T cells inhibit both the induction and effector function of autoreactive T cells and represent a unique lineage of immunoregulatory cells. Journal of immunology, 160(3), 1212–1218.

Sussman, D.A., Santaolalla, R., Strobel, S., Dheer, R. and Abreu, M.T. (2012). Cancer in inflammatory bowel disease: lessons from animal models. Current opinion in gastroenterology, 28(4), 327–333. doi:10.1097/MOG.0b013e328354cc36

Sveen, A., Bruun, J., Eide, P.W., Eilertsen, I.A., Ramirez, L., Murumägi, A., Arjama, M., Danielsen, S.A., Kryeziu, K., Elez, E., Tabernero, J., Guinney, J.,

Palmer, H.G., Nesbakken, A., Kallioniemi, O., Dienstmann, R. and Lothe, R.A. (2018). Colorectal Cancer Consensus Molecular Subtypes Translated to Preclinical Models Uncover Potentially Targetable Cancer Cell Dependencies. Clinical Cancer Research, 24(4), 794–806. doi:10.1158/1078-0432.CCR-17-1234

Syngal, S., Brand, R.E., Church, J.M., Giardiello, F.M., Hampel, H.L. and Burt, R.W. (2015). ACG Clinical Guideline: Genetic Testing and Management of Hereditary Gastrointestinal Cancer Syndromes. American Journal of Gastroenterology, 110(2), pp.223–262. doi:10.1038/ajg.2014.435.

Tahir, R., Renuse, S., Udainiya, S., Madugundu, A.K., Cutler, J.A., Nirujogi, R. S., Na, C.H., Xu, Y., Wu, X. and Pandey, A. (2021). Mutation-Specific and Common Phosphotyrosine Signatures of KRAS G12D and G13D Alleles. Journal of proteome research, 20(1), 670–683. doi:10.1021/acs.jproteome.0c00587

Takahashi, T., Morotomi, M. and Nomoto, K. (2004). A novel mouse model of rectal cancer established by orthotopic implantation of colon cancer cells. Cancer science, 95(6), 514–519. doi:10.1111/j.1349-7006.2004.tb03242.x

Takaku, K., Oshima, M., Miyoshi, H., Matsui, M., Seldin, M.F. and Taketo, M.M. (1998). Intestinal tumorigenesis in compound mutant mice of both Dpc4 (Smad4) and Apc genes. Cell, 92(5), 645–656. doi:10.1016/s0092-8674(00)81132-0

Takeshima, T., Chamoto, K., Wakita, D., Ohkuri, T., Togashi, Y., Shirato, H., Kitamura, H. and Nishimura, T. (2010). Local radiation therapy inhibits tumor growth through the generation of tumor-specific CTL: its potentiation by combination with Th1 cell therapy. Cancer research, 70(7), 2697–2706. doi:10.1158/0008-5472.CAN-09-2982

Tanaka, T., Kohno, H., Suzuki, R., Yamada, Y., Sugie, S. and Mori, H. (2003). A novel inflammation-related mouse colon carcinogenesis model induced by azoxymethane and dextran sodium sulfate. Cancer science, 94(11), 965–973. doi:10.1111/j.1349-7006.2003.tb01386.x

Tanaka, Y., Wu, A.Y., Ikekawa, N., Iseki, K., Kawai, M. and Kobayashi, Y. (1994). Inhibition of HT-29 human colon cancer growth under the renal capsule of severe combined immunodeficient mice by an analogue of 1,25-dihydroxyvitamin D3, DD-003. Cancer research, 54(19), 5148–5153.

Tang, H., Liang, Y., Anders, R.A., Taube, J.M., Qiu, X., Mulgaonkar, A., Liu, X., Harrington, S.M., Guo, J., Xin, Y., Xiong, Y., Nham, K., Silvers, W., Hao, G., Sun, X., Chen, M., Hannan, R., Qiao, J., Dong, H., Peng, H. and Fu, Y.X. (2018). PD-L1 on host cells is essential for PD-L1 blockade-mediated tumor regression. The Journal of clinical investigation, 128(2), 580–588. doi:10.1172/JCI96061

Taube, J.M., Klein, A., Brahmer, J.R., Xu, H., Pan, X., Kim, J.H., Chen, L., Pardoll, D.M., Topalian, S.L. and Anders, R.A. (2014). Association of PD-1, PD-1 ligands, and other features of the tumor immune microenvironment with response to anti-PD-1 therapy. Clinical cancer research, 20(19), 5064–5074. doi:10.1158/1078-0432.CCR-13-3271

Tauriello, D.V.F., Palomo-Ponce, S., Stork, D., Berenguer-Llergo, A., Badia-Ramentol, J., Iglesias, M., Sevillano, M., Ibiza, S., Cañellas, A., Hernando-Momblona, X., Byrom, D., Matarin, J.A., Calon, A., Rivas, E.I., Nebreda, A.R., Riera, A., Attolini, C.S. and Batlle, E. (2018). TGFβ drives immune evasion in

genetically reconstituted colon cancer metastasis. Nature, 554(7693), 538–543. doi:10.1038/nature25492

Taylor, F.G., Quirke, P., Heald, R.J., Moran, B., Blomqvist, L., Swift, I., Sebag-Montefiore, D.J., Tekkis, P., Brown, G. and MERCURY study group (2011). Preoperative high-resolution magnetic resonance imaging can identify good prognosis stage I, II, and III rectal cancer best managed by surgery alone: a prospective, multicenter, European study. Annals of surgery, 253(4), 711–719. doi:10.1097/SLA.0b013e31820b8d52

Taylor, M.A., Hughes, A.M., Walton, J., Coenen-Stass, A.M.L., Magiera, L., Mooney, L., Bell, S., Staniszewska, A.D., Sandin, L.C., Barry, S.T., Watkins, A., Carnevalli, L.S. and Hardaker, E.L. (2019). Longitudinal immune characterization of syngeneic tumor models to enable model selection for immune oncology drug discovery. Journal for immunotherapy of cancer, 7(1), 328. doi:10.1186/s40425-019-0794-7

Teicher B.A. (2021). TGFß-Directed Therapeutics: 2020. Pharmacology & therapeutics, 217, 107666. doi:10.1016/j.pharmthera.2020.107666

Tejpar, S. and Van Cutsem, E. (2002). Molecular and genetic defects in colorectal tumorigenesis. Best Practice & Research Clinical Gastroenterology, 16(2), 171–185. doi:10.1053/bega.2001.0279

Teng, F., Mu, D., Meng, X., Kong, L., Zhu, H., Liu, S., Zhang, J. and Yu, J. (2015). Tumor infiltrating lymphocytes (TILs) before and after neoadjuvant chemoradiotherapy and its clinical utility for rectal cancer. American journal of cancer research, 5(6), 2064–2074.

Teng, F., Meng, X., Kong, L., Mu, D., Zhu, H., Liu, S., Zhang, J. and Yu, J. (2015). Tumor-infiltrating lymphocytes, forkhead box P3, programmed death ligand-1, and cytotoxic T lymphocyte-associated antigen-4 expressions before and after neoadjuvant chemoradiation in rectal cancer. Translational research, 166(6), 721–732.e1. doi:10.1016/j.trsl.2015.06.019

Thomas, D.A. and Massagué, J. (2005). TGF-beta directly targets cytotoxic T cell functions during tumor evasion of immune surveillance. Cancer cell, 8(5), 369–380. doi:10.1016/j.ccr.2005.10.012

Tie, J., Cohen, J.D., Wang, Y., Li, L., Christie, M., Simons, K., Elsaleh, H., Kosmider, S., Wong, R., Yip, D., Lee, M., Tran, B., Rangiah, D., Burge, M., Goldstein, D., Singh, M., Skinner, I., Faragher, I., Croxford, M., Bampton, C., … Gibbs, P. (2019). Serial circulating tumour DNA analysis during multimodality treatment of locally advanced rectal cancer: a prospective biomarker study. Gut, 68(4), 663–671. doi:10.1136/gutjnl-2017-315852

Tiernan, J., Cook, A., Geh, I., George, B., Magill, L., Northover, J., Verjee, A., Wheeler, J. and Fearnhead, N. (2014). Use of a modified Delphi approach to develop research priorities for the Association of Coloproctology of Great Britain and Ireland. Colorectal Disease, 16(12), pp.965–970. doi:10.1111/codi.12790.

Tiriac, H., Belleau, P., Engle, D.D., Plenker, D., Deschênes, A., Somerville, T.D. D., Froeling, F.E.M., Burkhart, R.A., Denroche, R.E., Jang, G.H., Miyabayashi, K., Young, C.M., Patel, H., Ma, M., LaComb, J.F., Palmaira, R.L.D., Javed, A.A., Huynh, J.C., Johnson, M., Arora, K., … Tuveson, D.A. (2018). Organoid Profiling

Identifies Common Responders to Chemotherapy in Pancreatic Cancer. Cancer discovery, 8(9), 1112–1129. doi:10.1158/2159-8290.CD-18-0349

Torlakovic, E. and Snover, D. (1996). Serrated adenomatous polyposis in humans. Gastroenterology, 110(3), pp. 748–755. doi:10.1053/gast.1996.v110.pm8608884.

Torres-Roca, J.F., Eschrich, S., Zhao, H., Bloom, G., Sung, J., McCarthy, S., Cantor, A.B., Scuto, A., Li, C., Zhang, S., Jove, R. and Yeatman, T. (2005). Prediction of radiation sensitivity using a gene expression classifier. Cancer research, 65(16), 7169–7176. doi:10.1158/0008-5472.CAN-05-0656

Toyota, M., Ahuja, N., Ohe-Toyota, M., Herman, J.G., Baylin, S.B. and Issa, J.P. (1999). CpG island methylator phenotype in colorectal cancer. Proceedings of the National Academy of Sciences of the United States of America, 96(15), 8681–8686. doi:10.1073/pnas.96.15.8681

Trachtman, H., Fervenza, F.C., Gipson, D.S., Heering, P., Jayne, D.R., Peters, H., Rota, S., Remuzzi, G., Rump, L.C., Sellin, L.K., Heaton, J.P., Streisand, J. B., Hard, M.L., Ledbetter, S.R. and Vincenti, F. (2011). A phase 1, single-dose study of fresolimumab, an anti-TGF-ß antibody, in treatment-resistant primary focal segmental glomerulosclerosis. Kidney international, 79(11), 1236–1243. doi:10.1038/ki.2011.33

Trakarnsanga, A., Gönen, M., Shia, J., Nash, G.M., Temple, L.K., Guillem, J.G., Paty, P.B., Goodman, K.A., Wu, A., Gollub, M., Segal, N., Saltz, L., Garcia-Aguilar, J. and Weiser, M.R. (2014). Comparison of tumor regression grade systems for locally advanced rectal cancer after multimodality treatment. Journal of the National Cancer Institute, 106(10), dju248. doi:10.1093/jnci/dju248

Tran Chau, V., Liu, W., Gerbé de Thoré, M., Meziani, L., Mondini, M., O'Connor, M. J., Deutsch, E. and Clémenson, C. (2020). Differential therapeutic effects of PARP and ATR inhibition combined with radiotherapy in the treatment of subcutaneous versus orthotopic lung tumour models. British journal of cancer, 123(5), 762–771. doi:10.1038/s41416-020-0931-6

Tsai, C.S., Chen, F.H., Wang, C.C., Huang, H.L., Jung, S.M., Wu, C.J., Lee, C. C., McBride, W.H., Chiang, C.S. and Hong, J.H. (2007). Macrophages from irradiated tumors express higher levels of iNOS, arginase-I and COX-2, and promote tumor growth. International journal of radiation oncology, biology, physics, 68(2), 499–507. doi:10.1016/j.ijrobp.2007.01.041

Tsai, M.H., Cook, J.A., Chandramouli, G.V., DeGraff, W., Yan, H., Zhao, S., Coleman, C.N., Mitchell, J.B. and Chuang, E.Y. (2007). Gene expression profiling of breast, prostate, and glioma cells following single versus fractionated doses of radiation. Cancer research, 67(8), 3845–3852. doi:10.1158/0008-5472.CAN-06-4250

Tuveson, D.A., Shaw, A.T., Willis, N.A., Silver, D.P., Jackson, E.L., Chang, S., Mercer, K.L., Grochow, R., Hock, H., Crowley, D., Hingorani, S.R., Zaks, T., King, C., Jacobetz, M.A., Wang, L., Bronson, R.T., Orkin, S.H., DePinho, R.A. and Jacks, T. (2004). Endogenous oncogenic K-ras(G12D) stimulates proliferation and widespread neoplastic and developmental defects. Cancer cell, 5(4), 375–387. doi:10.1016/s1535-6108(04)00085-6

Twyman-Saint Victor, C., Rech, A.J., Maity, A., Rengan, R., Pauken, K.E., Stelekati, E., Benci, J.L., Xu, B., Dada, H., Odorizzi, P.M., Herati, R.S., Mansfield, K.D., Patsch, D., Amaravadi, R.K., Schuchter, L.M., Ishwaran, H., Mick, R., Pryma, D.A., Xu, X., Feldman, M.D., … Minn, A. J. (2015). Radiation and dual checkpoint blockade activate non-redundant immune mechanisms in cancer. Nature, 520(7547), 373–377. doi:10.1038/nature14292

Uchida, H., Yamazaki, K., Fukuma, M., Yamada, T., Hayashida, T., Hasegawa, H., Kitajima, M., Kitagawa, Y. and Sakamoto, M. (2010). Overexpression of leucine-rich repeat-containing G protein-coupled receptor 5 in colorectal cancer. Cancer science, 101(7), 1731–1737. doi:10.1111/j.1349-7006.2010.01571.x

Ungricht, R., Guibbal, L., Lasbennes, M.C., Orsini, V., Beibel, M., Waldt, A., Cuttat, R., Carbone, W., Basler, A., Roma, G., Nigsch, F., Tchorz, J.S., Hoepfner, D. and Hoppe, P.S. (2022). Genome-wide screening in human kidney organoids identifies developmental and disease-related aspects of nephrogenesis. Cell stem cell, 29(1), 160–175.e7. doi:10.1016/j.stem.2021.11.001

van der Valk, M.J.M., Hilling, D.E., Bastiaannet, E., Meershoek-Klein Kranenbarg, E., Beets, G.L., Figueiredo, N.L., Habr-Gama, A., Perez, R.O., Renehan, A.G., van de Velde, C.J.H. and IWWD Consortium (2018). Long-term outcomes of clinical complete responders after neoadjuvant treatment for rectal cancer in the International Watch & Wait Database (IWWD): an international multicentre registry study. Lancet, 391(10139), 2537–2545. doi:10.1016/S0140-6736(18)31078-X

Vanneman, M. and Dranoff, G. (2012). Combining immunotherapy and targeted therapies in cancer treatment. Nature Reviews Cancer, 12(4), 237–251. doi:10.1038/nrc3237

Vanpouille-Box, C., Diamond, J.M., Pilones, K.A., Zavadil, J., Babb, J.S., Formenti, S.C., Barcellos-Hoff, M.H. and Demaria, S. (2015). TGFβ Is a Master Regulator of Radiation Therapy-Induced Antitumor Immunity. Cancer research, 75(11), 2232–2242. doi:10.1158/0008-5472.CAN-14-3511

Varga, J., Nicolas, A., Petrocelli, V., Pesic, M., Mahmoud, A., Michels, B.E., Etlioglu, E., Yepes, D., Häupl, B., Ziegler, P.K., Bankov, K., Wild, P.J., Wanninger, S., Medyouf, H., Farin, H.F., Tejpar, S., Oellerich, T., Ruland, J., Siebel, C.W. and Greten, F.R. (2020). AKT-dependent NOTCH3 activation drives tumor progression in a model of mesenchymal colorectal cancer. The Journal of experimental medicine, 217(10), e20191515. doi:10.1084/jem.20191515

Vasen, H.F.A., Blanco, I., Aktan-Collan, K., Gopie, J.P., Alonso, A., Aretz, S., Bernstein, I., Bertario, L., Burn, J., Capella, G., Colas, C., Engel, C., Frayling, I.M., Genuardi, M., Heinimann, K., Hes, F.J., Hodgson, S.V., Karagiannis, J.A., Lalloo, F. and Lindblom, A. (2013). Revised guidelines for the clinical management of Lynch syndrome (HNPCC): recommendations by a group of European experts. Gut, [online] 62(6), pp.812–823. doi:10.1136/gutjnl-2012-304356.

Vatner, R.E. and Formenti, S. C. (2015). Myeloid-derived cells in tumors: effects of radiation. Seminars in radiation oncology, 25(1), 18–27. doi:10.1016/j.semradonc.2014.07.008

Veldkamp, R., Kuhry, E., Hop, W.C., Jeekel, J., Kazemier, G., Bonjer, H.J., Haglind, E., Påhlman, L., Cuesta, M.A., Msika, S., Morino, M., Lacy, A.M. and COlon cancer Laparoscopic or Open Resection Study Group (COLOR). (2005). Laparoscopic surgery versus open surgery for colon cancer: short-term outcomes of a randomised trial. The Lancet Oncology, 6(7), 477–484. doi:10.1016/S1470-2045(05)70221-7

Venderbosch, S., Nagtegaal, I.D., Maughan, T.S., Smith, C.G., Cheadle, J.P., Fisher, D., Kaplan, R., Quirke, P., Seymour, M.T., Richman, S.D., Meijer, G.A., Ylstra, B., Heideman, D.A., de Haan, A.F., Punt, C.J. and Koopman, M. (2014). Mismatch repair status and BRAF mutation status in metastatic colorectal cancer patients: a pooled analysis of the CAIRO, CAIRO2, COIN, and FOCUS studies. Clinical cancer research, 20(20), 5322–5330. doi:10.1158/1078-0432.CCR-14-0332

Verhaegen, F., Granton, P. and Tryggestad, E. (2011). Small animal radiotherapy research platforms. Physics in medicine and biology, 56(12), 55–R83. doi:10.1088/0031-9155/56/12/R01

Vidal-Lletjós, S., Andriamihaja, M., Blais, A., Grauso, M., Lepage, P., Davila, A. M., Gaudichon, C., Leclerc, M., Blachier, F. and Lan, A. (2019). Mucosal healing progression after acute colitis in mice. World journal of gastroenterology, 25(27), 3572–3589. doi:10.3748/wjg.v25.i27.3572

Vlachogiannis, G., Hedayat, S., Vatsiou, A., Jamin, Y., Fernández-Mateos, J., Khan, K., Lampis, A., Eason, K., Huntingford, I., Burke, R., Rata, M., Koh, D.M., Tunariu, N., Collins, D., Hulkki-Wilson, S., Ragulan, C., Spiteri, I., Moorcraft, S. Y., Chau, I., Rao, S., … Valeri, N. (2018). Patient-derived organoids model treatment response of metastatic gastrointestinal cancers. Science, 359(6378), 920–926. doi:10.1126/science.aao2774

Wang, D. and Dubois, R. N. (2006). Prostaglandins and cancer. Gut, 55(1), 115–122. doi:10.1136/gut.2004.047100

Wang, K. and Karin, M. (2015). Tumor-Elicited Inflammation and Colorectal Cancer. Advances in cancer research, 128, 173–196. doi:10.1016/bs.acr.2015.04.014

Wang, Y., Zhao, M., He, S., Luo, Y., Zhao, Y., Cheng, J., Gong, Y., Xie, J., Wang, Y., Hu, B., Tian, L., Liu, X., Li, C. and Huang, Q. (2019). Necroptosis regulates tumor repopulation after radiotherapy via RIP1/RIP3/MLKL/JNK/IL8 pathway. Journal of experimental & clinical cancer research, 38(1), 461. doi:10.1186/s13046-019-1423-5

Wang, Y.Q., Shen, L.J., Wan, J.F., Zhang, H., Wang, Y., Wu, X., Wang, J.W., Wang, R.J., Sun, Y.Q., Tong, T., Huang, D., Wang, L., Sheng, W.Q., Zhang, X., Cai, G.X., Xu, Y., Cai, S.J., Zhang, Z. and Xia, F. (2023). Chinese journal of gastrointestinal surgery, 26(5), 448–458. doi:10.3760/cma.j.cn441530-20230107-00010

Wei, S., Egenti, M.U., Teitz-Tennenbaum, S., Zou, W. and Chang, A.E. (2013). Effects of tumor irradiation on host T-regulatory cells and systemic immunity in the context of adoptive T-cell therapy in mice. Journal of immunotherapy (Hagerstown, Md. : 1997), 36(2), 124–132. doi:10.1097/CJI.0b013e31828298e6

Wei, S.C., Duffy, C.R. and Allison, J.P. (2018). Fundamental Mechanisms of Immune Checkpoint Blockade Therapy. Cancer discovery, 8(9), 1069–1086. doi:10.1158/2159-8290.CD-18-0367

Weichselbaum, R.R., Liang, H., Deng, L. and Fu, Y.X. (2017). Radiotherapy and immunotherapy: a beneficial liaison?. Nature reviews. Clinical oncology, 14(6), 365–379. doi:10.1038/nrclinonc.2016.211

van de Wetering, M., Francies, H.E., Francis, J.M., Bounova, G., Iorio, F., Pronk, A., van Houdt, W., van Gorp, J., Taylor-Weiner, A., Kester, L., McLaren-Douglas, A., Blokker, J., Jaksani, S., Bartfeld, S., Volckman, R., van Sluis, P., Li, V.S., Seepo, S., Sekhar Pedamallu, C., Cibulskis, K., … Clevers, H. (2015). Prospective derivation of a living organoid biobank of colorectal cancer patients. Cell, 161(4), 933–945. doi:10.1016/j.cell.2015.03.053

Wherry, E.J. and Kurachi, M. (2015). Molecular and cellular insights into T cell exhaustion. Nature reviews. Immunology, 15(8), 486–499. doi:10.1038/nri3862

Wilkins, A., Fontana, E., Nyamundanda, G., Ragulan, C., Patil, Y., Mansfield, D., Kingston, J., Errington-Mais, F., Bottomley, D., von Loga, K., Bye, H., Carter, P., Tinkler-Hundal, E., Noshirwani, A., Downs, J., Dillon, M., Demaria, S., Sebag-Montefiore, D., Harrington, K., West, N., … Sadanandam, A. (2021). Differential and longitudinal immune gene patterns associated with reprogrammed microenvironment and viral mimicry in response to neoadjuvant radiotherapy in rectal cancer. Journal for immunotherapy of cancer, 9(3), e001717. doi:10.1136/jitc-2020-001717

Willers, H., Dahm-Daphi, J. and Powell, S.N. (2004). Repair of radiation damage to DNA. British journal of cancer, 90(7), 1297–1301. doi:10.1038/sj.bjc.6601729

Wirtz, S., Popp, V., Kindermann, M., Gerlach, K., Weigmann, B., Fichtner-Feigl, S. and Neurath, M.F. (2017). Chemically induced mouse models of acute and chronic intestinal inflammation. Nature protocols, 12(7), 1295–1309. doi:10.1038/nprot.2017.044

Withers, H.R. (1975). The Four R's of Radiotherapy. Advances in Radiation Biology, 5, 241-271. doi:10.1016/B978-0-12-035405-4.50012-8.

Wong, J., Armour, E., Kazanzides, P., Iordachita, I., Tryggestad, E., Deng, H., Matinfar, M., Kennedy, C., Liu, Z., Chan, T., Gray, O., Verhaegen, F., McNutt, T., Ford, E. and DeWeese, T.L. (2008). High-resolution, small animal radiation research platform with x-ray tomographic guidance capabilities. International journal of radiation oncology, biology, physics, 71(5), 1591–1599. doi:10.1016/j.ijrobp.2008.04.025

Wong, M.H., Saam, J.R., Stappenbeck, T.S., Rexer, C.H. and Gordon, J.I. (2000). Genetic mosaic analysis based on Cre recombinase and navigated laser capture microdissection. Proceedings of the National Academy of Sciences of the United States of America, 97(23), 12601–12606. https://doi.org/10.1073/pnas.230237997

Wrana, J.L., Attisano, L., Cárcamo, J., Zentella, A., Doody, J., Laiho, M., Wang, X. F. and Massagué, J. (1992). TGF beta signals through a heteromeric protein kinase receptor complex. Cell, 71(6), 1003–1014. doi:10.1016/0092-8674(92)90395-s

Wrana, J.L., Attisano, L., Wieser, R., Ventura, F. and Massagué, J. (1994). Mechanism of activation of the TGF-beta receptor. Nature, 370(6488), 341–347. doi:10.1038/370341a0

Wrzesinski, S.H., Wan, Y.Y. and Flavell, R.A. (2007). Transforming growth factor-beta and the immune response: implications for anticancer therapy. Clinical cancer research, 13(18 Part 1), 5262–5270. doi:10.1158/1078-0432.CCR-07-1157

Wu, C.Y., Yang, L.H., Yang, H.Y., Knoff, J., Peng, S., Lin, Y.H., Wang, C., Alvarez, R.D., Pai, S.I., Roden, R.B., Hung, C.F. and Wu, T.C. (2014). Enhanced cancer radiotherapy through immunosuppressive stromal cell destruction in tumors. Clinical cancer research, 20(3), 644–657. doi:10.1158/1078-0432.CCR-13-1334

Wu, F., Yang, J., Liu, J., Wang, Y., Mu, J., Zeng, Q., Deng, S. and Zhou, H. (2021). Signaling pathways in cancer-associated fibroblasts and targeted therapy for cancer. Signal transduction and targeted therapy, 6(1), 218. doi:10.1038/s41392-021-00641-0

Xu, J., Escamilla, J., Mok, S., David, J., Priceman, S., West, B., Bollag, G., McBride, W. and Wu, L. (2013). CSF1R signaling blockade stanches tumor-infiltrating myeloid cells and improves the efficacy of radiotherapy in prostate cancer. Cancer research, 73(9), 2782–2794. doi:10.1158/0008-5472.CAN-12-3981

Xu, X.T., Hu, W.T., Zhou, J.Y. and Tu, Y. (2017). Celecoxib enhances the radiosensitivity of HCT116 cells in a COX-2 independent manner by up-regulating BCCIP. American journal of translational research, 9(3), 1088–1100.

Xue, Y., Johnson, R., Desmet, M., Snyder, P.W. and Fleet, J.C. (2010). Generation of a transgenic mouse for colorectal cancer research with intestinal cre expression limited to the large intestine. Molecular cancer research, 8(8), 1095–1104. doi:10.1158/1541-7786.MCR-10-0195

Yaeger, R., Shah, M.A., Miller, V.A., Kelsen, J.R., Wang, K., Heins, Z.J., Ross, J. S., He, Y., Sanford, E., Yantiss, R.K., Balasubramanian, S., Stephens, P.J., Schultz, N., Oren, M., Tang, L. and Kelsen, D. (2016). Genomic Alterations Observed in Colitis-Associated Cancers Are Distinct From Those Found in Sporadic Colorectal Cancers and Vary by Type of Inflammatory Bowel Disease. Gastroenterology, 151(2), 278–287.e6. doi:10.1053/j.gastro.2016.04.001

Yamazaki, T., Gunderson, A.J., Gilchrist, M., Whiteford, M., Kiely, M.X., Hayman, A., O'Brien, D., Ahmad, R., Manchio, J.V., Fox, N., McCarty, K., Phillips, M., Brosnan, E., Vaccaro, G., Li, R., Simon, M., Bernstein, E., McCormick, M., Yamasaki, L., Wu, Y., … Young, K.H. (2022). Galunisertib plus neoadjuvant chemoradiotherapy in patients with locally advanced rectal cancer: a single-arm, phase 2 trial. The Lancet. Oncology, 23(9), 1189–1200. doi:10.1016/S1470-2045(22)00446-6

Yan, Y., Kolachala, V., Dalmasso, G., Nguyen, H., Laroui, H., Sitaraman, S.V. and Merlin, D. (2009). Temporal and spatial analysis of clinical and molecular parameters in dextran sodium sulfate induced colitis. PloS one, 4(6), e6073. doi:10.1371/journal.pone.0006073

Yang, L., Wang, Y., Bao, H., Wan, J., Fan, X., Bao, H., Shen, L., Guan, Y., Wu, X., Shao, Y., Zhu, J. and Zhang, Z. (2019). ctDNA as a potential prognostic

marker for locally advanced rectal cancer patients with ‘watch and wait’ approach. Journal of Clinical Oncology, 37(15_suppl), 3544. doi:10.1200/JCO.2019.37.15_suppl.3544

Yang, M.Y., Lee, H.T., Chen, C.M., Shen, C.C. and Ma, H.I. (2014). Celecoxib suppresses the phosphorylation of STAT3 protein and can enhance the radiosensitivity of medulloblastoma-derived cancer stem-like cells. International journal of molecular sciences, 15(6), 11013–11029. doi:10.3390/ijms150611013

Yang, X., Li, C., Herrera, P.L. and Deng, C.X. (2002). Generation of Smad4/Dpc4 conditional knockout mice. Genesis, 32(2), 80–81. doi:10.1002/gene.10029

Yao, Y., Xu, X., Yang, L., Zhu, J., Wan, J., Shen, L., Xia, F., Fu, G., Deng, Y., Pan, M., Guo, Q., Gao, X., Li, Y., Rao, X., Zhou, Y., Liang, L., Wang, Y., Zhang, J., Zhang, H., Li, G., … Hua, G. (2020). Patient-Derived Organoids Predict Chemoradiation Responses of Locally Advanced Rectal Cancer. Cell stem cell, 26(1), 17–26.e6. doi:10.1016/j.stem.2019.10.010

Yasuda, K., Nirei, T., Sunami, E., Nagawa, H. and Kitayama, J. (2011). Density of CD4(+) and CD8(+) T lymphocytes in biopsy samples can be a predictor of pathological response to chemoradiotherapy (CRT) for rectal cancer. Radiation oncology, 6, 49. doi:10.1186/1748-717X-6-49

Yothers, G., O'Connell, M.J., Allegra, C.J., Kuebler, J.P., Colangelo, L.H., Petrelli, N.J. and Wolmark, N. (2011). Oxaliplatin as adjuvant therapy for colon cancer: updated results of NSABP C-07 trial, including survival and subset analyses. Journal of clinical oncology, 29(28), 3768–3774. doi:10.1200/JCO.2011.36.4539

Young, K.H., Newell, P., Cottam, B., Friedman, D., Savage, T., Baird, J.R., Akporiaye, E., Gough, M.J. and Crittenden, M. (2014). TGFβ inhibition prior to hypofractionated radiation enhances efficacy in preclinical models. Cancer immunology research, 2(10), 1011–1022. doi:10.1158/2326-6066.CIR-13-0207

Young, K.H., Baird, J.R., Savage, T., Cottam, B., Friedman, D., Bambina, S., Messenheimer, D.J., Fox, B., Newell, P., Bahjat, K.S., Gough, M.J. and Crittenden, M.R. (2016). Optimizing Timing of Immunotherapy Improves Control of Tumors by Hypofractionated Radiation Therapy. PloS one, 11(6), e0157164. doi:10.1371/journal.pone.0157164

Yuki, S., Bando, H., Tsukada, Y., Inamori, K., Komatsu, Y., Homma, S., Uemura, M., Kato, T., Kotani, D., Fukuoka, S., Nakamura, N., Fukui, M., Wakabayashi, M., Kojima, M., Togashi, Y., Sato, A., Nishikawa, H., Ito, M. and Yoshino T. (2020). Short-term results of VOLTAGE-A: Nivolumab monotherapy and subsequent radical surgery following preoperative chemoradiotherapy in patients with microsatellite stable and microsatellite instability-high locally advanced rectal cancer. J Clin Oncol, 38(15_suppl):4100.

Zhang, H., Koch, C.J., Wallen, C.A. and Wheeler, K.T. (1995). Radiation-induced DNA damage in tumors and normal tissues. III. Oxygen dependence of the formation of strand breaks and DNA-protein crosslinks. Radiation research, 142(2), 163–168.

Zhang, S., Bai, W., Tong, X., Bu, P., Xu, J. and Xi, Y. (2019). Correlation between tumor microenvironment-associated factors and the efficacy and

prognosis of neoadjuvant therapy for rectal cancer. Oncology letters, 17(1), 1062–1070. doi:10.3892/ol.2018.9682

Zheng, H., Bai, Y., Wang, J., Chen, S., Zhang, J., Zhu, J., Liu, Y. and Wang, X. (2021). Weighted Gene Co-expression Network Analysis Identifies CALD1 as a Biomarker Related to M2 Macrophages Infiltration in Stage III and IV Mismatch Repair-Proficient Colorectal Carcinoma. Frontiers in molecular biosciences, 8, 649363. doi:10.3389/fmolb.2021.649363

Zhong, Y., Lin, Z., Lin, X., Lu, J., Wang, N., Huang, S., Wang, Y., Zhu, Y., Shen, Y., Jiang, J. and Lin, S. (2019). IGFBP7 contributes to epithelial-mesenchymal transition of HPAEpiC cells in response to radiation. Journal of cellular biochemistry, 120(8), 12500–12507. doi:10.1002/jcb.28516

Zhou, B.B. and Elledge, S.J. (2000). The DNA damage response: putting checkpoints in perspective. Nature, 408(6811), 433–439. doi:10.1038/35044005

Zhao, X., Li, L., Starr, T.K. and Subramanian, S. (2017). Tumor location impacts immune response in mouse models of colon cancer. Oncotarget, 8(33), 54775–54787. doi:10.18632/oncotarget.18423

Zhong, W., Myers, J.S., Wang, F., Wang, K., Lucas, J., Rosfjord, E., Lucas, J., Hooper, A.T., Yang, S., Lemon, L.A., Guffroy, M., May, C., Bienkowska, J.R. and Rejto, P.A. (2020). Comparison of the molecular and cellular phenotypes of common mouse syngeneic models with human tumors. BMC genomics, 21(1), 2. doi:10.1186/s12864-019-6344-3

Zhu, J., Sun, X., Zhang, T., Liu, A., Zhu, Y., Jia, J., Zhu, Y., Tan, S., Zhou, J., Zhang, C., Wang, X., Cai, G., Luo, B., Wu, J., Yang, J. and Zhang Z. 2017. A randomized phase III trial of capecitabine with or without irinotecan driven by UGT1A1 in neoadjuvant chemoradiation of locally advanced rectal cancer (CinClare). J. Clin. Oncol., 35(15_suppl), p. TPS3632. doi:10.1200/JCO.2017.35.15_suppl.TPS3632

Zhulai, G. and Oleinik, E. (2022). Targeting regulatory T cells in anti-PD-1/PD-L1 cancer immunotherapy. Scandinavian journal of immunology, 95(3), e13129. doi:10.1111/sji.13129

Zigmond, E., Halpern, Z., Elinav, E., Brazowski, E., Jung, S. and Varol, C. (2011). Utilization of murine colonoscopy for orthotopic implantation of colorectal cancer. PloS one, 6(12), e28858. doi:10.1371/journal.pone.0028858

Zitvogel, L., Pitt, J.M., Daillère, R., Smyth, M.J. and Kroemer, G. (2016). Mouse models in oncoimmunology. Nature reviews. Cancer, 16(12), 759–773. doi:10.1038/nrc.2016.91

Zou, W., Wolchok, J.D. and Chen, L. (2016). PD-L1 (B7-H1) and PD-1 pathway blockade for cancer therapy: Mechanisms, response biomarkers, and combinations. Science translational medicine, 8(328), 328rv4. doi:10.1126/scitranslmed.aad7118

Appendix - GPOL Mutation Panel Gene List

AIM2

ALK

AMER1

APC

AR

ARAF

ARID1A

ARID1B

ARID2

ASTE1

ASXL1

ATM

ATR

ATRX

BLM

BRAF

BRCA1

BRCA2

CDK12

CDKN2A

CHEK2

CHIITA

CREBBP

CTCF

CTNNB1

DAXX

DICER1

DNMT3A

EGFR

EP300

ERBB2

ERBB3

ERBB4

FBXW7

FGFR1

FGFR2

FGFR3

FGFR4

GATA3

GNA11

GNAQ

GNAS

HGF

IDH1

IDH2

JAK2

JAK3

KDR

KMT2A

KRAS

MAP2K4

MAP3K1

MEN1

MET

MSH2

MSH6

MTOR

MYC

NBN

NF1

NOTCH1

NOTCH2

NOTCH3

NOTCH4

NRAS

NTRK1

PALB2

PBRM1

PDGFRA

PHF6

PIK3CA

PIK3CB

PIK3R1

POLE

POLQ

PPP2R1A

PTCH1

PTEN

QKI

RAC1

RAD50

RAF1

RB1

RET

RNF43

ROS1

RPL22

RUNX1

SETD2

SF3B1

SLC23A2

SMAD4

SMARCA4

SMO

STAG2

TAF1B

TEAD2

TGFBR2

TMBIM4

TP53

TSC1

TSC2

TTK

WT1